FOSSIL

DOE/MC/24264-2786
IDE90000442)

Re-Analysis of the MWX Fracture Stimulation Data From the Fluvial Zone of the Mesaverde Formation and Comparison With Paludal and Coastal Zone Behavior

Final Report

M.B. Smith
W.K. Miller II

October 1989

Work Performed Under Contract No.: DE-AC21-87MC24264

For
U.S. Department of Energy
Office of Fossil Energy
Morgantown Energy Technology Center
Morgantown, West Virginia

By
Nolte-Smith, Inc.
Tulsa, Oklahoma

DISCLAIMER

This report was prepared as an account of work sponsored by an agency of the United States Government. Neither the United States Government nor any agency thereof, nor any of their employees, makes any warranty, express or implied, or assumes any legal liability or responsibility for the accuracy, completeness, or usefulness of any information, apparatus, product, or process disclosed, or represents that its use would not infringe privately owned rights. Reference herein to any specific commercial product, process, or service by trade name, trademark, manufacturer, or otherwise does not necessarily constitute or imply its endorsement, recommendation, or favoring by the United States Government or any agency thereof. The views and opinions of authors expressed herein do not necessarily state or reflect those of the United States Government or any agency thereof.

DISCLAIMER

Portions of this document may be illegible in electronic image products. Images are produced from the best available original document.

DISCLAIMER

This report was prepared as an account of work sponsored by an agency of the United States Government. Neither the United States Government nor any agency thereof, nor any of their employees, makes any warranty, express or implied, or assumes any legal liability or responsibility for the accuracy, completeness, or usefulness of any information, apparatus, product, or process disclosed, or represents that its use would not infringe privately owned rights. Reference herein to any specific commercial product, process, or service by trade name, trademark, manufacturer, or otherwise does not necessarily constitute or imply its endorsement, recommendation, or favoring by the United States Government or any agency thereof. The views and opinions of authors expressed herein do not necessarily state or reflect those of the United States Government or any agency thereof.

This report has been reproduced directly from the best available copy.

Available to DOE and DOE contractors from the Office of Scientific and Technical Information, P.O. Box 62, Oak Ridge, TN 37831; prices available from (615)576-8401, FTS 626-8401.

Available to the public from the National Technical Information Service, U. S. Department of Commerce, 5285 Port Royal Rd., Springfield, VA 22161.

Price: Printed Copy A21
Microfiche A01

Printed in the United States of America, Office of Scientific and Technical Information, Oak Ridge , Tennessee

DOE/MC/24264--2786

DE90 000442

Re-Analysis of the MWX Fracture Stimulation Data From the Fluvial Zone of the Mesaverde Formation and Comparison With Paludal and Coastal Zone Behavior

Final Report

M.B. Smith
W.K. Miller II

Work Performed Under Contract No.: DE-AC21-87MC24264

For
U.S. Department of Energy
Office of Fossil Energy
Morgantown Energy Technology Center
P.O. Box 880
Morgantown, West Virginia 26507-0880

By
Nolte-Smith, Inc.
7030 South Yale
Suite 502
Tulsa, Oklahoma 74136

October 1989

TABLE OF CONTENTS

	Page
LIST OF FIGURES AND TABLES	ii
INTRODUCTION	1
SUMMARY	2
DISCUSSION	5
In Situ Stress Analysis	5
Stress Correlation Analysis	6
Stress v. Lithology	6
Stress v. Acoustic Velocity	7
Stress Profiling	9
Fluvial B Sand Fracture Analysis	10
Closure Pressure Determination	10
Minifrac Pressure Decline Analysis	10
Minifrac Pressure History Match	11
Main Fracture Treatment History Match	11
Fluvial C Sand Fracture Analysis	13
Closure Pressure Determination	13
Minifrac No. 1 Pressure Decline Analysis	13
Minifrac No. 1 Pressure History Match	14
Minifrac No. 2 Pressure Decline Analysis	15
Minifrac No. 2 Pressure History Match	16
Fluvial E Sand Fracture Analysis	17
Closure Pressure Determination	17
Minifrac Pressure Decline Analysis	18
Minifrac Pressure History Match	19
Main Fracture Treatment History Match	20
CONCLUSIONS	22
REFERENCES	24
FIGURES AND TABLES	25
APPENDICES	119
APPENDIX A - Stress Test Analysis	120
APPENDIX B - Calculations for Lithology and Acoustic Derived In Situ Stress Logs.	359
APPENDIX C - Fracture Analysis Simulator I/O	394

LIST OF FIGURES AND TABLES

FIGURES

		Page
1.	Geologic Cross-Section of MWX-1	26
2.	VOLAN Log Showing Fluvial Zone Stress Test Intervals	27
3.	Comparison of NSI and Sandia Fracture Gradients	34
4.	Characteristic of Backstress Effect (Shale 5757-5759')	35
5.	Comparison of NSI and Sandia Fracture Gradients for All MWX Stress Test Data	36
6.	"K-Factor" v. Gamma-Ray API Units for Fluvial Stress Data	39
7.	"K-Factor" v. Gamma-Ray for All MWX Data Showing the Bi-Linear Correlation	40
8.	Measured K-Factor v. Sonic Log K-Factor for Fluvial Stress Data	41
9.	Measured K-Factor v. Sonic Log K-Factor for All MWX Stress Data	42
10.	Measured Stress v. Sonic Log Derived Stress Comparing MWX Results to Other Industry Results	43
11.	Derived Stress Log from Bi-Linear GR Correlation as Compared to Measured Stresses, MWX-2	44
12.	Derived Stress Log from the Sonic Correlation as Compared to Measured Stresses, MWX-2	50
13.	Stress Profile Used for Matching the Fluvial Zone Frac Tests	56

FLUVIAL "B" SAND TESTS:

14.	Nitrogen Step-Rate Test	57
15.	Nitrogen Step-Rate Test Flowback Decline	58
16.	Nitrogen Pump-In/Flowback No. 2 Decline	59
17.	Nitrogen Pump-In/Flowback No. 3 Decline	60
18.	Nitrogen Pump-In/Flowback No. 4 Decline	61
19.	KCL Pump-In/Flowback Decline	62
20.	Minifrac Shut-In Pressure Decline	63
21.	MInifrac Pressure Decline Type-Curve Match	64
22.	Core Fracture Frequency and Width Distribution With Respect to Depth in MWX-1	66
23.	Foam Minifrac Injection/Decline Pressure History Match	67
24.	Simulator Predicted Gross Fracture Height at Wellbore for Foam Minifrac	68
25.	Pressure History Match of Fluvial "B" Foam Fracture Treatment Using Same Input Parameters Used to History Match the Minifrac	69
26.	Pressure History Match of Fluvial "B" Foam Fracture Treatment With Increased Boundary Stress, Constant, Pressure Mode, and Extended Mid-Treatment Shut-In Decline	70
27.	Stimulation of Extended Constant Pressure Mode for Foam Fracture Treatment to Evaluate Excess Leak-Off	71
28.	Simulator Predicted Gross Fracture Height at Wellbore For Foam Fracture Treatment at the Time of the Mid-Treatment Shut-Down	72
29.	Post-Frac Gamma-Ray Log for Foam Fracture Treatment	73
30.	Estimated Lens Size/Orientation for the Fluvial "B" Sand	74

FIGURES (CONT.) Page

FLUVIAL "C" SAND TESTS:

31. KCL Pump-In/Flowback Test Pressure Decline 76
32. KCL Step-Rate Test Injection 77
33. KCL Step-Rate Test/Flowback 78
34. KCL Pump-In/Flowback Test No. 2 79
35. KCL Pump-In/Flowback Test No. 3 80
36. KCL Pump-In/Flowback Test No. 4 81
37. Foam Minifrac No.1 Pressure Decline (Without 100 Mesh Sand) 82
38. Foam Minifrac No.1 Pressure Type Curve Match 83
39. Pressure History Match of Foam Minifrac No.1 Without Constant Pressure Mode 85
40. Simulator Predicted Gross Fracture Height at Wellbore for Foam Minifrac No.1 Without Constant Pressure Mode 86
41. Pressure History Match of Foam Minifrac No. 1 With Constant Pressure Mode 87
42. Simulator Predicted Gross Height at Wellbore for Foam Minifrac No.1 With Constant Pressure Mode 88
43. Foam Minifrac No. 1 Pressure Decline (With 100 Mesh Sand) 89
44. Foam Minifrac No. 2 Pressure Decline Type Curve Match, With 100 Mesh Sand 90
45. Pressure History Match of Foam Minifrac No. 2 With 100 Mesh Sand .. 92
46. Simulator Predicted Gross Height at Wellbore for Foam Minifrac No. 2 With 100 Mesh Sand 93
47. Pressure History Match of Foam Minifrac No. 2 With Increased Fluid Viscosity Through Constant Pressure Mode 94
48. Pressure History Match of Foam Minifrac No. 2 With Increased Fluid Viscosity Through Constant Pressure Mode and Decreased Viscosity in Early Time 95
49. Simulator Predicted Gross Fracture Height at Wellbore for Foam Minifrac No. 2 With Viscosity Changes 96
50. History Match of Pressure Decline for Foam Minifrac No. 2 97
51. Comparison of Pressure Decline Behavior for Two Foam Minifracs 98

FLUVIAL "E" SAND TESTS:

52. KCL Pump-In/Shut-In Decline 100
53. Horner Plot of KCL Pump-In/Shut-In Decline 101
54. KCL Step-Rate Test Injection 102
55. KCL Step-Rate Test/Flowback Decline 103
56. KCL Pump-In/Flowback No. 2 Decline 104
57. KCL Pump-In/Flowback No. 3 Decline 105
58. KCL Pump-In/Flowback No. 4 Decline 106
59. Foam Minifrac Shut-In Pressure Decline 107
60. Foam Minifrac Pressure Decline Type Curve Match, Pump Time = 16.5 Minutes 108
61. Foam Minifrac Pressure Decline Type Curve Match, Pump Time = 25.9 Minutes 109
62. Foam Minifrac Pressure Decline History Match 111
63. Initial Attempt to History Match the Foam Minifrac Injection/ Decline Pressures 112

FIGURES (CONT.) Page

64. Foam Minifrac Pressure History Match With Changes in Fluid Viscosity 113
65. Simulator Predicted Gross Fracture Height at Wellbore for Foam Minifrac 114
66. Foam Fracture Treatment Pressure History Match 115
67. Estimated Sand Lens Size/Orientation 116
68. Post-Frac Temperature Log for Foam Fracture Treatment 117
69. Post-Frac Gamma-Ray Log for Foam Fracture Treatment 118

TABLES:

1. Comparison of NSI and Sandia Fluvial Zone Stress Results 31
2. Summary of Stress, Sonic Log, and Mean Gamma-Ray Data Considered for Correlation Analysis 37
3. Comparison of Lithology Correlation Stress With Measured Stress for Fluvial Zone 49
4. Comparison of Sonic Correlation Stress With Measured Stress for Fluvial Data 55
5. Worksheet for Fluvial "B" Minifrac Pressure Decline Analysis 65
6. Results of Fluvial "C" Closure Stress Tests 75
7. Worksheet for Fluvial "C" Minifrac No. 1 Pressure Decline Analysis. 84
8. Worksheet for Fluvial "C" Minifrac No. 2 Pressure Decline Analysis. 91
9. Results of Fluvial "E" Closure Stress Tests 99
10. Worksheet for Fluvial "E" Minifrac Pressure Decline Analysis 110

INTRODUCTION

Historically, producing natural gas from low permeability formations has been uneconomical and inefficient due to the low natural flow rates. While massive hydraulic fracturing has resulted in significant improvements in production from blanket sand, the results have been disappointing for lenticular tight gas reservoirs. In 1980, the National Petroleum Council estimated that these lenticular reservoirs contained in excess of 370 Tcf of gas, or over 40 percent of the estimated reserves in the U.S. tight gas basins. More recently (1987), the U.S. Geological Survey estimated that gas-in-place in the Piceance Basin lenticular sands alone exceeded 400 Tcf with estimated recoverable gas at 68 Tcf.

For a number of years the U.S. Department of Energy has been engaged in research to enhance gas recovery from "tight gas sands," particularly the lenticular sandstone formations common to the Western United States. The purpose of this research is to establish the production potential from lenticular reservoirs, improve existing production technology; and ultimately, to demonstrate the economic feasibility of drilling and completing wells in this unconventional gas source.

To investigate these Western U.S tight gas sands, DOE established the Multi-Well Experiment (MWX), a field research facility near Rifle, Colorado, where three closely spaced wells were drilled through the lenticular Mesaverde formation in the Piceance basin. Testing included extensive coring and core analysis, production testing, and instrumented fracture stimulation experiments. Because one of the more important aspects of the MWX project was to establish the predictability of well stimulation procedures, extensive fracture testing was conducted in the Paludal, Coastal, and Fluvial zones.

This report focuses on a review and re-analysis of the MWX stimulation data obtained in the Fluvial zone. This follows a similar re-analysis of the Paludal and Coastal zone data which compared stress analysis methods, defined a relationship between stress and lithology, identified weaknesses in the fluid loss pressure decline analysis, and demonstrated a methodology for combining history matching of injection/decline pressures with the pressure decline analysis to better characterize the leak-off and geometry associated with the hydraulic fracture. Many of these same analytical techniques are used to evaluate the Fluvial data, comparing the correlations and methods previously devised to those required in this evaluation. Where appropriate, the techniques and results from the analysis of the three Mesaverde zones are compared and discussed, helping to set forth guidelines for future testing in this formation.

SUMMARY

In situ stress tests were performed on 26 Fluvial intervals in well MWX-2 using the pump-in/shut-in micro-frac procedure. For each interval anywhere from 3 to 7 tests were performed to determine closure stress. Each of these tests were re-analyzed using a plot of pressure versus the square-root of shut-in time to determine closure pressure. While there was reasonably good agreement with previous results estimated from ISIP's;, the "reservoir type" analysis allowed for a more definitive, less subjective pick of closure pressure. In addition to the small volume tests; larger volume step-rate tests, pump-in/shut-ins, and pump-in/flowback tests were performed in the Fluvial B, C, and E sands. These results were also considered in the stress analysis.

Similar to the prior re-analysis of the data from the Paludal and Coastal zones, a "K-factor" was calculated from the stress results to normalize out the effects of depth and pore pressure in comparing the stress results. Using the K-factor, correlation analysis was performed with both the gamma-ray (lithology) log and the acoustic (sonic) log resulting in equations for calculating stress from either the gamma-ray or acoustic log response. When the lithology calculated stresses were compared to the actual measured stresses there was mixed agreement; there being reasonably good agreement in the sandstones, but, very poor agreement in the mudstones. While the lithology correlation appeared to be an accurate tool for predicting closure stress in the Paludal and Coastal zones, its use for the Fluvial zone was found to be unacceptable. The sonic correlation, in this case, was found to give the better results and was thus used to derive a stress profile for modeling subsequent Fluvial fracture injections.

For each of the three Fluvial zones (B, C, and E sands) the minifracs were analyzed both with pressure decline type-curve analysis and through history matching of the injection and decline pressures using the derived stress profile. As alluded to in the original analysis of this data, there appeared to be a dual leak-off system present - probably due to natural fissures. This was not evident in the type-curve analysis, however it was quite apparent in trying to history match the minifrac pressure declines with the simulator. Once again, as discussed in the Paludal and Coastal reports; the pressure decline type-curve analysis has certain weaknesses for complex environments and needs to be used in conjunction with history matching to achieve a meaningful analysis.

In history matching the Fluvial B main fracture treatment, a good match was obtained up to the time of the abnormal pressure increase. Several attempts were made to model the

abnormal pressure behavior and no logical cause could be obtained with the simulator. Once again, as seen in the analysis of the Paludal and Coastal treatments; proppant bridging at the lens boundary due to lateral variations in stress is the most likely cause. The estimated lens geometry and fracture azimuth were consistent with this evaluation.

On the Fluvial "C" sand a main fracture treatment was not performed. However, two minifracs were performed to evaluate the dual leak-off system; one with and one without 100-mesh sand for leak-off control to natural fissures. From NSI's analysis it appeared that the 100-mesh sand was effective in going into the fissures to reduce leak-off during injection. However, there was also a corresponding higher net treating pressure on the 100-mesh minifrac which may have contributed to more height growth and the opening of additional leak-off sources. Without fracture evaluation logs to compare to the simulator results it was difficult to determine if this happened or not and how effective the 100-mesh sand was. It did appear from this analysis, though, that a secondary leak-off source was present.

While the fracture injection pressures for the B and C sands could be explained fairly straight forward, i.e. no indication of "abnormally" high treating pressures; the minifrac and main fracture injection pressures on the Fluvial "E" sand could not. At about the same time in both injections (about 10 minutes) there was a sharp pressure rise which could not be attributed to changes in rate, viscosity, height growth, etc. The only way to model this was to severely increase viscosity; however, since it was on both treatments, it was not thought to be viscosity related but, instead related to the formation. Since there were two lenses present (E1 and E2 with the E2 lens being very small and narrow in comparison to the E1 lens) it is possible that both lenses were taking fluid initially and the fracture in the E2 lens reached a lateral stress barrier causing this portion of the fracture to stop growing and in effect reducing the "effective" fracture height and increasing the injection rate into the remaining E1 sand. The abnormal pressure rise in the later part of the main fracture treatment was reasonably consistent with the fracture reaching the E1 lens boundary as per the estimated lens geometry.

The analysis of the Fluvial fracture data completes the re-analysis of the MWX stimulation data. Several significant finding have surfaced from this work, including

* a comparison of analysis techniques for analyzing the micro-frac stress tests, with the "reservoir type" method giving more definitive, less subjective results,

* a comparison of stress derived profiles from both lithology and acoustic logs and the potential error in using

this technique for stress profiling,

* the weaknesses in the pressure decline type-curve analysis for complex environments such as the Mesaverde formation,

* the need to perform both the type-curve analysis and pressure history matching of both injection and decline pressures to quantify fluid leak-off, and

* a reasonably simple explanation for the "apparent" high fracture treating pressures based on lateral stress variations at the sand lens boundaries.

In addition, much of the previous analyses was confirmed, however, two significant differences emerged. First, with one exception, no indication of abnormal treating pressure was noted. In fact, net pressure for the minifracs and pad stages of the fracture treatments was very predictable using stress profiles generated from in situ stress tests, laboratory data for modulus, and published fluid rheology values. The exception was the Fluvial "E" sand, where an unexpected pressure increase occurred about 10 minutes into pumping (prior to starting proppant) and this exception is discussed herein.

Second, some of the "abnormal" pressure data and treatment screenouts was previously related to a significant effect of natural fractures on the treatment pumping behavior. This analysis found evidence for this only in the Fluvial zones, which, based on core analysis, was the zone containing the majority of the observed natural fractures. Instead of fluid loss to natural fractures, the pre-mature screenout of several treatments correlated closely with proppant reaching the boundary of the limited, lenticular sands. This implies that propped fracture stimulations, at least using "normal, conventional" procedures, cannot be used to connect remote lenses to the wellbore.

DISCUSSION

The Fluvial zone of the Mesaverde Formation, present from about 4,400 to 6,000 feet in the MWX Wells (Figure 1), is comprised of lenticular, cross-bedded, channel-form sandstones and rare carbonaceous shales, mudstones, and siltstones.[1] The lower part of the fluvial interval (between 5,000 and 6,000 feet) is of greatest interest for its gas potential. In addition, numerous cored sandstone intervals in the fluvial interval contain interconnected, partly open, vertical fractures which greatly enhance permeability in otherwise very low-permeability rock.

To evaluate hydraulic fracturing as a means of stimulating the Fluvial zone, extensive research was performed at the MWX site. Testing included in situ stress tests in twenty-six different intervals and step-rate tests, injection decline tests, and minifracs in the Fluvial "B", "C", and "E" sands. Main foam fracturing treatments were performed in the "B" and "E" sands.

The following focuses on a review/re-analysis of the Fluvial stimulation data, the goal being to provide an independent engineering evaluation of the data and treatment results. Also, where appropriate the results from the previous analyses of the Paludal and Coastal Zones are interjected into the Fluvial analysis.

IN-SITU STRESS ANALYSIS

In-situ stress tests were performed on 26 Fluvial intervals in well MWX-2 using the small volume (micro-frac) procedure, which typically consists of pumping low volumes of low viscosity fluid into a 1-2 foot interval at 5-20 gpm and measuring the shut-in pressure (instantaneous shut-in pressure, ISIP).[1,2,3,4] Because of the small volume injected and the apparent small fracture volume created, theoretically the fracture should close quickly and the closure stress will be approximated by the ISIP. In addition to the small volume stress tests; larger volume step-rate tests, pump-in/shut-ins, and pump-in/flowback tests were performed in the Fluvial B, C, and E sands. These results are discussed later as part of the modeling of the minifracs and fracture treatments and compared with the predicted stress profile generated from the small volume stress tests.

Figure 2 shows the VOLAN log from MWX-2 with the microfrac test intervals and different Fluvial zone sands indicated. The designation for the stress intervals is "well number-zone-test interval, e.g. 2F1 indicates MWX-2, Fluvial zone, and test

interval no. 1. As seen from the log, the test intervals sampled both sands and shales, providing a good basis for stress profiling and fracture modeling.

The data and interpretation of the Fluvial zone in situ stress tests is included in Appendix A. As for the previous analysis of the "Paludal" and "Coastal" zone data, the "reservoir type" analysis was used in this evaluation.[5,6] As indicated in the previous analyses, although the "ISIP" method yields repeatable results, there is no clear, quantitative method for picking this ISIP. The "reservoir type" method, using the square-root of shut-in time plot, provides a more definitive pick of closure stress. Because of this difference in analysis techniques, NSI's closure stresses are consistently lower than the previous stress analysis; but by less than 100 psi in most cases. Table 1 shows this comparison. Figure 3 shows a good comparison of Fluvial fracture gradients calculated from NSI's and the previous stress results. In this same figure an attempt was made to determine the existence of backstress effects. Such an effect would be evident from a stress systematically increasing with each subsequent injection on the same interval. This was not evident from Figure 3; however, when the data was evaluated closer, one zone from 5757 to 5759 feet (shale-mudstone) showed evidence of backstress as seen in Figure 4. Because this is virtually a non-permeable zone, though, this is thought to be purely coincidental and of no significance to the Fluvial analysis. Thus, it was concluded that backstress effects were not a factor in the analysis of the Fluvial zone stress data.

Figure 5, shows a comparison of fracture gradients calculated from NSI's and the previous stress results for all MWX data from the Paludal, Coastal, and Fluvial zones. While there are a few points that deviated from a 1:1 correlation, most fall within a reasonable margin of error; NSI's results falling, for the most part, just below the line because of the analysis technique used.

STRESS CORRELATION ANALYSIS

STRESS VERSUS LITHOLOGY

Similar to the re-analysis of the Paludal and Coastal data,[5,6] a "K factor" was calculated from the results of each Fluvial stress test to normalize out the effects of depth and pore pressure in comparing the stress results. These are shown in the last two columns of Table 1. With the exception of the first zone; the results compared favorably. To perform the lithology correlation analysis, the stress results in Table 2 were considered, including twenty-six intervals from the Fluvial, eleven from the Coastal, twelve from the Paludal, and eleven from the Marine zone. The "Gamma-Ray" column in Table 2

gives the average GR over the two foot perforated test interval and the "Mean Gamma Ray" is the mean GR value over the eleven foot interval surrounding the test zone. The "Std Dev" column gives the standard deviation in gamma-ray associated with the mean GR results. "Frac Grad" and "K (Stress)" are based on NSI's re-analysis verification of the previously determined results. "K (Sonic)" is K factor results based on acoustic log data from the respective wells. The Poisson's Ratio (ν), obtained from the sonic log and averaged over the eleven foot interval, was used to calculated "K" using the relationship $K = \nu / (1-\nu)$.

When K-factor was plotted versus the mean GR values for only the Fluvial results, Figure 6, the correlation was not very good, with significantly more scatter than was evident from the similar Paludal and Coastal analyses. As seen in Figure 6, the results were sub-divided into those with GR standard deviations greater than and less than 10. This did not seem to affect the scatter, both high and low standard deviation values falling outside the acceptable range of a "good" correlation.

Plotting only the lower standard deviation (i.e. < 10) results for all four zones (Paludal, Coastal, Fluvial, and Marine), Figure 7, a reasonably good bi-linear lithology correlation still existed. As for the previous Paludal and Coastal analyses, the correlation was defined by the equation

$$K = MGR * 0.01532 - 0.458 \qquad (1)$$

for GR less than 90 API Units and K = 1.0 for GR greater than 90 API Units. K equal to 1.0 implies that closure stress is equal to the overburden pressure. As shown in the previous Paludal and Coastal analyses,[5,6] this lithology correlation enables the stress value for any zone to be estimated based on its mean GR value, overburden stress, and local pore pressure using the equation

$$K = (\sigma_c - P_o) / (OB - P_o). \qquad (2)$$

The stress profile derived with the lithology correlation is presented later and compared with the sonic derived stress profile.

STRESS VERSUS ACOUSTIC VELOCITY

A linear relation generally exists between depth, pore pressure, and closure stress as expressed by a K factor - and this factor is often assumed linked to the Poisson's Ratio by

$$K = \nu / (1 - \nu). \qquad (3)$$

This relation has led to the use of sonic logs which measure compressional and shear wave velocities from which Poisson's

Ratio is calculated.[7,8] While the theoretical validity of such a calculation might be questioned, it has been used empirically in several areas with good success.[9] Also, some empirical evidence exists that suggests that sonic log derived stress generally correlates (not 1:1) with actual measured stress.[10]

Based on this empirical procedure, the long-spaced-sonic log from MWX-2 was used to determine "K-factor" independent of the stress analysis. As with the development of the GR lithology correlation, the heterogeneity of each test interval was evaluated and those zones with a low GR standard deviation were separated out and plotted as shown in Figure 8. As was the case with the Coastal data, significant scatter existed, with a hint of a correlation, yet potential for large error. Plotting all low standard deviation (i.e. less than 10) results for the Fluvial, Coastal, Paludal, and Marine zones; the correlation was strengthened as shown in Figure 9. While there still appears to be potential for large error, the best-fit "dashed" line was used to formulate a stress profile for comparison to the stress profile derived from the lithology correlation to access which more closely approximates the results obtained on the Fluvial minifracs and main fracture treatments. The correlation in Figure 9 can be defined by the equation

$$K_{corr} = 3.495\ K_{log} - 0.458, \tag{4}$$

where "K_{corr}" would be that calculated to more closely approximate the actual measured stress. The resultant slope from this correlation is shallower than that previously determined for the analysis of the Coastal data; this previous correlation being defined by the equation

$$K_{corr} = 5.31\ K_{log} - 0.87 \tag{5}$$

Equation 4 was used to derive the sonic stress profile in the subsequent analysis.

To look at the sonic stress versus measured stress correlation for the MWX data in comparison to other available industry data,[10] all data was plotted in Figure 10. While the combination of this data appears to yield a very tight correlation, the scales are somewhat deceiving. Taking a closer look, many of the sonic derived stresses are as much as 500 to 1000 psi different than the actual stresses. The point to be made here is that a generalized correlation such as this can not be used for all fields and lithologies with confidence. The only time where this correlation, defined by the equation

$$\sigma_{corr} = 1.195\ \sigma_{log} - 403, \tag{6}$$

should be used is when no other stress information is available. Then, and only then, might it provide a "ball park" stress profile.

In summary, two correlations have been developed, lithology and acoustic velocity, for deriving closure stress in the Fluvial zone of the Mesaverde formation from commonly run logs. While the "tightness" of both correlations are not as good as one might desire, they still provide a reasonably sound method for developing stress profiles. In the next section, stress profiles are developed for both correlations and a comparison made to determine which is most accurate for modeling the Fluvial fracture injections. In previous analyses of the Paludal and Coastal data, the GR lithology correlation was found to be the most accurate.

STRESS PROFILING

The "Bi-linear" lithology correlation described previously and based on the gamma-ray log was used to developed the stress log shown in Figure 11. This was developed from calculating closure pressure every two feet using the corresponding gamma-ray values (Appendix B). When the actual measured stress values (the MWX-2 "average" stress test results from NSI's re-analysis) were "plotted" on the log, there was mixed agreement as shown in Table 3. There seemed to be reasonably good agreement for the sandstones (average error equal 250 psi); but, very poor agreement in the mudstones (average error equal 609 psi). While the lithology correlation appeared to be an accurate tool for predicting closure stress in the Paludal and Coastal zones, its use for the Fluvial zone was found to be unacceptable. This emphasizes the extreme caution necessary in deriving and using such correlations, especially across a large geographic region with varying lithology.

Figure 12 shows the stress log developed with acoustic velocity (Sonic) correlation. Once again the actual measured stresses (as interpreted by NSI) were "plotted" on the log for comparison. Once again, the comparison was not as good as desired as shown in Table 4. While the sonic correlation was almost twice as accurate as the lithology correlation, the average error between sonic derived and measured stresses was still 320 psi. Overall, though, the same average error existed for both sandstones and mudstones, unlike the lithology correlation.

Based on the comparative results of the two correlations, the acoustic velocity correlation was found most suitable for subsequent analysis of the Fluvial fracturing injections. As shown in Figure 13, this correlation was used to create a smoothed stress profile for use as a starting point in the modeling.

FLUVIAL B SAND FRACTURE ANALYSIS

CLOSURE PRESSURE DETERMINATION

As part of the Fluvial "B" fracture diagnostics, several pre-frac tests were conducted including a nitrogen step-rate test, three nitrogen pump-in/flowback tests and one KCL pump-in/flowback test. The step-rate test injection (Figure 14) resulted in a fairly well defined fracture extension pressure of 4750 psi. Fracture extension pressure is the pressure required to extend an existing fracture and is usually 100-300 psi above closure pressure providing an upper bound for closure pressure determination. From the step-rate test decline and the subsequent nitrogen PI/FB tests there was no indication of closure pressure as seen in Figures 15-18. In each case, the formation appeared to have been broken-down and extending a fracture; however, these was no evidence of reverse curvature on the flowback pressures which would indicate closure. The problem seemed to be too slow of a flowback rate. Also, the nitrogen gas may have been expanding and contributing to an "apparent" slow pressure decline. Unfortunately, the one KCL PI/FB test conducted was unsuccessful due to a varying flowback rate. When shut-in following the KCL flowback, the bottomhole pressure rebounded to about 4250 psi prior to the end of data acquisition (Figure 19). While the pressure had not rebounded to closure pressure, this indicates that closure is greater than 4250 psi and less than 4750 psi from the step-rate test. A value of 4550 psi, or 200 psi less than fracture extension pressure, was used in the subsequent analysis. For comparison, the stress predicted from the sonic correlation was approximately 4100 psi.

MINIFRAC PRESSURE DECLINE ANALYSIS

An 8,000 gallon 75 quality nitrogen foam minifrac was pumped in the Fluvial "B" sand at an average injection rate of 10 BPM. The shut-in pressure decline (Figure 20) showed a distinct slope change at about 5040 psi on a square-root of shut-in time plot. While this is indicative of fracture closure, it is thought to be that of a higher stressed boundary layer and not the main sand. The pressure decline was only monitored down to about 4850 psi or still 100 psi above the fracture extension pressure measured on the step-rate test. Had the pressure decline been extended, it is likely that a second closure would have been evident below 4750 psi. From the sonic derived stress log, the indicated stress for the upper boundary is around 5100 psi and the lower boundary between 5500 and 6000 psi.

Using a closure pressure of 4550 psi (estimated) and a closure time of 173 minutes from an extrapolation of the data in Figure 20; the pressure decline type curve match in Figure 21 was obtained. The match pressure (P*) of 215 psi was used

in Table 5 to calculate the fluid efficiency and estimate the fluid leak-off coefficient. Calculation of fluid efficiency based on the pump time and estimated time-to-close resulted in a value of 0.78. Based on the efficiency analysis from pressures, an efficiency of 0.71 was calculated or relatively the same; indicating none or only slight leak-off to a secondary source such as natural fissures. This is consistent with the core analysis fracture frequency shown in Figure 22 through the "B" sand interval 5822 to 5845 feet, which shows only slight to moderate fracture frequency through this interval and its boundary layers. The initial calculation of leak-off coefficient was based on a gross created height of 40 feet and a leak-off height of 25 feet, resulting in a coefficient of 0.00047 ft/ $\sqrt{\text{min}}$. Also shown in Table 6 are coefficients calculated for gross heights of 60 and 80 feet, resulting in values of 0.0011 and 0.0019 ft/ $\sqrt{\text{min}}$.

MINIFRAC PRESSURE HISTORY MATCH

Using the stress profile derived from the acoustic log and a leak-off coefficient of 0.0005 ft/ $\sqrt{\text{min}}$, a reasonably good history match of the minifrac pressures was obtained as shown in Figure 23. Sensitivities of the post-minifrac decline were performed and this was also matched with C = 0.0005 ft/ $\sqrt{\text{min}}$. The input/output from NSI's fracture model for this and subsequent simulations is included in Appendix C.

Figure 24 shows the predicted created height for the minifrac injection, which shows a total height of about 160 feet or much greater than the 40 feet used to calculate the leak-off coefficient. The simulated fluid efficiency was very close to that calculated in the prior pressure decline analysis. As was evident in both the Paludal and Coastal stimulation data reviews, evaluating leak-off using the decline analysis is a function of the complexity of the environment. As seen in Figure 24, there is significant stress difference between the sands and adjacent layers, i.e. greater than 1000 psi. Also, from the width profile, it is evident that a "pinch point" exists below the "B" sand. If this region of the fracture were to close quickly after shut-down and squeeze the slurry back into the pay, the "effective" height for analyzing the pressure decline would be only that part of the fracture above this closed portion and in communication with the perforations.

MAIN FRACTURE TREATMENT HISTORY MATCH

Using the same parameters used in history matching the minifrac pressures, an attempt was made to history match the Fluvial "B" main fracture treatment. As shown in Figure 25, a fair match was obtained through the shut-in pressure decline at 30 minutes which occurred due to surface sand handling

problems. Beyond this time, though, when pumping was resumed; the abnormal pressure increase could not be matched. The simulator predicted that even with the 12 minute shut-in period, there was enough pad fluid to resume fracture extension; unlike the actual behavior indicating a screen-out (restriction) mode.

To further check the model's evaluation of leak-off during the shut-in period, a second simulation was performed where the treatment was only pumped to the point of the shut-in and then allowed to decline past the point where pumping was resumed. Additional changes included (1) increasing the immediate upper and lower boundary stresses from 5700 psi (original acoustic derived stress profile) to 6000 psi to increase the treating pressure during the first 11 minutes and (2) running the program in a constant pressure mode from 11 to 20 minutes to simulate the nearly flat pressure record during this period. In addition to simulating the near constant pressure behavior, leak-off is accelerated during this period by the simulator to maintain the constant pressure.

As shown by Figure 26, the above mentioned changes resulted in a much better history match of the first 20 minutes. Also, the simulation of the extended shut-in decline indicated that the fracture had not closed after a shut-in of 45 minutes. In fact, the simulator predicted the pressure at this point was still over 500 psi above closure. This extended shut-in analysis indicates that the shut-in pressure decline rate during the 9 minute shut-in was too slow to have resulted in enough leak-off for this to have been the cause of the screen-out. If natural fissures were opened during the constant pressure period, causing accelerated leak-off, they apparently closed quickly upon shut-down and did not contribute significantly to leak-off during the shut-in period.

Taking the analysis one step further, the simulator was allowed to run in an extended constant pressure mode throughout the remainder of the treatment (without the 9 minute shut-in period) to determine if the accelerated leak-off would predict the screen-out behavior. As seen in Figure 27, the screen-out still did not occur; leading to the conclusion that the abnormal pressure increase was not caused by pad depletion alone.

Excessive height growth was also evaluated as a possible cause of the abnormal pressure increase. As part of the second history match (Figure 26), the created height at the point of shut-down during the treatment was about 45 feet as seen in Figure 28. This is consistent with the gross height used to calculate the leak-off coefficient and also the results seen on the post-frac gamma-ray log (Figure 29). This is also consistent with the abnormally increasing pressure behavior after the shut-in period, since moderate to excessive height growth during this period would have resulted in a near flat or slightly declining pressure behavior.

In summary, there is no logical cause for the abnormal pressure increase based on the treatment pumped. Pad depletion was not a factor. Once again, as seen in the analyses of the Paludal and Coastal fracture treatments; proppant bridging at the lens boundary due to lateral variations in stress is the most obvious explanation. From the second history match (Figure 26), the created fracture half-length at the time of shut-in (11 minutes) was 1088 feet, but with proppant only out to about 100 feet. This is reasonable consistent with the dimensions obtained in the previous analysis of 1060 feet of hydraulic length and 318 feet of propped length. As seen from Figure 30, the estimated lens size/orientation for the Fluvial "B" sand shows the nearest lens boundary in the general azimuth trend to be on the order of 225 feet. This is between the propped lengths from the two analyses and lends support to the lateral stress variation theory.

FLUVIAL C SAND FRACTURE ANALYSIS

CLOSURE PRESSURE DETERMINATION

The Fluvial "C" fracture diagnostics included one KCL pump-in/shut-in decline test, a KCL step-rate/flowback test, and three KCL pump-in/flowback tests for determining fracture closure pressure. The results from the two minifrac pressure declines were also considered in this evaluation. The Fluvial "C" fracture tests were all performed through perforations from 5720 to 5738 feet in well MWX-1. Table 6 summarizes NSI's re-analysis of these tests and plots of the step-rate test injection and pressure declines are included in Figures 31 through 36. In each case the formation appeared to have been broken down and fractured and much better results were obtained with the KCL PI/FB tests than the nitrogen PI/FB tests performed in the Fluvial "B" sand.

From Table 6, closure pressure appears to be at 4727 psi (average of the four highest values). From the step-rate test fracture extension pressure was well defined at 5052 psi or about 325 above closure. The closure pressure of 4727 psi was used in the subsequent analysis of the two minifracs performed in this sand. This compared very close with the acoustic derived stress for the lower part of the "C" sand of 4700 psi (see Figure 13).

MINIFRAC NO. 1 PRESSURE DECLINE ANALYSIS

Because of the expected possible dual leak-off system thought to exist for the Fluvial "B" fracture treatment, i.e. the constant pressure mode and screen-out caused by opening natural fissures; two minifracs were designed for the

Fluvial "C" fracture diagnostics testing - one with and one without 100-mesh sand.[11] The "C" sand was not a major target sand and a fracture treatment was not performed in this zone.

Minifrac no. 1 consisted of pumping 12,860 gallons of 75 quality nitrogen foam with 20 lb/1000 gal gel at an average injection rate of 11 BPM. No 100-mesh sand was included in this test, nor was any breaker added to the foam. Figure 37 shows the pressure decline following the injection. From the available data, it appears that data acquisition was stopped too soon, i.e. at approximately 5140 psi, to see if closure pressure could be detected at around 4725 psi. Since there is strong evidence from the other stress tests and minifrac no.2 that closure is at 4727 psi and the data was declining on at a near constant rate, the data was extrapolated to 4727 psi to determine closure time for use in the pressure decline analysis.

The type curve match is shown in Figure 38, resulting in a P^* match pressure of 117 psi. Using this pressure, the fluid efficiency and leak-off coefficient were calculated as shown in Table 7. From injection and closure time, an efficiency of 0.77 was determined, which compared very close with the efficiency of 0.79 calculated from pressures. This indicates little or no leak-off to a secondary source such as natural fissures. As shown in Figure 22, the estimated core fracture frequency through the Fluvial "C" sand interval 5715 to 5735 feet shows only slight to moderate fracturing. In fact, the frequency is less in the boundary layers of this zone than on the "B" sand. Using a leak-off height of 22 feet and an estimated gross height of 50 feet (from geophone results and offset stress tests), a fluid leak-off coefficient of 0.00043 ft/$\sqrt{\text{min}}$ was calculated. This is reasonably close to the coefficient of 0.0005 ft/$\sqrt{\text{min}}$ determined for the "B" sand and required to history match the "B" sand minifrac and fracture treatment.

MINIFRAC NO. 1 PRESSURE HISTORY MATCH

As was evident on the Fluvial "B" fracture treatment, there was a near constant pressure mode reached on the Fluvial "C" minifrac no. 1 at about 16 minutes (Figure 39). In fact, the pressures appeared to be slightly declining for the last 7 minutes of injection. The first history match of this test is shown in Figure 39, which was obtained using a leak-off coefficient of 0.00043 ft/$\sqrt{\text{min}}$ and the stresses below the "C" sand required to history match the "B" zone minifrac and fracture treatment. Only slight alterations in the acoustic derived stresses above the "C" sand were required as shown in the simulator I/O in Appendix C. The simulated fluid efficiency was 0.73 as compared to 0.78 from the pressure decline analysis.

As was evident in the previous analyses, the simulator predicted height growth was considerably greater than used in the pressure decline analysis to calculate the leak-off coefficient. For the history match in Figure 39, the height reached 185 feet as compared to 50 feet used in the leak-off calculation. As seen in Figure 40, most of the simulated height growth was in an upward direction into the shale (mudstone) of much higher stress than the "C" sand. As alluded to before, if the higher stress region were to close quickly upon shut-down, the "effective" height during the pressure decline would be closer to the 50 feet used in the original analysis. As evident from the decline pressures in Figure 39, the steeper early-time decline slope was indicative of higher leak-off, followed by a shallower slope. This could be representative of one of two things or both - (1) natural fissures open early in the decline and closing fairly quick and/or (2) early-time leak-off to the greater height which lessens as the higher stress zones close.

To further the evaluation of minifrac no.1, a second history match was performed with the simulator in a constant pressure mode for the last 12-13 minutes of injection. As seen in Figure 41, this match was equally good or even slightly better than the first match. The simulated height was also much closer to that used in the pressure decline analysis, i.e. 53 feet (Figure 42). However, the fluid efficiency was only 0.69 as compared to 0.78 from the pressure decline analysis. This is due to the increased leak-off caused by the simulator's handling of the constant pressure mode.

As evident from the pressure decline in Figure 41, a very good match was obtained for the early-time decline data, but a very poor match of the latter decline. This is supportive of the original analysis of this data which suggested a dual leak-off system. Since leak-off increased in NSI's simulation during the constant pressure mode, the resultant decline was more rapid. However, the simulator is not capable of simulating changing leak-off during the decline. It is apparent that a secondary leak-off source existed in the later time of injection and early-time decline due to either opening of natural fissures and/or excessive height growth. Once again, this evaluation points out the weaknesses present in the pressure decline analysis for complex environments.

MINIFRAC NO. 2 PRESSURE DECLINE ANALYSIS

The second minifrac performed in the Fluvial "C" sand consisted of 15,000 gallons of 75 quality foam pumped at an average rate of 10 BPM and preceded by a nitrogen "pre-pad" to pump up the pressure high enough to maintain a stable foam. The purpose of this second minifrac was to determine if 100 mesh sand could control the extra leak-off evident on the previous minifrac. 100-mesh sand was added at concentrations of 0.25 to 1.0 ppg throughout the middle stages.

Figure 43 shows the pressure decline following the second minifrac, indicating closure pressure at 4718 psi and closure time at 182 minutes. The type curve match of this data (Figure 44) gave a P* match pressure of 255 psi. Using these values in Table 8, the fluid efficiency and leak-off coefficient were determined. A pump-time of 37.9 minutes was used as determined from the injection time for only the foam, the pure nitrogen expected to leak-off very quick and not be a factor in the analysis. Using the injection time and the time-to-close, a fluid efficiency of 0.69 was determined. This once again compared favorably to the efficiency calculated from pressures of 0.66, indicating little or no extra leak-off to a secondary source such as natural fissures during the decline. Using a gross and leak-off height of 50 and 22 feet, the leak-off coefficient calculated was 0.00082 ft/ $\sqrt{min}$ or almost twice that calculated from minifrac no. 1. As indicated from the previous analysis, this increase in leak-off may be due to the 100-mesh sand either propping open the natural fissures within the zone or holding open the shales sufficiently that other leak-off zones were available.[11] This would also explain the lower fluid efficiency calculated for the second minifrac.

MINIFRAC NO. 2 PRESSURE HISTORY

Using a leak-off coefficient of 0.00082 ft/ $\sqrt{min}$ and the same stress profile used to history match minifrac no. 1, a fairly good match of the second minifrac was obtained with the exception of the constant pressure mode being 75 to 100 psi low (Figure 45). However, the simulator predicted efficiency was only 0.52 at the end of injection as compared to 0.67 from the pressure decline analysis. When the nitrogen prepad was removed from the schedule, the simulator predicted an efficiency of 0.61; which is within acceptable error.

The match of the pressure decline was also very close as seen in Figure 45. Height growth appeared to be a problem, though; the estimated height at the end of injection being 286 feet as seen in Figure 46. Most of the growth was in an upward direction and intersected the Fluvial "E" sand interval at 5525 to 5565 feet. However, upon shut-down the higher stress zone between the "C" and "E" sands probably closed fairly quick, leaving a much smaller "effective" height for the pressure decline analysis. Since growth into the "E" sand occurred fairly late in the simulation, it probably did not contribute significantly to leak-off.

To try to get a better match through the constant pressure mode the foam viscosity was increased. This resulted in a good match through the constant pressure period (Figure 47), however the early injection pressures were too high and the pressure decline was more rapid than measured. To lower the early pressures, foam viscosity was reduced during this period and

also, the leak-off coefficient was reduced to 0.00075 ft/ $\sqrt{min}$ to try to better match the decline pressures (Figures 48). This resulted in a very good match of the foam injection period; however, the match of the decline pressures was still not very good, the simulator predicted efficiency being 0.57 as compared to 0.67 from the pressure decline analysis. The simulator predicted height for this history match was 179 feet as seen in Figure 49. As shown in the Figure, without the prepad nitrogen injection, the fracture did not grow into the "E" sand. Regardless of whether it did or did not, the "E" sand probably did not contribute significantly to leak-off or to the behavior of the decline.

To further the evaluation of the minifrac no. 2 pressure decline, the measured pressures were compared to simulator predicted declines for several leak-off coefficients (maintaining all other parameters constant). As seen in Figure 50, the early time portion of the decline indicates high leak-off, i.e. > 0.001 ft/ $\sqrt{min}$ and the later portion indicates low leak-off, i.e. less than 0.0005 ft/ $\sqrt{min}$. This suggests that maybe the natural fissures were still open during the early decline (due to proppant?) but closed back with time. The other possibility is that there was still communication with other permeable sand layers during the early decline, which were isolated from the "C" sand in the later decline as the higher stress boundary layers closed. The late time leak-off behavior in Figure 50 is nearly the same as the leak-off coefficient determined for the first minifrac. Figure 51 shows the two pressure declines for comparison. While both show early sharp declines, the second minifrac continued to decline at a slightly faster rate.

In summary, it appears that the 100-mesh sand in minifrac no. 2 was effective in doing what it was designed for, i.e. going into the natural fissures to reduce leak-off during injection. However, there was also a corresponding higher net treating pressure than on minifrac no. 1 which may have contributed to more height growth and the opening of additional leak-off sources. The higher leak-off during the early decline indicates open, propped fractures; however, the decreasing leak-off rate during the decline could also be explained by changing "effective" leak-off height. Without fracture height evaluation logs to compare to the simulator results, it is difficult to say which is most representative of what really happened. It does appear, though, that a secondary leak-off source existed.

FLUVIAL E SAND FRACTURE ANALYSIS

CLOSURE PRESSURE DETERMINATION

The Fluvial "E" fracture diagnostic tests included a pump-in/shut-in test, a step-rate/flowback test, and three pump-

in/flowback tests; all using KCL water. Although, a minifrac/shut-in decline was also performed, the decline was not monitored long enough to detect closure pressure. These tests were all performed through perforations 5535 to 5565 feet.

A summary of the results from the pre-frac tests are included in Table 9. The analysis of each test is presented in Figure 52 through 58. The only truly definitive results were obtained from the initial pump-in/shut-in decline and the step-rate test injection. The PI/SI test showed a distinct fracture closure at 4522 psi (Figure 52). Because of the extended shut-in, a Horner-type plot was also possible indicating reservoir pressure, P*, at 3275 psi. This compared favorably with the previous analysis estimate of 3200 psi, indicating that these small volume injection/decline tests might have merit in determining reservoir properties, i.e. reservoir pressure and formation permeability.

The step-rate test injection showed a well defined fracture extension pressure at 4875 psi (Figure 54) or about 250 psi above the closure pressure from the PI/SI test. From the flowback following the step-rate test and the other three flowbacks, there was no clear indication of closure pressure. It is NSI's assessment that the problems in not obtaining good repeatable data from these tests was (1) too low a flowback rate and (2) not maintaining the flowback rate constant. The flowback declines on the step-rate test and PI/FB tests 3 and 4 (Figures 55, 57, & 58) showed slight reverse curvature (indicative of closure); but, it was too subtle to pick a definitive value. Higher, constant flowback rates, i.e. 2-3 BPM, would have provided definition to the curvature reversal. This is usually best achieved through trial-and-error using an adjustable choke; and then leaving the choke set (with only minor adjustments) and opening the flowback with a ball-value.

MINIFRAC PRESSURE DECLINE ANALYSIS

The minifrac performed on the Fluvial "E" sand consisted of pumping 20,000 gallons of foamed water followed by 10,000 gallons of 75 quality foam with 20 lb/1000 gallons gel. The average calculated injection rate was 21.5 BPM. The foam was immediately preceded by a nitrogen pump-up stage to rid the perforations of any residual water and increase the wellbore pressure to aid in foam stability. In the pressure decline analysis, fluid efficiency and leak-off coefficient were calculated with and without this pump-up stage included.

Figure 59 shows the pressure decline following the minifrac. While possible breaks in the decline, i.e. slope changes, may seem evident; these are all well above the fracture extension pressure of 4875 psi and could not possibly be the fracture closure. Still assuming closure at around 4520

psi, the minifrac decline was not left shut-in long enough to reach this pressure. Thus for the leak-off analysis, the final slope of the data in Figure 59 was extrapolated to this pressure to determine the closure time of 94 minutes.

As mentioned previously, the pressure decline analysis was performed both with and without the nitrogen pump-in included in the pump time to access its affect on the results. Figures 60 and 61 show the type curve matches for the two cases, the resultant P* match pressure being about the same at 320 psi. Table 10 shows the calculations. Not including the pump-up stage, a fluid efficiency of 0.73 was determined from the time-to close. With the pump-up stage included the efficiency was 0.62. Using the pressures, efficiency was calculated to be 0.60. This once again indicates no secondary leak-off source; however, this is inconsistent with the core fracture frequency shown in Figure 22, which shows the "E" sand to have a much higher degree of fracturing than either the "B" or "C" sands.

Using a gross and leak-off height of 30 and 15 feet, respectively; a leak-off coefficient of 0.00066 ft/ $\sqrt{min}$ was calculated for the injection excluding the pump-up stage. With the pump-up stage, a leak-off coefficient of 0.00053 ft/ $\sqrt{min}$ was calculated. To look at the leak-off analysis further, the minifrac pressure decline was plotted versus simulator predicted declines based on leak-off coefficients ranging from 0.0005 to 0.003 ft/ $\sqrt{min}$ (Figure 62). It is apparent from this that, once again, a dual leak-off system is present with the early decline indicating greater than 0.003 ft/ $\sqrt{min}$ and the later decline flattening out and paralleling the leak-off curve of 0.0005 ft/ $\sqrt{min}$. This indicates the presence of open natural fractures closing during the decline.

MINIFRAC PRESSURE HISTORY MATCH

Figure 63 shows the initial attempt at history matching the Fluvial "E" minifrac injection using the same approximate stress profile from previous analyses, a leak-off coefficient of 0.002 ft/ $\sqrt{min}$ (some mid-point between range of leak-offs determined from Figure 62), and foam rheology data as reported by the service company. The sharp pressure rise starting at about 10 minutes, could not be explained as a result of reaching a higher stress layer. Also, the injection rate was nearly constant through this period, leaving increased viscosity as a possible cause. To get the sharp pressure rise required increasing the viscosity from around 75 to 400 cp for a short period of time and then tapering back to the normal 75 quality foam viscosity. This match is shown in Figure 64. It is evident from the decline that a leak-off coefficient of 0.002 ft/ $\sqrt{min}$ does not match very well since leak-off is higher in the early portion and lower in the later portion. Irregardless, slight differences in the leak-off coefficient would not affect the injection pressures significantly.

Figure 65 shows the simulator predicted fracture height for the history match in Figure 64. The predicted total height from the simulator was 102 feet; however, it is evident in the figure that fracture width above about 5515 feet and below 5590 feet was negligible leaving, at most, an "effective" height of 75 feet. Keeping the leak-off height fixed at 15 feet, the leak-off coefficient that would be calculated for this gross height would be 0.004 ft/ $\sqrt{min}$ or on the order of that evident in Figure 62 for the early part of the decline. To calculate a leak-off coefficient of 0.002 ft/ $\sqrt{min}$ would require a gross height of 52 feet, certainly conceivable from Figure 65 after early closure of the higher stress zones.

It is evident from this analysis that the leak-off rate is changing throughout the decline and probably varied during the injection due to a dual leak-off system. It also points out the weakness in using only the pressure decline analysis to determine the leak-off coefficient in complex situations. When coupled with history matching of the minifrac injection and decline pressures, a more complete and accurate analysis is achieved.

MAIN FRACTURE TREATMENT HISTORY MATCH

The sharp pressure rise measured on the minifrac at about 10 minutes was also evident in the main fracture treatment (Figure 66). Once again to match this rise, fluid viscosity was increased the same as on the minifrac and then tapered back to the original viscosity. This repeatability indicates that the pressure rise was not fluid viscosity related; but instead, a formation - fracture related phenomenon. This behavior suggests some anomaly in the fracture flow path at about 10 minutes which would cause a sharp rise in fracture friction pressure and as pumping continues and the fracture widens, the friction pressure goes down resulting in the slower rise in pressure. This could also have been caused, in part, by the opening of natural fissures.

At 10 minutes the simulator predicted a fracture penetration of 825 feet; however, pumping of proppant had not been started. As shown in Figure 67, the "E" sand is broken up into two lenses, the E1 and E2 lenses. The E2 lens is very narrow and small in comparison to the E1 lens. This may have been a possible cause for the sharp pressure rise. If both lenses were taking fluid initially and the fracture in the E2 lens reached some lateral stress barrier, this portion of the fracture would have stopped growing and in effect reduced the "effective" fracture height and increased slightly the injection rate into the larger E1 sand.

The abnormal pressure rise in the later part of the treatment might be explained by the proppant reaching the E1

lens boundary. As seen in Figure 67, the estimated boundary to the northwest of well MWX-1 is about 1000 feet. From the simulator the first proppant would have reached this distance after about 40 minutes. After 30 minutes, proppant would have been approximately 600 feet from the wellbore. Looking at higher leak-off as a possible cause of the abnormal pressure increase; even with a leak-off coefficient of 0.01 ft/$\sqrt{\text{min}}$ the pad fluid was not totally depleted. Besides, a good match of the pressure decline following the fracture treatment was achieved using a leak-off coefficient of 0.0015 ft/$\sqrt{\text{min}}$.

Because of the two abnormal pressure increases during the treatment and the other possible extension anomalies caused by the two lens boundaries, the simulator prediction of fracture height was probably invalid. From the post-temperature and post-gamma ray logs (Figures 68 and 69) it appears that the majority of fluid and proppant stayed in zone, with most or all of the proppant going into the lower sand lens.

CONCLUSIONS

The re-analysis of the Fluvial stress data, plotting pressure versus the square-root of shut-in time, showed reasonably good agreement with the previous results estimated from the ISIP's. As in the Paludal and Coastal re-analysis, though, the "square-root or reservoir-type" method yielded clearer, more definitive results. In this same evaluation back-stress effects were investigated and the conclusion made that backstress was not a factor in the Fluvial zone, as was also the case for the Paludal and Coastal data.

Similar to the Paludal and Coastal correlation analysis, both lithology and acoustic velocity correlations were investigated with respect to stress for the Fluvial. Unlike the first two zones, though, which showed the gamma-ray lithology correlation to be superior; the acoustic velocity correlation was more accurate with respect to actual stress measurements in the Fluvial. This emphasizes the extreme caution necessary in deriving such empirical type correlations, especially for a large geographical region with varying lithology. The acoustic correlation was used to develop a detailed stress profile for modeling of the Fluvial minifrac and fracture treatments.

Once again, as was found to be the case in analyzing the Paludal and Coastal data; it was evident in the minifrac pressure decline analysis that certain limitations exist in the type curve analysis for determining fluid leak-off properties. The principal problems are (1) varying closure times for different lithologies intersected by the fracture and how this affects the injection of fluid from non-permeable to permeable zones during the shut-in period, (2) what gross and leak-off heights to use if these are changing during the decline, and (3) how natural fractures might affect the decline behavior. If was evident from this and the previous analyses, that leak-off is also probably changing during the decline making it difficult to determine the most representative fluid leak-off coefficient for use in design and post-treatment analysis. It was only through coupling of the type-curve pressure decline analysis with history matching of both the minifrac injection and decline that a somewhat meaningful evaluation was obtained. This should be the approach in analyzing minifrac data for any complex environment such as the Mesaverde Formation.

Using the results of the Fluvial "B" Sand minifrac analysis and pressure history match a leak-off coefficient was determined and a reasonably good model match of the minifrac obtained. Using the "calibrated" parameters from the minifrac, a good match of the main fracture treatment was also obtained through the point at which the treatment was shut-in due to

proppant handling problems. The abnormally increasing pressure behavior when pumping resumed could not be explained by excessive leak-off. Once again, as seen in the analysis of the Paludal and Coastal treatments; proppant bridging at the lens boundary provided the most obvious explanation. The modeled fracture dimensions at the time of the unexpected shut-down during the treatment were fairly consistent with the lens geometry and estimated fracture azimuth for the "B" Sand.

The evaluation of 100-mesh sand in the Fluvial "C" Sand appeared to be successful, i.e. indications from the minifrac injection/decline pressures that the 100-mesh sand did go into the natural fissures to reduce leak-off during injection. However, there was also a corresponding higher net treating pressure with the 100-mesh sand as compared to the minifrac without this additive; this possibly contributing to additional height growth and the opening of additional leak-off sources. Without fracture height logs it was difficult to make this evaluation. It did appear, from this work, that a secondary leak-off source existed. Model pressure history matching of the two minifracs on this zone were relatively straight forward, with no indication of abnormally high treating pressures.

The injections on the Fluvial "E" Sand minifrac and main fracture treatment included a sharp pressure increase at about 10 minutes. This was really the first case in analyzing all of the MWX stimulation data of "abnormally" high treating pressures. Pressure history matches were obtained by changing fluid viscosity; however, since the behavior was repeatable on both injections it was not thought to be viscosity related but instead a function of the formation. With initial injection into both the E2 and E1 lenses, one way to explain this abnormal behavior was if the fluid reached a lateral stress barrier in the smaller narrower E2 lens causing this portion of the fracture to stop growing. If, in fact, this happened, the effective fracture height would have been reduced and the injection rate into the remaining E1 lens increased, both causing fracture injection pressure to increase.

As for the Paludal and Coastal stimulation analyses, the Fluvial analysis also indicated that proppant could not be carried beyond the sand lens boundaries with conventional fracturing techniques in the Mesaverde Formation.

REFERENCES

1. Pitman, J. K. and Spencer, C. W.: "Petrology of Selected Sandstones in the MWX Wells (Northwest Colorado) and its Relationship to Borehole Geophysical-Log-Analysis and Reservoir Quality," date unknown.

2. Kehle, R. O: "The Determination of Tectonic Stresses Through Analysis of Hydraulic Well Fracturing," J. of Geophysical Research, Vol.69, No.2, Jan. 15, 1964.

3. McLennan, J. D. and Rogiers, J. C.: "How Instantaneous Are Instantaneous Shut-In Pressures,: SPE 11064 presented at 57th ANN. Conf. of SPE, New Orleans, LA., Sept. 26-29, 1982.

4. Warpinski, N. R.: "Investigation of the Accuracy and Reliability of In Situ Stress Measurements Using Hydraulic Fracturing in Perforated Cased Holes, "Proceedings 24th U.S. Symposium on Rock Mechanics, June 1983.

5. Smith, M. B. and Miller II, W. K.: "Re-Analysis of the MWX Fracture Stimulation Data From the Paludal Zone of the Mesaverde Formation," Annual Report, FY 1988, Doe Contract DE-AC21-87 MC24264, November, 1988.

6. Smith, M. B. and Miller II, W. K.: "Re-Analysis of the MWX Fracture Stimulation Data From the Coastal Zone of the Mesaverde Formation," Topical Report, Doe Contract DE-AC21-87 MC24264, April, 1989.

7. Nolte, K. G.: "Fracture Design Considerations Based on Pressure Analysis," SPE 10911 presented at 1982 Cotton Valley Symposium, Tyler, TX., May 20.

8. Warpinski, N. R. and Teufel, L. W.: "In Situ Stresses in Low-Permeability, Nonmarine Rocks," SPE/DOE 16402.

9. Breckels, I. M. and Van Eekelen, H. A. M.: "Relationship Between Horizontal Stress and Depth in Sedimentary Basins," SPE 10336 presented at 56th Ann. Conf. of SPE, San Antonio, TX., Oct. 5-7, 1981.

10. Veatch, R. W., Jr., and Moschovidis, Z. A.: "An Overview of Recent Advances in Hydraulic Fracturing Technology," SPE 14085 presented at 1986 SPE International Mtg. Beijing, China, March 17-20, 1986.

11. Warpinski, N. R.: "Fluvial C Leakoff Experiments at MWX," Sandia National Laboratory Report, December 10, 1987.

FIGURES AND TABLES

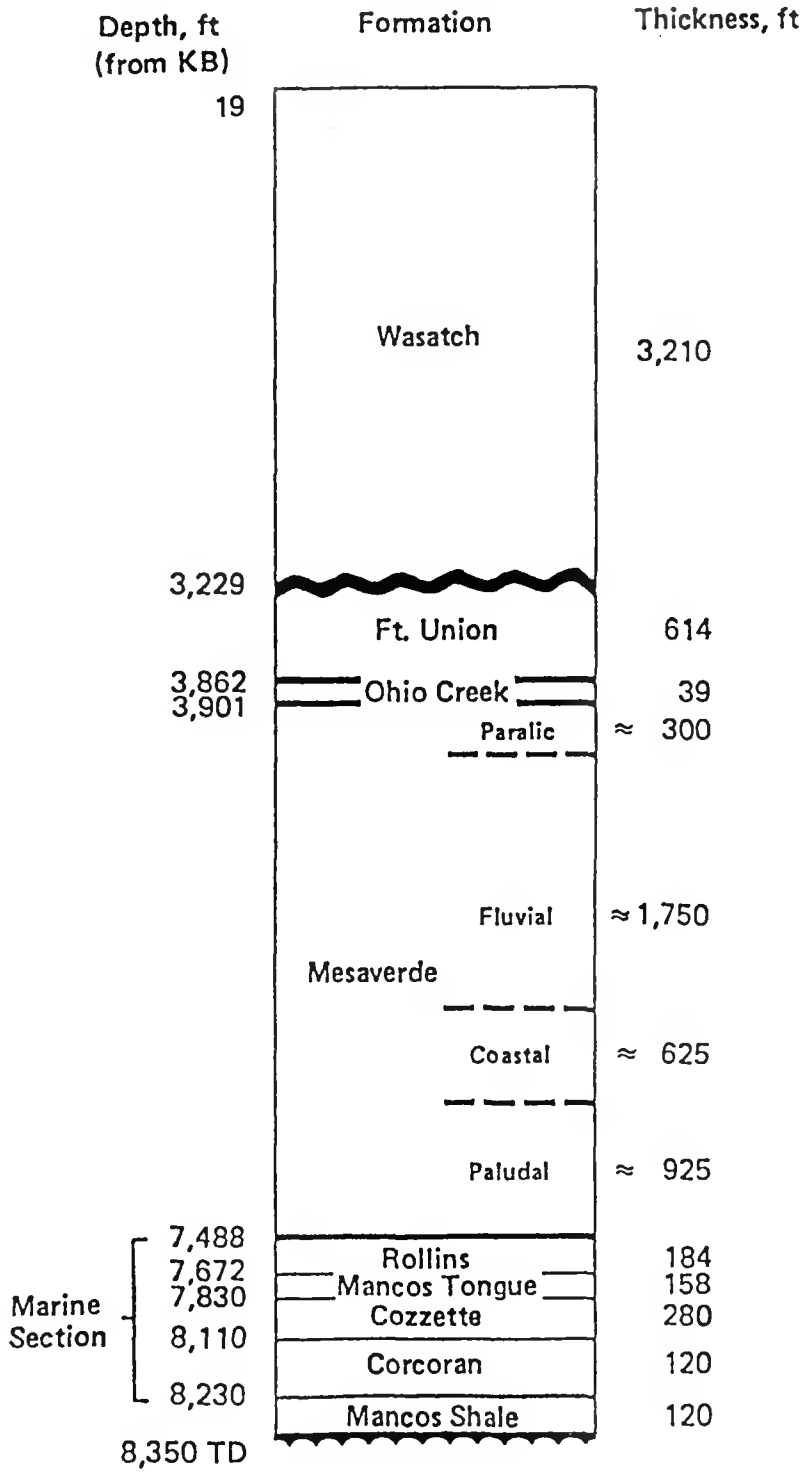
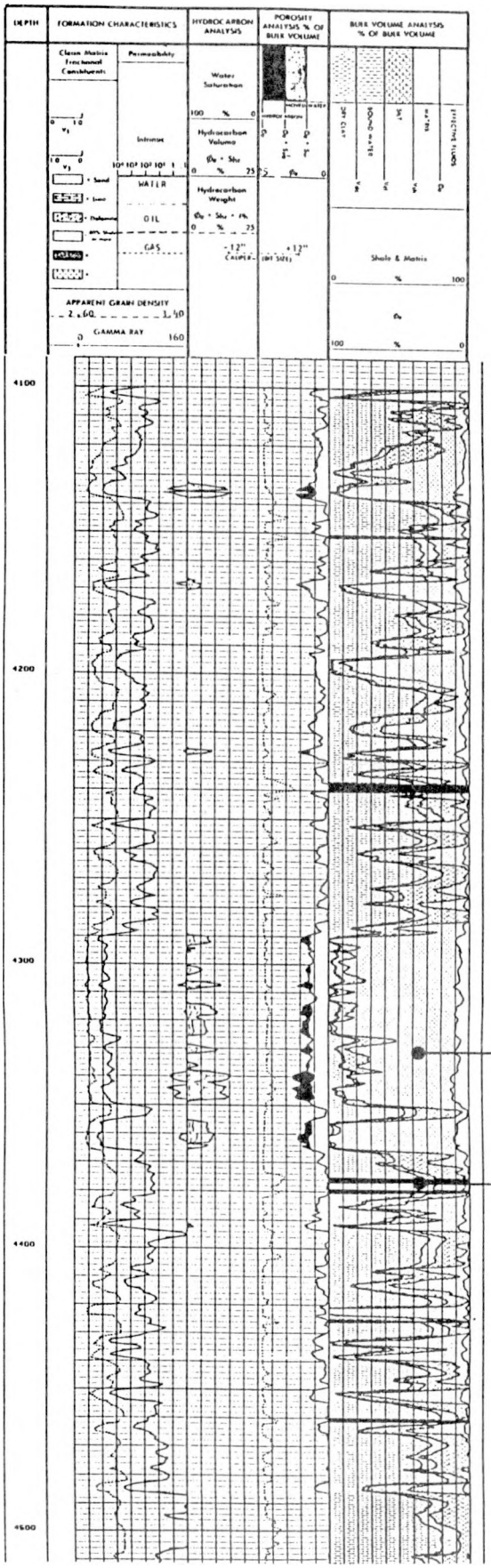


FIGURE 1: Geologic Cross-Section of MWX-1.

FIGURE 2: VOLAN Log Showing Fluvial Zone Stress Test Intervals.



Test Zone (Stress)

2F1 (2983)

2F2 (3852)

FIGURE 2 - Continued

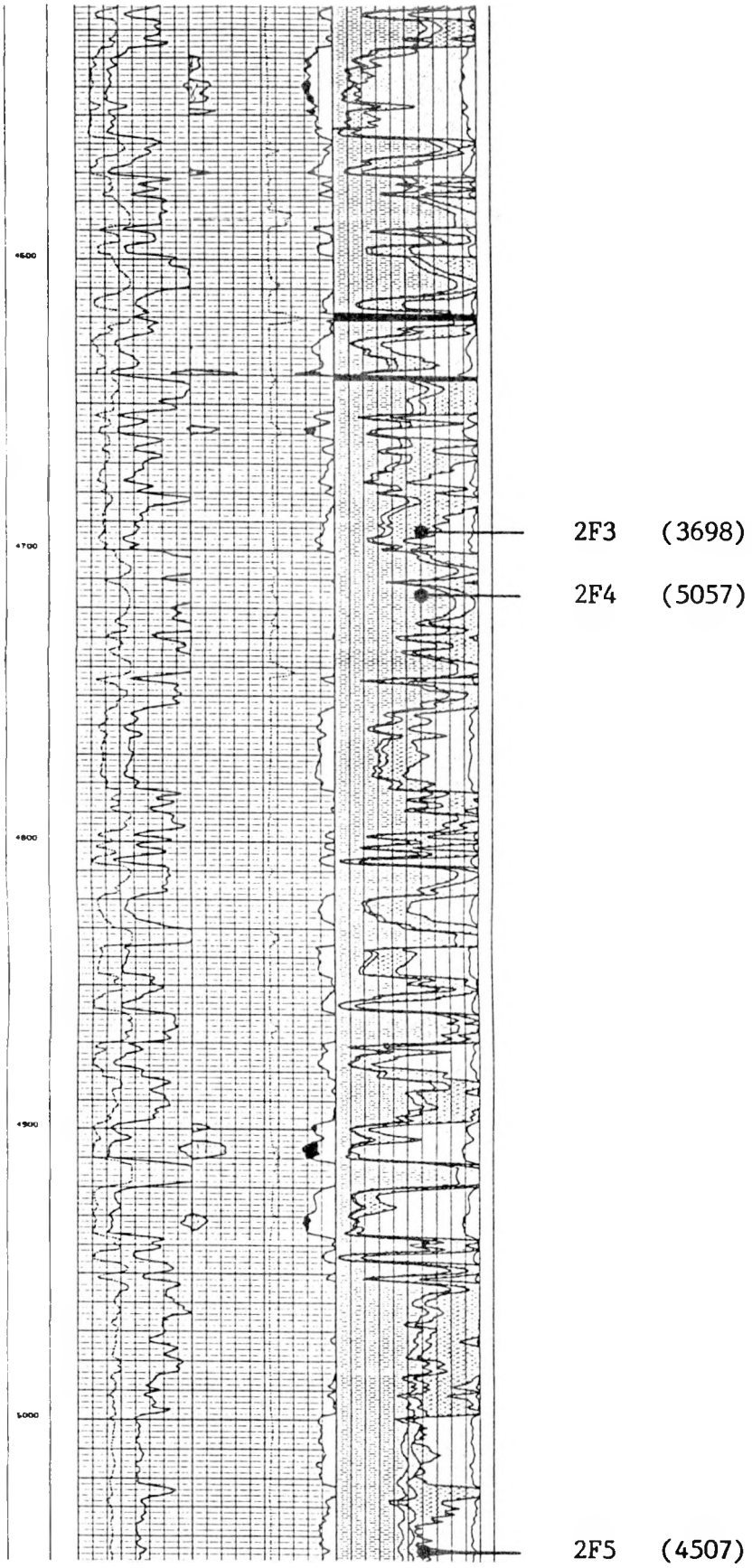


FIGURE 2 – Continued

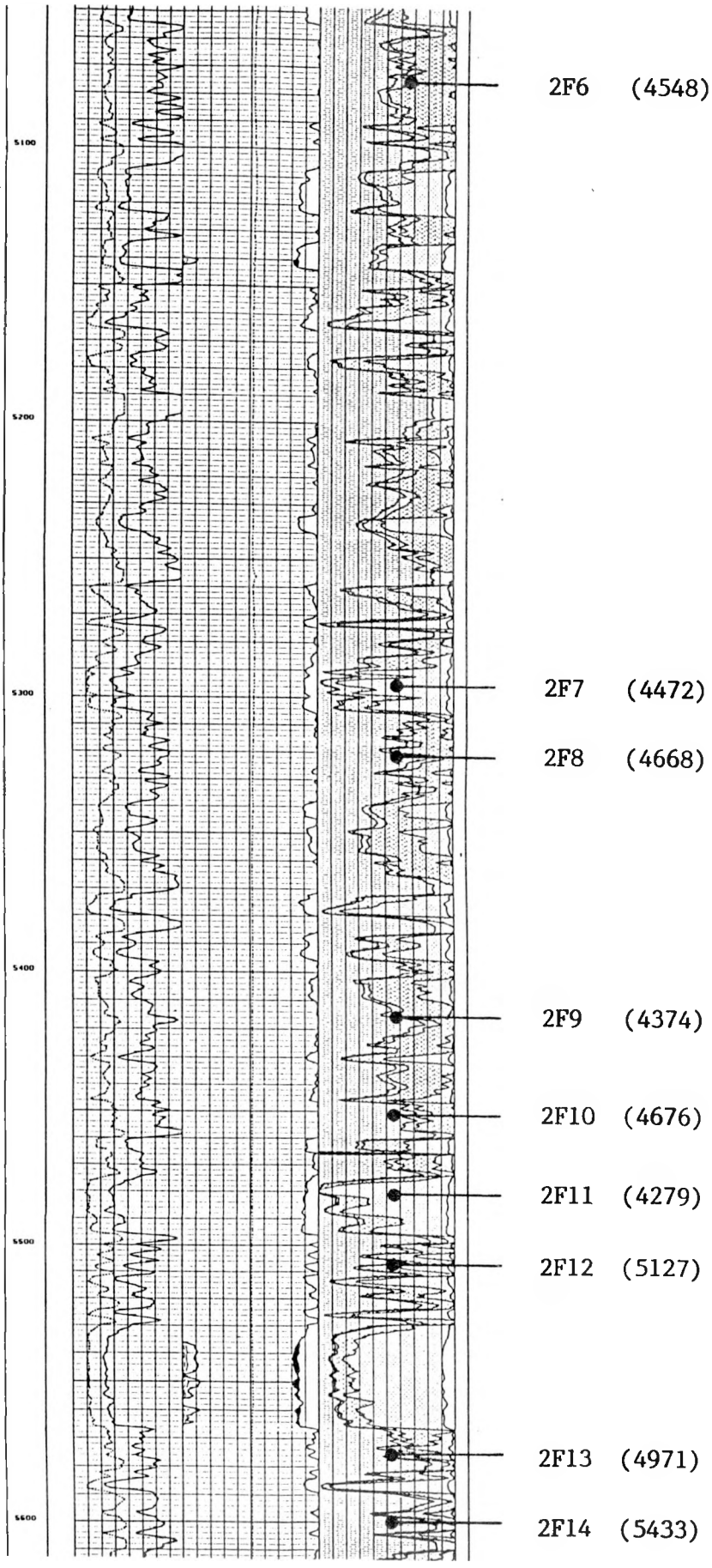


FIGURE 2: Continued

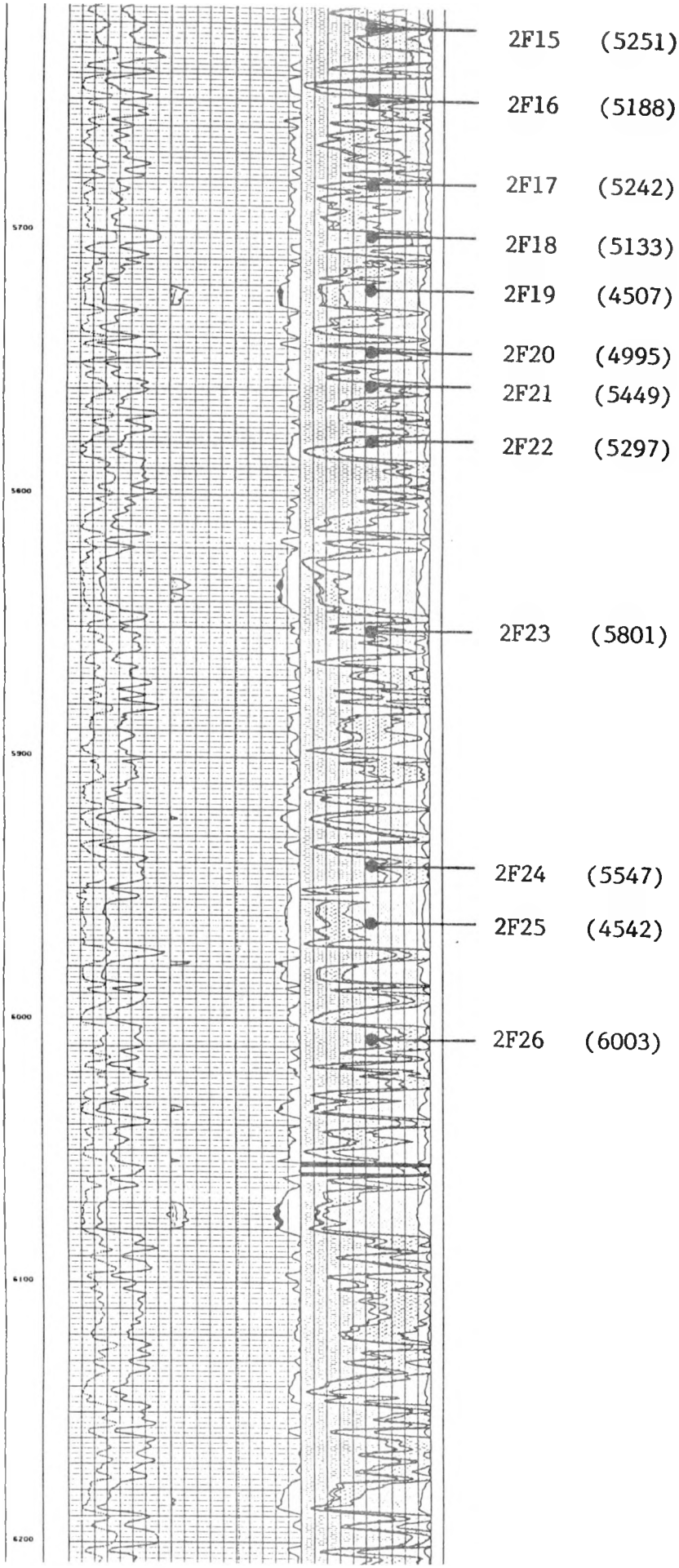


TABLE 1: Comparison of NSI and Sandia Fluvial Zone Stress Results.

TEST	DEPTH	SANDIA CLOSURE	NSI CLOSURE	PORE PRESSURE	OB PRES.	SANDIA GRAD.	NSI GRAD.	SANDIA K	NSI K
2F1TST2	4330	3350	2959	2510	4547	0.77	0.68	0.41	0.22
2F1TST3	4330	3350	3006	2510	4547	0.77	0.69	0.41	0.24
2F2TST2	4376	4050	3887	2535	4595	0.93	0.89	0.74	0.66
2F2TST3	4376	4050	3835	2535	4595	0.93	0.88	0.74	0.63
2F2TST4	4376	4050	3833	2535	4595	0.93	0.88	0.74	0.63
2F3TST1	4692	3730	3717	2720	4927	0.79	0.79	0.46	0.45
2F3TST2	4692	3730	3727	2720	4927	0.79	0.79	0.46	0.46
2F3TST4	4692	3730	3702	2720	4927	0.79	0.79	0.46	0.44
2F3TST5	4692	3730	3673	2720	4927	0.79	0.78	0.46	0.43
2F3TST6	4692	3730	3671	2720	4927	0.79	0.78	0.46	0.43
2F4TST1	4714	5250	5031	2730	4950	1.11	1.07	1.14	1.04
2F4TST2	4714	5250	5075	2730	4950	1.11	1.08	1.14	1.06
2F4TST3	4714	5250	5076	2730	4950	1.11	1.08	1.14	1.06
2F4TST4	4714	5250	5044	2730	4950	1.11	1.07	1.14	1.04
2F5TST1	5044	4460	3655	2925	5296	0.88	0.72	0.65	0.31
2F5TST2	5044	4460	4588	2925	5296	0.88	0.91	0.65	0.70
2F5TST3	5044	4460	4584	2925	5296	0.88	0.91	0.65	0.70
2F5TST4	5044	4460	4375	2925	5296	0.88	0.87	0.65	0.61
2F5TST5	5044	4460	4406	2925	5296	0.88	0.87	0.65	0.62
2F5TST6	5044	4460	4451	2925	5296	0.88	0.88	0.65	0.64
2F6TST1	5074	4650	4409	2940	5328	0.92	0.87	0.72	0.62
2F6TST2	5074	4650	4552	2940	5328	0.92	0.90	0.72	0.68
2F6TST3	5074	4650	4559	2940	5328	0.92	0.90	0.72	0.68
2F6TST4	5074	4650	4584	2940	5328	0.92	0.90	0.72	0.69
2F6TST5	5074	4650	4495	2940	5328	0.92	0.89	0.72	0.65
2F7TST2	5294	4530	4450	3070	5559	0.86	0.84	0.59	0.55
2F7TST3	5294	4530	4474	3070	5559	0.86	0.85	0.59	0.56
2F7TST4	5294	4530	4491	3070	5559	0.86	0.85	0.59	0.57
2F8TST1	5320	4800	4683	3085	5586	0.90	0.88	0.69	0.64
2F8TST2	5320	4800	4652	3085	5586	0.90	0.87	0.69	0.63
2F9TST1	5414	4450	4208	3120	5685	0.82	0.78	0.52	0.42
2F9TST2	5414	4450	4356	3120	5685	0.82	0.80	0.52	0.48
2F9TST4	5414	4450	4395	3120	5685	0.82	0.81	0.52	0.50
2F9TST5	5414	4450	4370	3120	5685	0.82	0.81	0.52	0.49

TABLE 1 - Continued

TEST	DEPTH	SANDIA CLOSURE	NSI CLOSURE	PORE PRESSURE	OB PRES.	SANDIA GRAD.	NSI GRAD.	SANDIA K	NSI K
2F10TST1	5450	4715	4659	3140	5723	0.87	0.85	0.59	0.59
2F10TST2	5450	4715	4661	3140	5723	0.87	0.86	0.59	0.59
2F10TST4	5450	4715	4673	3140	5723	0.87	0.86	0.59	0.59
2F10TST6	5450	4715	4709	3140	5723	0.87	0.86	0.59	0.61
2F11TST1	5480	4520	4272	3200	5754	0.82	0.78	0.52	0.42
2F11TST2	5480	4520	4272	3200	5754	0.82	0.78	0.52	0.42
2F11TST4	5480	4520	4285	3200	5754	0.82	0.78	0.52	0.42
2F11TST5	5480	4520	4288	3200	5754	0.82	0.78	0.52	0.43
2F12TST1	5506	5230	4600	3200	5781	0.95	0.84	0.79	0.54
2F12TST3	5506	5230	5122	3200	5781	0.95	0.93	0.79	0.74
2F12TST4	5506	5230	5133	3200	5781	0.95	0.93	0.79	0.75
2F13TST1	5575	5125	5021	3200	5853	0.92	0.90	0.73	0.69
2F13TST2	5575	5125	4936	3200	5853	0.92	0.89	0.73	0.65
2F13TST3	5575	5125	4957	3200	5853	0.92	0.89	0.73	0.66
2F14TST1	5600	5480	5434	3200	5880	0.98	0.97	0.85	0.83
2F14TST2	5600	5480	5433	3200	5880	0.98	0.97	0.85	0.83
2F14TST3	5600	5480	5431	3200	5880	0.98	0.97	0.85	0.83
2F14TST4	5600	5480	5414	3200	5880	0.98	0.97	0.85	0.83
2F15TST1	5620	5320	5252	3240	5901	0.95	0.93	0.78	0.76
2F15TST2	5620	5320	5239	3240	5901	0.95	0.93	0.78	0.75
2F15TST3	5620	5320	5250	3240	5901	0.95	0.93	0.78	0.76
2F15TST4	5620	5320	5264	3240	5901	0.95	0.94	0.78	0.76
2F16TST2	5649	5210	5182	3260	5931	0.92	0.92	0.73	0.72
2F16TST3	5649	5210	5181	3260	5931	0.92	0.92	0.73	0.72
2F16TST4	5649	5210	5201	3260	5931	0.92	1.00	0.73	0.73
2F17TST1	5680	5275	5292	3280	5964	0.93	0.93	0.74	0.75
2F17TST2	5680	5275	5276	3280	5964	0.93	0.93	0.74	0.74
2F17TST3	5680	5275	5247	3280	5964	0.93	0.92	0.74	0.74
2F17TST4	5680	5275	5199	3280	5964	0.93	0.92	0.74	0.71
2F17TST5	5680	5275	5196	3280	5964	0.93	0.92	0.74	0.71
2F18TST1	5700	5150	5139	3290	5985	0.90	0.90	0.69	0.69
2F18TST3	5700	5150	5126	3290	5985	0.90	0.90	0.69	0.68

TABLE 1 - Continued

TEST	DEPTH	SANDIA CLOSURE	NSI CLOSURE	PORE PRESSURE	OB PRES.	SANDIA GRAD.	NSI GRAD.	SANDIA K	NSI K
2F19TST1	5721	4575	4514	3300	6007	0.80	0.79	0.47	0.45
2F19TST2	5721	4575	4494	3300	6007	0.80	0.79	0.47	0.44
2F19TST3	5721	4575	4565	3300	6007	0.80	0.80	0.47	0.47
2F19TST4	5721	4575	4540	3300	6007	0.80	0.79	0.47	0.46
2F19TST5	5721	4575	4420	3300	6007	0.80	0.77	0.47	0.41
2F20TST2	5744	5050	5020	3300	6031	0.88	0.87	0.64	0.63
2F20TST3	5744	5050	5031	3300	6031	0.88	0.88	0.64	0.63
2F20TST4	5744	5050	4947	3300	6031	0.88	0.86	0.64	0.60
2F20TST5	5744	5050	4983	3300	6031	0.88	0.87	0.64	0.62
2F21TST2	5757	5440	5121	3330	6045	0.94	0.89	0.78	0.66
2F21TST3	5757	5440	5218	3330	6045	0.94	0.91	0.78	0.70
2F21TST4	5757	5440	5343	3330	6045	0.94	0.93	0.78	0.74
2F21TST5	5757	5440	5416	3330	6045	0.94	0.94	0.78	0.77
2F21TST6	5757	5440	5435	3330	6045	0.94	0.94	0.78	0.78
2F21TST7	5757	5440	5486	3330	6045	0.94	0.95	0.78	0.79
2F21TST8	5757	5440	5457	3330	6045	0.94	0.95	0.78	0.78
2F22TST2	5778	5315	5252	3450	6067	0.92	0.91	0.71	0.69
2F22TST3	5778	5315	5308	3450	6067	0.92	0.92	0.71	0.71
2F22TST4	5778	5315	5220	3450	6067	0.92	0.90	0.71	0.68
2F22TST5	5778	5315	5269	3450	6067	0.92	0.91	0.71	0.70
2F22TST6	5778	5315	5328	3450	6067	0.92	0.92	0.71	0.72
2F22TST7	5778	5315	5310	3450	6067	0.92	0.92	0.71	0.71
2F22TST8	5778	5315	5280	3450	6067	0.92	0.91	0.71	0.70
2F23TST1	5850	5925	5749	3450	6143	1.01	0.98	0.92	0.85
2F23TST2	5850	5925	5854	3450	6143	1.01	1.00	0.92	0.89
2F24TST1	5940	5750	5582	3510	6237	0.97	0.94	0.82	0.76
2F24TST3	5940	5750	5512	3510	6237	0.97	0.93	0.82	0.73
2F25TST1	5962	4600	4439	3530	6260	0.77	0.74	0.39	0.33
2F25TST2	5962	4600	4554	3530	6260	0.77	0.76	0.39	0.38
2F25TST3	5962	4600	4529	3530	6260	0.77	0.76	0.39	0.37
2F26TST2	6006	6200	6003	3550	6306	1.03	1.00	0.96	0.89

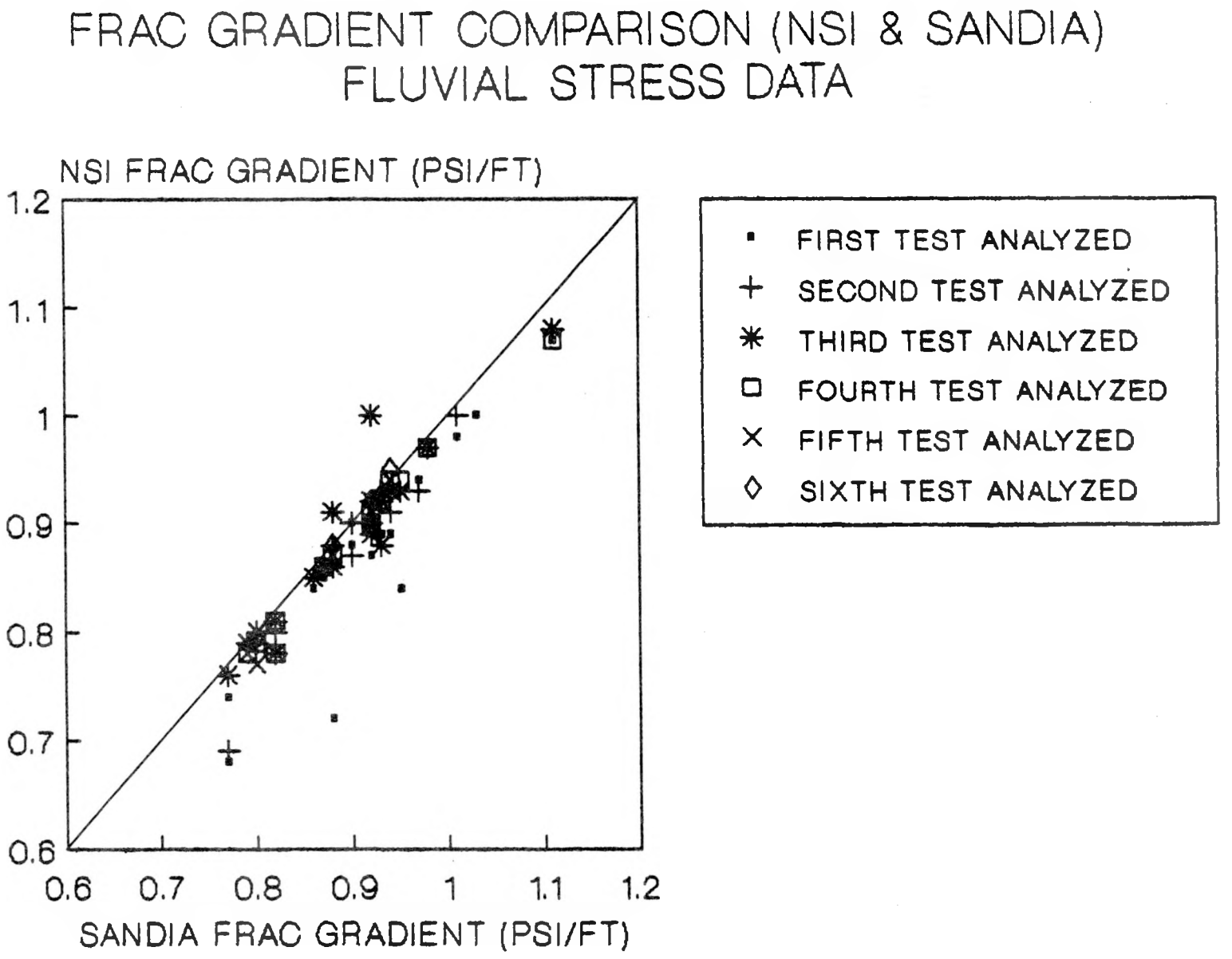


FIGURE 3: Comparison of NSI and Sandia Fracture Gradients from Fluvial Stress Data.

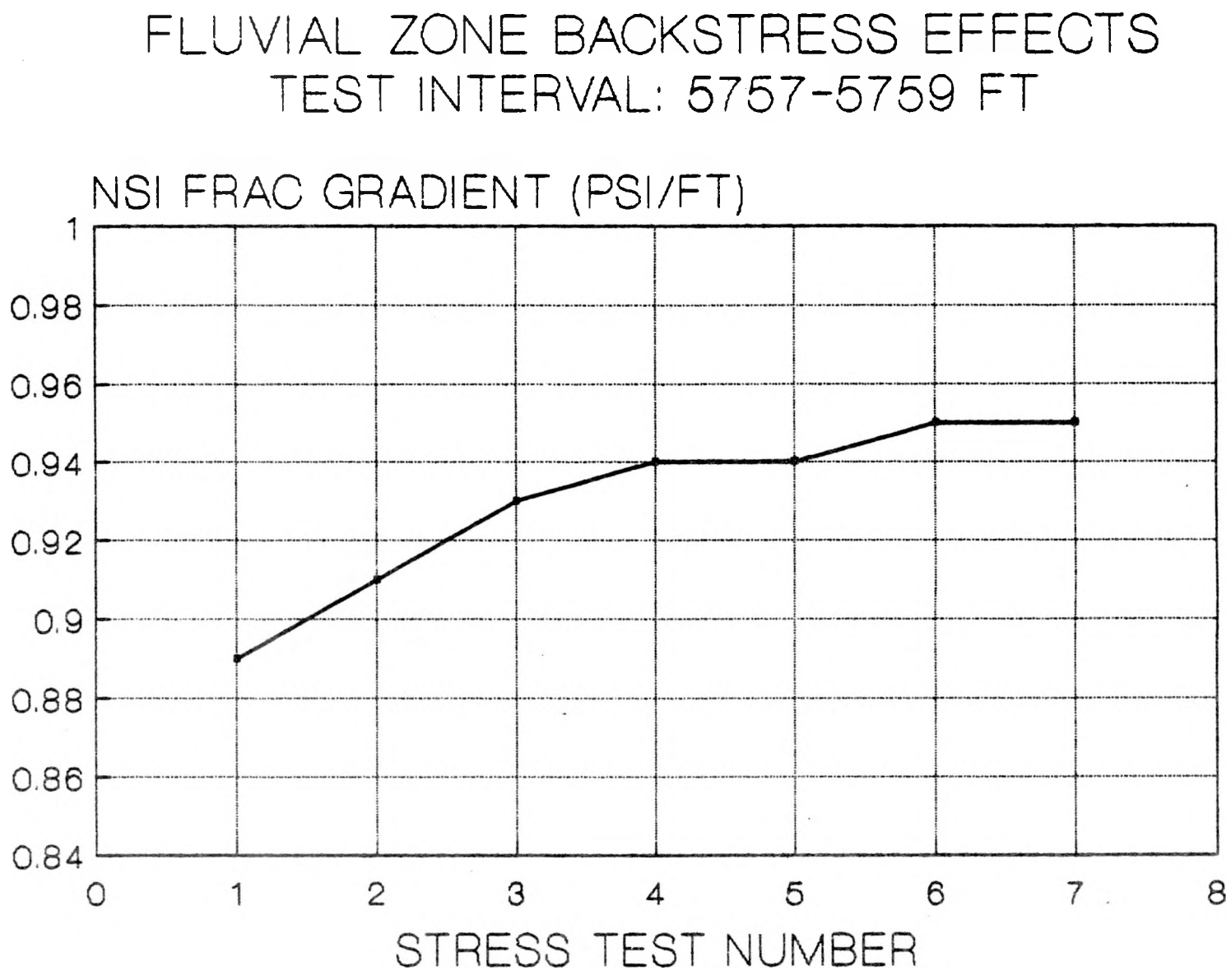


FIGURE 4: Characteristic of Backstress Effect (shale 5757-5759').

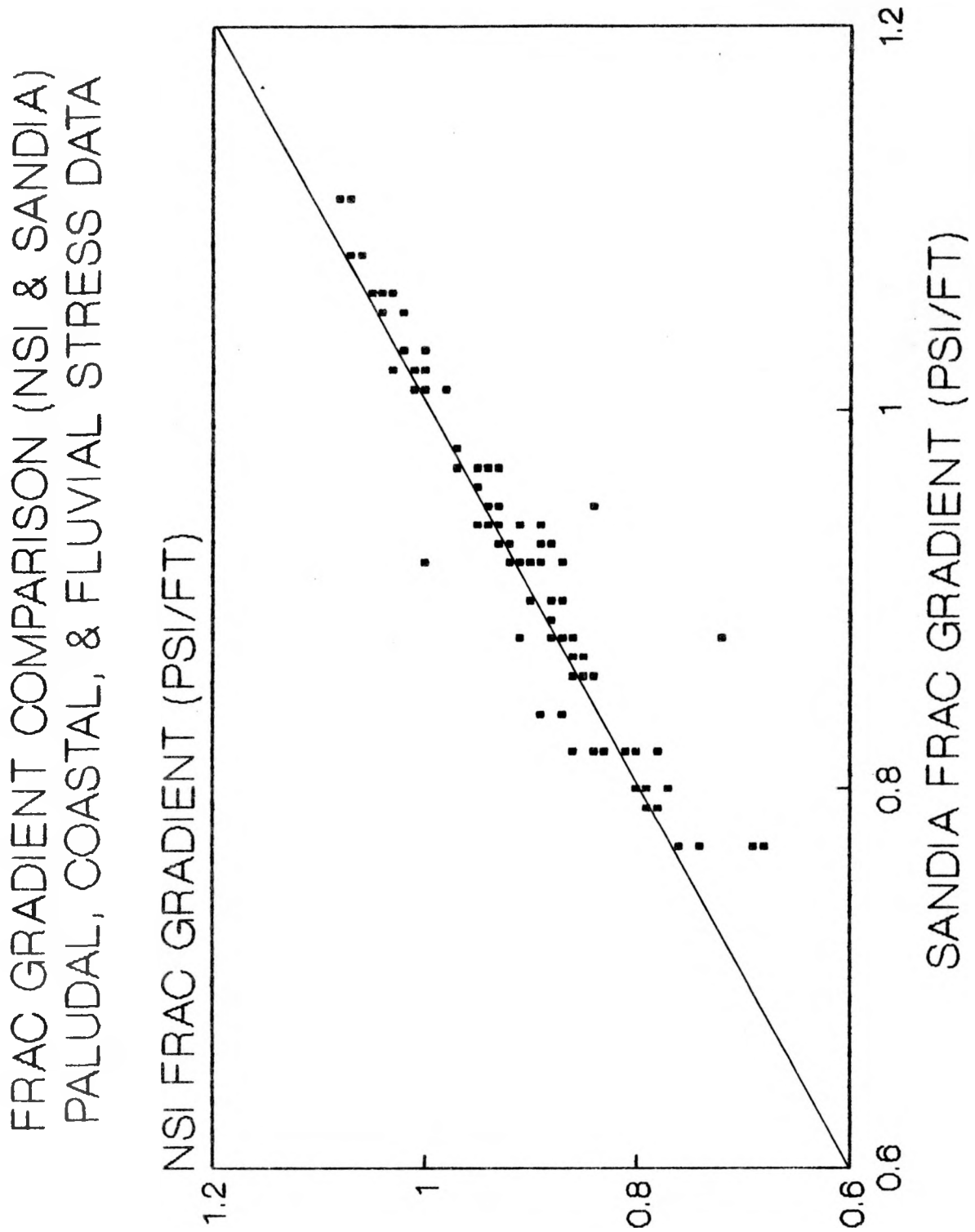


FIGURE 5: Comparison of NSI and Sandia Fracture Gradients for All MWX Stress Test Data.

TABLE 2: Summary of Stress, Sonic Log, and Mean Gamma-Ray Data Considered for Correlation Analysis.

TEST ZONE	DEPTH	GR	MEAN GR	STD DEV.	FRAC GRAD	K (STRESS)	K (SONIC)
2F1	4331	45	51	7	0.77	0.41	NA
2F2	4377	110	106	8	0.93	0.74	NA
2F3	4693	85	81	9	0.79	0.46	0.344
2F4	4715	160	151	14	1.11	1.14	0.397
2F5	5045	90	85	4	0.88	0.65	0.283
2F6	5075	130	127	13	0.92	0.72	0.370
2F7	5295	60	70	11	0.86	0.59	0.358
2F8	5321	140	128	10	0.90	0.69	0.362
2F9	5415	120	121	15	0.82	0.52	0.365
2F10	5451	130	125	8	0.87	0.59	0.378
2F11	5481	55	61	9	0.82	0.52	0.300
2F12	5507	100	99	18	0.95	0.79	0.356
2F13	5576	95	105	13	0.92	0.73	0.363
2F14	5601	125	113	15	0.98	0.85	0.376
2F15	5621	115	101	11	0.95	0.78	0.362
2F16	5650	100	100	20	0.92	0.73	0.362
2F17	5681	75	90	13	0.93	0.74	0.327
2F18	5701	140	107	30	0.90	0.69	0.336
2F19	5722	50	57	8	0.80	0.47	0.219
2F20	5745	130	99	33	0.88	0.64	0.401
2F21	5758	120	100	22	0.94	0.78	0.316
2F22	5779	90	96	21	0.92	0.71	0.354
2F23	5851	90	100	10	1.01	0.92	0.353
2F24	5941	115	112	11	0.97	0.82	0.345
2F26	6007	110	108	9	1.03	0.96	0.326
3C1	6375	125	121	18	1.03	0.94	0.379
3C2	6399	140	125	20	1.01	0.89	0.379
3C3	6421	140	132	15	1.06	1.03	0.290
3C4	6443	55	60	7	0.89	0.56	0.325
3C5	6461	65	65	2	0.88	0.53	0.250
3C6	6513	75	74	8	0.90	0.59	0.250
3C7	6528	145	118	21	1.02	0.92	0.370
3C8	6549	53	57	4	0.86	0.50	0.266
3C9	6566	120	113	15	1.06	1.03	0.389
3C10	6607	120	119	18	1.08	1.08	0.300
3C11U	6707	90	89	7	1.06	1.02	0.370
3C11L	6766	90	112	23	1.05	1.00	0.429

TABLE 2 - Continued

TEST ZONE	DEPTH	GR	MEAN GR	STD DEV.	FRAC GRAD	K (STRESS)	K (SONIC)
2P1	6929	115	101	8	0.84	0.38	*
2P2	6964	70	77	17	0.82	0.31	*
2P3	7011	90	94	13	0.90	0.53	0.416
3P1	7033	160	109	36	0.97	0.73	-
3P2	7049	30	56	30	1.02	0.91	-
3P3	7069	115	115	18	0.82	0.23	-
2P4	7170	80	85	5	0.98	0.76	0.300
2P5	7207	75	72	10	0.96	0.68	0.410
2P6	7264	50	60	11	0.93	0.59	0.230
2P7	7304	110	103	9	0.88	0.42	0.387
2P8	7395	65	68	7	0.91	0.52	0.341
2P9	7424	30	35	13	0.92	0.58	*
2M1	7467	50	53	4	0.91	0.49	0.239
2M2	7531	55	56	2	0.88	0.36	0.291
2M3	7601	85	81	2	1.00	0.82	0.290
2M4	7665	105	102	3	1.06	1.06	0.364
2M5	7766	105	105	2	1.11	1.23	0.354
2M6	7850	50	50	8	0.85	0.24	0.178
2M7	7895	80	87	8	0.87	0.27	0.279
2M8	7924	90	90	2	0.98	0.74	0.300
2M9	7971	60	60	1	0.86	0.28	0.233
2M10	8015	110	110	7	1.02	0.84	0.330
2M11	8061	90	92	2	1.02	0.86	0.298

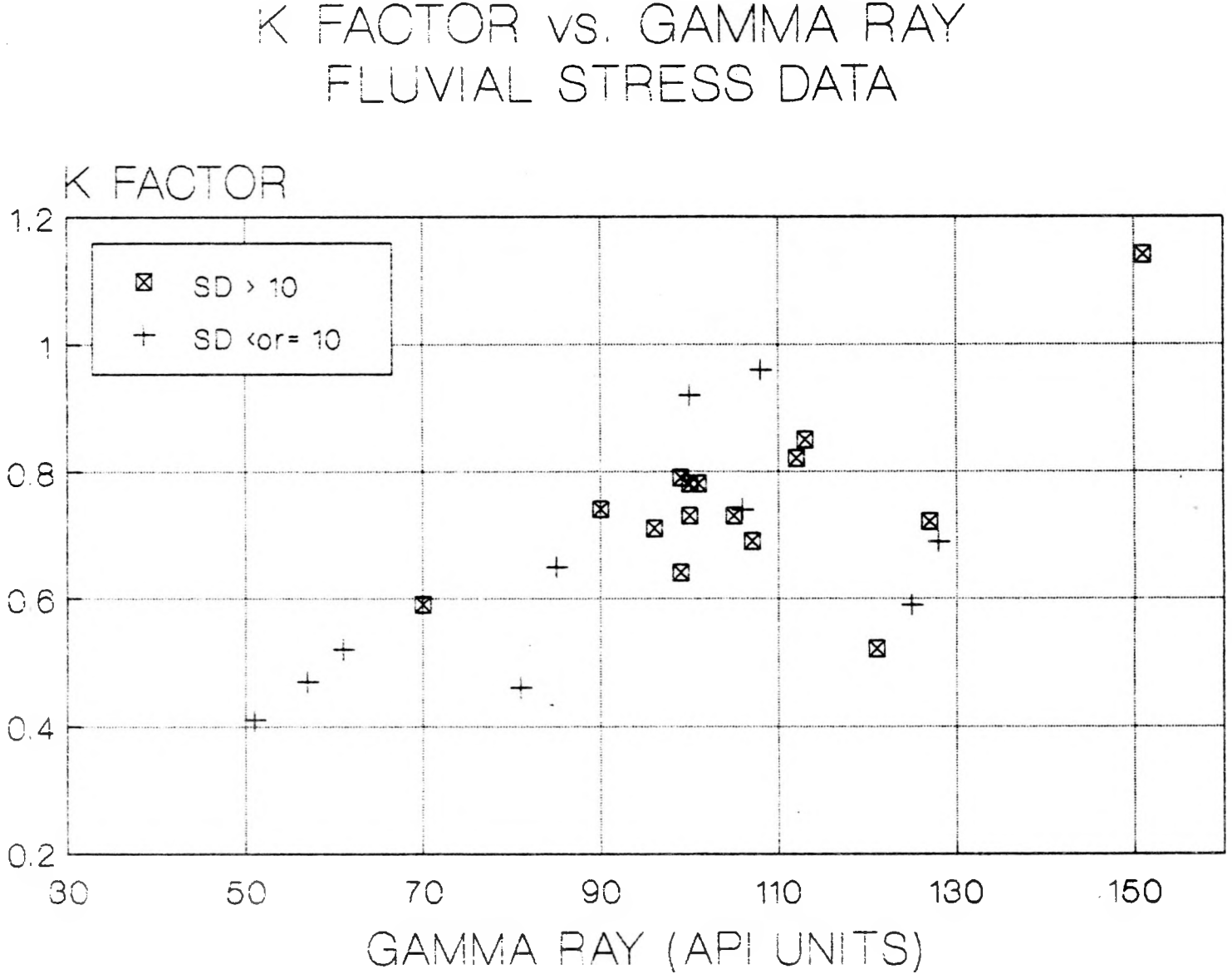


FIGURE 6: "K-Factor" v. Gamma-Ray API Units for Fluvial Stress Data.

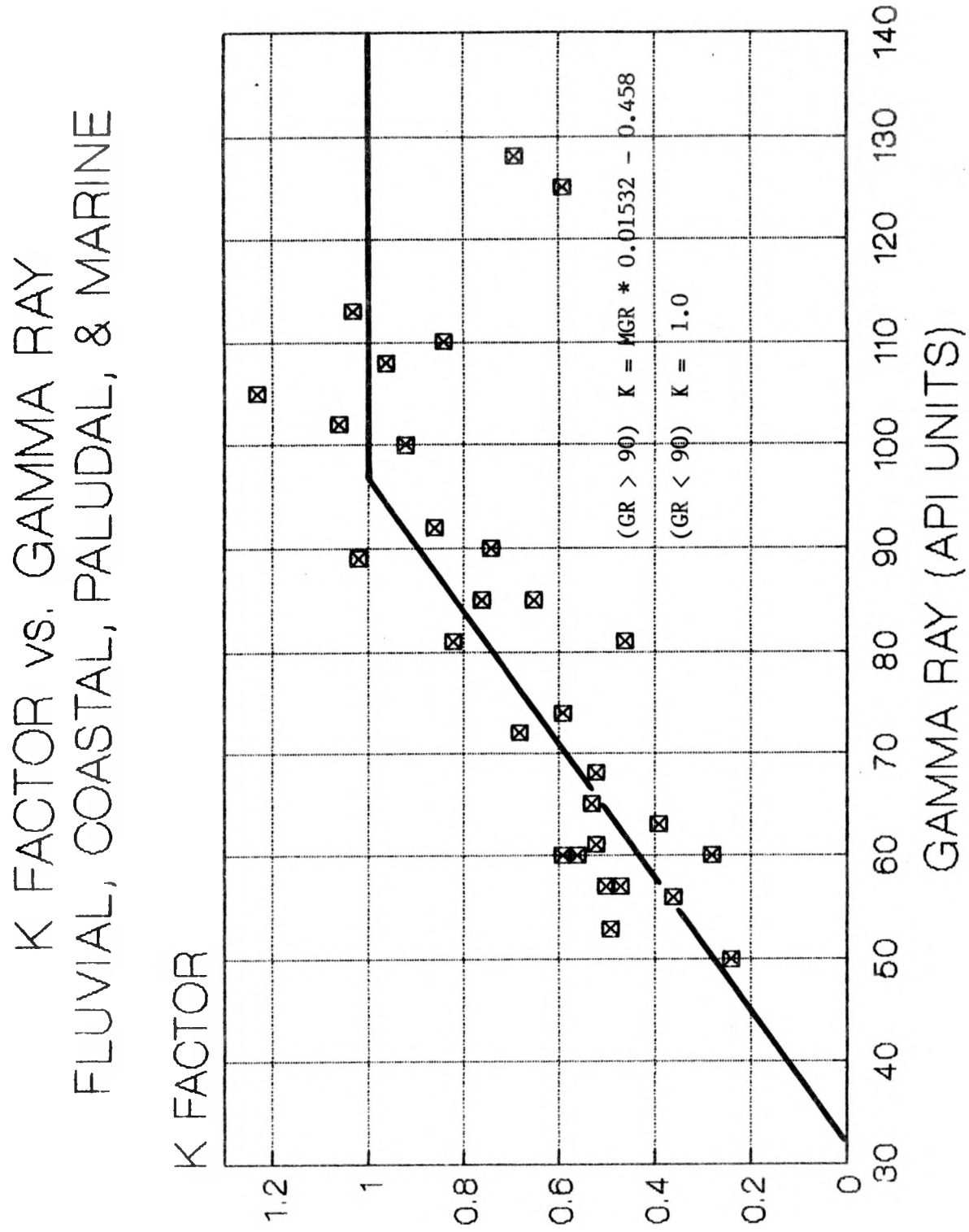


FIGURE 7: "K-Factor" v. Gamma-Ray for All MWX Data Showing the Bi-Linear Correlation.

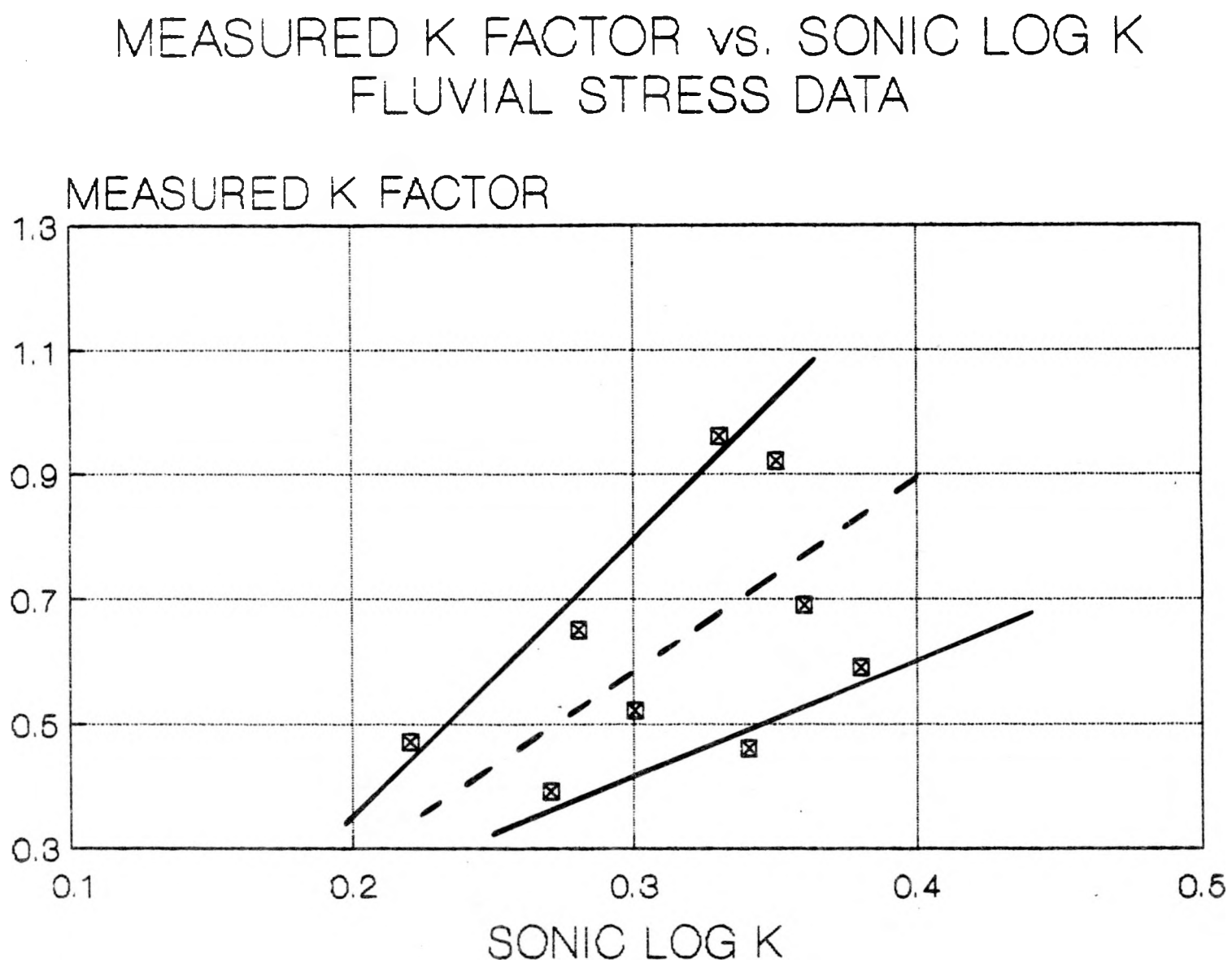


FIGURE 8: Measured K-Factor v. Sonic Log K-Factor for Fluvial Stress Data.

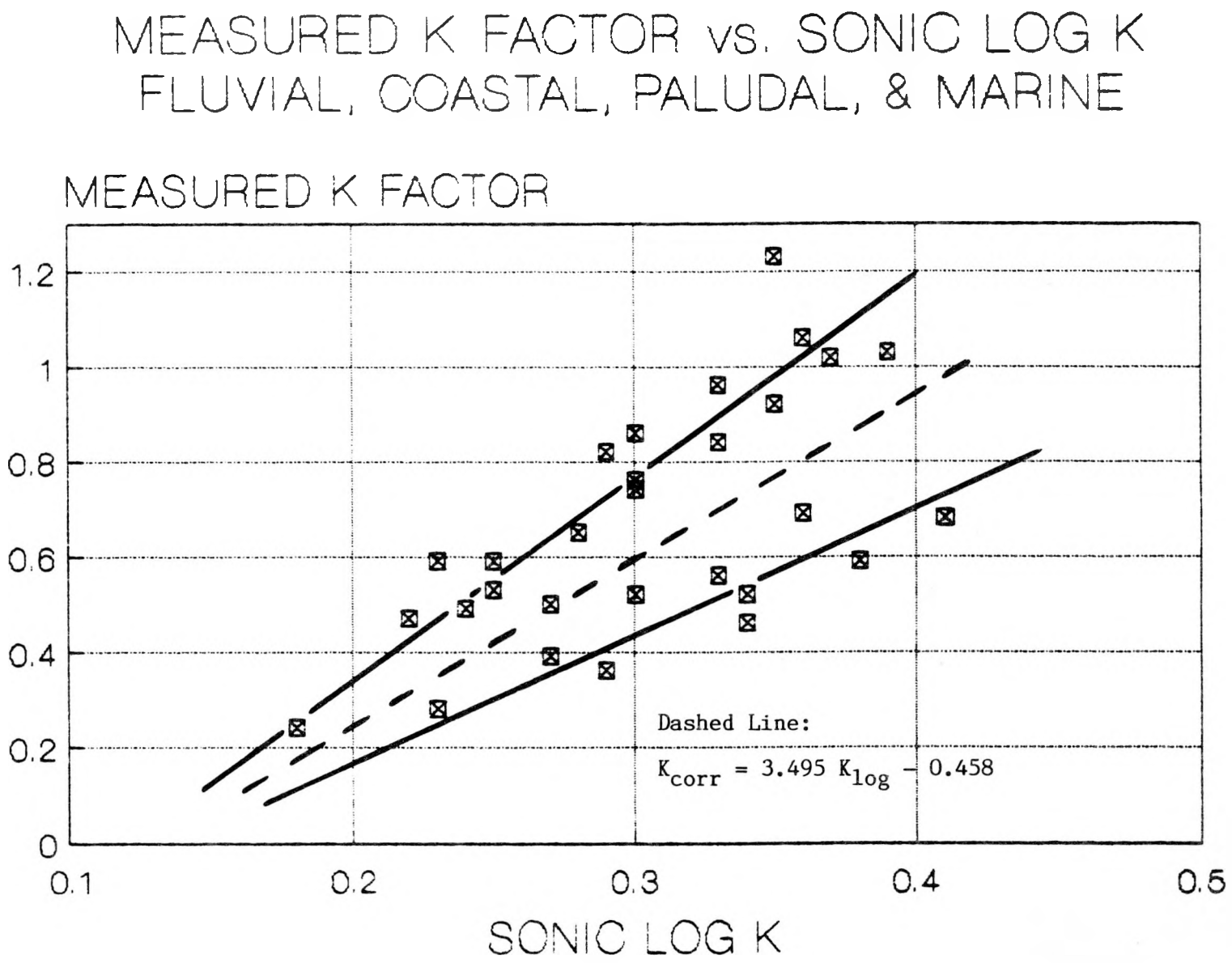


FIGURE 9: Measured K-Factor v. Sonic Log K-Factor for All MWX Stress Data.

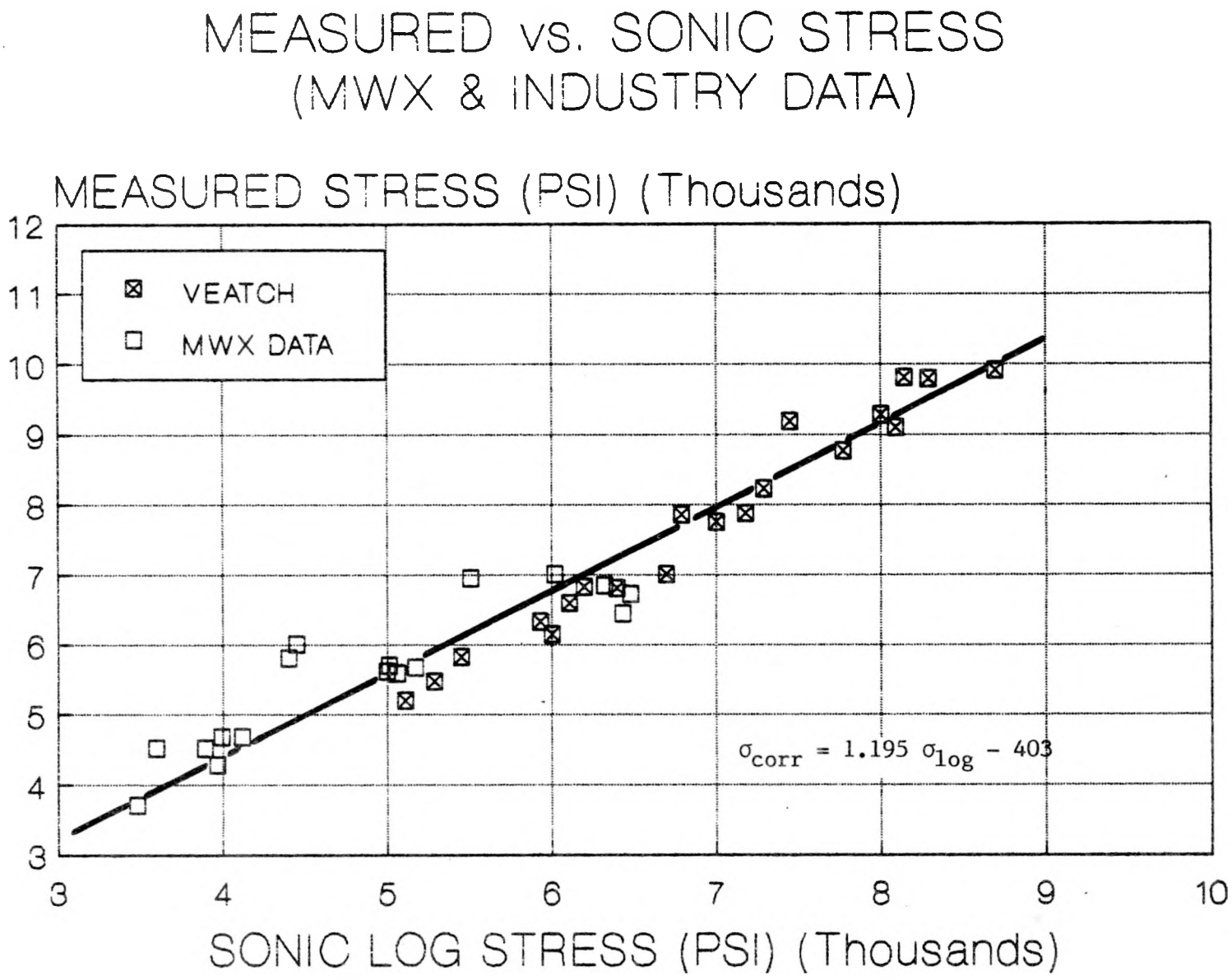


FIGURE 10: Measured Stress v. Sonic Log Derived Stress Comparing MWX Results to Other Industry Results.

FIGURE 11: Derived Stress Log from Bi-Linear GR Correlation as Compared to Measured Stresses, MWX-2.

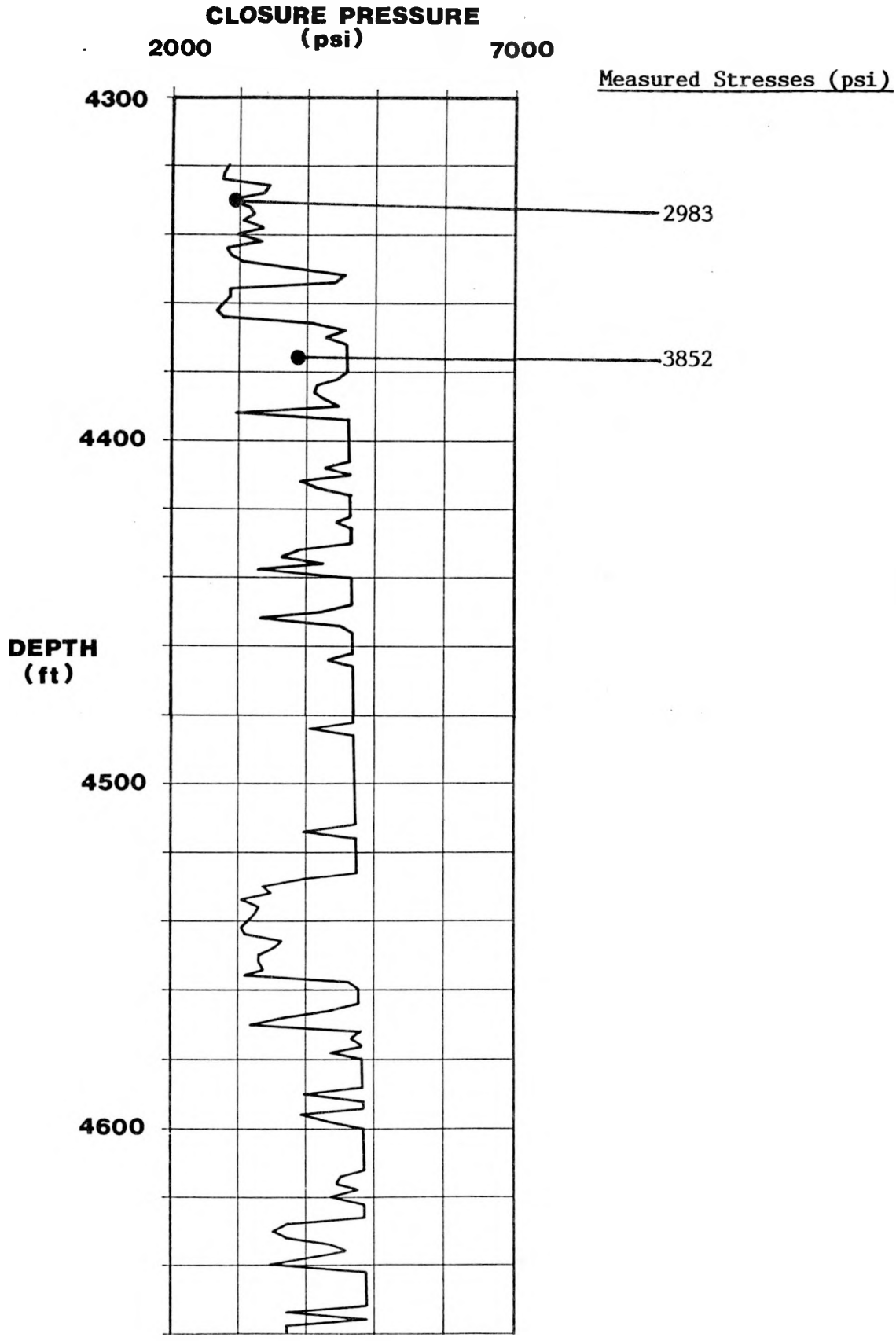


FIGURE 11 - Continued

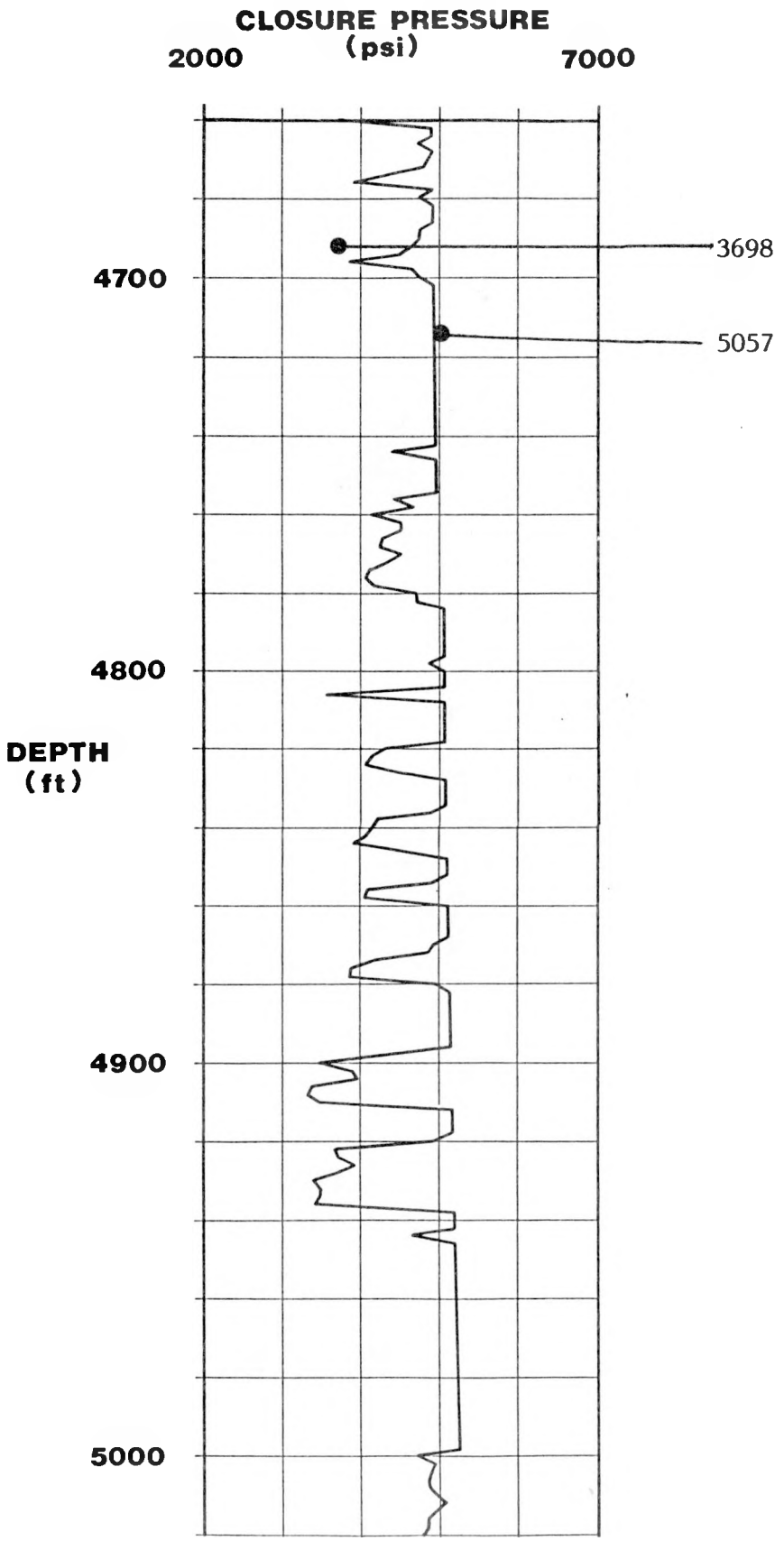


FIGURE 11 - Continued

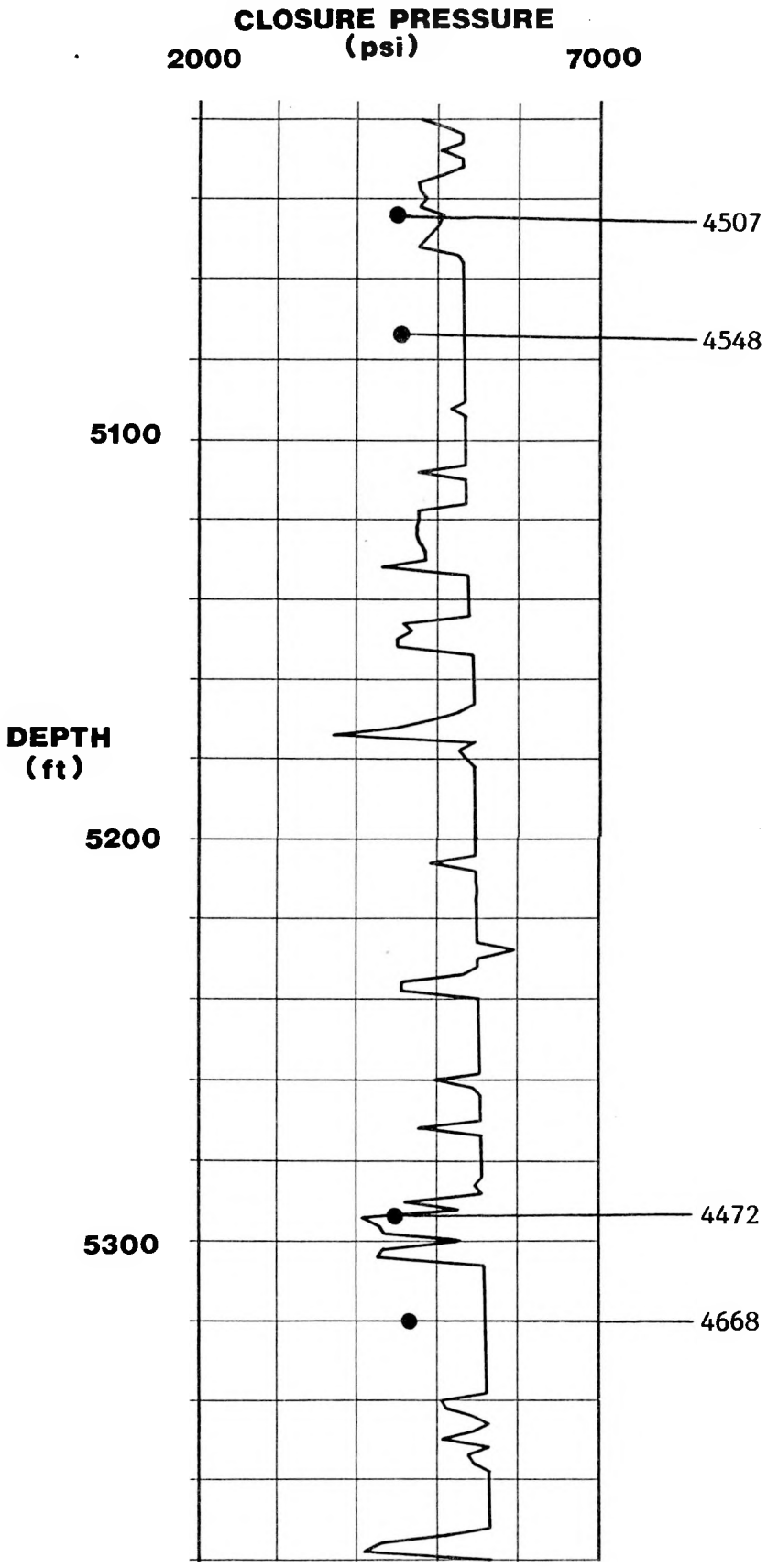


FIGURE 11 - Continued

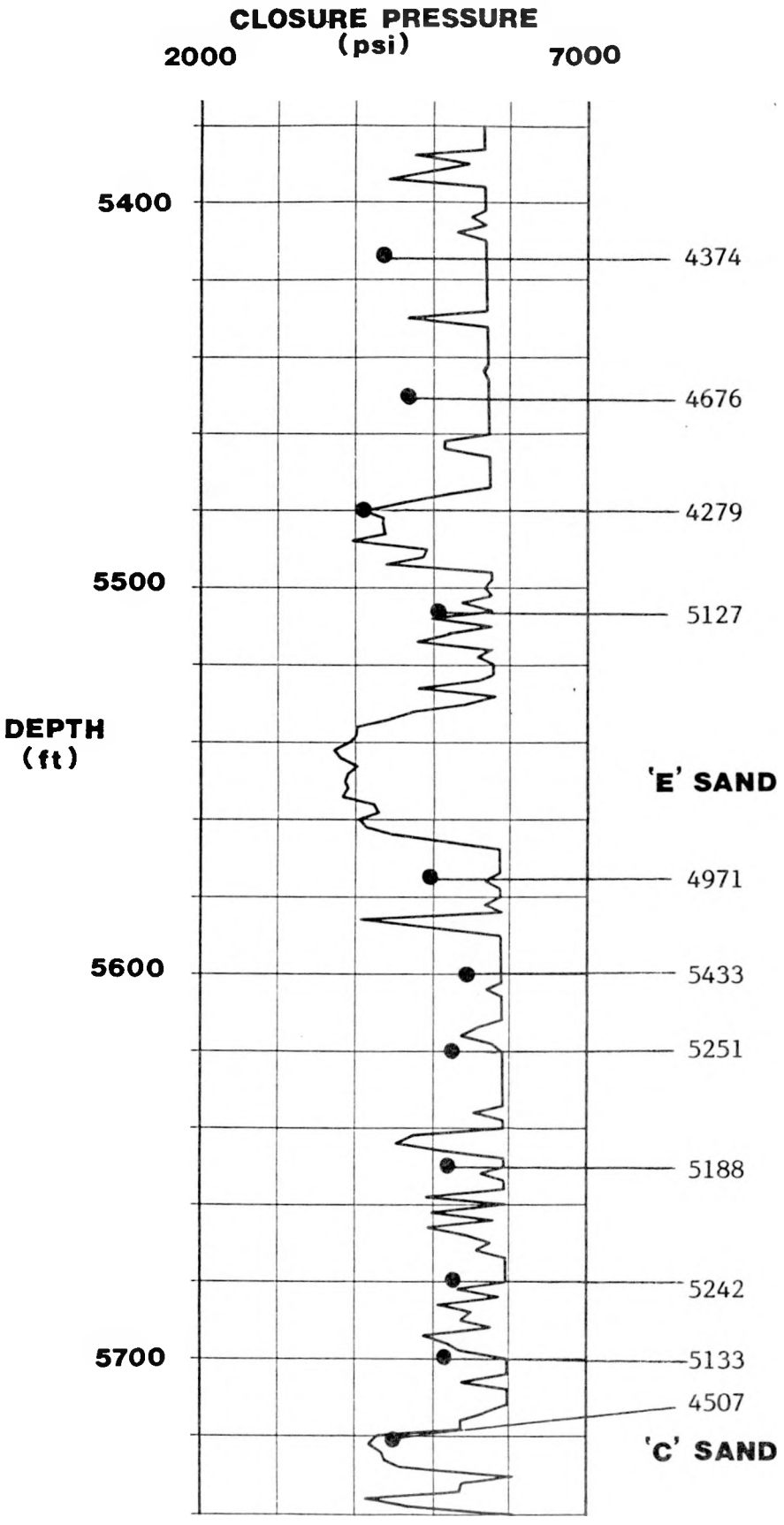


FIGURE 11 – Continued

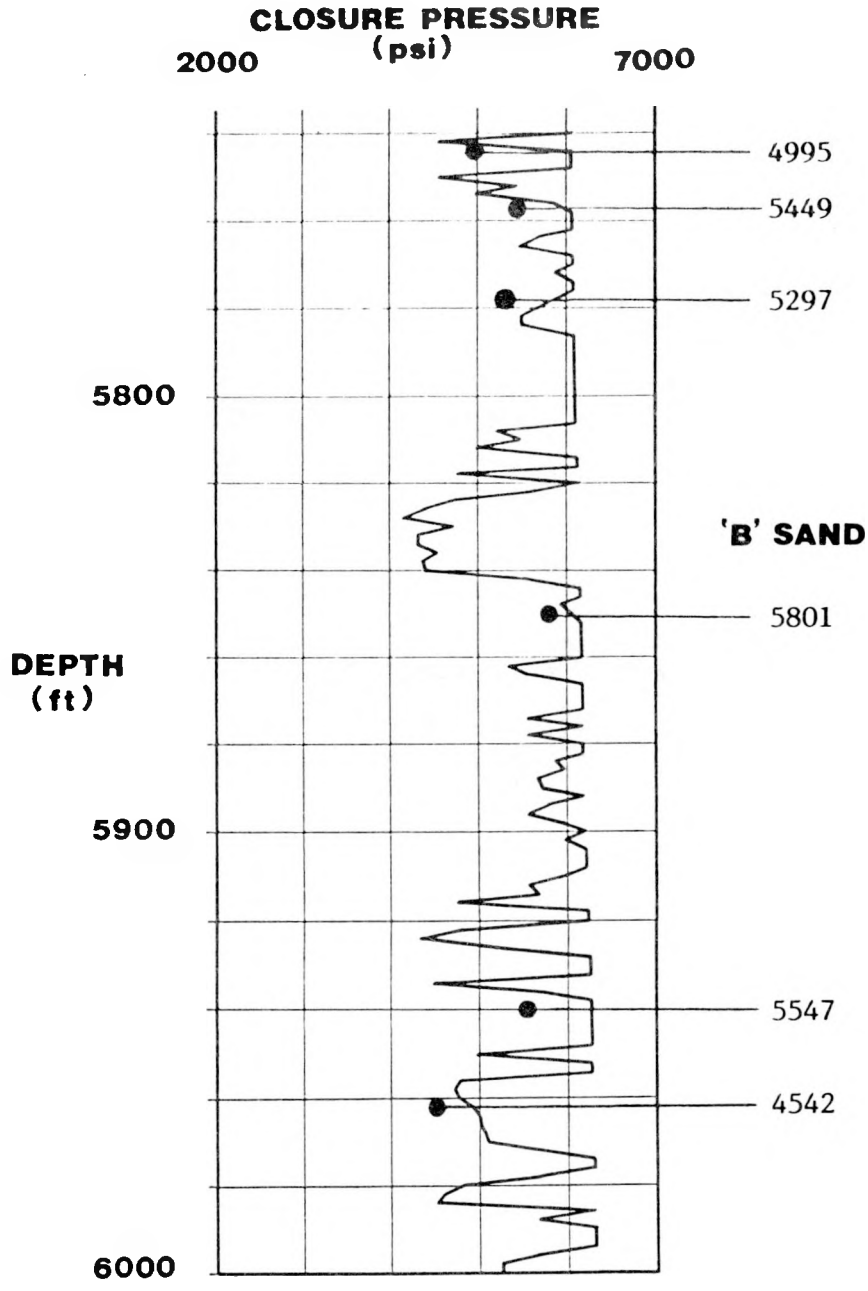


TABLE NO. 3

Comparison of Lithology Correlation Stress With Measured Stress for Fluvial Data

DEPTH (Ft)	LITHOLOGY	GR CORR. (psi)	MEAS. σ (psi)	σ DIFF. (psi)
4331	Sandstone	3146	2983	163
4377	Mudstone	4596	3852	741
4693	Sandstone	4392	3698	694
4715	Mudstone	4951	5057	106
5045	Sandstone	4946	4507	439
5075	Mudstone	5329	4548	781
5295	Sandstone	4476	4472	4
5321	Mudstone	5587	4668	919
5415	Mudstone	5686	4374	1,312
5451	Mudstone	5724	4676	1,048
5481	Sandstone	4339	4279	60
5507	Mudstone	5482	5127	355
5576	Mudstone	5811	4971	840
5601	Mudstone	5828	5433	395
5621	Mudstone	5870	5251	619
5650	Mudstone	5701	5188	513
5681	Mudstone	5766	5242	524
5701	Mudstone	5819	5133	686
5722	Sandstone	4491	4507	16
5745	Mudstone	5664	4995	669
5758	Mudstone	5793	5449	344
5779	Mudstone	5762	5297	465
5851	Mudstone	6068	5801	267
5941	Mudstone	6238	5547	691
5963	Sandstone	4916	4542	374
6007	Mudstone	6307	6003	304

AVG. DIFF. FOR SANDSTONES = 250 psi

AVG. DIFF. FOR MUDSTONES = 609 psi

AVG. DIFF. FOR ALL = 513 psi

FIGURE 12: Derived Stress Log from the Sonic Correlation as Compared to Measured Stresses, MWX-2.

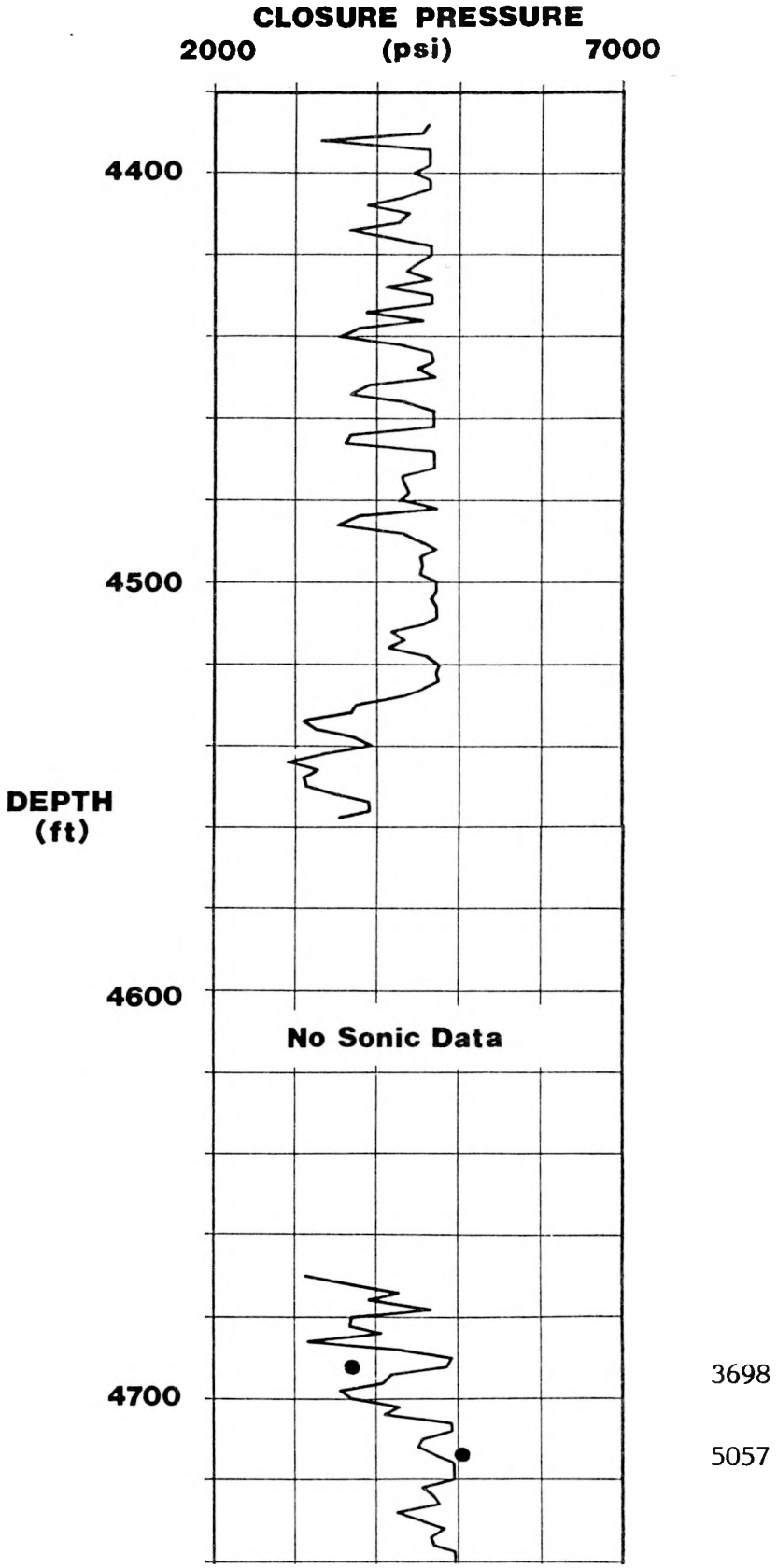


FIGURE 12 – Continued

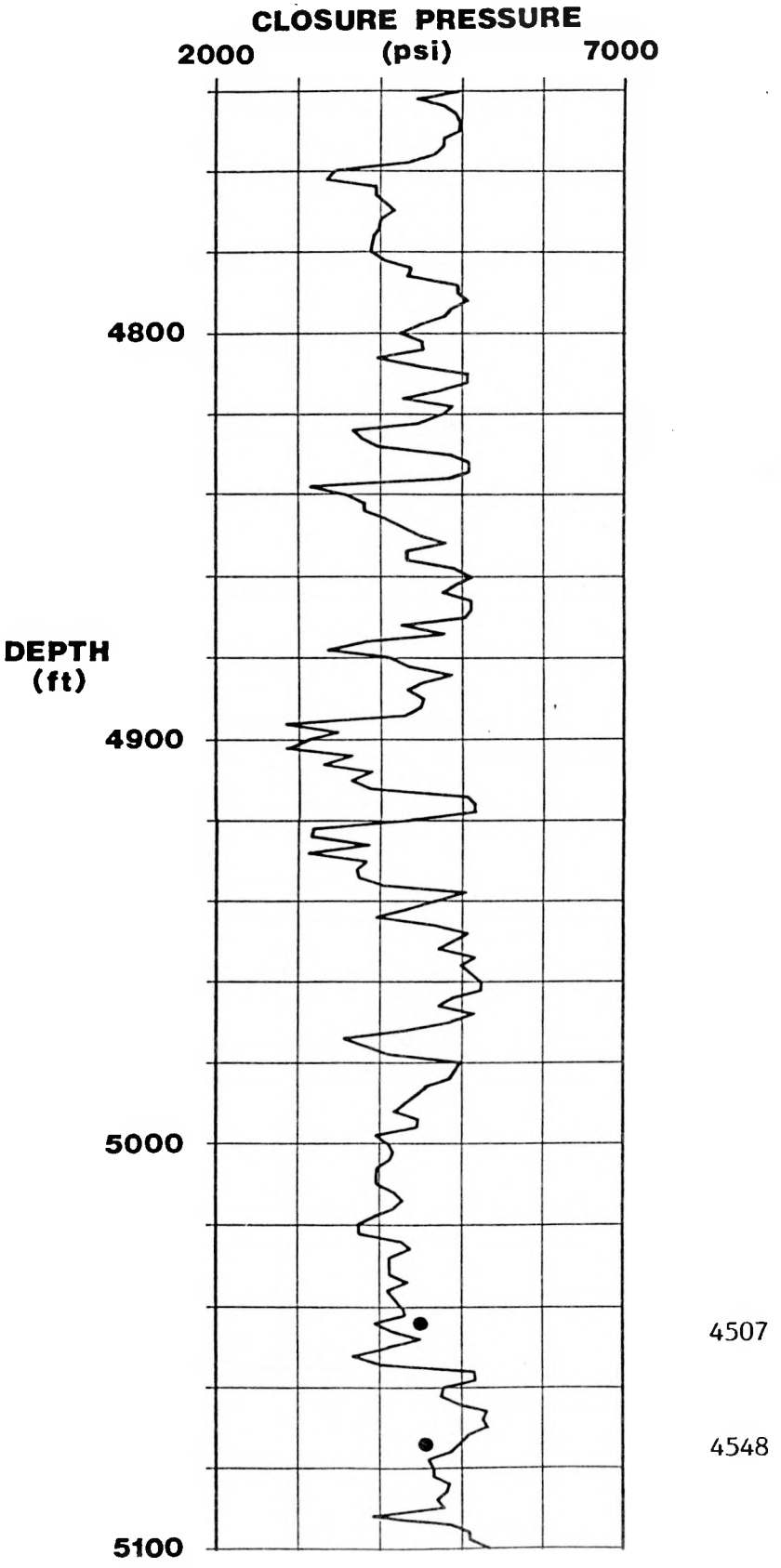


FIGURE 12 - Continued

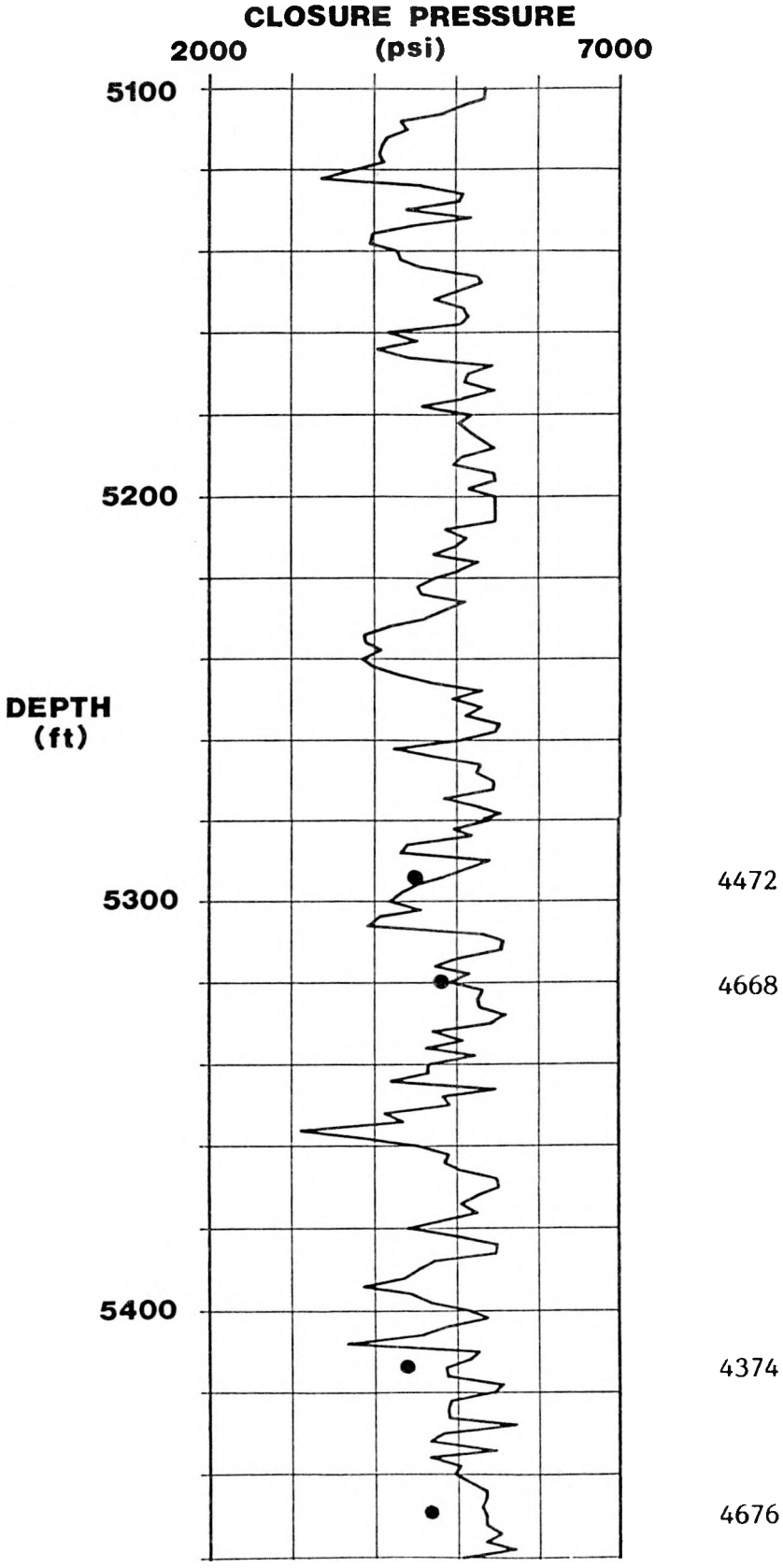


FIGURE 12 - Continued

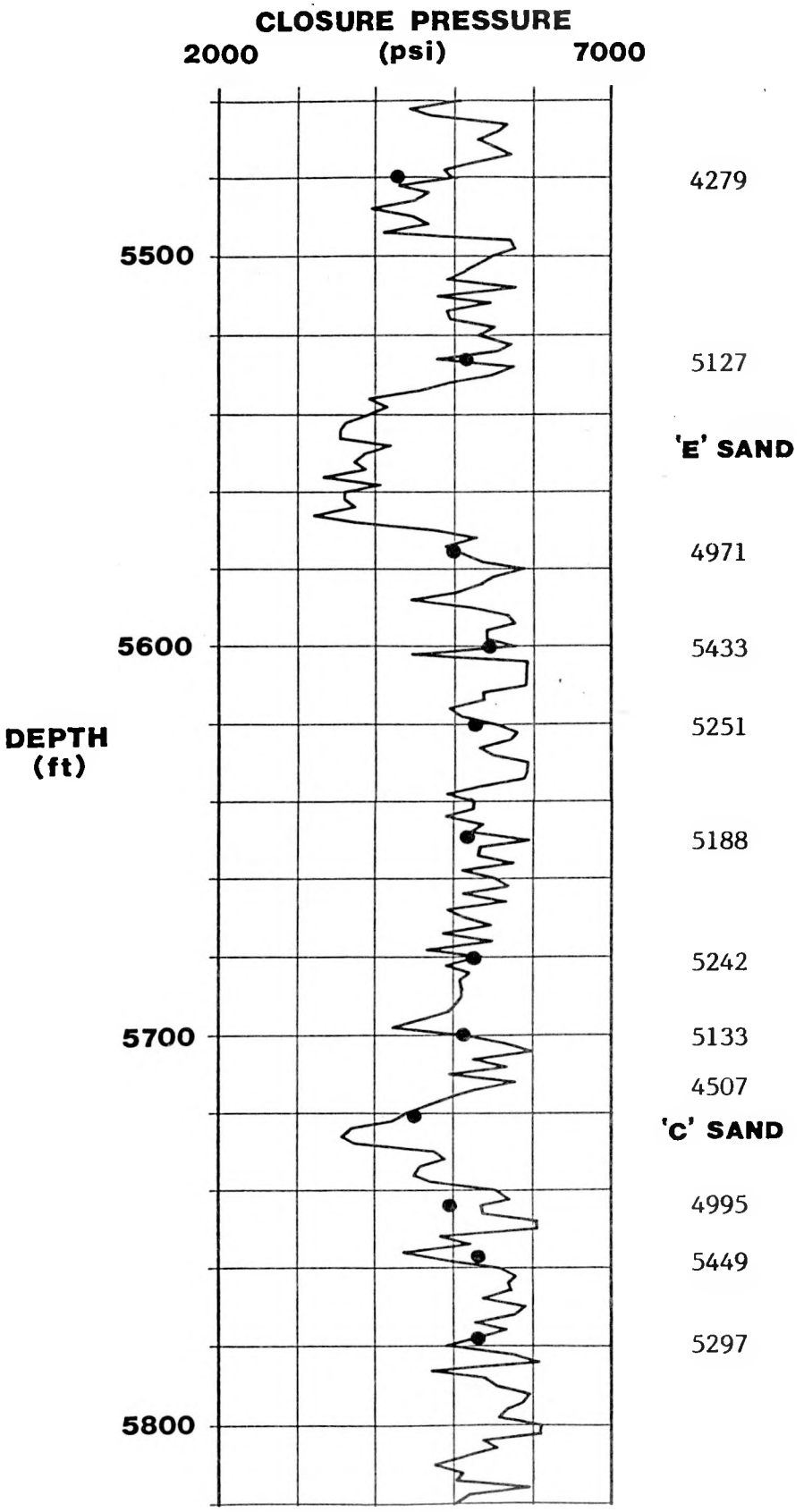


FIGURE 12 – Continued

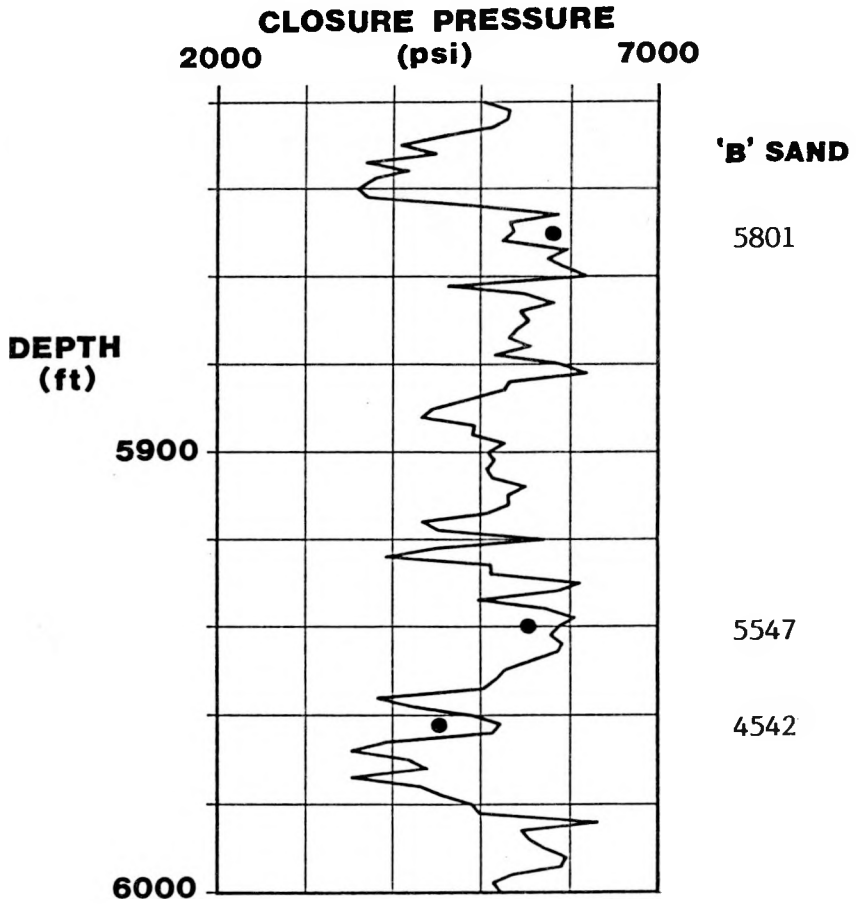


TABLE NO. 4

Comparison of Sonic Correlation Stress With Measured Stress for Fluvial Data

DEPTH (Ft)	LITHOLOGY	SONIC (psi)	MEAS. σ (psi)	σ DIFF. (psi)
4693	Sandstone	4318	3698	620
4715	Mudstone	4782	5057	275
5045	Sandstone	4183	4507	324
5075	Mudstone	4905	4548	357
5295	Sandstone	4723	4472	251
5321	Mudstone	5093	4668	425
5415	Mudstone	5187	4374	813
5451	Mudstone	5374	4676	698
5481	Sandstone	4757	4279	478
5507	Mudstone	5217	5127	90
5576	Mudstone	5314	4971	343
5601	Mudstone	5460	5433	27
5621	Mudstone	5386	5251	135
5650	Mudstone	5472	5188	284
5681	Mudstone	5095	5242	147
5701	Mudstone	5125	5133	8
5722	Sandstone	4030	4507	447
5745	Mudstone	5654	4995	659
5758	Mudstone	5242	5449	207
5779	Mudstone	5483	5297	186
5851	Mudstone	5584	5801	217
5941	Mudstone	5855	5547	308
5962	Sandstone	4478	4542	64

AVG. DIFF. FOR SANDSTONES = 364 psi

AVG. DIFF. FOR MUDSTONES = 305 psi

AVG. DIFF. FOR ALL = 320 psi

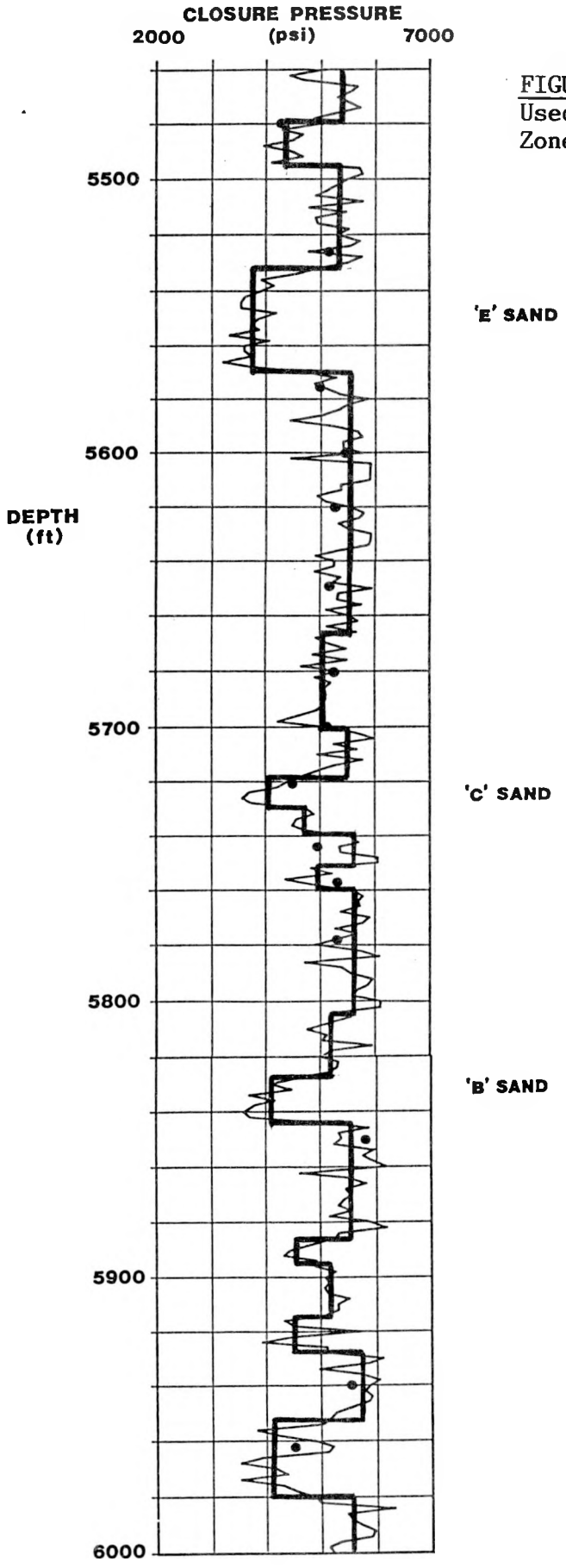


FIGURE 13: Stress Profile Used for Matching the Fluvial Zone Fracturing Tests.

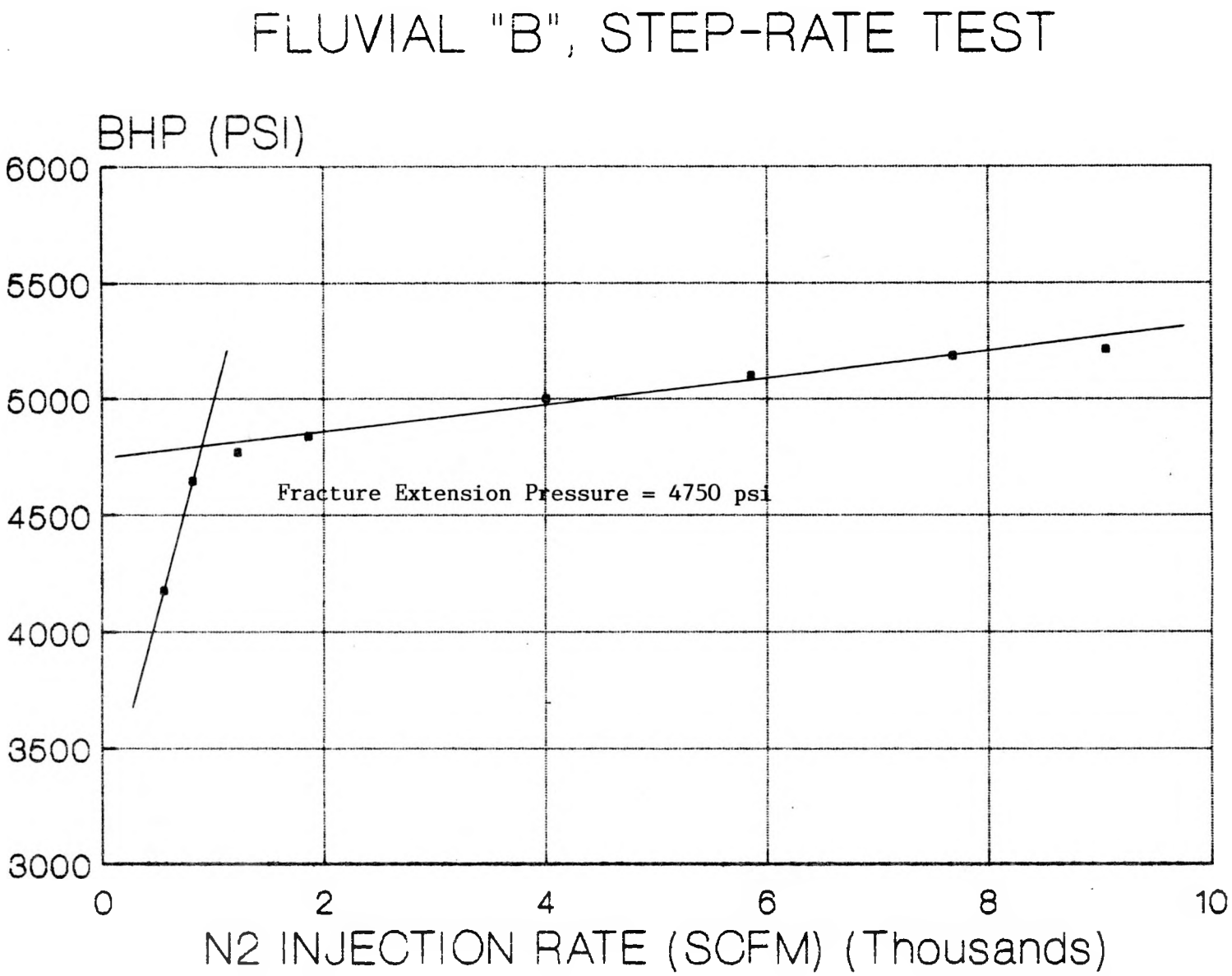


FIGURE 14: Fluvial "B" Sand Nitrogen Step-Rate Test.

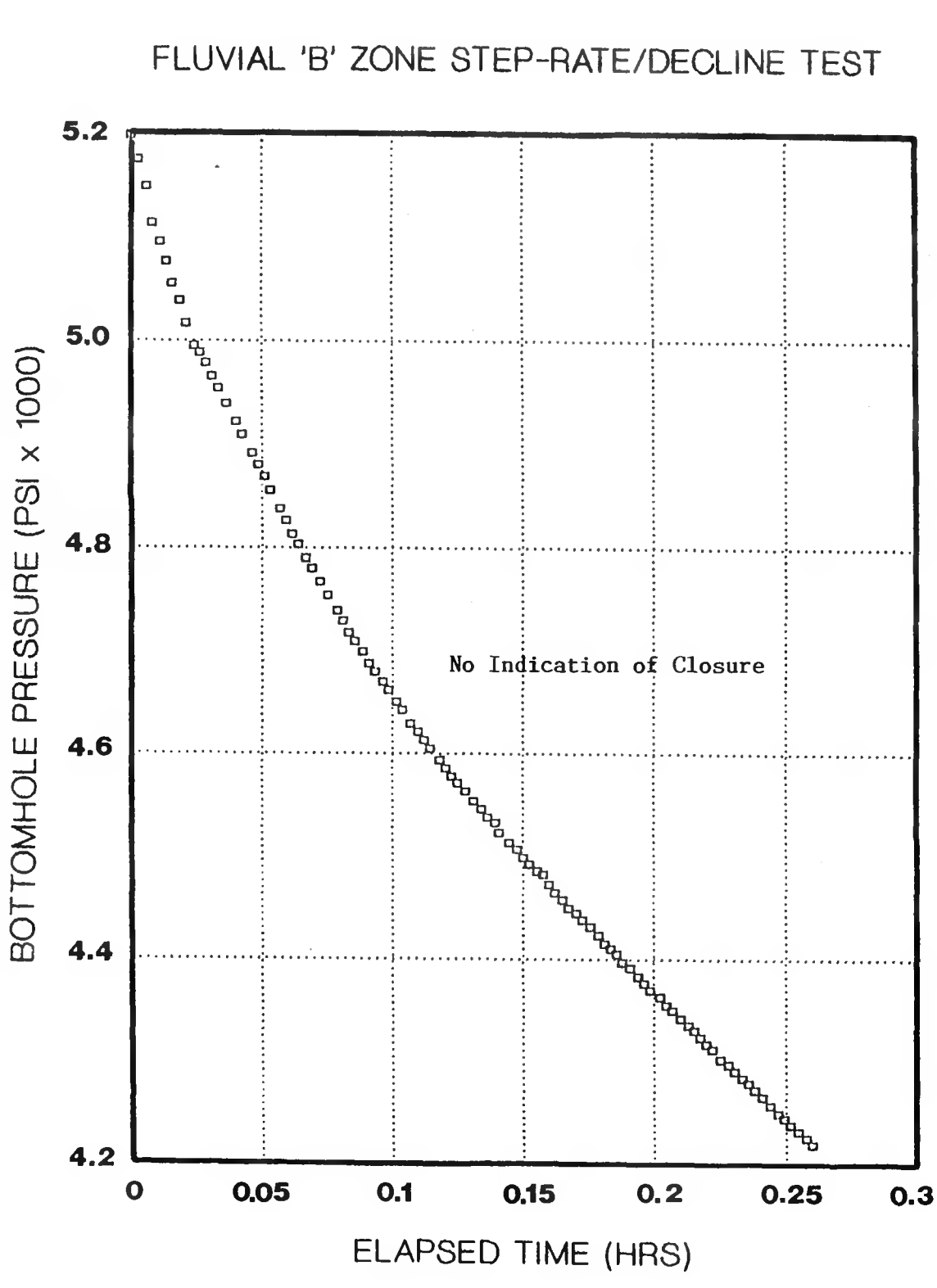


FIGURE 15: Fluvial "B" Sand Nitrogen Step-Rate Test Flowback Decline.

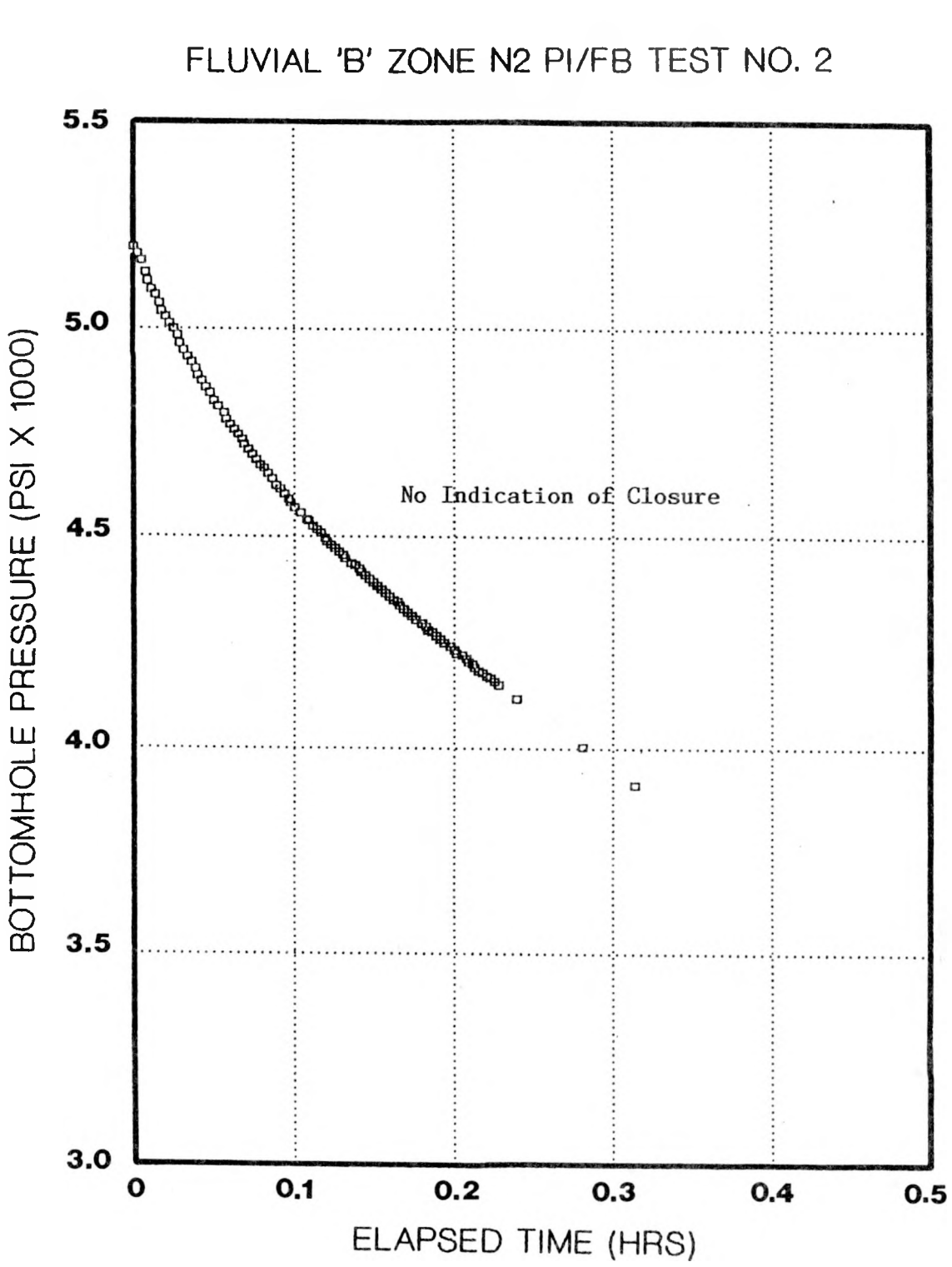


FIGURE 16: Fluvial "B" Sand Nitrogen Pump-In/Flowback No. 2 Decline.

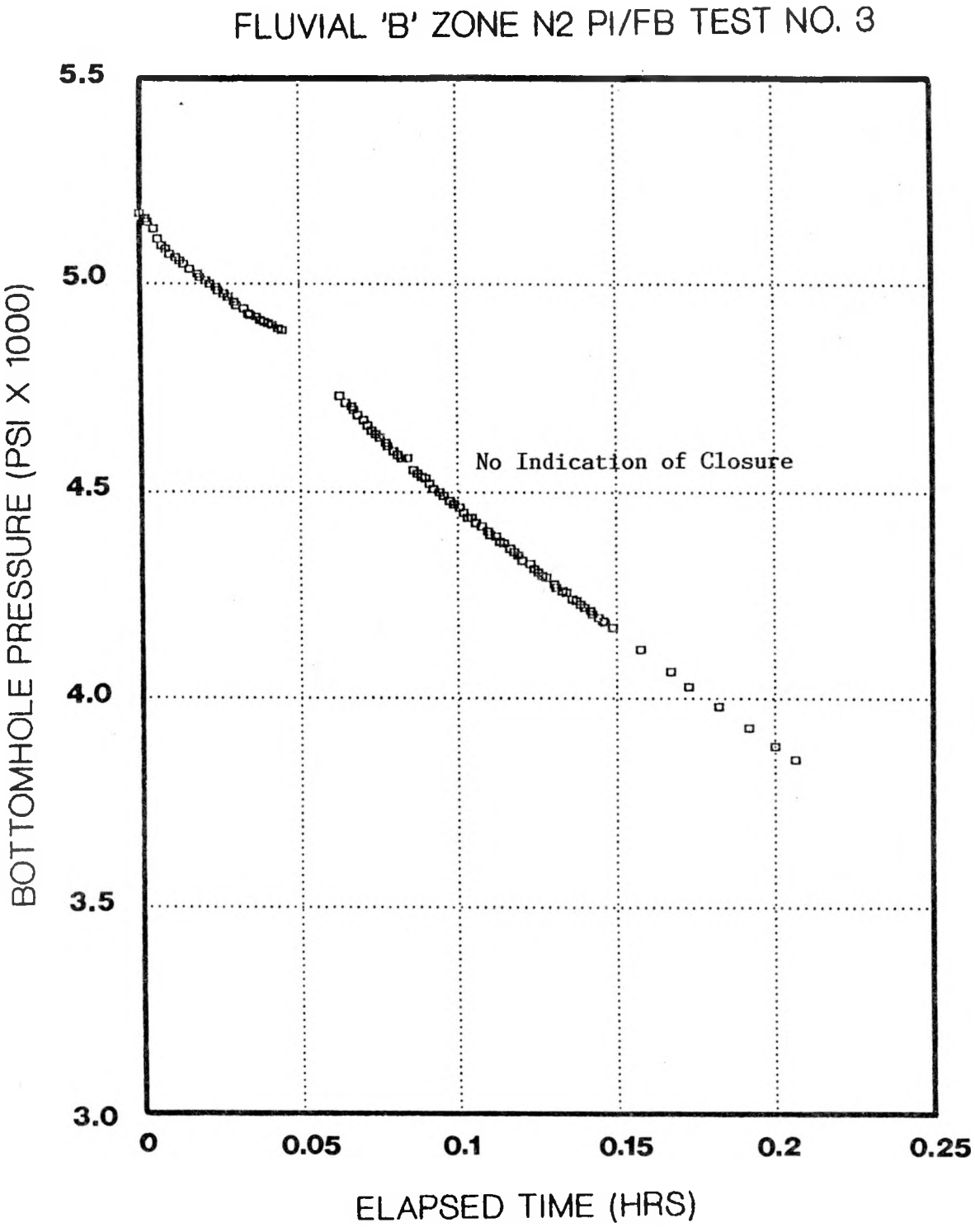


FIGURE 17: Fluvial "B" Sand Nitrogen Pump-In/Flowback No. 3 Decline.

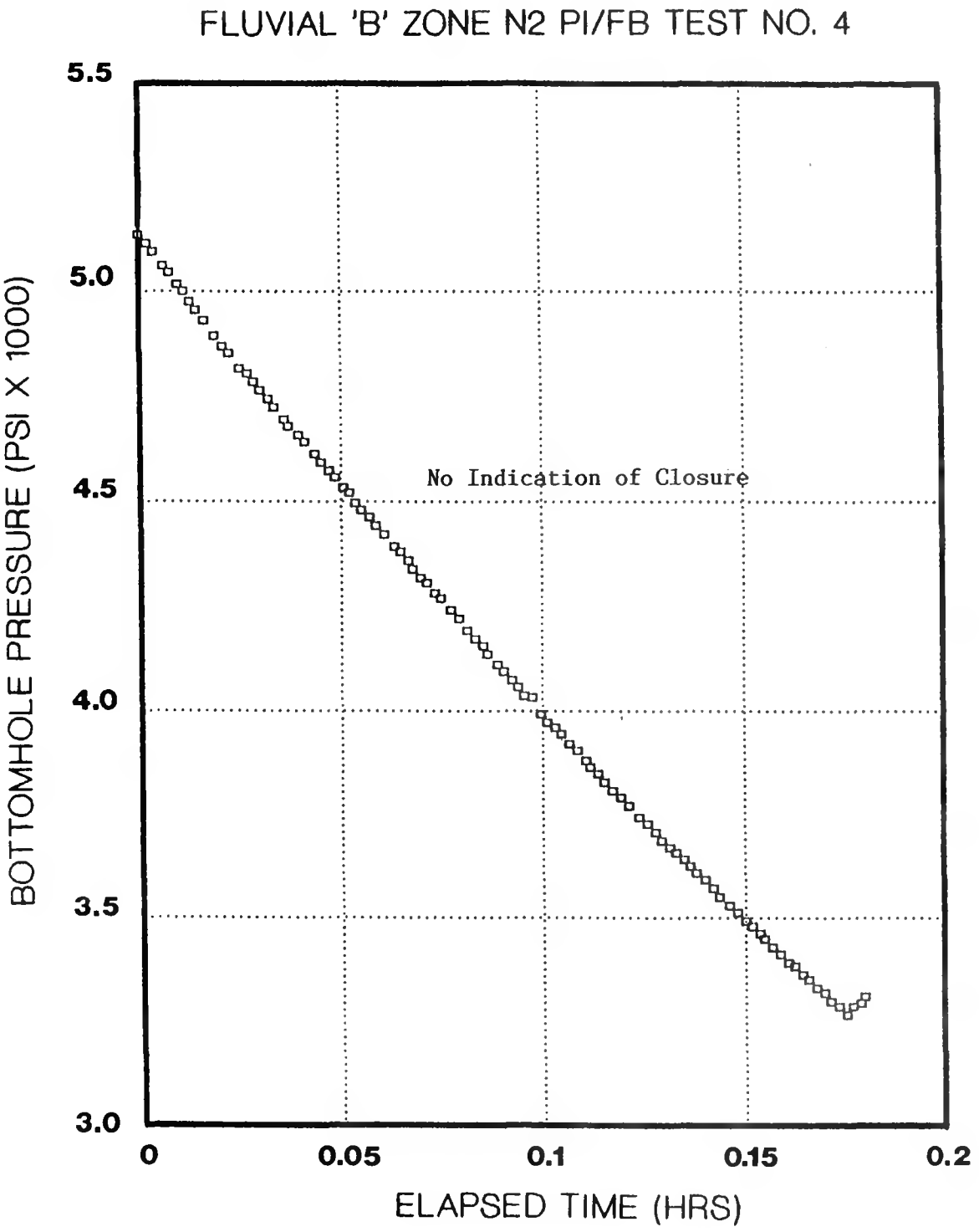


FIGURE 18: Fluvial "B" Sand Nitrogen Pump-In/Flowback No. 4 Decline.

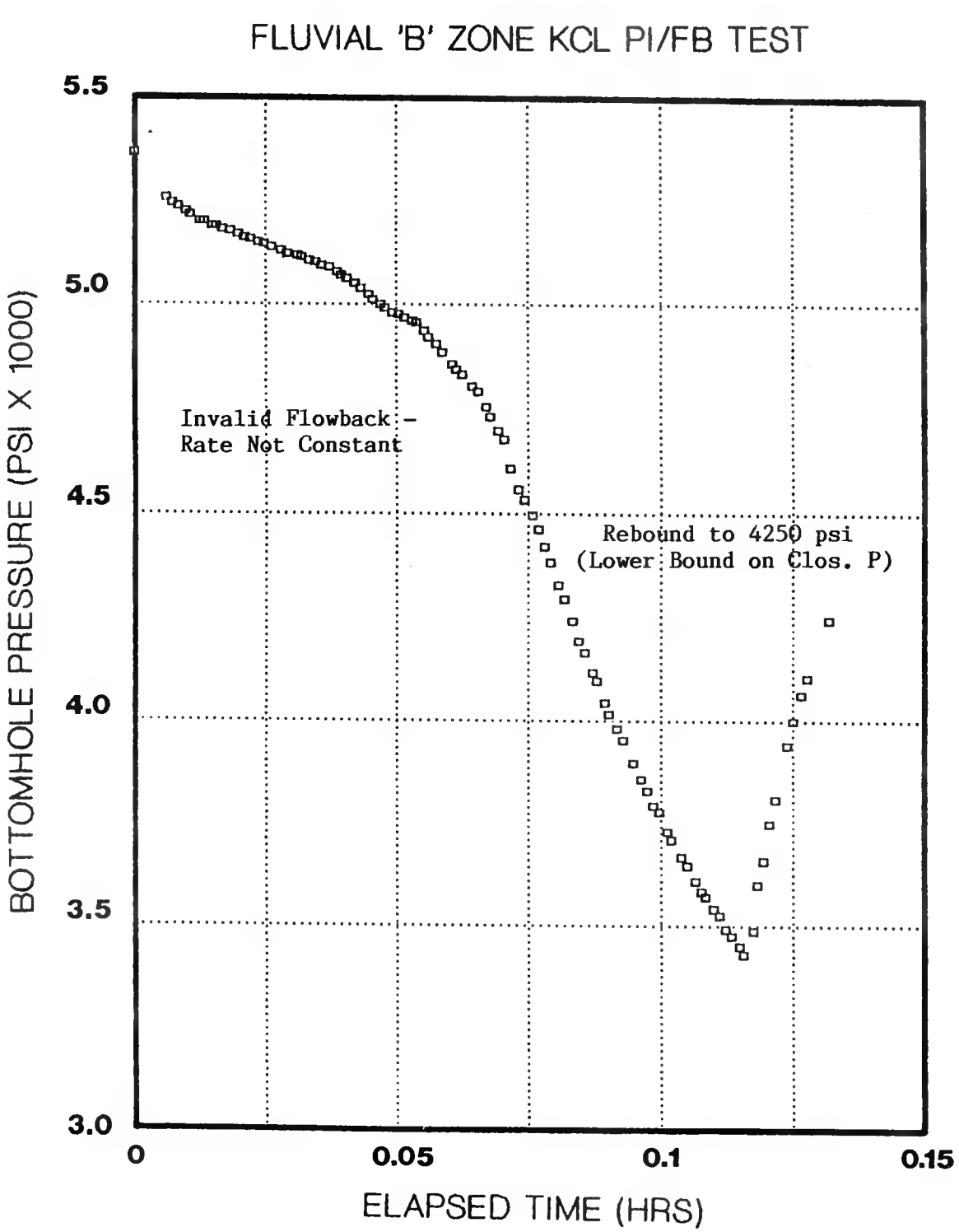


FIGURE 19: Fluvial "B" Sand KCL Pump-In/Flowback Test Decline.

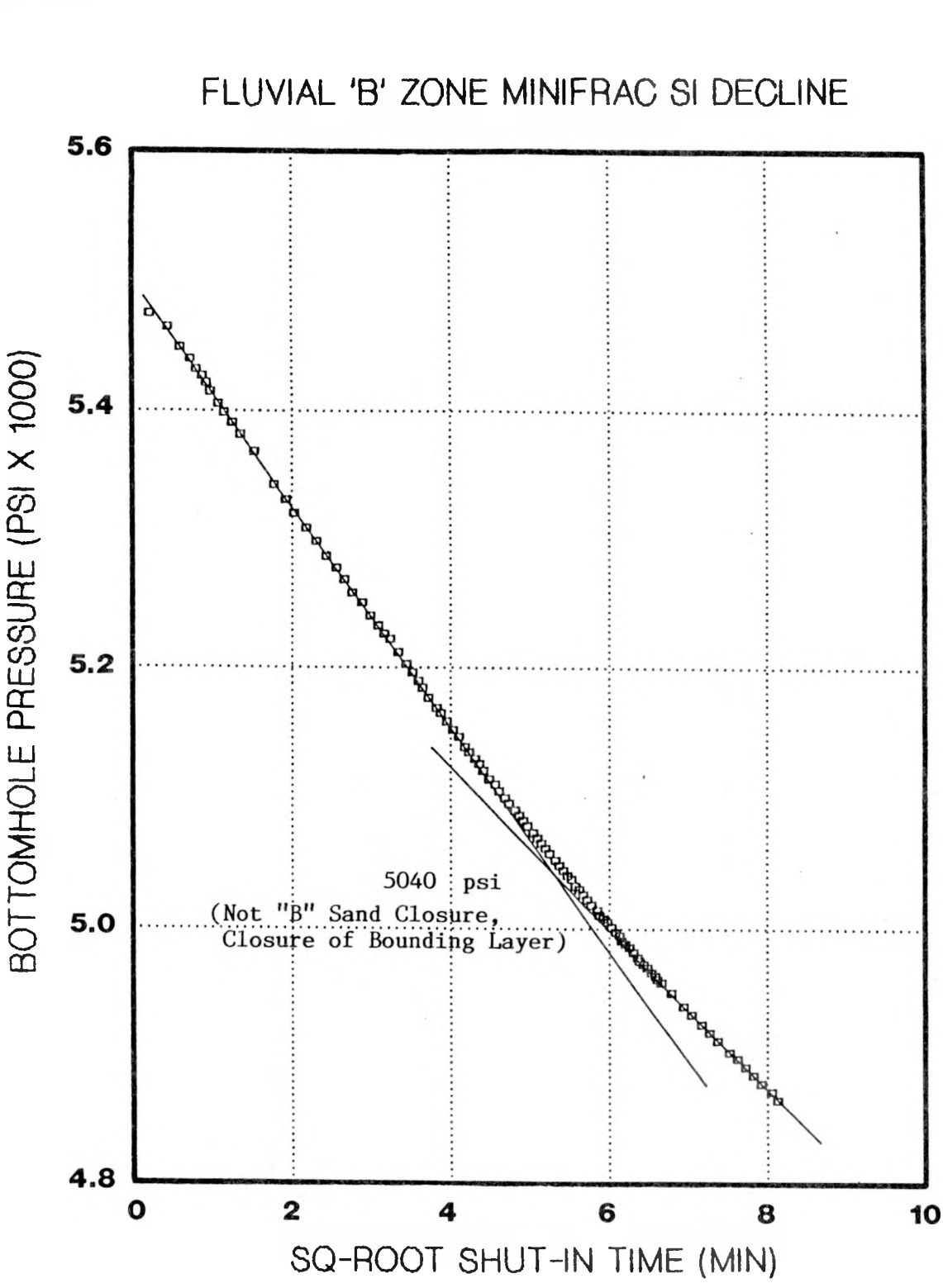


FIGURE 20: Fluvial "B" Sand Minifrac Shut-In Pressure Decline.

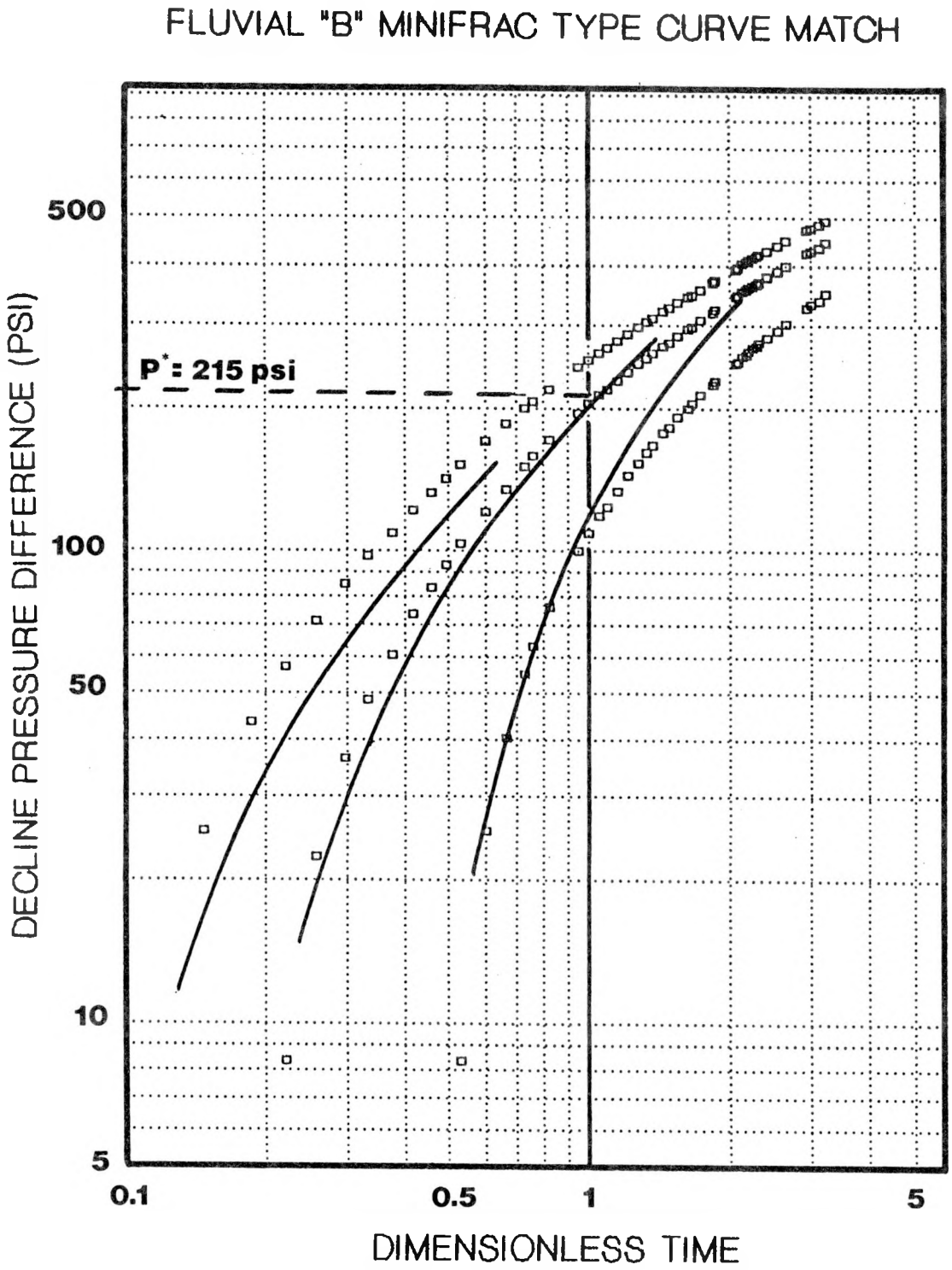


FIGURE 21: Fluvial "B" Sand Minifrac Pressure Decline Type-Curve Match.

TABLE NO. 5

WORKSHEET FOR PRESSURE DECLINE ANALYSIS - PERKINS & KERN GEOMETRY

Input Data:

Young's Modulus = E' =	5×10^6	psi	(Source - Sandia	)
Pump Time = t_p =	19	min	(Source - Minifrac Data	)
Volume Pumped = V =	8,000	gal	(Source - Minifrac Data	)
ISIP =	5,540	psi	(Source - NSI	)
Closure Pressure = σ_c =	4,550	psi	(Source - NSI	)
Closure time = Δt_c =	173	min	(Source - NSI	)

Net $p = p_s$ = ISIP - Closure Pressure = 990 psi

Match p = P* (from Type Curves) = 215 psi

Geometry Parameters:

$g_o = 1.45$, $g_c = 1.00$, $\beta' = 0.75$, $K = 1.00$, $h_p = 25'$, $h = 40'$, $r_p = 0.625$

EFFICIENCY ANALYSIS

from time-to-close and graph

efficiency = e_f = 0.78

* from pressures

* $\rho = \pi\, p_s / 4\, K\, g_o\, P^* = 2.494$

* $e_f = \rho / (1 + \rho) = 0.71$

use efficiency e_f =

LEAK-OFF COEFFICIENT

Leak-Off Coefficient (ft/min**0.5) = $C = P^* \beta'\ h / r_p\ t_p^{**0.5}\ E'$; $r_p = h_p/h$

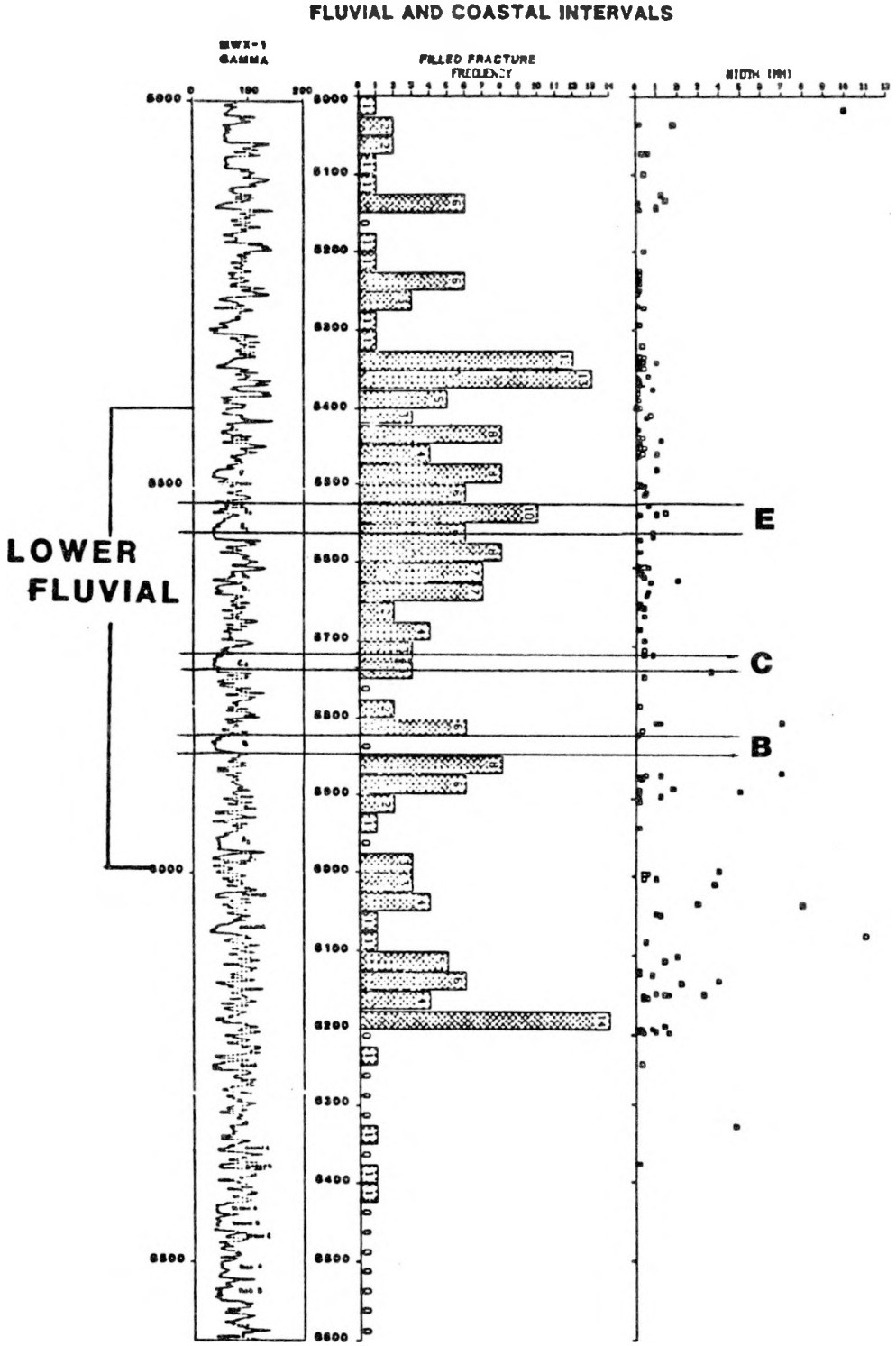
$C = [(215)(0.75)(40)]/[(0.625)(4.36)(5 \times 10^6)]$

$C = 0.00047$ ft/ min

h	r_p	C
40'	0.625	0.00047
60'	0.417	0.0011
80'	0.313	0.0019

FIGURE 22

CORE FRACTURE FREQUENCY AND WIDTH DISTRIBUTION WITH RESPECT TO DEPTH IN MWX-1



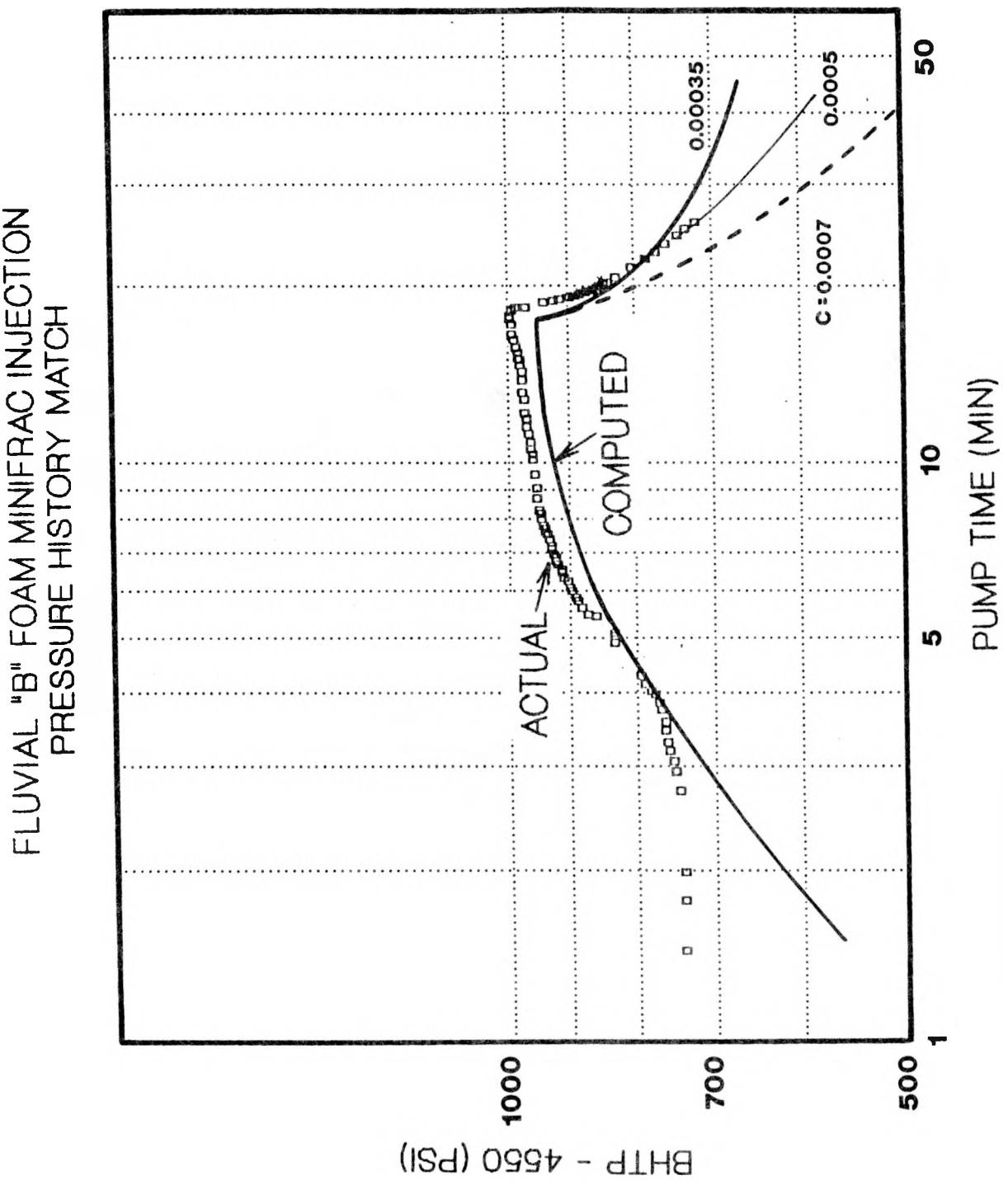


FIGURE 23: Fluvial "B" Sand Foam Minifrac Injection/Decline Pressure History Match.

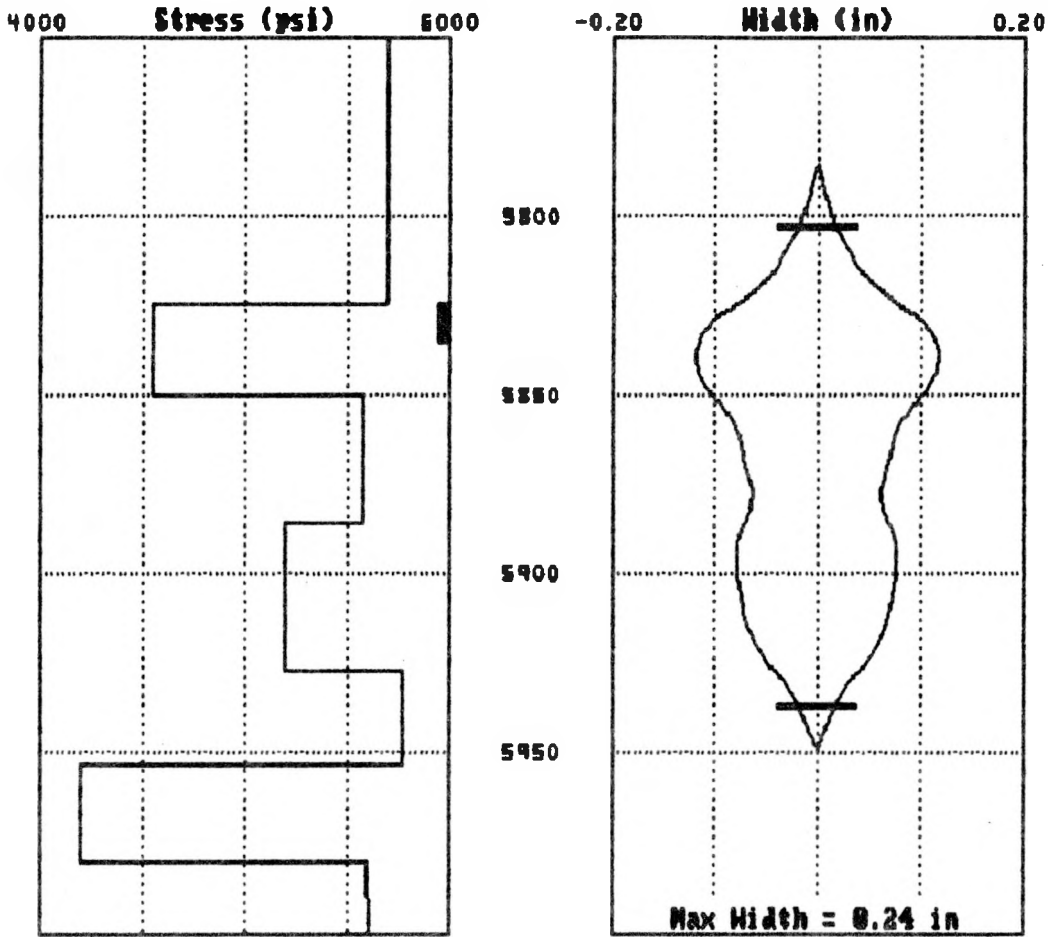


FIGURE 24: Simulator Predicted Gross Fracture Height at Wellbore for Fluvial "B" Sand Foam Minifrac.

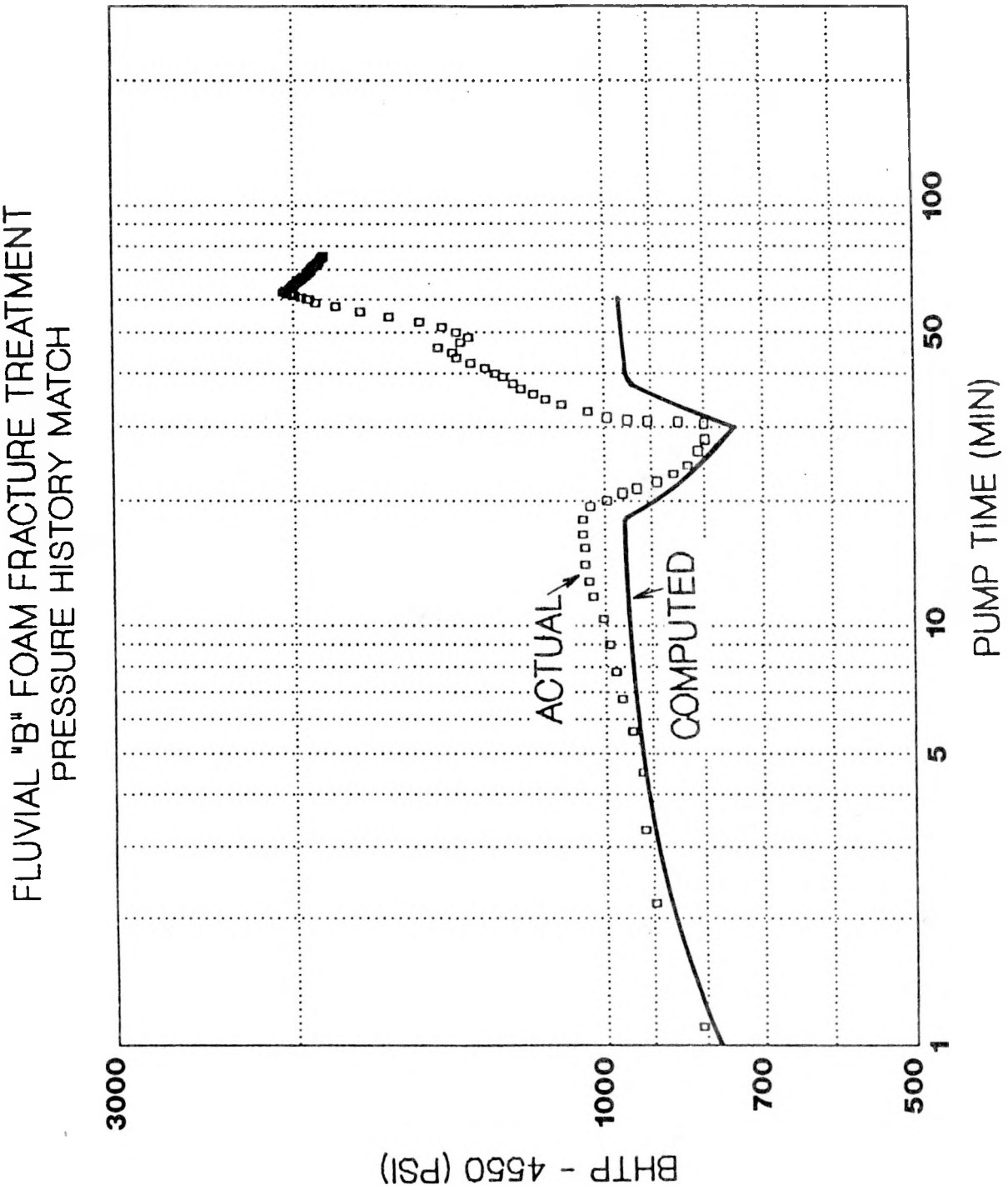


FIGURE 25: Pressure History Match of Fluvial "B" Foam Fracture Treatment Using Same Input Parameters Used to History Match the Minifrac.

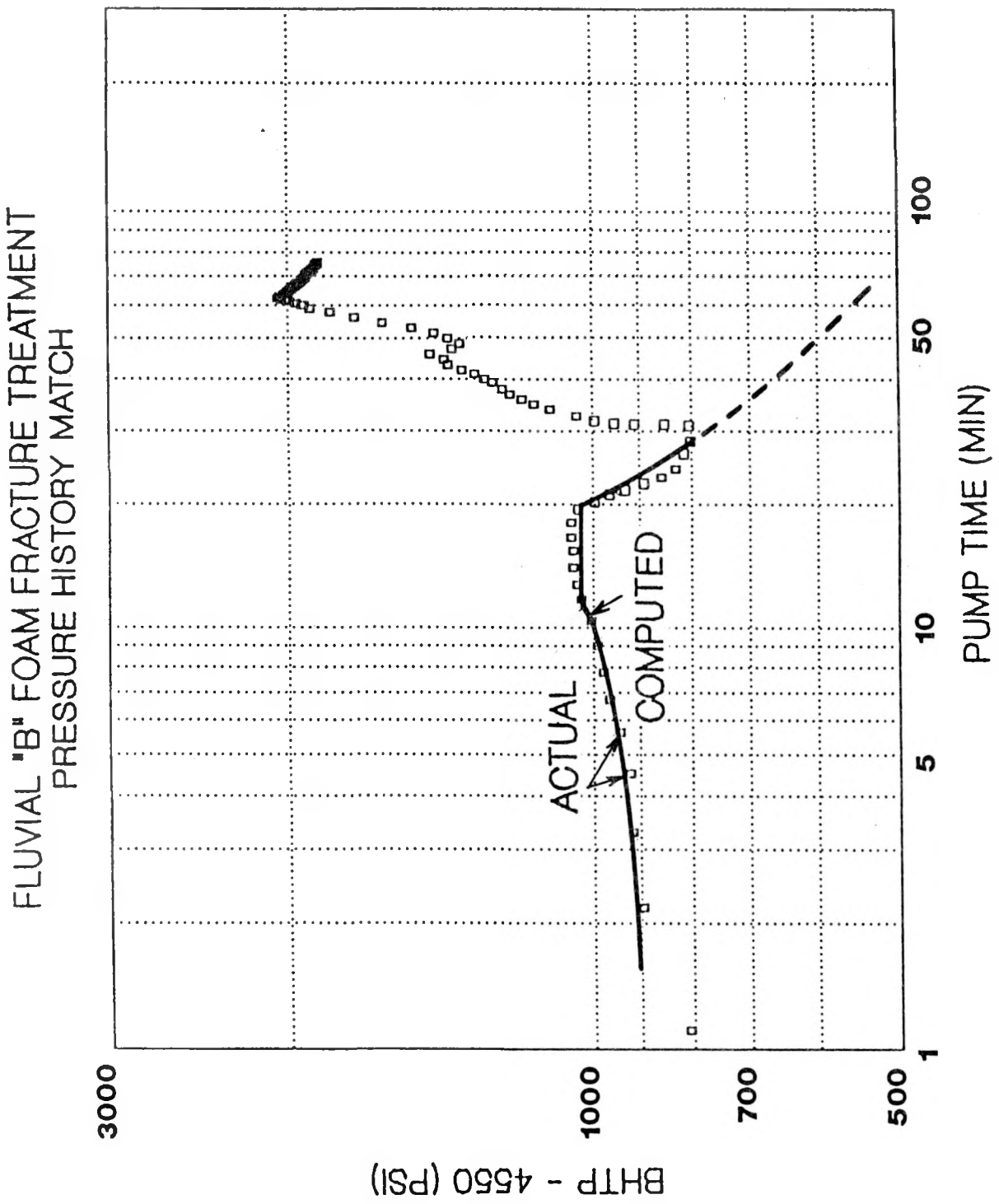


FIGURE 26: Pressure History Match of Fluvial "B" Foam Fracture Treatment With Increased Boundary Stress, Constant Pressure Mode, and Extended Mid-Treatment Shut-In Decline.

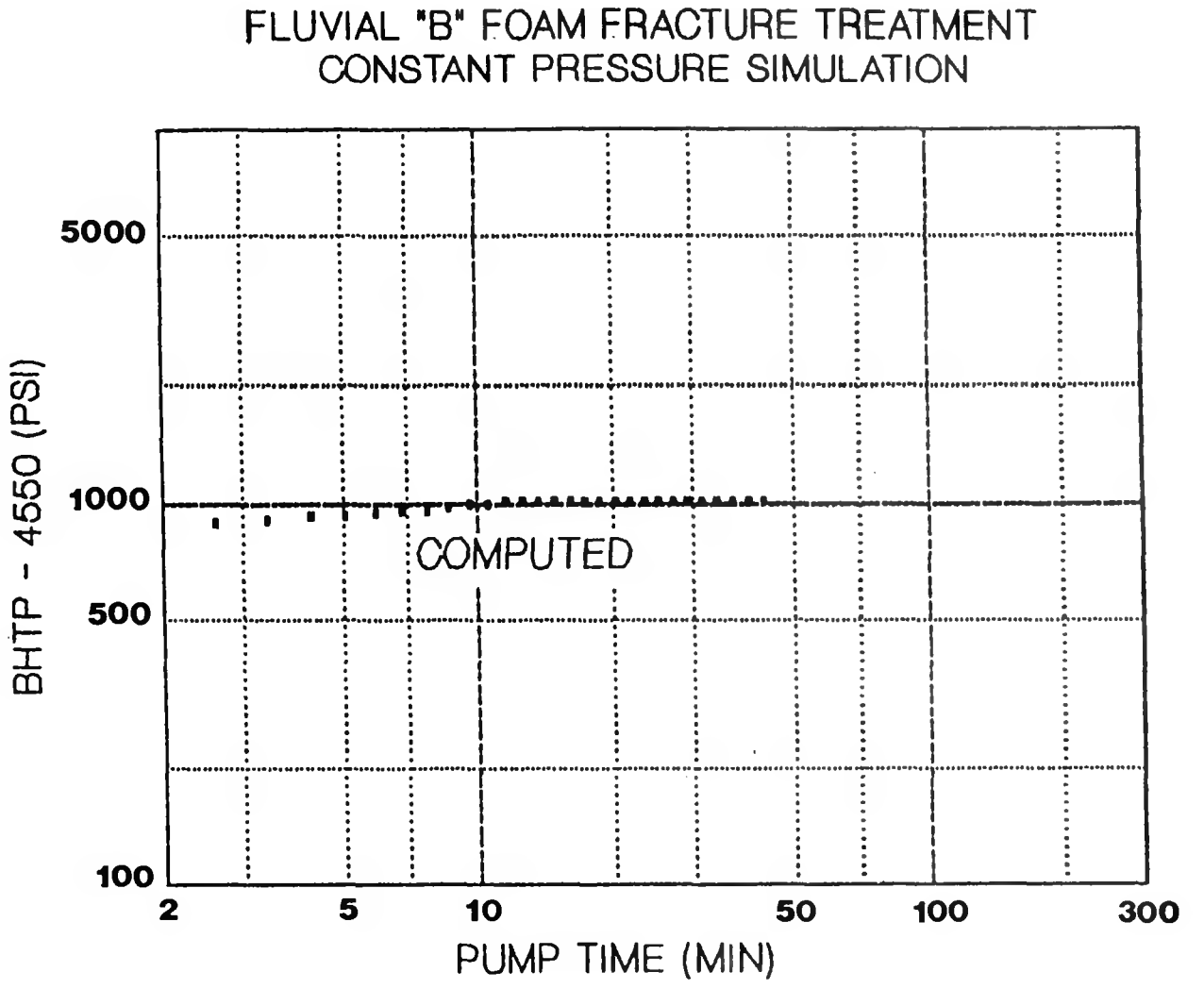


FIGURE 27: Simulation of Extended Constant Pressure Mode for Fluvial "B" Foam Fracture Treatment to Evaluate Excess Leak-Off as Reason for Abnormal Pressure Increase.

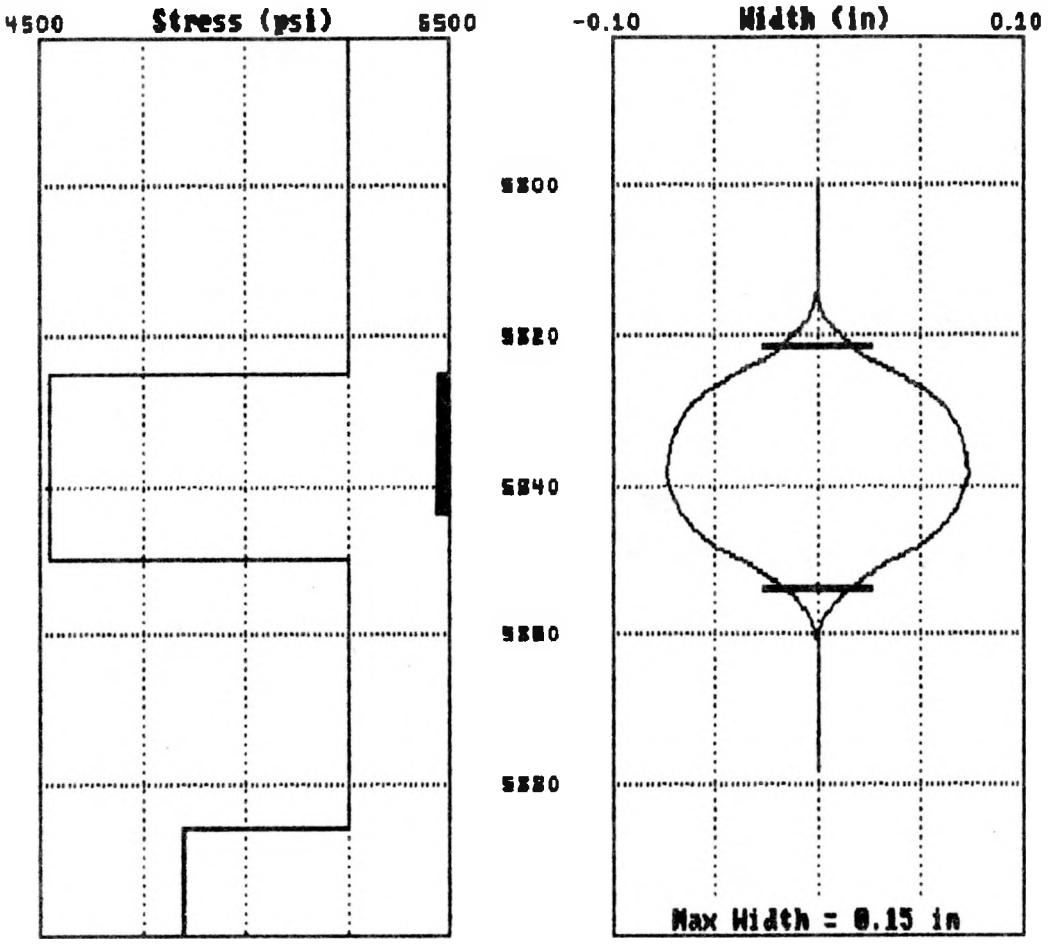
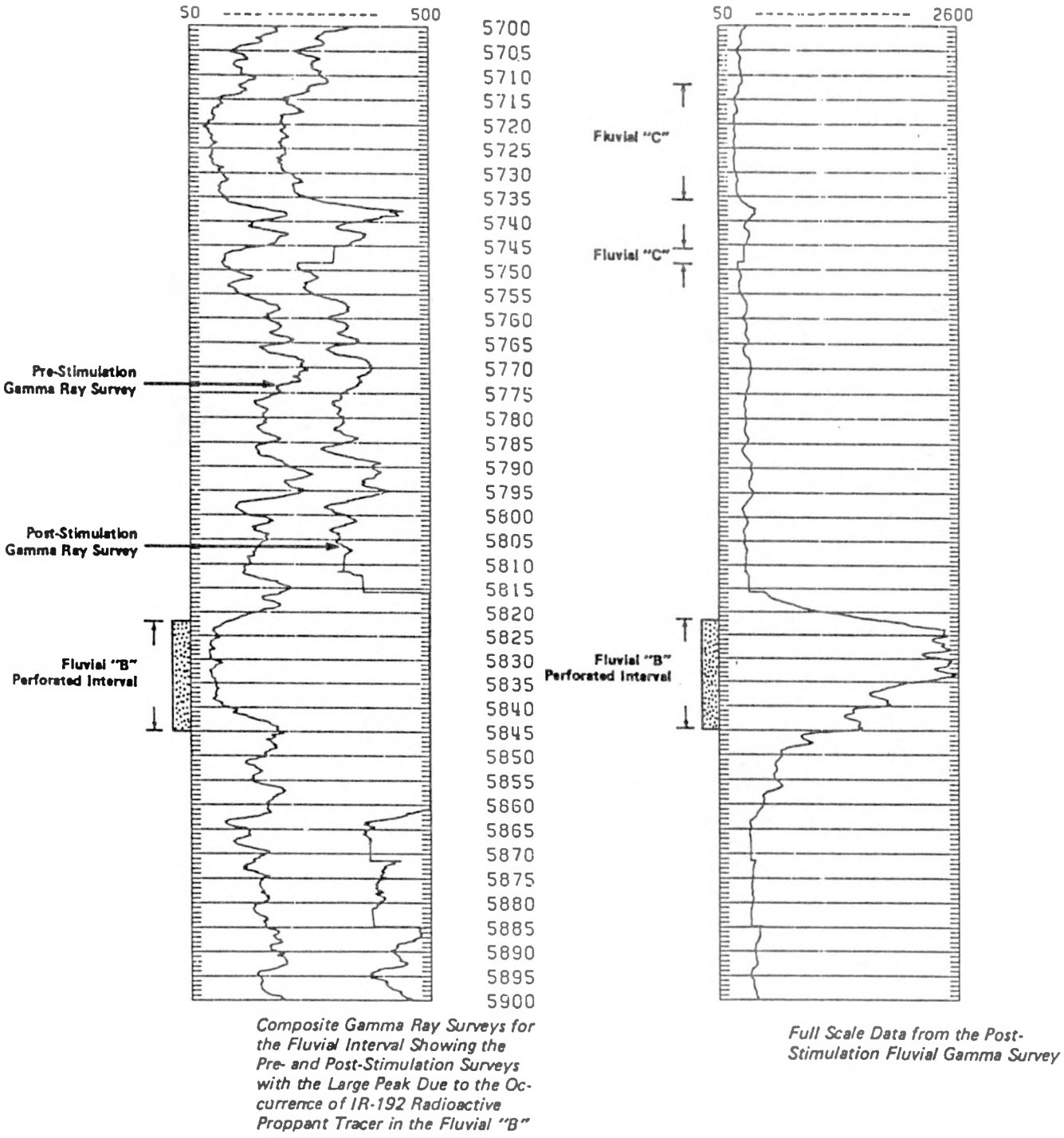


FIGURE 28: Simulator Predicted Gross Fracture Height at Wellbore for Fluvial "B" Foam Fracture Treatment at the Time of the Mid-Treatment Shut-Down.



Composite Gamma Ray Surveys for the Fluvial Interval Showing the Pre- and Post-Stimulation Surveys with the Large Peak Due to the Occurrence of IR-192 Radioactive Proppant Tracer in the Fluvial "B"

Full Scale Data from the Post-Stimulation Fluvial Gamma Survey

FIGURE 29: Post-Frac Gamma-Ray Log for Fluvial "B" Foam Fracture Treatment.

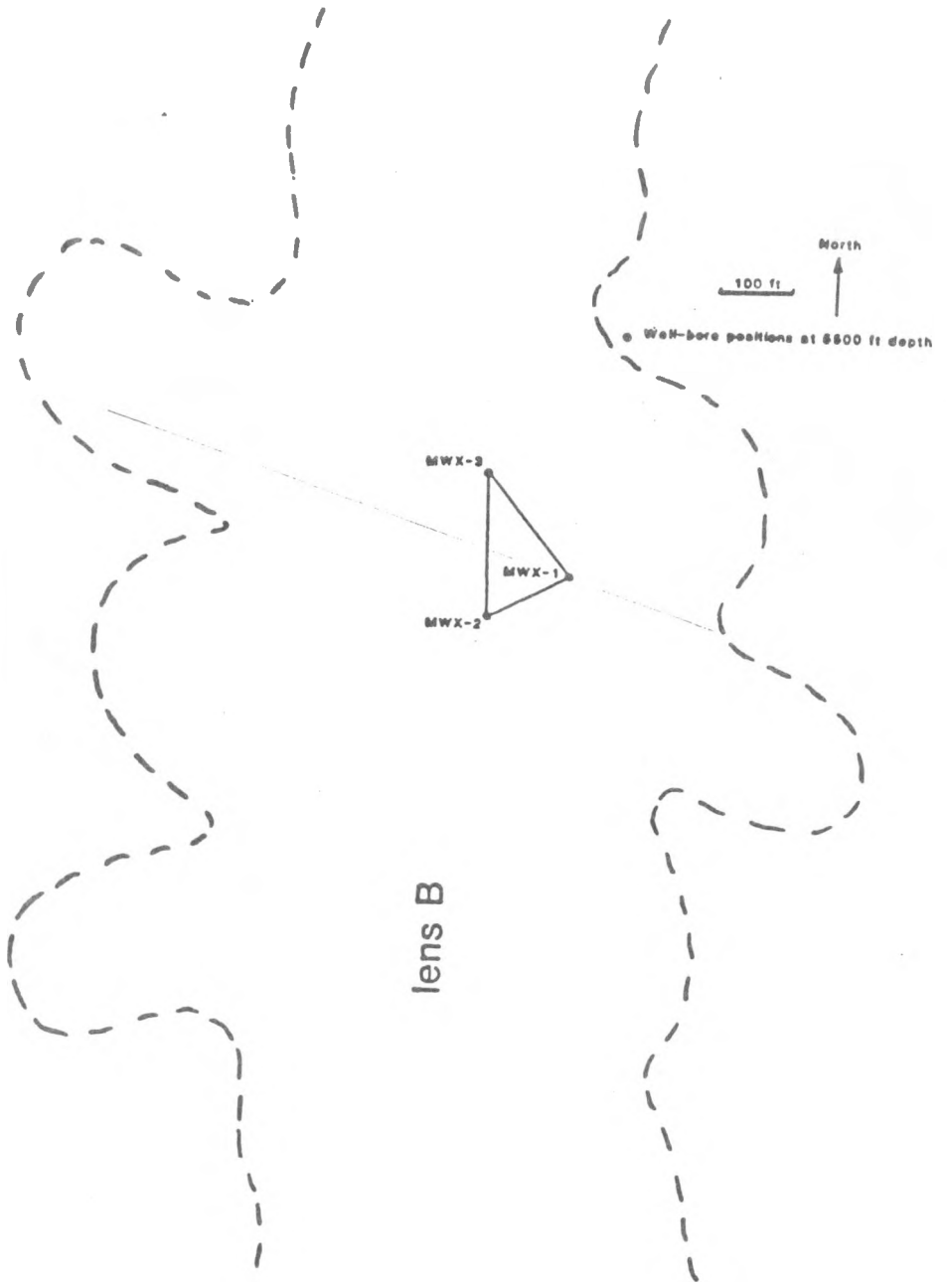


FIGURE 30: Estimated Lens Size/Orientation for the Fluvial "B" Sand.

TABLE NO.6

Results of Fluvial "C" Closure Stress Tests

Test	Frac Ext. P (psi)	Closure P (psi)
PI/SI	-	4517
SRT/FB-1	5052	4708
PI/FB-2	-	4706
PI/FB-3	-	4766
PI/FB-4	-	4488
MF/SI-1	-	-
MF/SI-2	-	4718

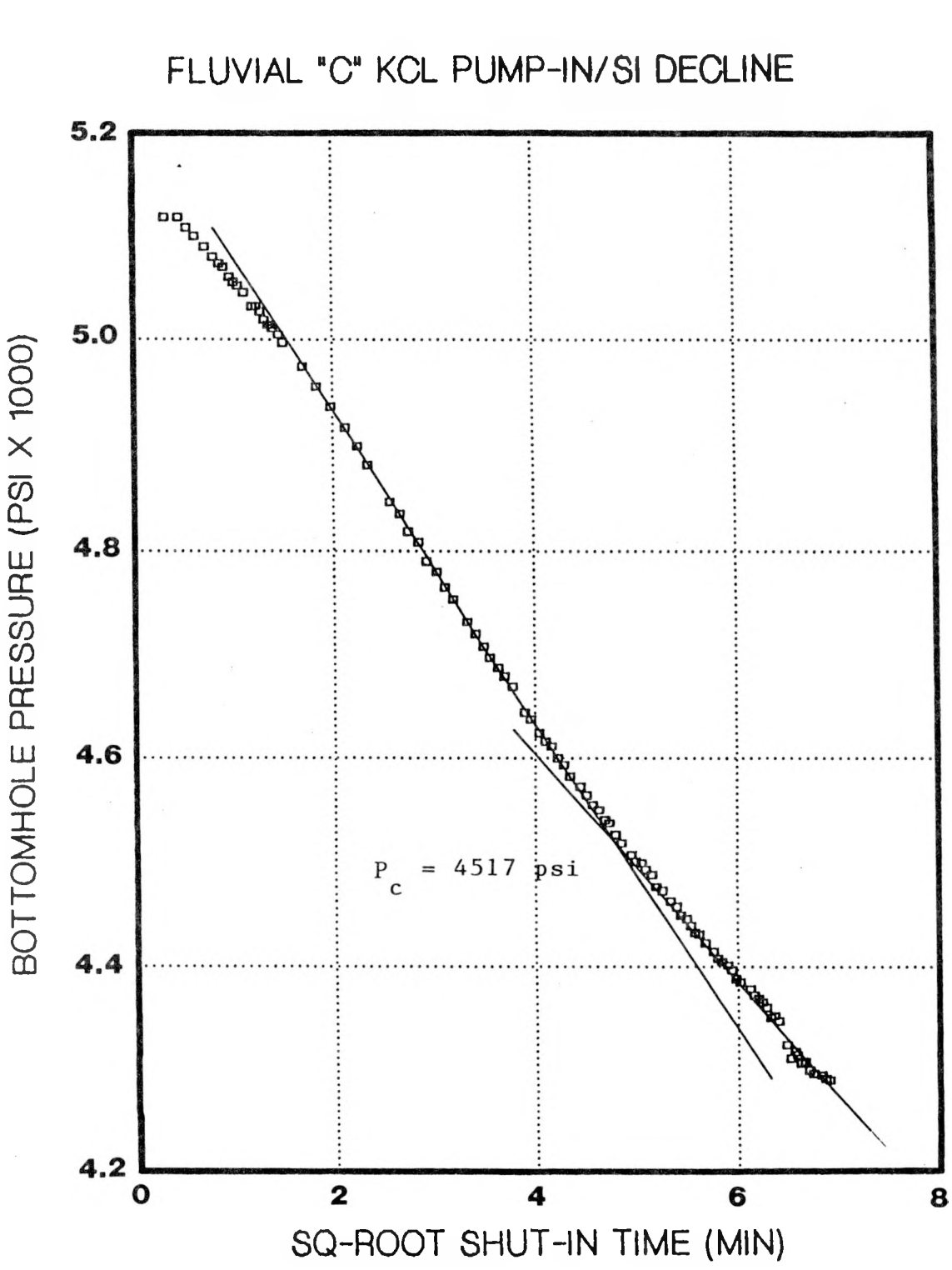


FIGURE 31: Fluvial "C" Sand KCl Pump-In/ Shut-In Test Pressure Decline.

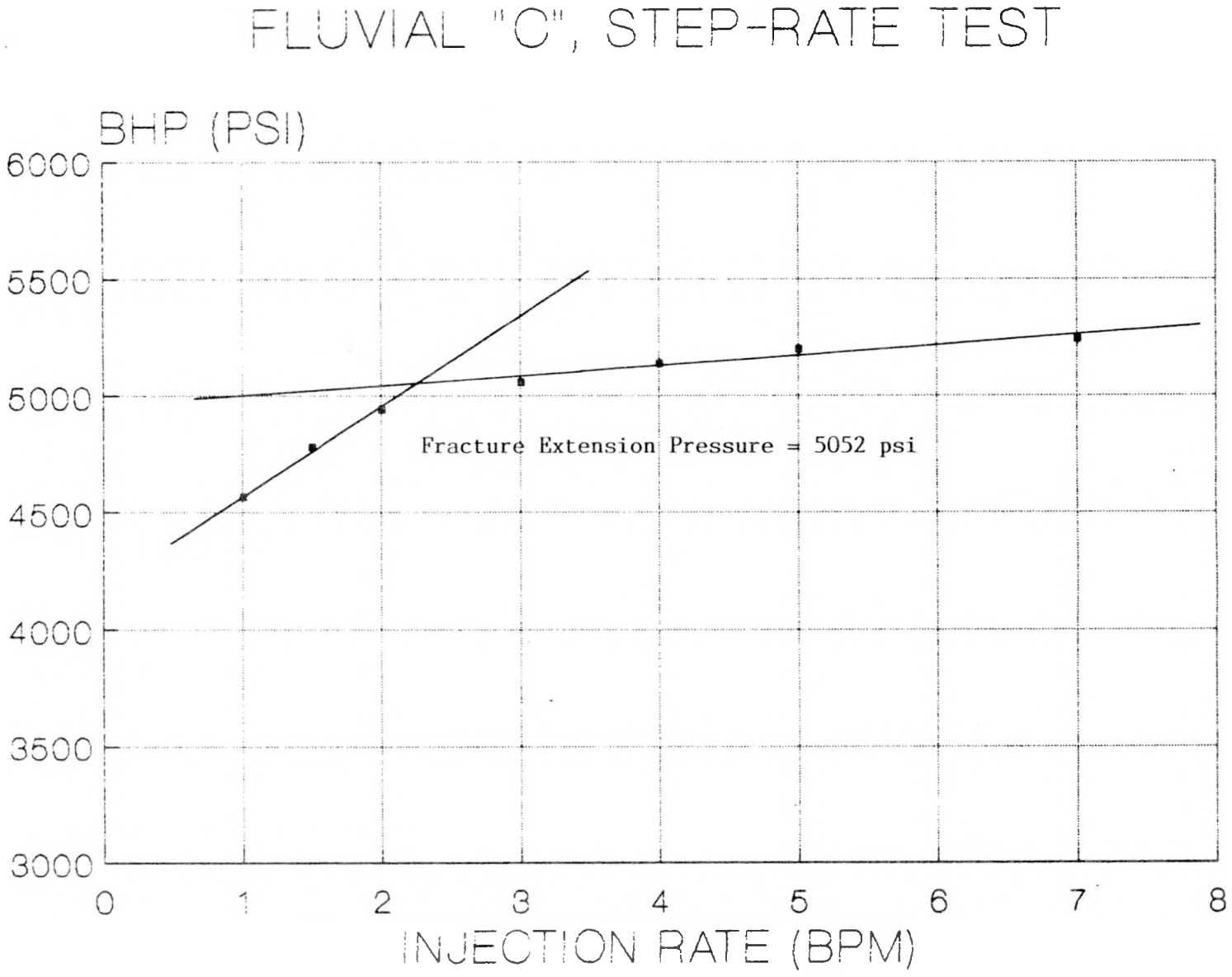


FIGURE 32: Fluvial "C" Sand KCl Step-Rate Test Injection.

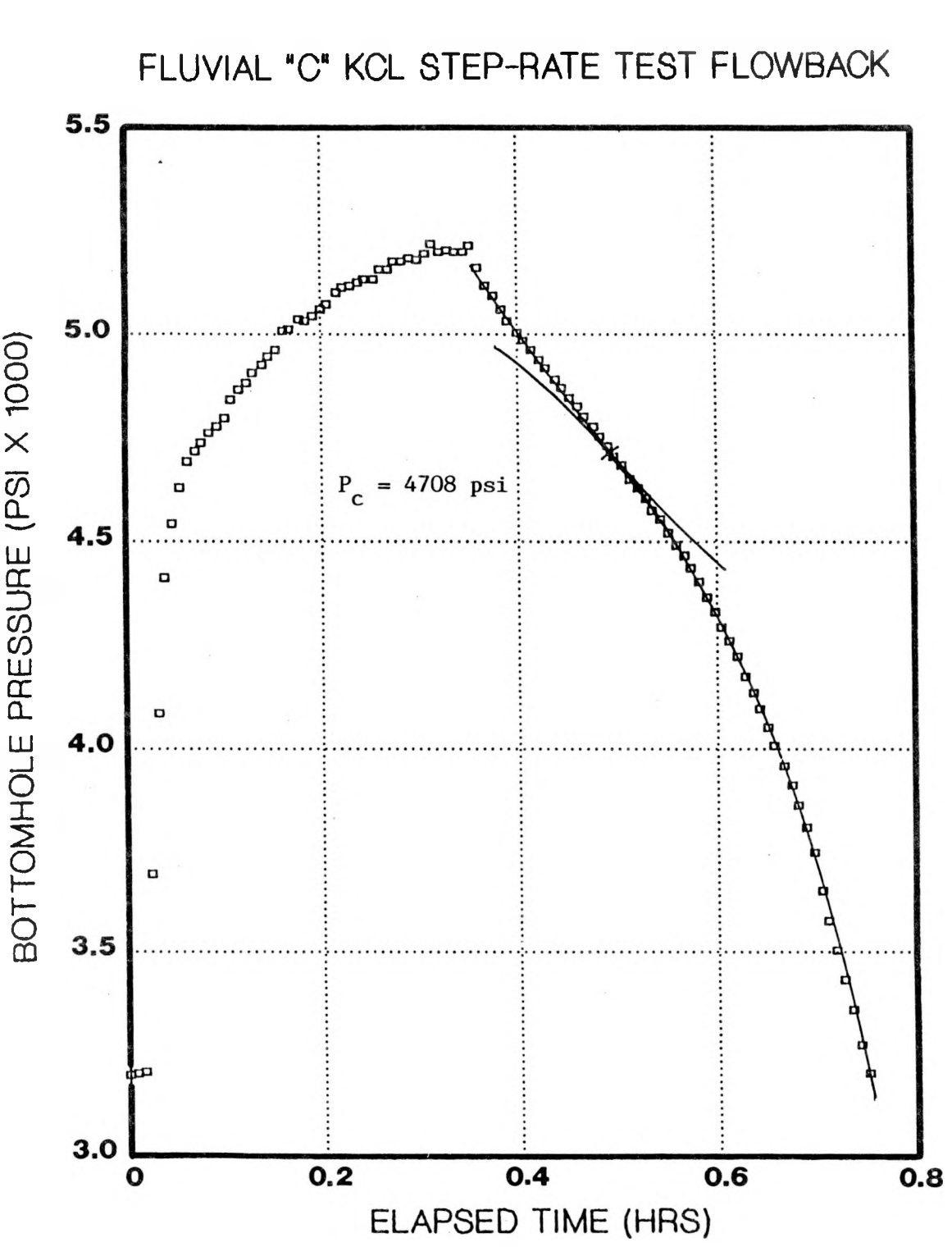


FIGURE 33: Fluvial "C" Sand KCl Step-Rate Test/Flowback.

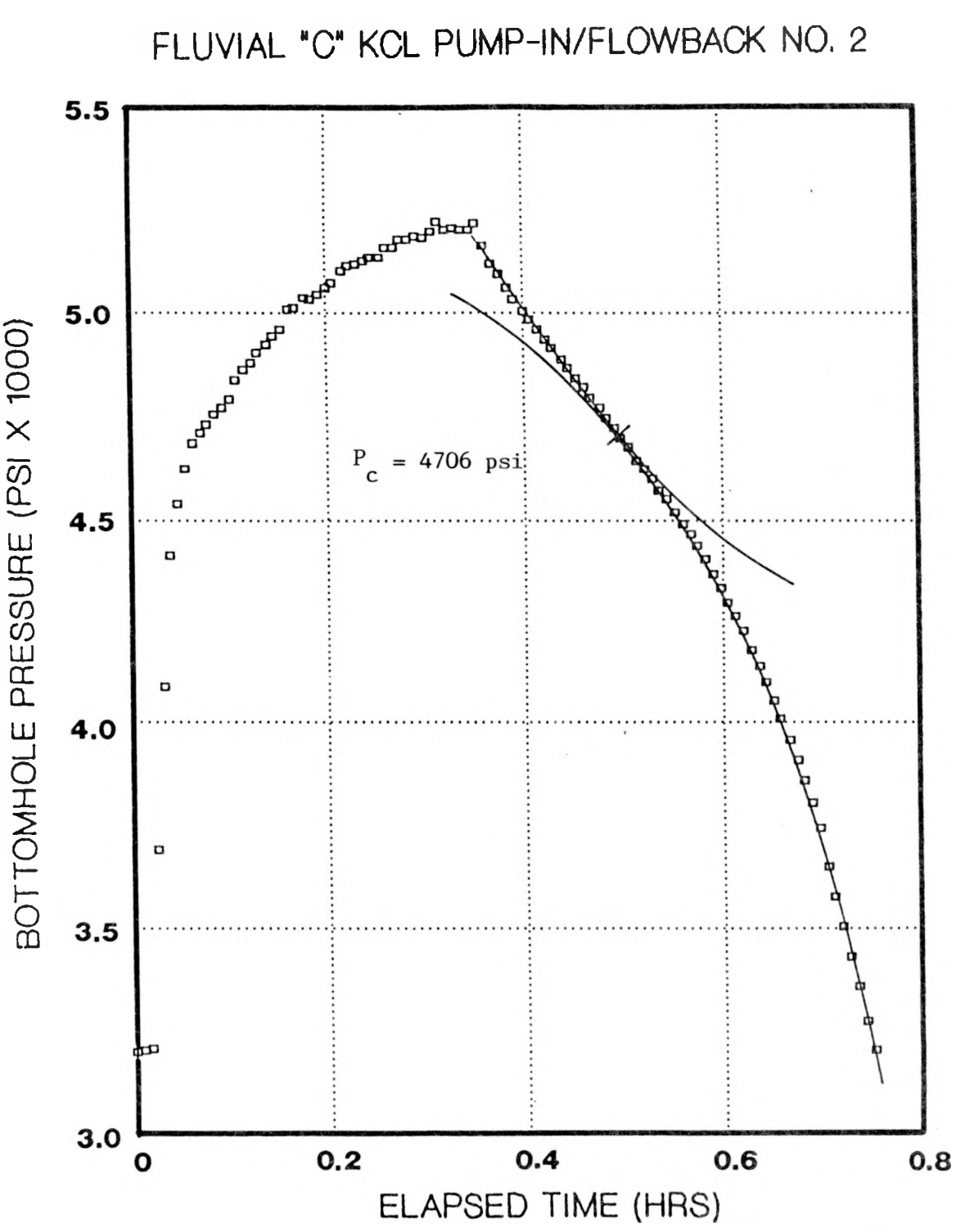


FIGURE 34: Fluvial "C" Sand KCl Pump-In/Flowback Test No. 2.

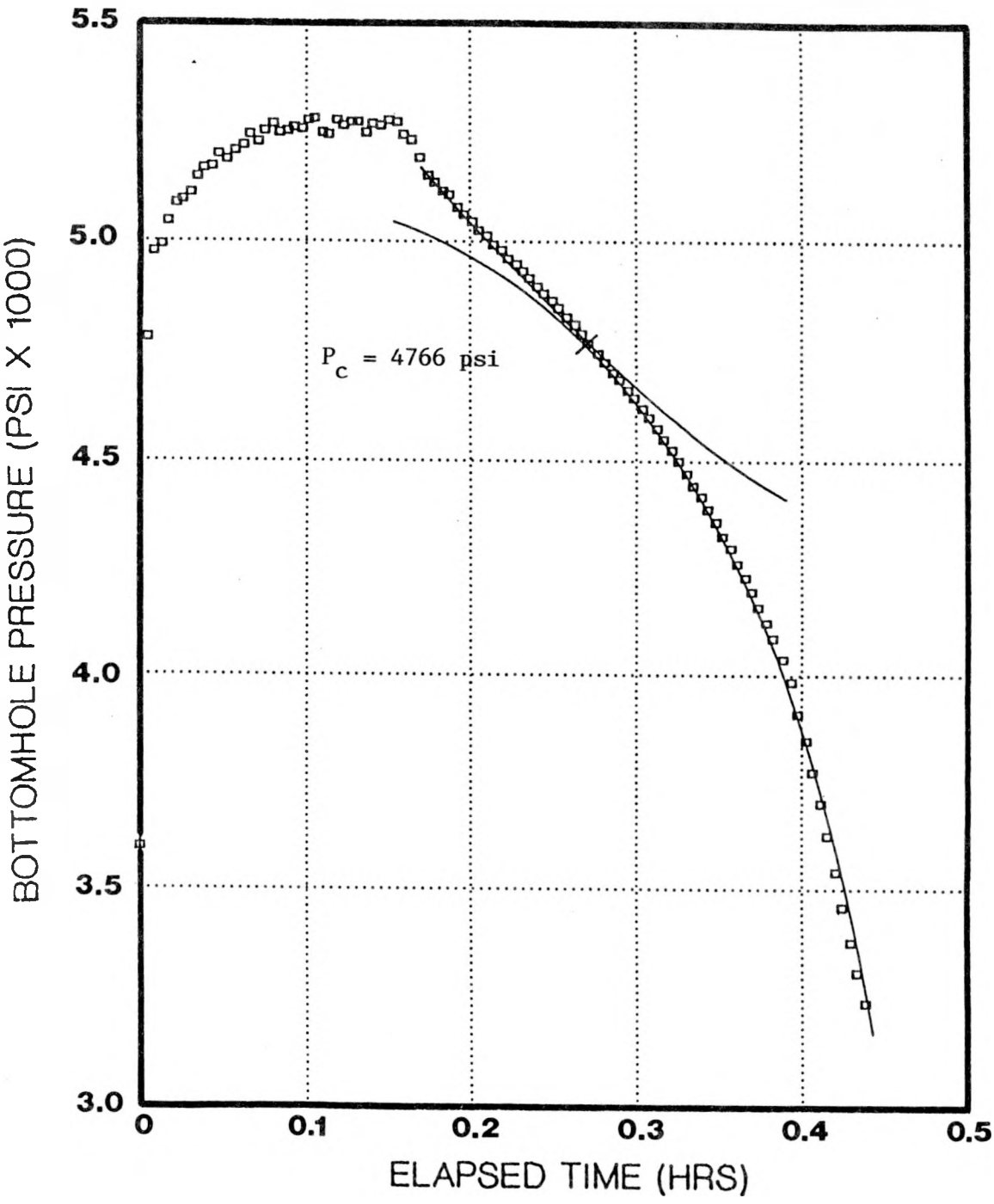


FIGURE 35: Fluvial "C" Sand KCl Pump-In/Flowback Test No. 3.

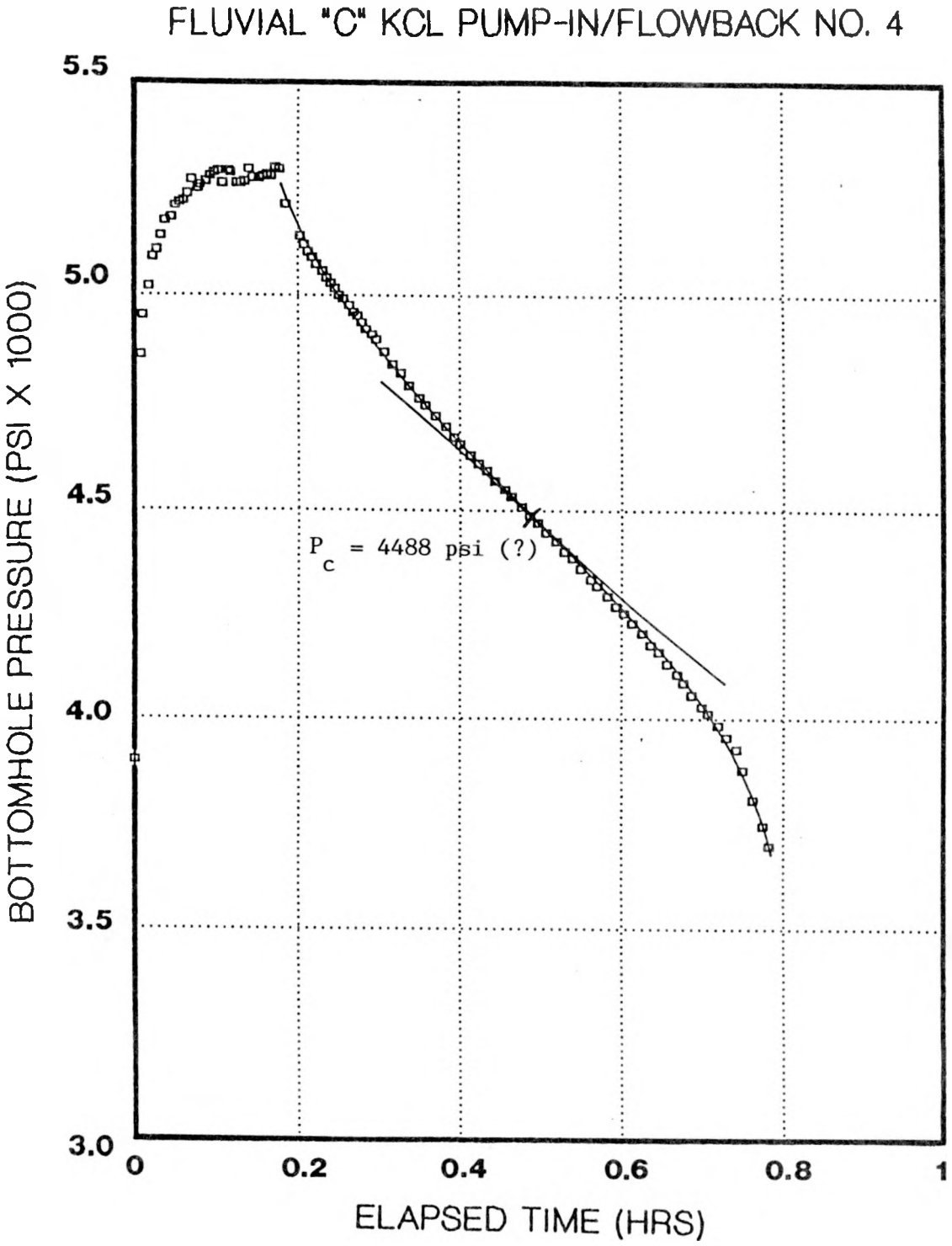


FIGURE 36: Fluvial "C" Sand KCl Pump-In/Flowback Test No. 4.

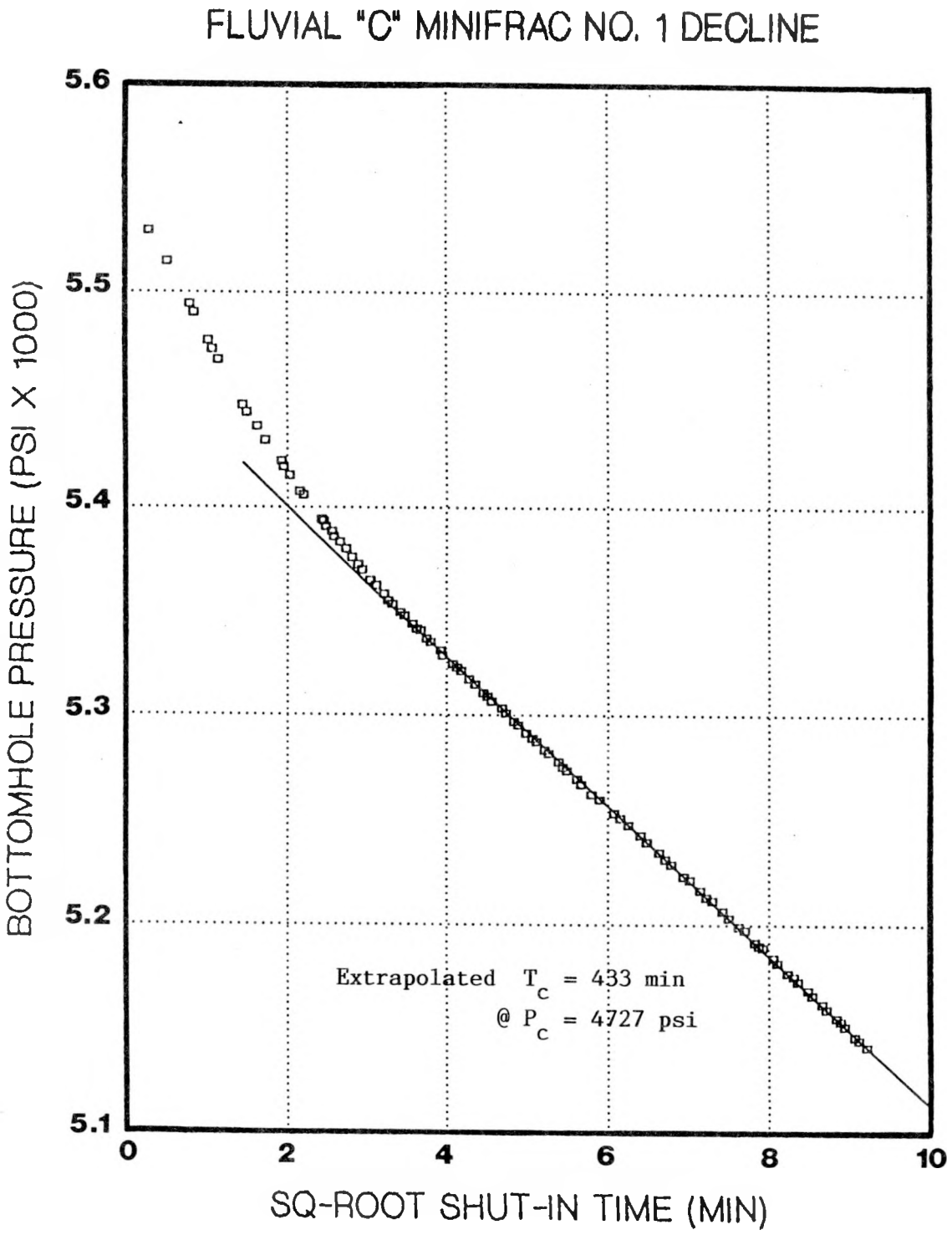


FIGURE 37: Fluvial "C" Sand Foam Minifrac No. 1 Pressure Decline (Without 100 Mesh Sand).

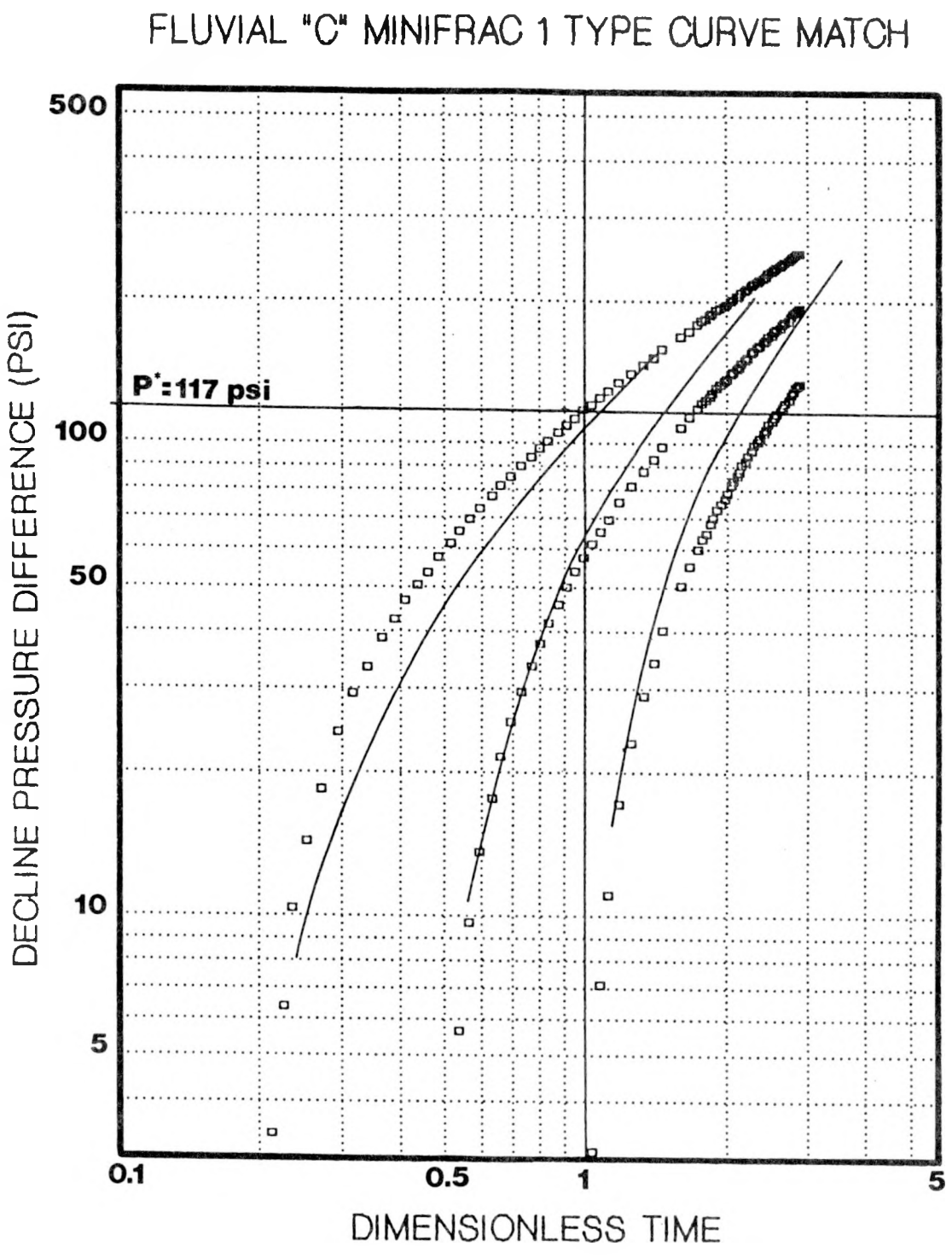


FIGURE 38: Fluvial "C" Sand Foam Minifrac No. 1 Pressure Decline Type Curve Match, Without 100 Mesh Sand.

TABLE NO. 7

WORKSHEET FOR PRESSURE DECLINE ANALYSIS - PERKINS & KERN GEOMETRY

Input Data:

Young's Modulus = E' =	4×10^6	psi	(Source - Sandia	)
Pump Time = t_p =	29.4	min	(Source - Minifrac Data	)
Volume Pumped = V =	6,300	gal	(Source - Minifrac Data	)
ISIP =	5537	psi	(Source - NSI	)
Closure Pressure = σ_c =	4727	psi	(Source - NSI	)
Closure time = Δt_c =	241	min	(Source - NSI	)

Net p = p_s = ISIP - Closure Pressure = 810 psi

Match p = P* (from Type Curves) = 117 psi

Geometry Parameters:

$g_o = 1.45$, $g_c = 1.00$, $\beta' = 0.7$, $K = 1.00$

EFFICIENCY ANALYSIS

from time-to-close and graph

efficiency = $e_f = 0.$

$t_c/t_o = 241/29.4 = 8.2$

$e_f = 0.77$

* from pressures

* $\rho = \pi\, p_s/4\, K\, g_o\, P^* = 3.75$

* $e_f = \rho / (1 + \rho) = 0.79$

use efficiency e_f =

LEAK-OFF COEFFICIENT

Leak-Off Coefficient (ft/min**0.5) = $C = P^* \beta'\ h / r_p\, t_p^{**0.5}\, E'$; $r_p = h_p/h = 22/50 = 0.44$

$r_p = 22/75 = 0.29$

$c = [(117)(0.7)(50)]/[(0.44)(5.42)(4 \times 10^6)]$

$c = 0.00043$ ft/$\sqrt{\text{min}}$ (h = 50')

$c = 0.001$ ft/$\sqrt{\text{min}}$ (h = 75')

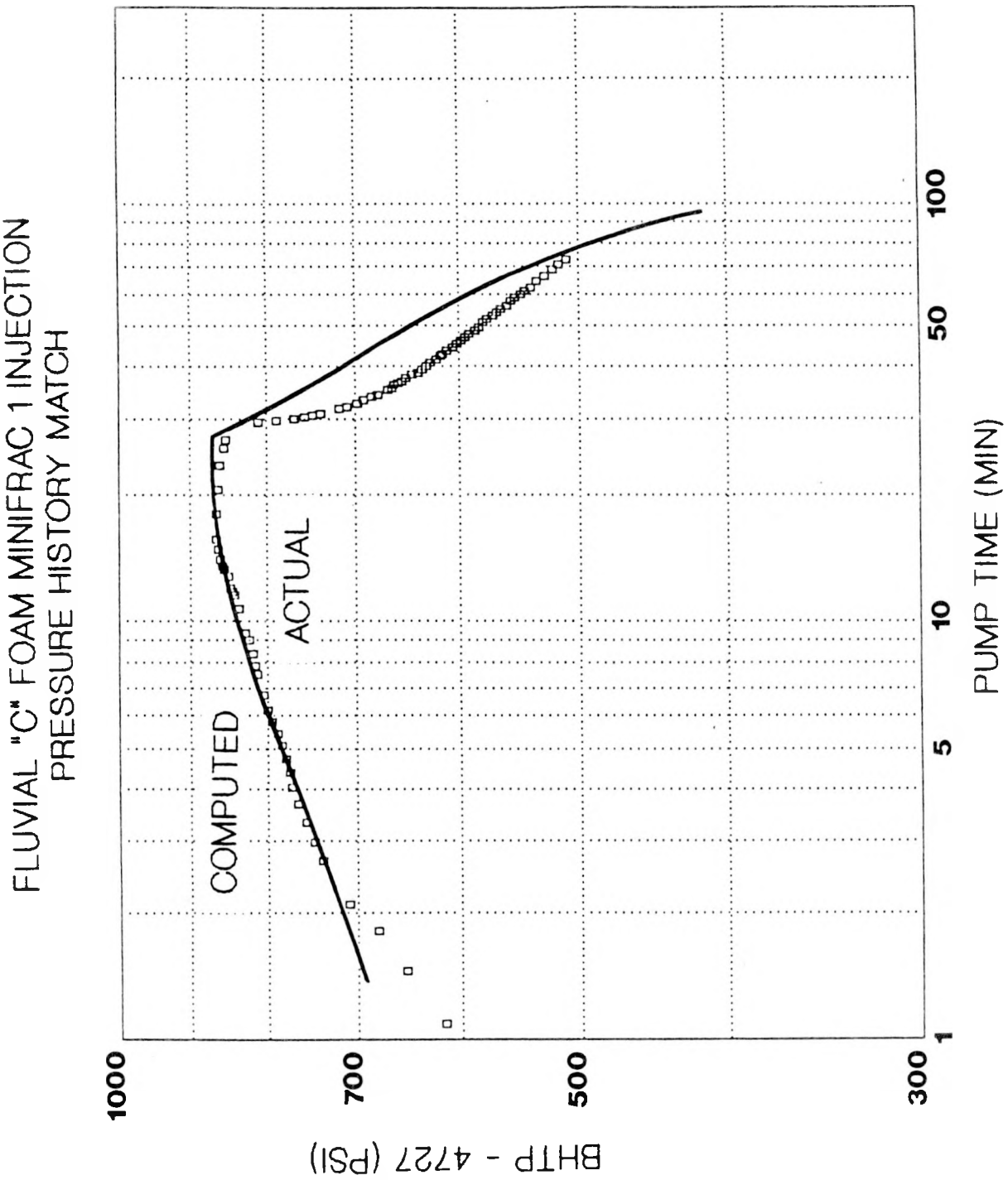


FIGURE 39: Pressure History Match of Fluvial "C" Foam Minifrac No. 1 Without Constant Pressure Mode.

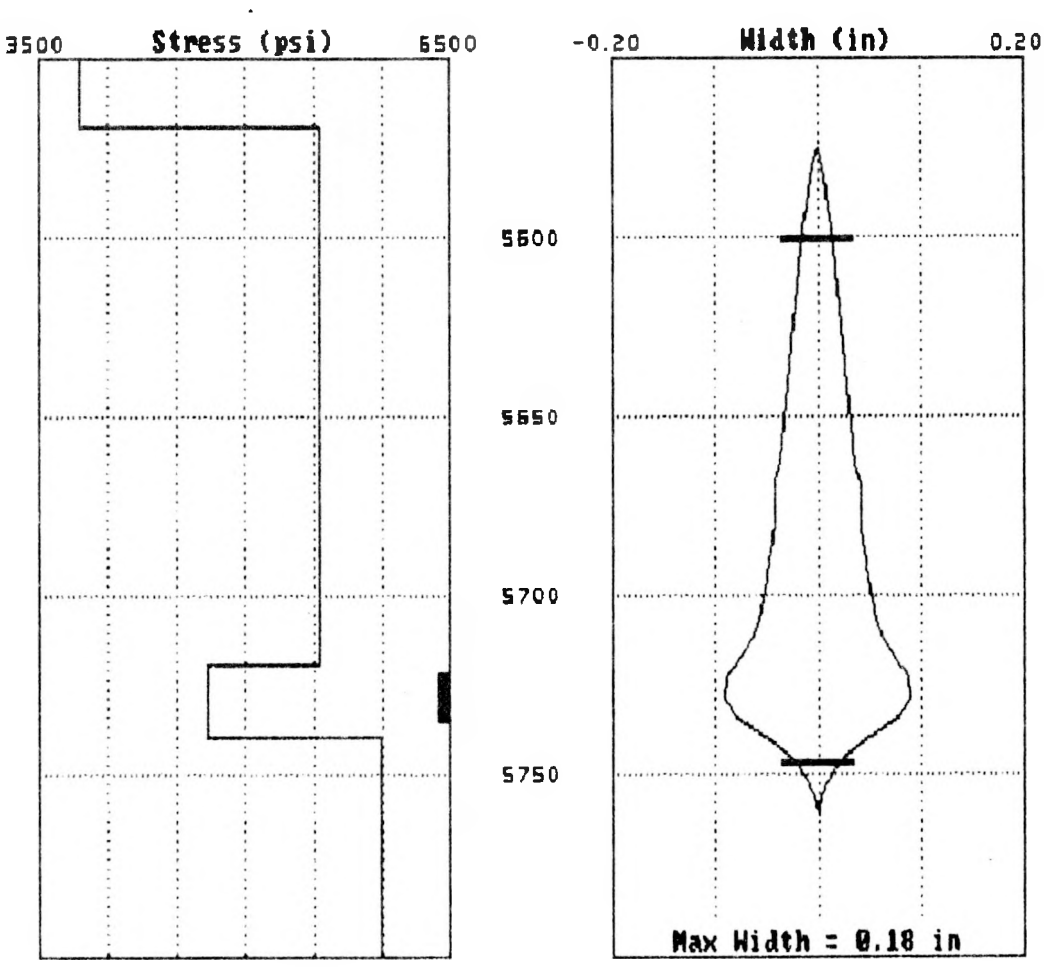


FIGURE 40: Simulator Predicted Gross Fracture Height at Wellbore for Fluvial "C" Foam Minifrac No. 1 Without Constant Pressure Mode.

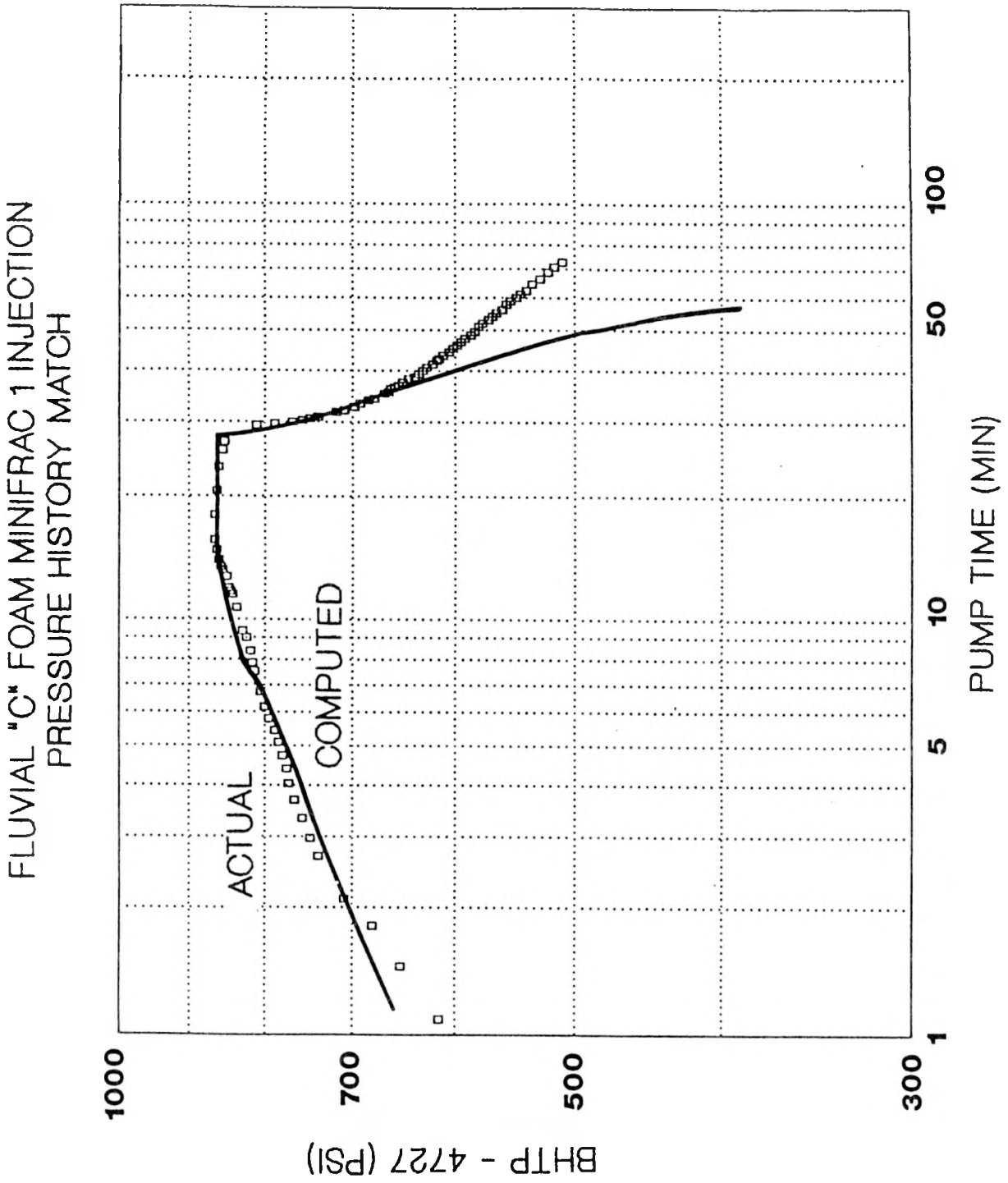


FIGURE 41: Pressure History Match of Fluvial "C" Foam Minifrac No. 1 With Constant Pressure Mode From About 15 Minutes to the End of Injection.

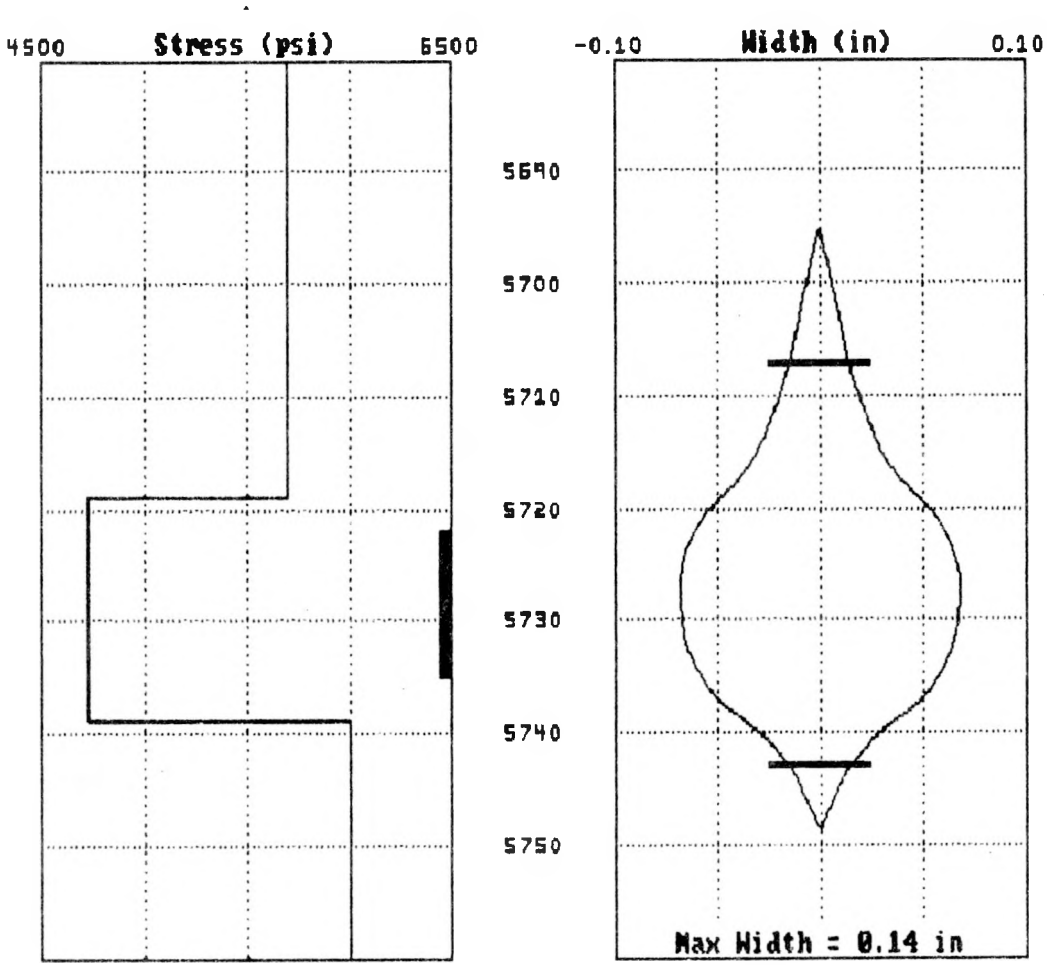


FIGURE 42: Simulator Predicted Gross Fracture Height at Wellbore for Fluvial "C" Foam Minifrac No. 1 With Constant Pressure Mode.

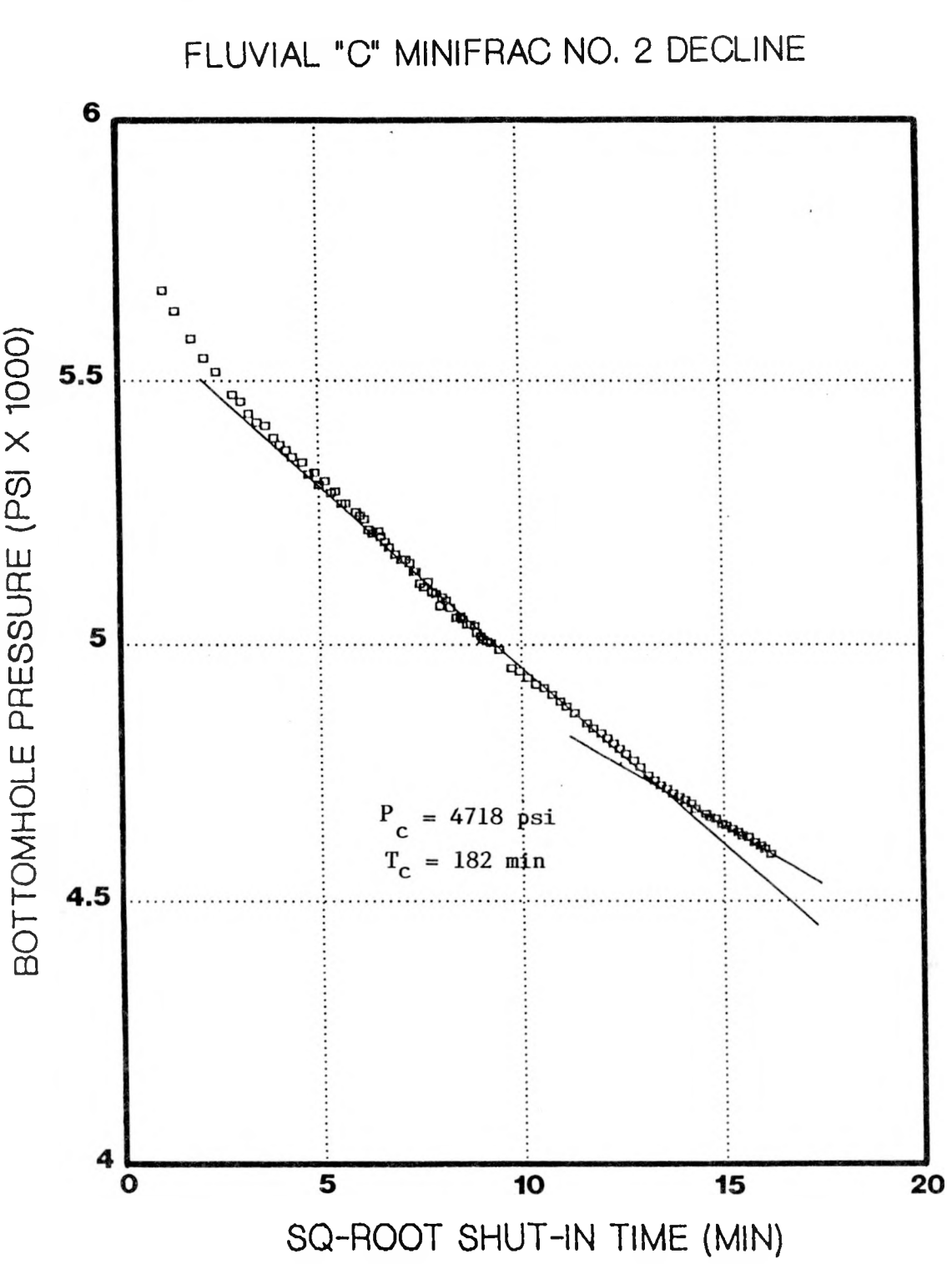


FIGURE 43: Fluvial "C" Sand Foam Minifrac No. 1 Pressure Decline (With 100 Mesh Sand).

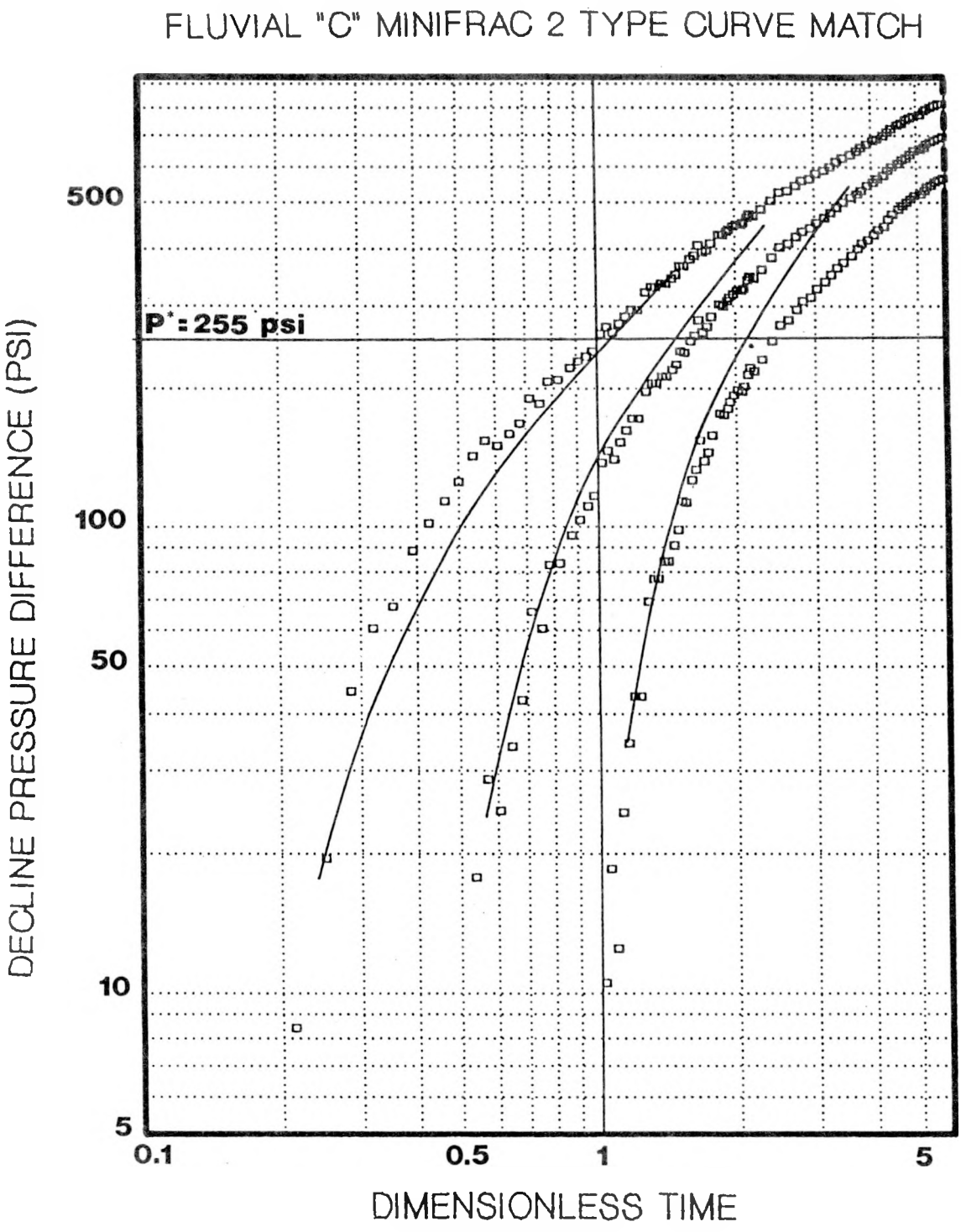


FIGURE 44: Fluvial "C" Sand Foam Minifrac No. 2 Pressure Decline Type Curve Match, With 100 Mesh Sand.

TABLE NO. 8

WORKSHEET FOR PRESSURE DECLINE ANALYSIS - PERKINS & KERN GEOMETRY

Input Data:

Young's Modulus = E' =	4×10^6	psi	(Source - Sandia	)
Pump Time = t_p =	37.9	min	(Source - Minifrac Data	)
Volume Pumped = V =	15,000	gal	(Source - Minifrac Data	)
ISIP =	5642	psi	(Source - NSI	)
Closure Pressure = σ_c =	4718	psi	(Source - NSI	)
Closure time = Δt_c =	182	min	(Source - NSI	)

Net p = p_s = ISIP - Closure Pressure = 924 psi

Match p = P* (from Type Curves) = 255 psi

Geometry Parameters:

$g_o = 1.45$, $g_c = 1.00$, $\beta' = 0.7$, $K = 1.00$

EFFICIENCY ANALYSIS

from time-to-close and graph

efficiency = $e_f = 0.$

$t_c/t_o = 4.8$

$e_f = 0.69$

* from pressures

* $\rho = \pi\, p_s/4\, K\, g_o\, P^* = 1.96$

* $e_f = \rho / (1 + \rho) = 0.66$

use efficiency e_f =

LEAK-OFF COEFFICIENT

Leak-Off Coefficient (ft/min**0.5) = $C = P^* \beta'\ h / r_p\ t_p^{**0.5}\ E'$; $r_p = h_p/h = 22/50 = 0.44$

$r_p = 22/75 = 0.29$

$c = [(255)(0.7)(50)]/[(0.44)(6.16)(4 \times 10^6)]$

$c = 0.00082$ ft/$\sqrt{\text{min}}$ (h = 50')

$c = 0.0019$ ft/$\sqrt{\text{min}}$ (h = 75')

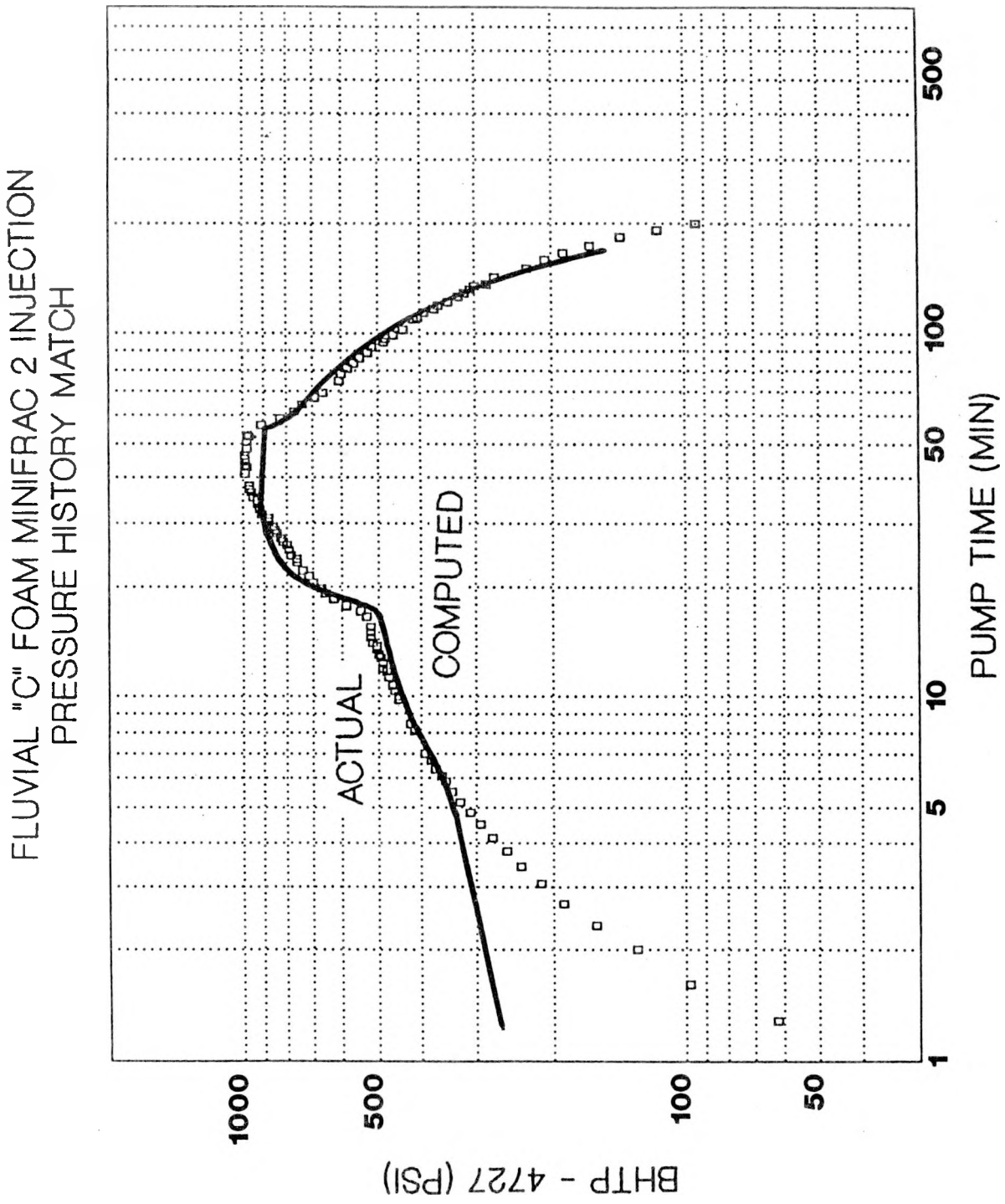


FIGURE 45: Pressure History Match of Fluvial "C" Foam Minifrac No. 2 With 100 Mesh Sand.

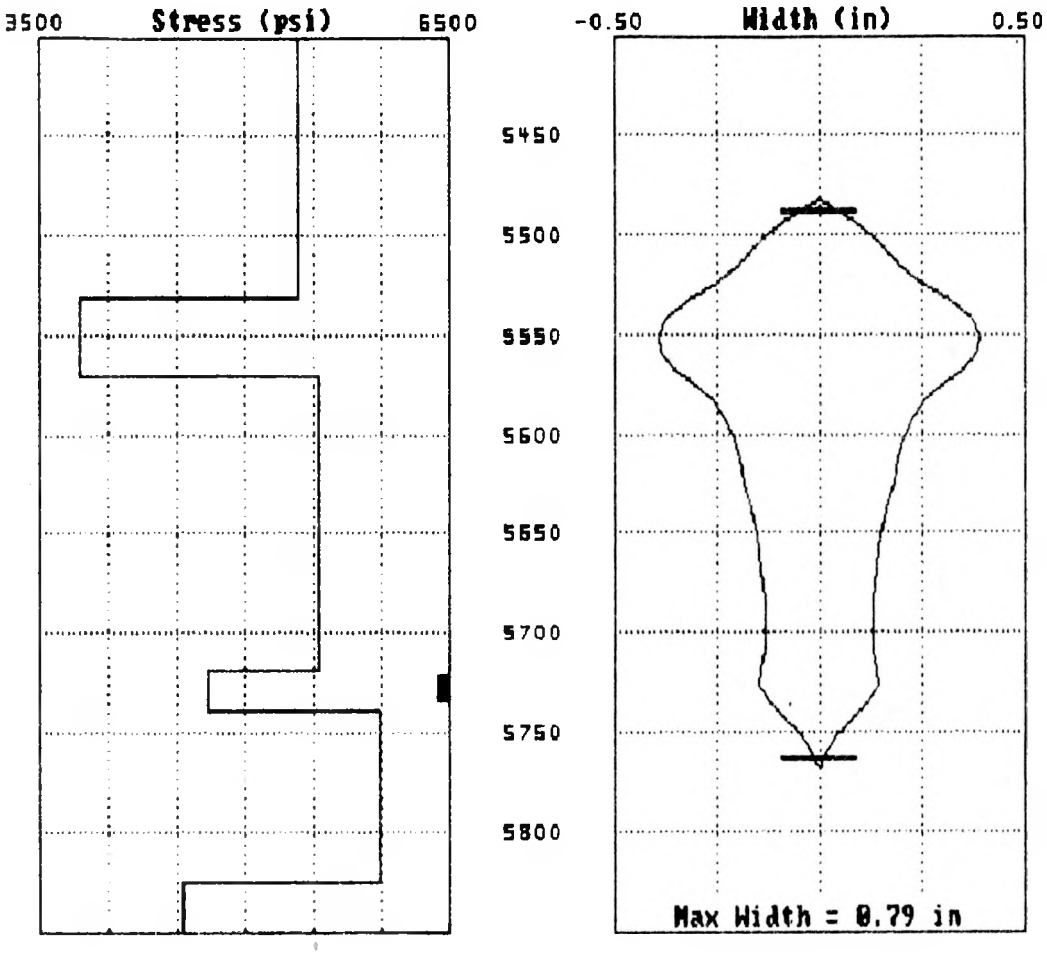


FIGURE 46: Simulator Predicted Gross Fracture Height at Wellbore for Fluvial "C" Foam Minifrac No. 2 With 100 Mesh Sand.

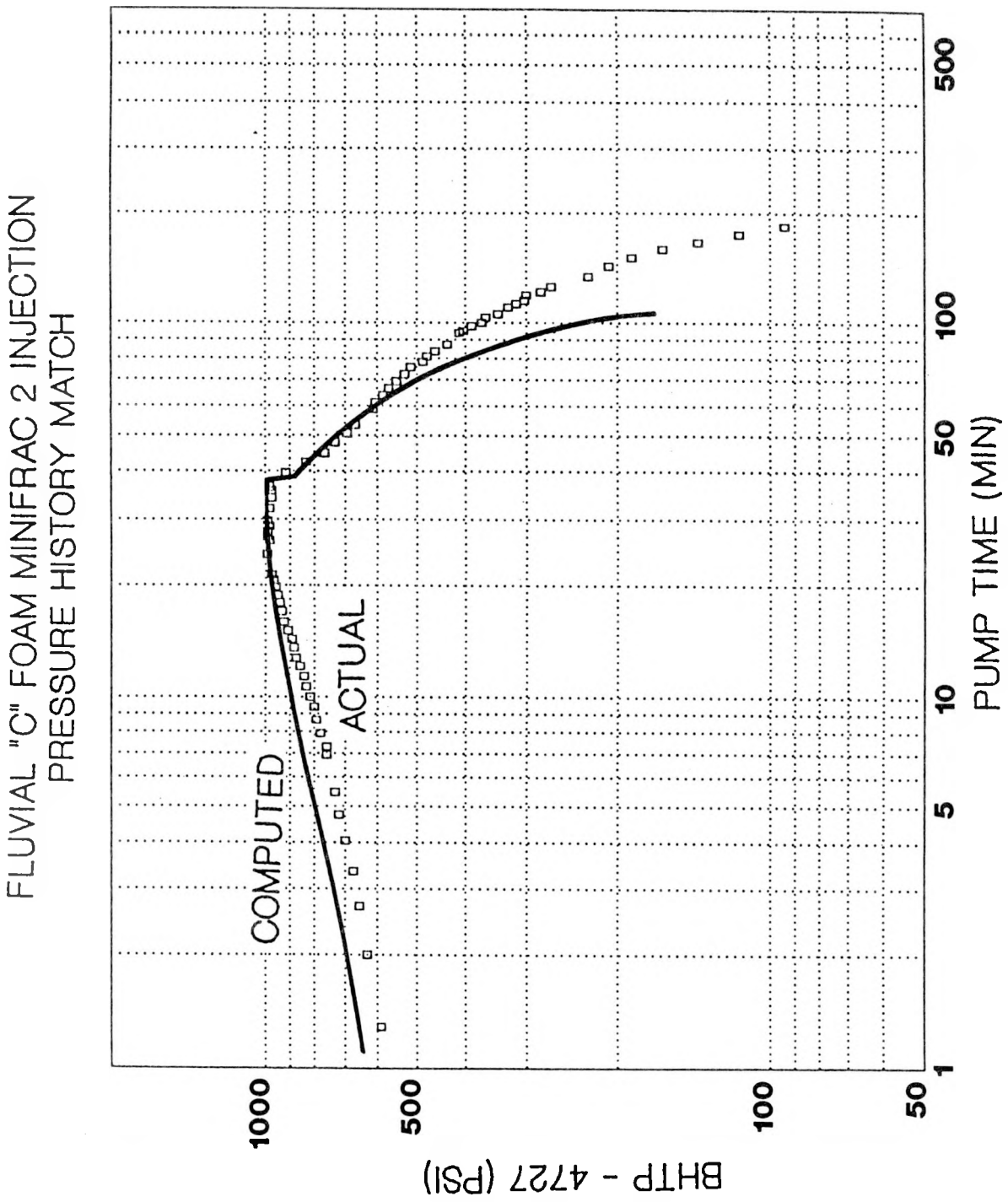


FIGURE 47: Pressure History Match of Fluvial "C" Foam Minifrac No. 2 With Increased Fluid Viscosity Through Constant Pressure Mode.

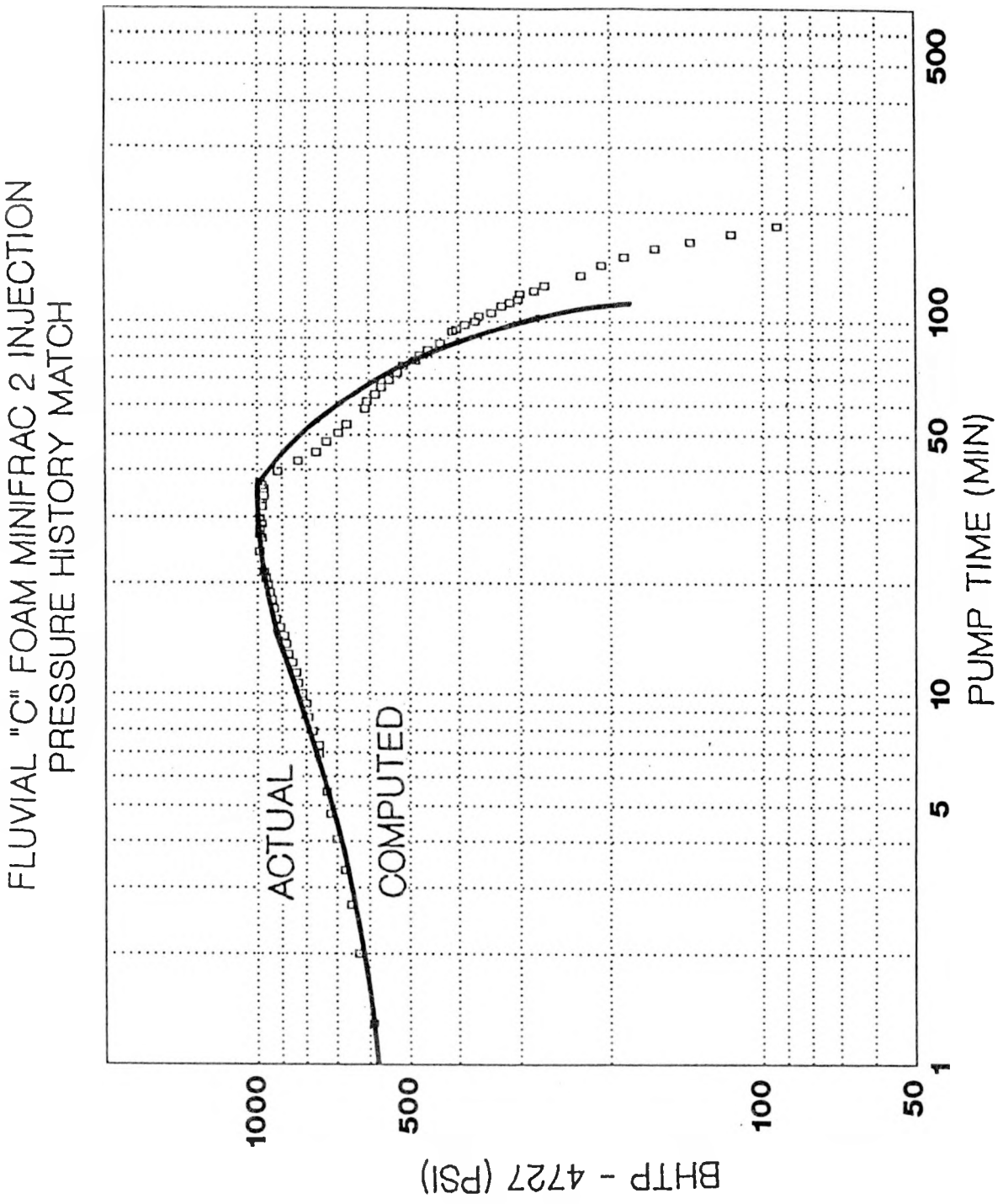


FIGURE 48: Pressure History Match of Fluvial "C" Foam Minifrac No. 2 With Increased Fluid Viscosity Through Constant Pressure Mode and Decreased Viscosity in Early Time.

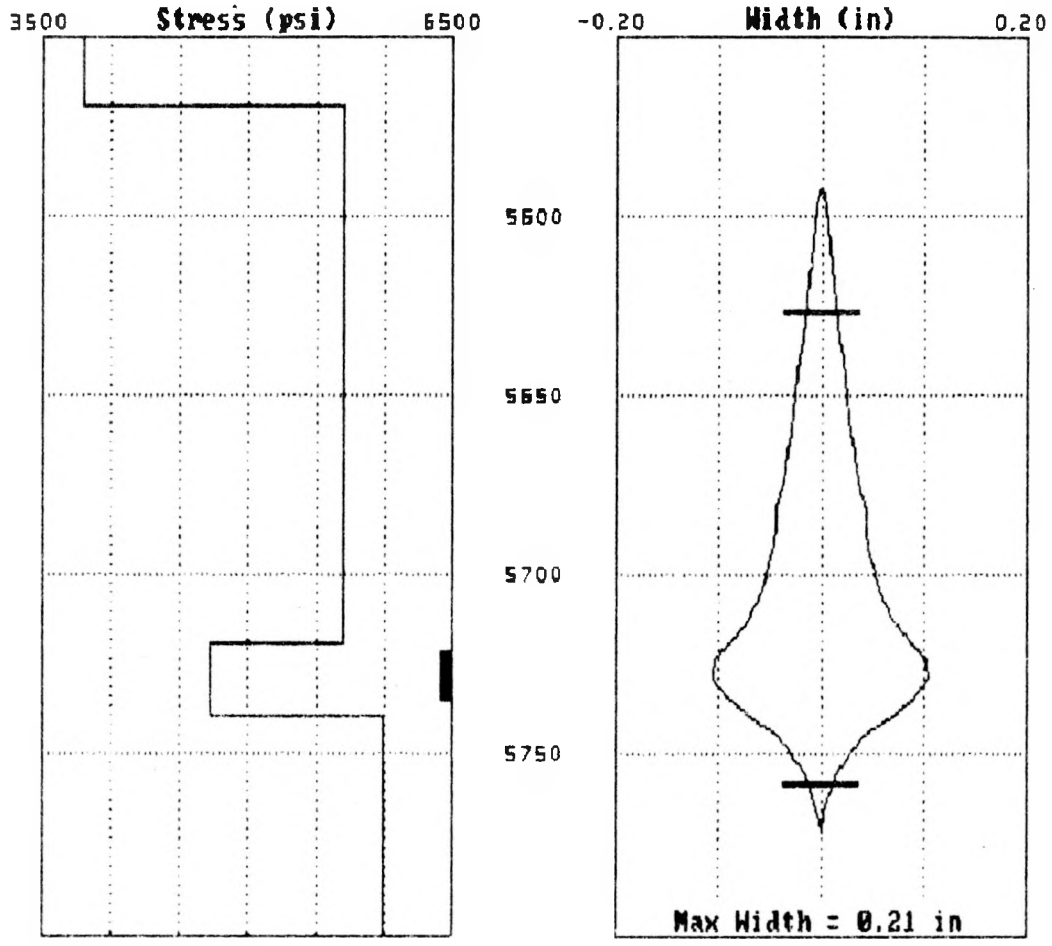


FIGURE 49: Simulator Predicted Gross Fracture Height at Wellbore for Fluvial "C" Foam Minifrac No. 2 With Increased Fluid Viscosity Through Constant Pressure Mode and Decreased Viscosity in Early Time.

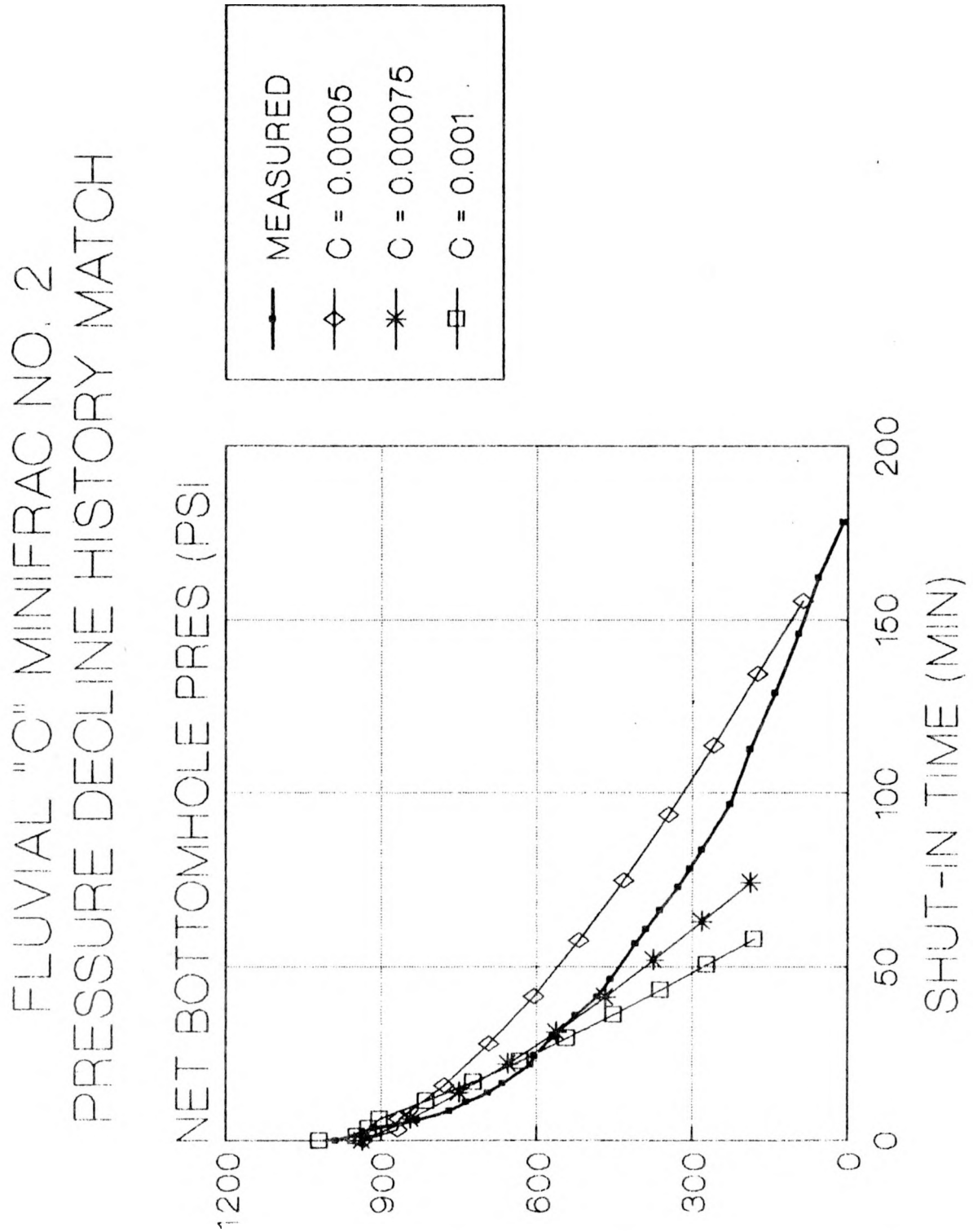


FIGURE 50: History Match of Pressure Decline for Fluvial "C" Foam Minifrac No. 2.

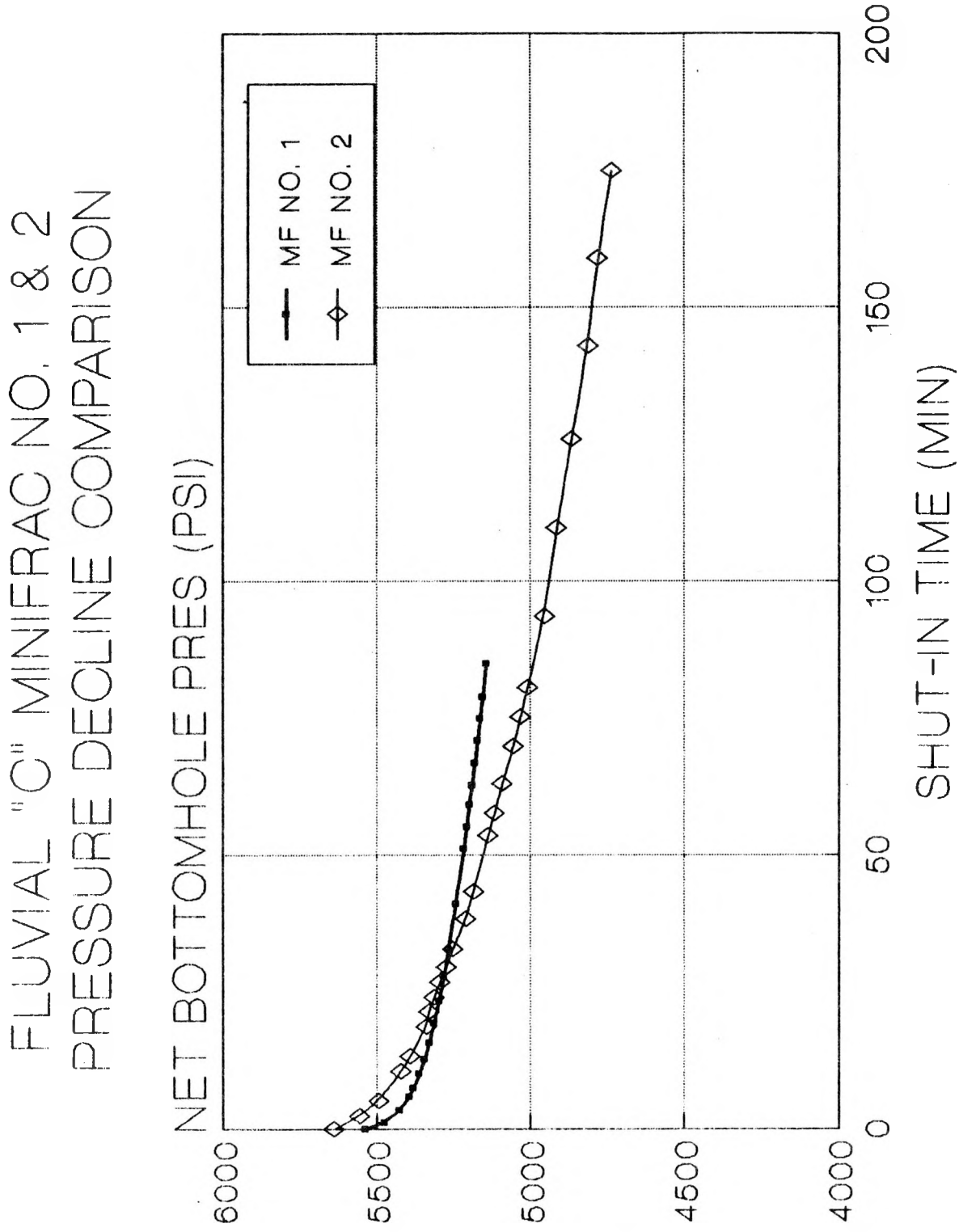


FIGURE 51: Comparison of Pressure Decline Behavior for the Two Fluvial "C" Foam Minifracs.

TABLE NO. 9

Results of Fluvial "E" Closure Stress Tests

Test	Frac Ext. P (psi)	Closure P (psi)
PI/SI	-	4522
SRT/FB-1	4875	4315
PI/FB-2	-	-
PI/FB-3	-	4406
PI/FB-4	-	4450
MF/SI	-	-

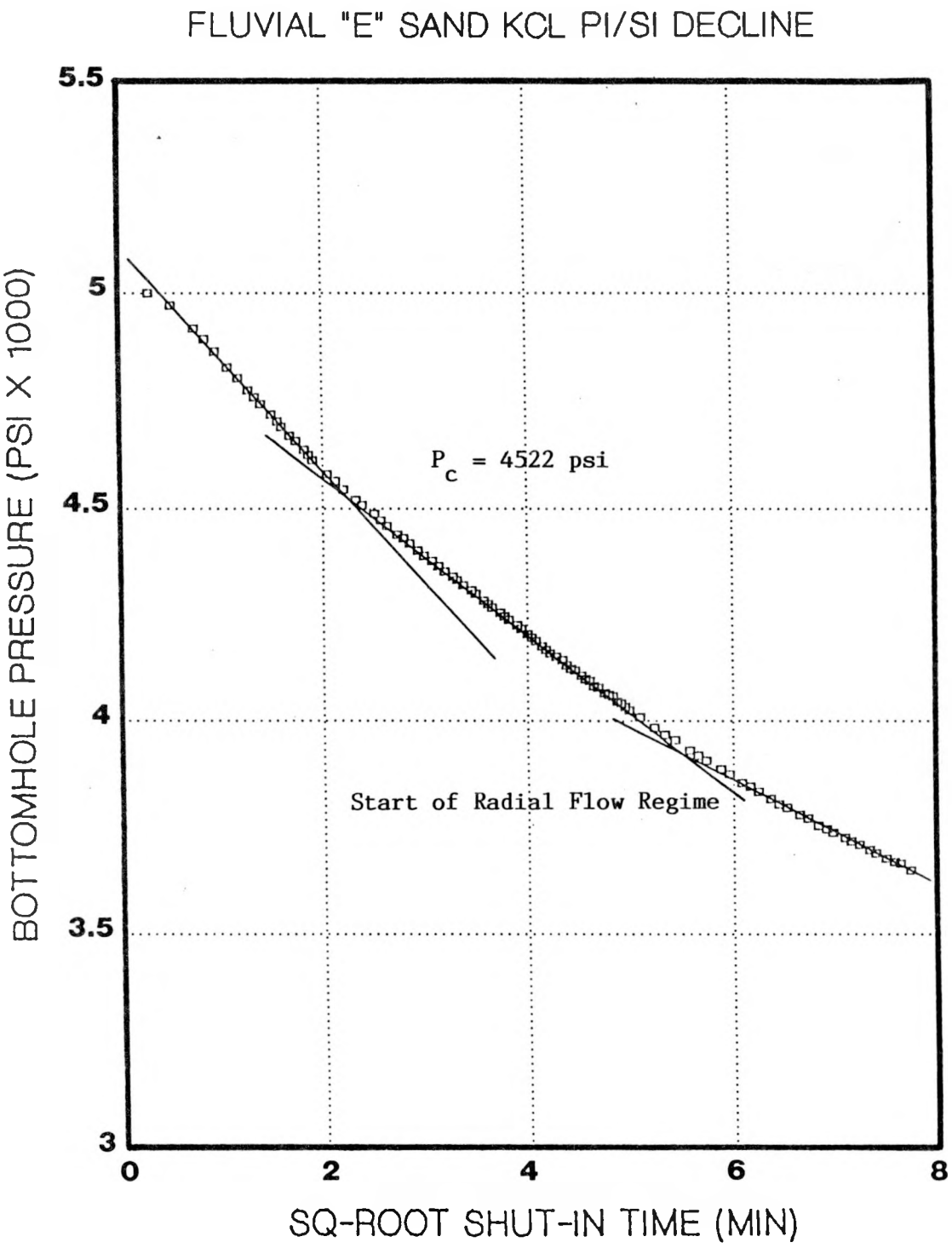


FIGURE 52: Fluvial "E" Sand KCl Pump-In/Shut-In Decline.

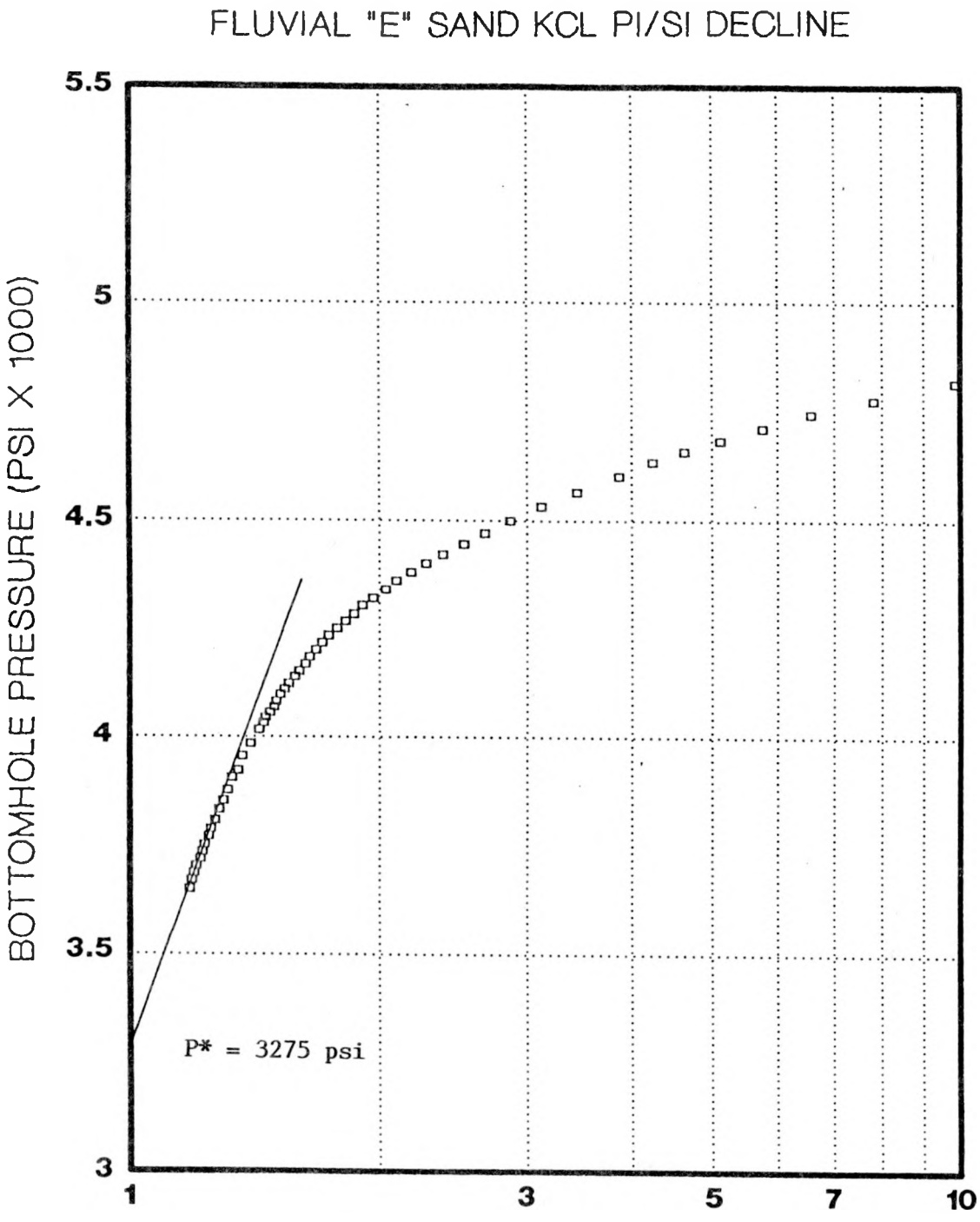


FIGURE 53: Horner Plot of Fluvial "E" Sand KCl Pump-In/Shut-In Decline.

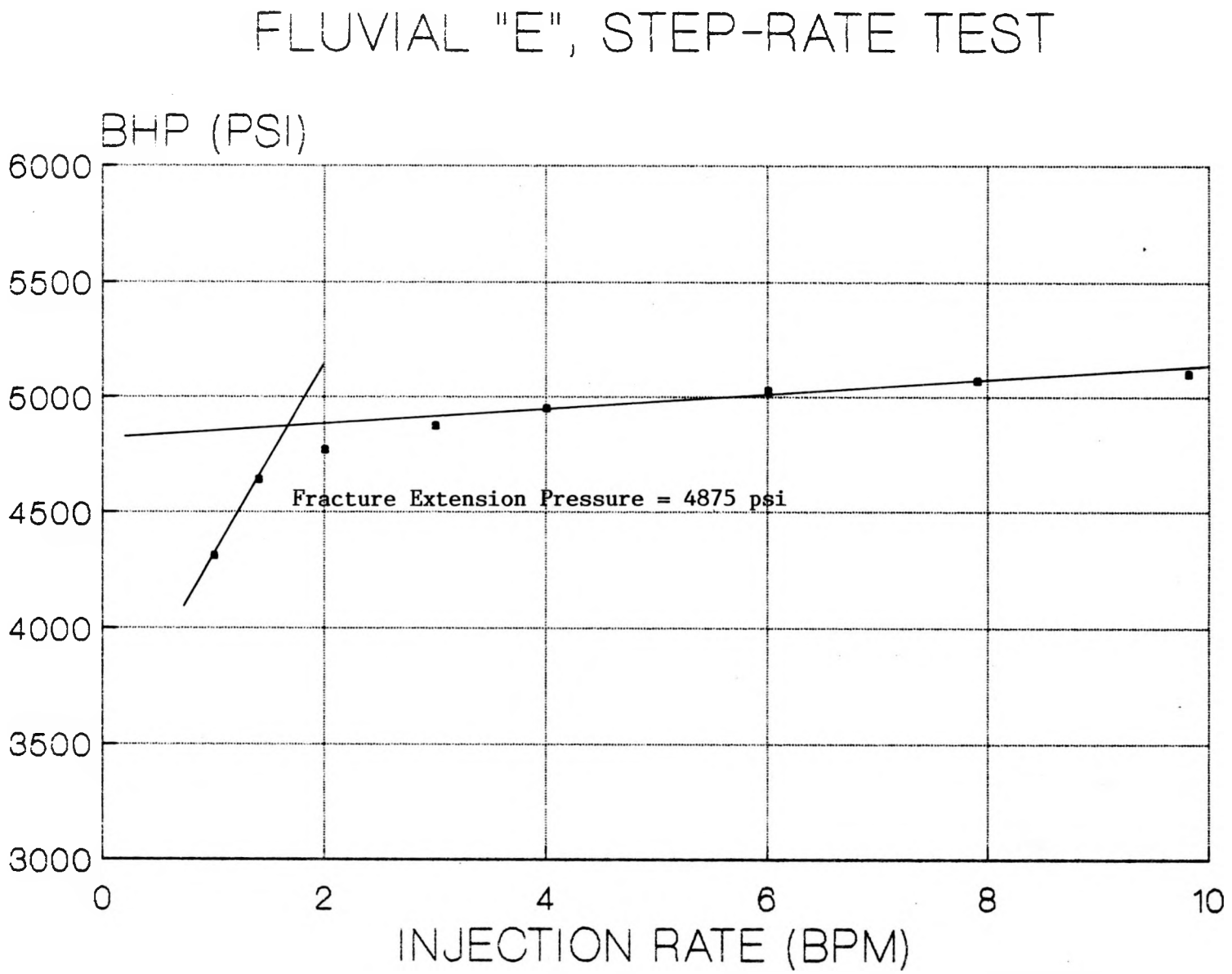


FIGURE 54: Fluvial "E" Sand KCl Step-Rate Test Injection.

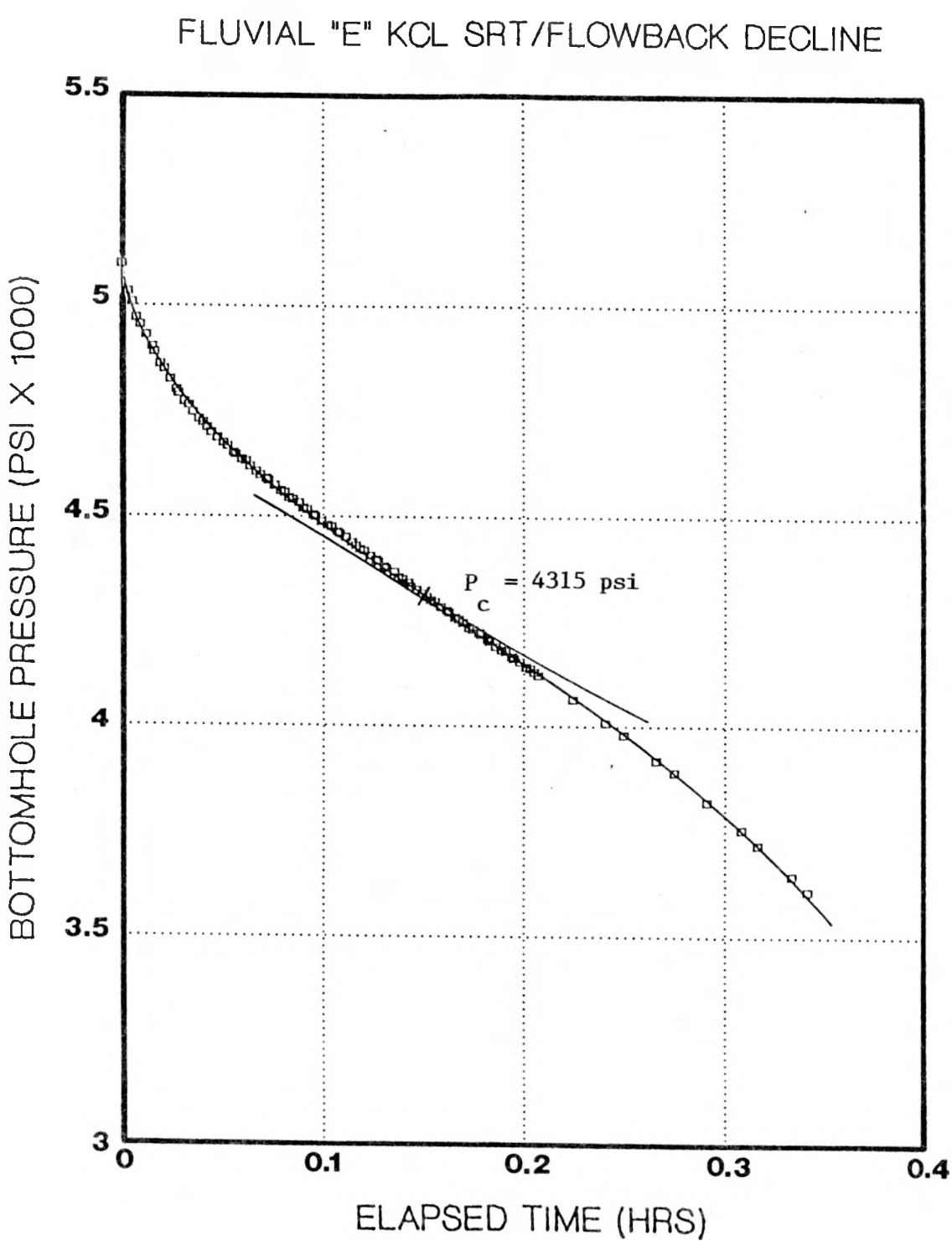


FIGURE 55: Fluvial "E" Sand KCl Step-Rate Test/Flowback Decline.

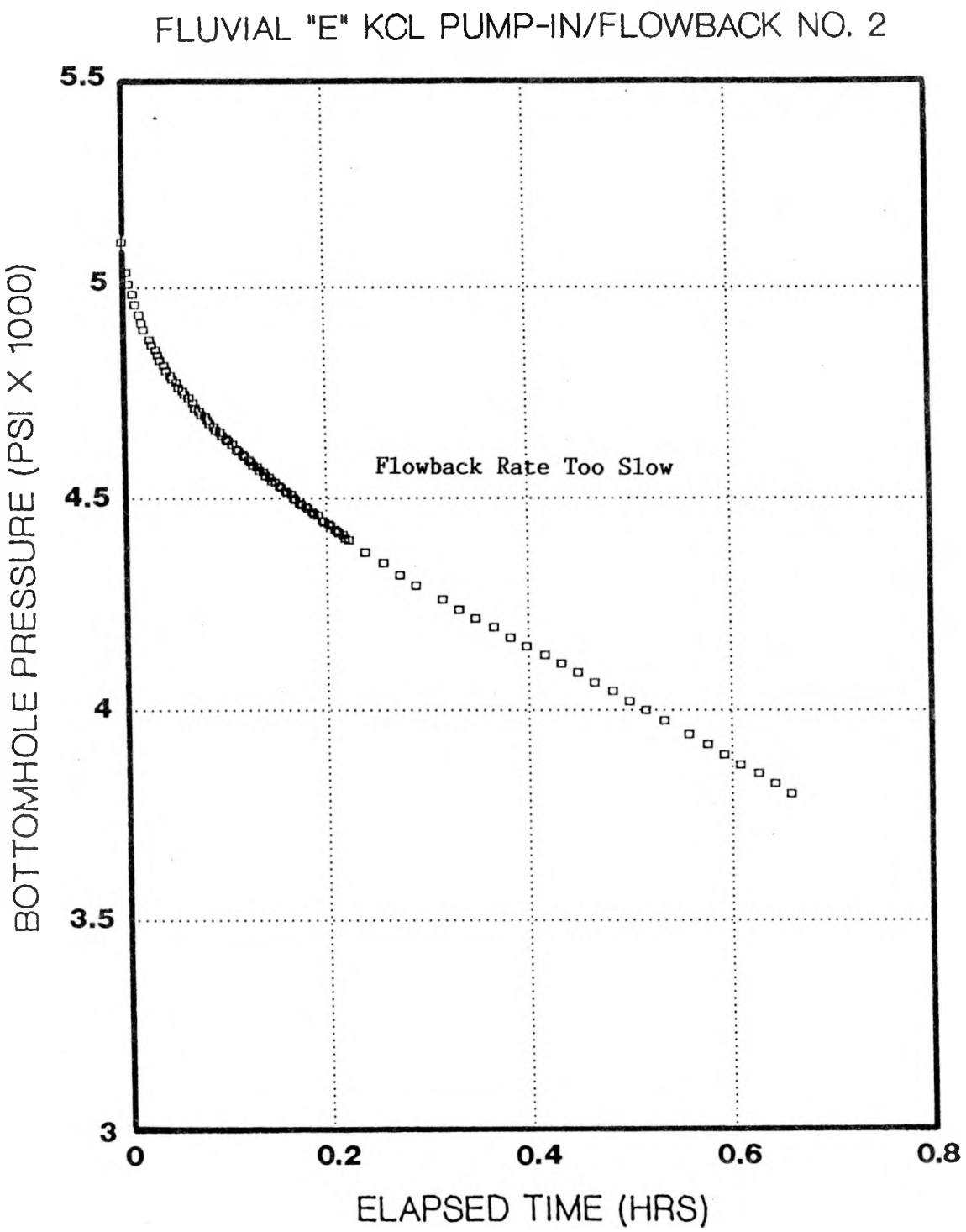


FIGURE 56: Fluvial "E" Sand KCl Pump-In/Flowback No. 2 Decline.

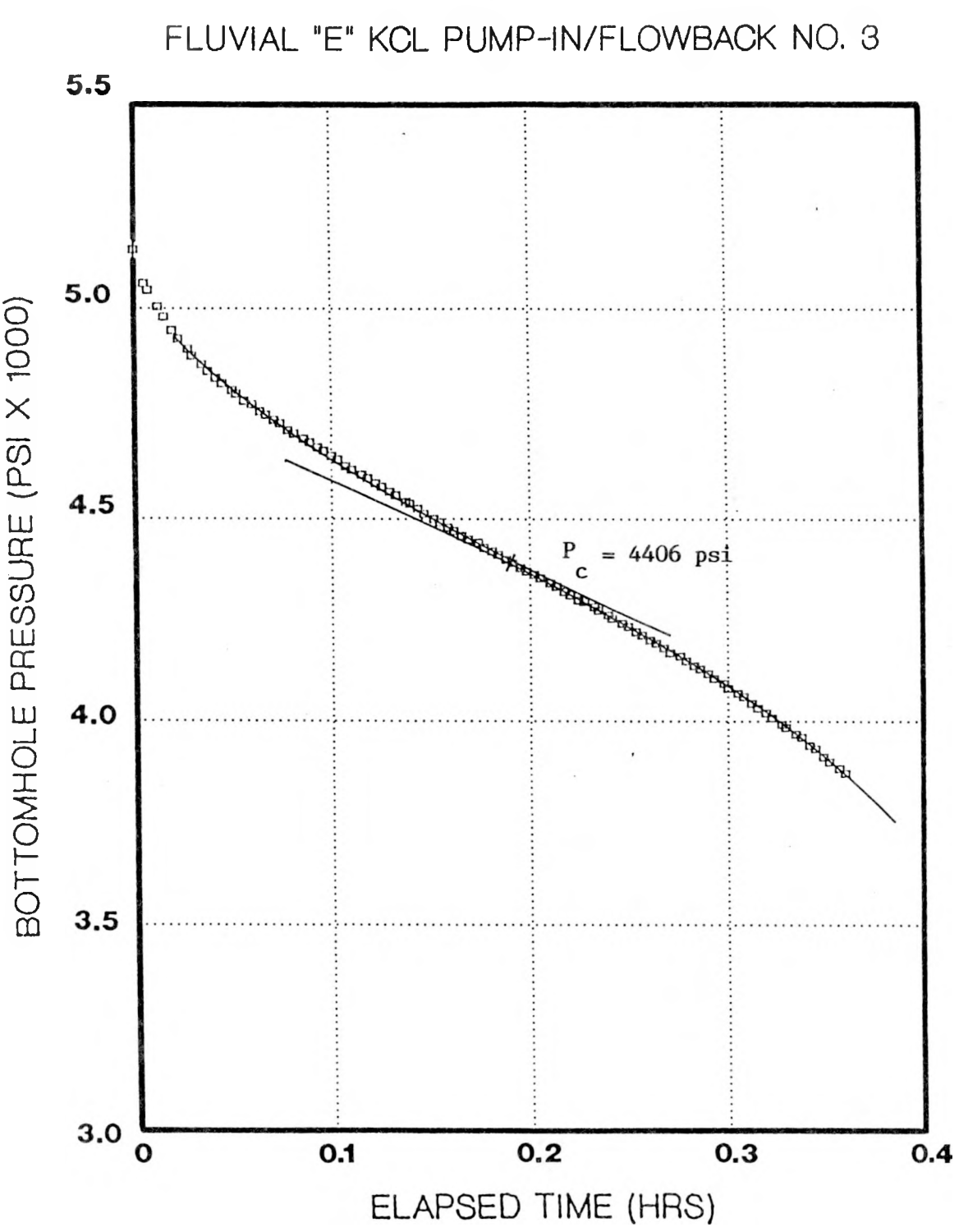


FIGURE 57: Fluvial "E" Sand KCl Pump-In/Flowback No. 3 Decline.

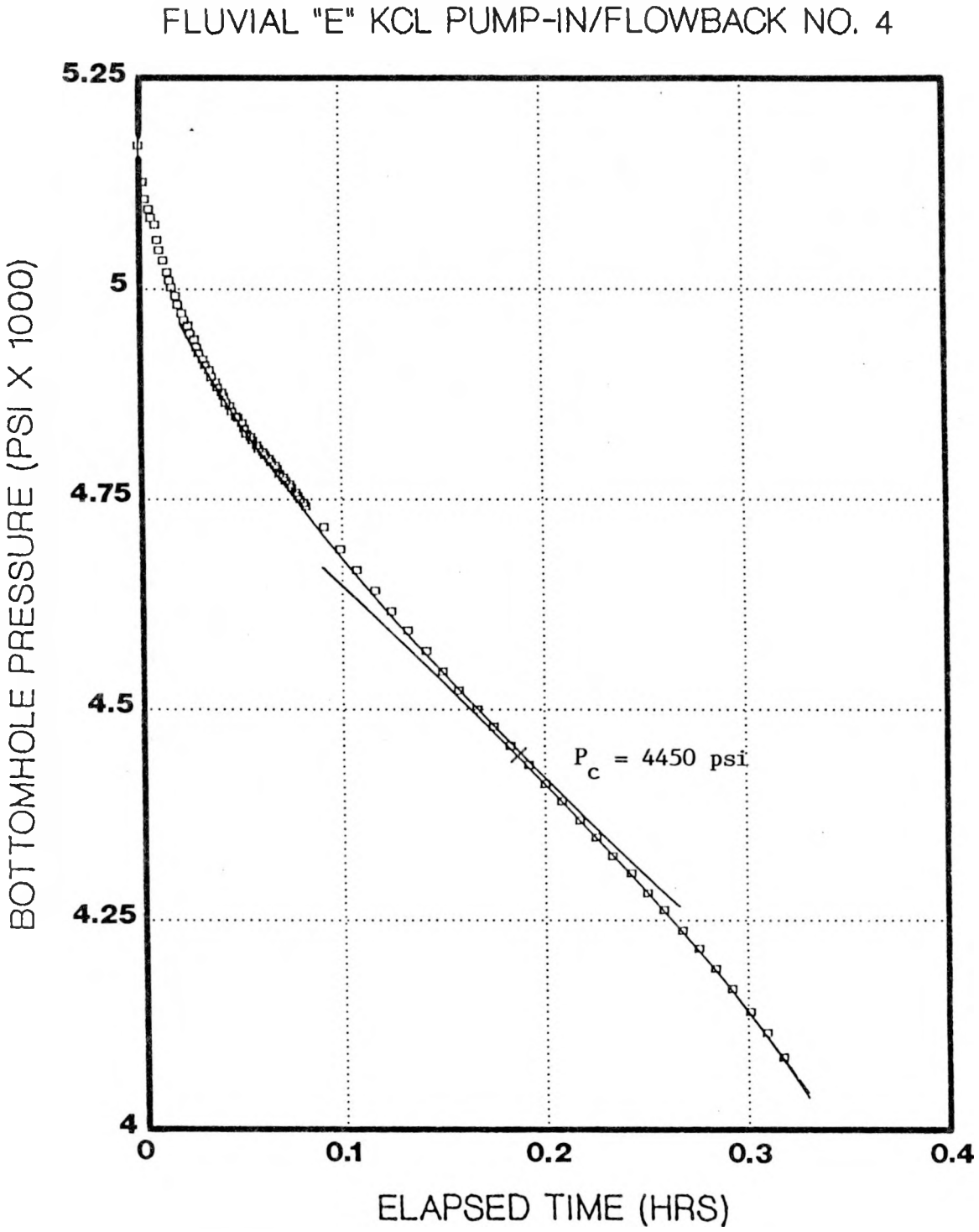


FIGURE 58: Fluvial "E" Sand KCl Pump-In/Flowback No. 4 Decline.

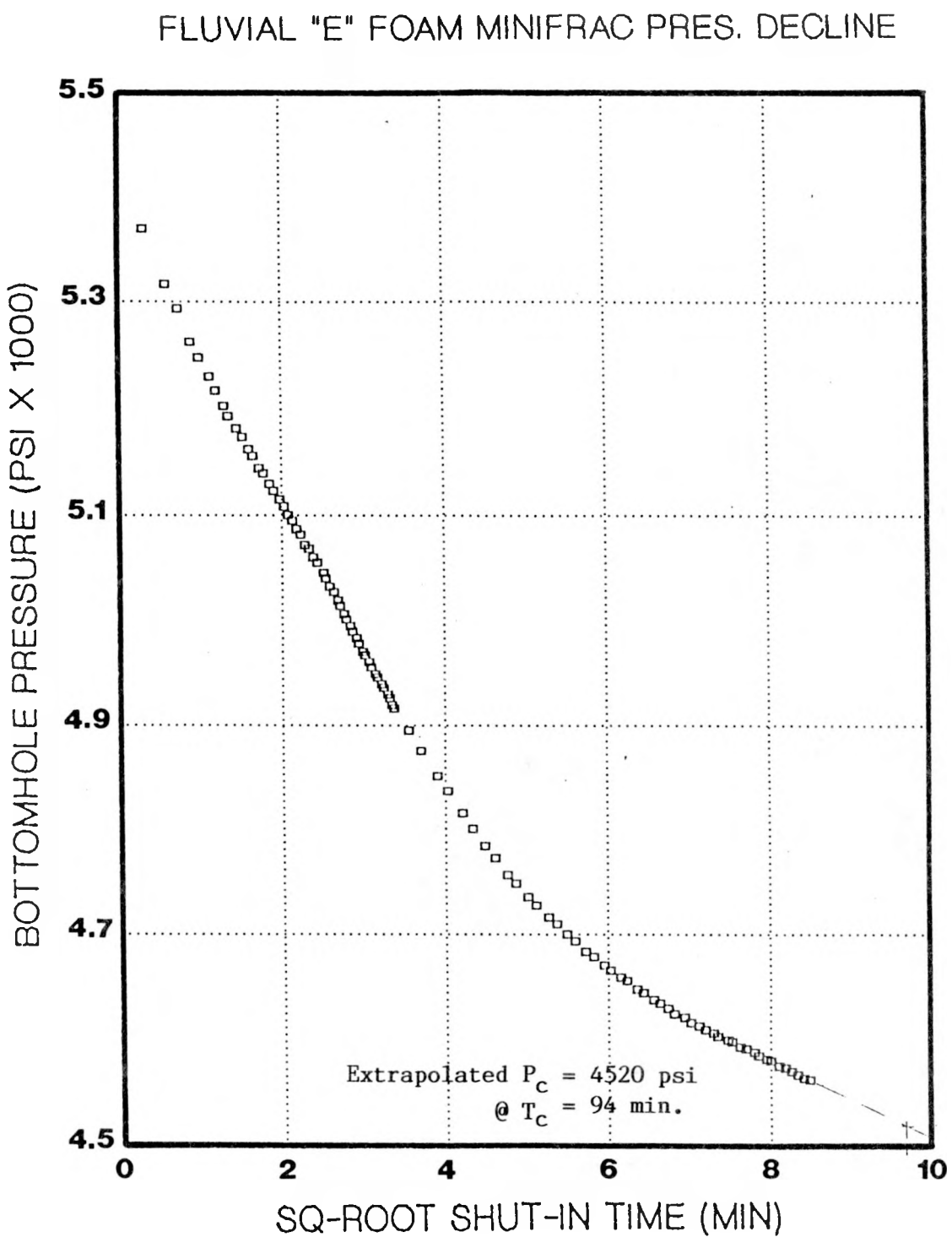


FIGURE 59: Fluvial "E" Sand Foam Minifrac Shut-In Pressure Decline.

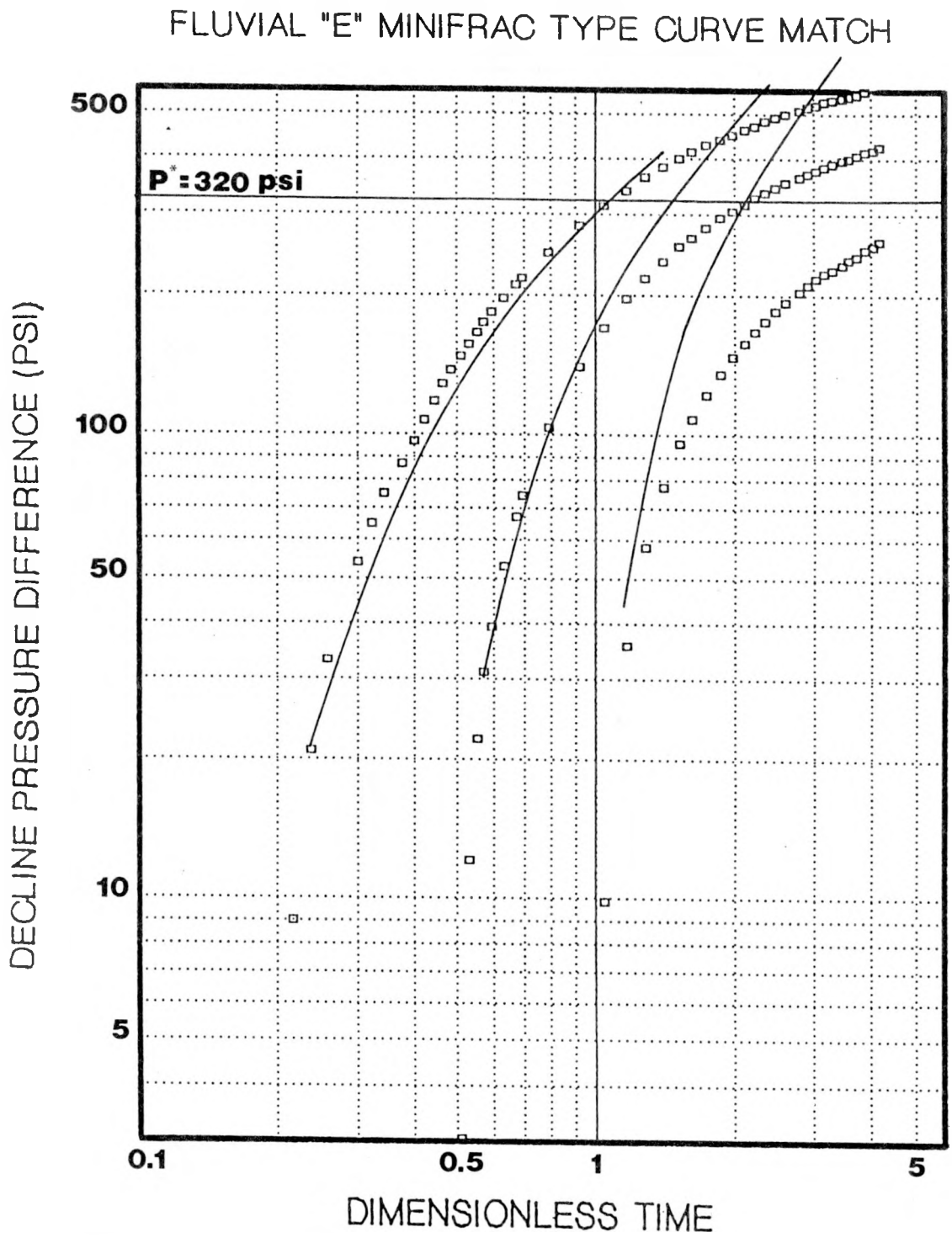


FIGURE 60: Fluvial "E" Sand Foam Minifrac Pressure Decline Type Curve Match, Pump Time = 16.5 minutes.

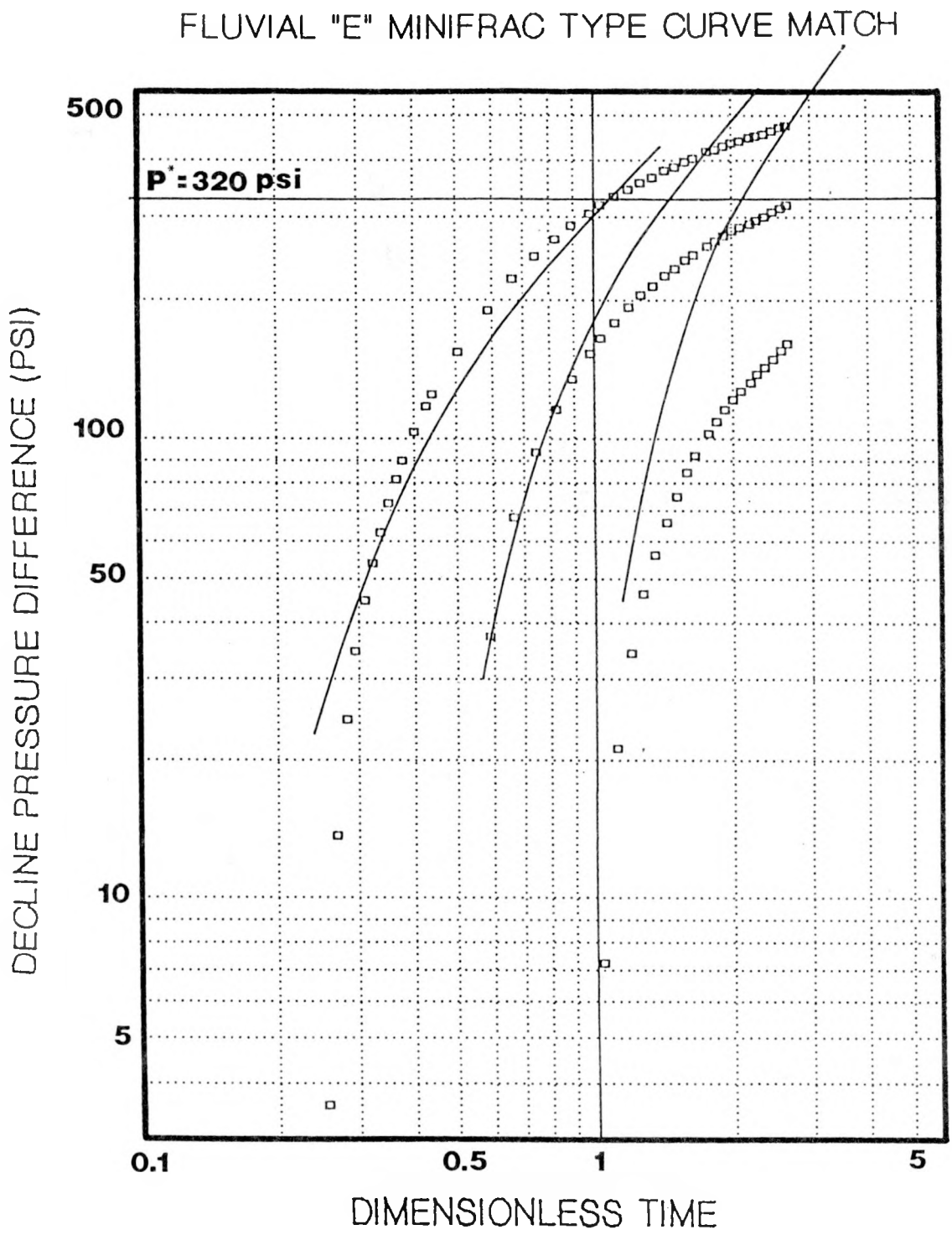


FIGURE 61: Fluvial "E" Sand Foam Minifrac Pressure Decline Type Curve Match, Pump Time = 25.9 minutes.

TABLE NO. 10

WORKSHEET FOR PRESSURE DECLINE ANALYSIS - PERKINS & KERN GEOMETRY

Input Data:

Young's Modulus = E' =	5×10^6	psi	(Source - Sandia	)
Pump Time = t_p =	16.55/25.92	min	(Source - Minifrac Data	)
Volume Pumped = V =	14,905	gal	(Source - Minifrac Data	)
ISIP =	5385	psi	(Source - NSI	)
Closure Pressure = σ_c =	4520	psi	(Source - NSI	)
Closure time = Δt_c =	94	min	(Source - NSI	)

Net $p = p_s$ = ISIP - Closure Pressure = 865 psi

Match p = P* (from Type Curves) = 320 psi

Geometry Parameters:

$g_o = 1.45$, $g_c = 1.00$, $\beta' = 0.7$, $K = 1.00$

EFFICIENCY ANALYSIS

from time-to-close and graph

efficiency = e_f = 0.

$t_c/t_o = 94/16.55 = 5.7$

$e_f = 0.73$

$t_c/t_o = 94/25.92 = 3.6$

$e_f = 0.62$

* from pressures

* $\rho = \pi\, p_s/4\, K\, g_o\, P^* = 1.54\ (1.46)$

* $e_f = \rho / (1 + \rho) = 0.60$ k↑, e_f↓

use efficiency e_f =

LEAK-OFF COEFFICIENT

Leak-Off Coefficient (ft/min**0.5) = $C = P^* \beta'\ h / r_p\, t_p^{**0.5}\, E'$; $r_p = h_p/h$

$t_p = 16.55$: $c = [(320)(0.7)(30)]/[(0.5)(4.07)(5 \times 10^6)]$

$c = 0.00066$ ft/ min

$t_p = 25.92$*: $c = [(320)(0.7)(30)]/[(0.5)(5.09)(5 \times 10^6)]$

$c = 0.00053$ ft/ min

*Includes nitrogen pump-up stage.

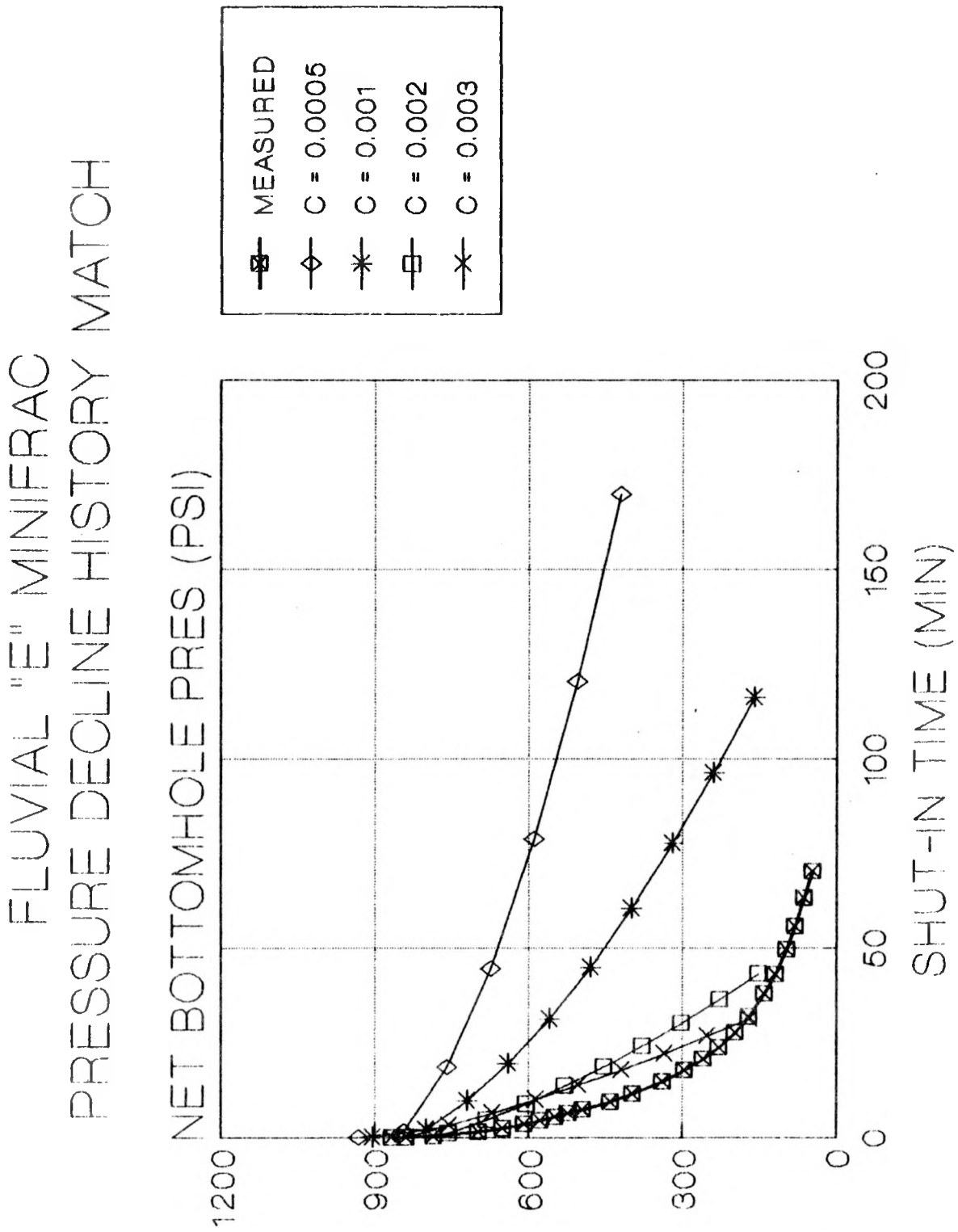


FIGURE 62: Fluvial "E" Sand Foam Minifrac Pressure Decline History Match.

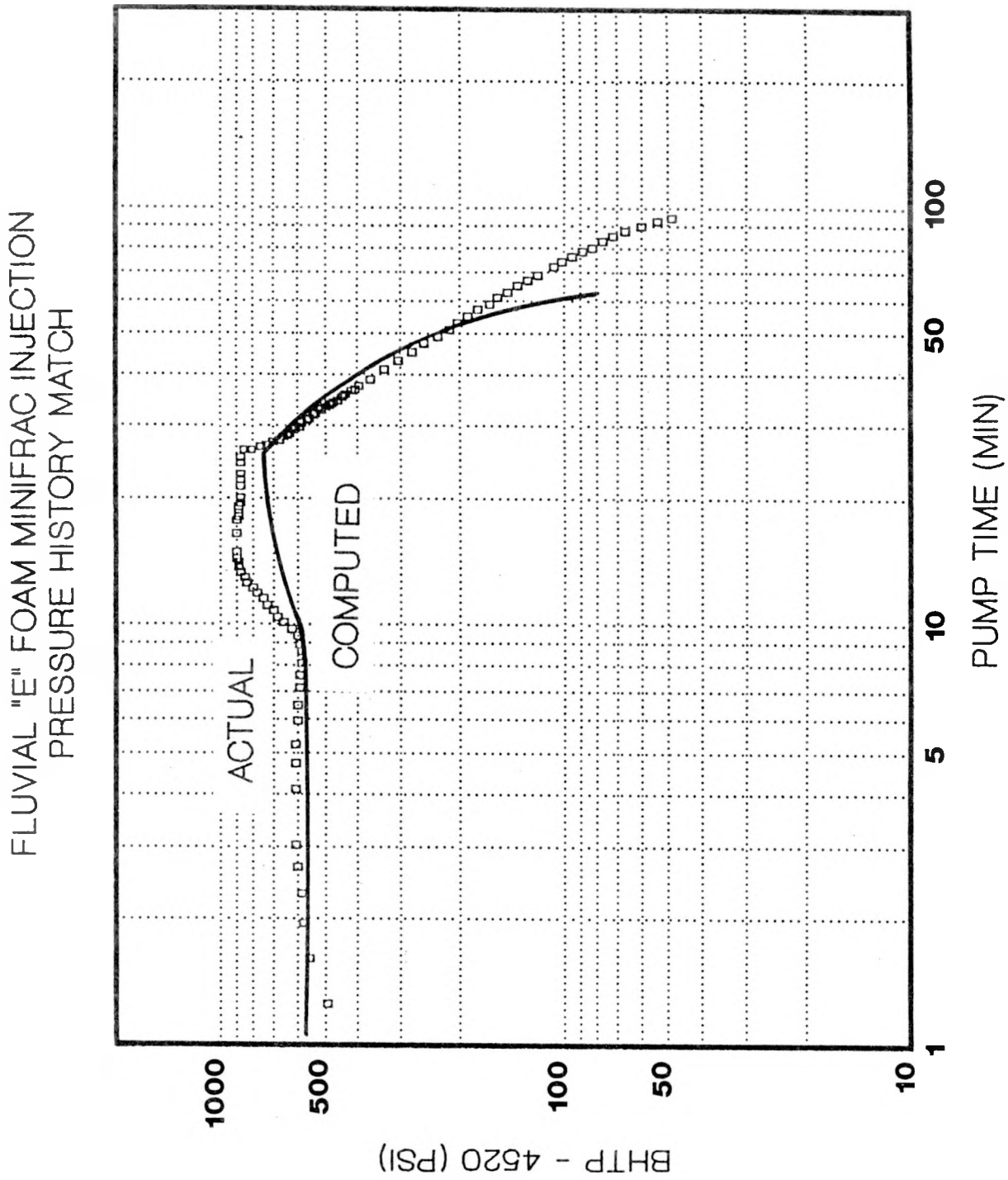


FIGURE 63: Initial Attempt to History Match the Fluvial "E" Sand Foam Minifrac Injection/Decline Pressures.

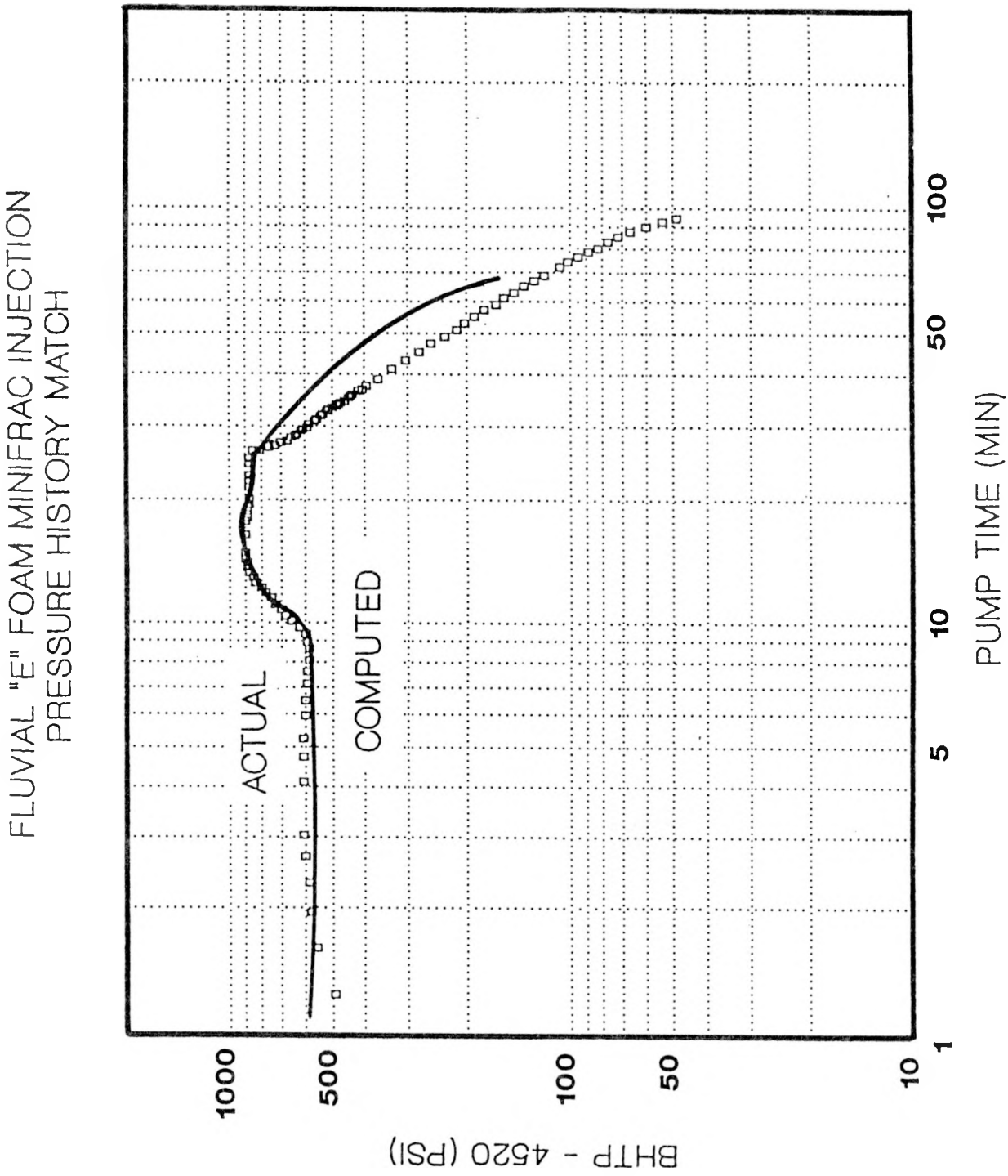


FIGURE 64: Fluvial "E" Foam Minifrac Pressure History Match With Changes in Fluid viscosity.

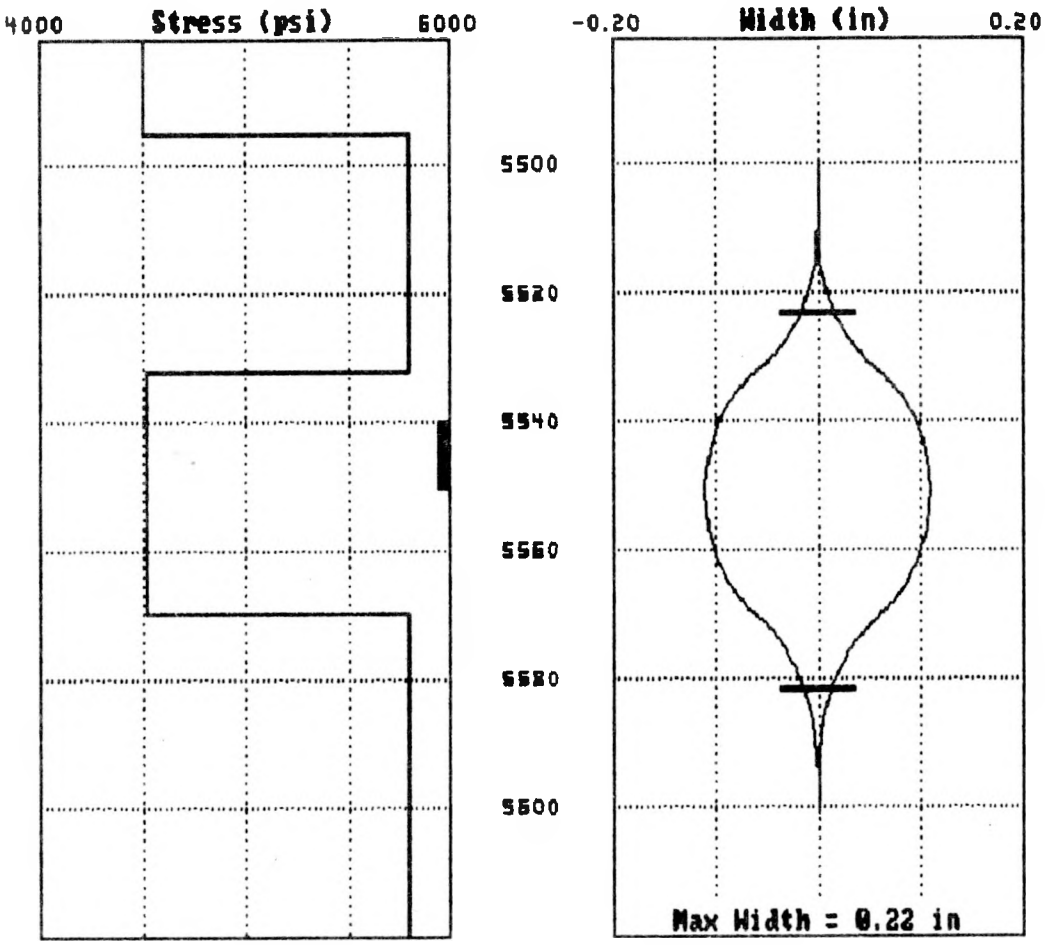


FIGURE 65: Simulator Predicted Gross Fracture Height at Wellbore for the Fluvial "E" Sand Foam Minifrac.

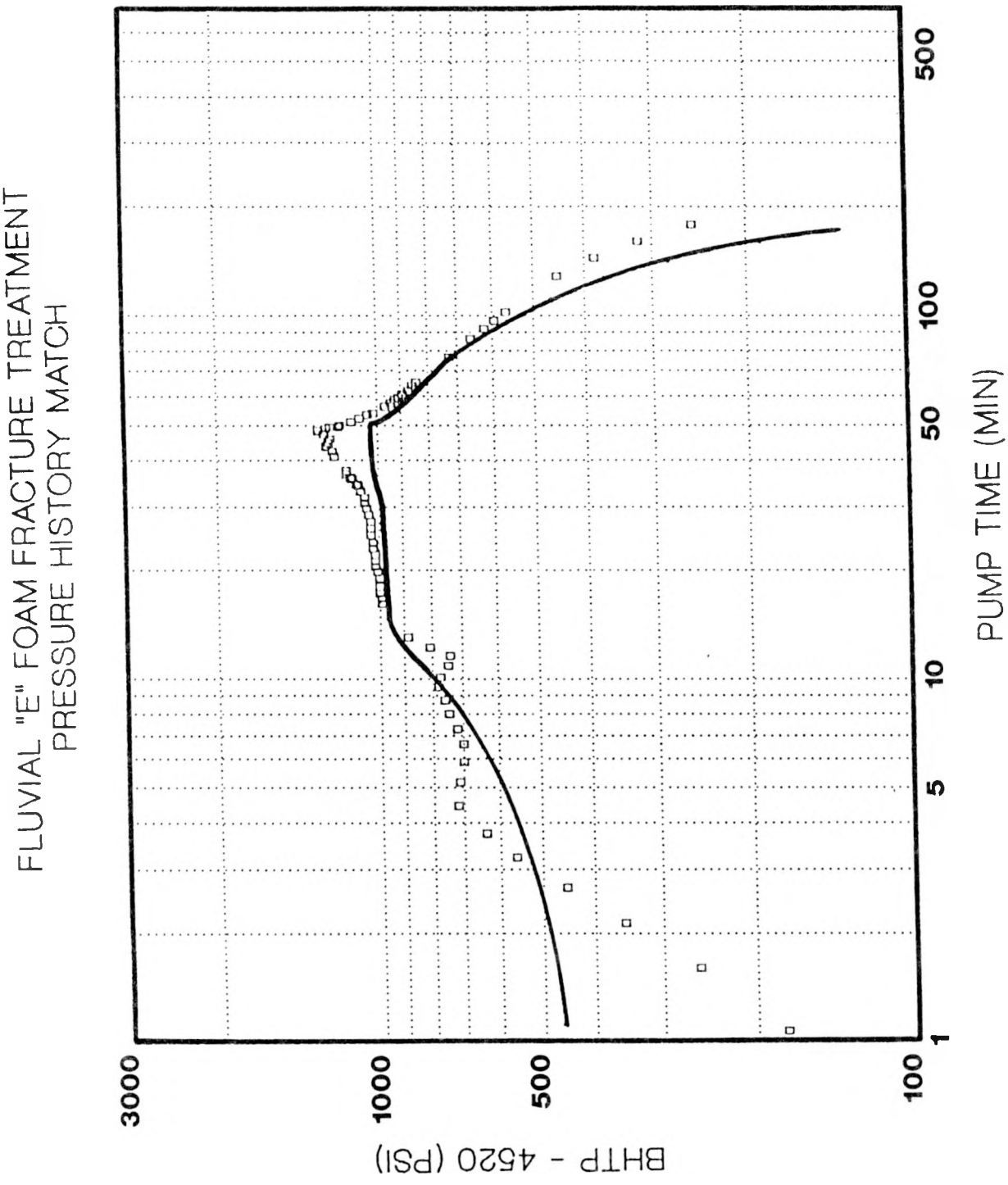


FIGURE 66: Fluvial "E" Sand Foam Fracture treatment Pressure History Match.

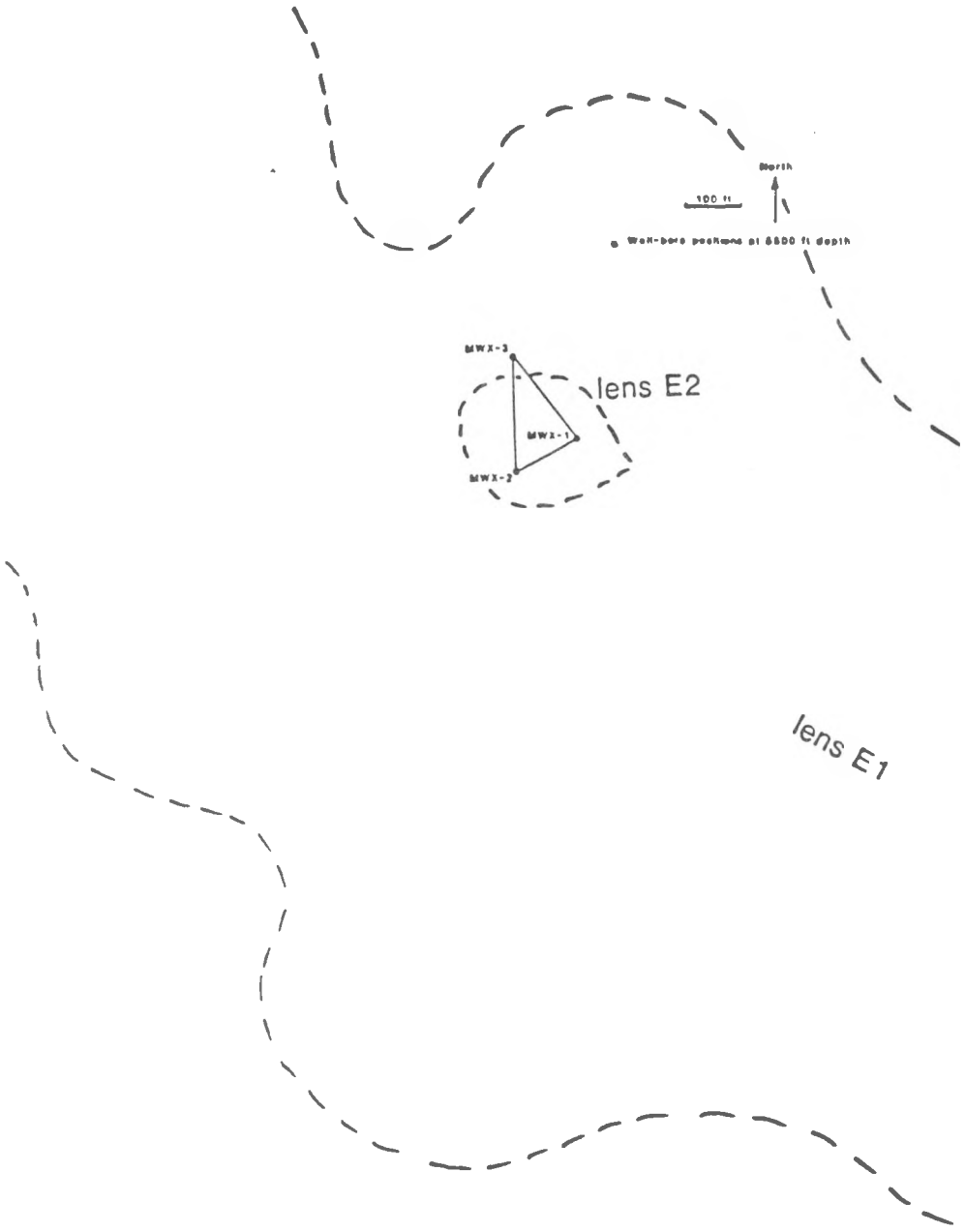


FIGURE 67: Estimated Fluvial "E" Sand Lens Size/Orientation.

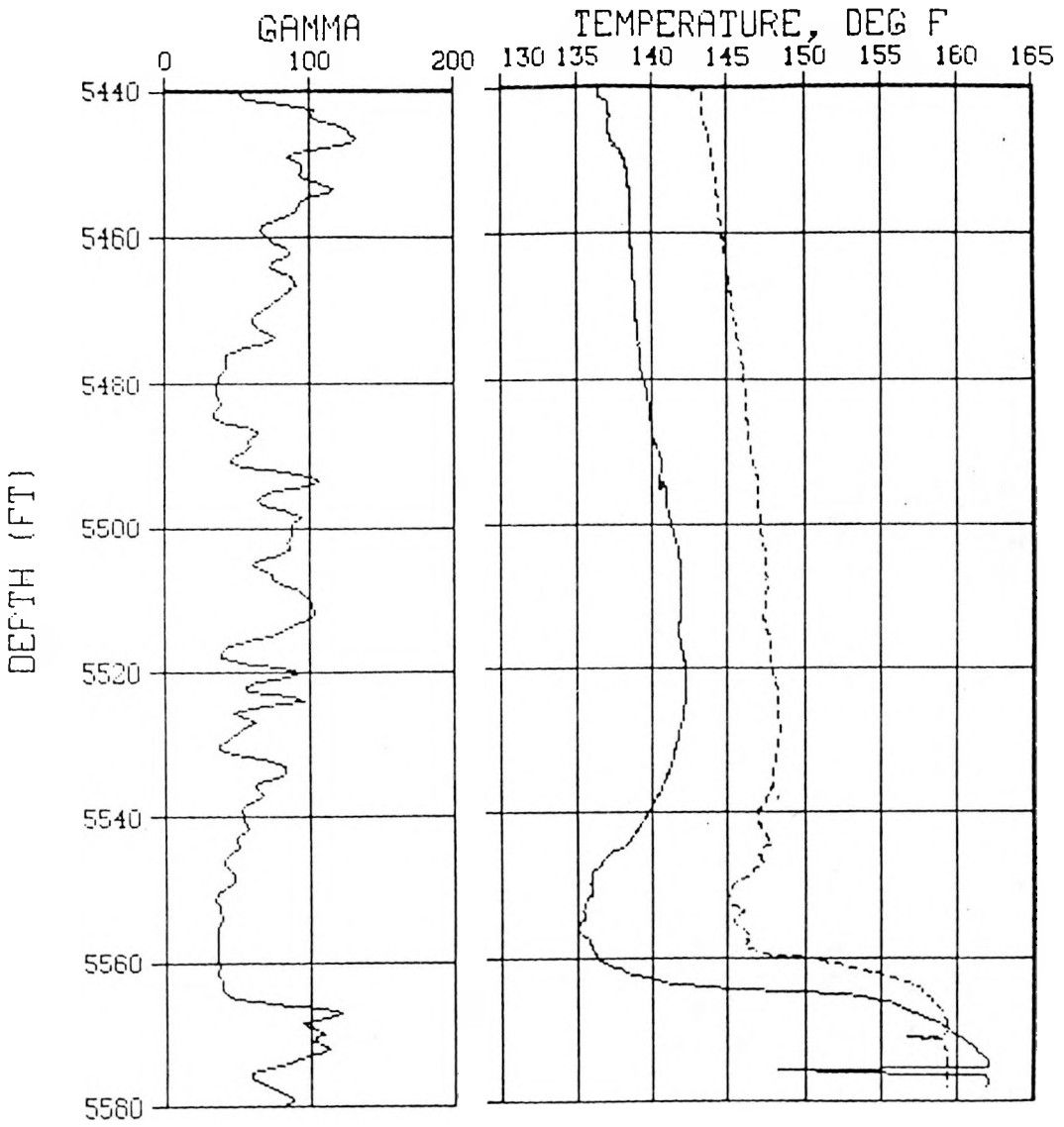


FIGURE 68: Post-Frac Temperature Log for the Fluvial "E" Foam Fracture Treatment.

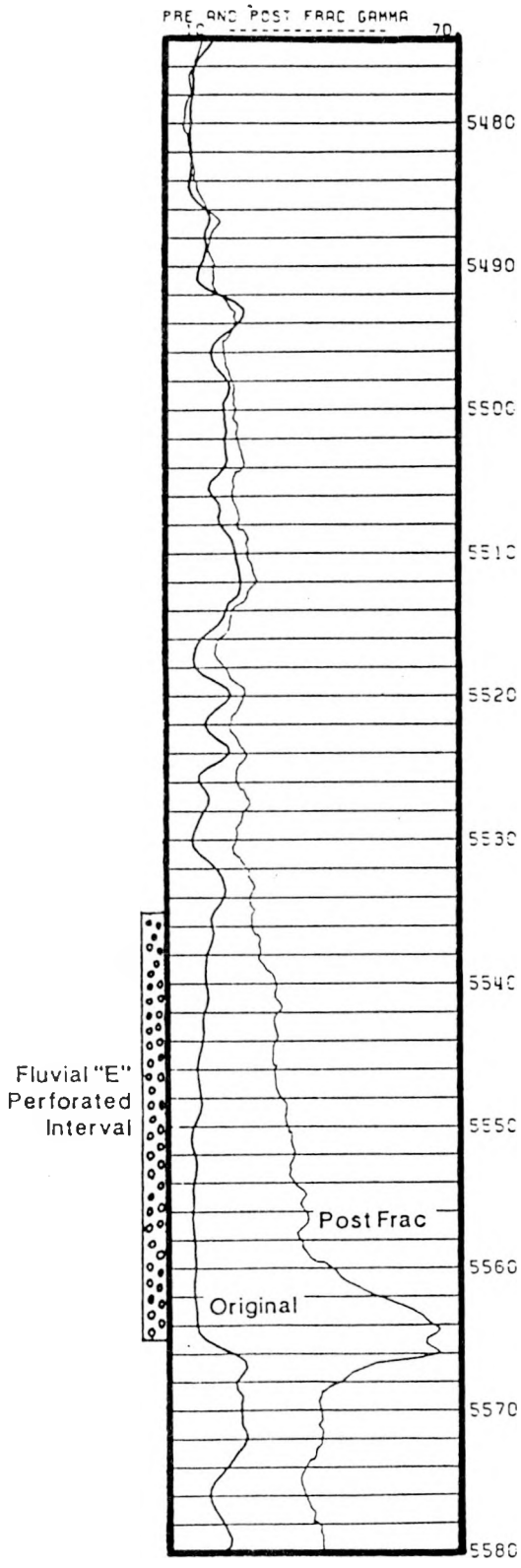


FIGURE 69: Post-Frac Gamma-Ray Log for the Fluvial "E" Foam Fracture Treatment.

APPENDICES

APPENDIX A

STRESS TEST ANALYSIS

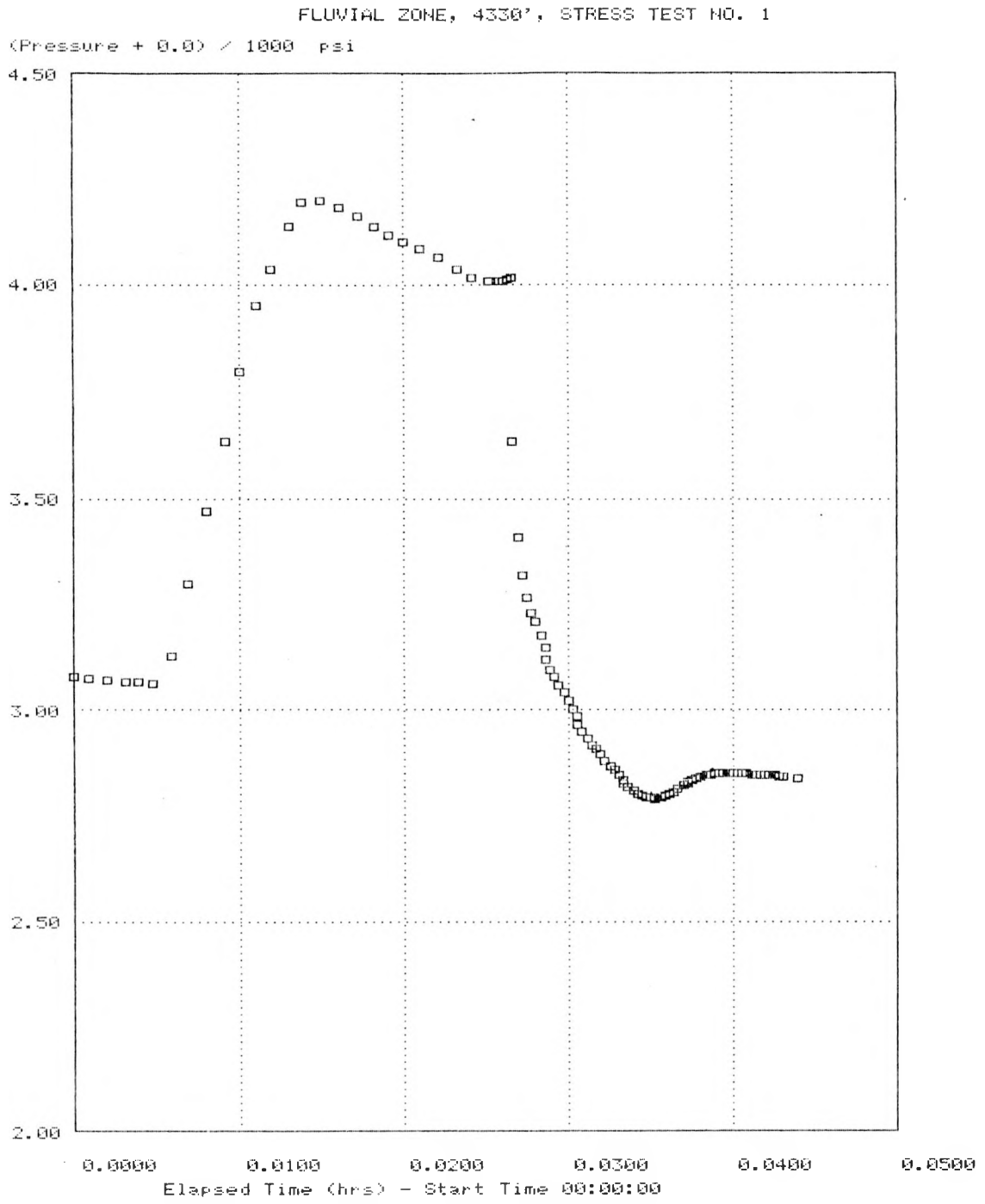


FIGURE A.1: Sandstone Stress Test (4330-4332'), Linear Plot of Test No. 1 Injection/Decline.

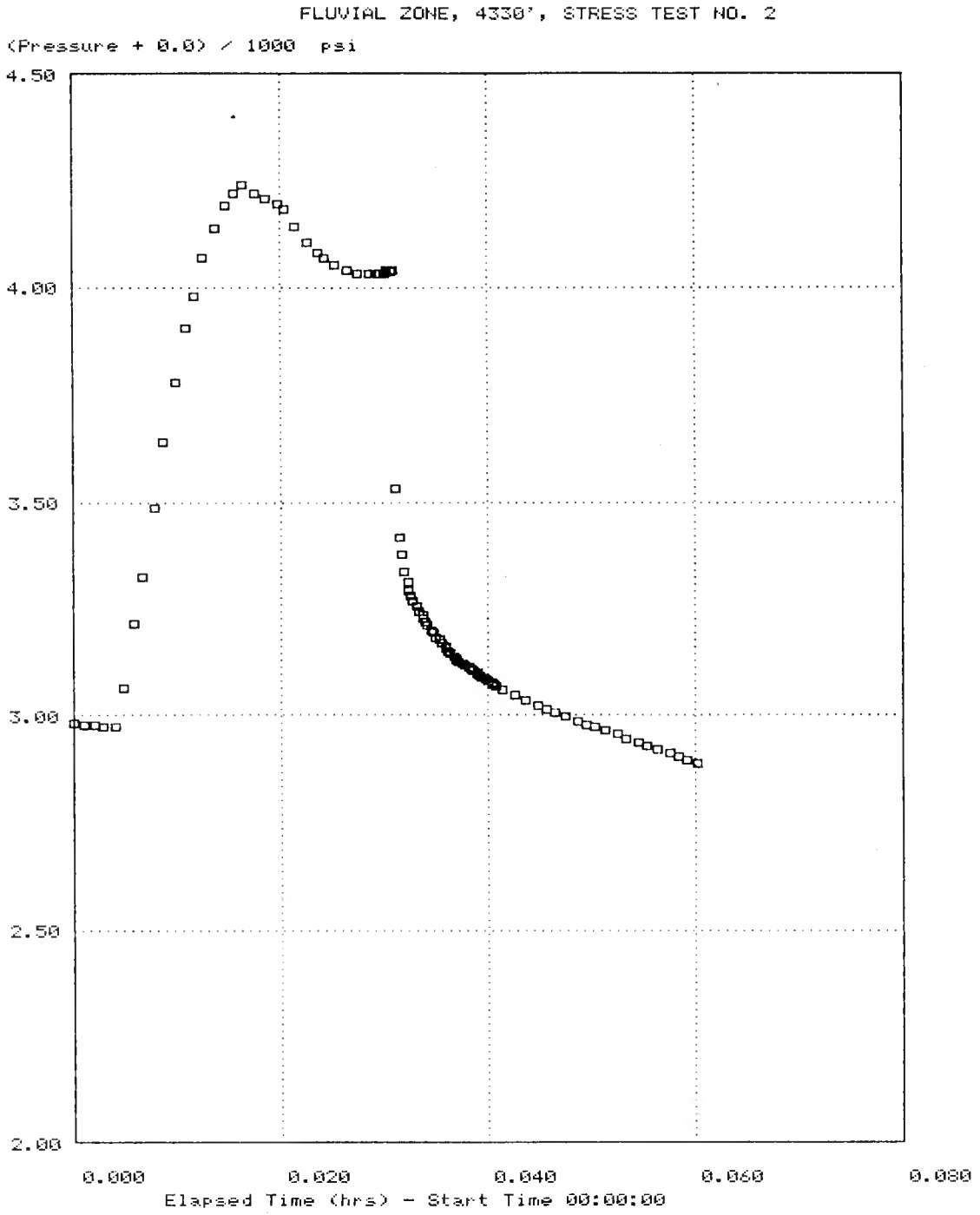


FIGURE A.2: Sandstone Stress Test (4330–4332'), Linear Plot of Test No. 2 Injection/Decline.

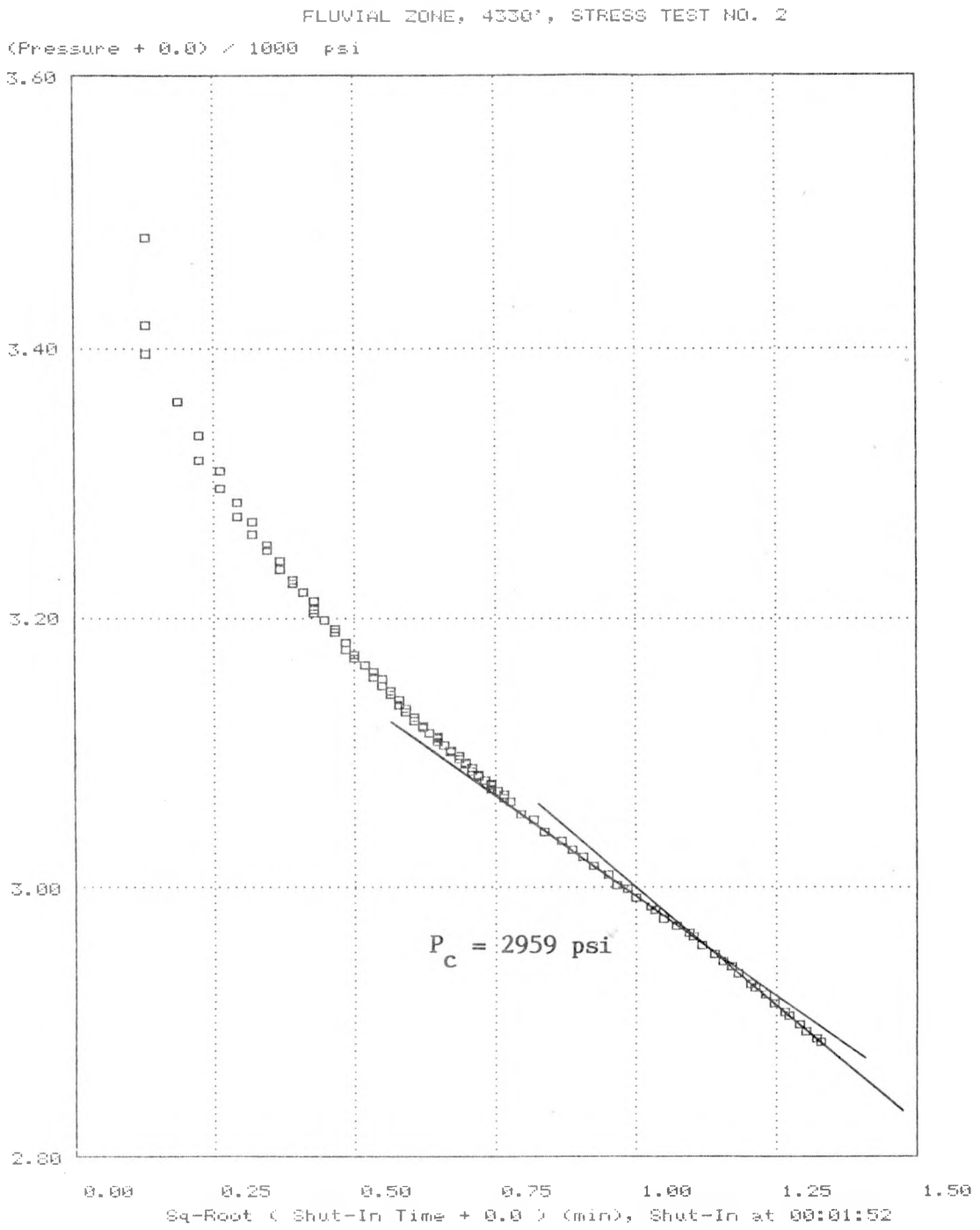


FIGURE A.3: Sandstone Stress Test (4330–4332'), Square-Root of Shut-In Time Plot of Test No. 2 Pressure Decline.

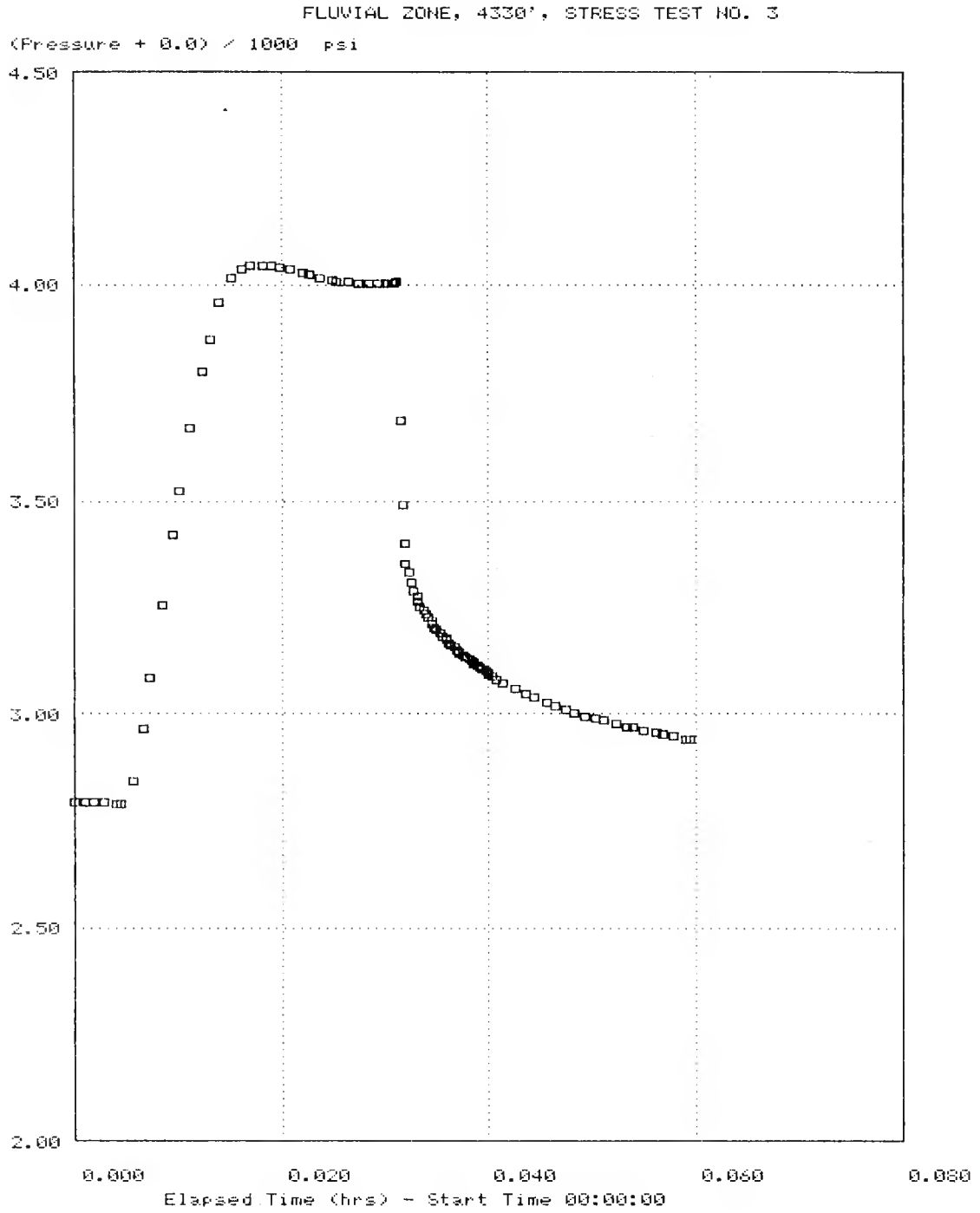


FIGURE A.4: Sandstone Stress Test (4330-4332'), Linear Plot of Test No. 3 Injection/Decline.

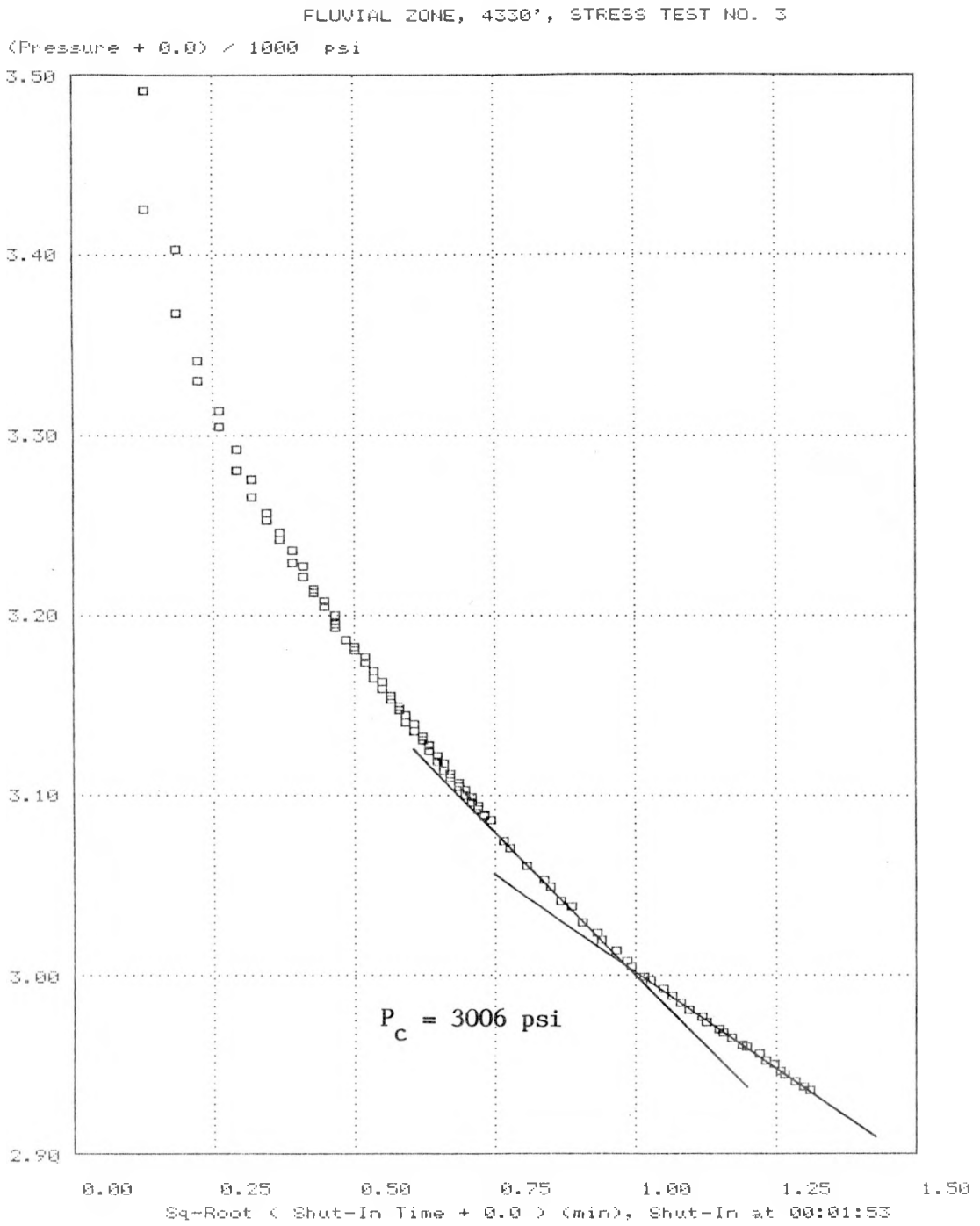


FIGURE A.5: Sandstone Stress Test (4330-4332'), Square-Root of Shut-In Time Plot of Test No. 3 Pressure Decline.

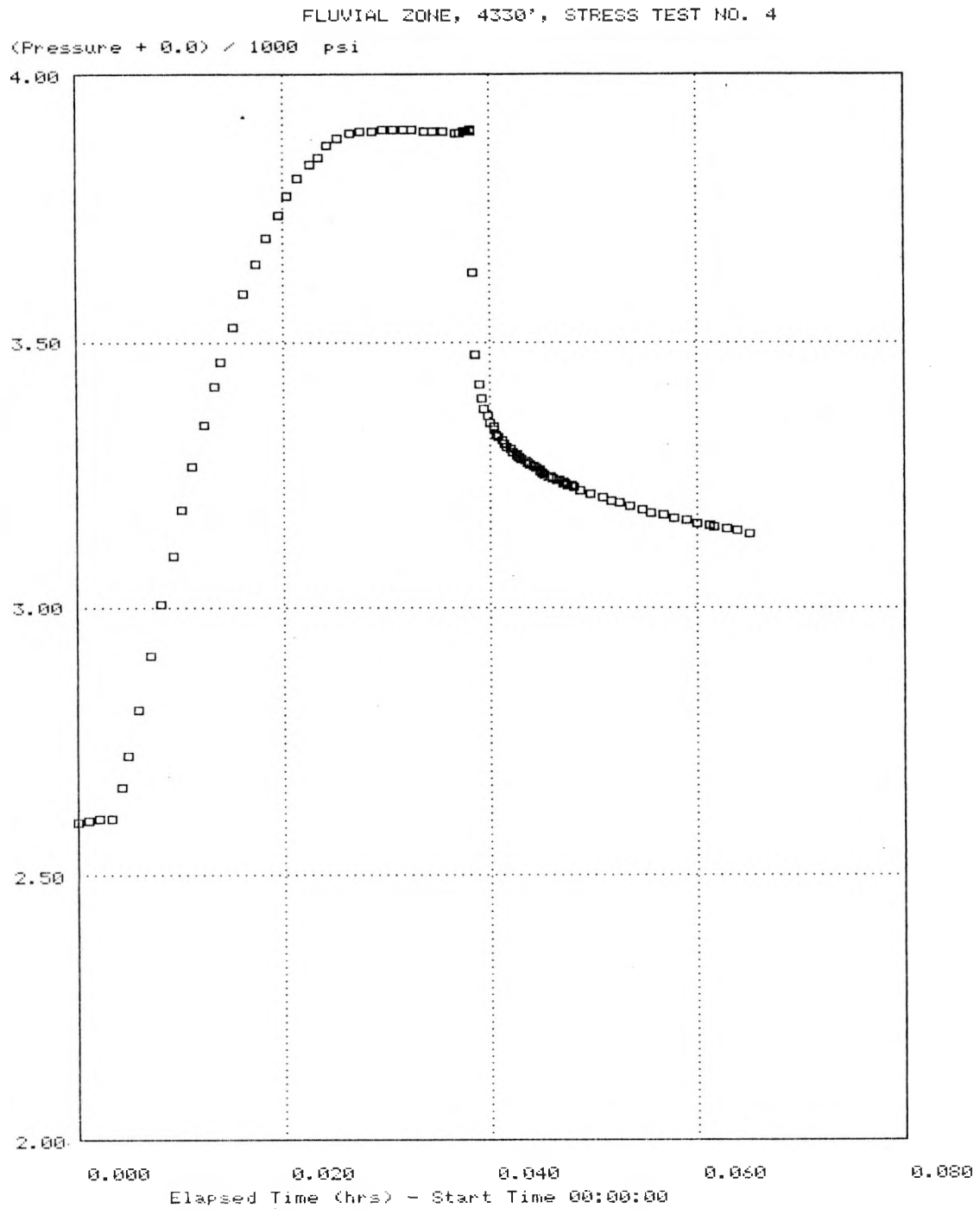


FIGURE A.6: Sandstone Stress Test (4330-4332'), Linear Plot of Test No. 4 Injection/Decline.

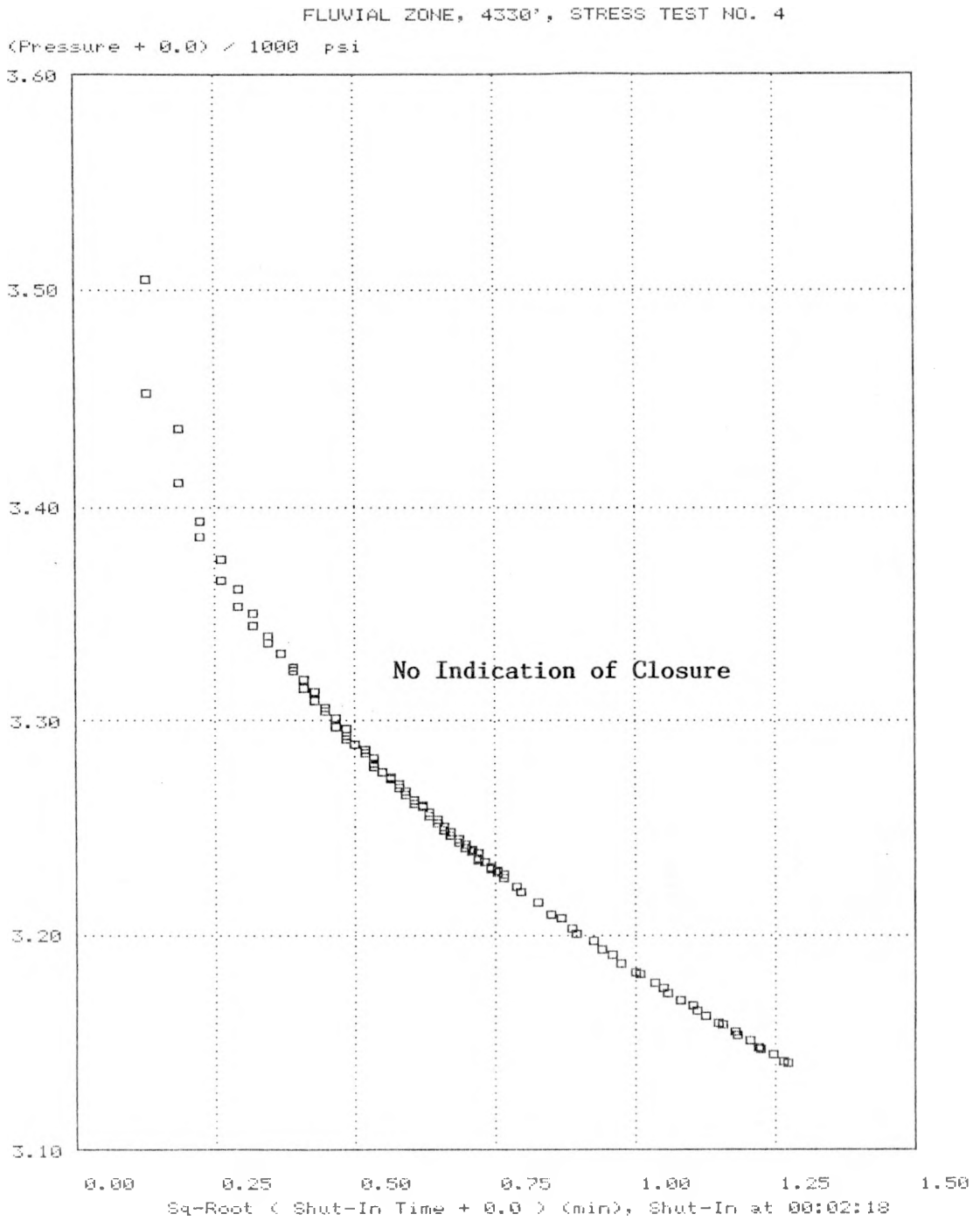


FIGURE A.7: Sandstone Stress Test (4330–4332'), Square-Root of Shut-In Time Plot of Test No. 4 Pressure Decline.

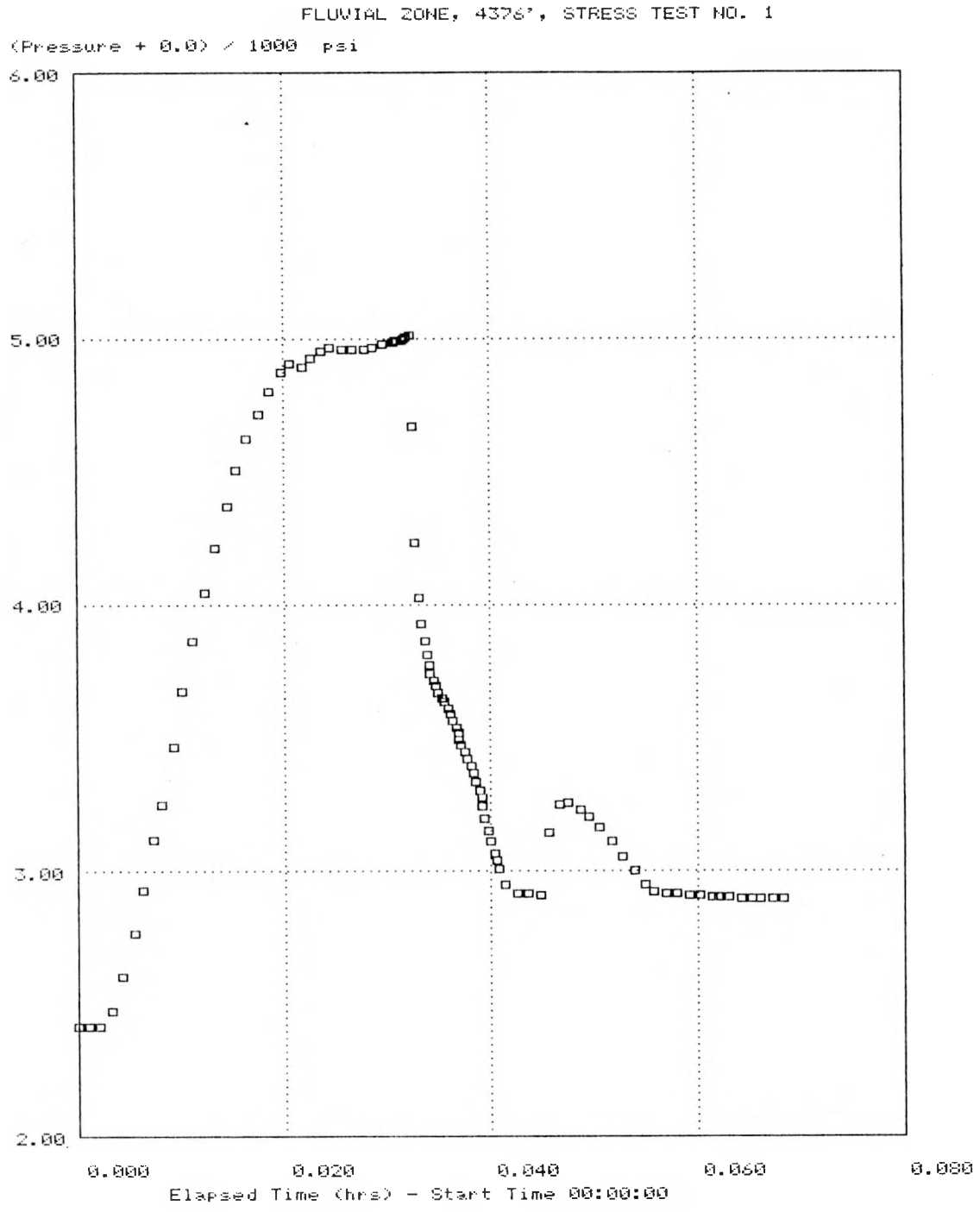


FIGURE A.8: Shale Stress Test (4376-4378'), Linear Plot of Test No. 1 Injection/Decline.

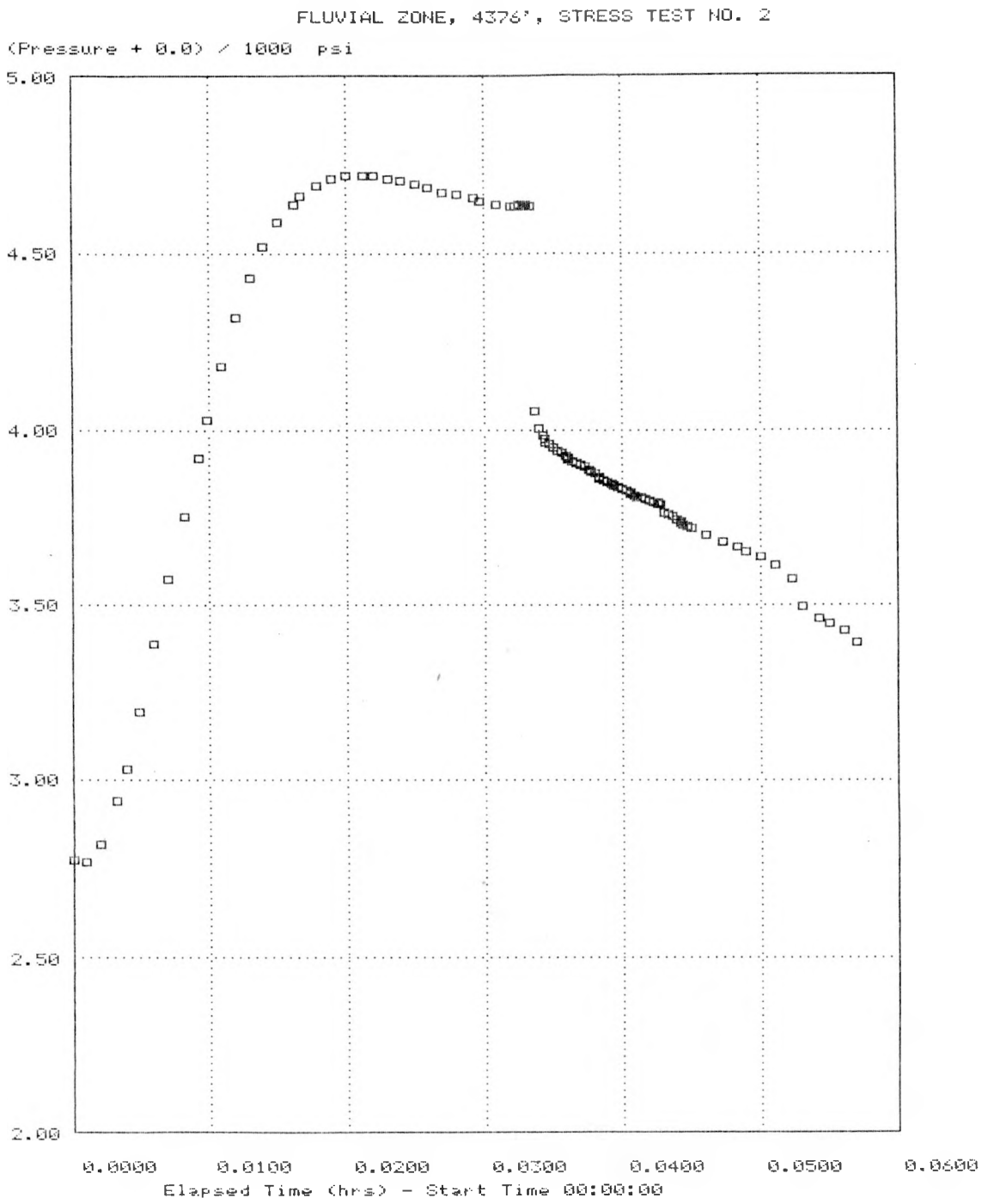


FIGURE A.9: Shale Stress Test (4376-4378'), Linear Plot of Test No. 2 Injection/Decline.

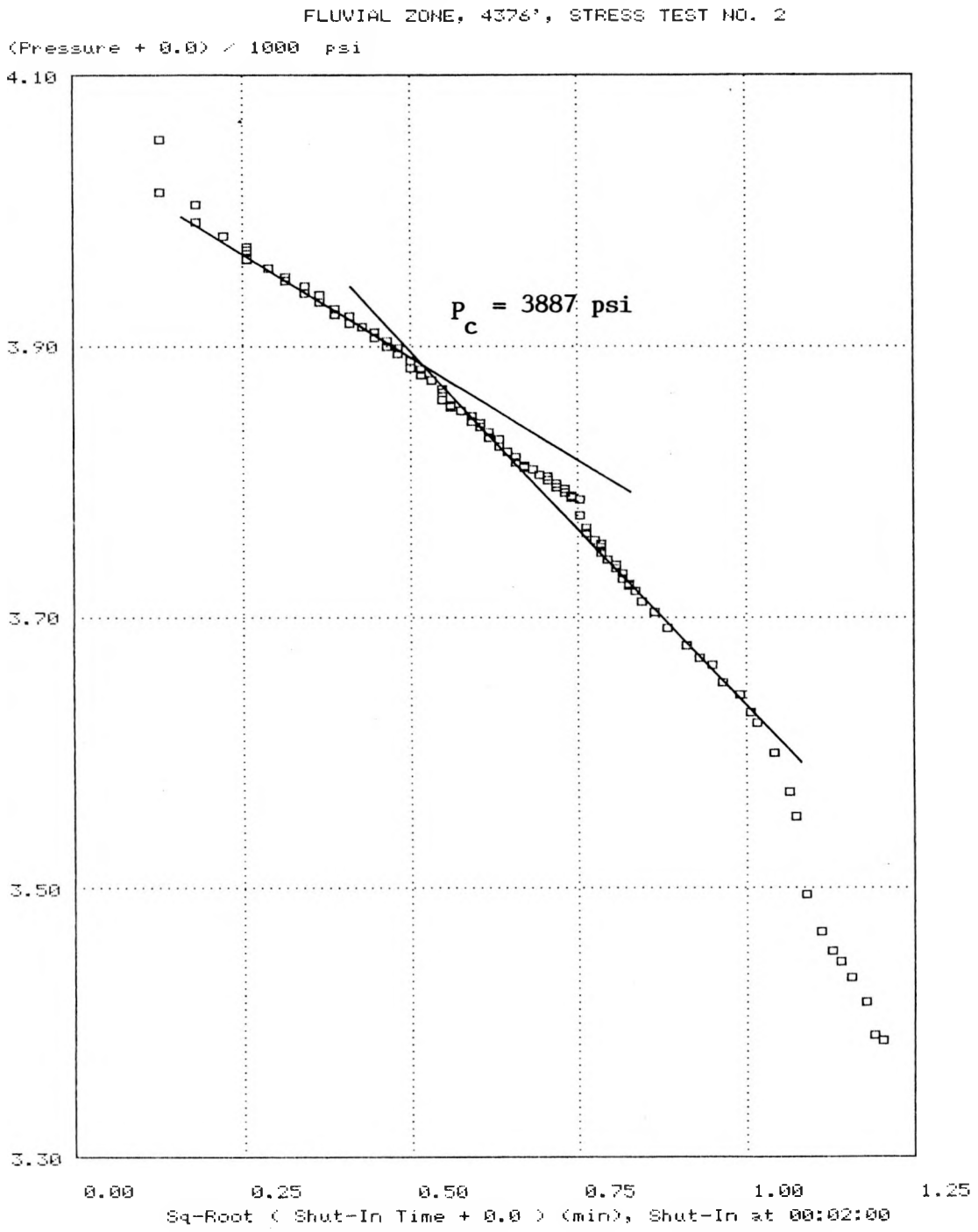


FIGURE A.10: Shale Stress Test (4376-4378'), Square-Root of Shut-In Time Plot of Test No. 2 Pressure Decline.

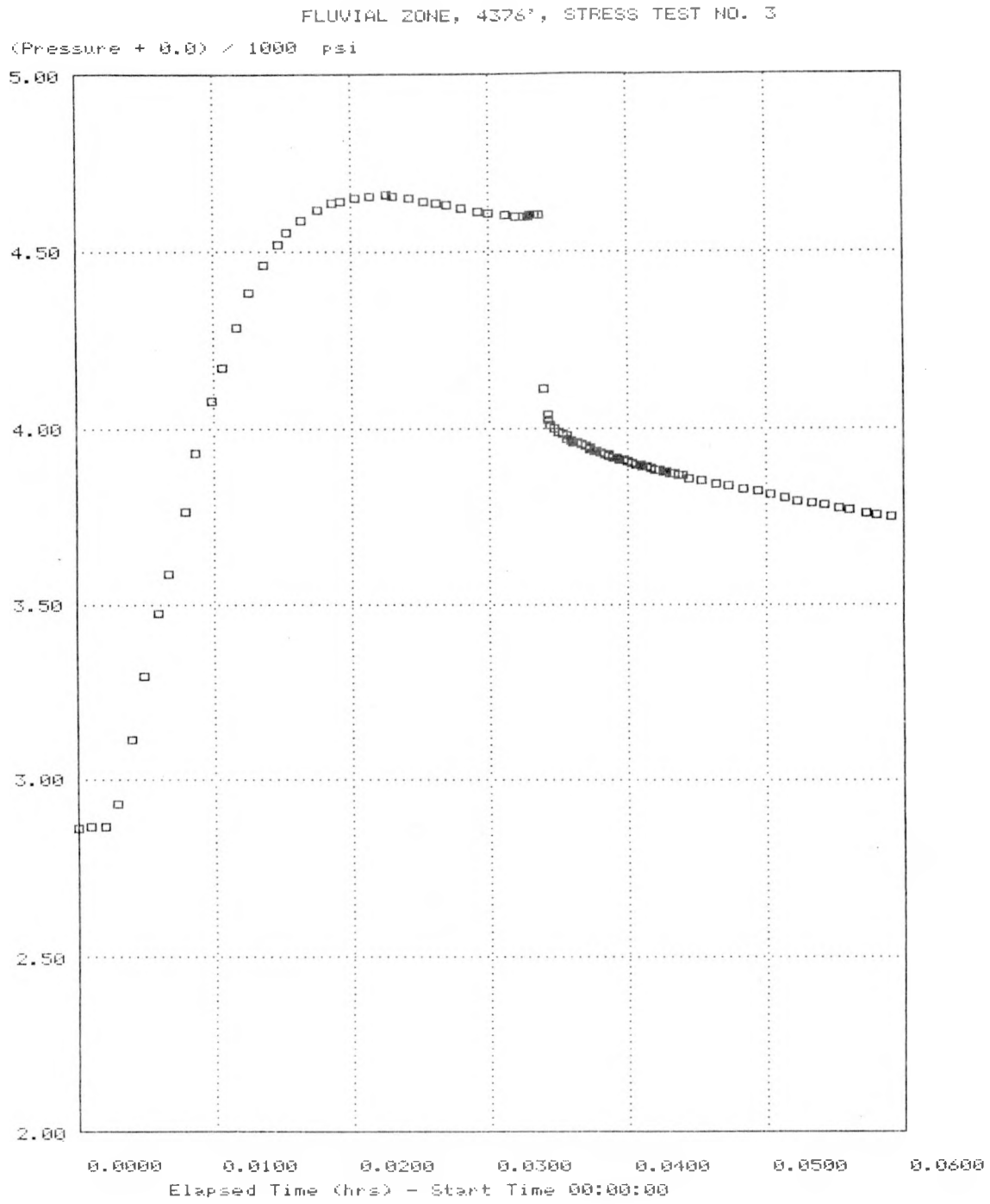


FIGURE A.11: Shale Stress Test (4376-4378'), Linear Plot of Test No. 3 Injection/Decline.

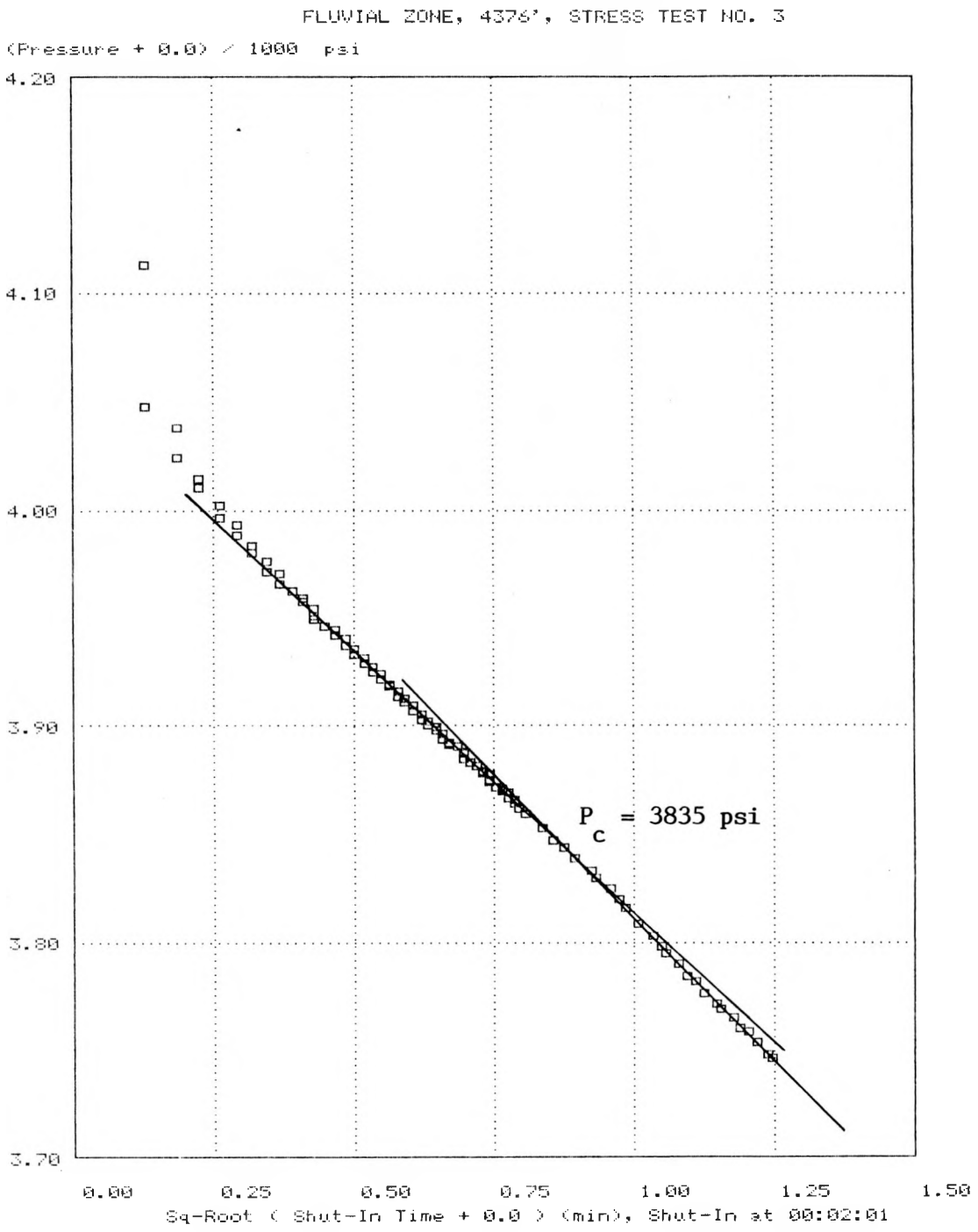


FIGURE A.12: Shale Stress Test (4376–4378'), Square-Root of Shut-In Time Plot of Test No. 3 Pressure Decline.

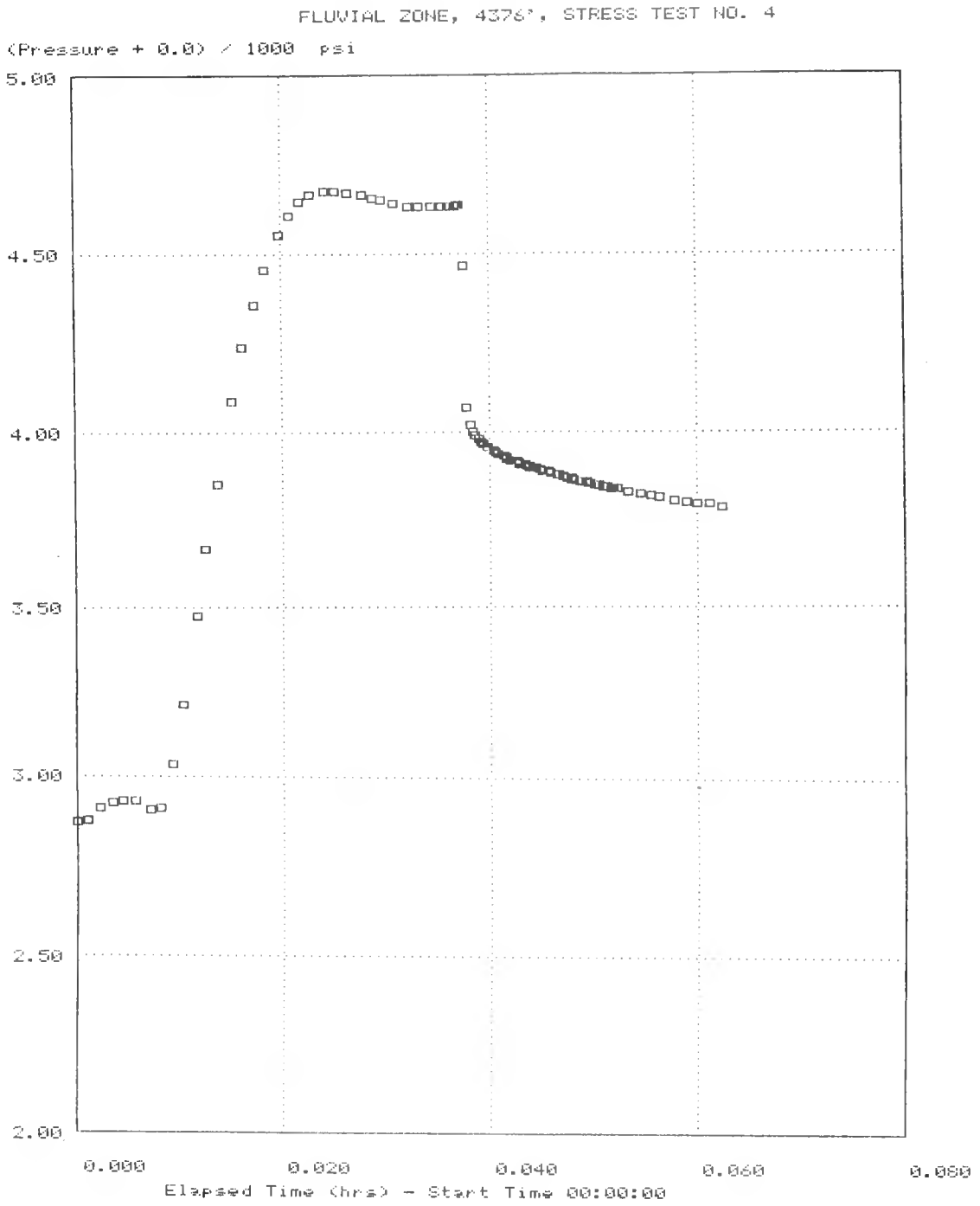


FIGURE A.13: Shale Stress Test (4376-4378'), Linear Plot of Test No. 4 Injection/Decline.

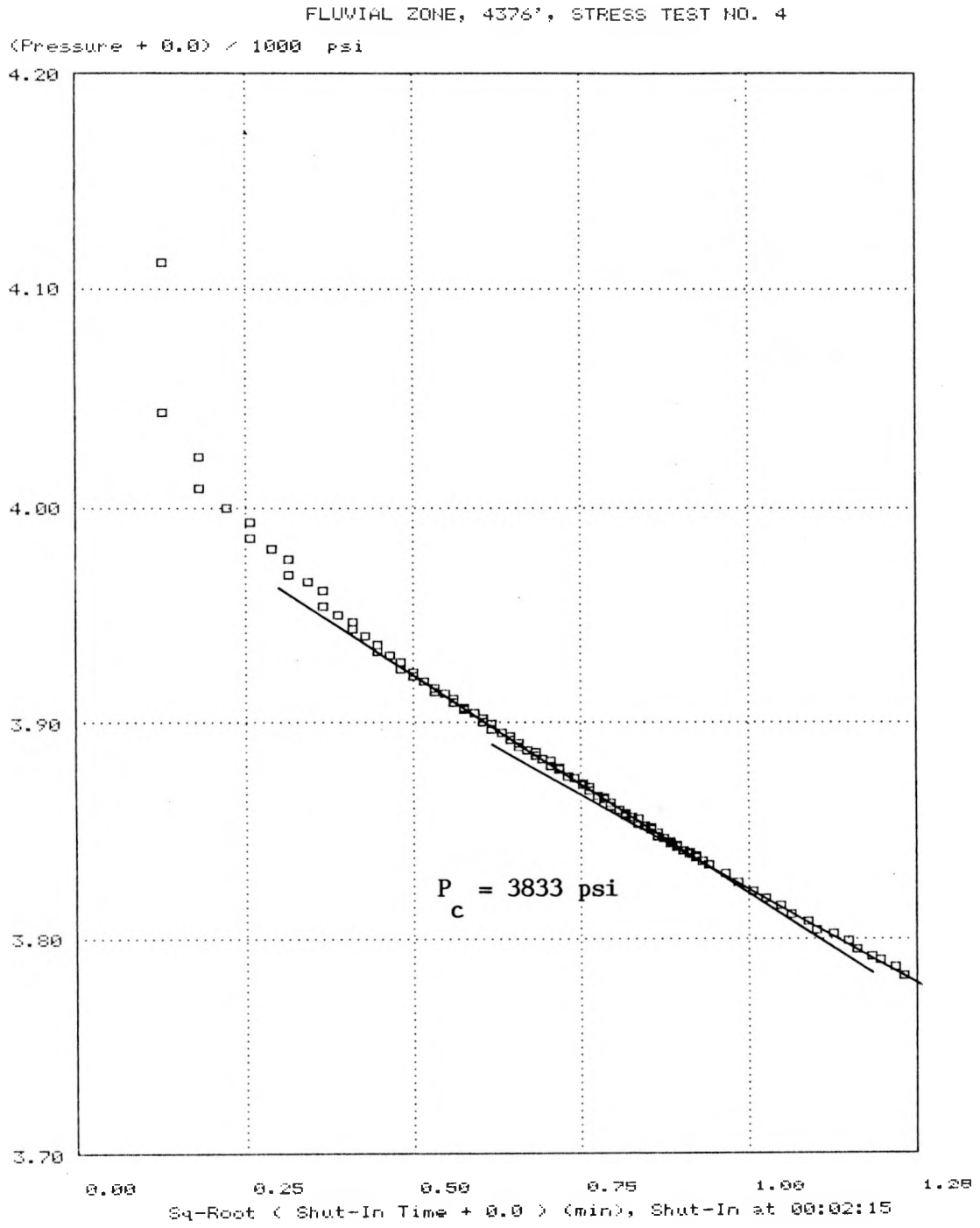


FIGURE A.14: Shale Stress Test (4376-4378'), Square-Root of Shut-In Time Plot of Test No. 4 Pressure Decline.

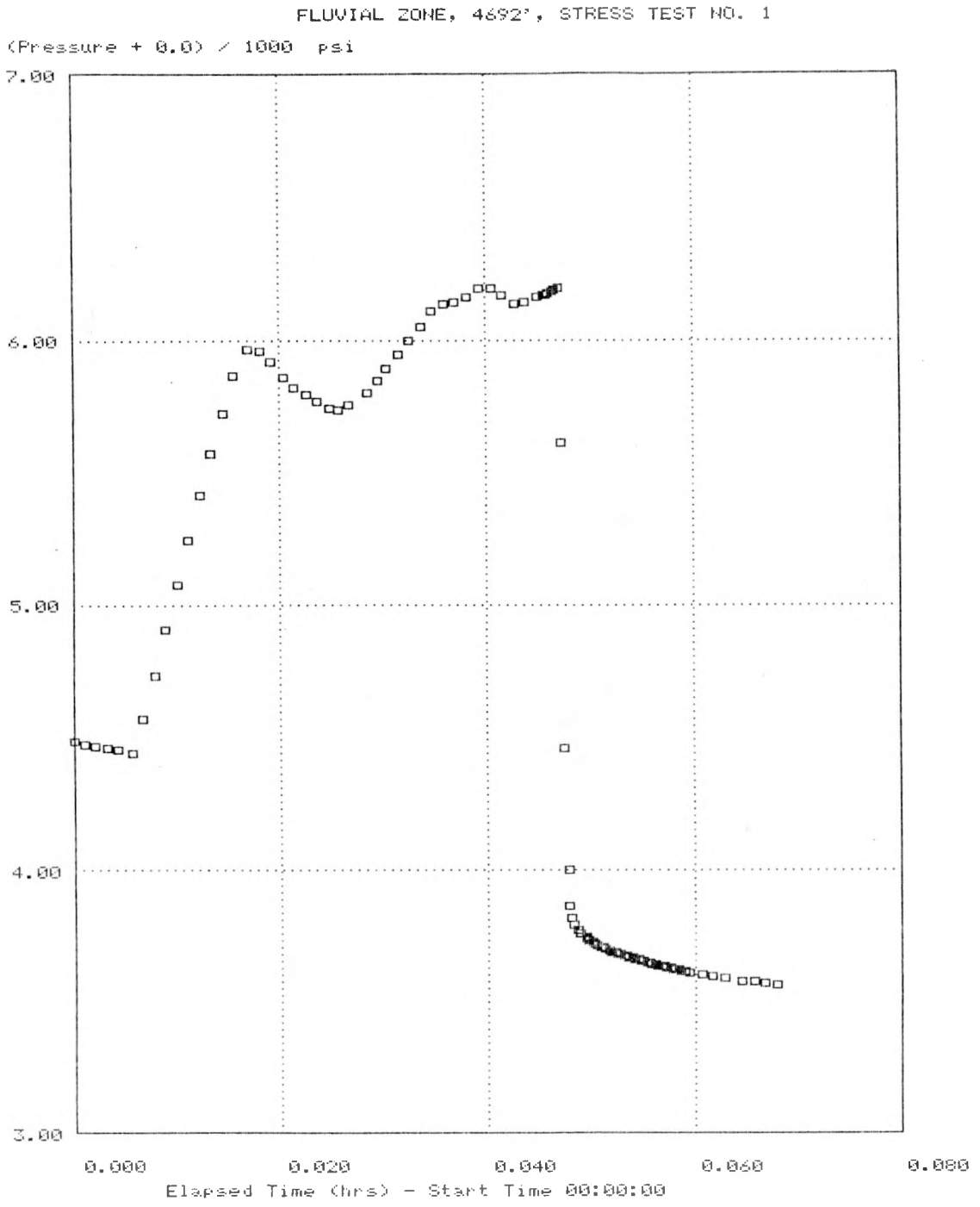


FIGURE A.15: Sandstone Stress Test (4692-4694'), Linear Plot of Test No. 1 Injection/Decline.

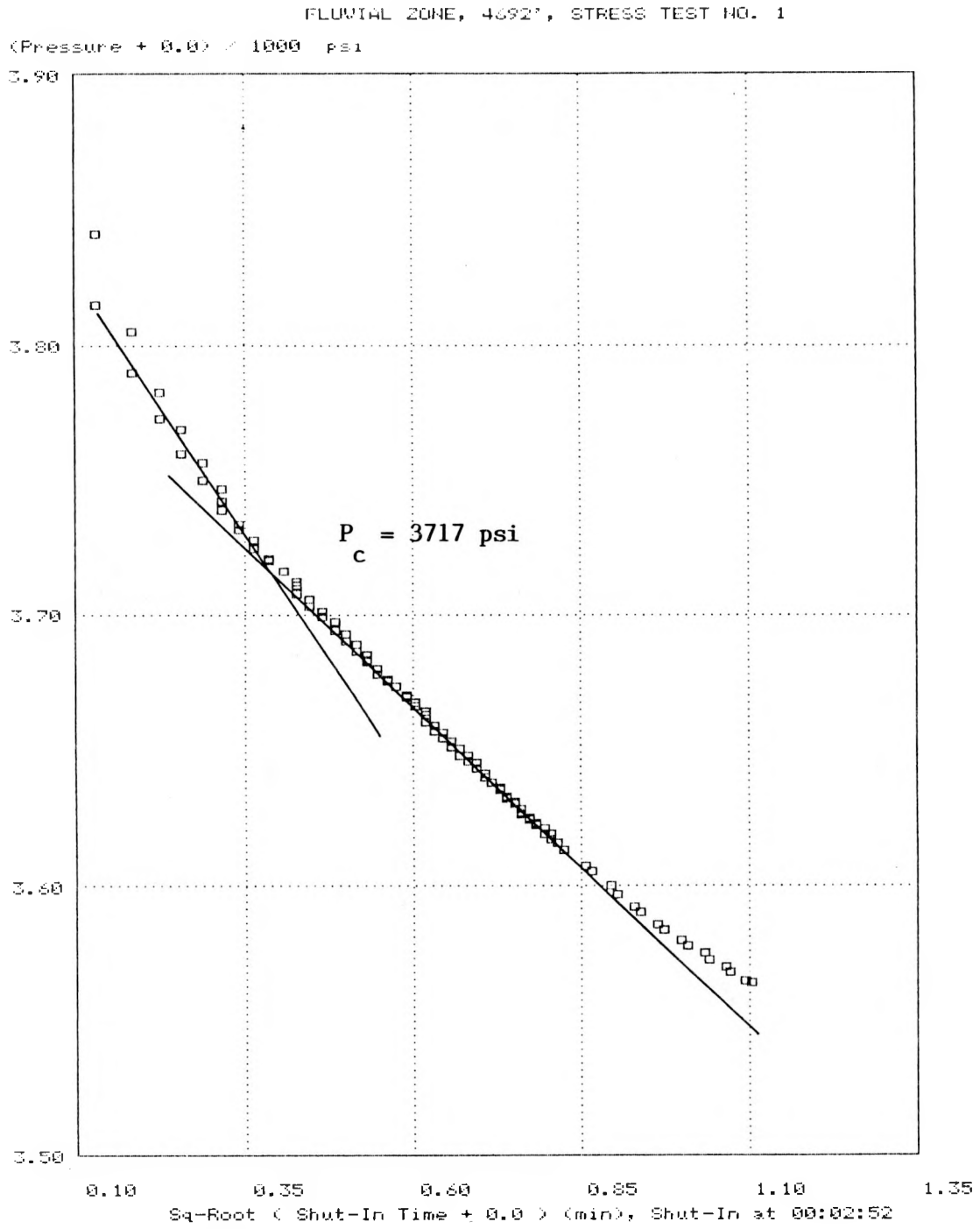


FIGURE A.16: Sandstone Stress Test (4692-4694'), Square-Root of Shut-In Time Plot of Test No. 1 Pressure Decline.

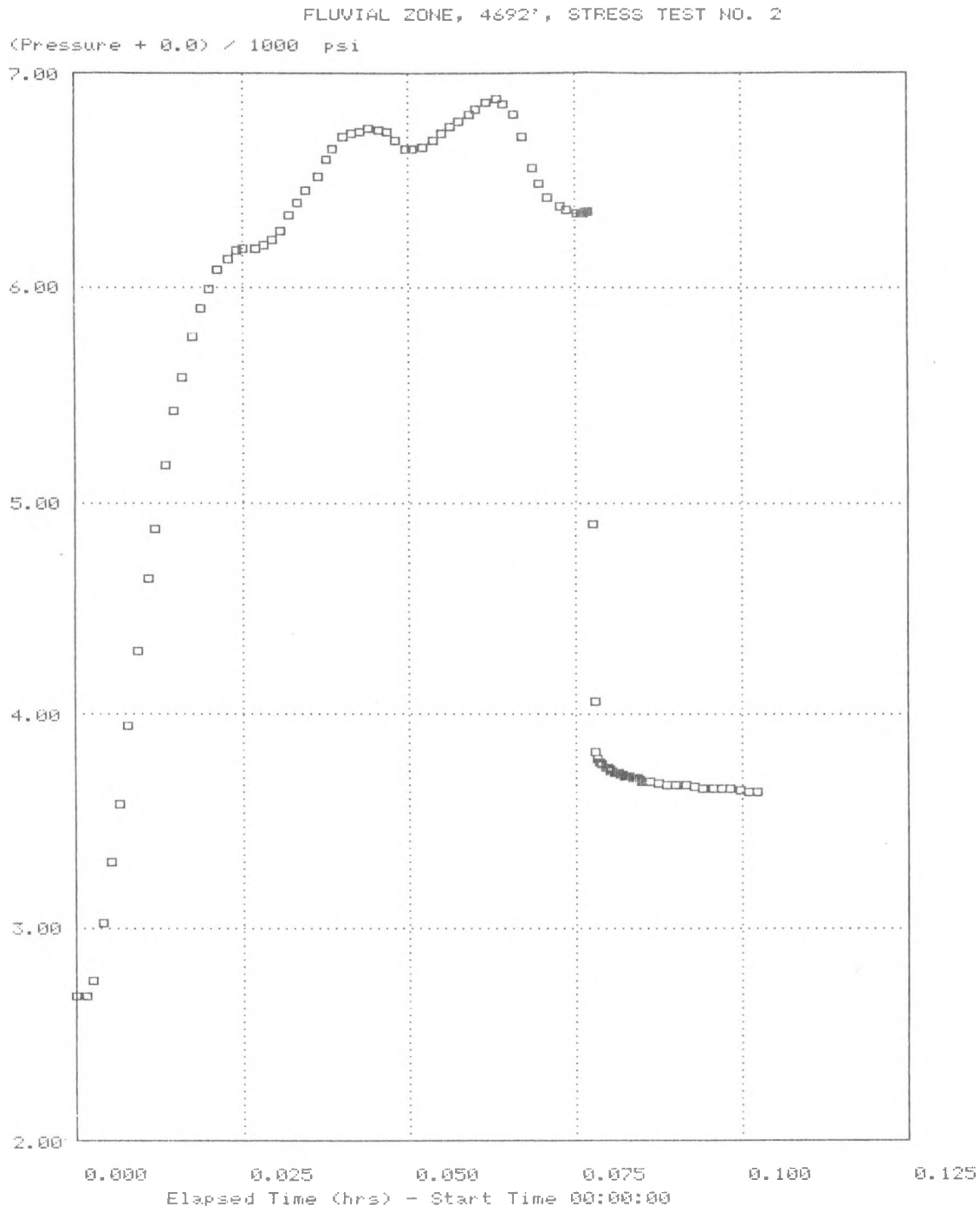


FIGURE A.17: Sandstone Stress Test (4692-4694'), Linear Plot of Test No. 2 Injection/Decline.

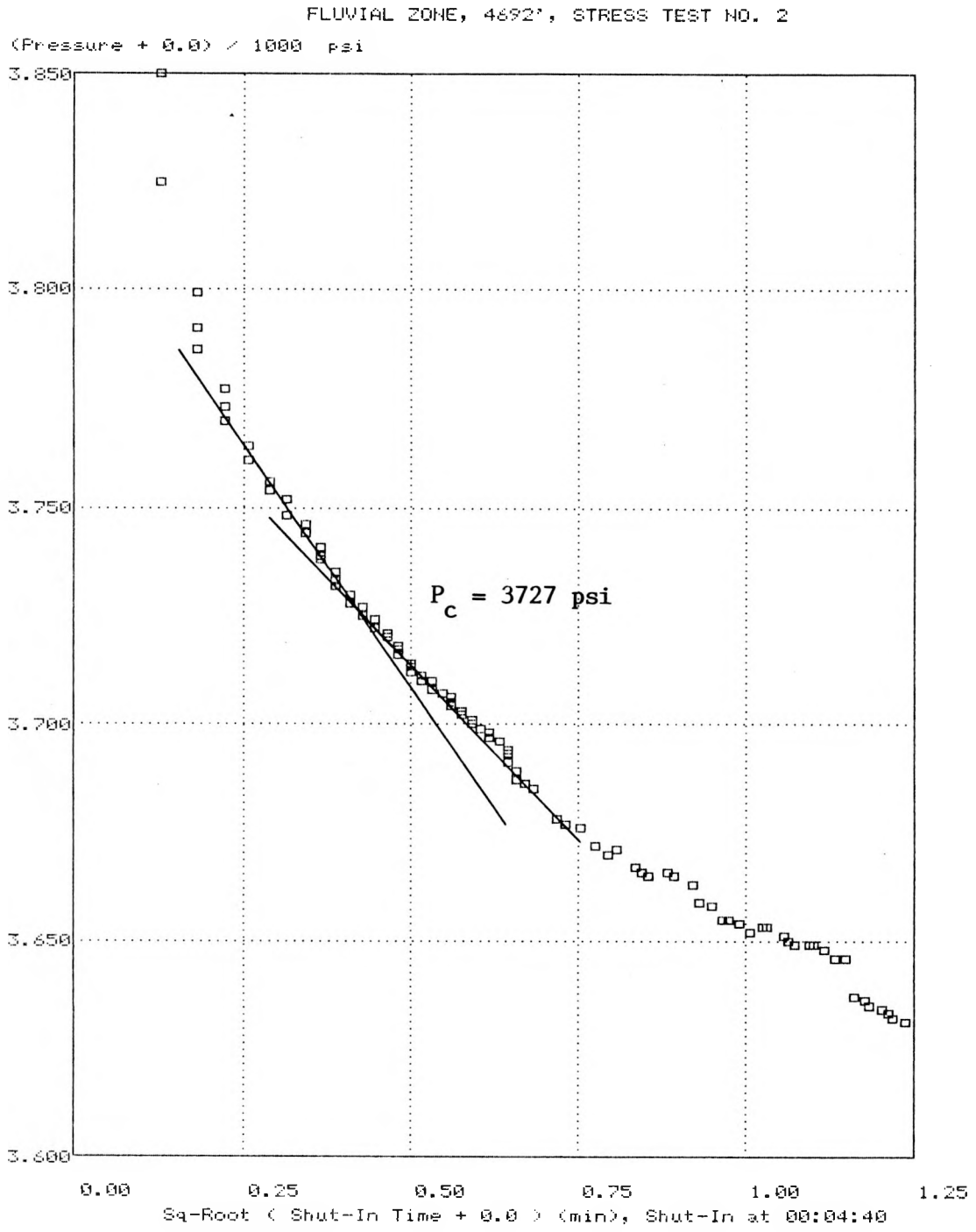


FIGURE A.18: Sandstone Stress Test (4692-4694'), Square-Root of Shut-In Time Plot of Test No. 2 Pressure Decline.

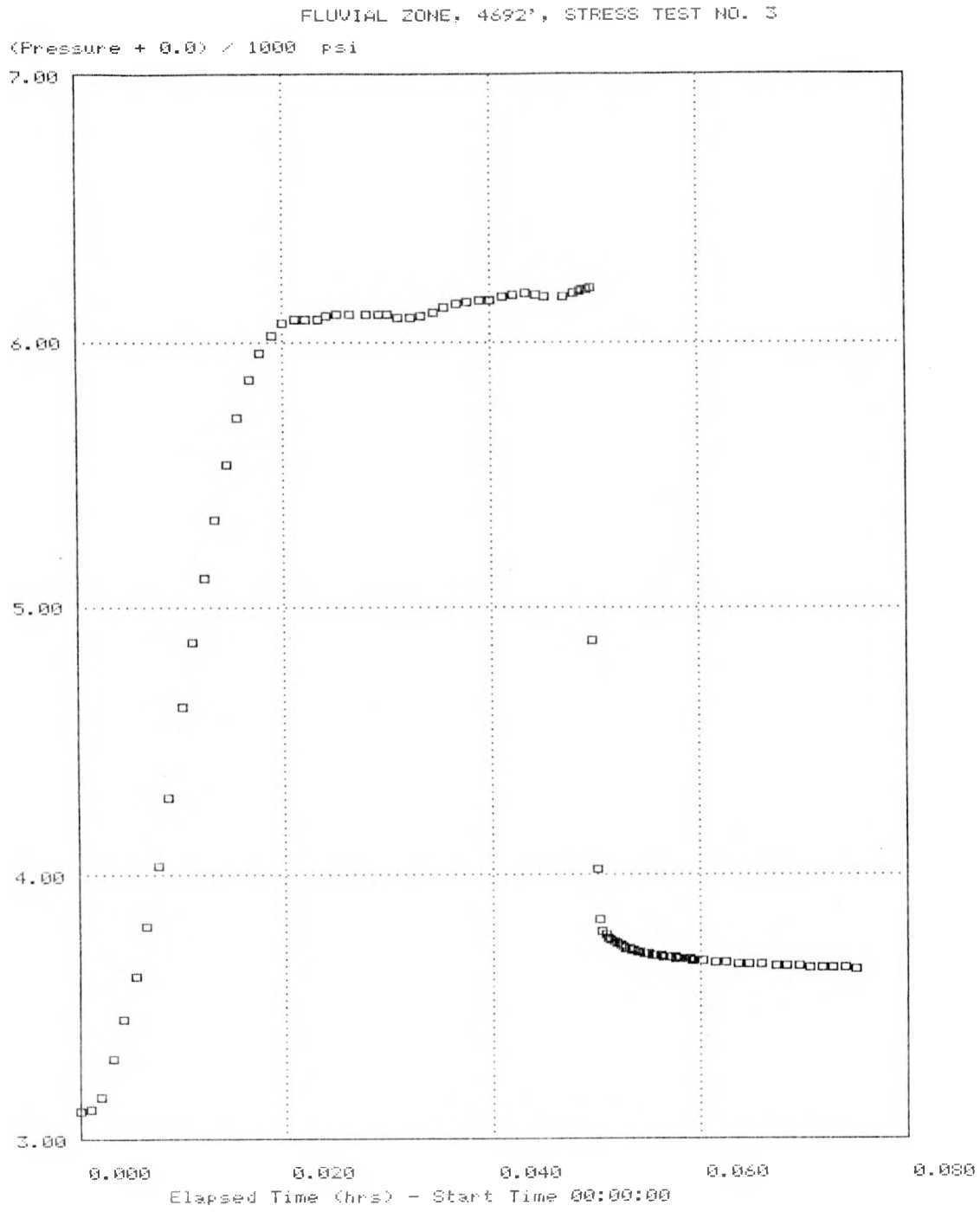


FIGURE A.19: Sandstone Stress Test (4692-4694'), Linear Plot of Test No. 3 Injection/Decline.

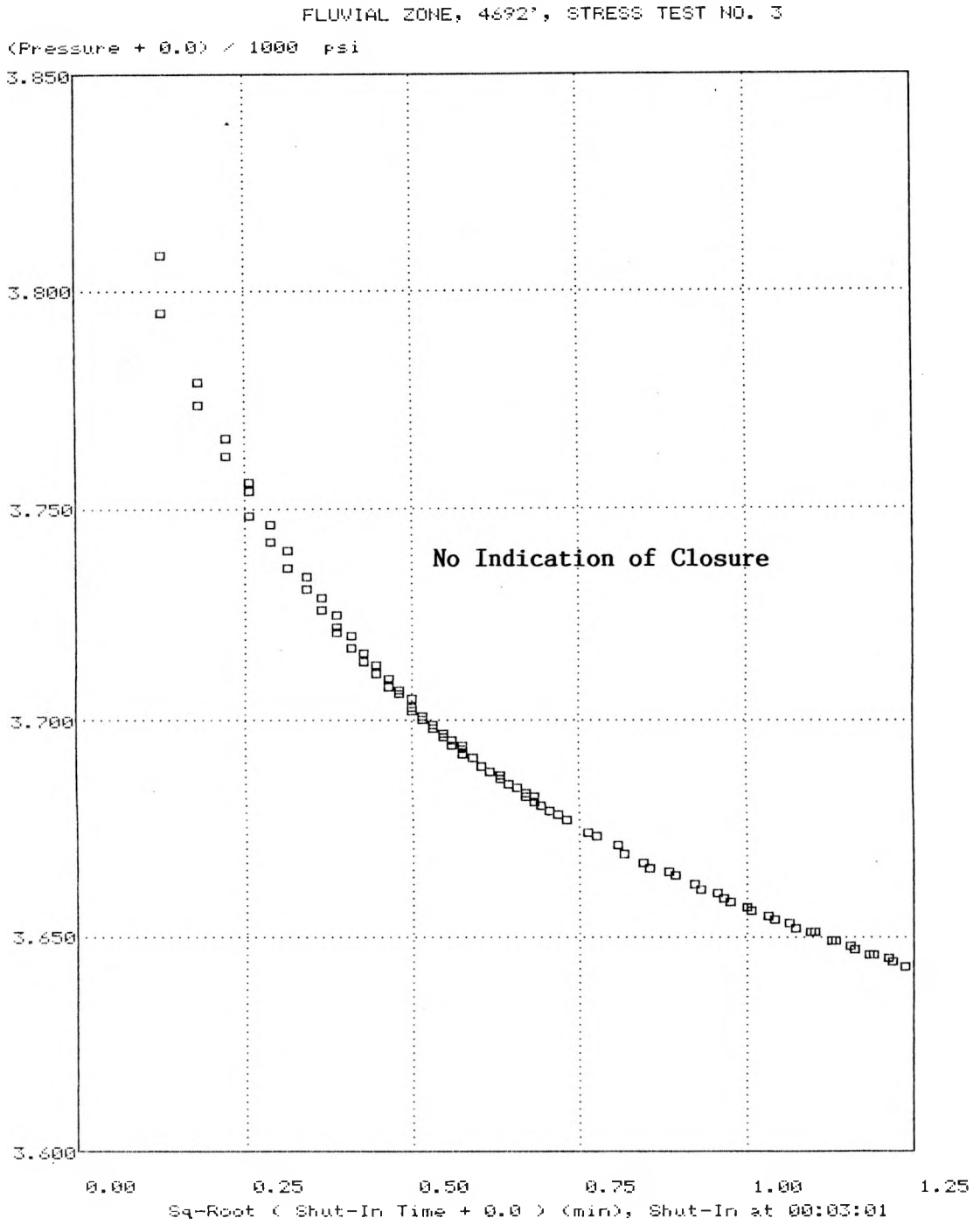


FIGURE A.20: Sandstone Stress Test (4692-4694'), Square-Root of Shut-In Time Plot of Test No. 3 Pressure Decline.

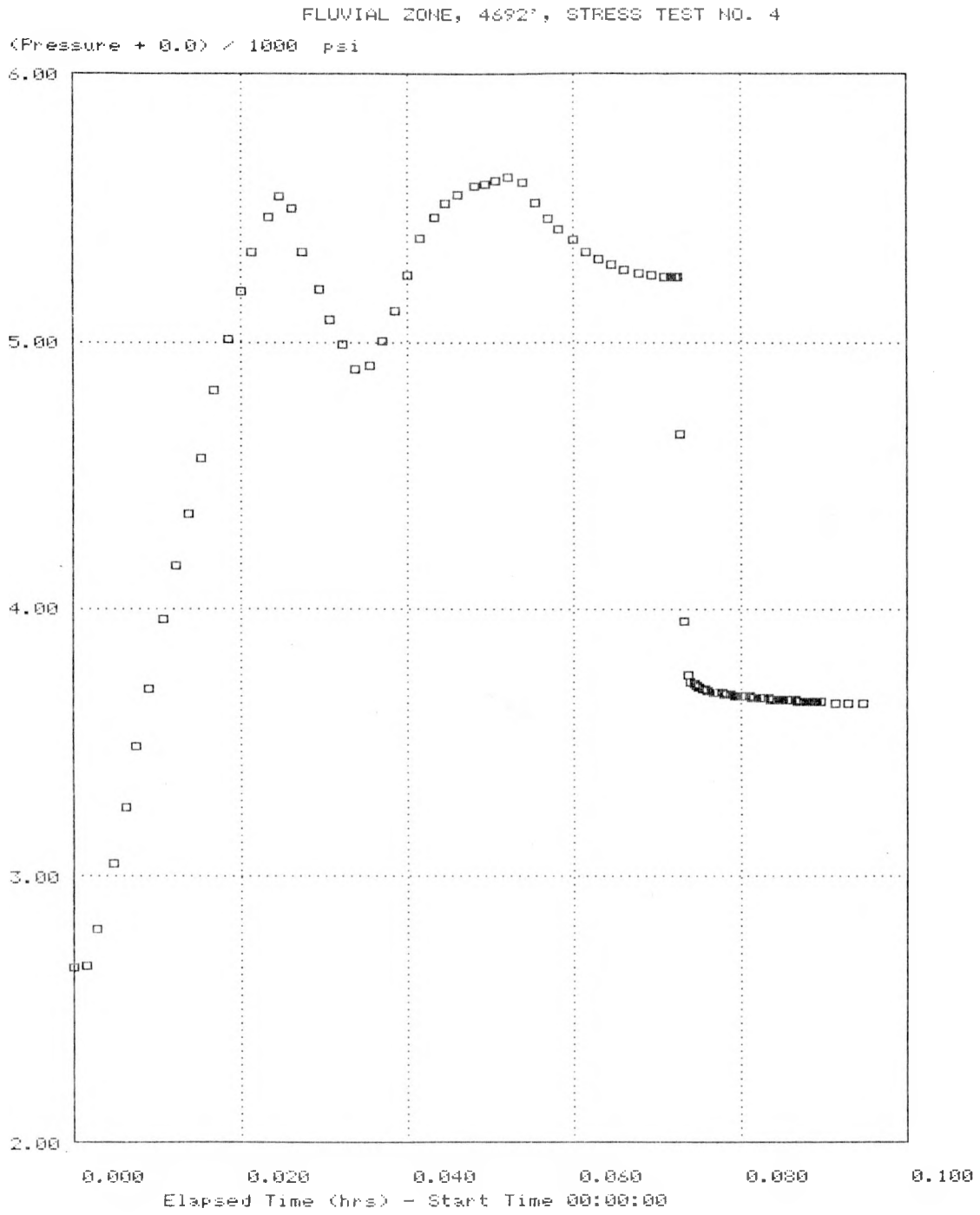


FIGURE A.21: Sandstone Stress Test (4692-4694'), Linear Plot of Test No. 4 Injection/Decline.

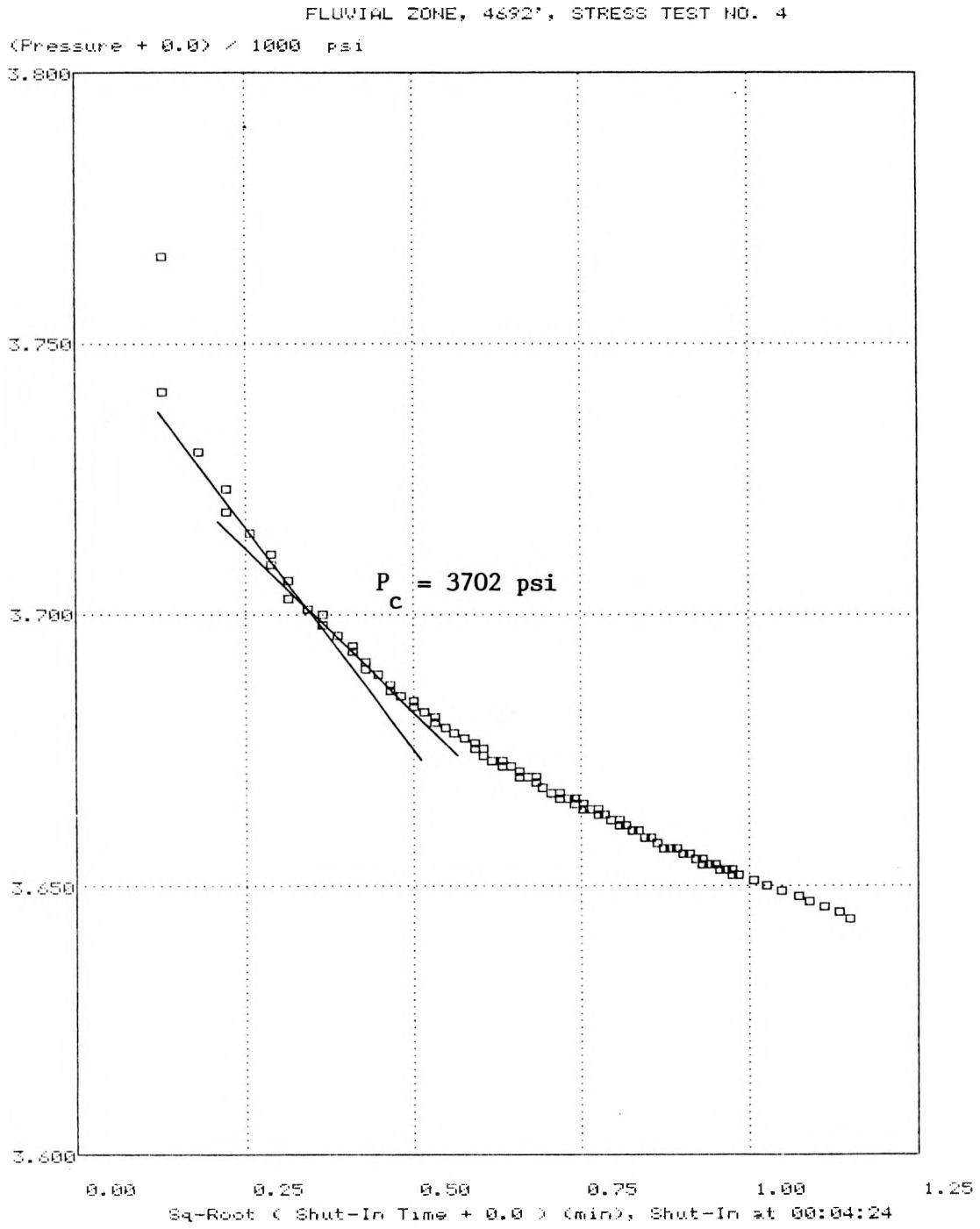


FIGURE A.22: Sandstone Stress Test (4692-4694'), Square-Root of Shut-In Time Plot of Test No. 4 Pressure Decline.

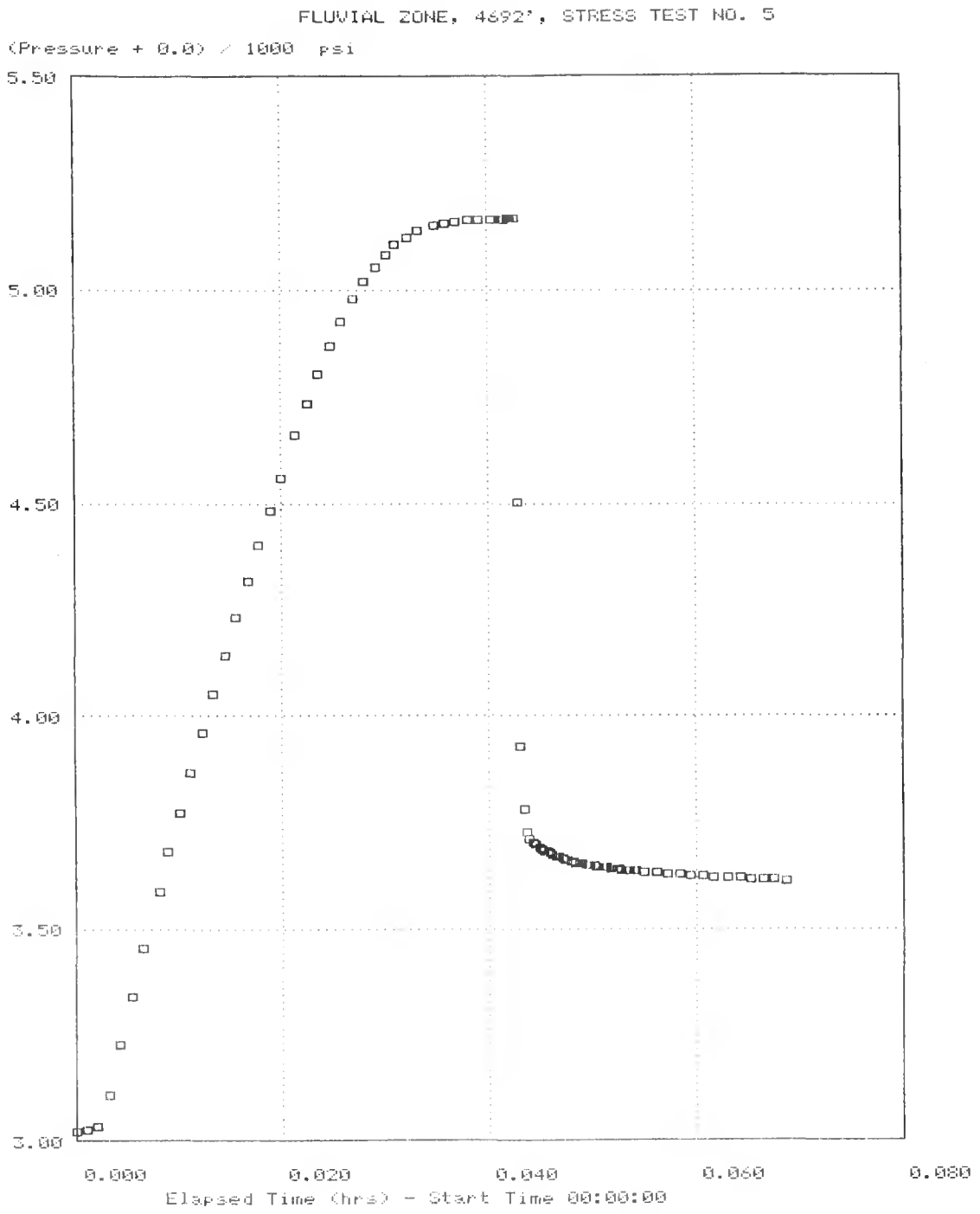


FIGURE A.23: Sandstone Stress Test (4692-4694'), Linear Plot of Test No. 5 Injection/Decline.

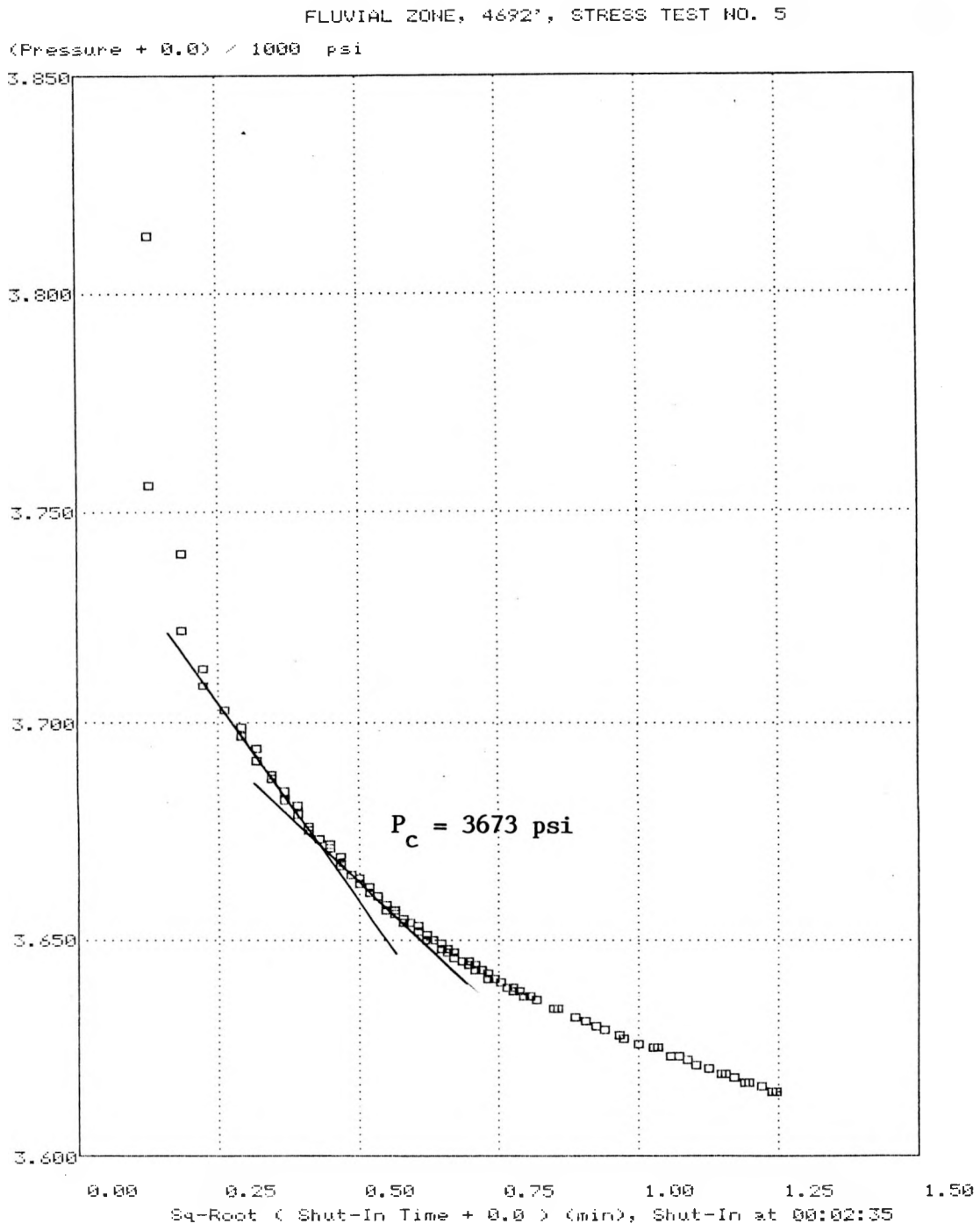


FIGURE A.24: Sandstone Stress Test (4692-4694'), Square-Root of Shut-in Time Plot of Test No. 5 Pressure Decline.

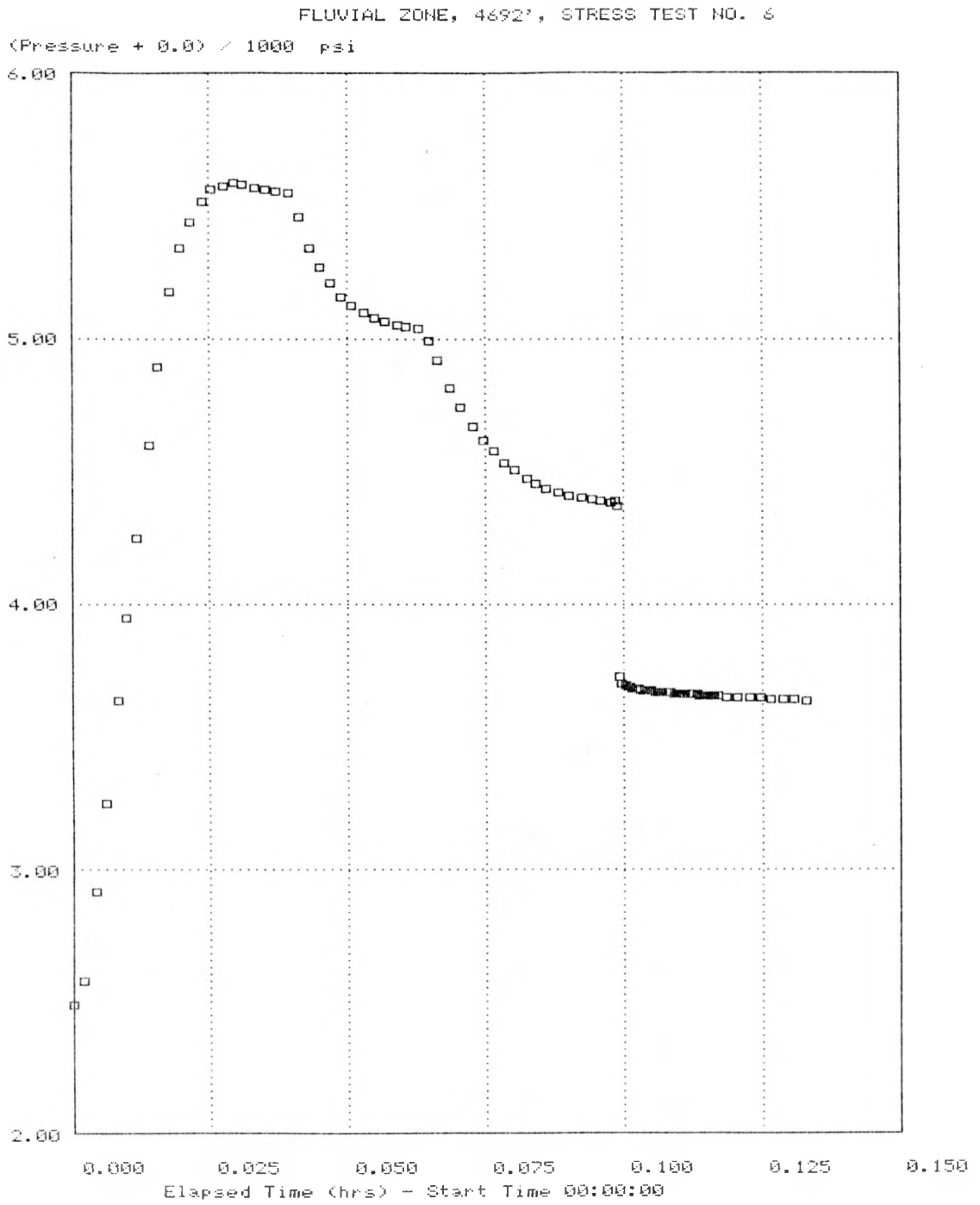


FIGURE A.25: Sandstone Stress Test (4692-4694'), Linear Plot of Test No. 6 Injection/Decline.

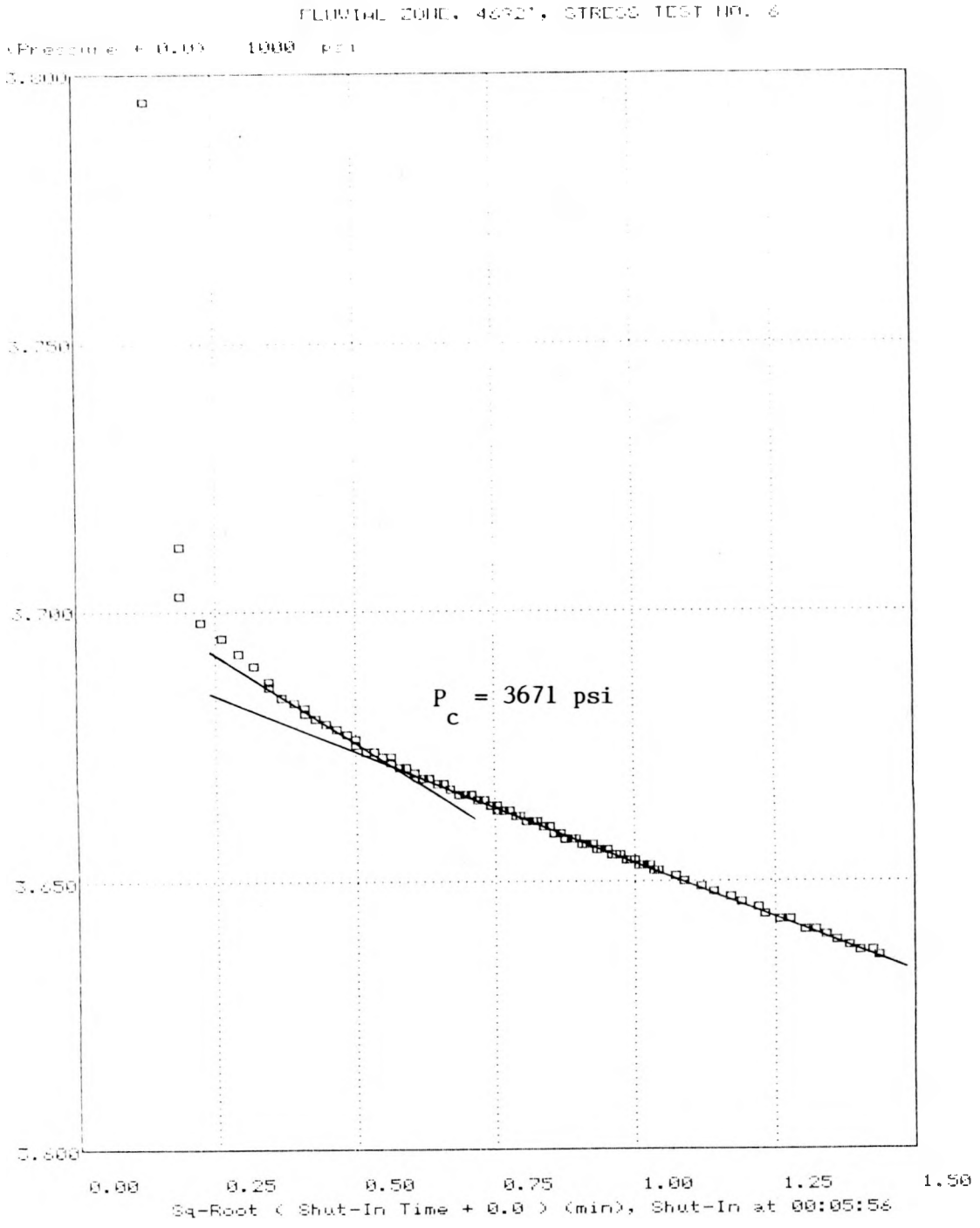


FIGURE A.26: Sandstone Stress Test (4692-4694'), Square-Root of Shut-In Time Plot of Test No. 6 Pressure Decline.

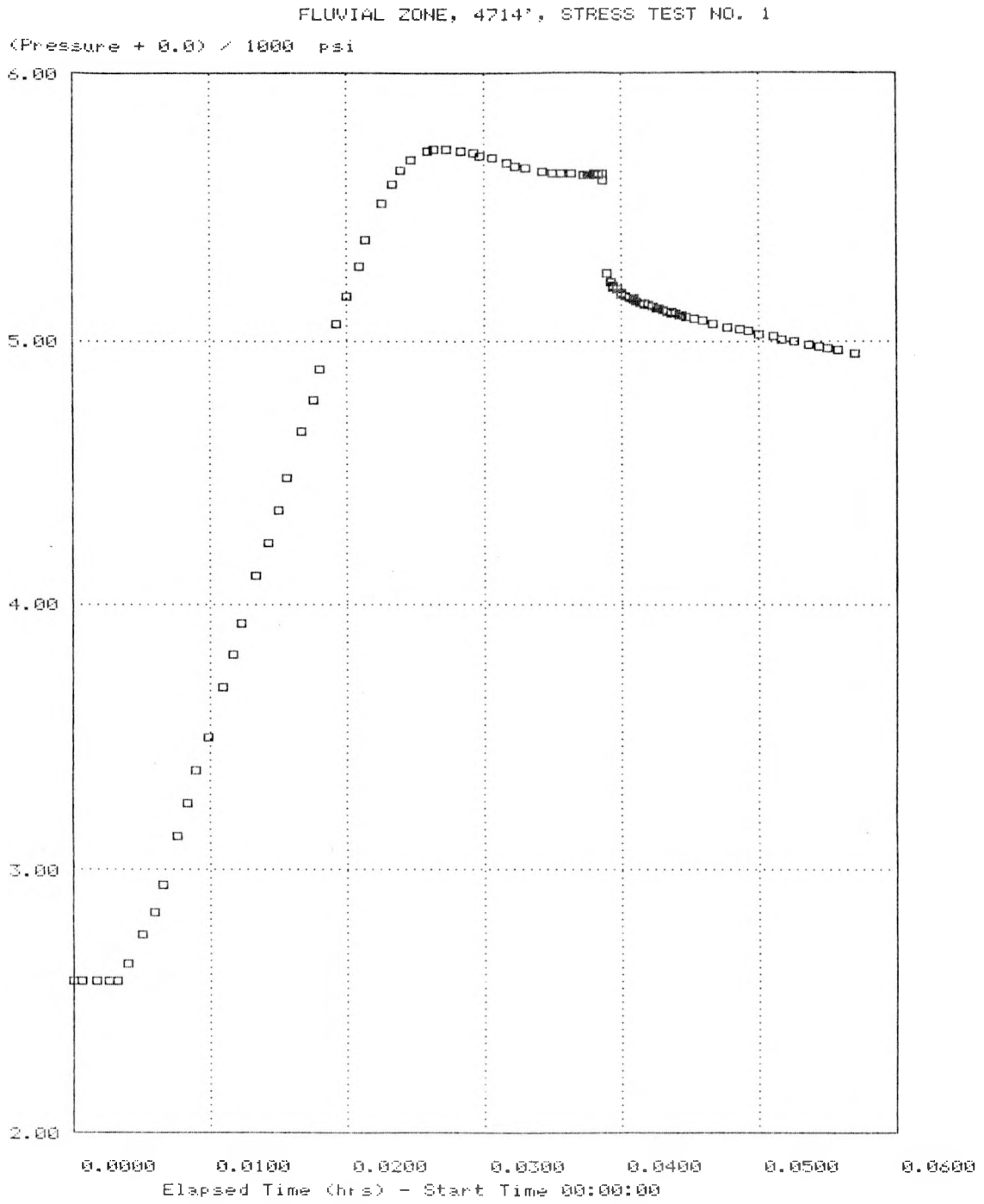


FIGURE A.27: Shale Stress Test (4714-4716'), Linear Plot of Test No. 1 Injection/Decline.

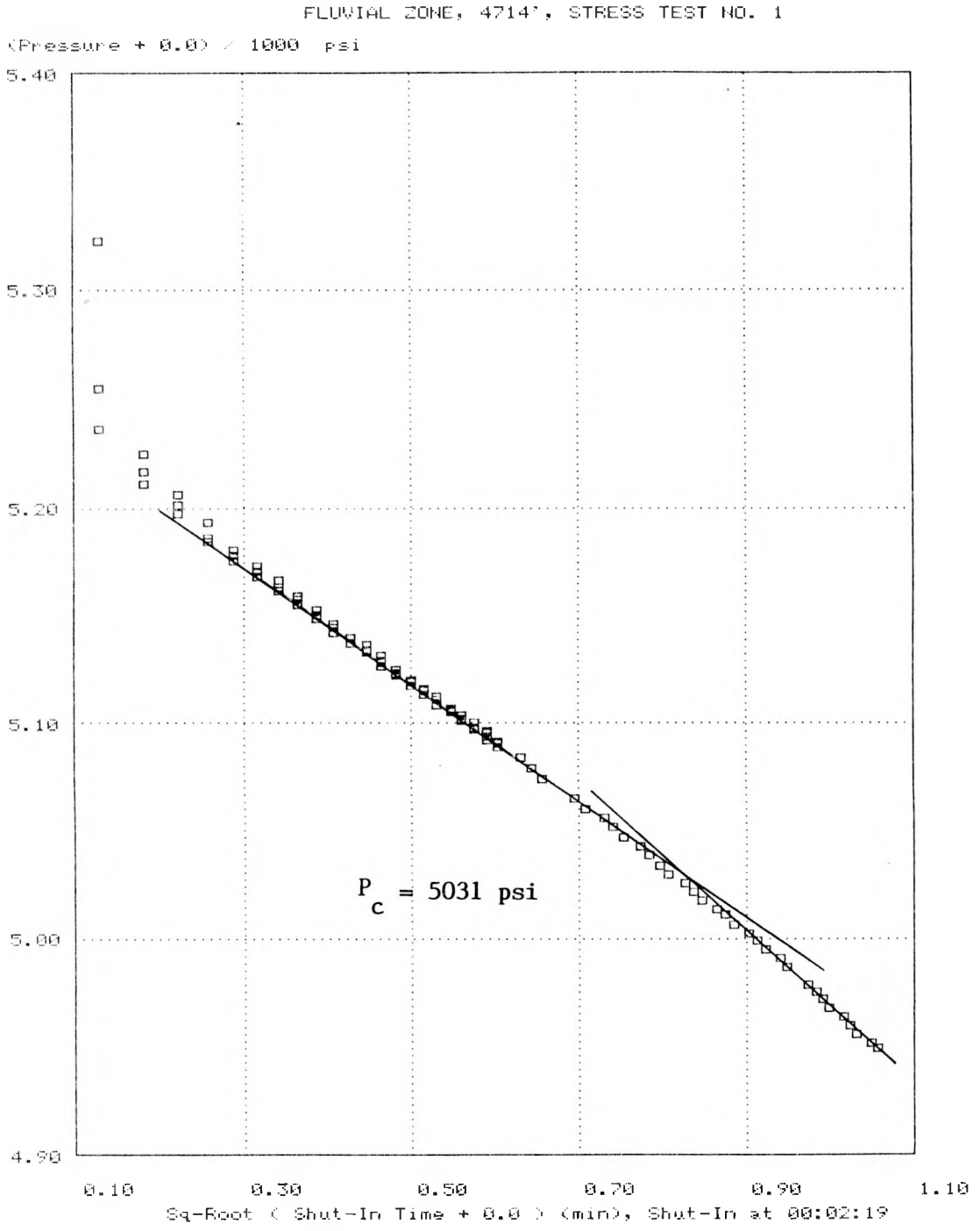


FIGURE A.28: Shale Stress Test (4714-4716'), Square-Root of Shut-In Time Plot of Test No. 1 Pressure Decline.

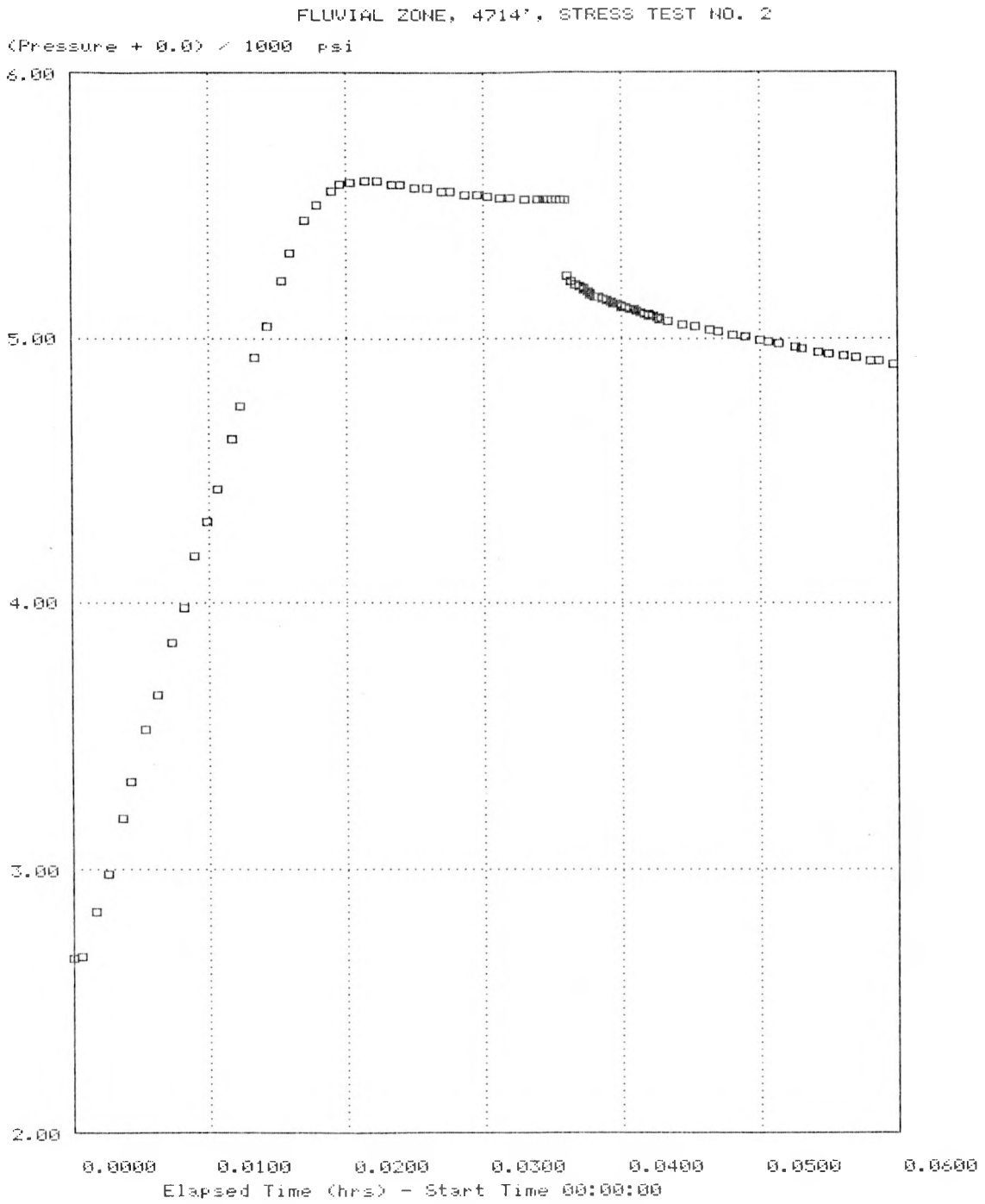


FIGURE A.29: Shale Stress Test (4714-4716'), Linear Plot of Test No. 2 Injection/Decline.

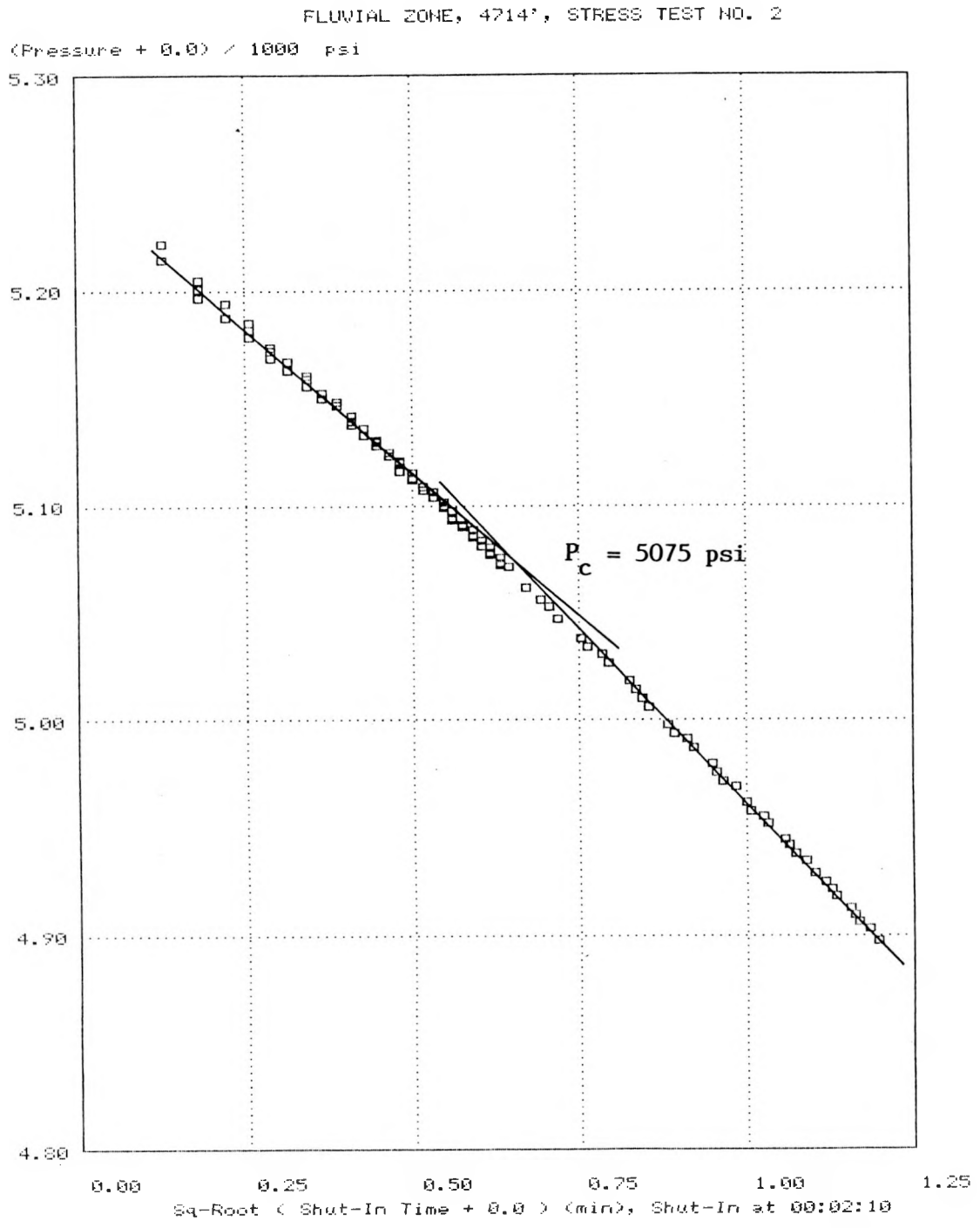


FIGURE A.30: Shale Stress test (4714-4716'), Square-Root of Shut-In Time Plot of Test No. 2 Pressure Decline.

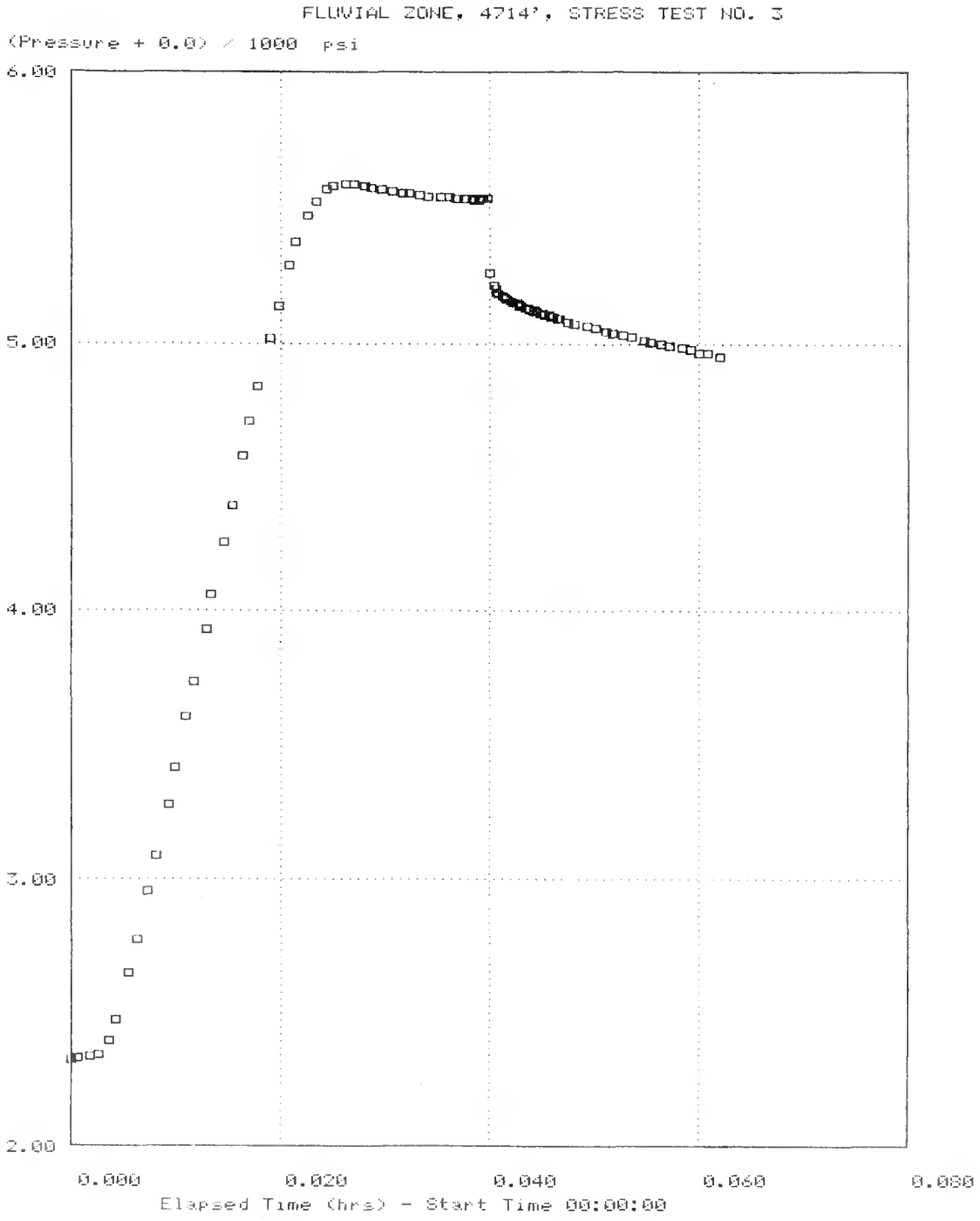


FIGURE A.31: Shale Stress Test (4714-4716'), Linear Plot of Test No. 3 Injection/Decline.

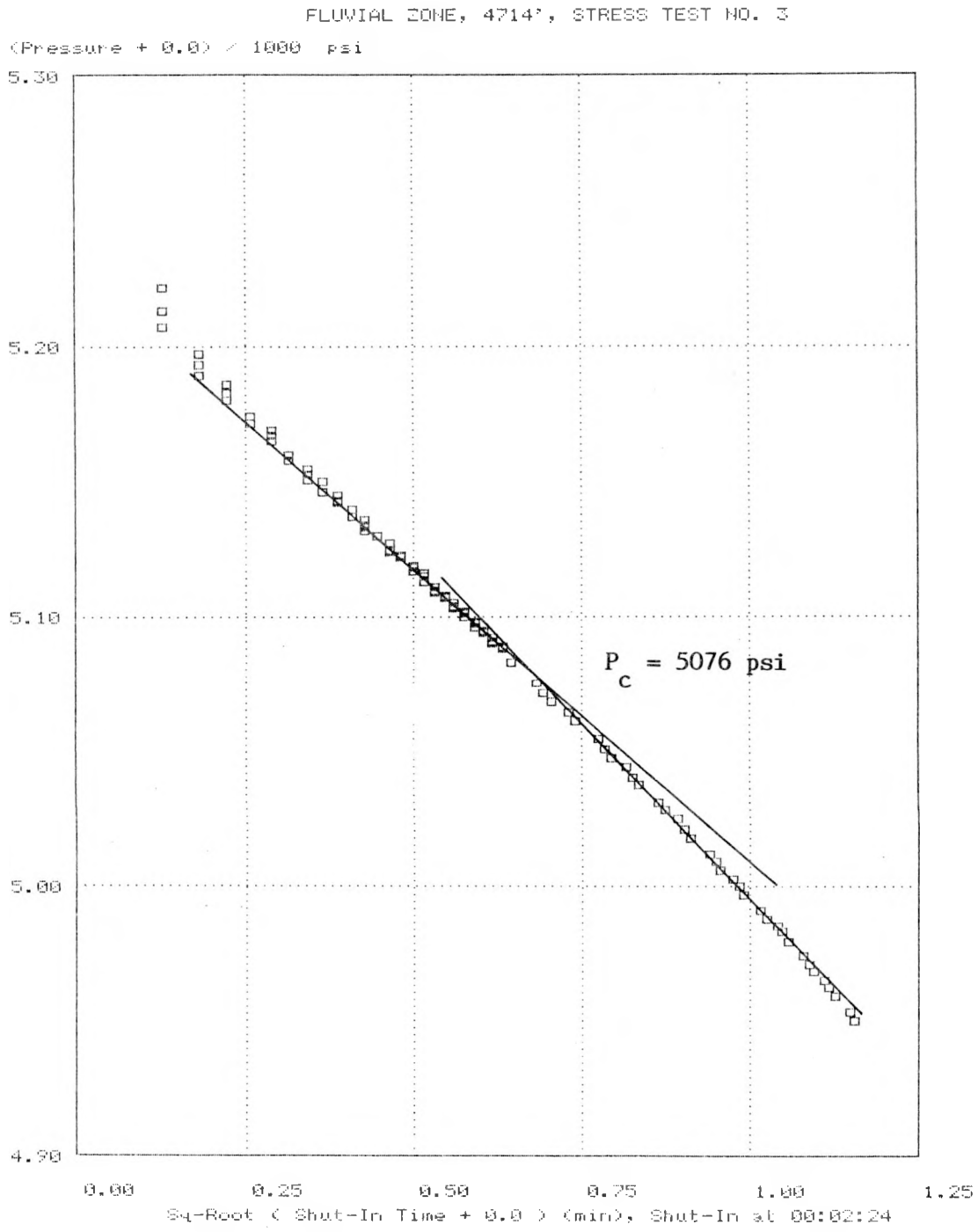


FIGURE A.32: Shale Stress Test (4714-4716'), Square-Root of Shut-In Time Plot of Test No. 3 Pressure Decline.

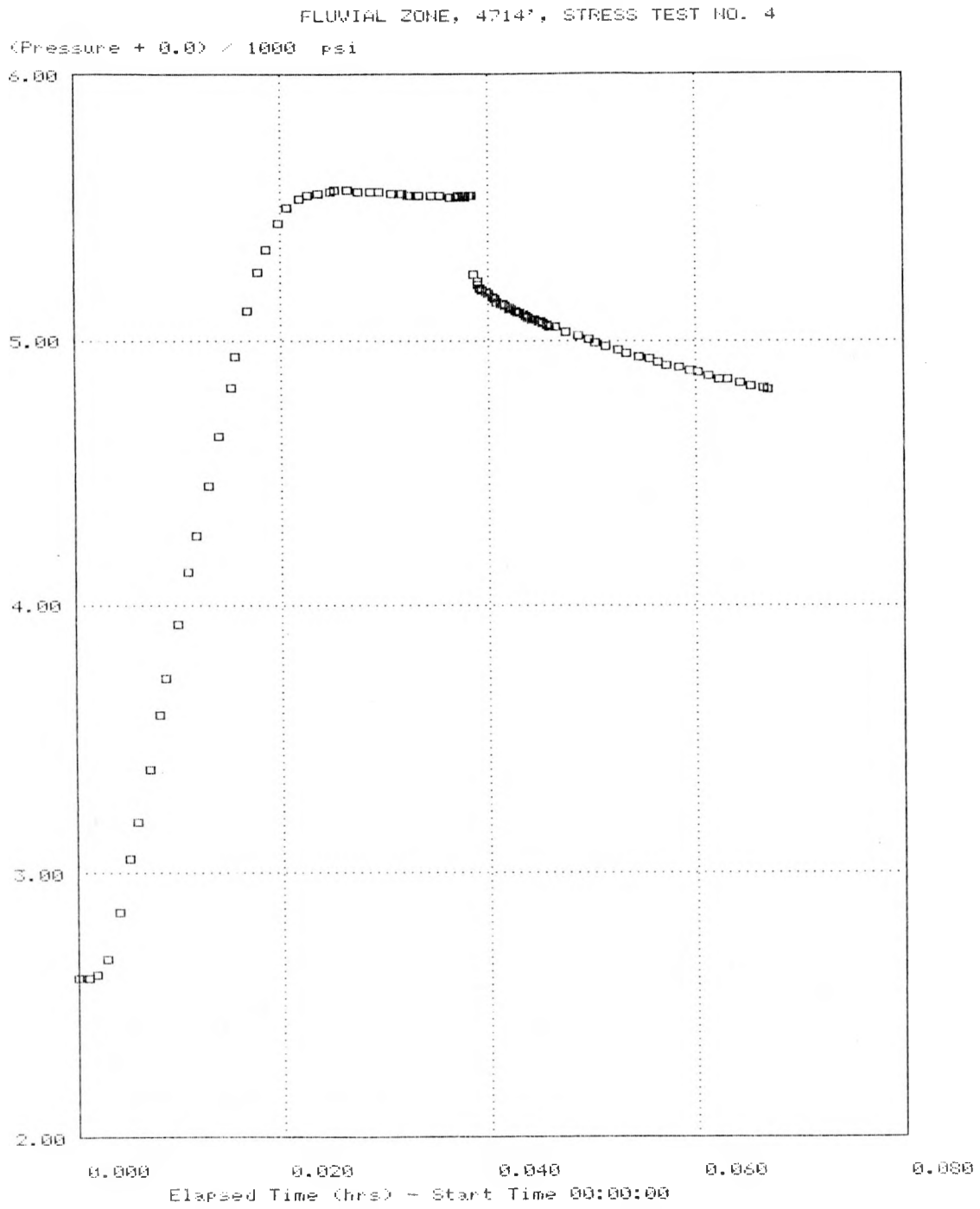


FIGURE A.33: Shale Stress Test (4714-4716'), Linear Plot of Test No. 4 Injection/Decline.

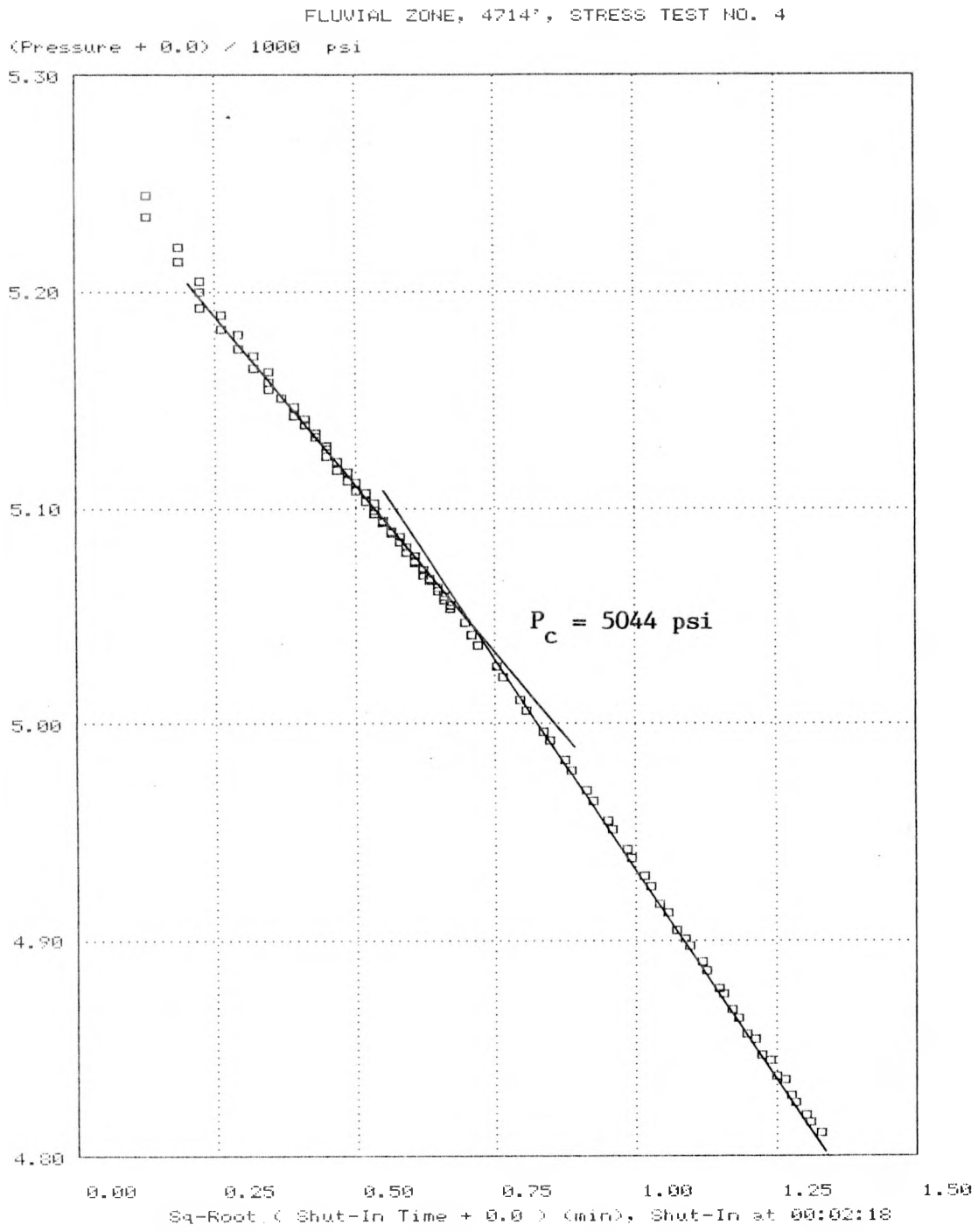


FIGURE A.34: Shale Stress Test (4714-4716'), Square-Root of Shut-In Time Plot of Test No. 4 Pressure Decline.

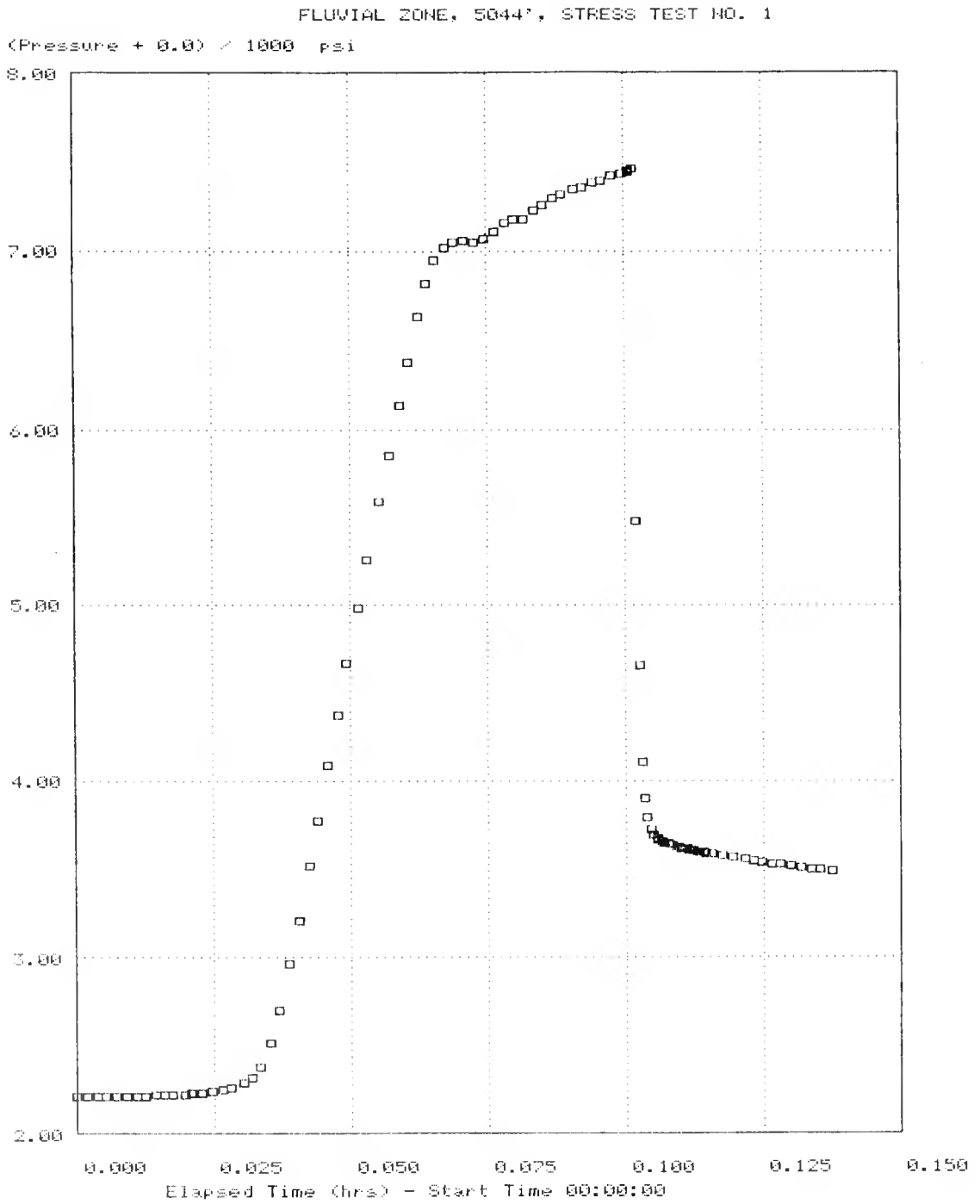


FIGURE A.35: Sandstone Stress Test (5044–5046'), Linear Plot of Test No. 1 Injection/Decline.

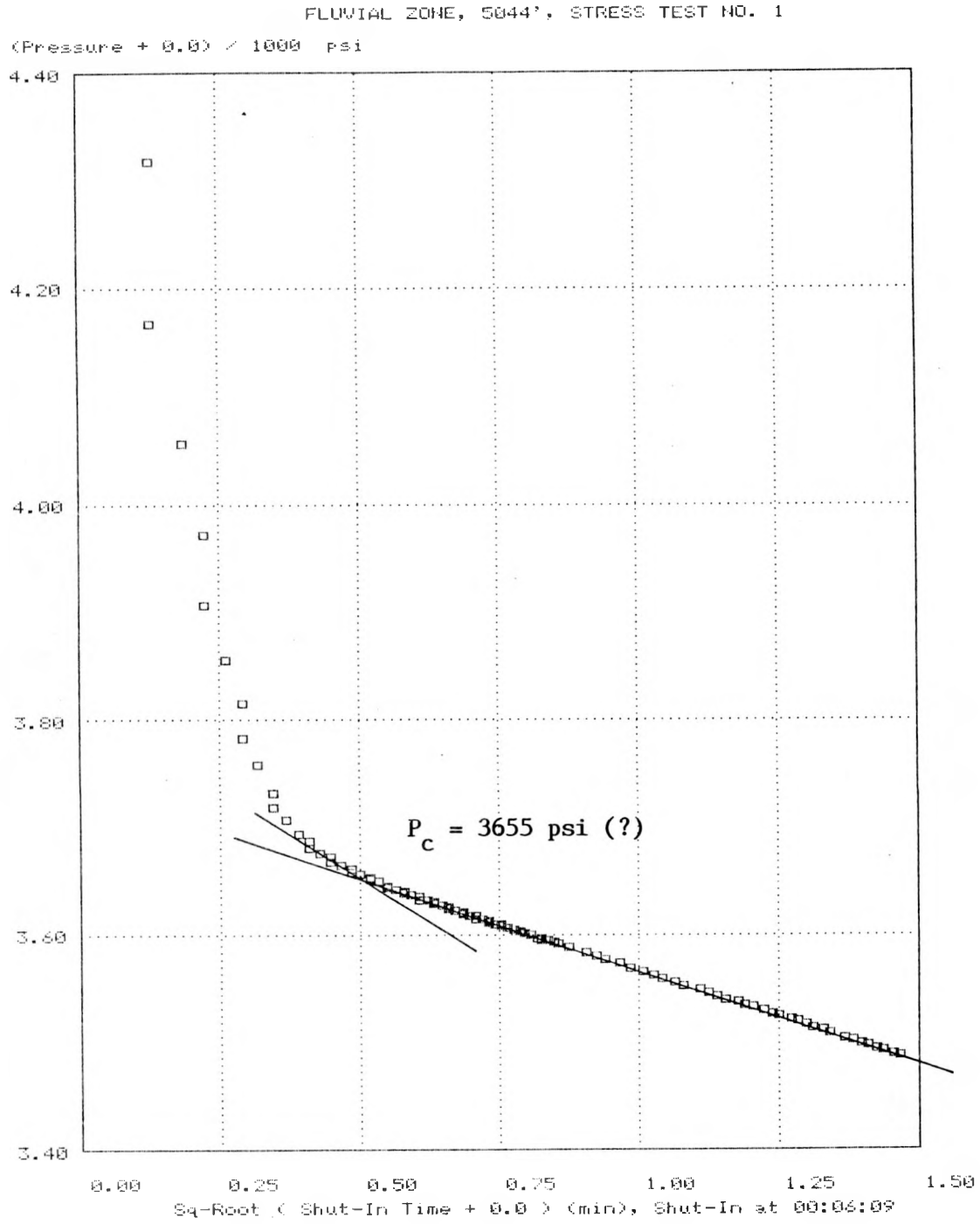


FIGURE A.36: Sandstone Stress Test (5044-5046'), Square-Root of Shut-In Time Plot of Test No. 1 Pressure Decline.

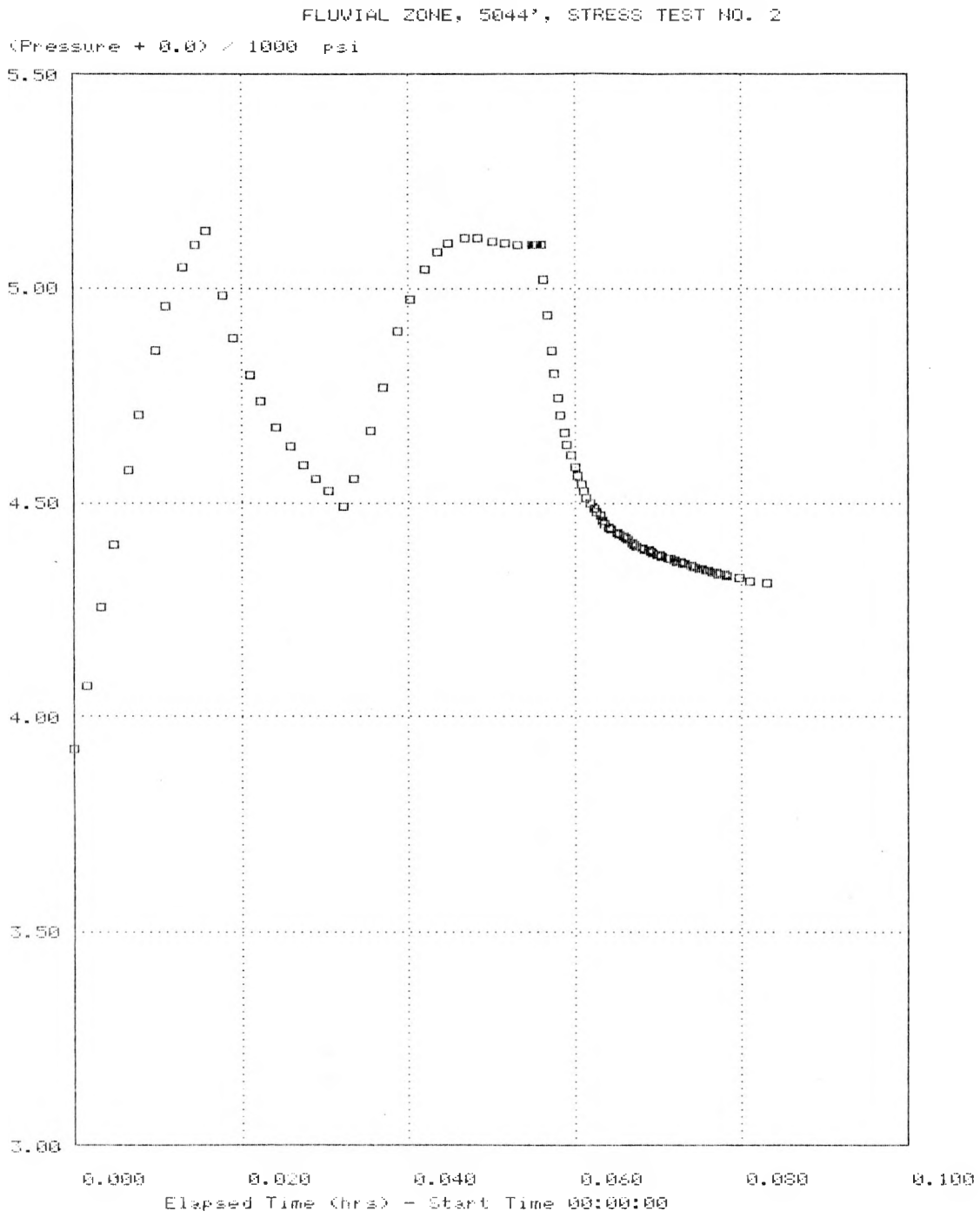


FIGURE A.37: Sandstone Stress Test (5044-5046'), Linear Plot of Test No. 2 Injection/Decline.

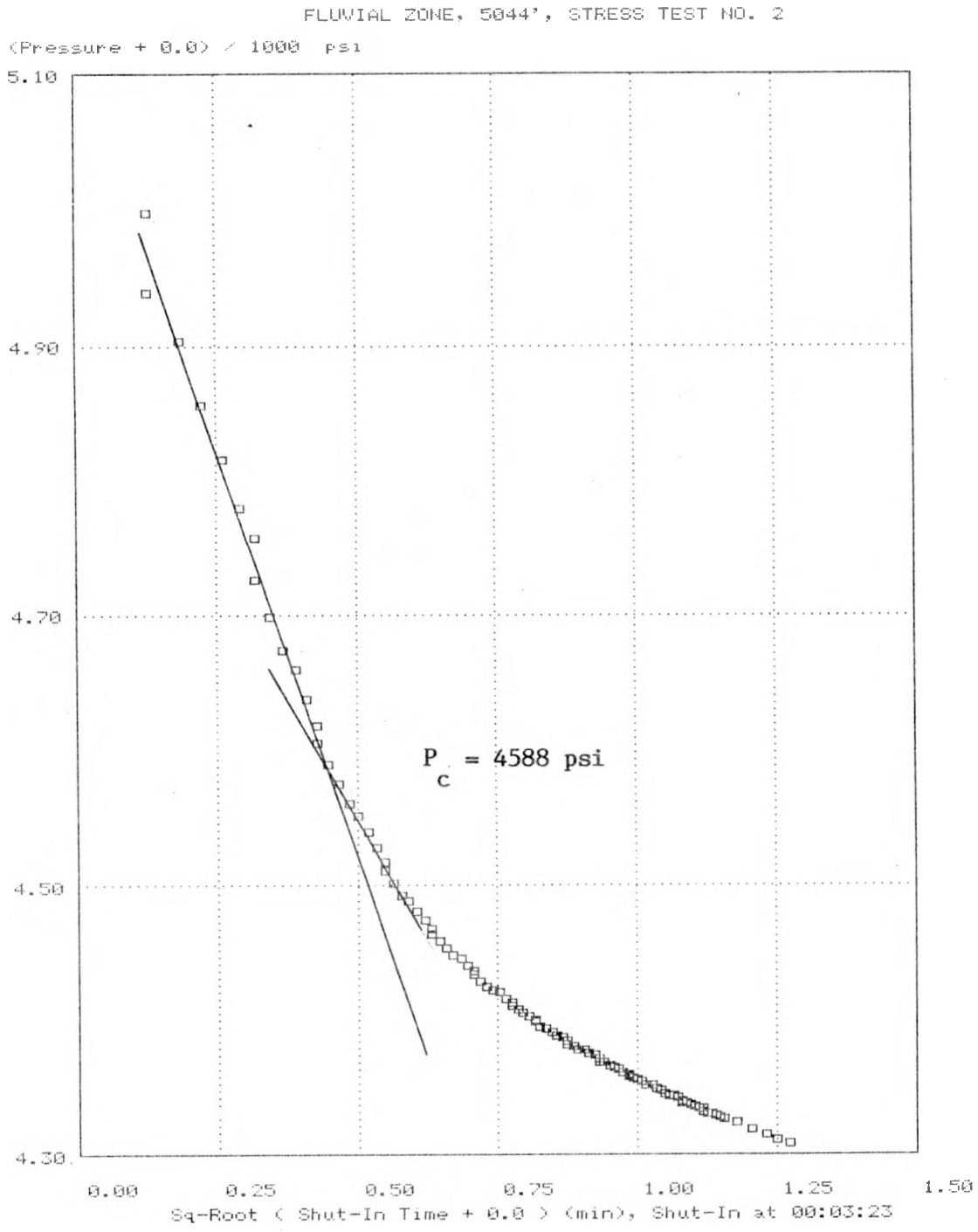


FIGURE A.38: Sandstone Stress Test (5044-5046'), Square-Root of Shut-In Time Plot of Test No. 2 Pressure Decline.

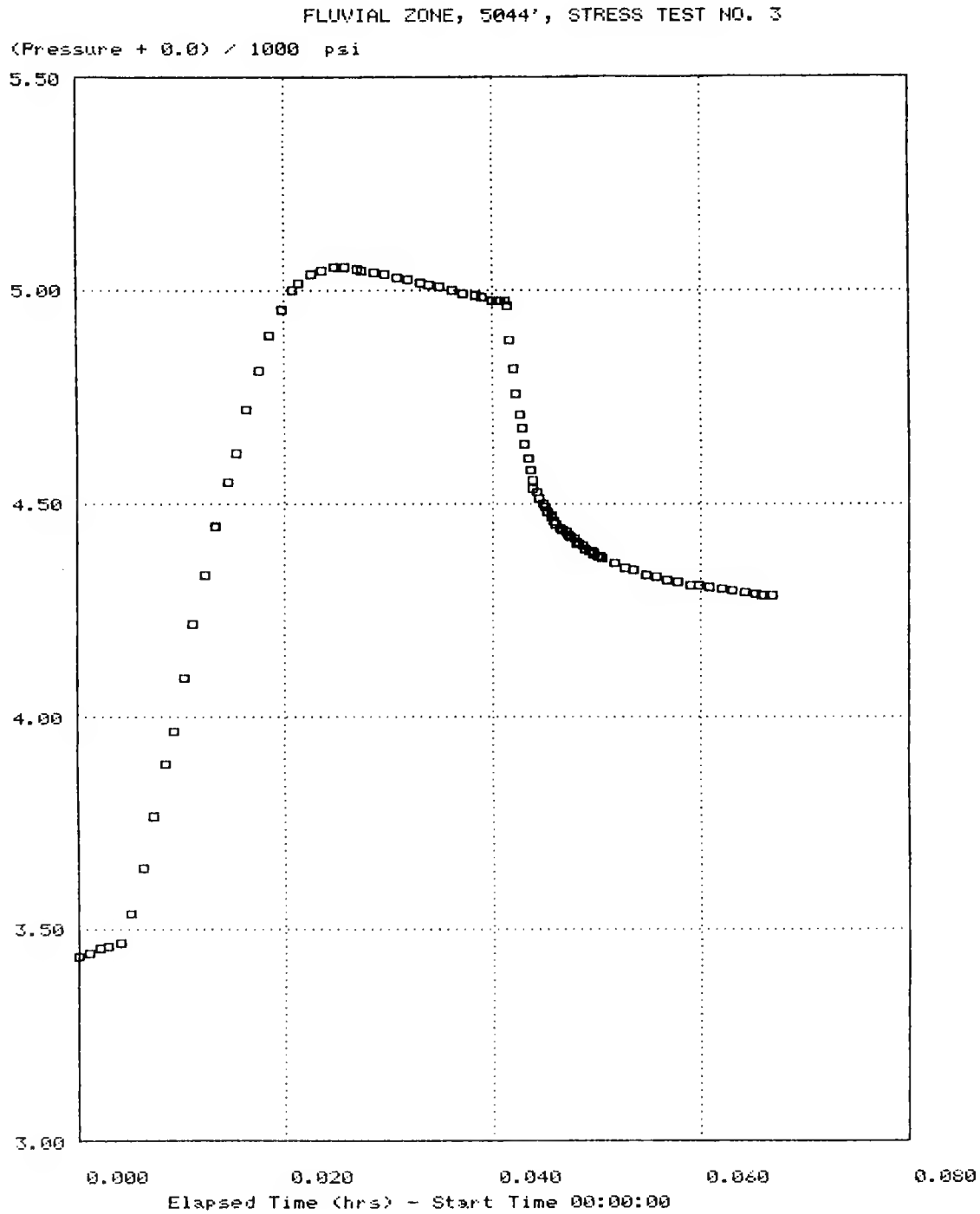


FIGURE A.39: Sandstone Stress Test (5044-5046'), Linear Plot of Test No. 3 Injection/Decline.

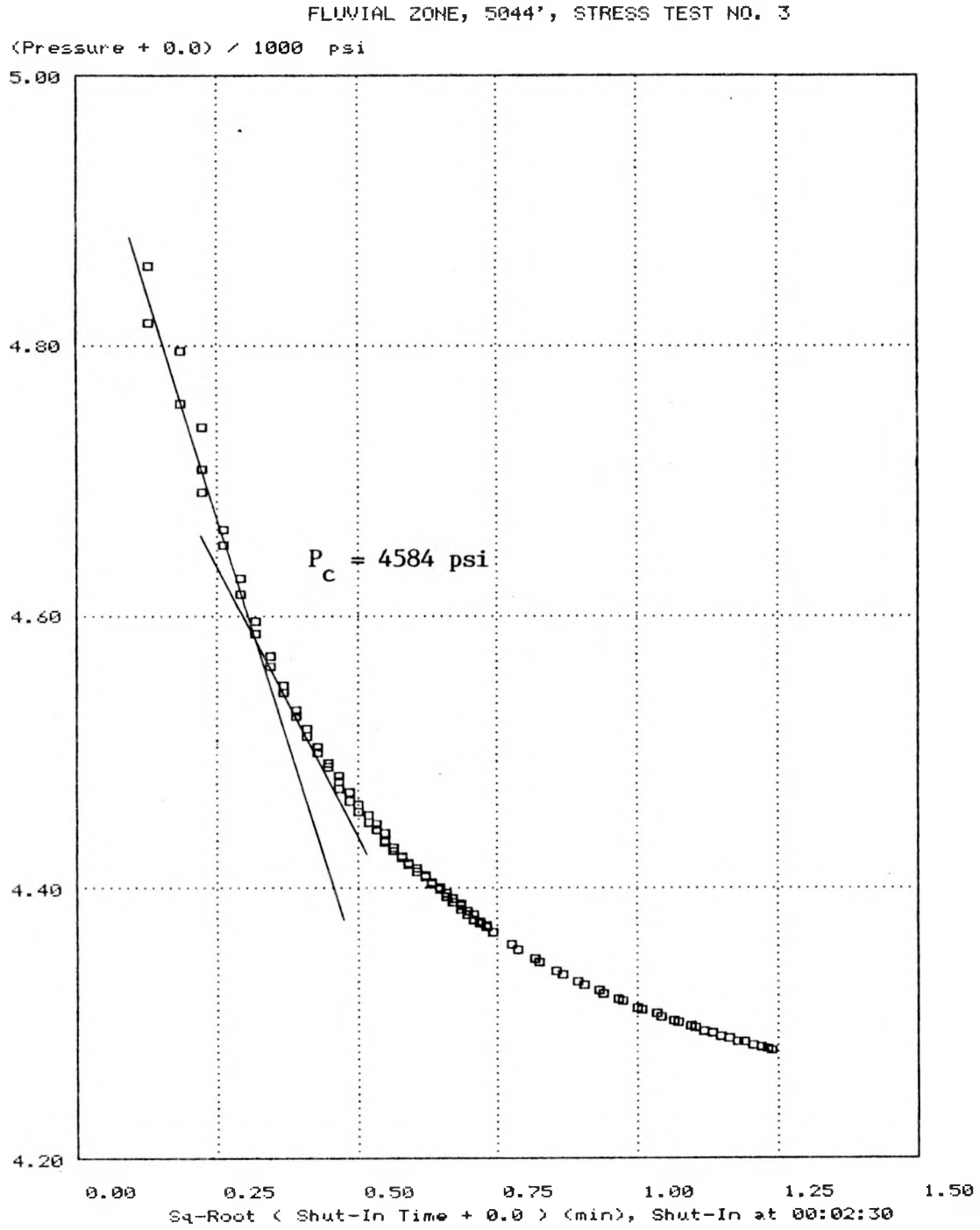


FIGURE A.40: Sandstone Stress Test (5044-5046'), Square-Root of Shut-In Time Plot of Test No. 3 Pressure Decline.

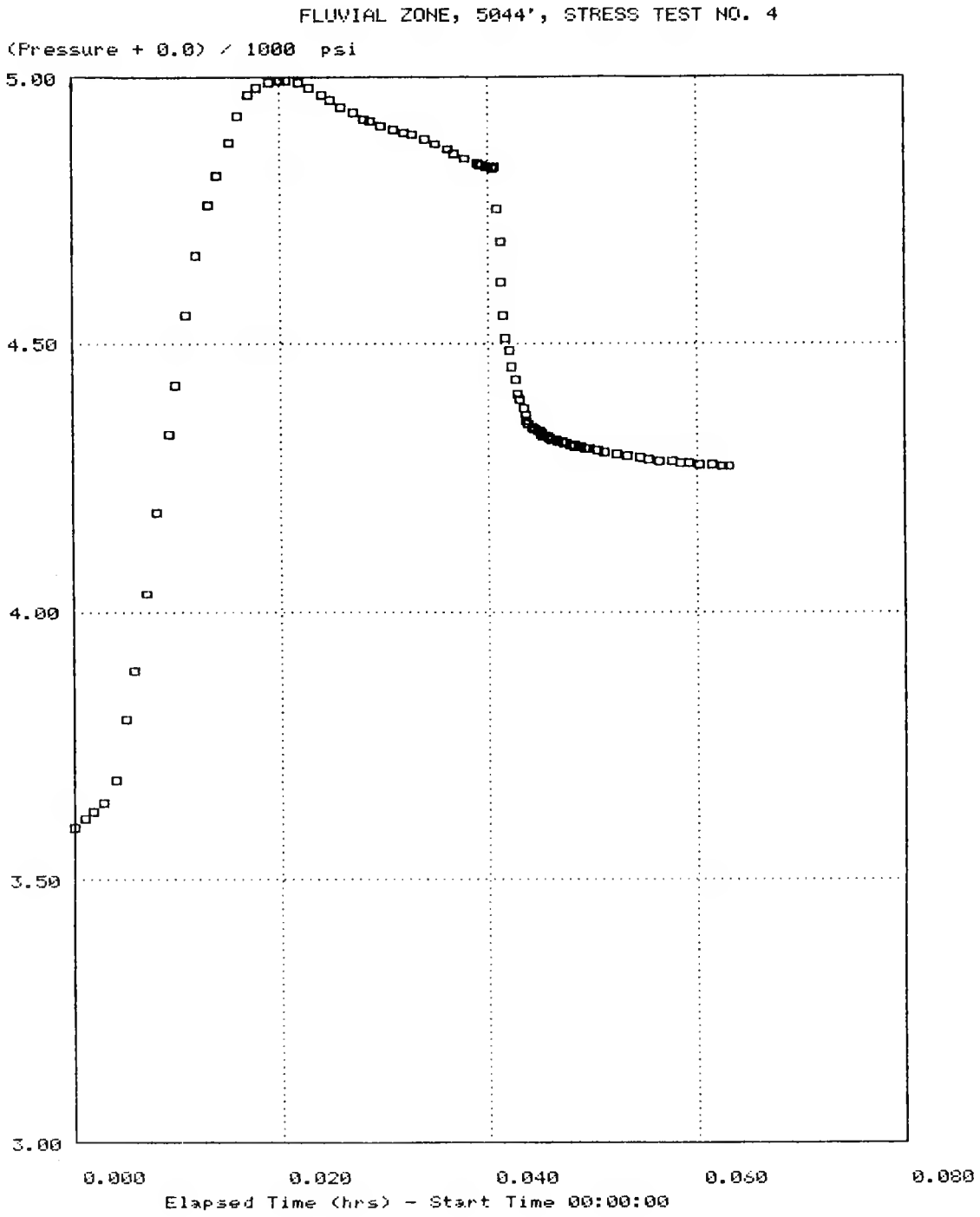


FIGURE A.41: Sandstone Stress Test (5044-5046'), Linear Plot of Test No. 4 Injection/Decline.

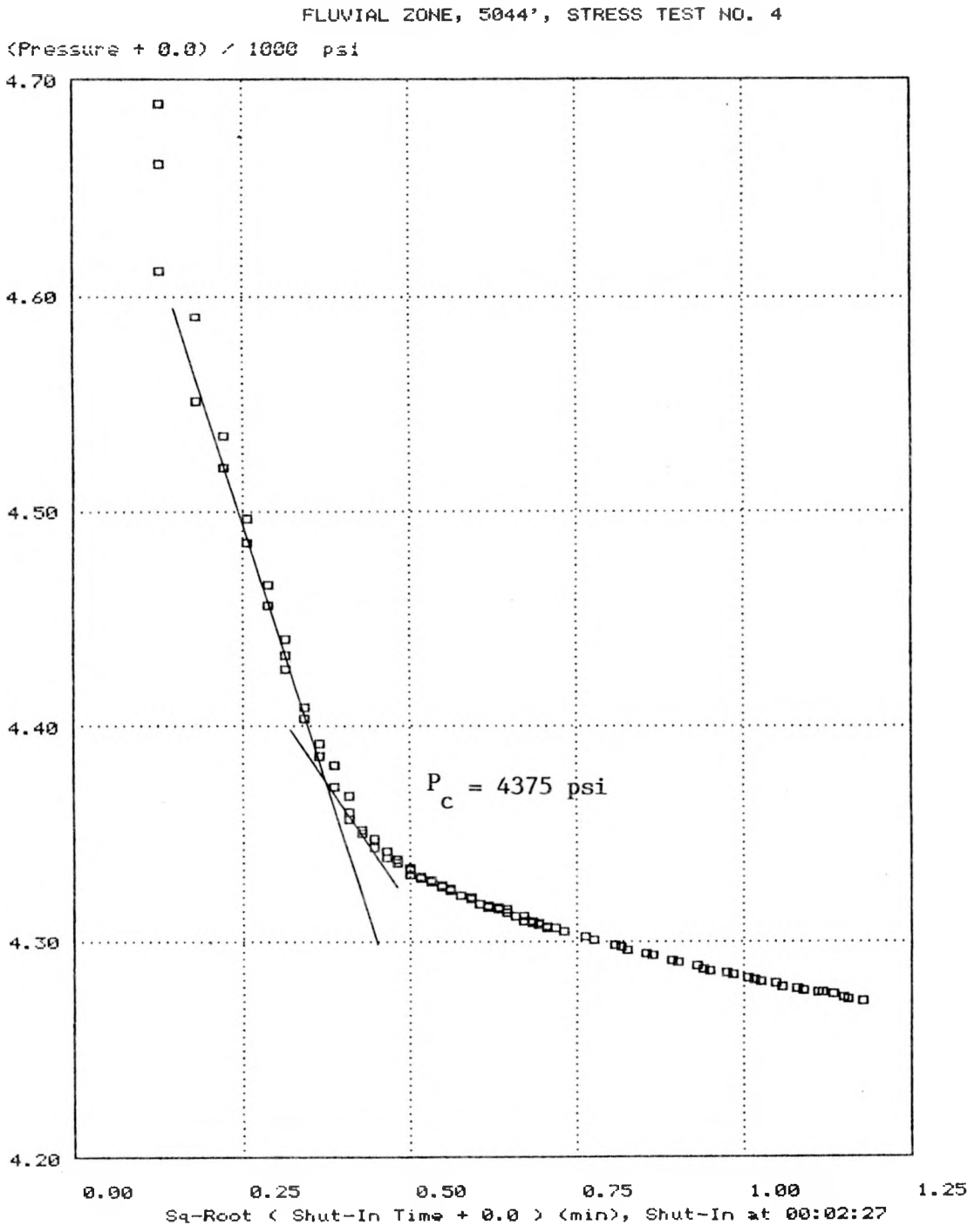


FIGURE A.42: Sandstone Stress Test (5044-5046'), Square-Root of Shut-In Time Plot of Test No. 4 Pressure Decline.

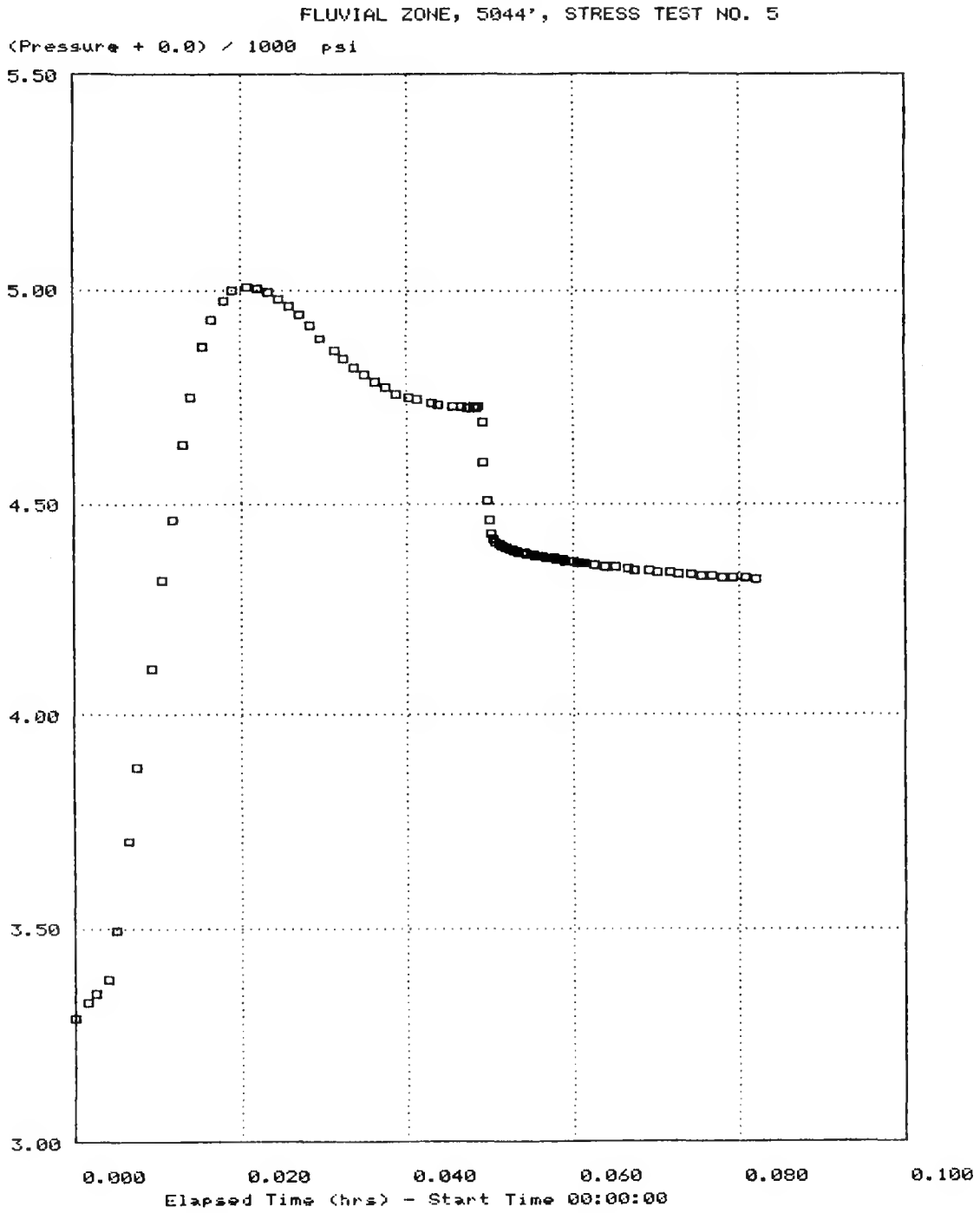


FIGURE A.43: Sandstone Stress Test (5044-5046'), Linear Plot of Test No. 5 Injection/Decline.

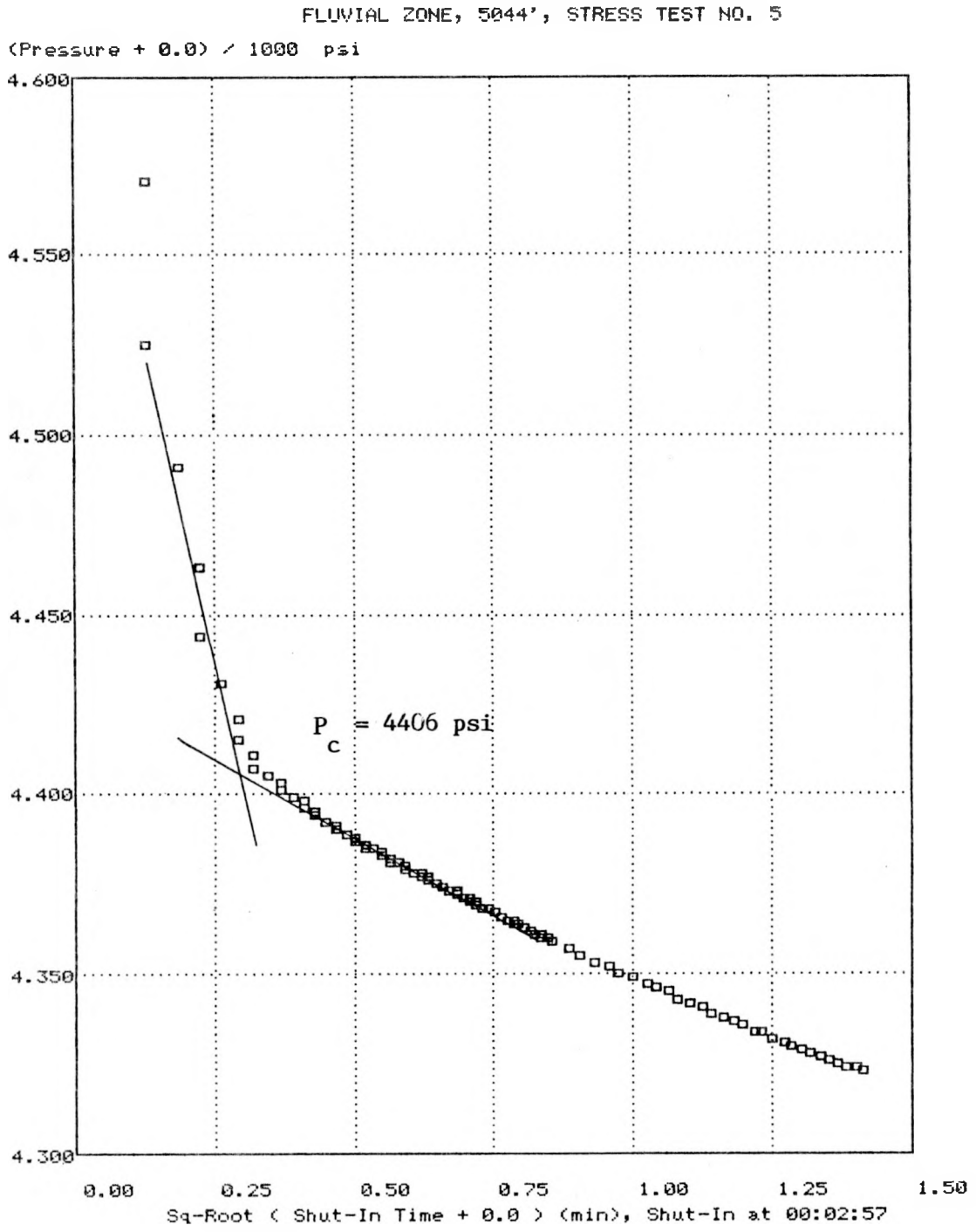


FIGURE A.44: Sandstone Stress Test (5044-5046'), Square-Root of Shut-In Time Plot of Test No. 5 Pressure Decline.

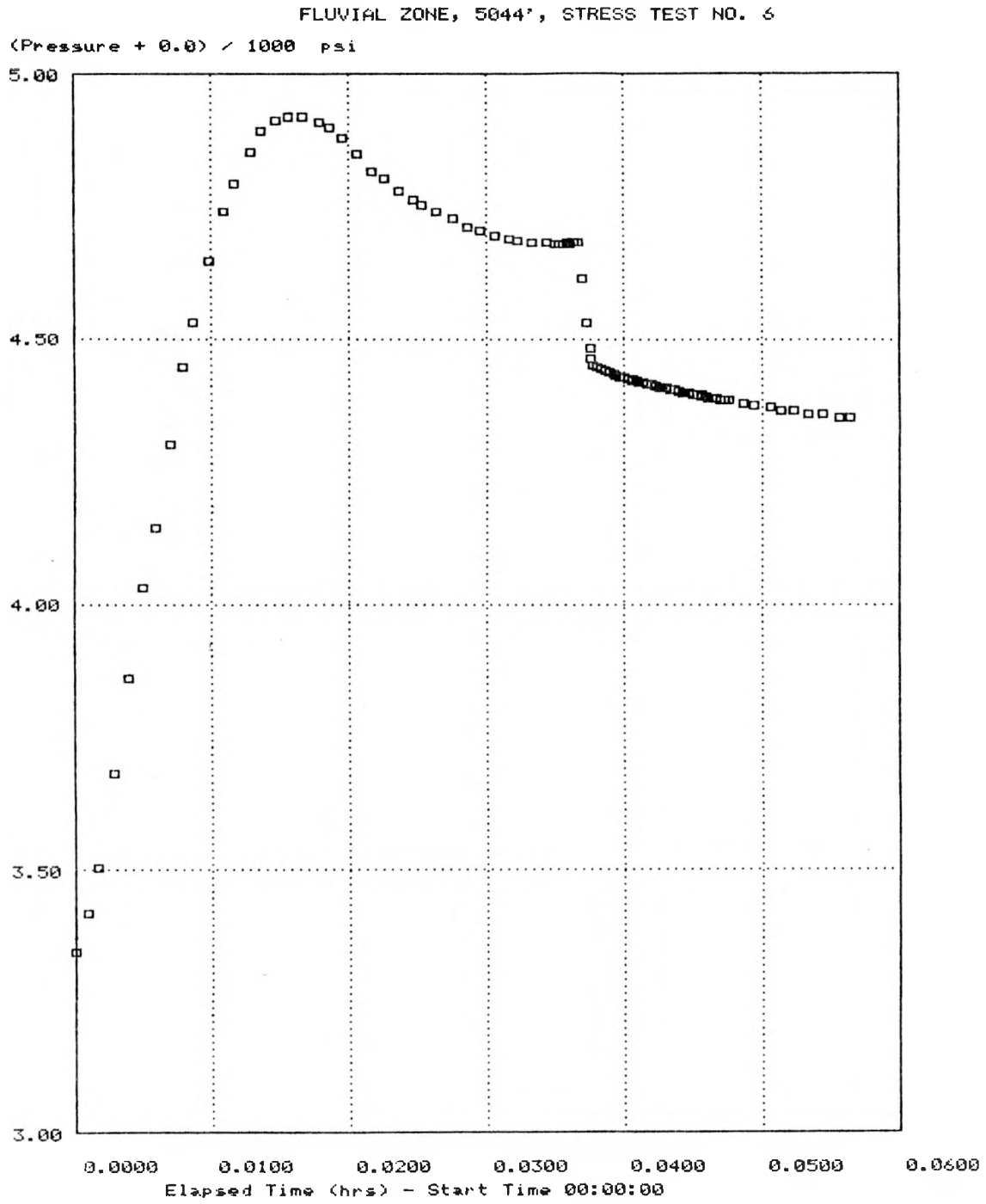


FIGURE A.45: Sandstone Stress Test (5044-5046'), Linear Plot of Test No. 6 Injection/Decline.

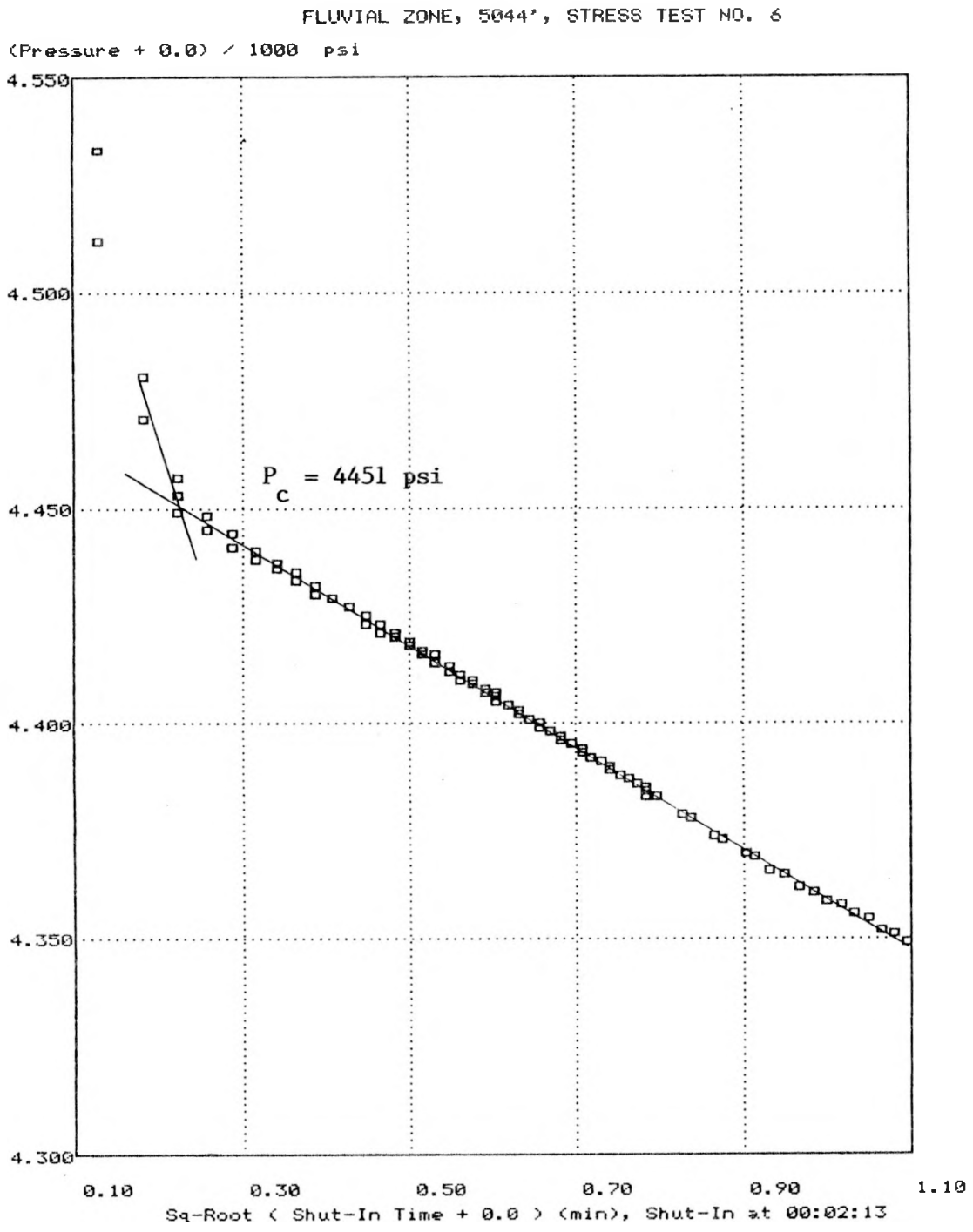


FIGURE A.46: Sandstone Stress Test (5044-5046'), Square-Root of Shut-In Time Plot of Test No. 6 Pressure Decline.

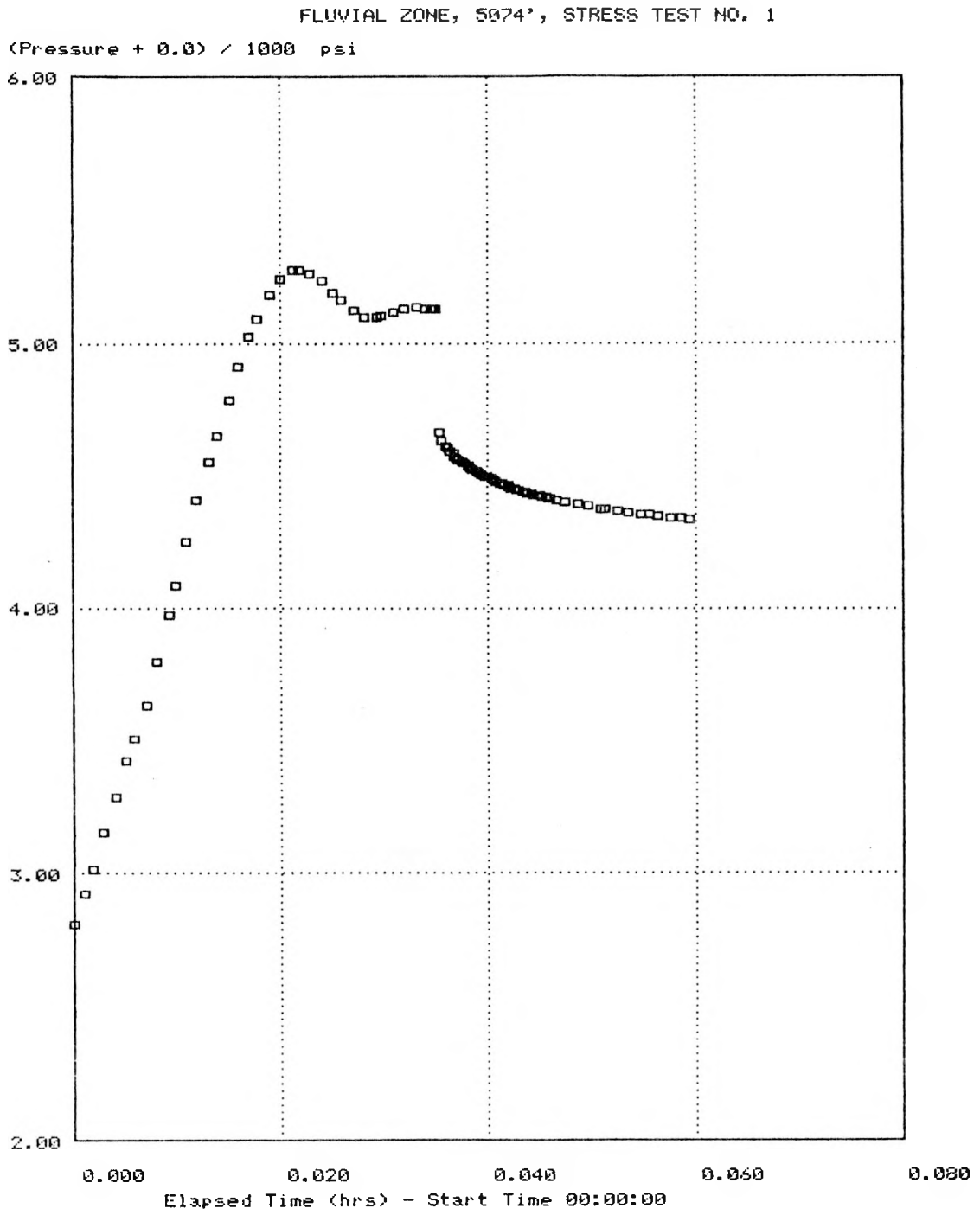


FIGURE A.47: Shale Stress Test (5074-5076'), Linear Plot of Test No. 1 Injection/Decline.

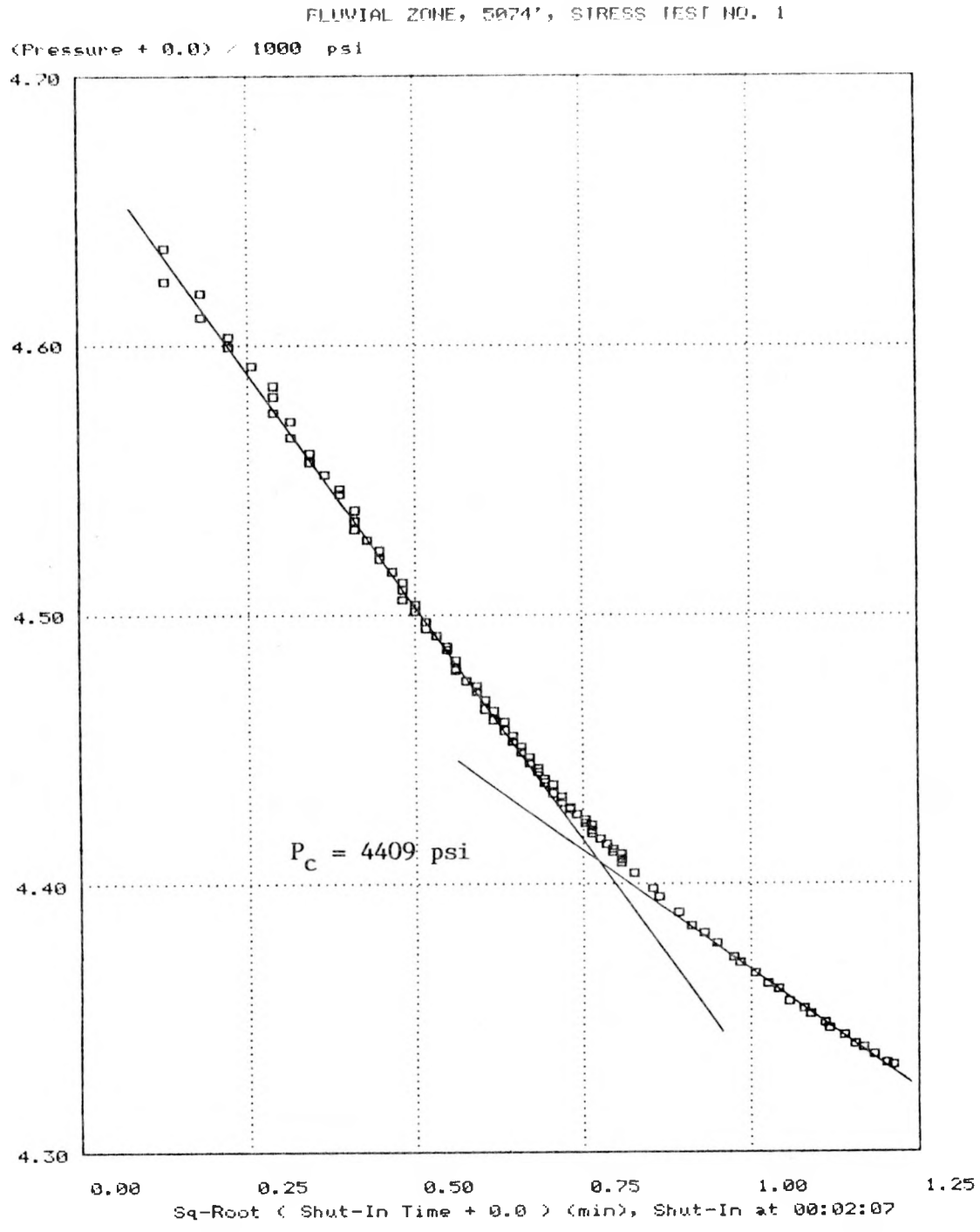


FIGURE A.48: Shale Stress Test (5074-5076'), Square-Root of Shut-In Time Plot of Test No. 1 Pressure Decline.

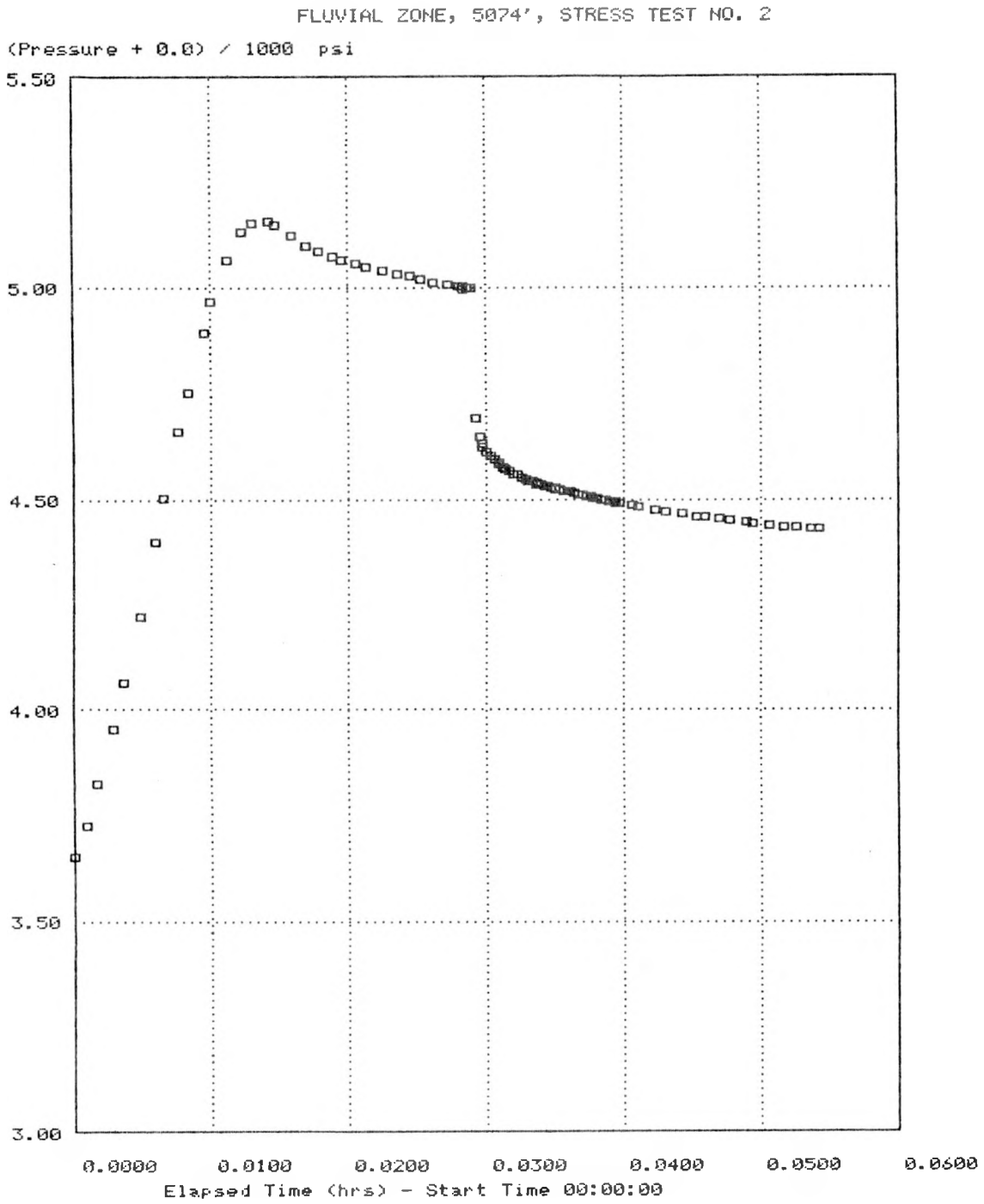


FIGURE A.49: Shale Stress Test (5074-5076'), Linear Plot of Test No. 2 Injection/Decline.

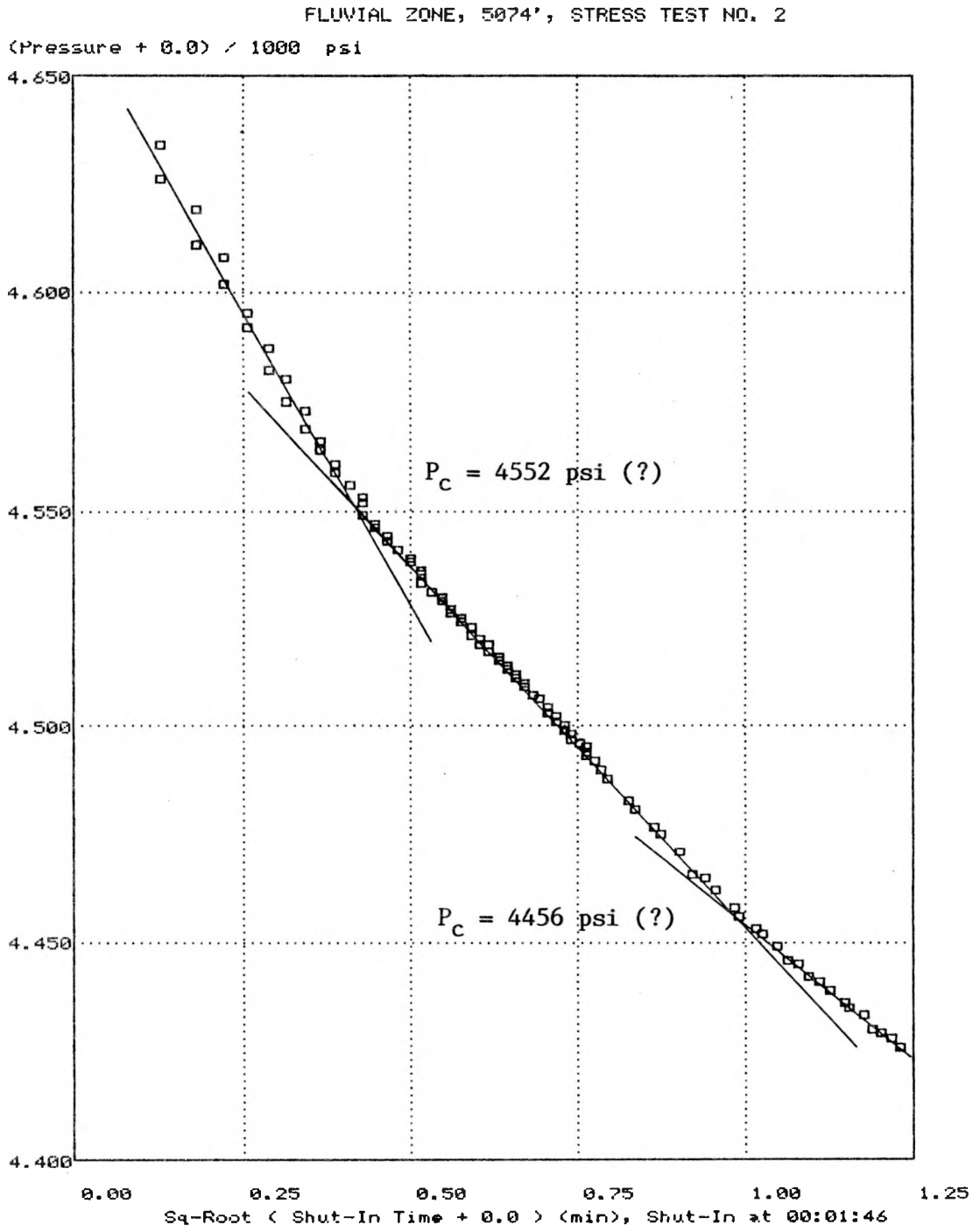


FIGURE A.50: Shale Stress Test (5074-5076'), Square-Root of Shut-In Time Plot of Test No. 2 Pressure Decline.

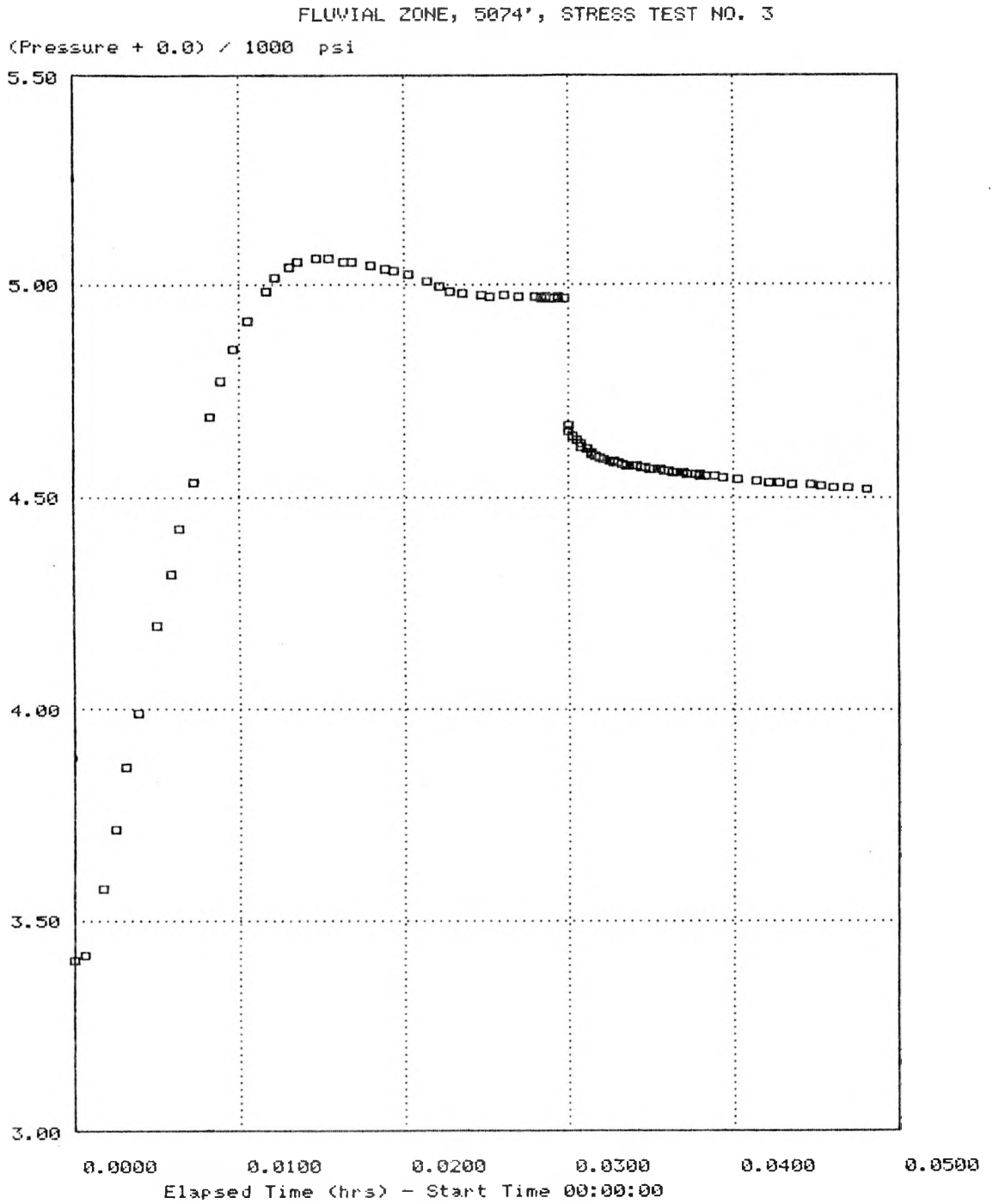


FIGURE A.51: Shale Stress Test (5074-5076'), Linear Plot of Test No. 3 Injection/Decline.

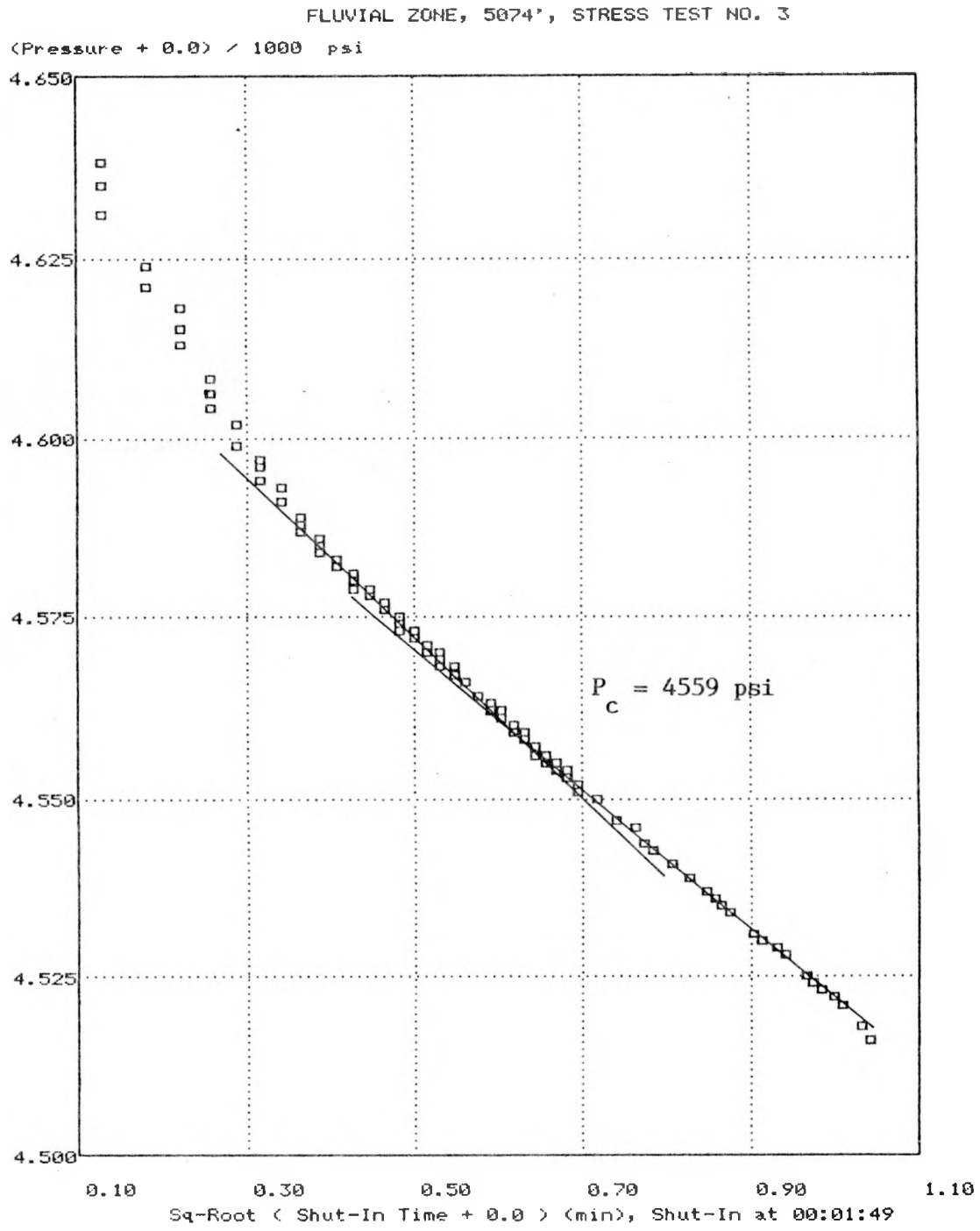


FIGURE A.52: Shale Stress Test (5074-5076'), Square-Root of Shut-In Time Plot of Test No. 3 Pressure Decline.

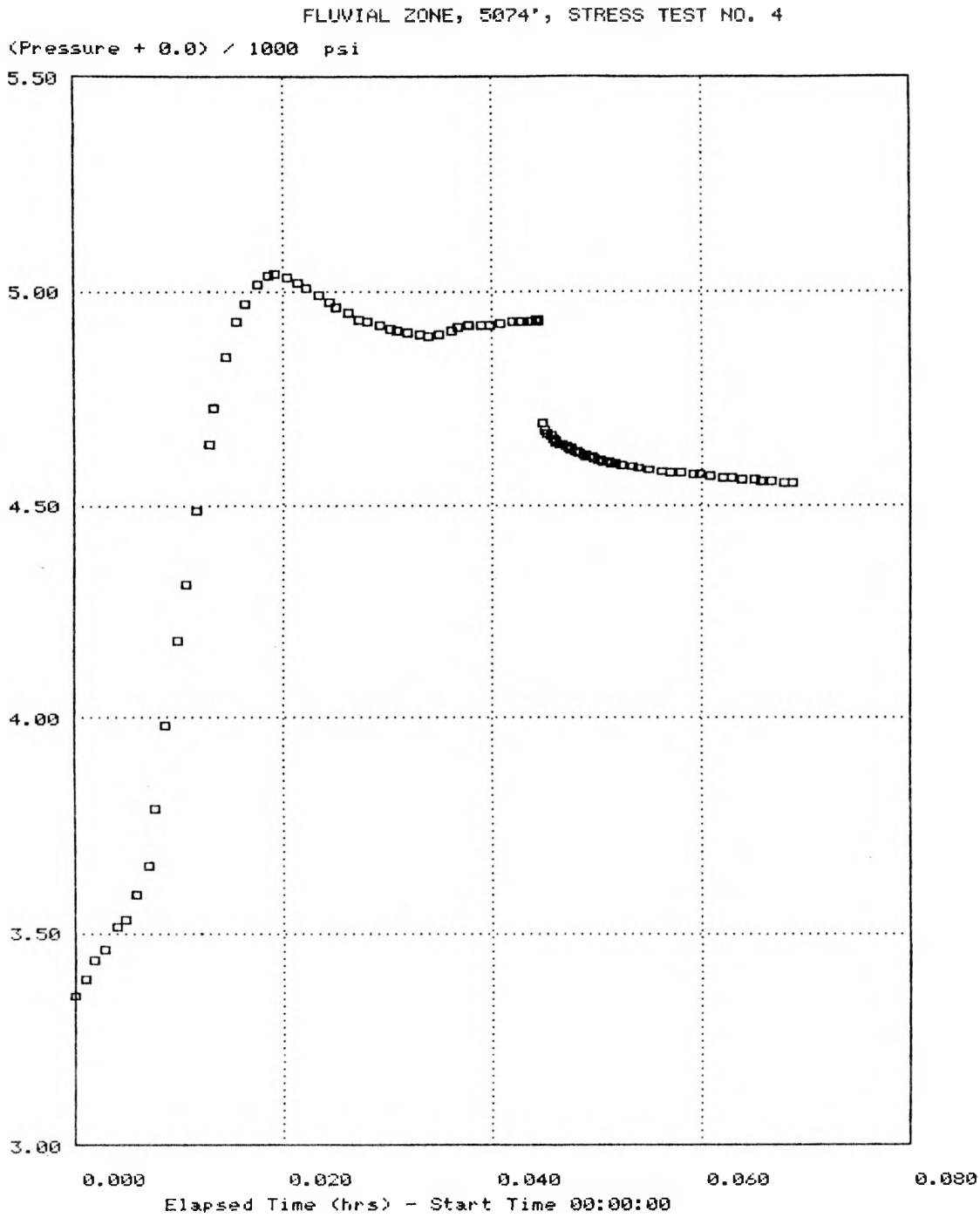


FIGURE A.53: Shale Stress Test (5074-5076'), Linear Plot of Test No. 4 Injection/Decline.

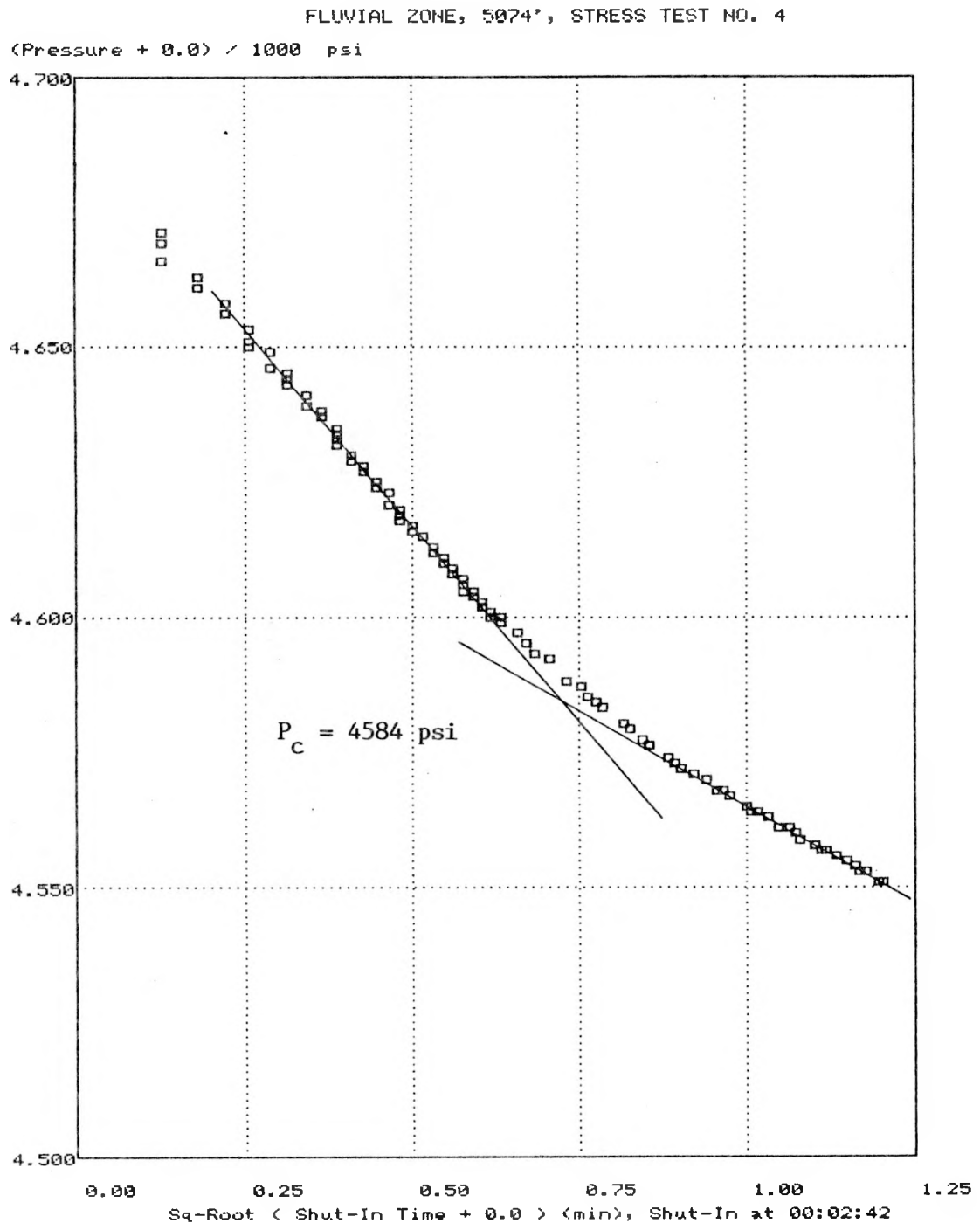


FIGURE A.54: Shale Stress Test (5074-5076'), Square-Root of Shut-In Time Plot of Test No. 4 Pressure Decline.

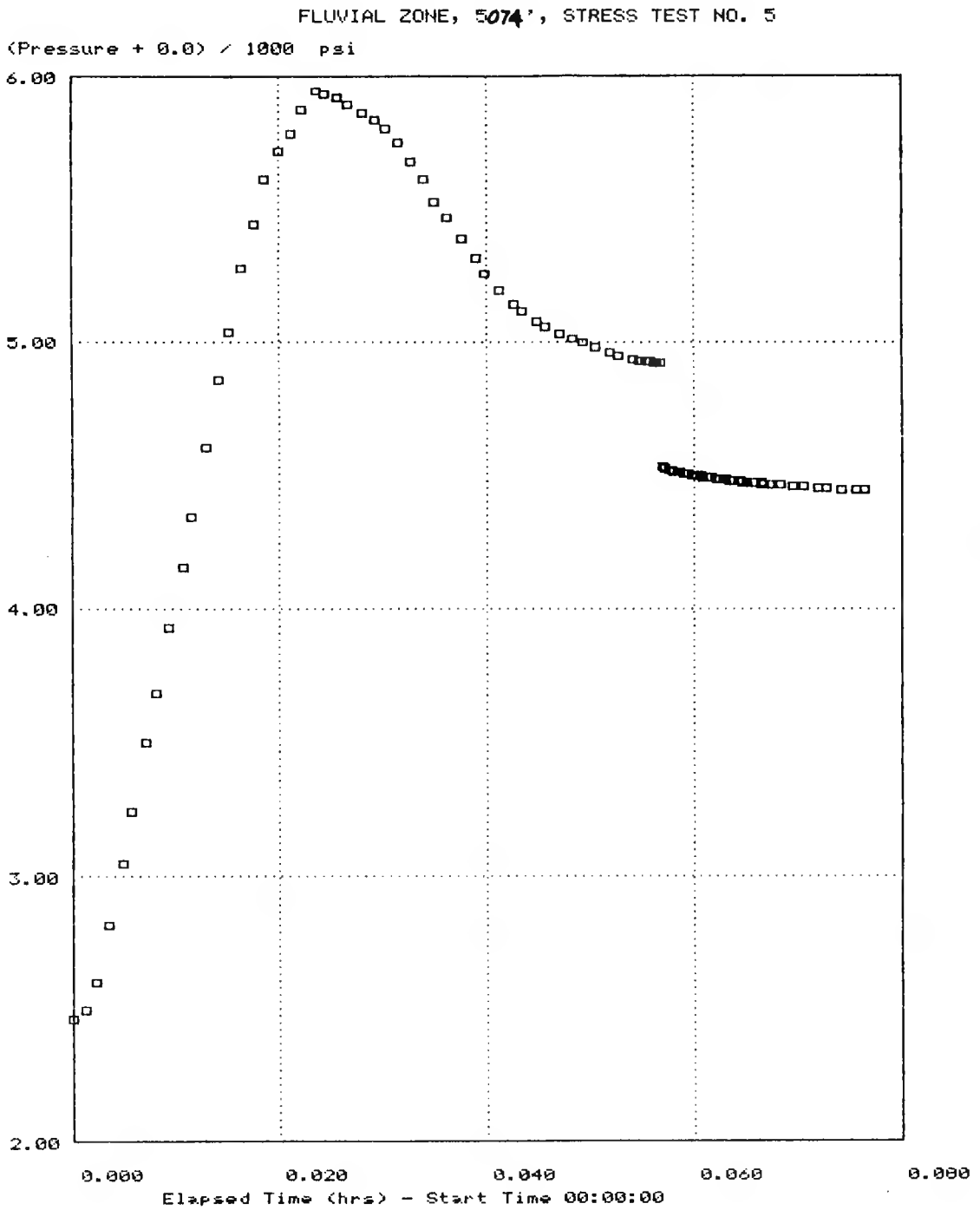


FIGURE A.55: Shale Stress Test (5074-5076'), Linear Plot of Test No. 5 Injection/Decline.

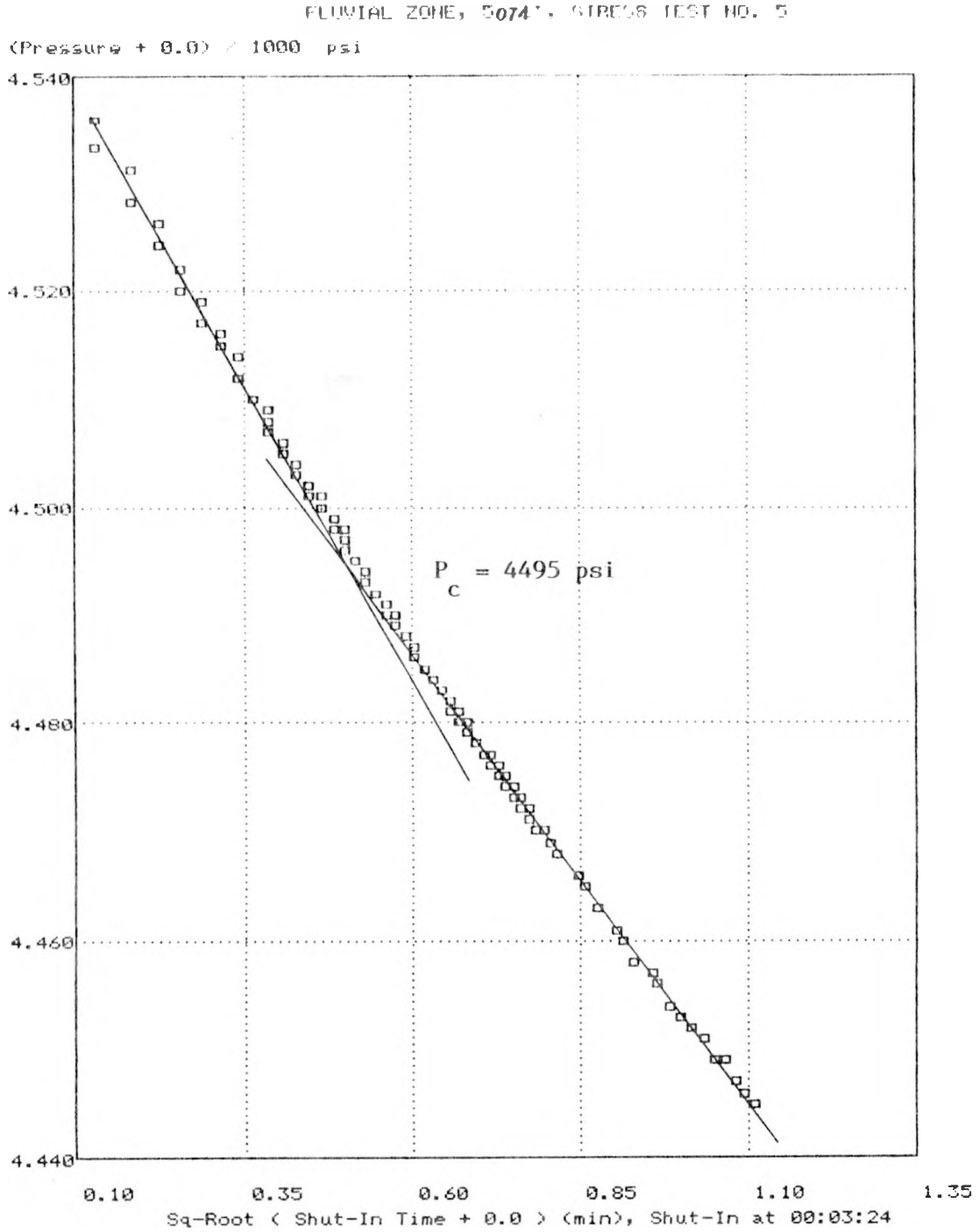


FIGURE A.56: Shale Stress Test (5074-5076'), Square-Root of Shut-In Time Plot of Test No. 5 Pressure Decline.

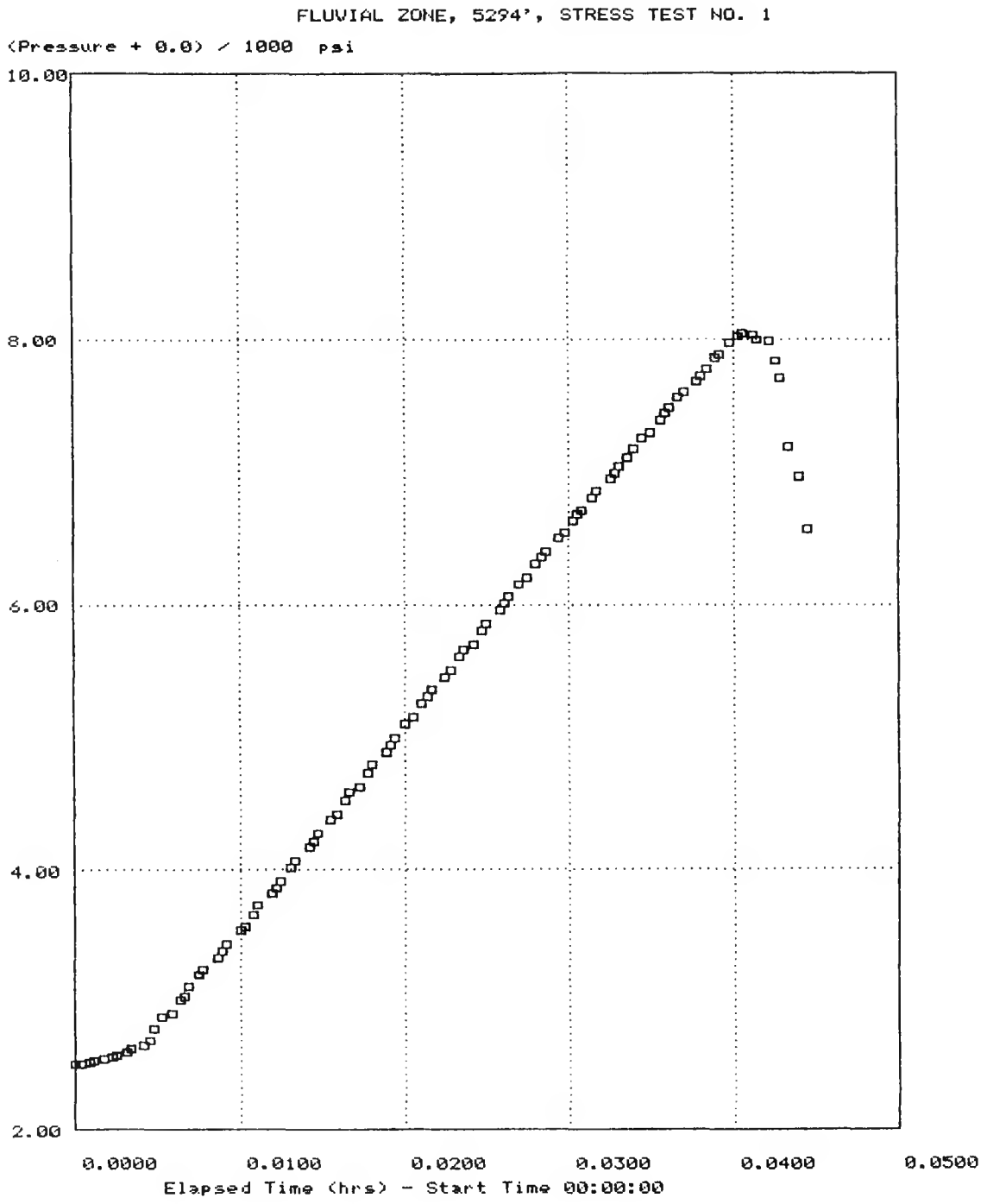


FIGURE A.57: Sandstone Stress Test (5294-5296'), Linear Plot of Test No. 1 Injection/Decline.

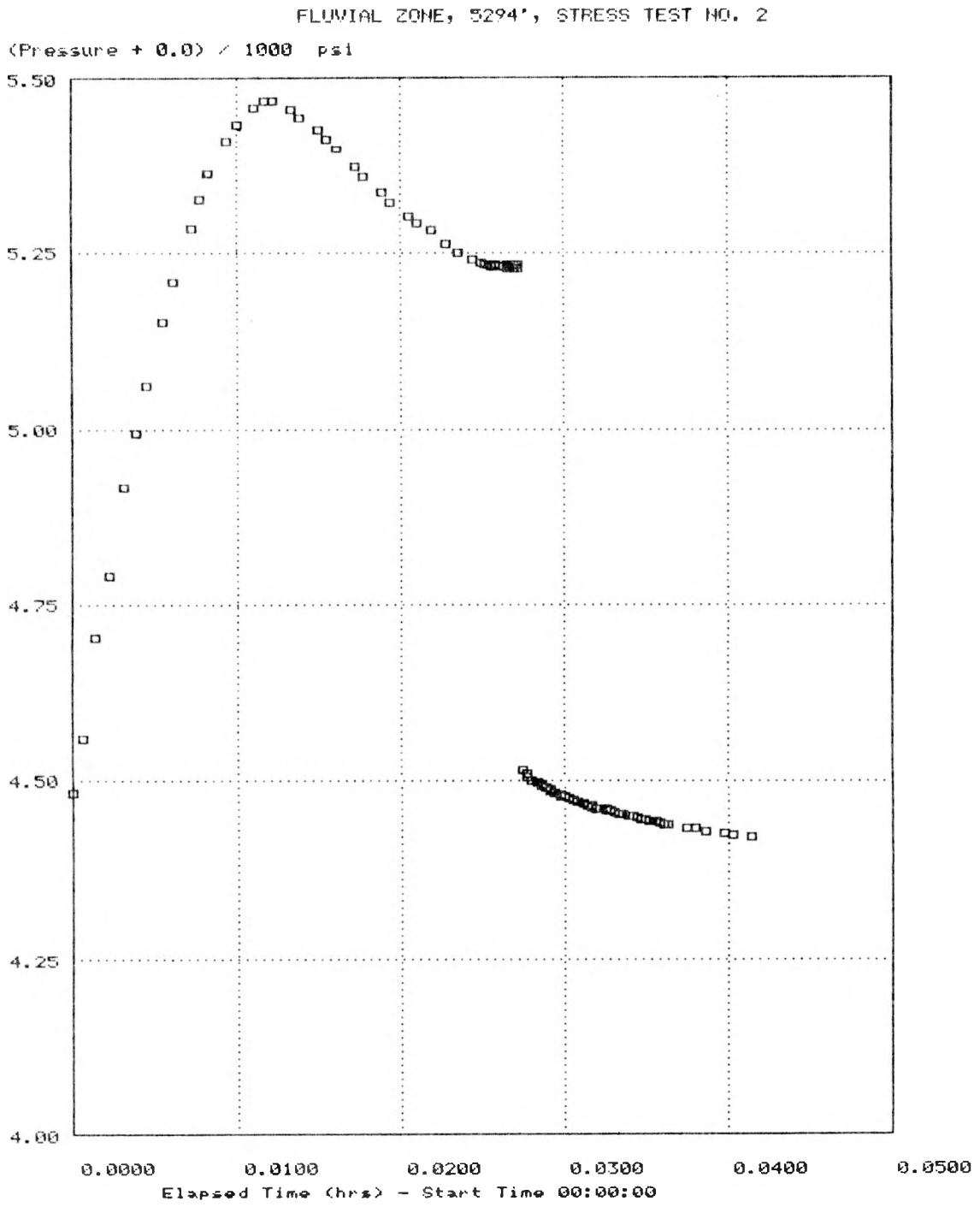


FIGURE A.58: Sandstone Stress Test (5294-5296'), Linear Plot of Test No. 2 Injection/Decline.

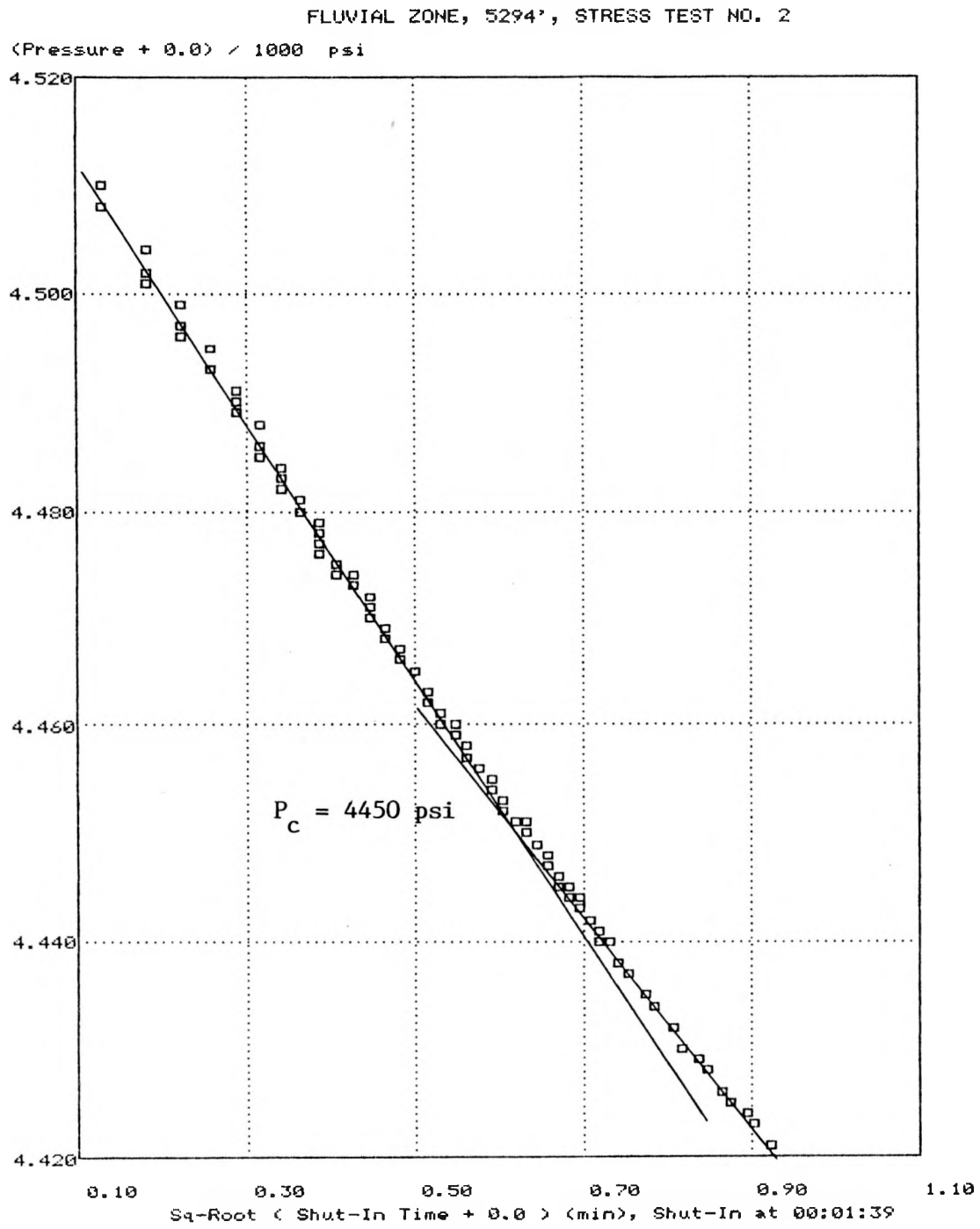


FIGURE A.59: Sandstone Stress Test (5294-5296'), Square-Root of Shut-In Time Plot of Test No. 2 Pressure Decline.

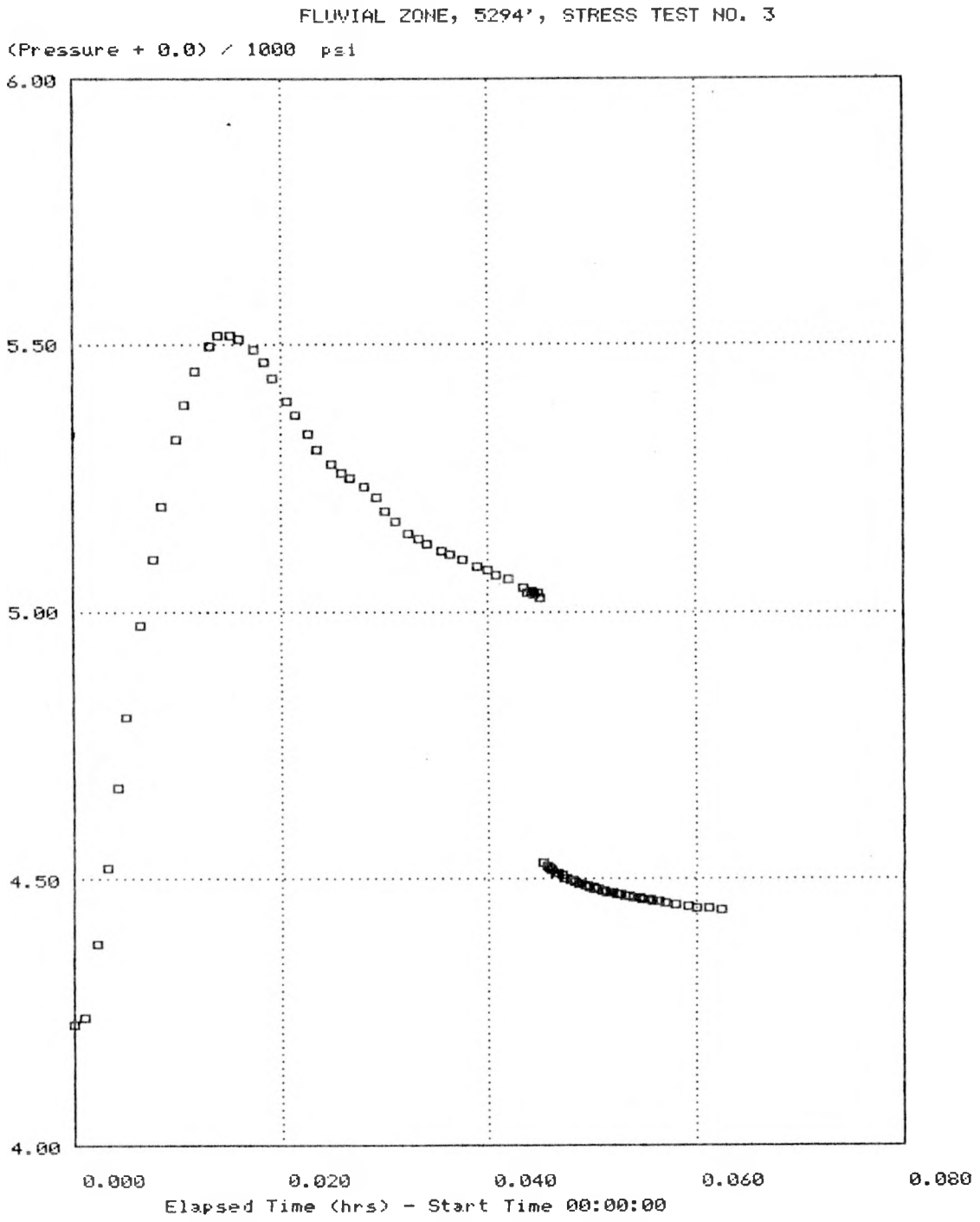


FIGURE A.60: Sandstone Stress Test (5294-5296'), Linear Plot of Test No. 3 Injection/Decline.

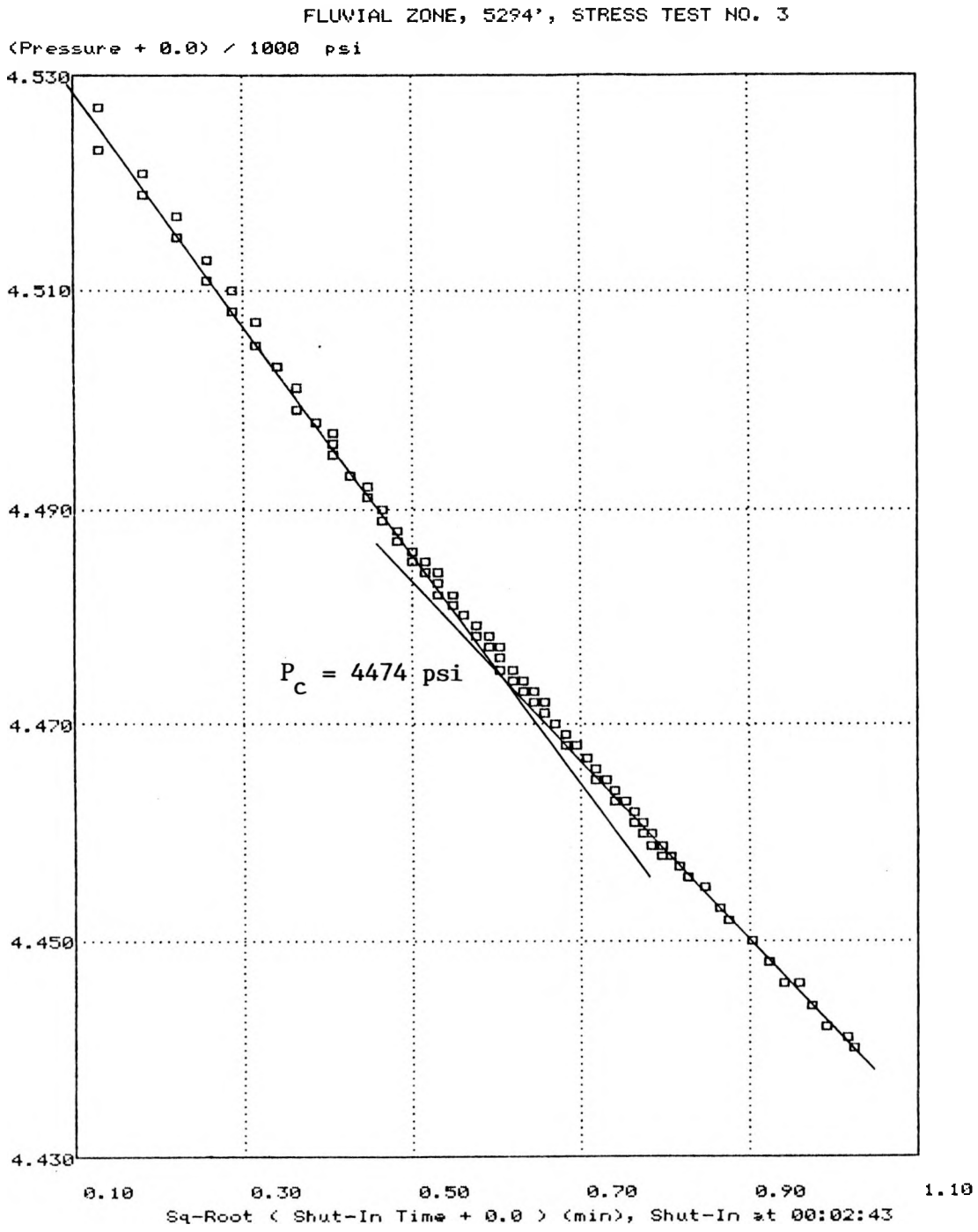


FIGURE A.61: Sandstone Stress Test (5294–5296'), Square-Root of Shut-In Time Plot of Test No. 3 Pressure Decline.

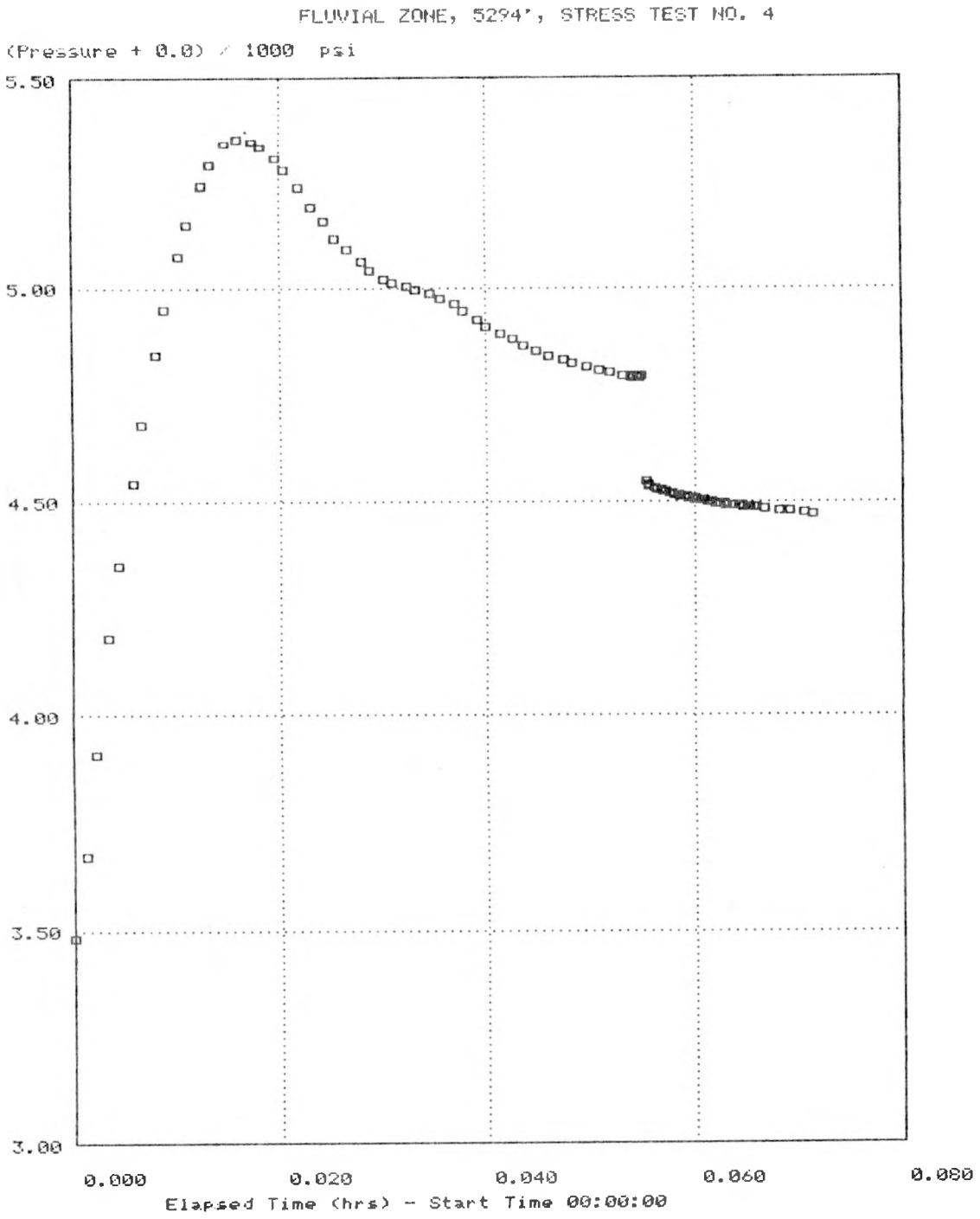


FIGURE A.62: Sandstone Stress Test (5294-5296'), Linear Plot of Test No. 4 Injection/Decline.

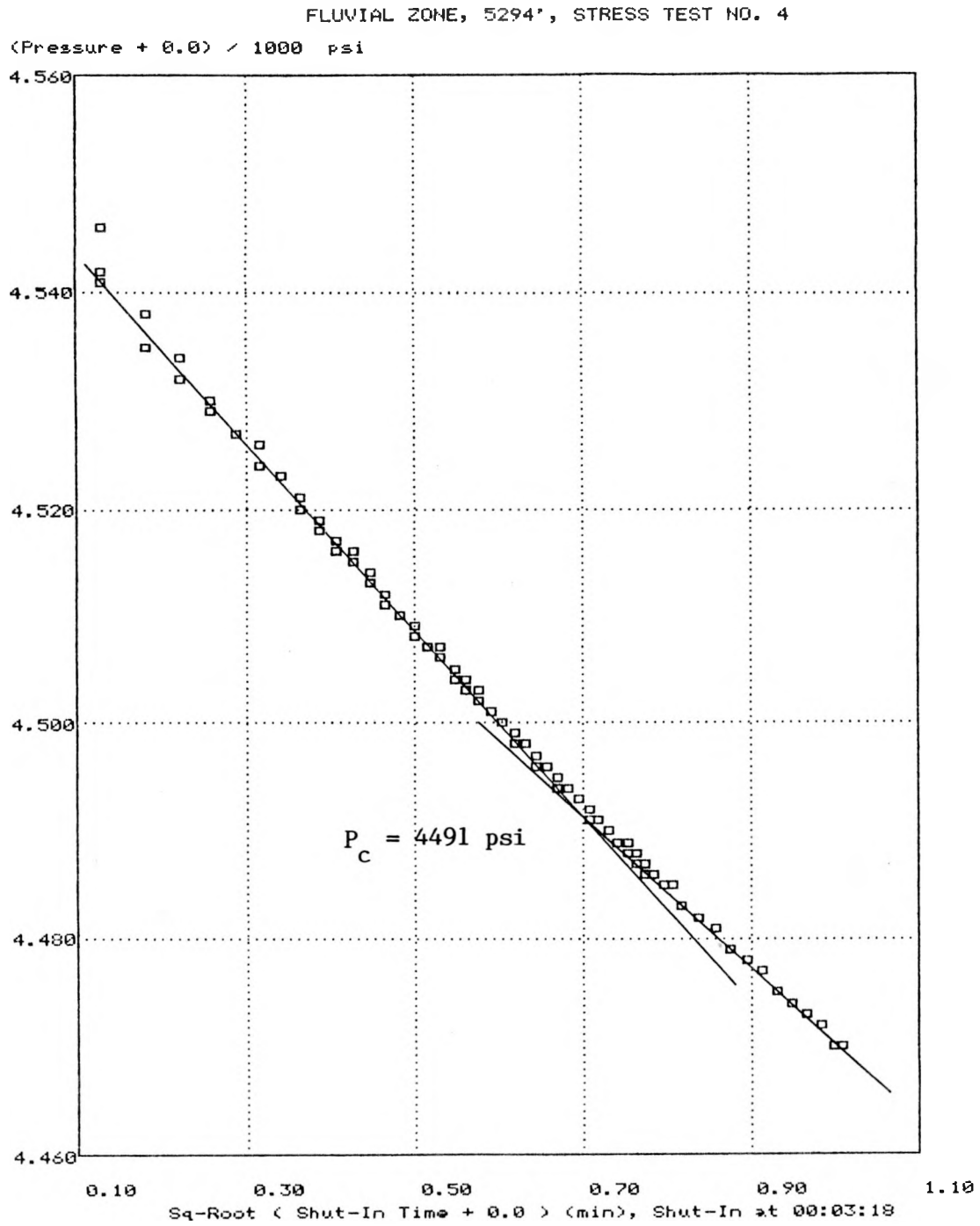


FIGURE A.63: Sandstone Stress Test (5294-5296'), Square-Root of Shut-In Time Plot of Test No. 4 Pressure Decline.

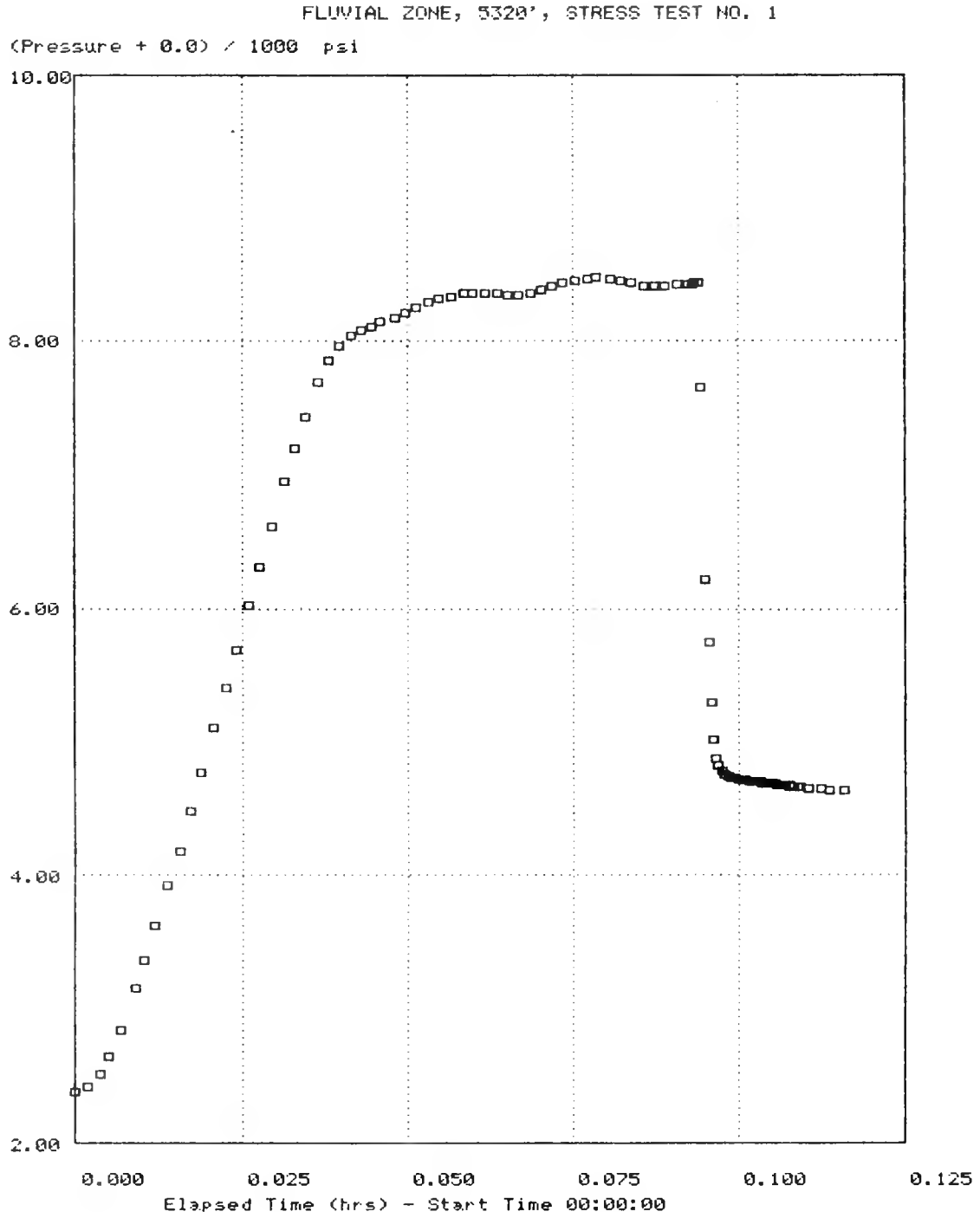


FIGURE A.64: Shale Stress Test (5320-5322'), Linear Plot of Test No. 1 Injection/Decline.

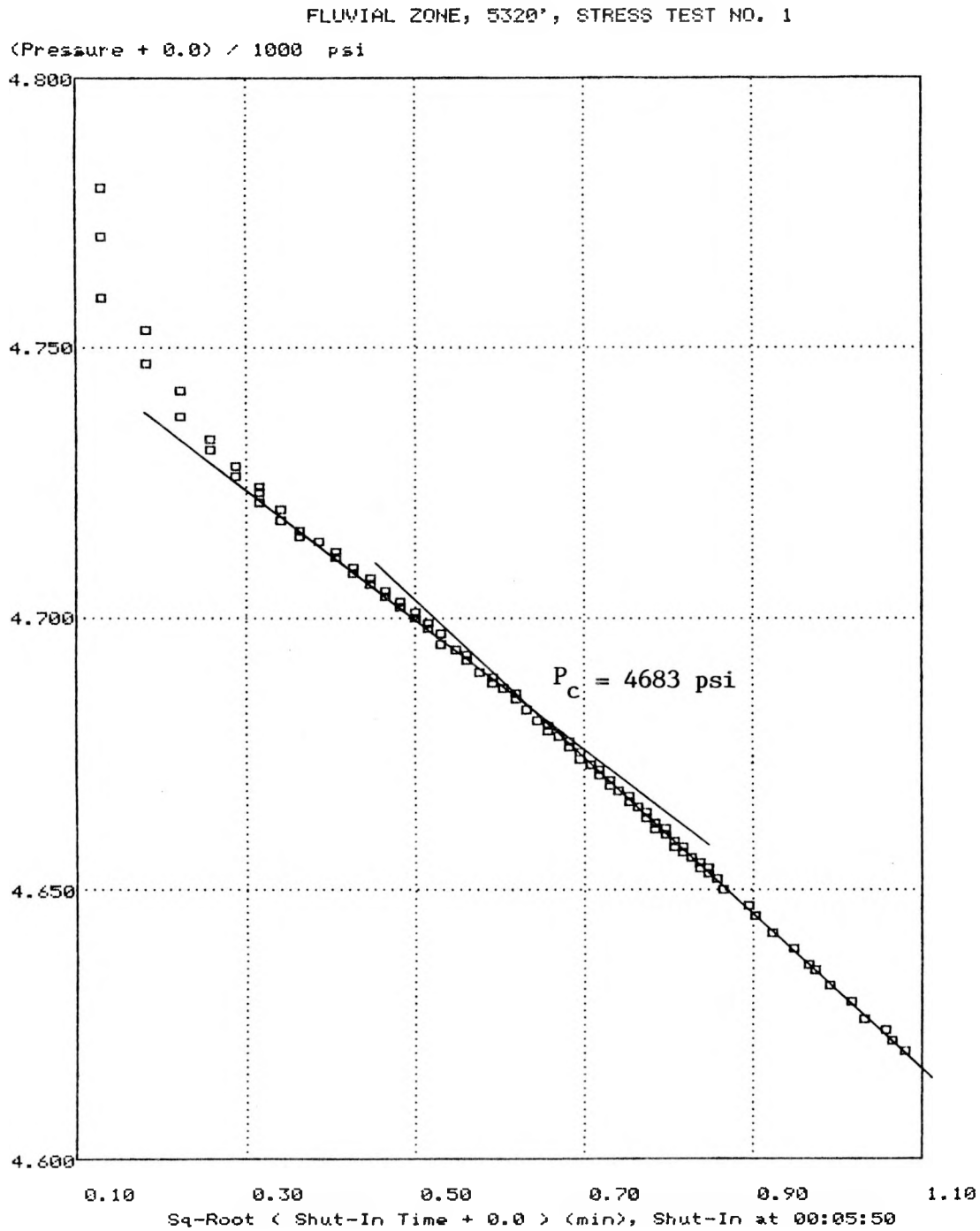


FIGURE A.65: Shale Stress Test (5320-5322'), Square-Root of Shut-In Time Plot of Test No. 1 Pressure Decline.

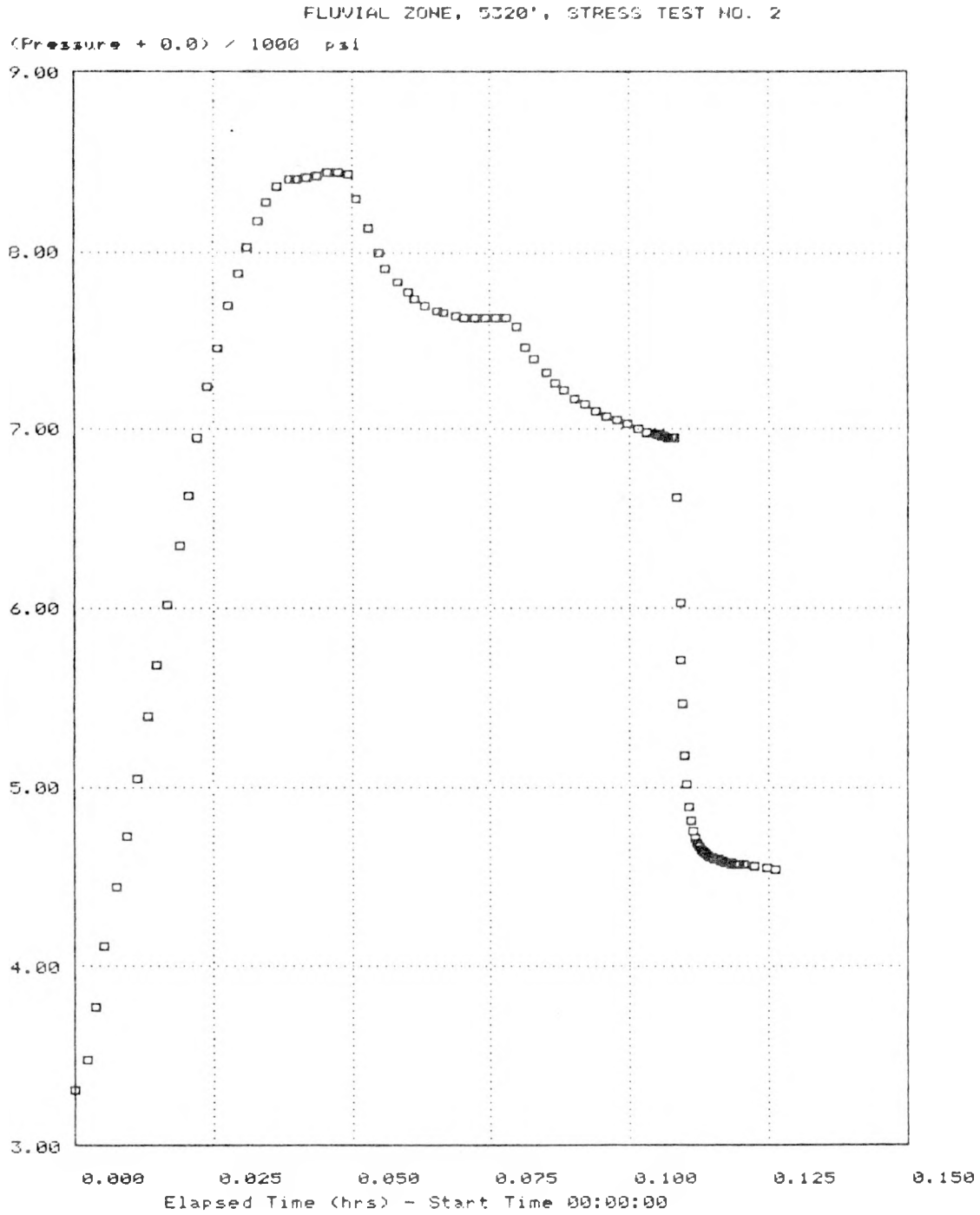


FIGURE A.66: Shale Stress Test (5320–5322'), Linear Plot of Test no. 2 Injection/Decline.

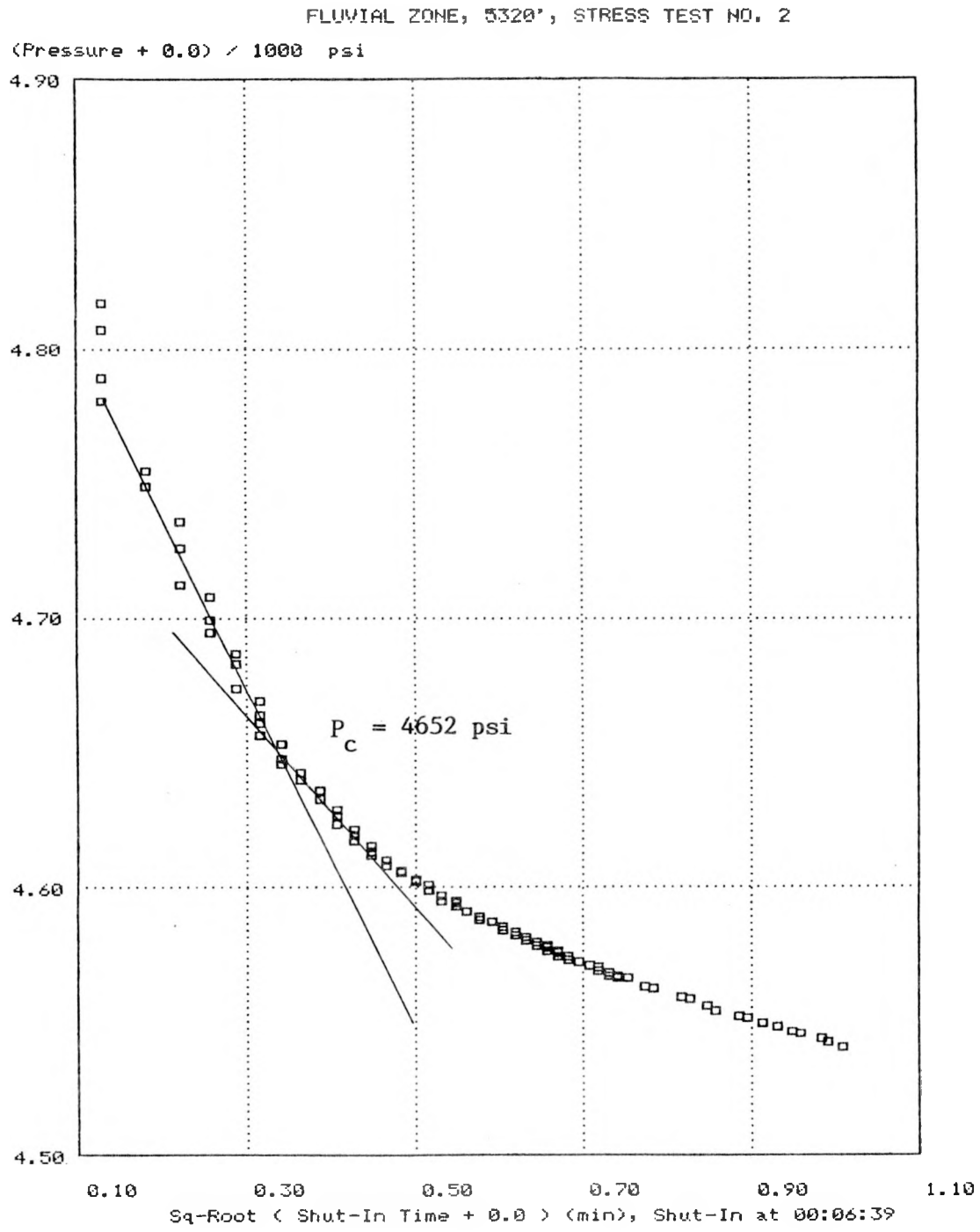


FIGURE A.67: Shale Stress Test (5320-5322'), Square-Root of Shut-In Time Plot of Test No. 2 Pressure Decline.

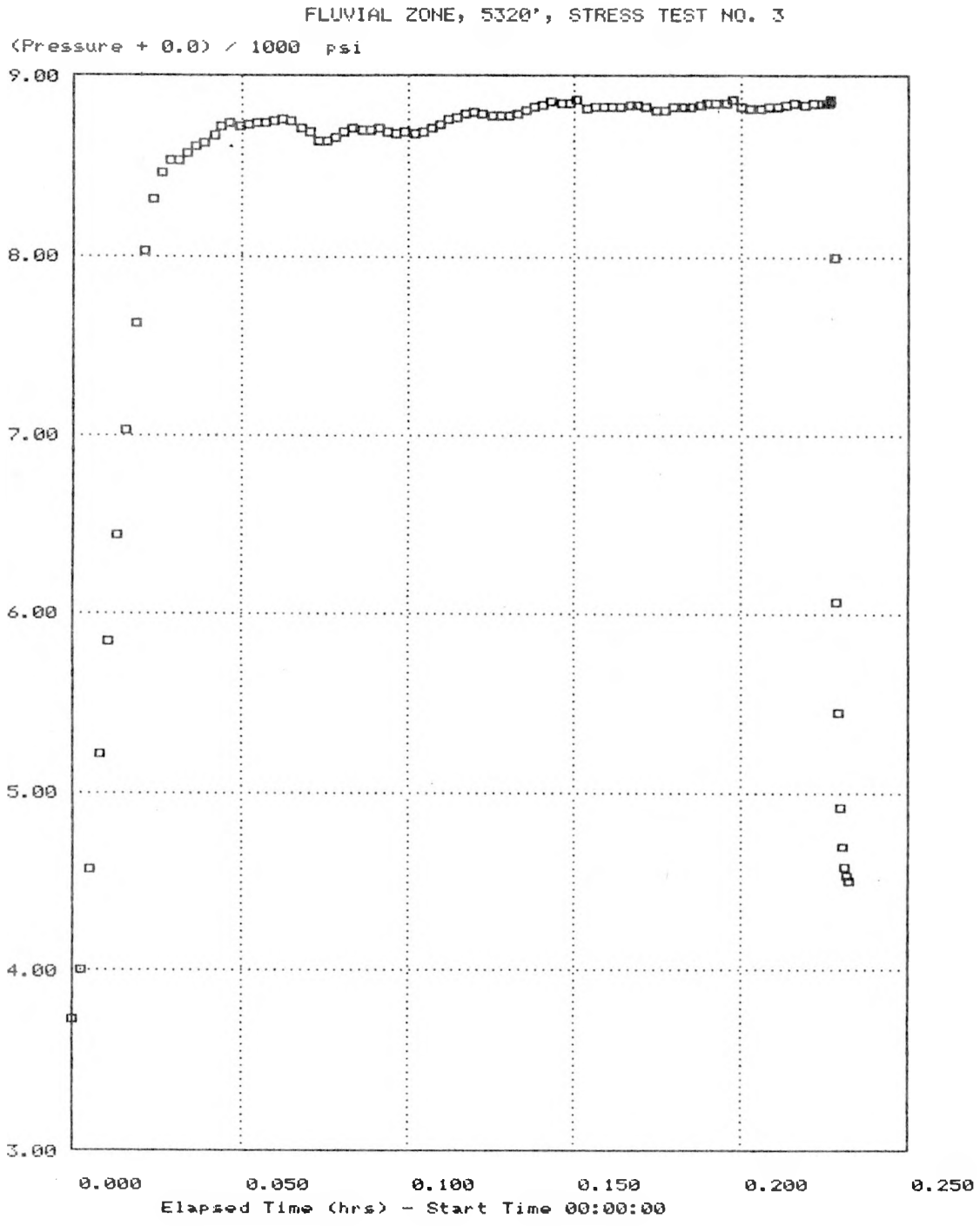


FIGURE A.68: Shale Stress Test (5320–5322'), Linear Plot of Test No. 3 Injection/Decline.

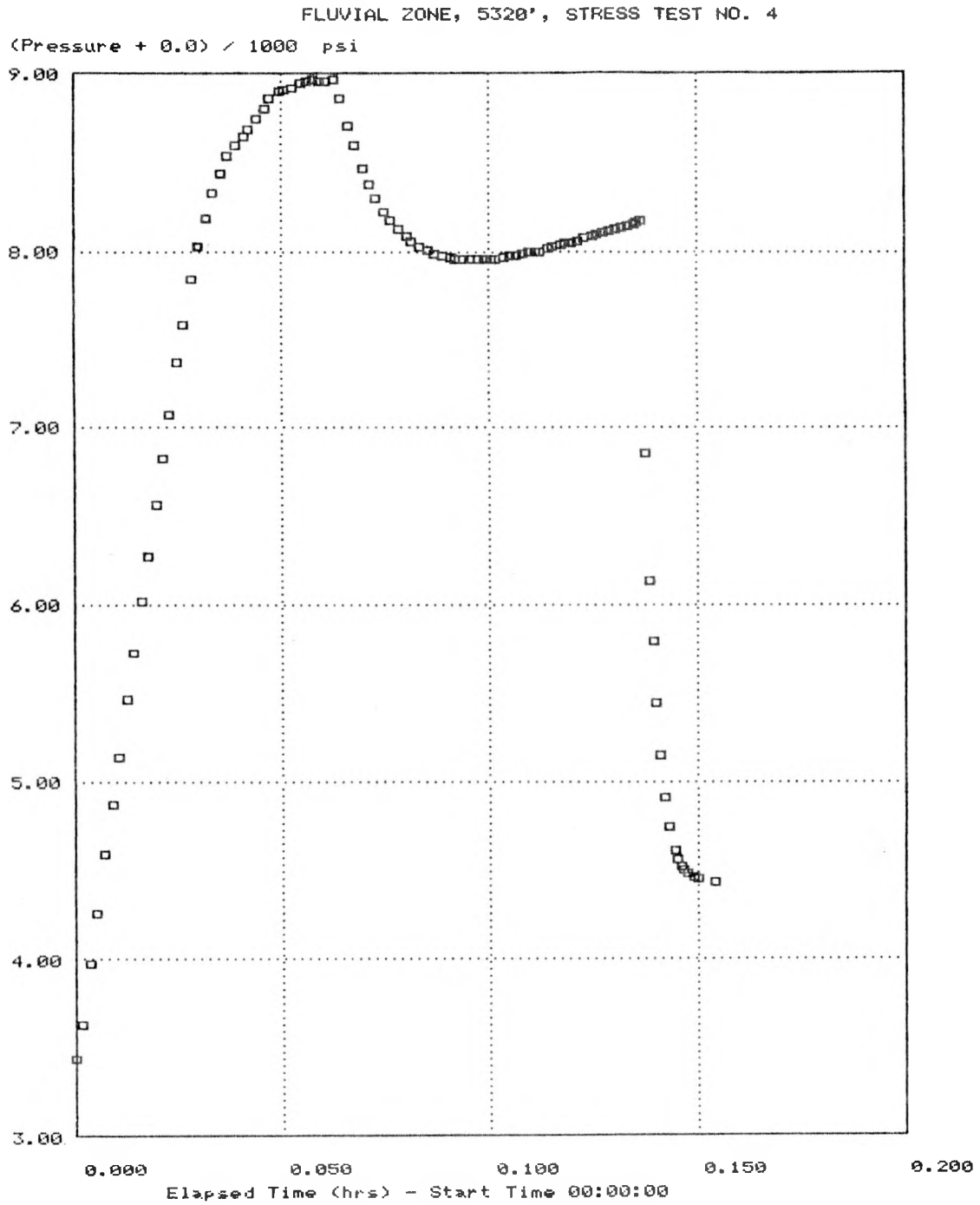


FIGURE A.69: Shale Stress Test (5320–5322'), Linear Plot of Test No. 4 Injection/Decline.

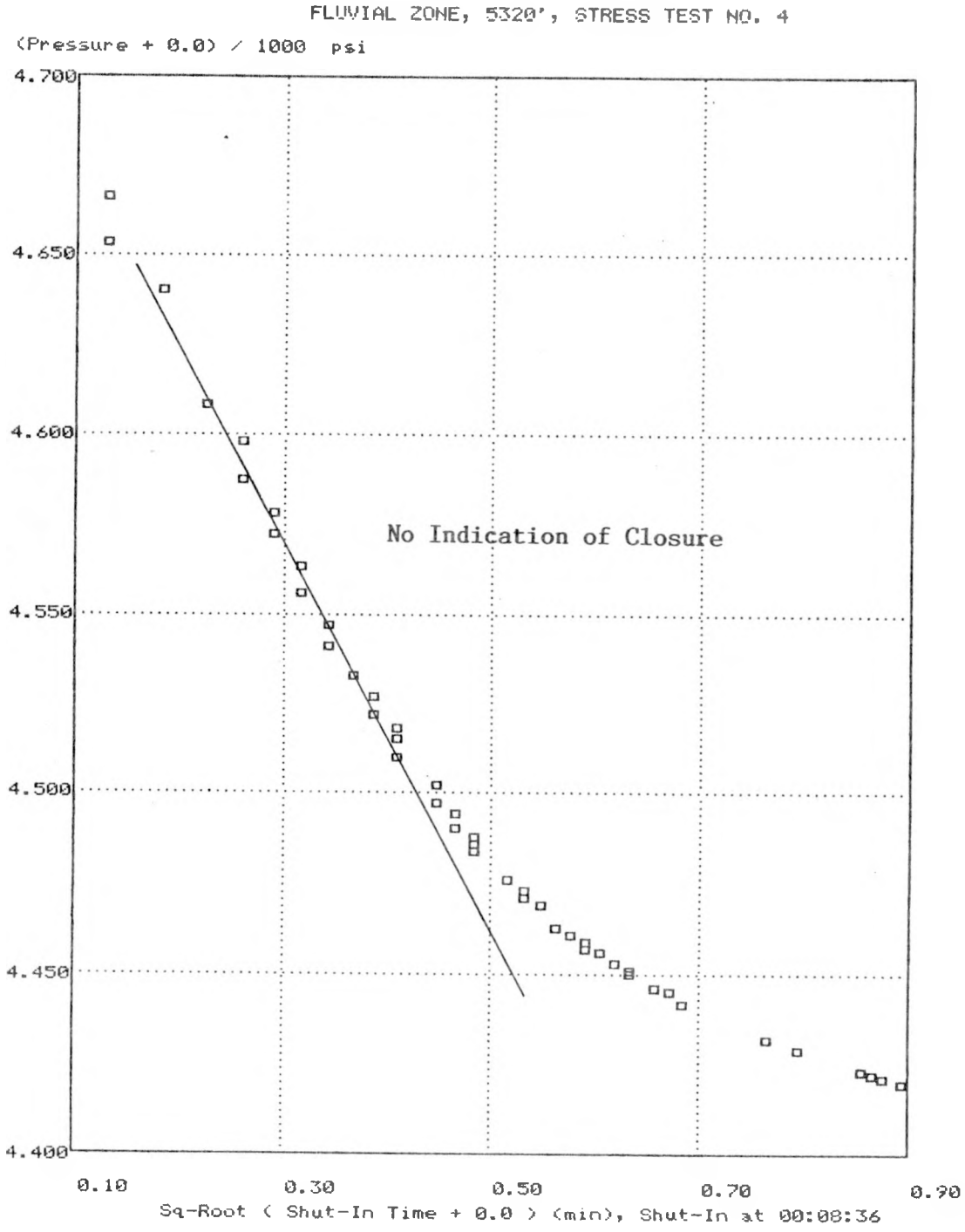


FIGURE A.70: Shale Stress Test (5320–5322'), Square-Root of Shut-In Time Plot of Test No. 4 Pressure Decline.

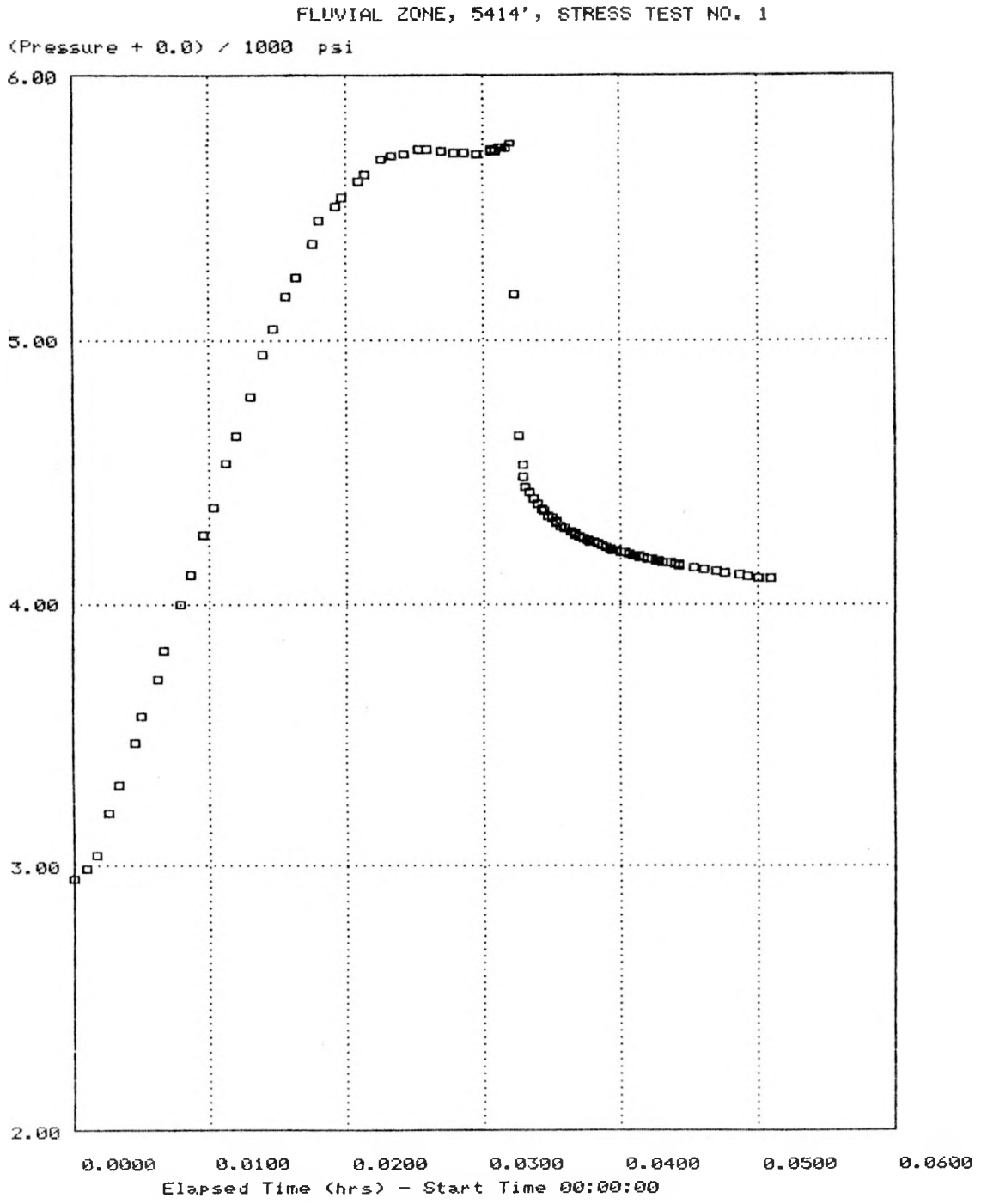


FIGURE A.71: Shale Stress Test (5414-5416'), Linear Plot of Test No. 1 Injection/Decline.

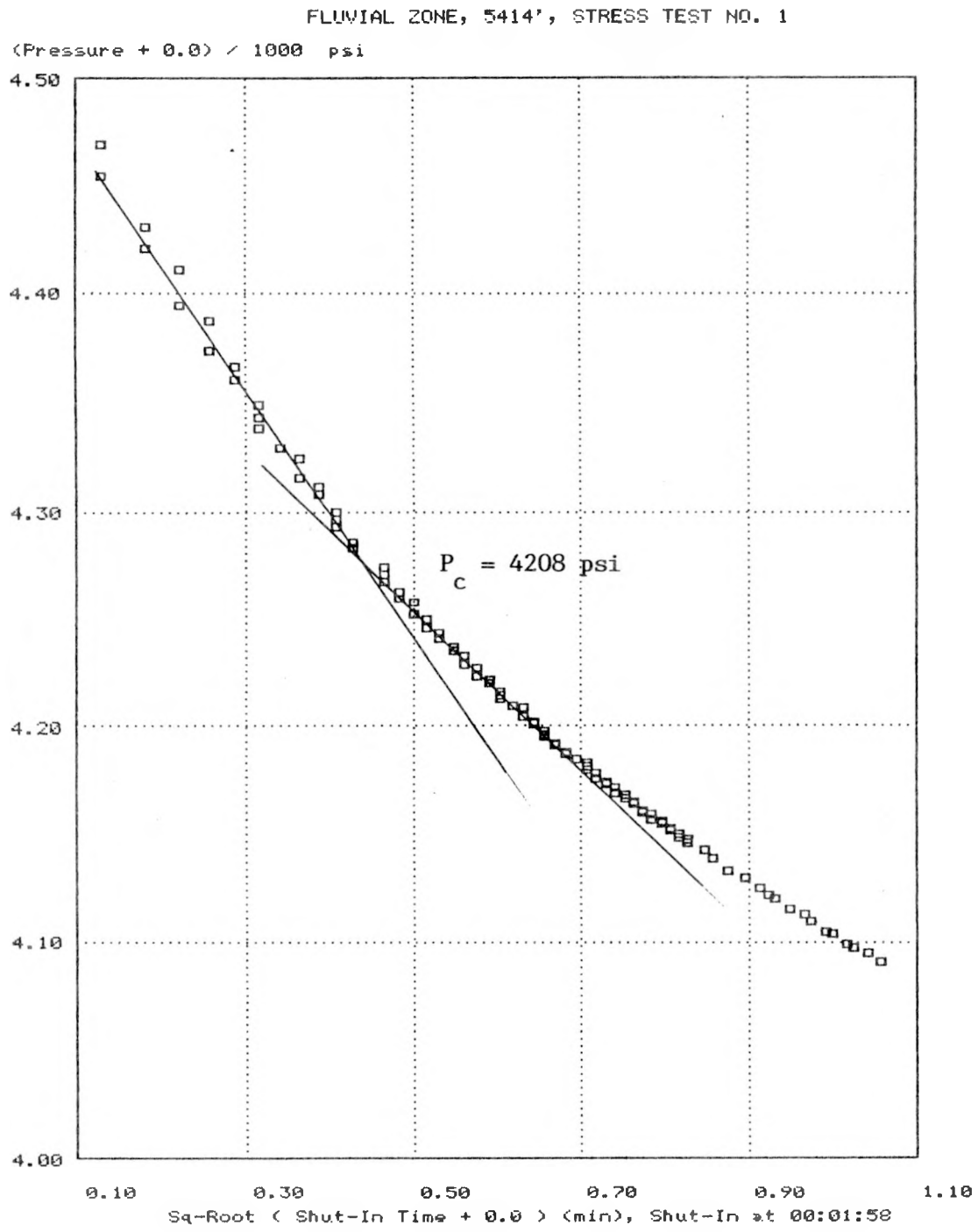


FIGURE A.72: Shale Stress Test (5414-5416'), Square-Root of Shut-In Time Plot of Test No. 1 Pressure Decline.

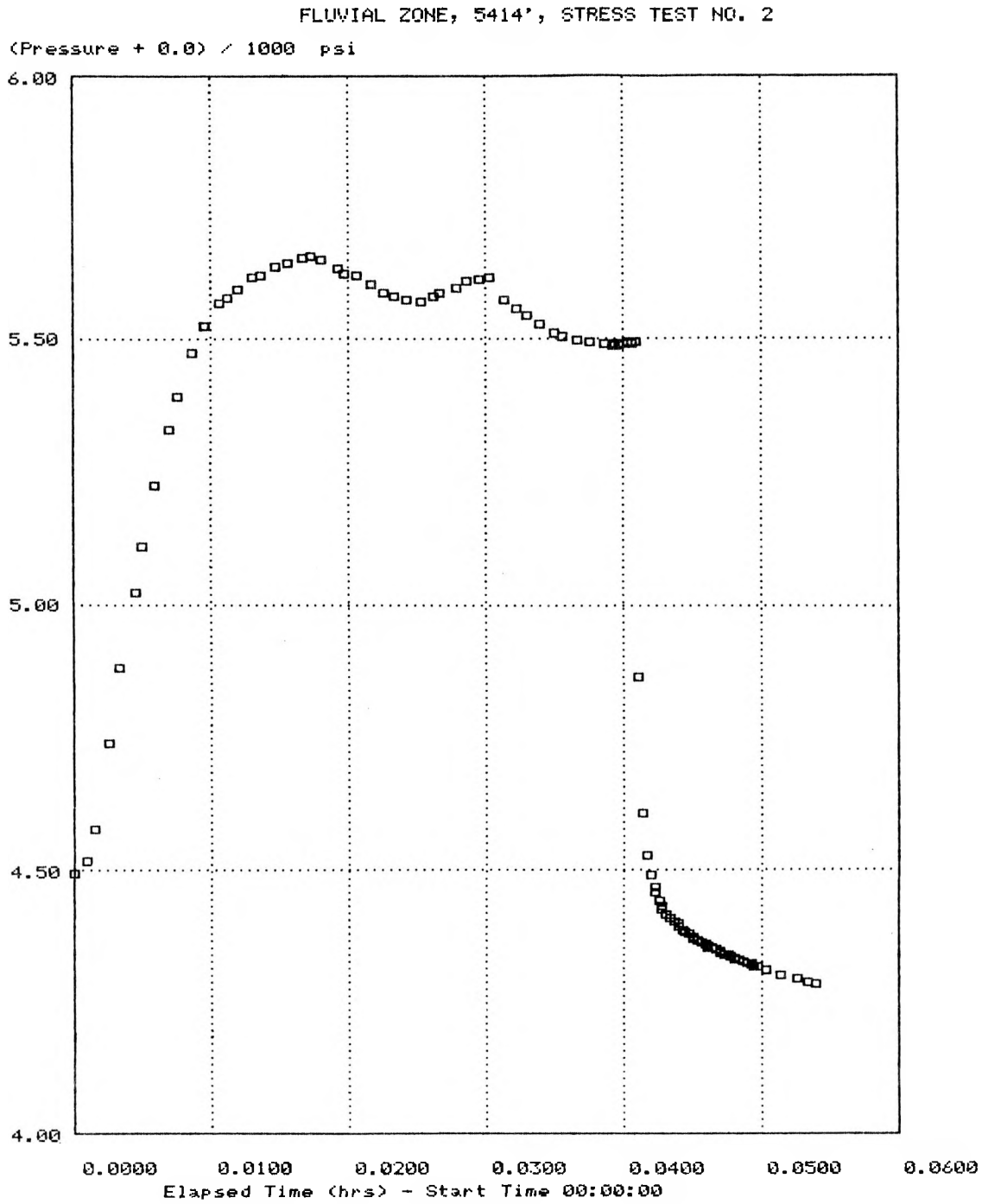


FIGURE A.73: Shale Stress Test (5414-5416'), Linear Plot of Test No. 2 Injection/Decline.

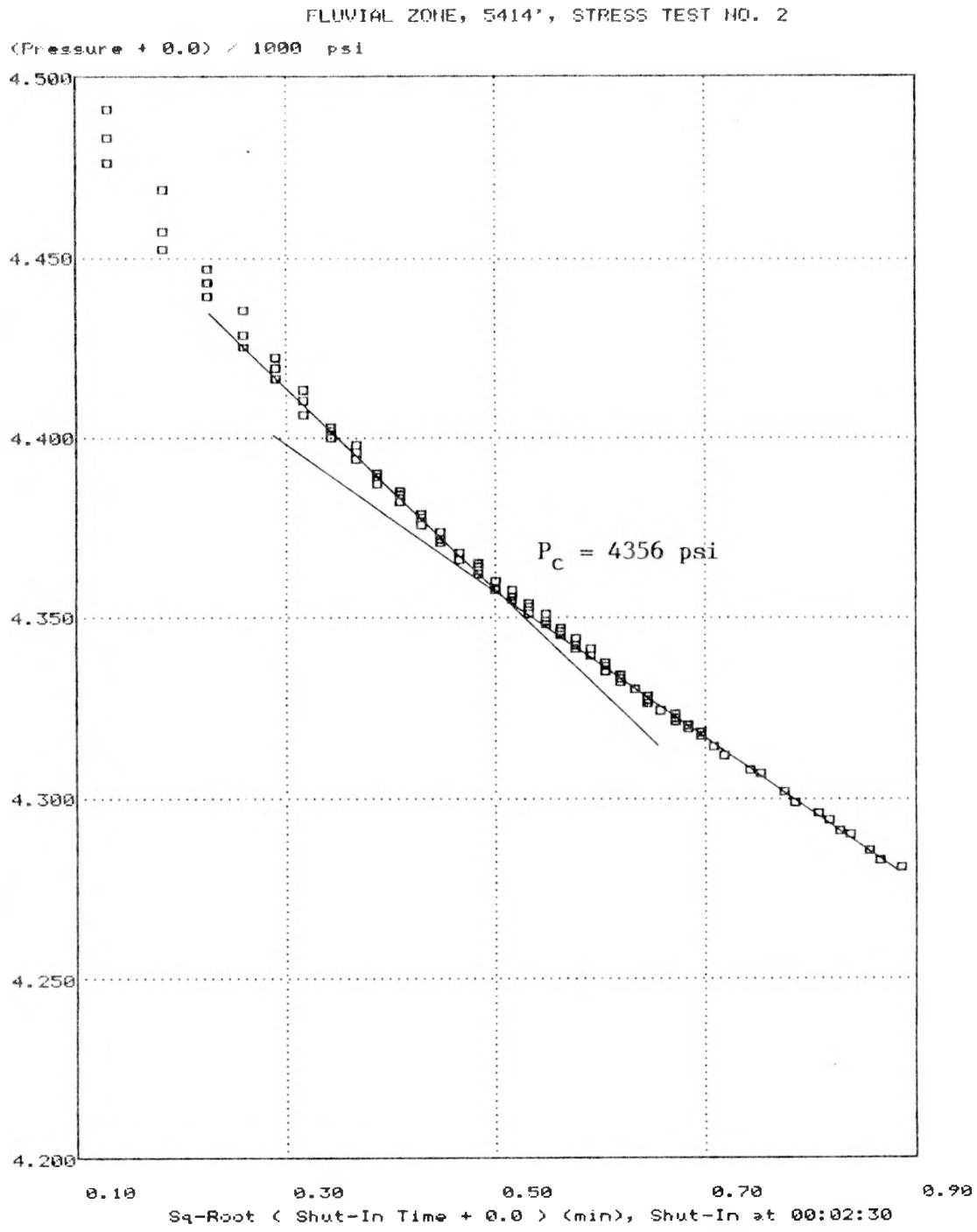


FIGURE A.74: Shale Stress Test (5414-5416'), Square-Root of Shut-In Time Plot of Test No. 2 Pressure Decline.

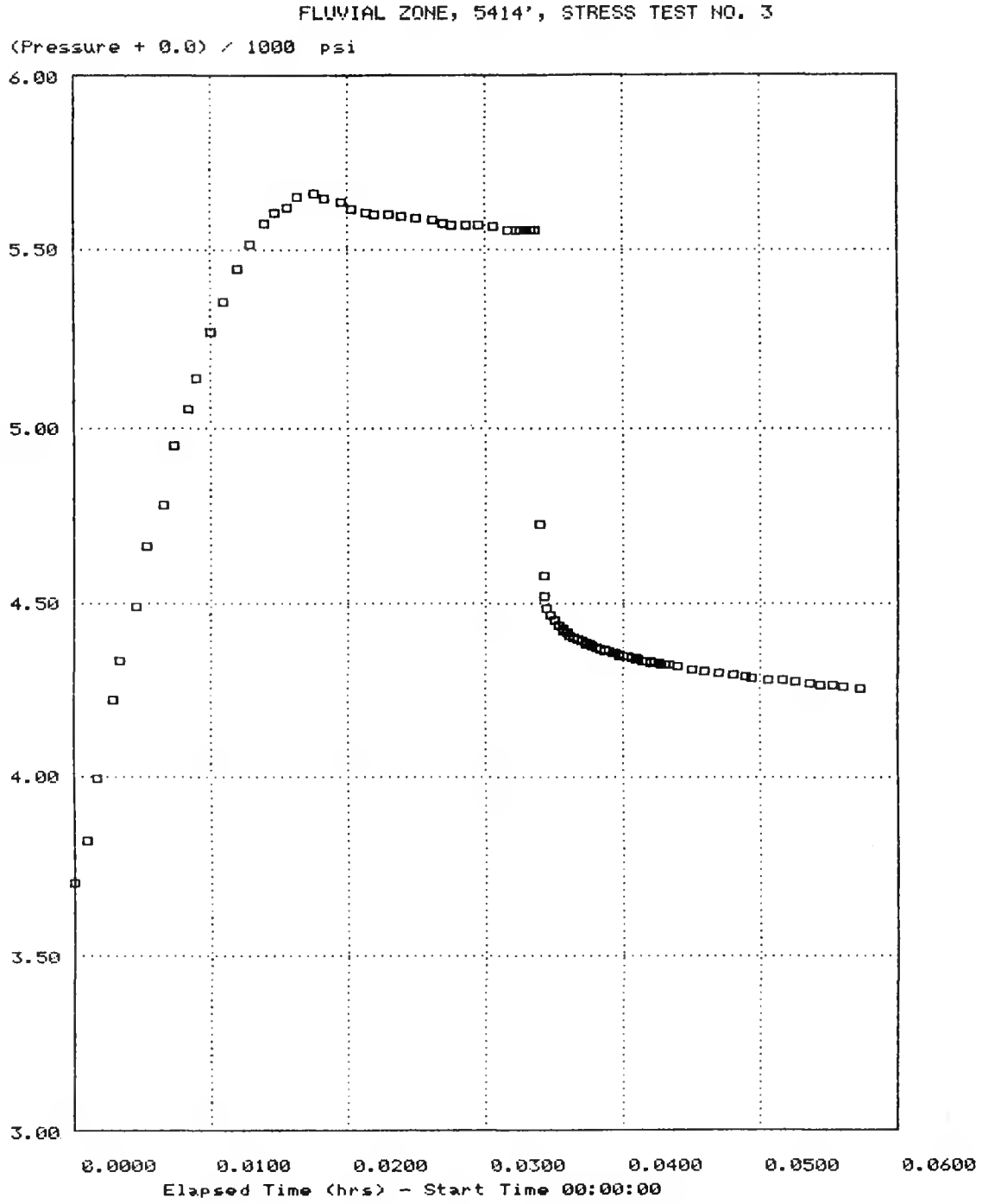


FIGURE A.75: Shale Stress Test (5414-5416'), Linear Plot of Test No. 3 Injection/Decline.

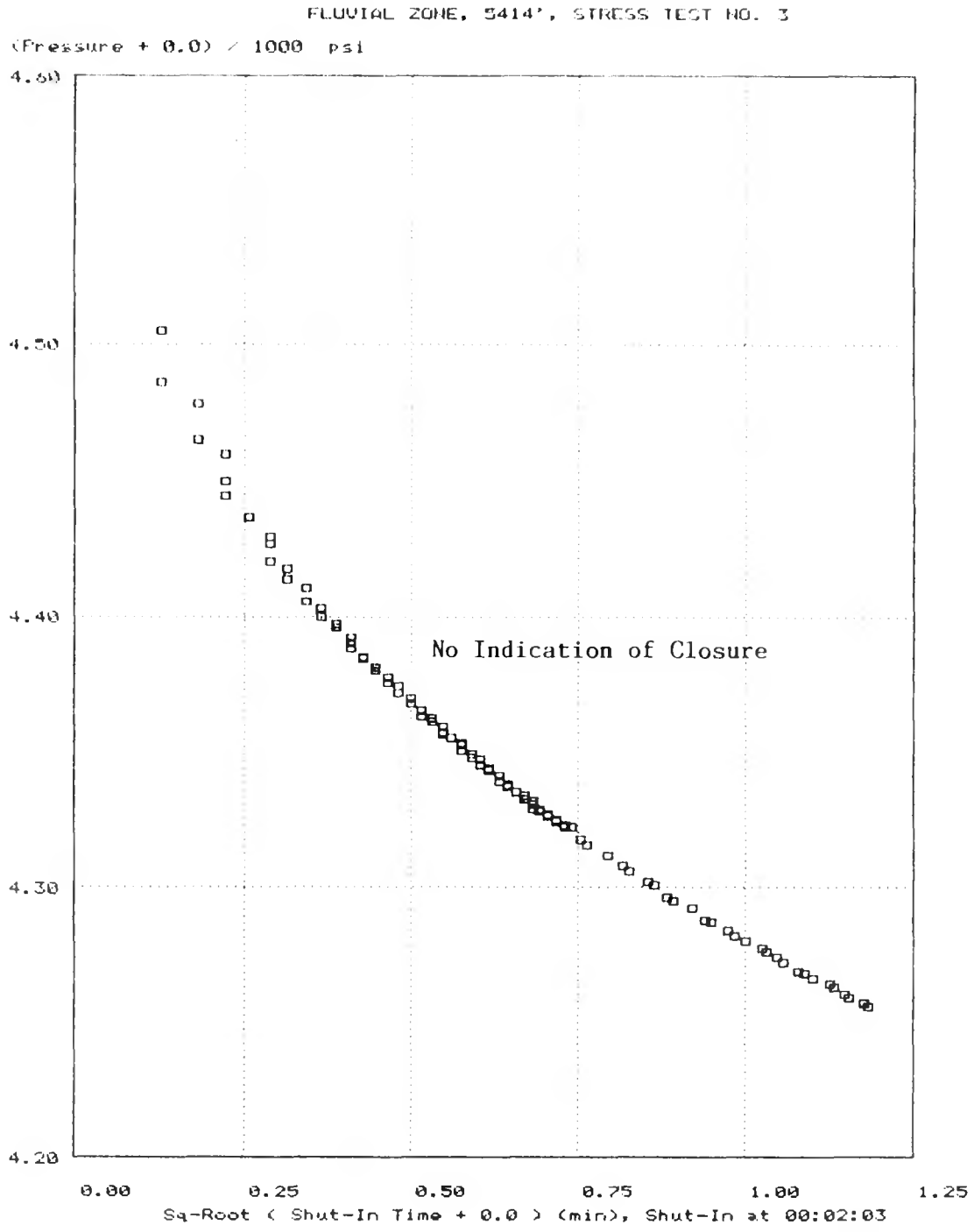


FIGURE A.76: Shale Stress Test (5414-5416'), Square-Root of Shut-In Time Plot of Test No. 3 Pressure Decline.

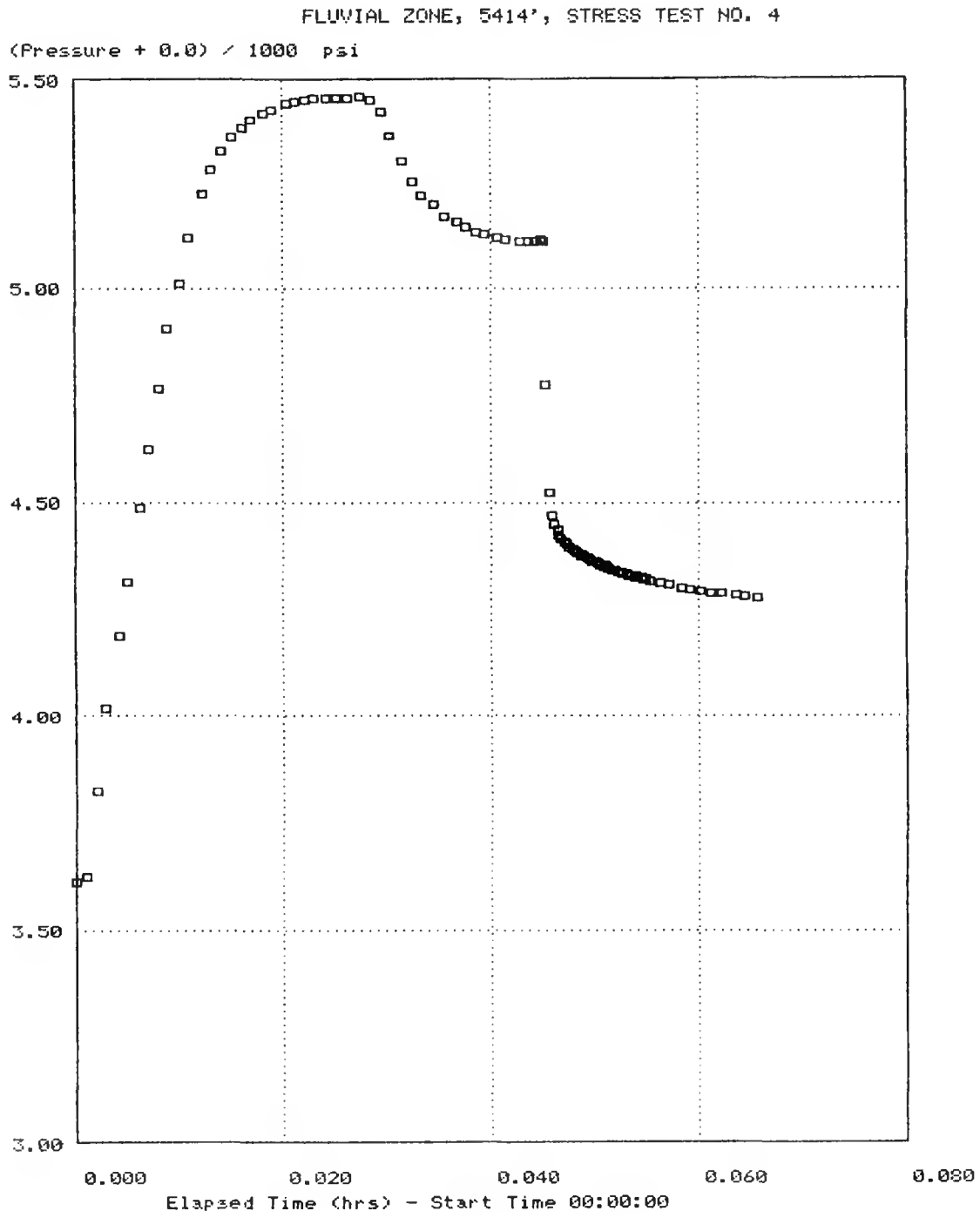


FIGURE A.77: Shale Stress Test (5414-5416'), Linear Plot of Test No. 4 Injection/Decline.

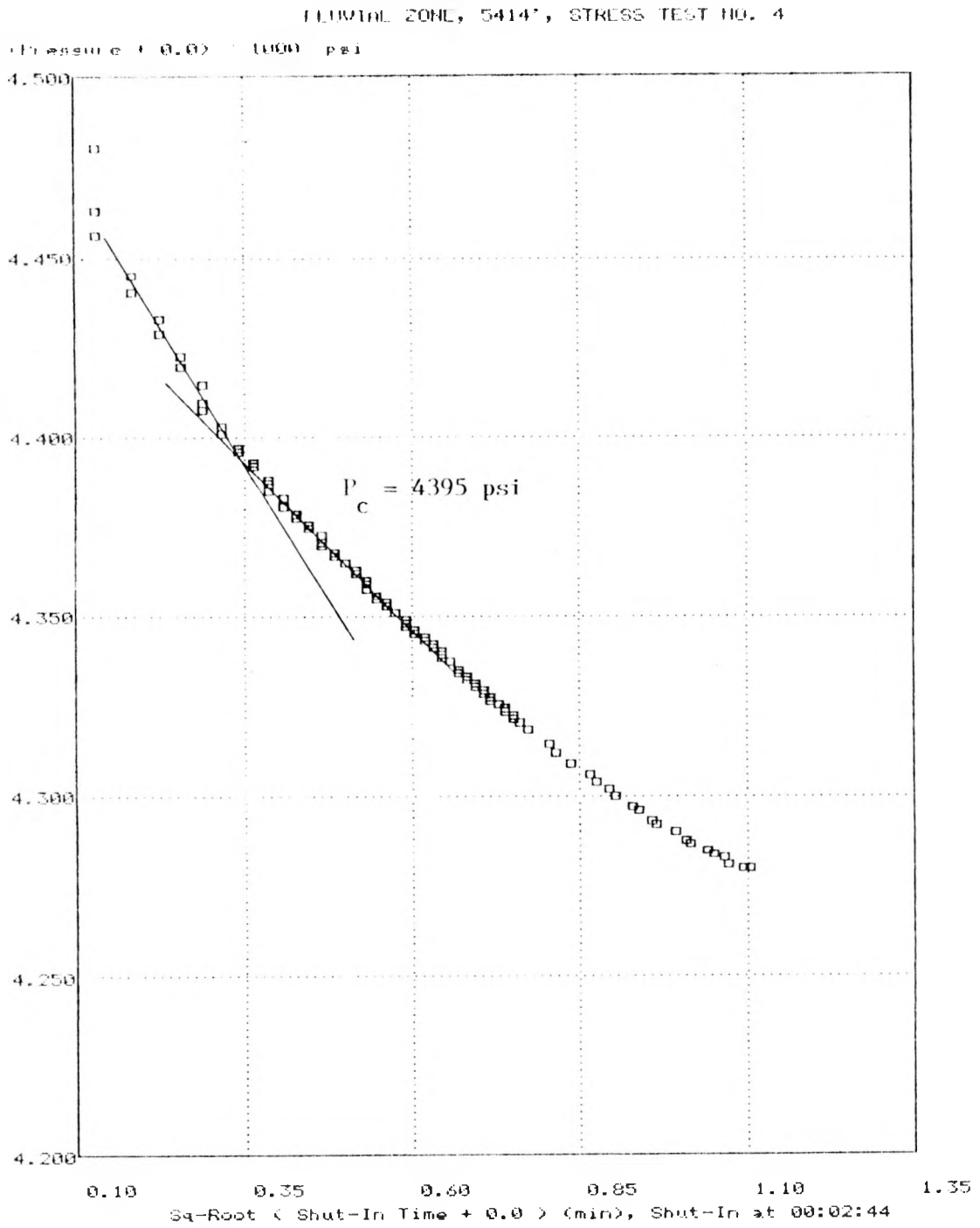


FIGURE A.78: Shale Stress Test (5414-5416'), Square-Root of Shut-In Time Plot of Test No. 4 Pressure Decline.

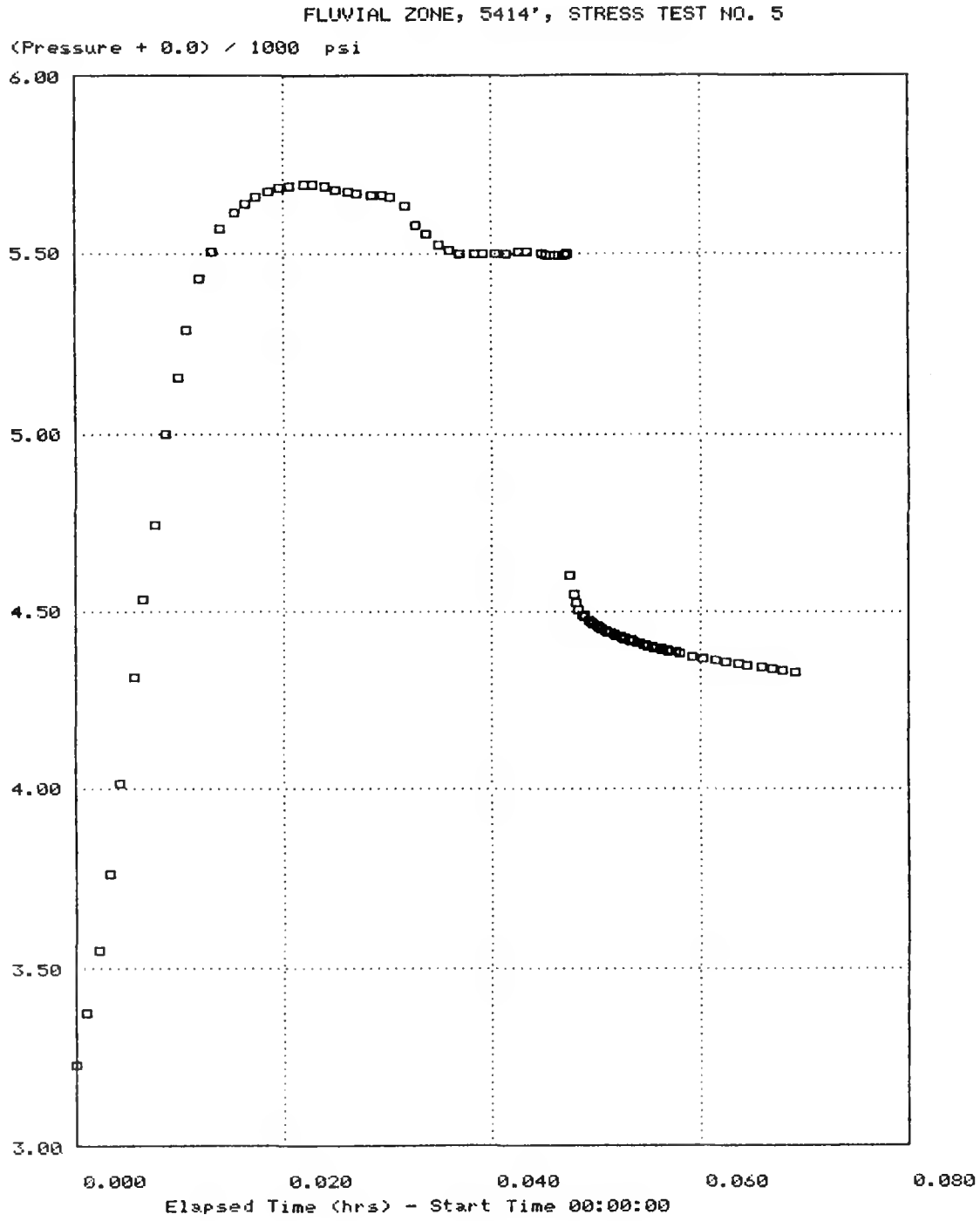


FIGURE A.79: Shale Stress Test (5414-5416'), Linear Plot of Test No. 5 Injection/Decline.

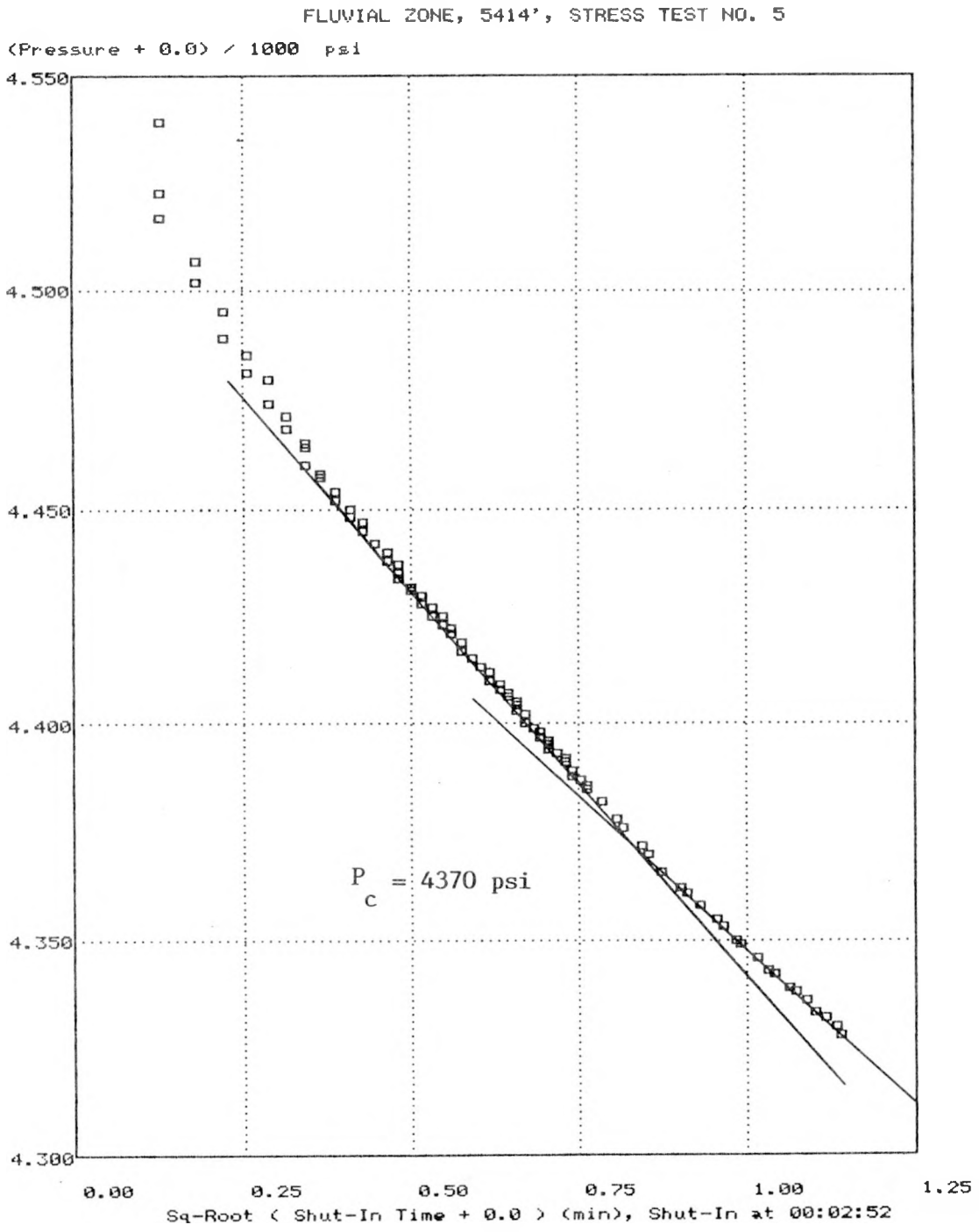


FIGURE A.80: Shale Stress Test (5414-5416'), Square-Root of Shut-In Time Plot of Test No. 5 Pressure Decline.

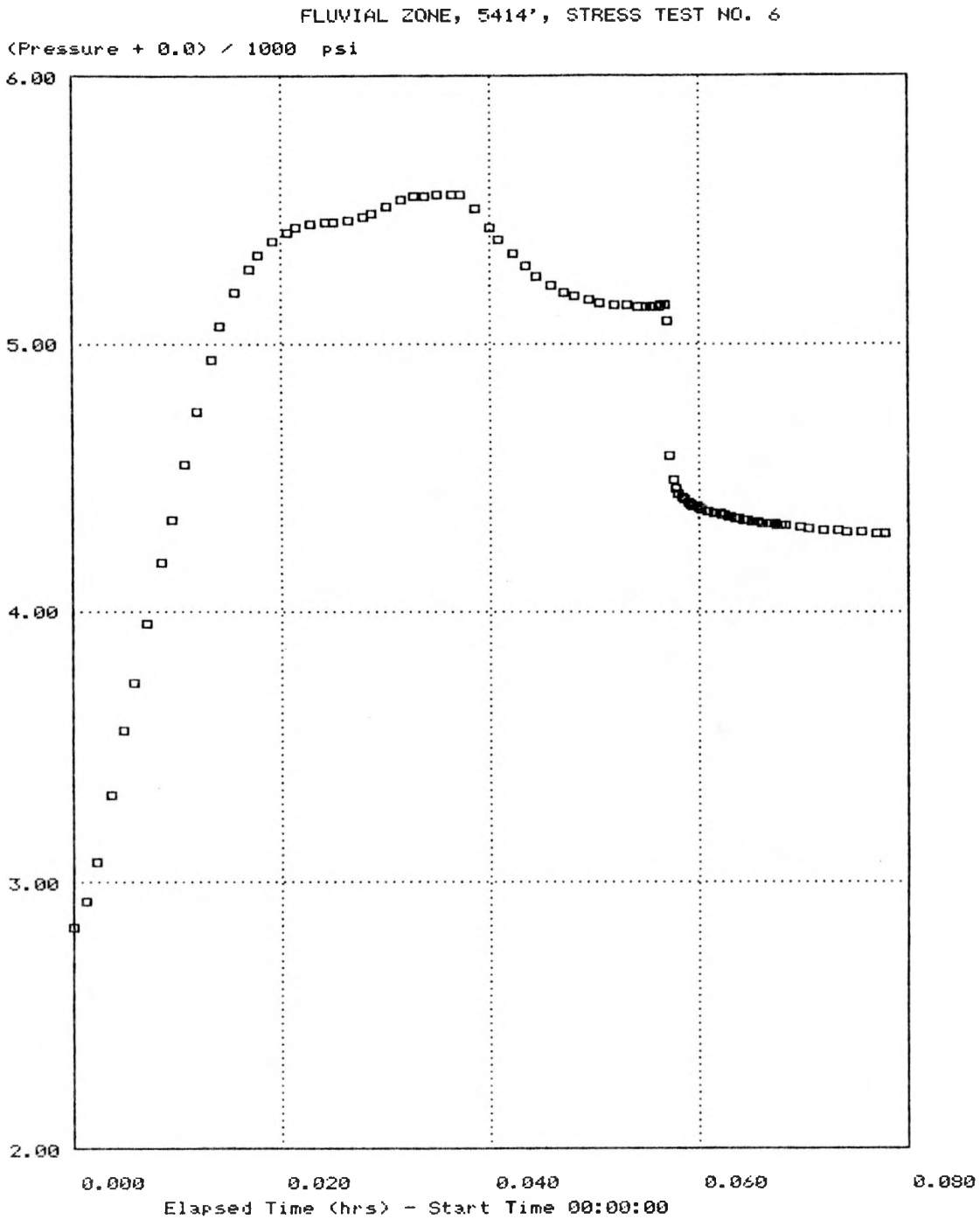


FIGURE A.81: Shale Stress Test (5414-5416'), Linear Plot of Test No. 6 Injection/Decline.

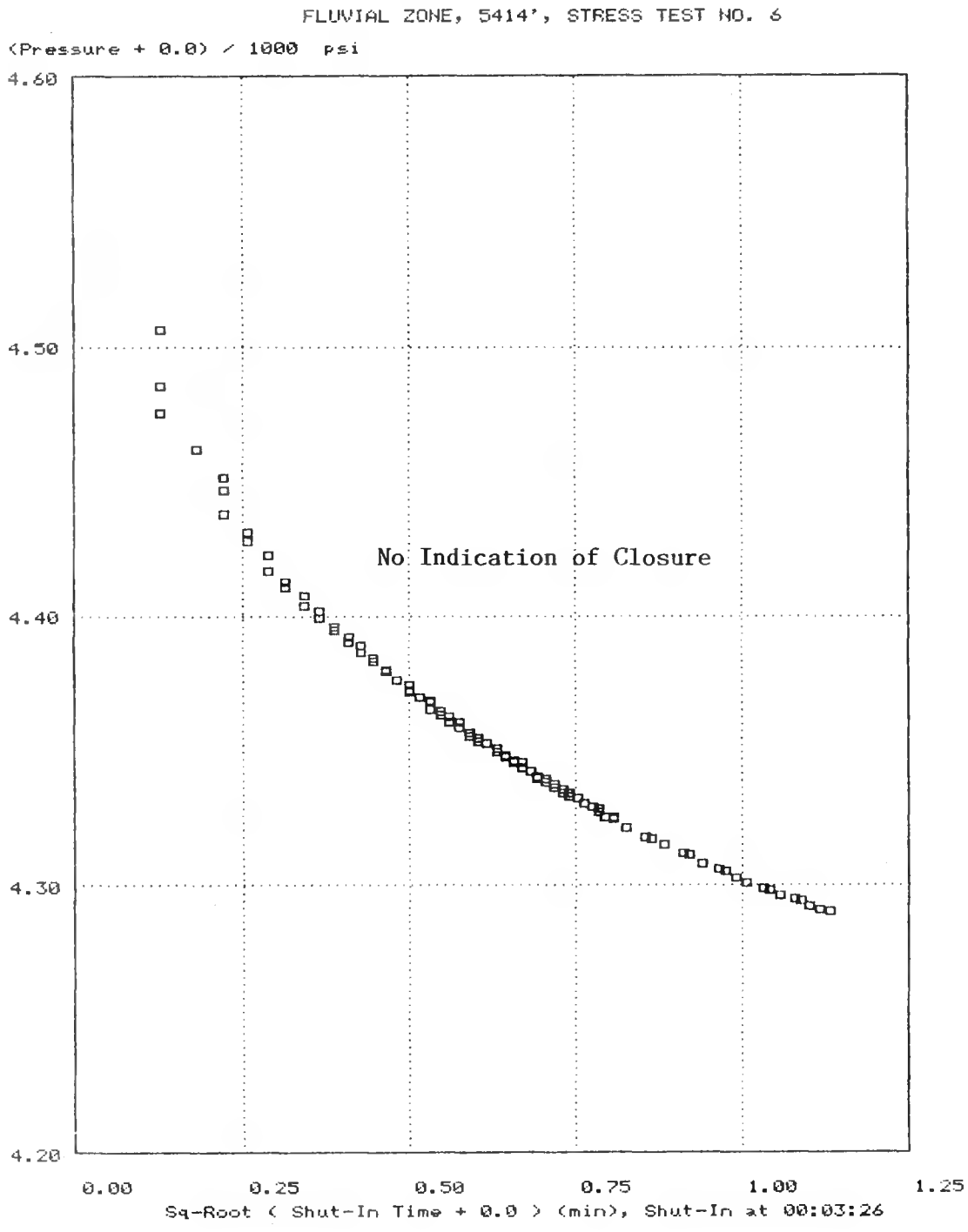


FIGURE A.82: Shale Stress Test (5414-5416'), Square-Root of Shut-In Time Plot of Test No. 6 Pressure Decline.

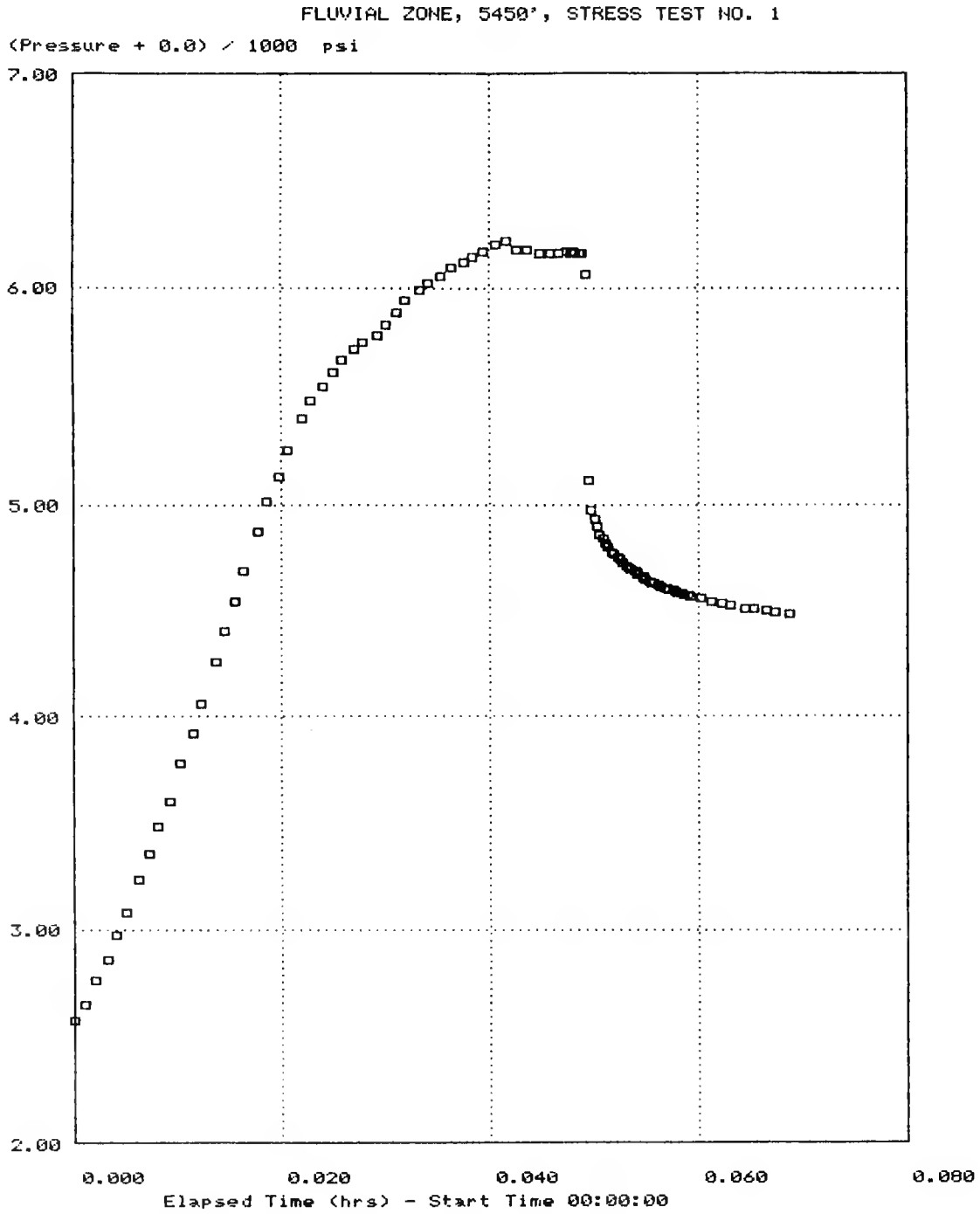


FIGURE A.83: Shale Stress Test (5450-5452'), Linear Plot of Test No. 1 Injection/Decline.

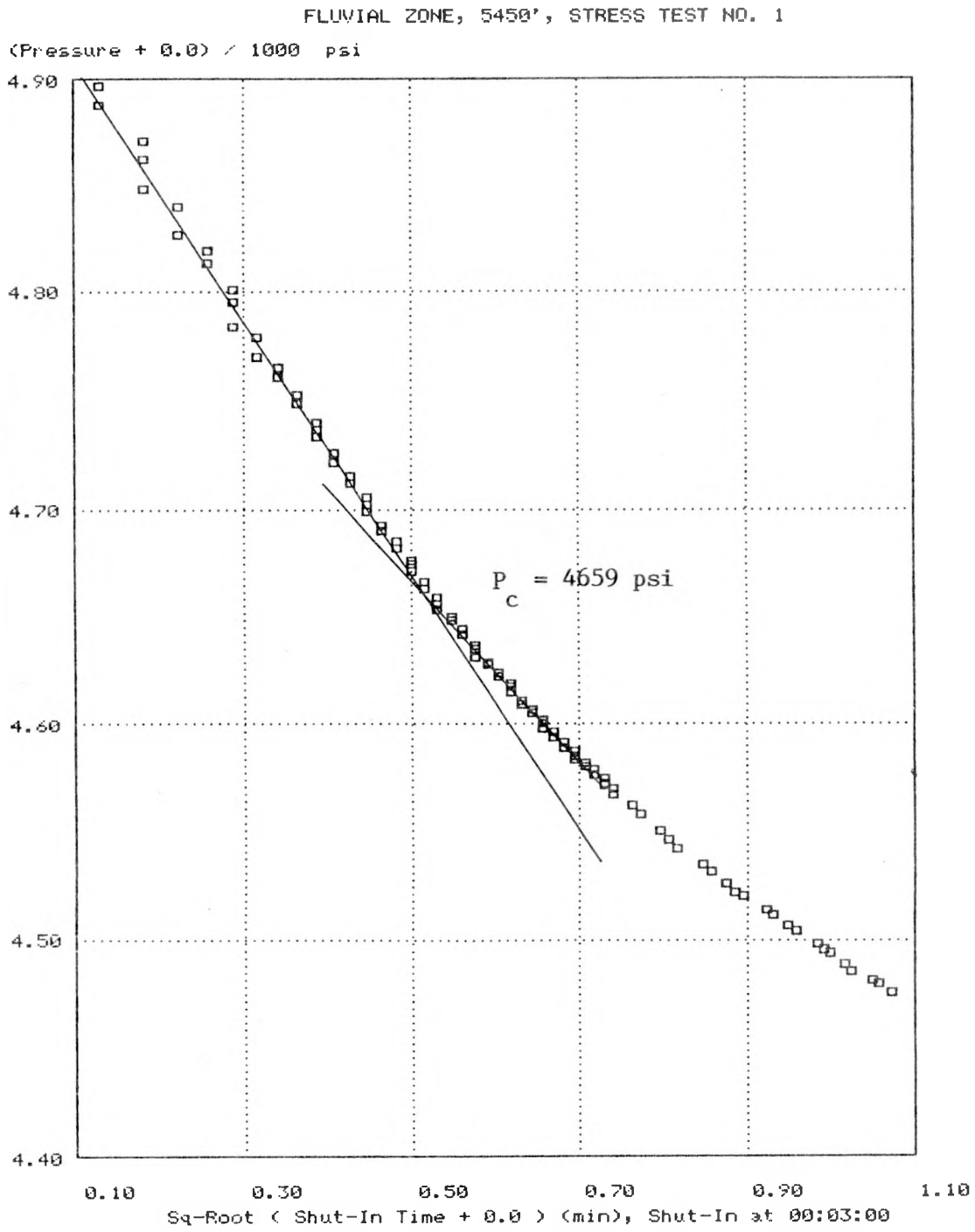


FIGURE A.84: Shale Stress Test (5450-5452'), Square-Root of Shut-In Time Plot of Test No. 1 Pressure Decline.

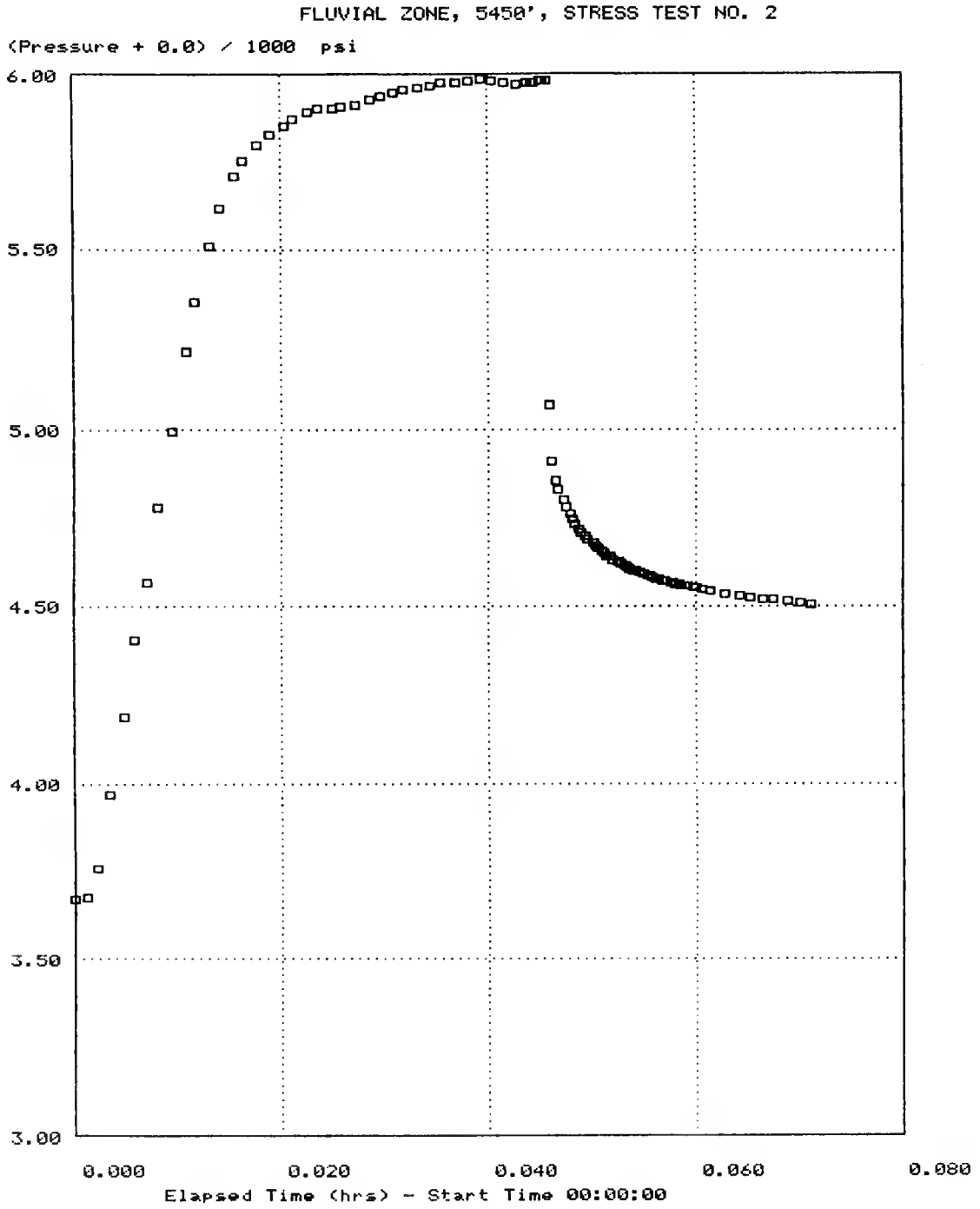


FIGURE A.85: Shale Stress Test (5450-5452'), Linear Plot of Test No. 2 Injection/Decline.

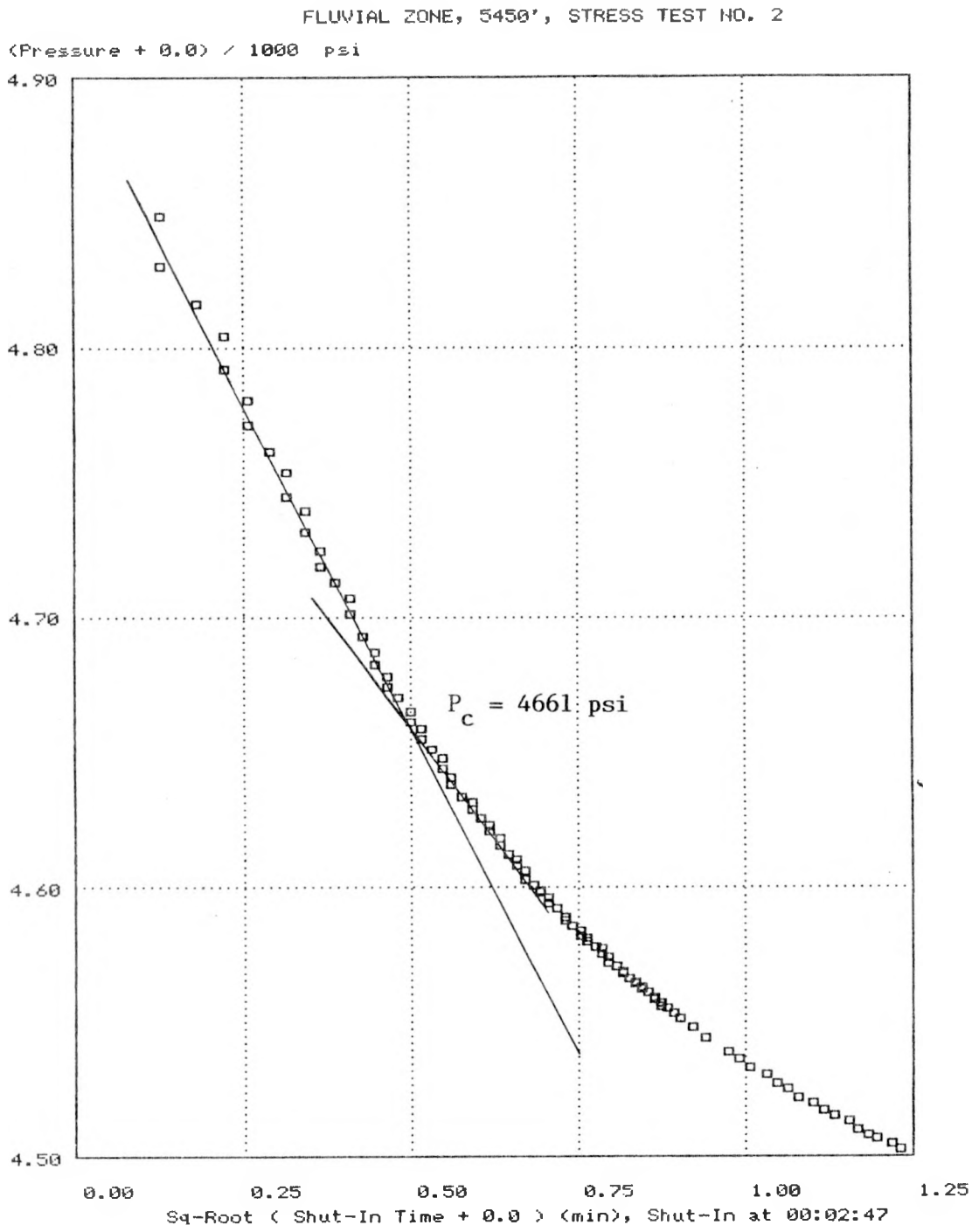


FIGURE A.86: Shale Stress Test (5450-5452'), Square-Root of Shut-In Time Plot of Test No. 2 Pressure Decline.

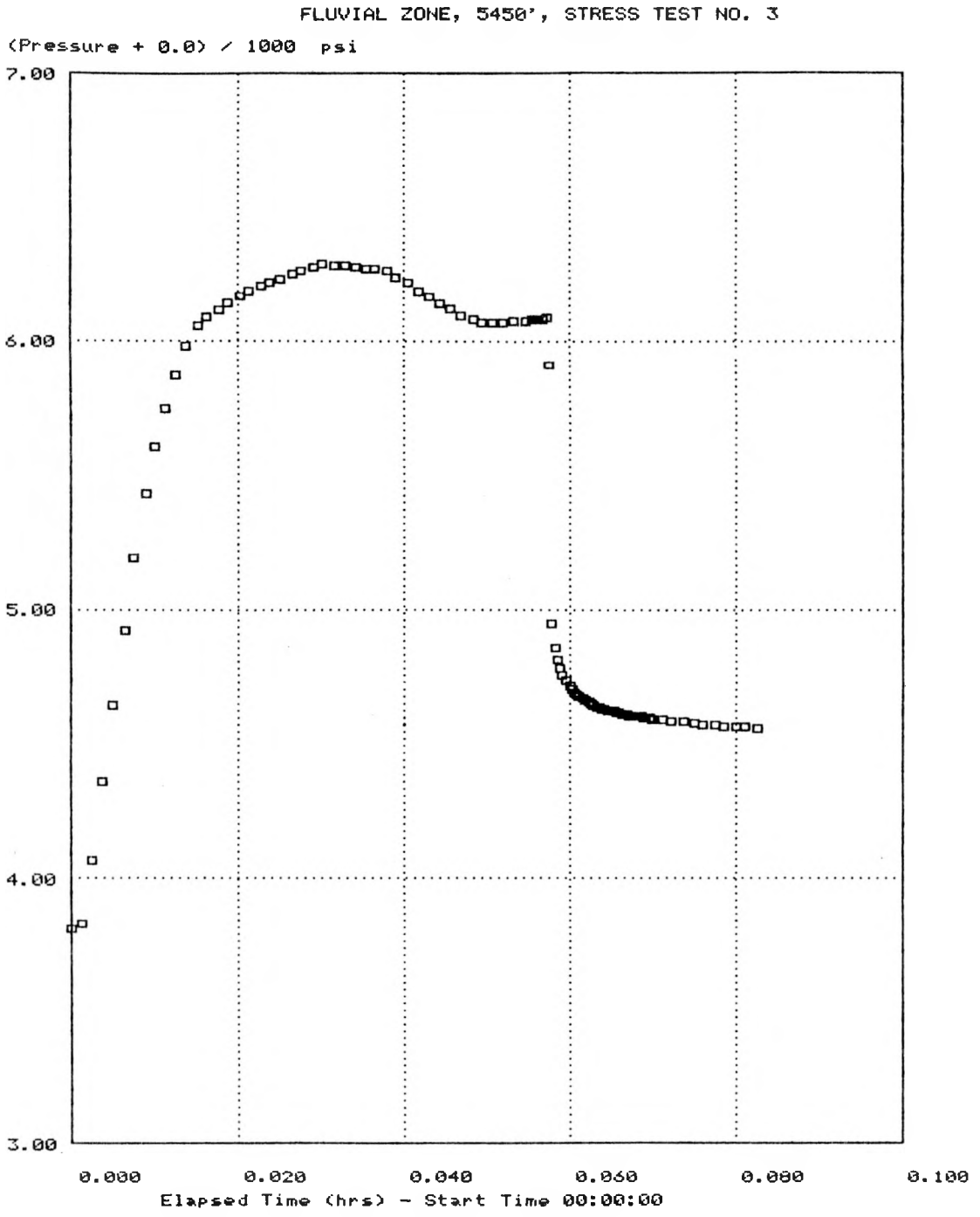


FIGURE A.87: Shale Stress Test (5450–5452'), Linear Plot of Test No. 3 Injection/Decline.

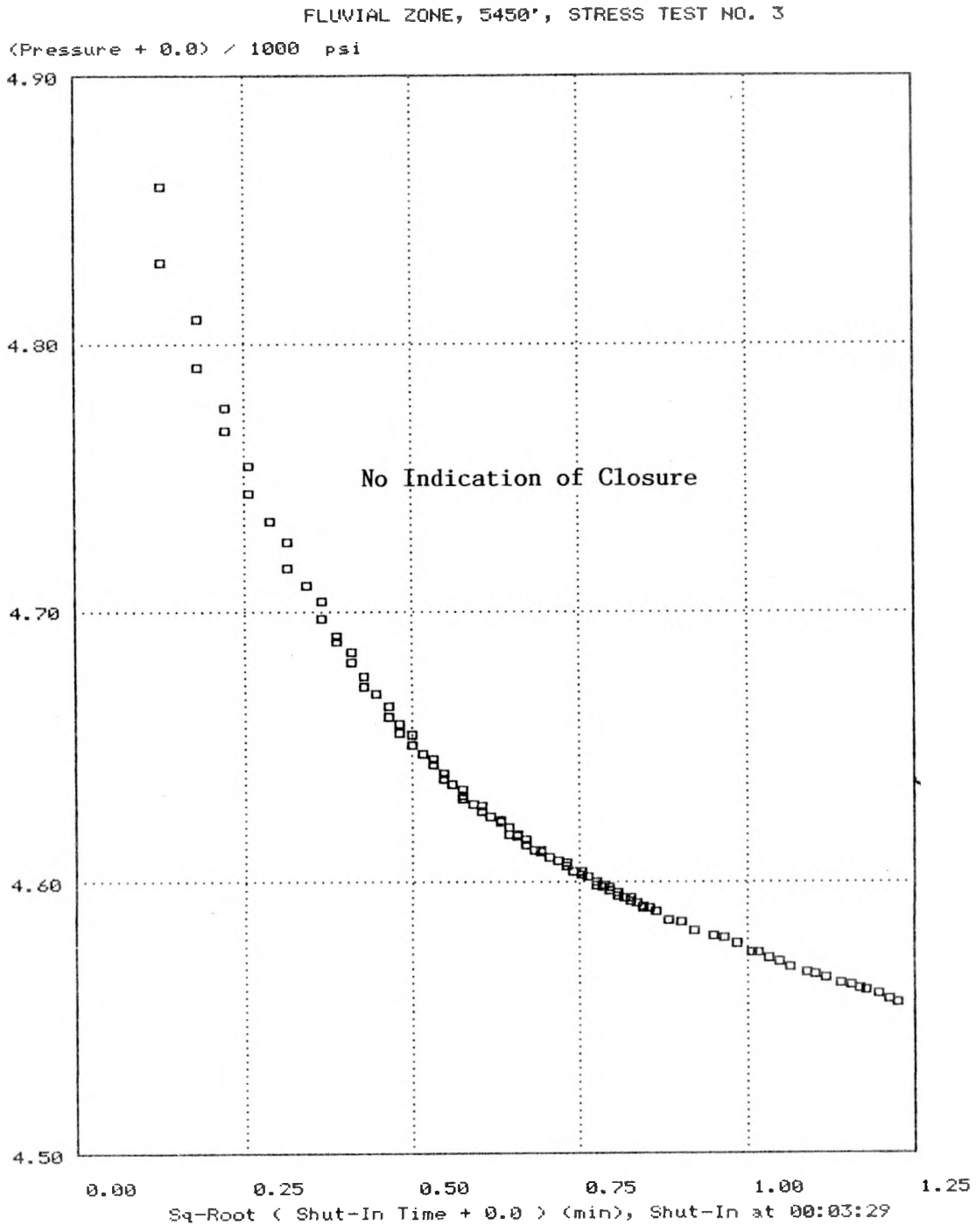


FIGURE A.88: Shale Stress Test (5450-5452'), Square-Root of Shut-In Time Plot of Test No. 3 Pressure Decline.

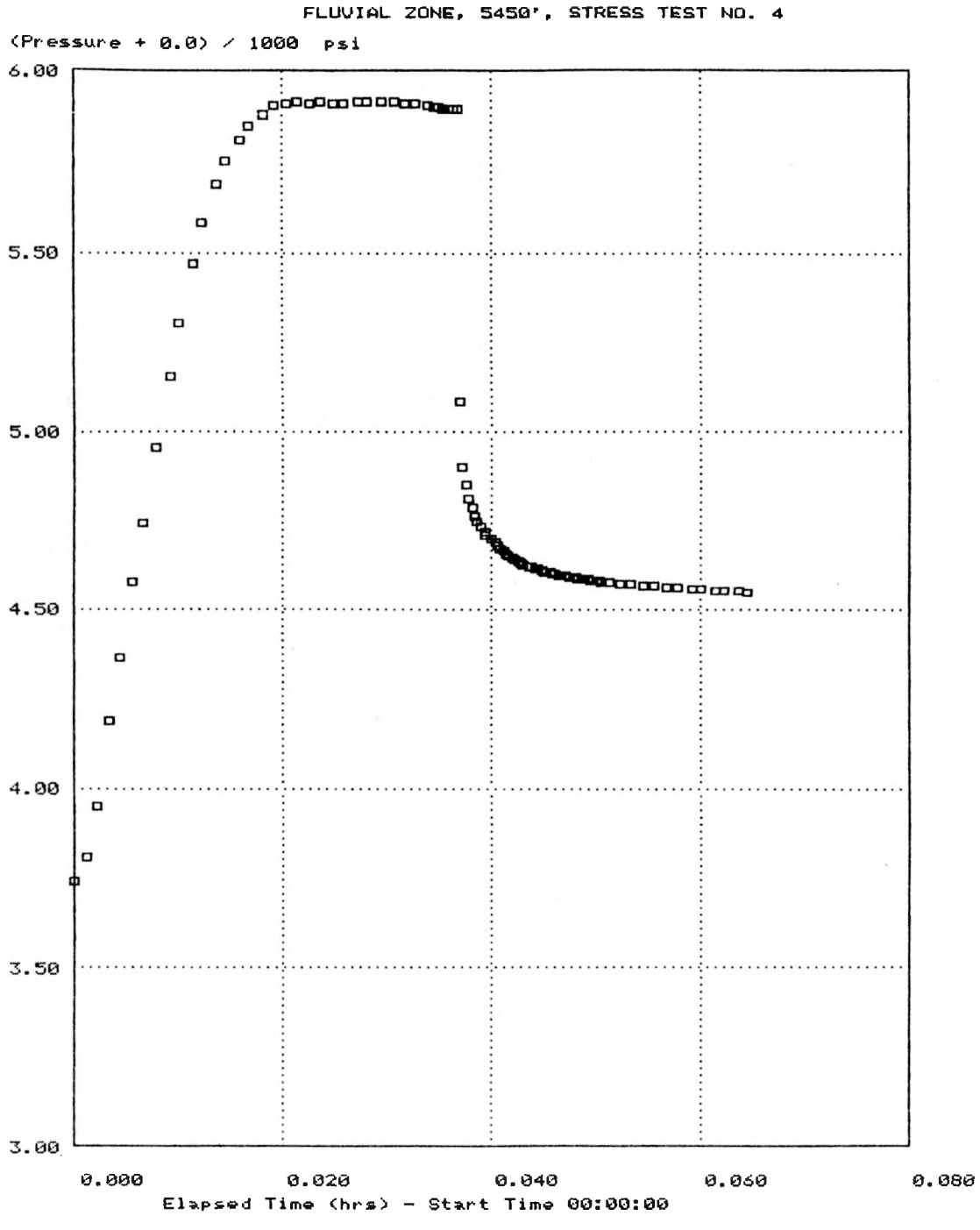


FIGURE A.89: Shale Stress Test (5450-5452'), Linear Plot of Test No. 4 Injection/Decline.

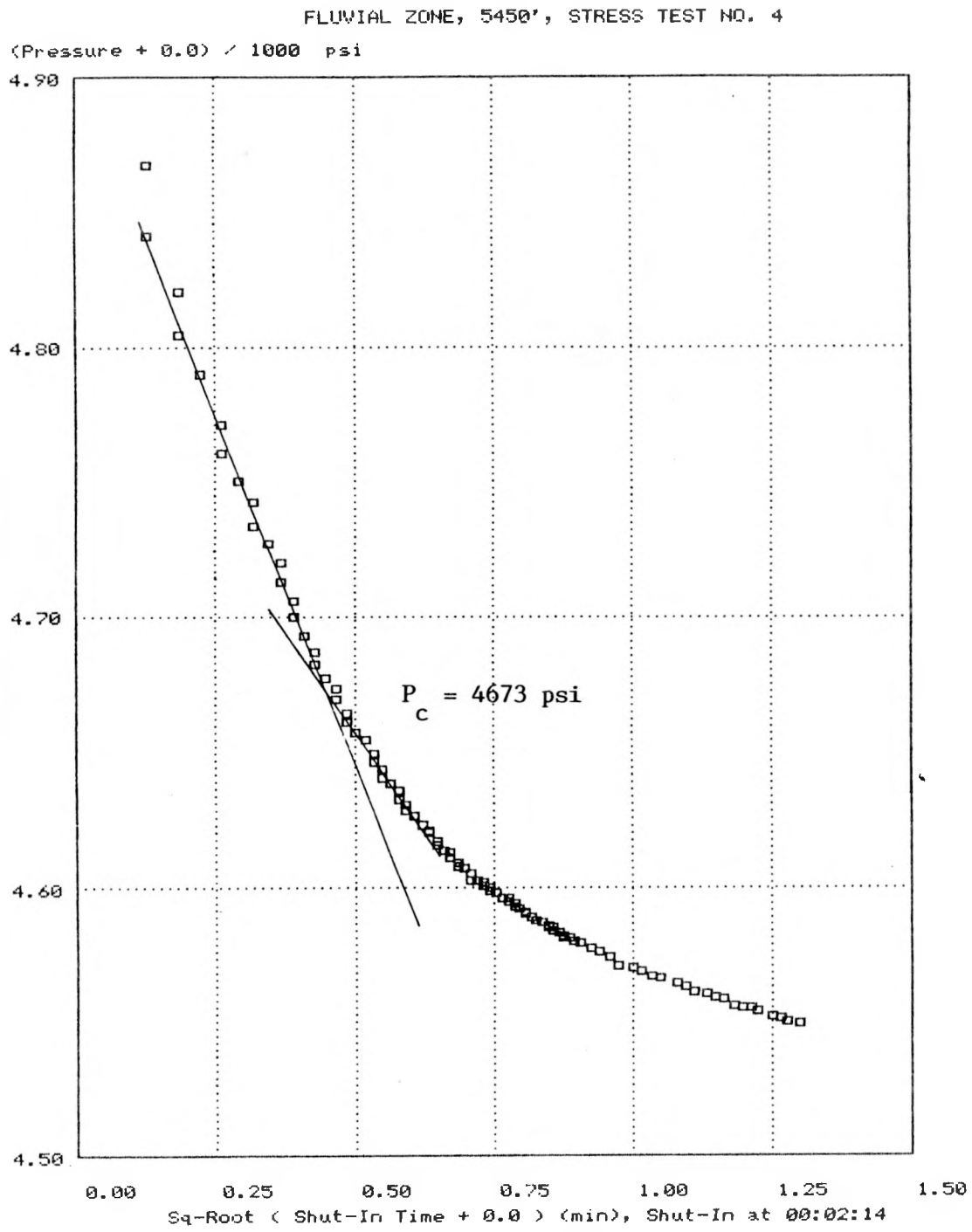


FIGURE A.90: Shale Stress Test (5450-5452'), Square-Root of Shut-In Time Plot of Test No. 4 Pressure Decline.

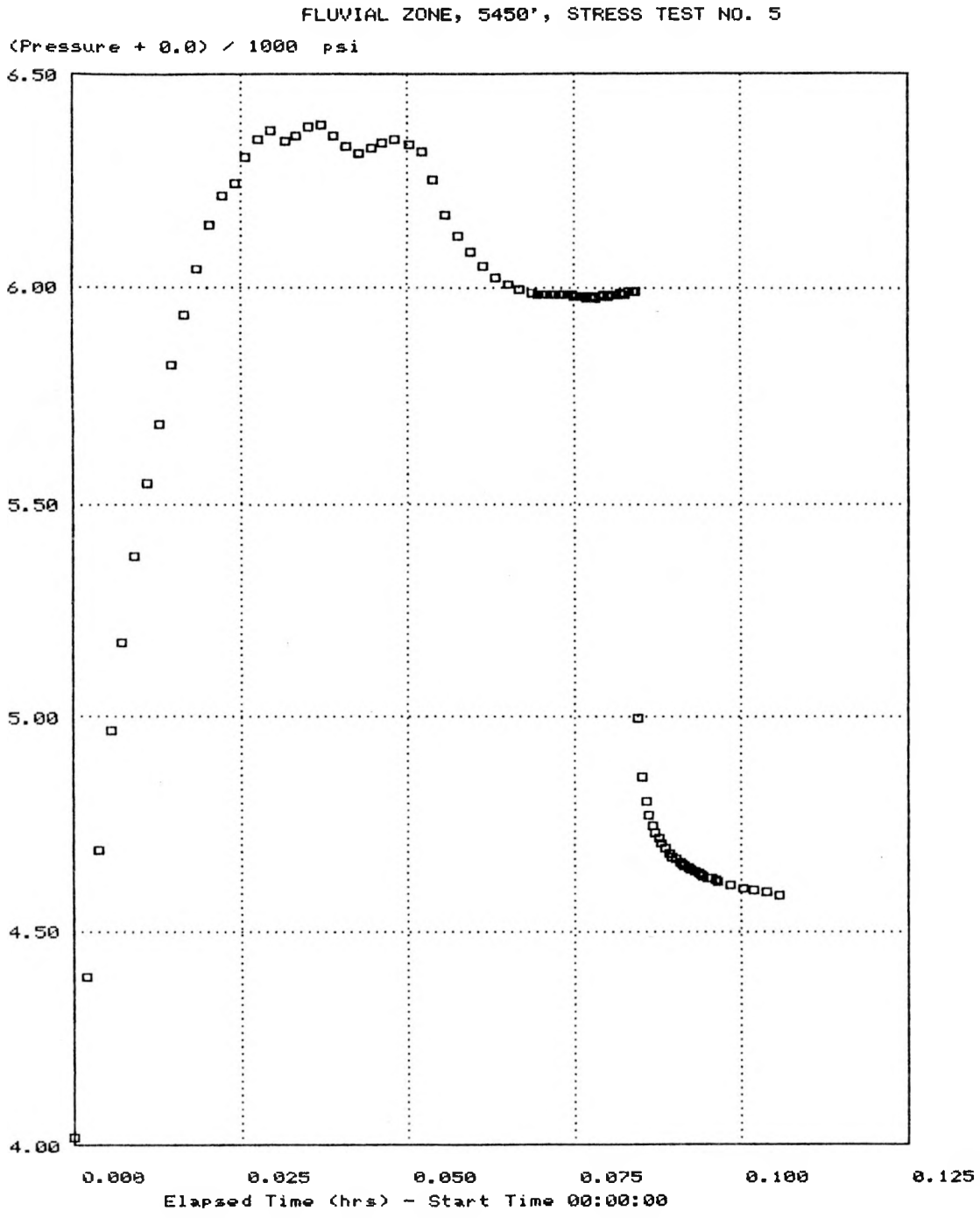


FIGURE A.91: Shale Stress Test (5450-5452'), Linear Plot of Test No. 5 Injection/Decline.

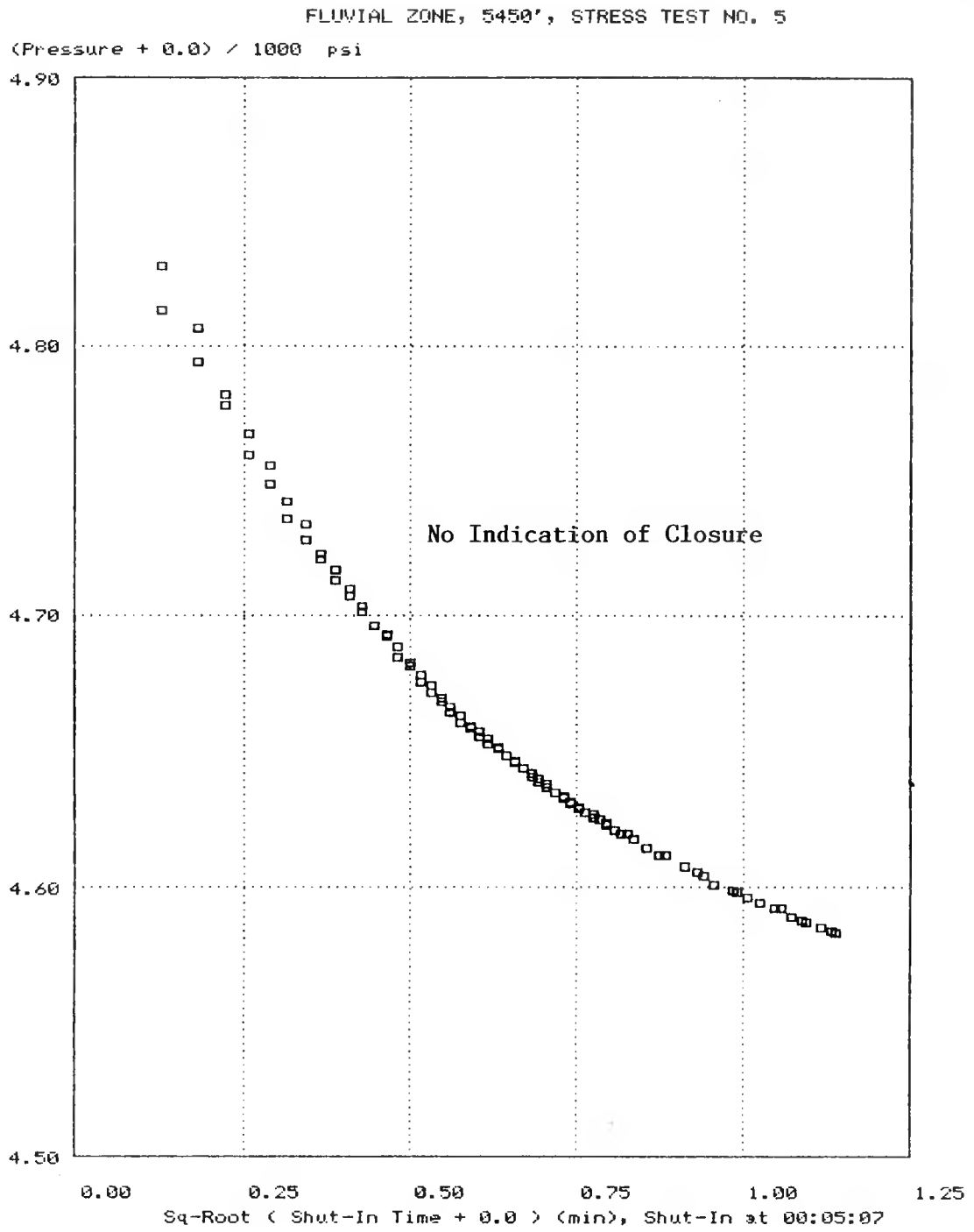


FIGURE A.92: Shale Stress Test (5450-5452'), Square-Root of Shut-In Time Plot of Test No. 5 Pressure Decline.

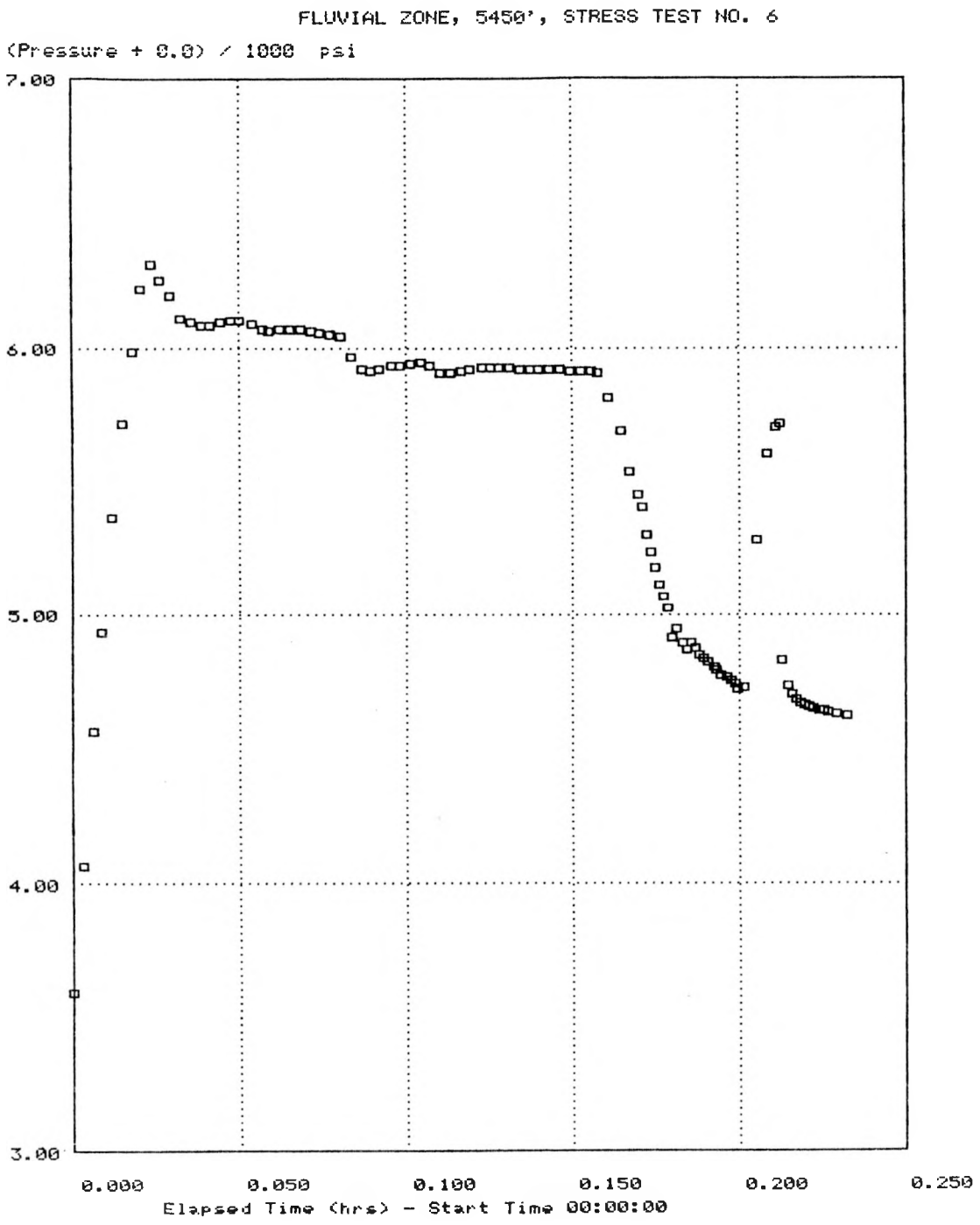


FIGURE A.93: Shale Stress Test (5450–5452'), Linear Plot of Test No. 6 Injection/Decline.

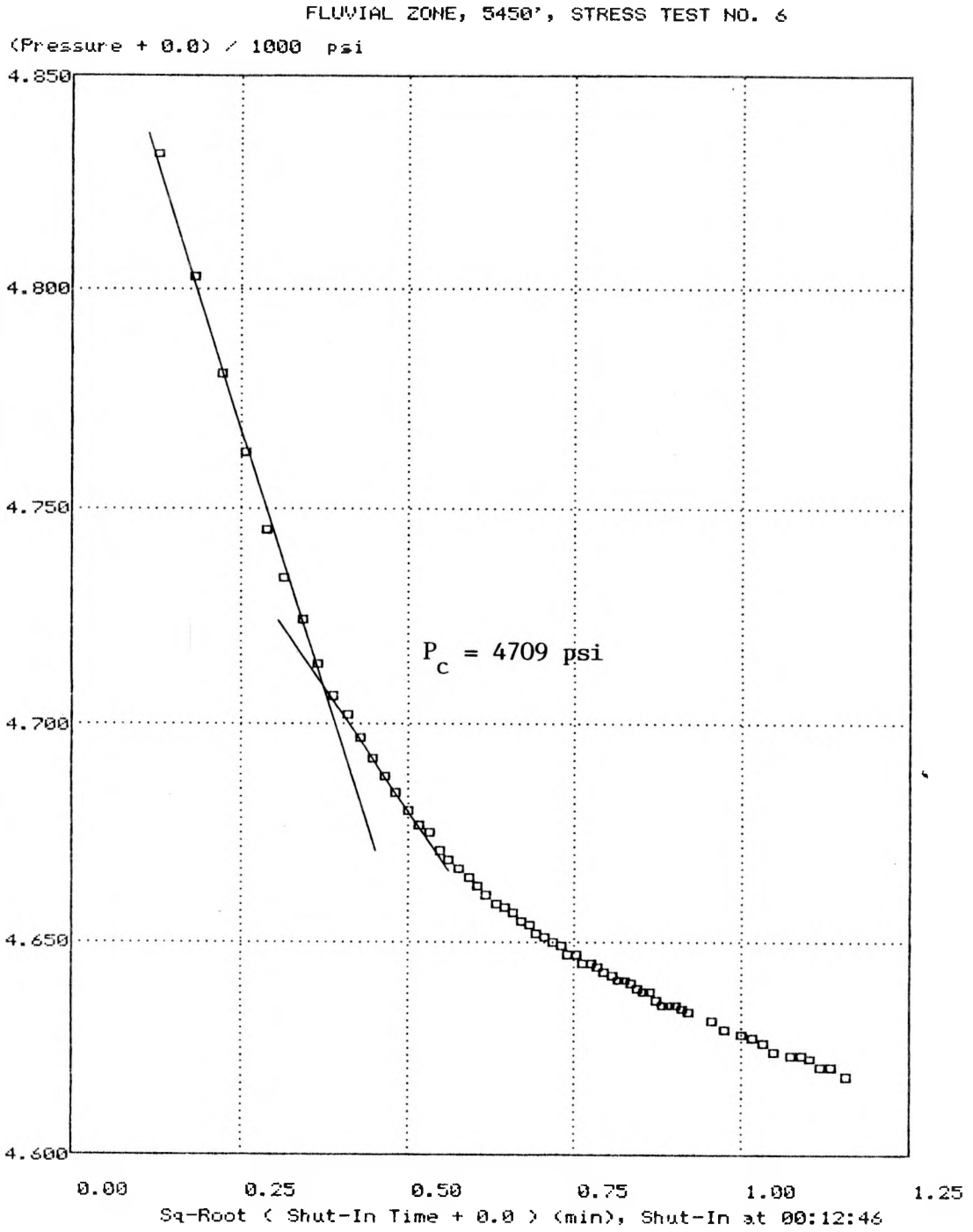


FIGURE A.94: Shale Stress Test (5450-5452'), Square-Root of Shut-In Time Plot of Test No. 6 Pressure Decline.

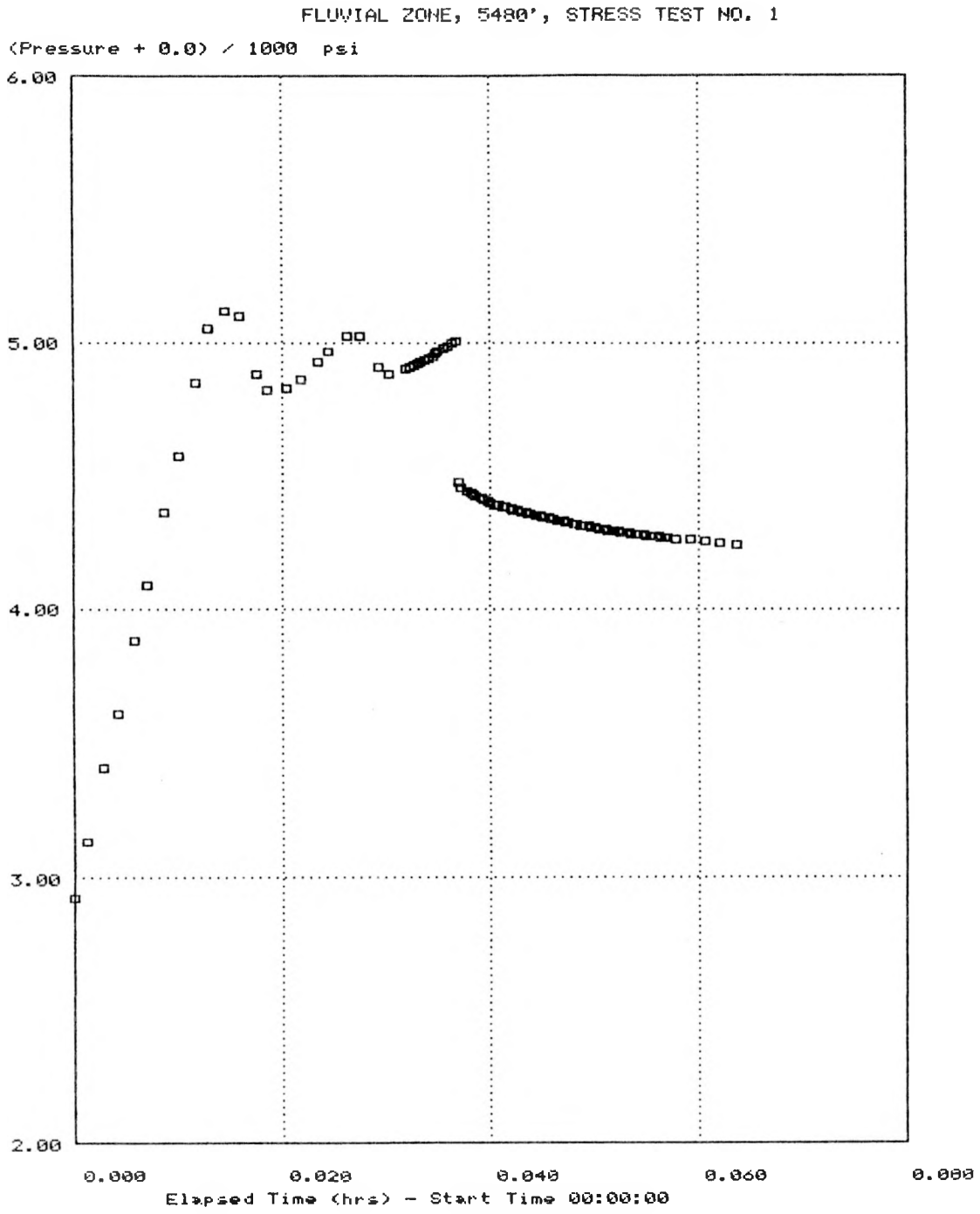


FIGURE A.95: Sandstone Stress Test (5480–5482'), Linear Plot of Test No. 1 Injection/Decline.

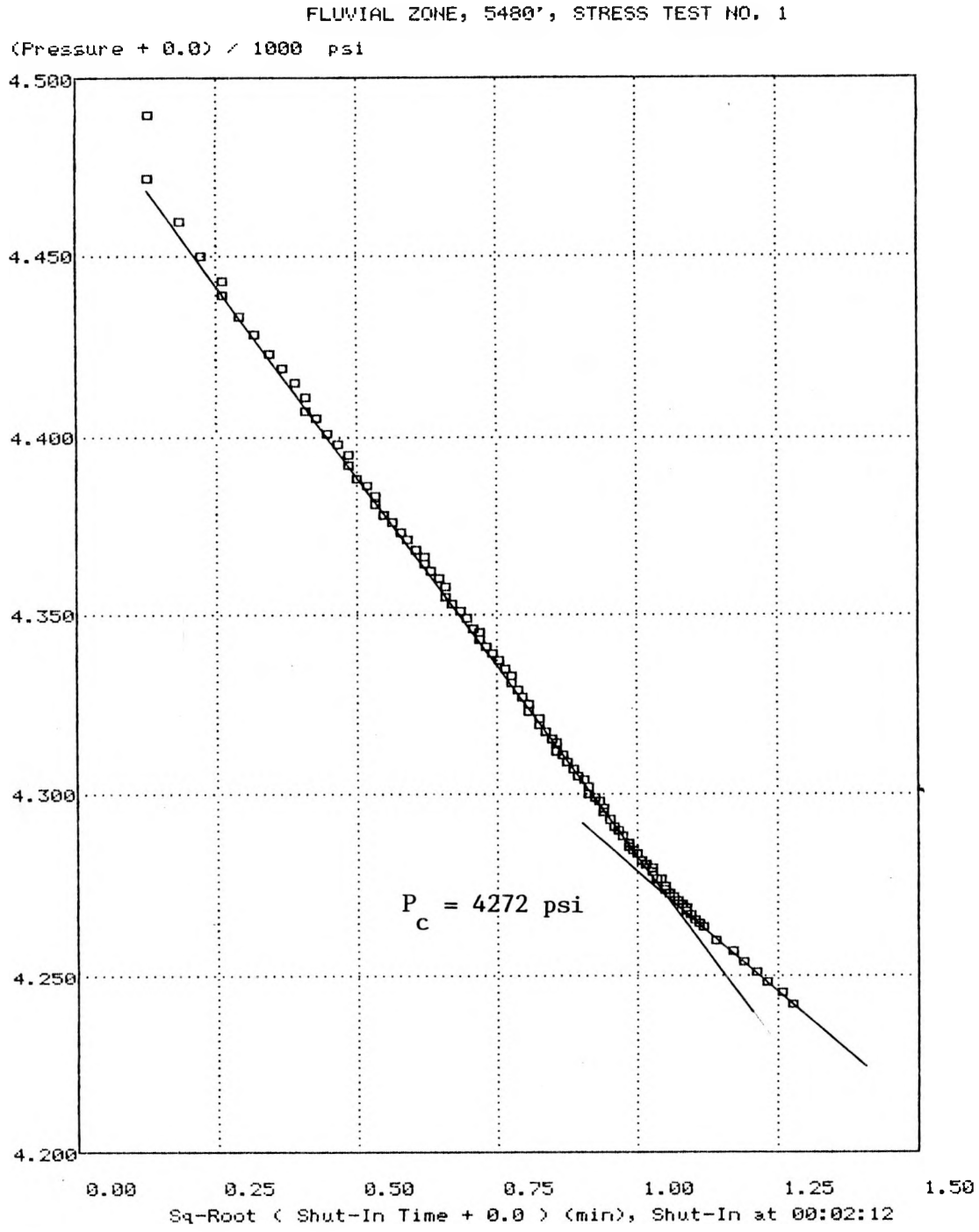


FIGURE A.96: Sandstone Stress Test (5480–5482'), Square-Root of Shut-In Time Plot of Test No. 1 Pressure Decline.

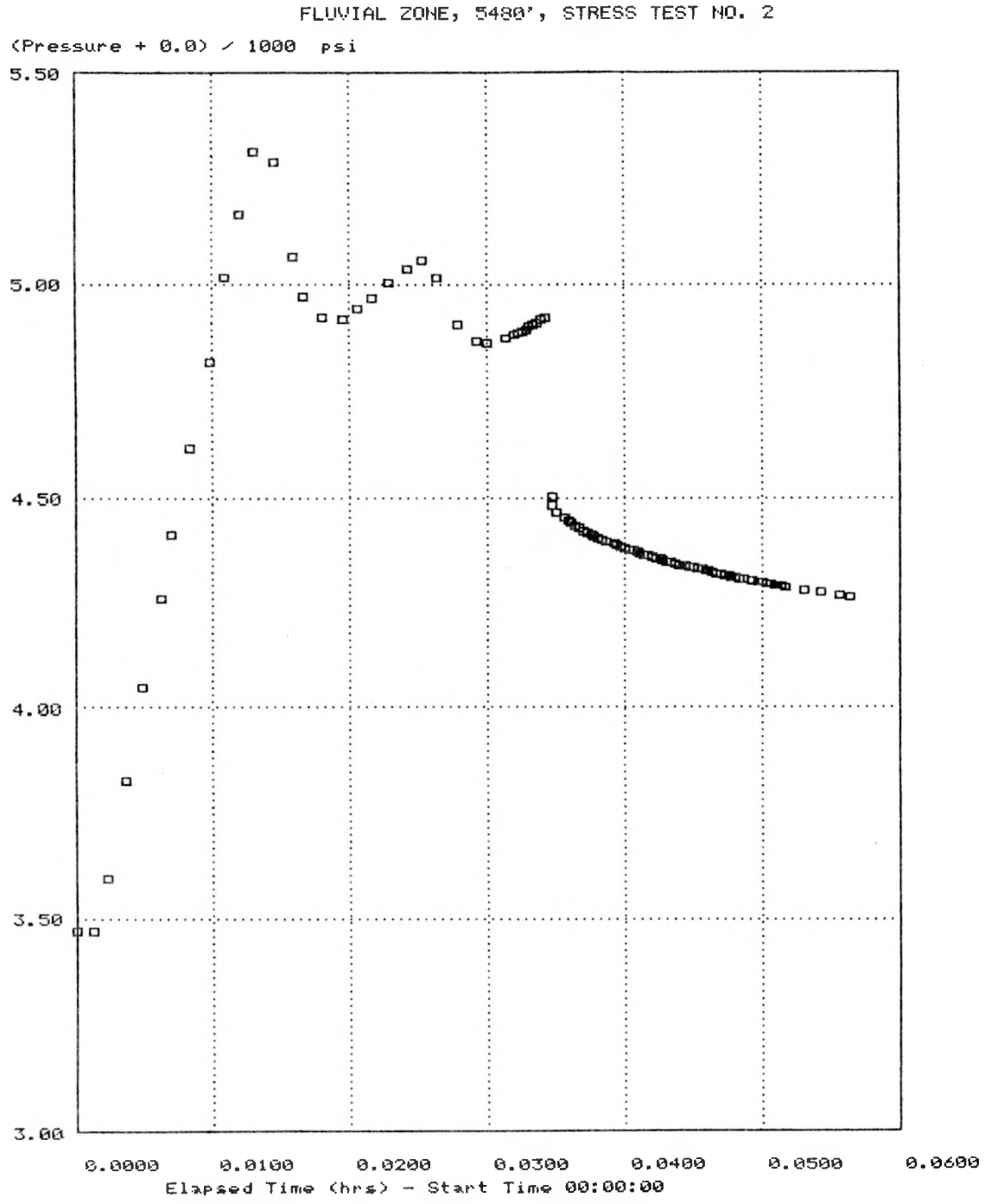


FIGURE A.97: Sandstone Stress Test (5480-5482'), Linear Plot of Test No. 2 Injection/Decline.

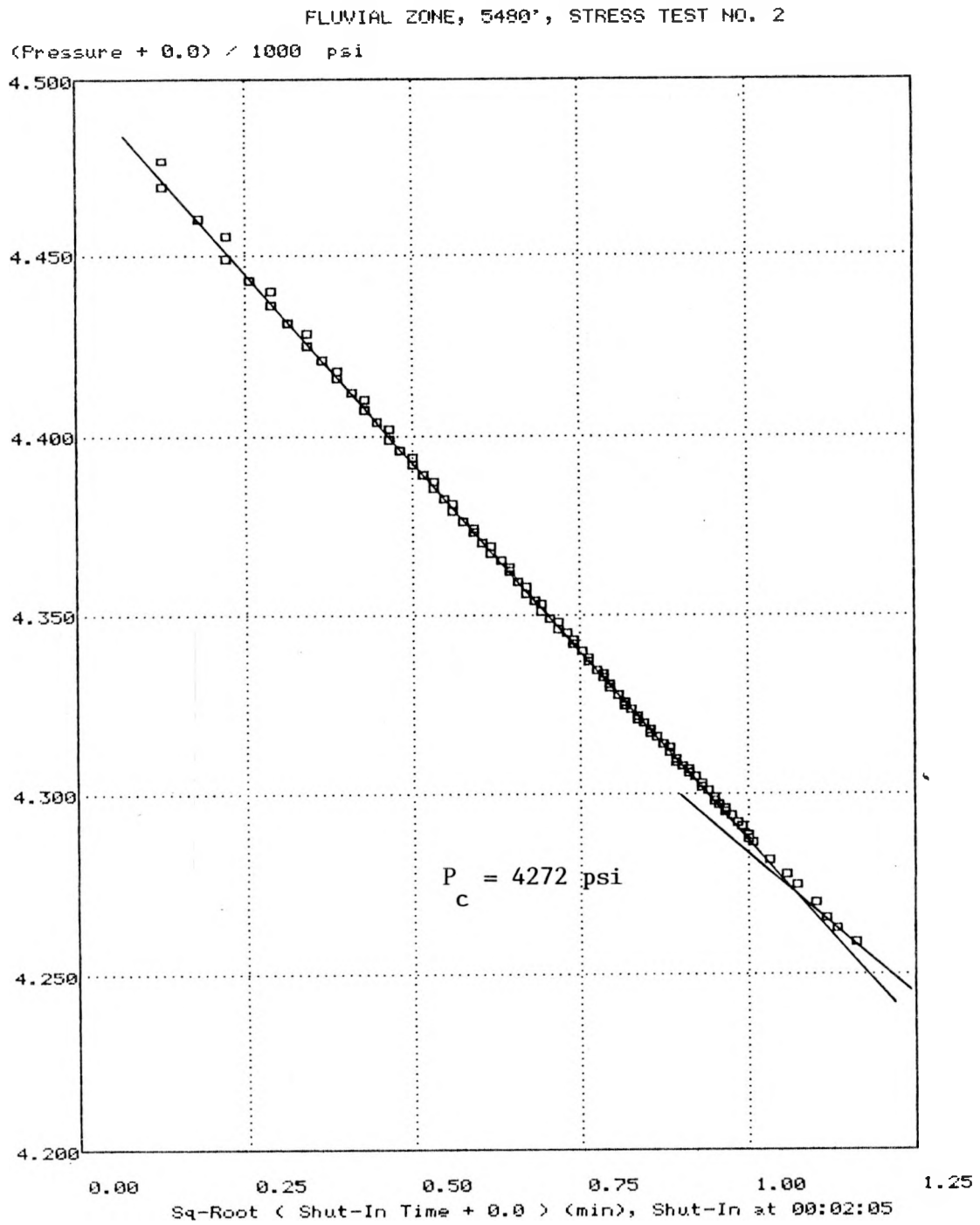


FIGURE A.98: Sandstone Stress Test (5480–5482'), Square-Root of Shut-In Time Plot of Test No. 2 Pressure Decline.

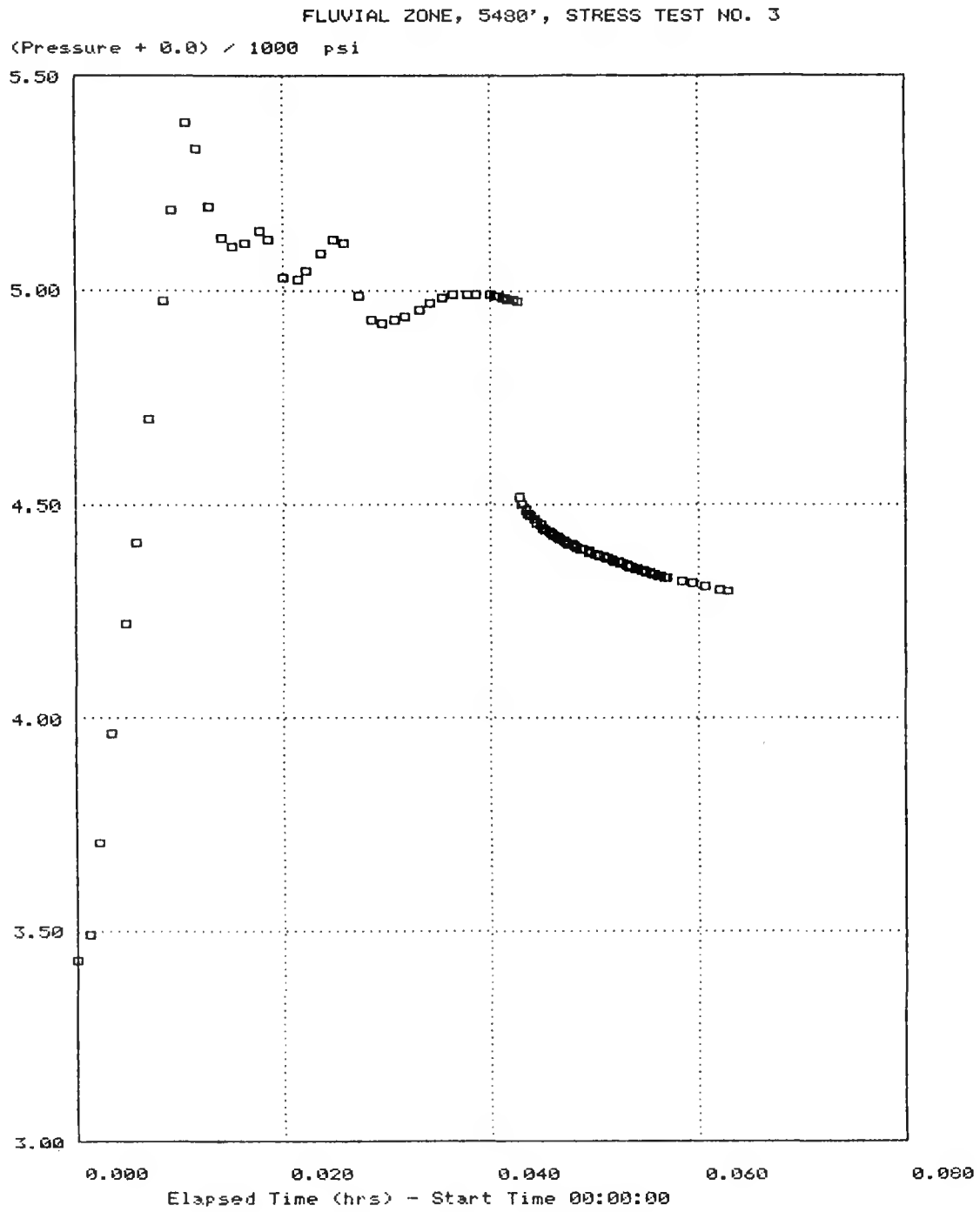


FIGURE A.99: Sandstone Stress Test (5480–5482'), Linear Plot of Test No. 3 Injection/Decline.

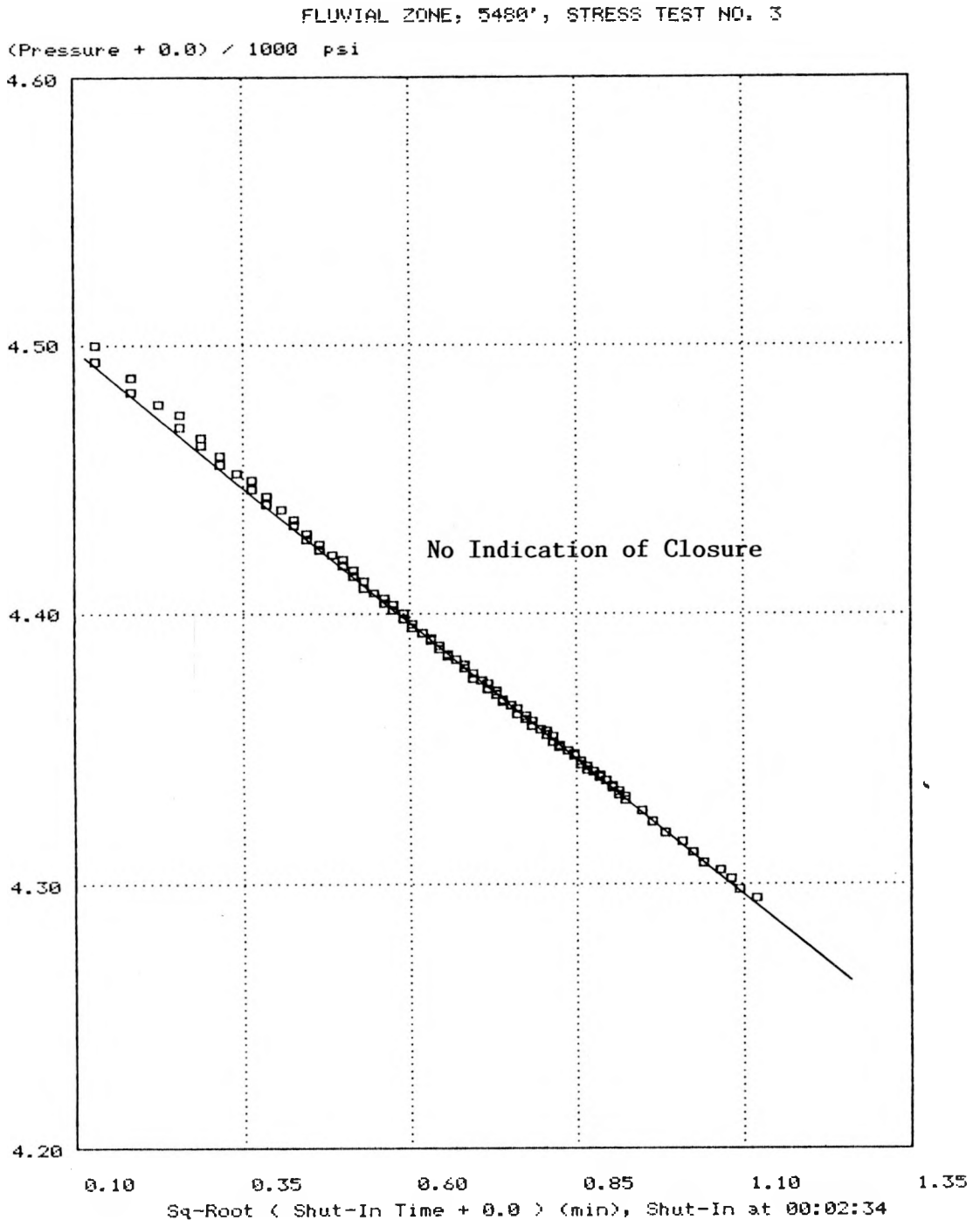


FIGURE A.100: Sandstone Stress Test (5480–5482'), Square-Root of Shut-In Time Plot of Test No. 3 Injection/Decline.

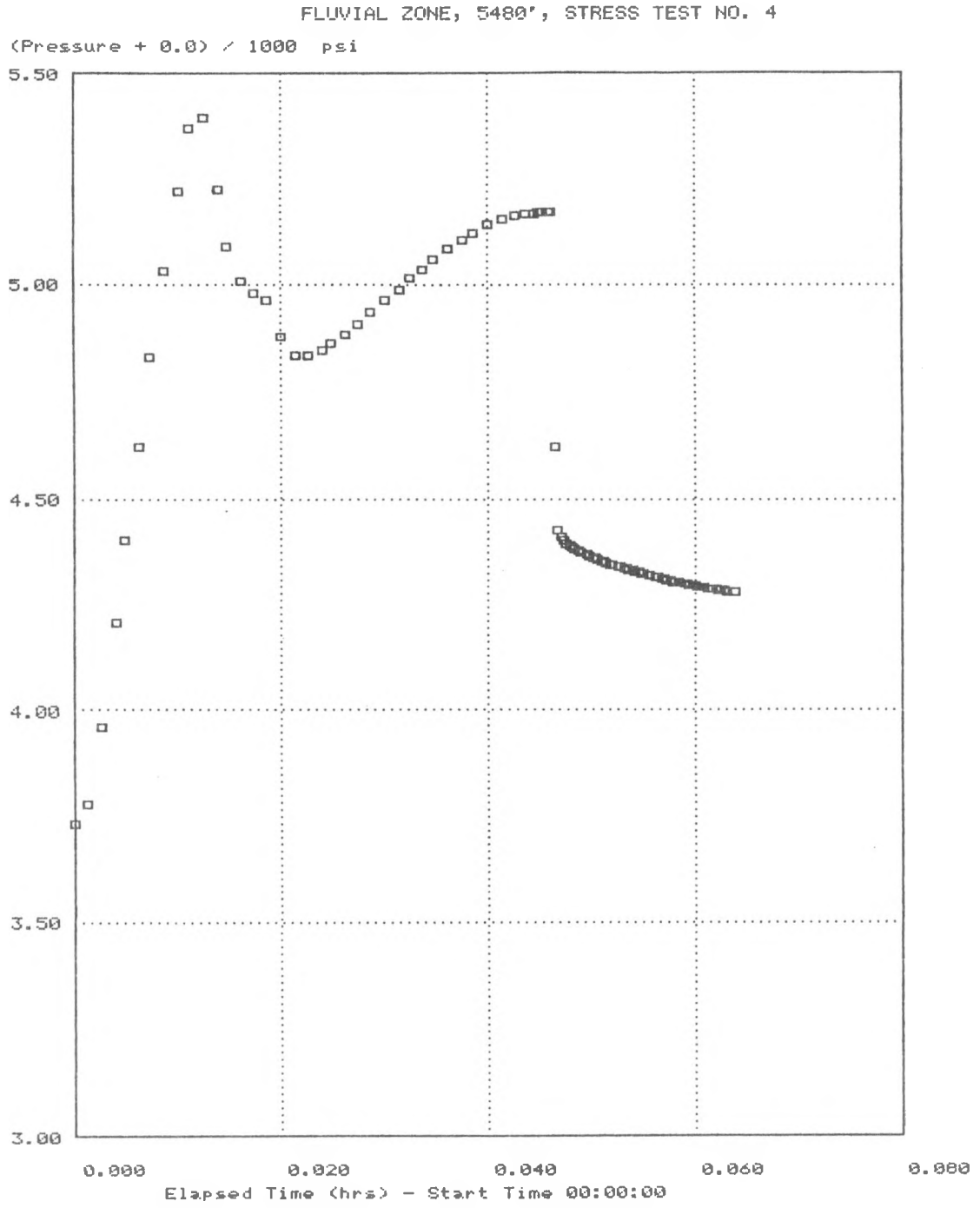


FIGURE A.101: Sandstone Stress Test (5480-5482'), Linear Plot of Test No. 4 Injection/Decline.

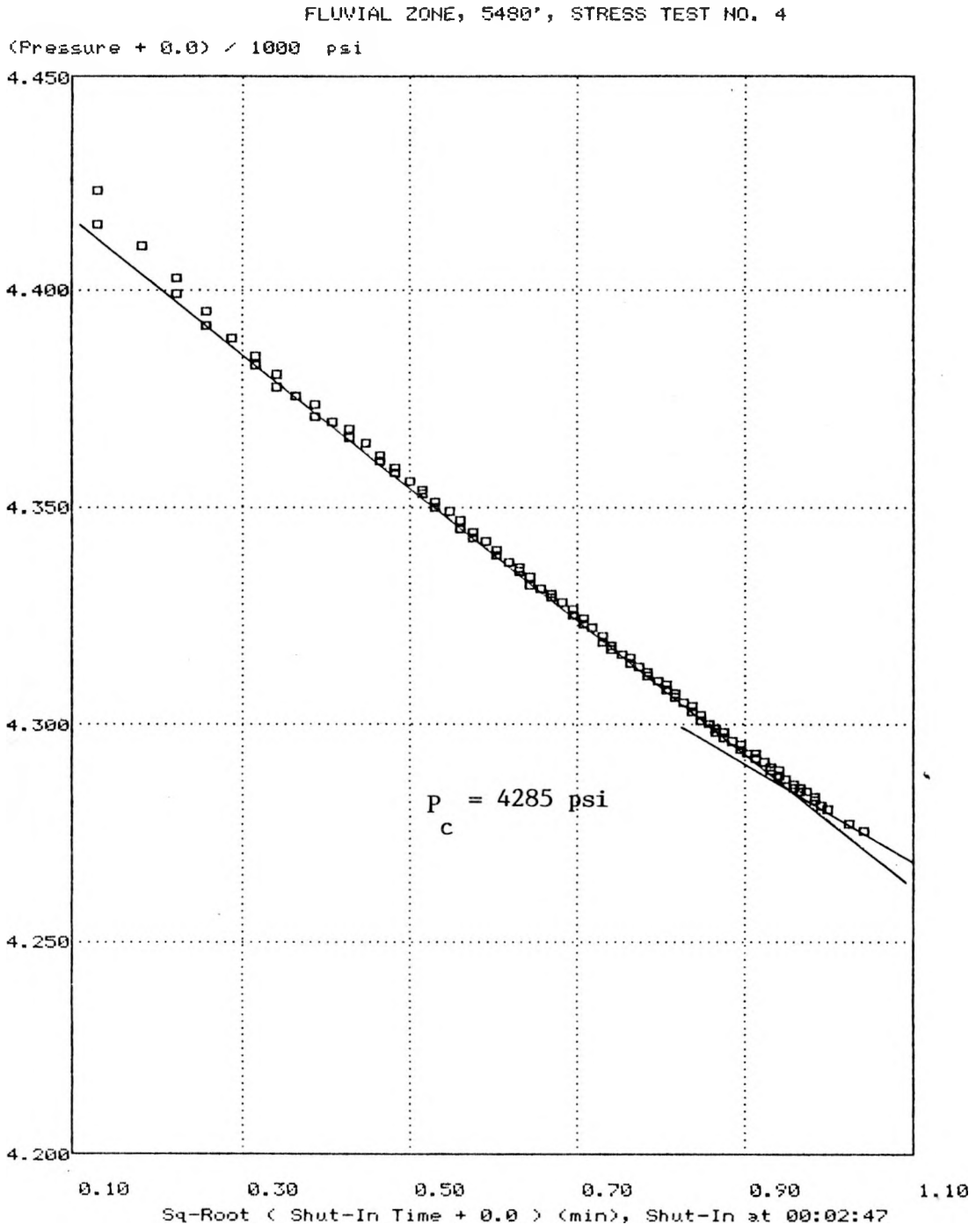


FIGURE A.102: Sandstone Stress Test (5480-5482'), Square-Root of Shut-In Time Plot of Test No. 4 Pressure Decline.

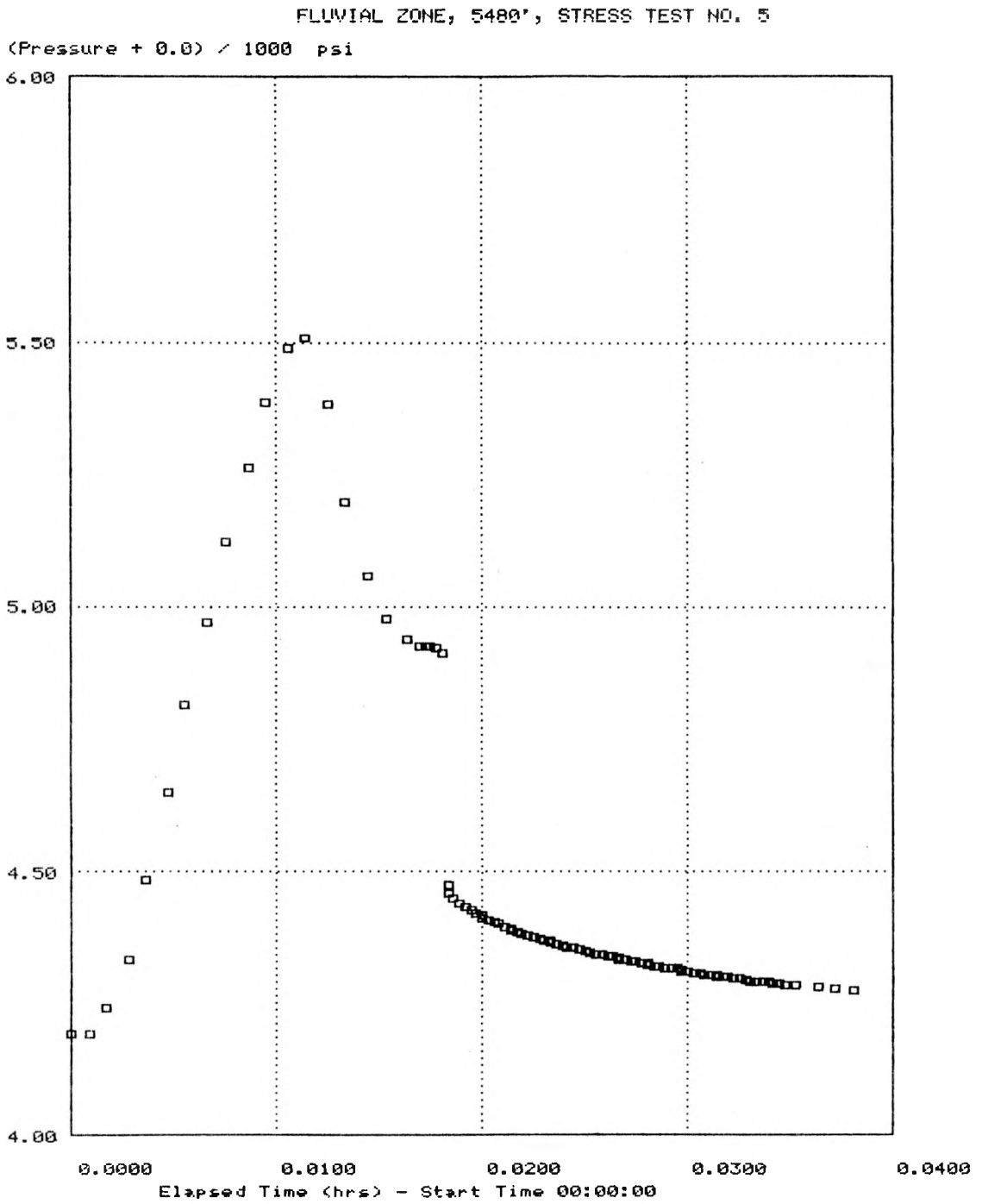


FIGURE A.103: Sandstone Stress Test (5480-5482'), Linear Plot of Test No. 5 Injection/Decline.

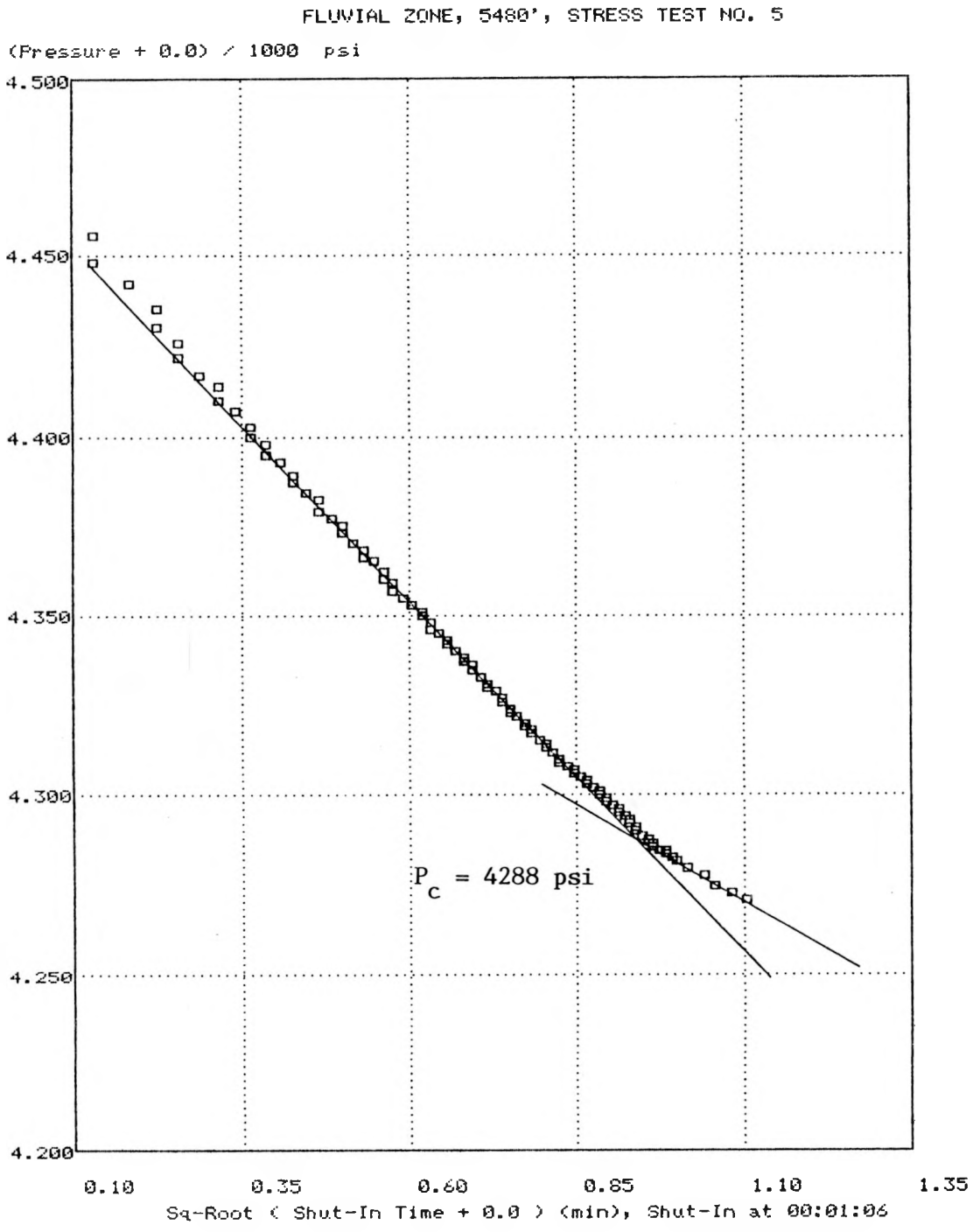


FIGURE A.104: Sandstone Stress Test (5480–5482'), Square-Root of Shut-In Time Plot of Test No. 5 Pressure Decline.

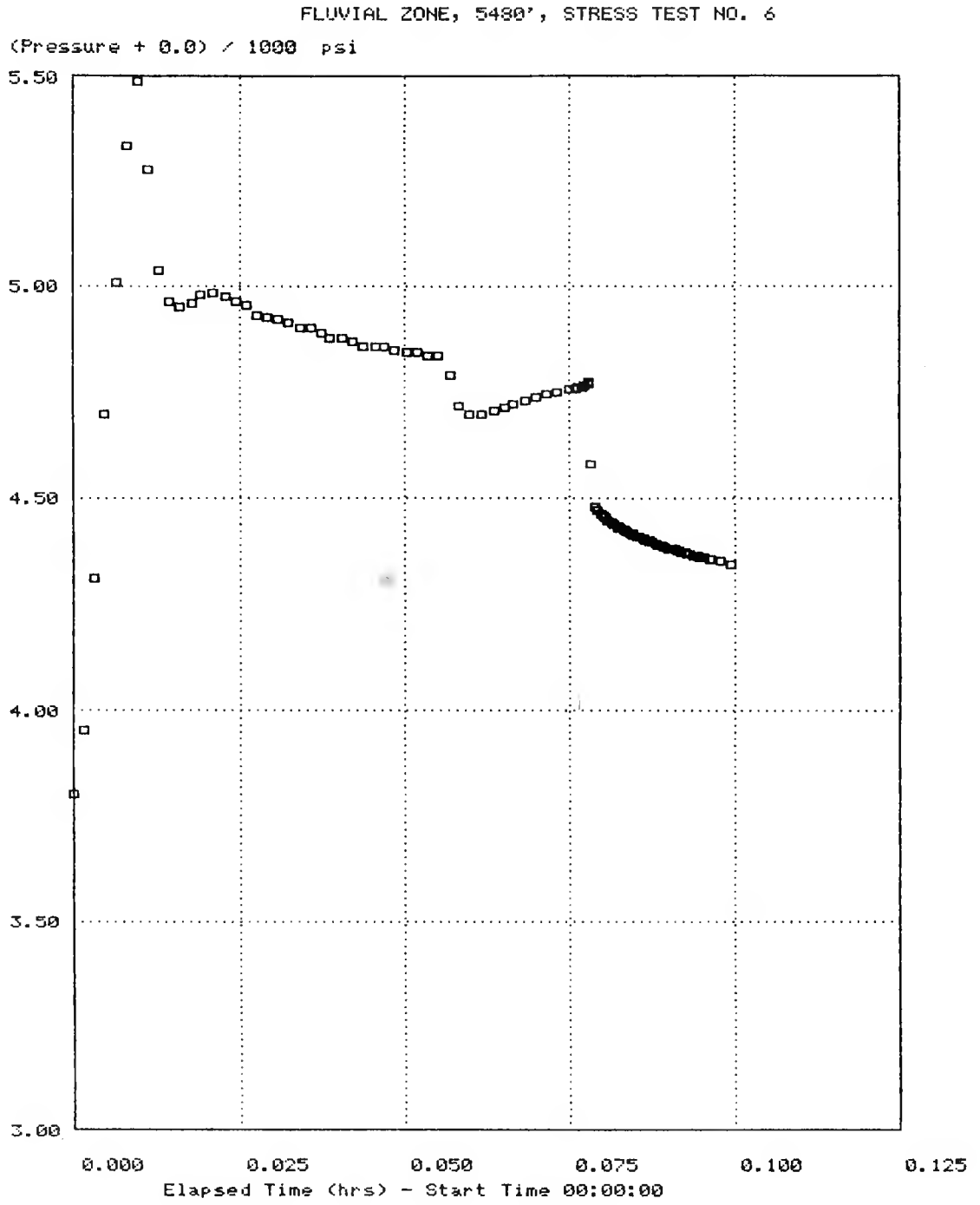


FIGURE A.105: Sandstone Stress Test (5480–5482'), Linear Plot of Test No. 6 Injection/Decline.

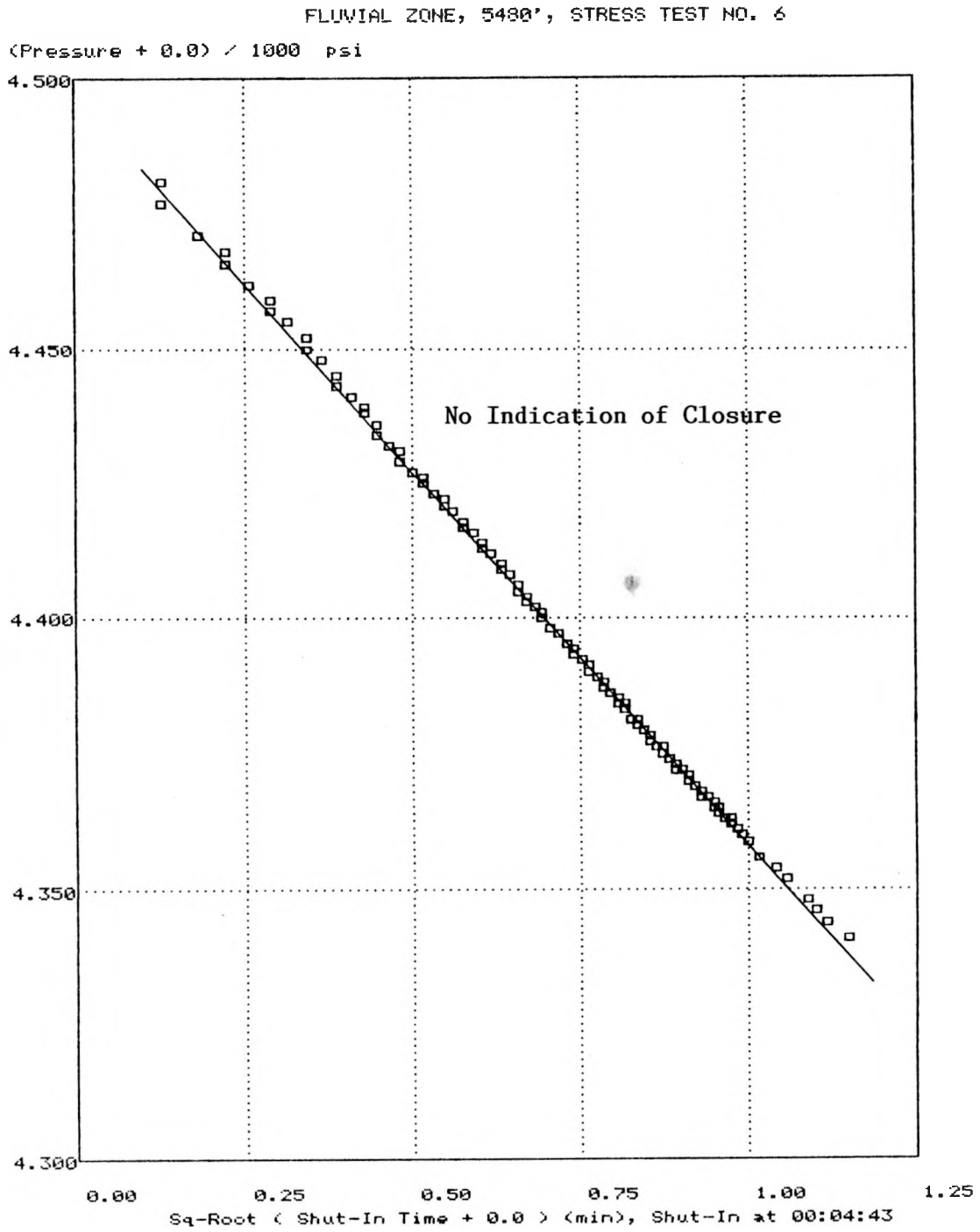


FIGURE A.106: Sandstone Stress Test (5480-5482'), Square-Root of Shut-In Time Plot of Test No. 6 Pressure Decline.

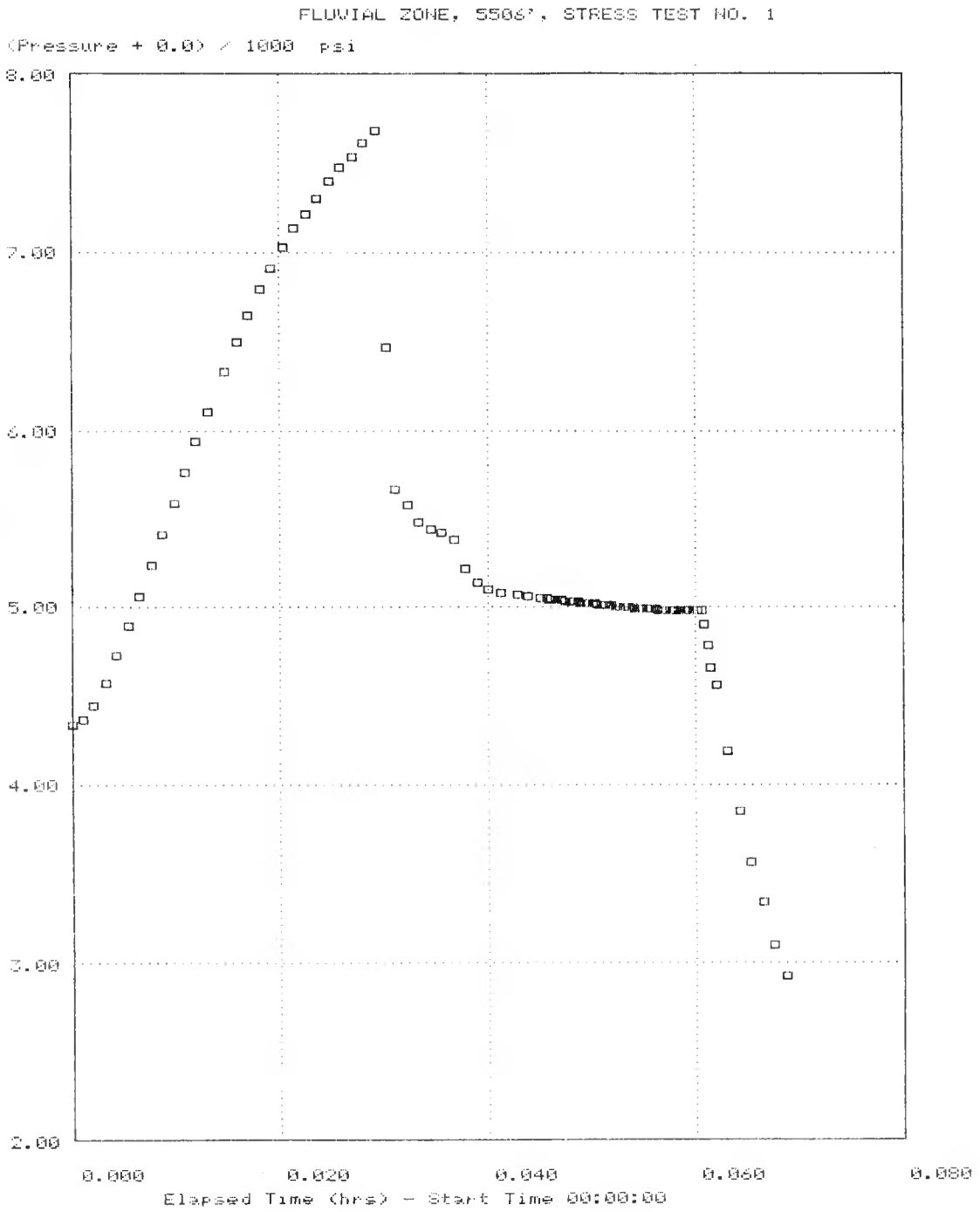


FIGURE A.107: Shale Stress Test (5506-5508'), Linear Plot of Test No. 1 Injection/Decline.

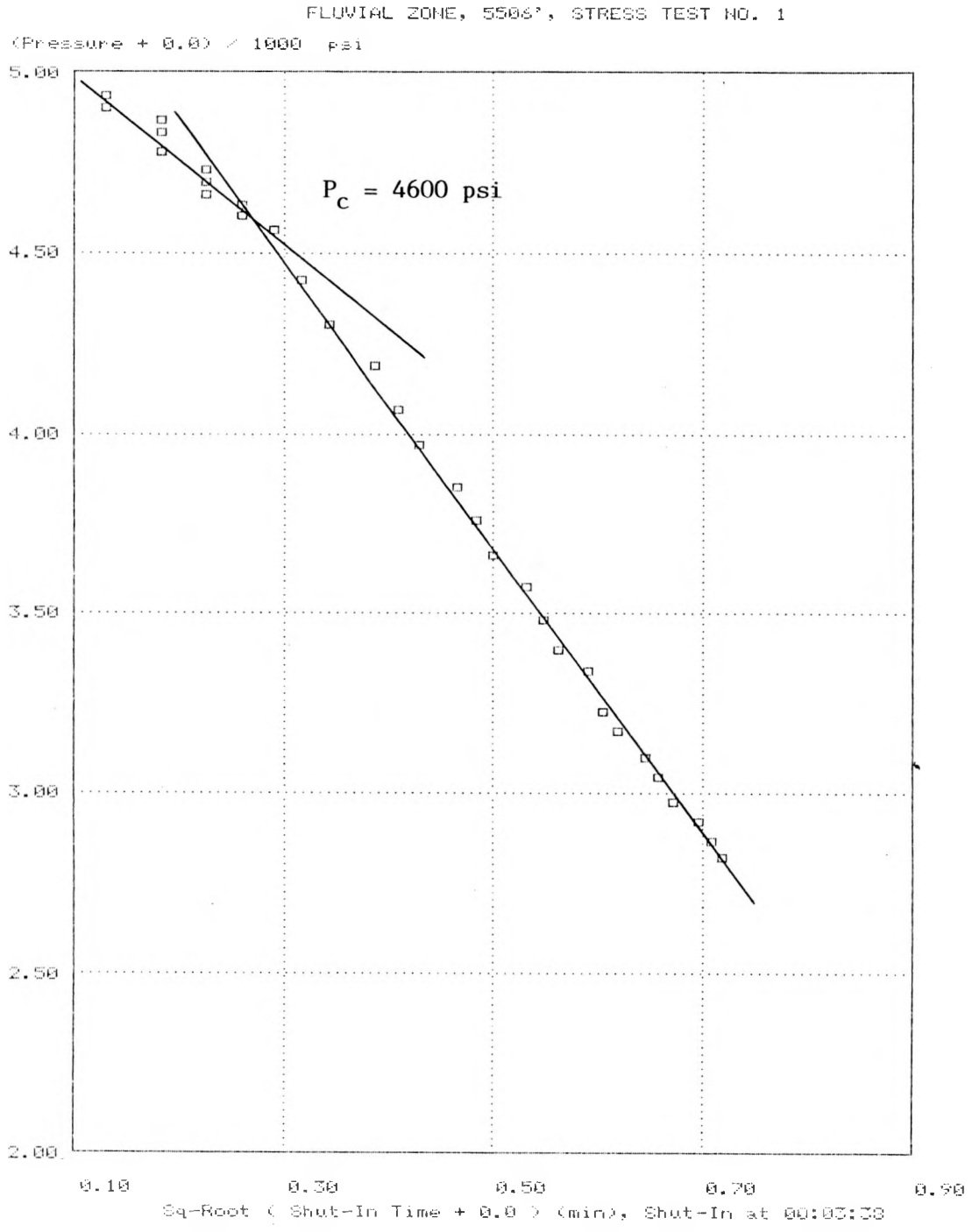


FIGURE A.108: Shale Stress Test (5506-5508'), Square-Root of Shut-In Time Plot of Test No. 1 Pressure Decline.

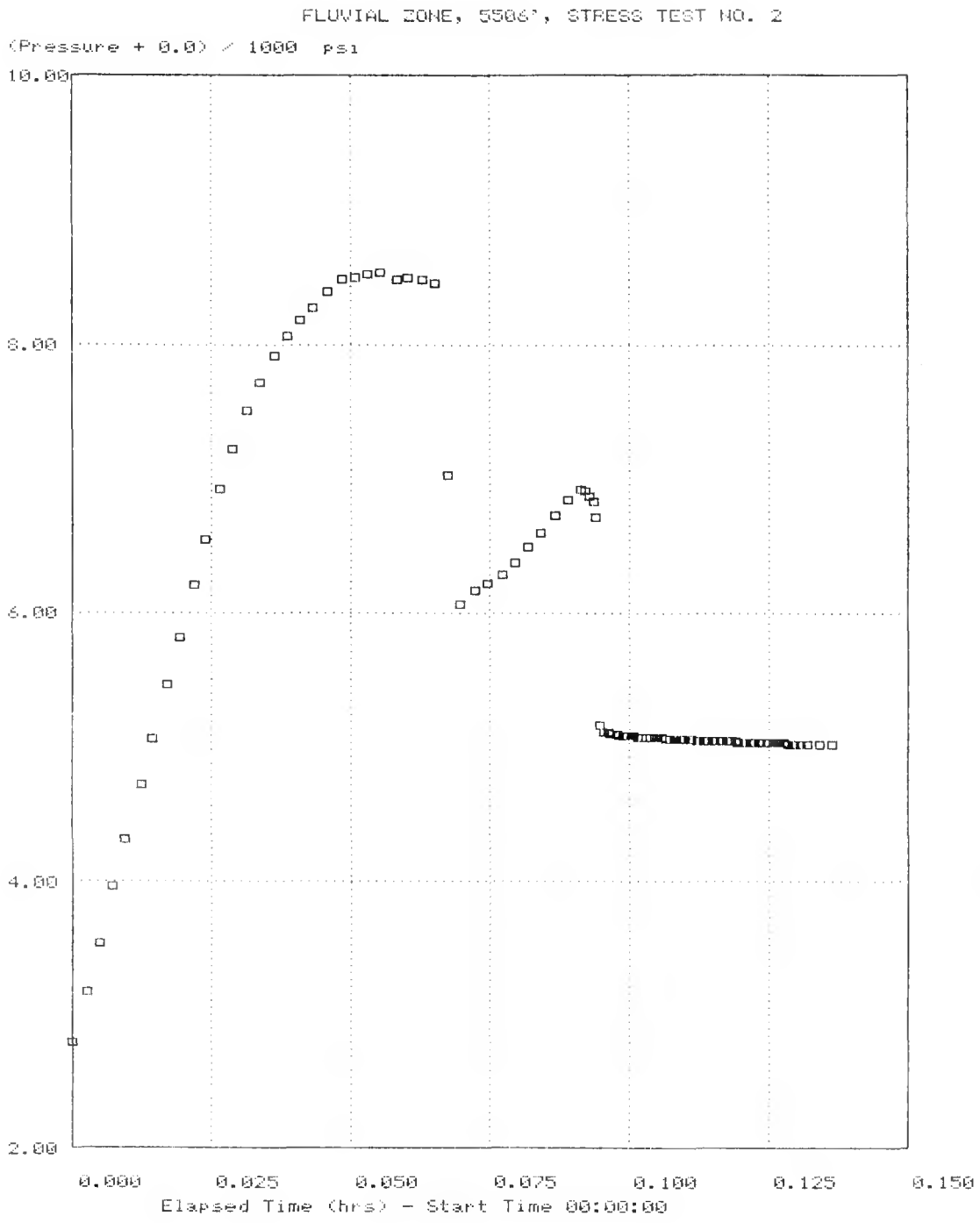


FIGURE A.109: Shale Stress Test (5506-5508'), Linear Plot of Test No. 2 Injection/Decline.

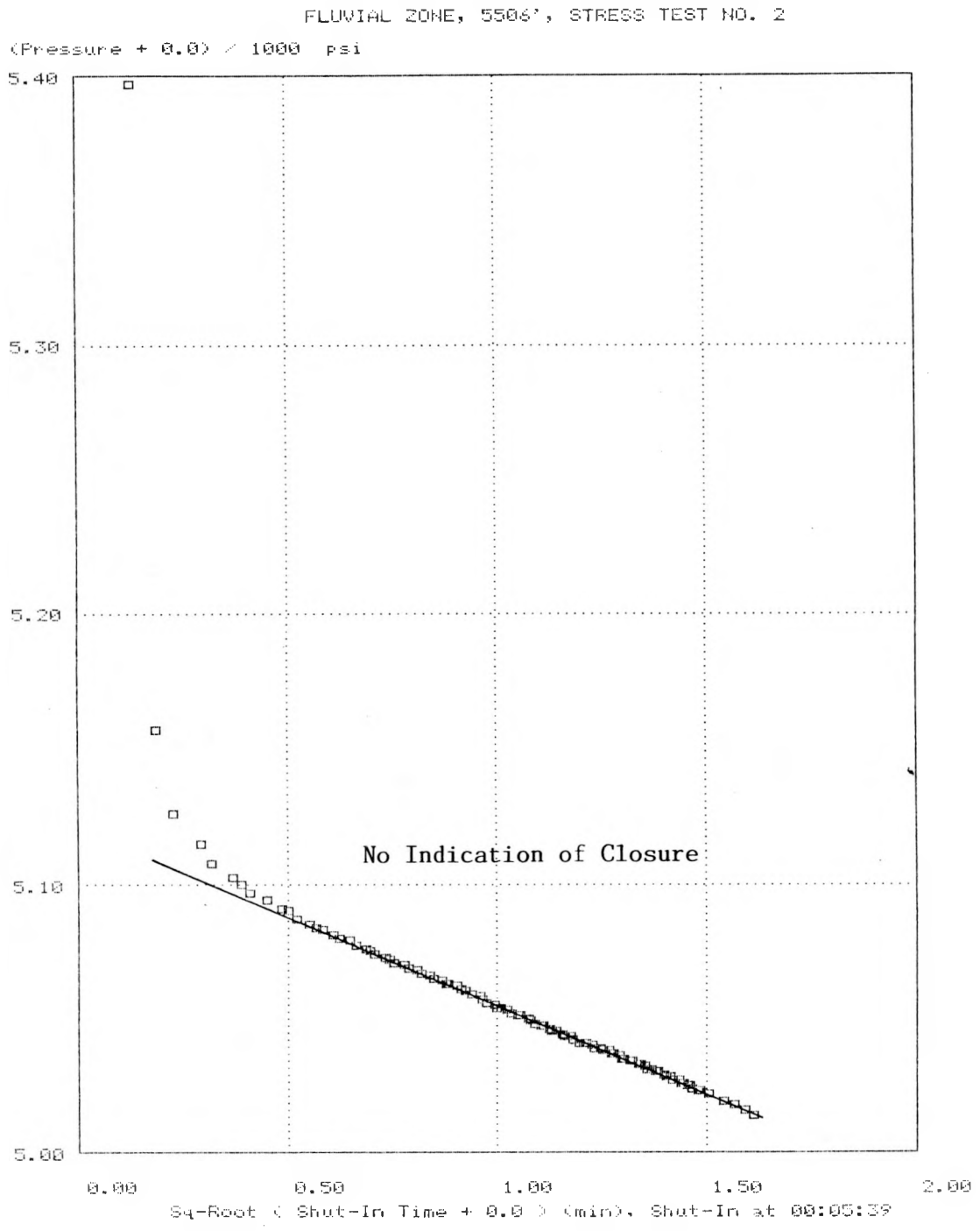


FIGURE A.110: Shale Stress Test (5506-5508'), Square-Root of Shut-In Time Plot of Test No. 2 Pressure Decline.

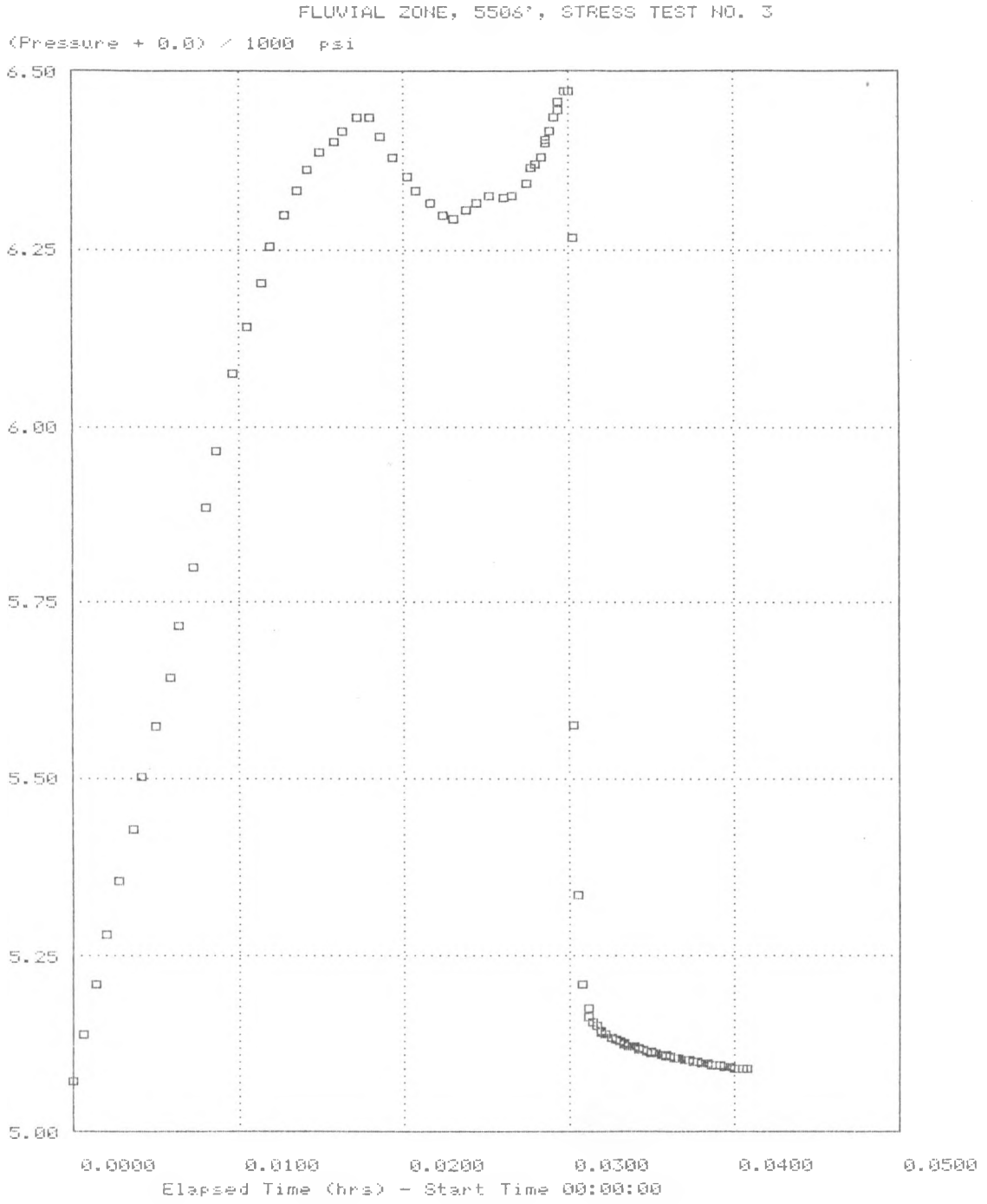


FIGURE A.111: Shale Stress Test (5506-5508'), Linear Plot of Test No. 3 Injection/Decline.

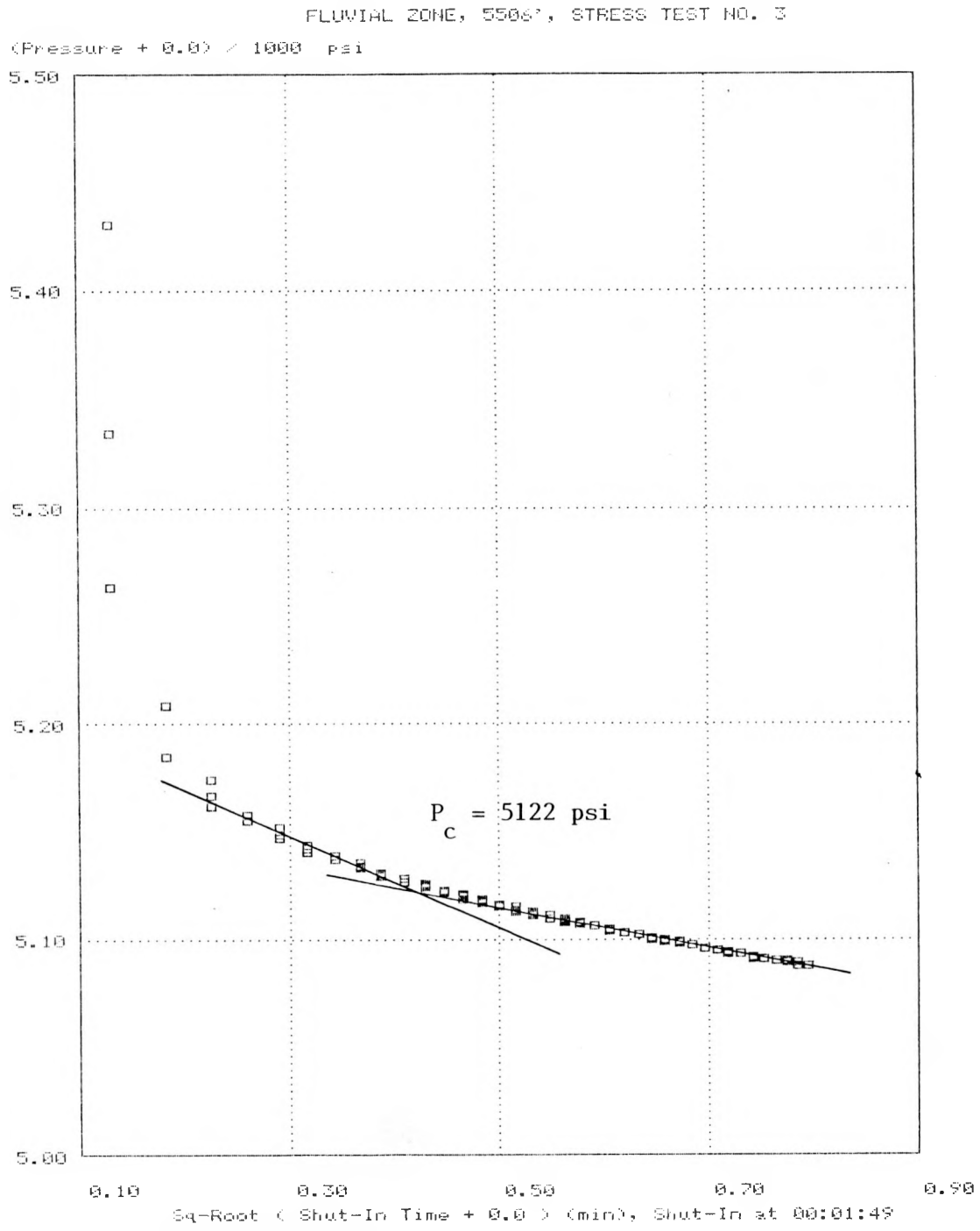


FIGURE A.112: Shale Stress Test (5506-5508'), Square-Root of Shut-In Time Plot of Test No. 3 Pressure Decline.

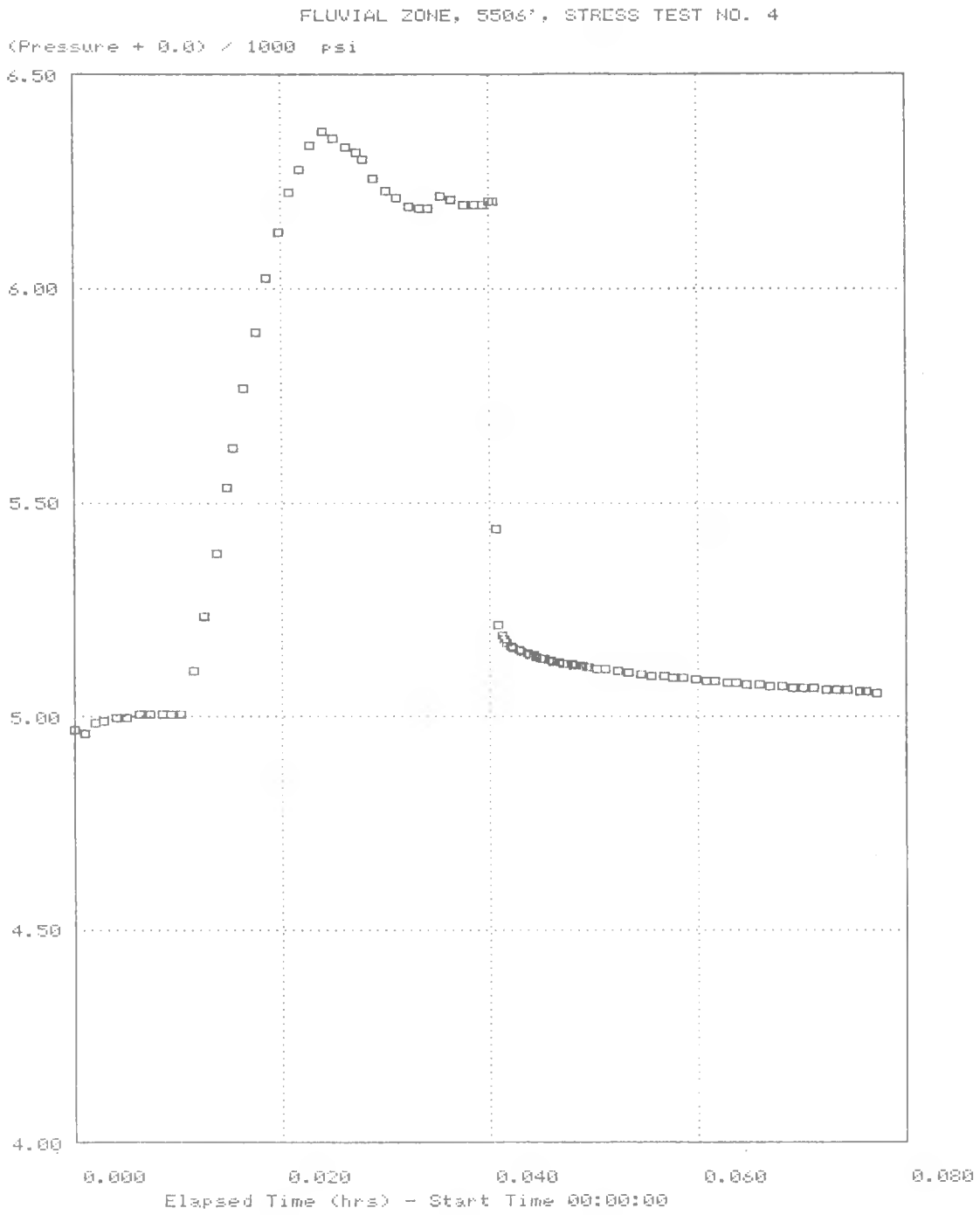


FIGURE A.113: Shale Stress Test (5506-5508'), Linear Plot of Test No. 4 Injection/Decline.

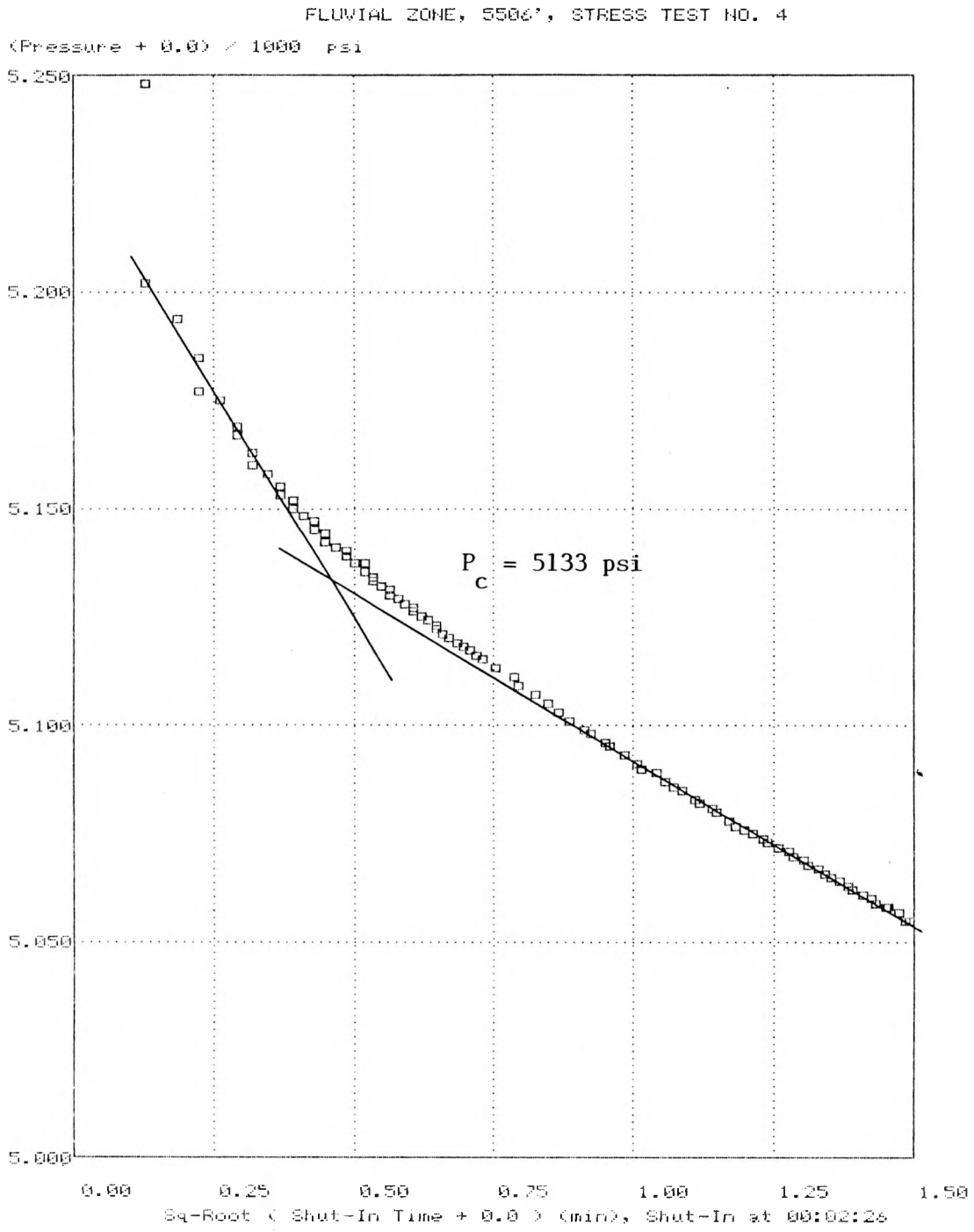


FIGURE A.114: Shale Stress Test (5506-5508'), Square-Root of Shut-In Time Plot of Test No. 4 Pressure Decline.

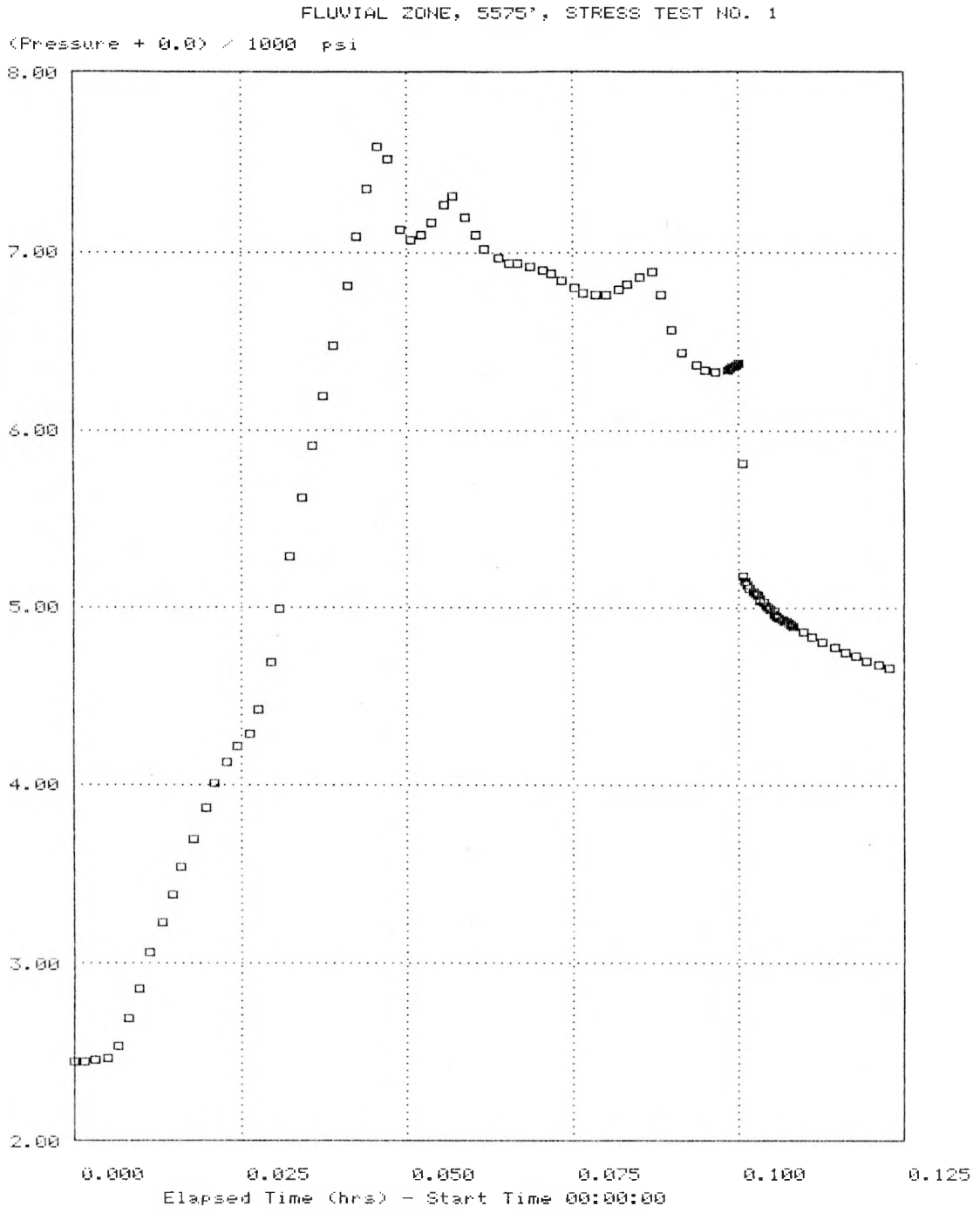


FIGURE A.115: Shale Stress Test (5575-5577'), Linear Plot of Test No. 1 Injection/Decline.

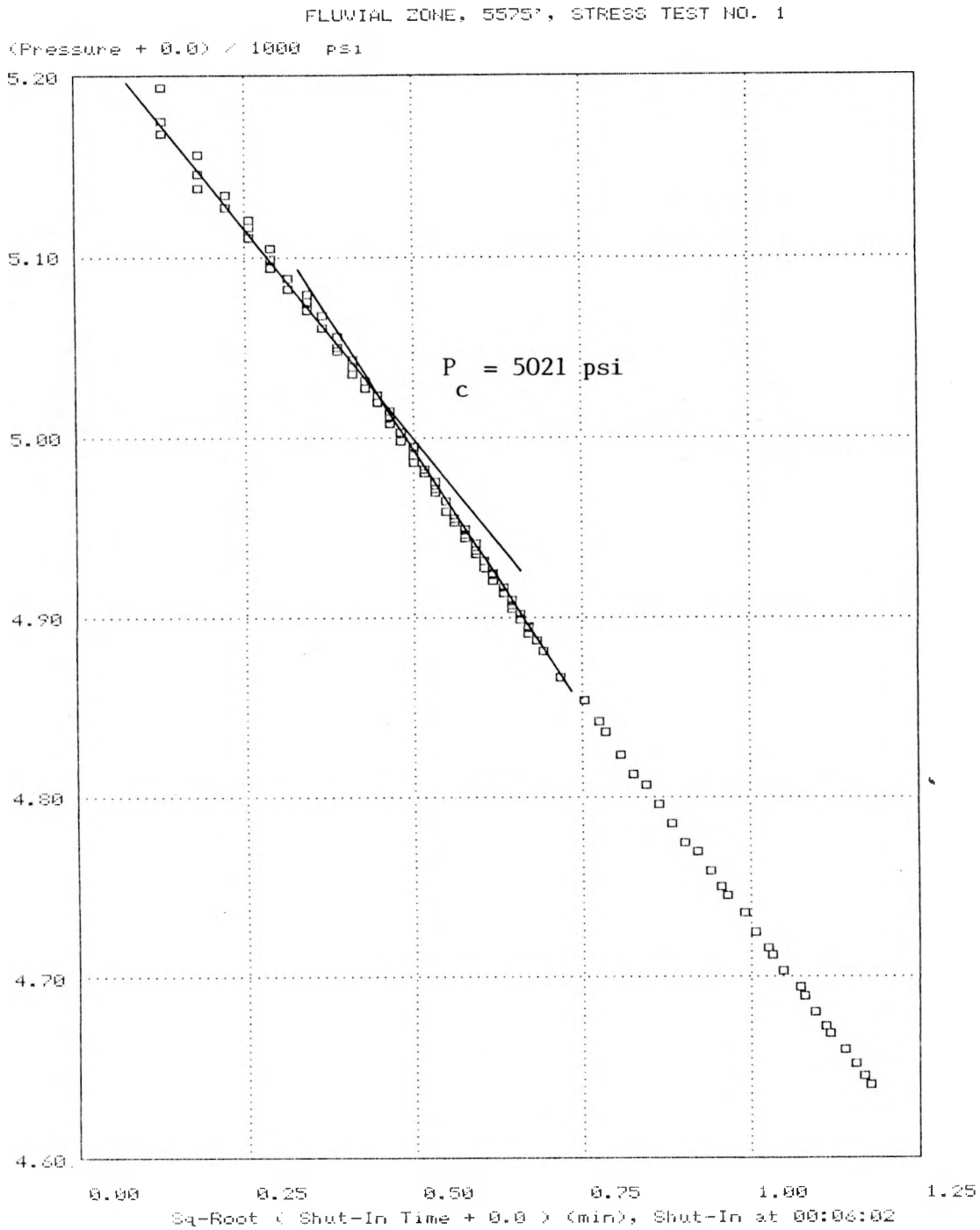


FIGURE A.116: Shale Stress Test (5575-5577'), Square-Root of Shut-In Time Plot of Test No. 1 Pressure Decline.

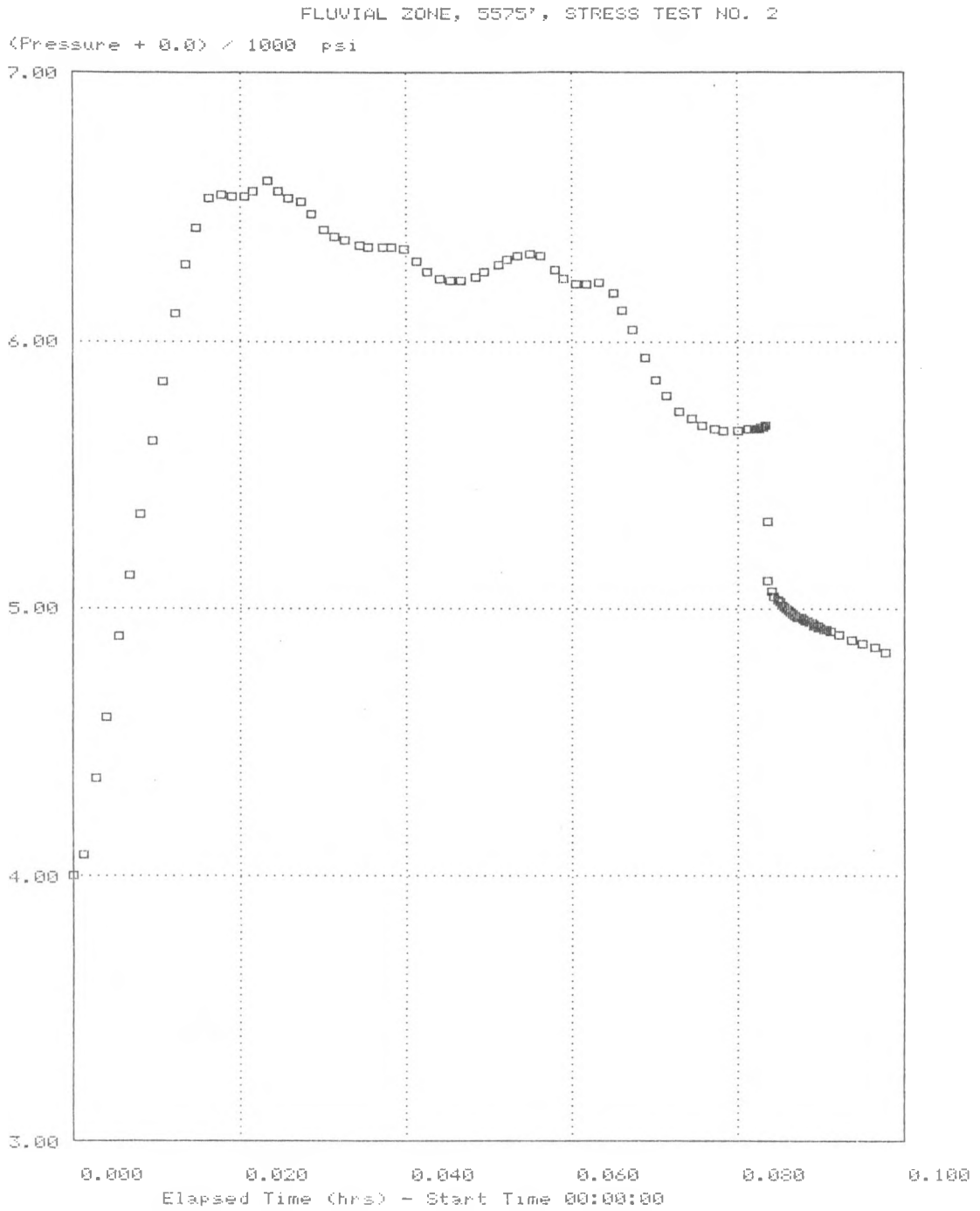


FIGURE A.117: Shale Stress Test (5575–5577'), Linear Plot of Test No. 2 Injection/Decline.

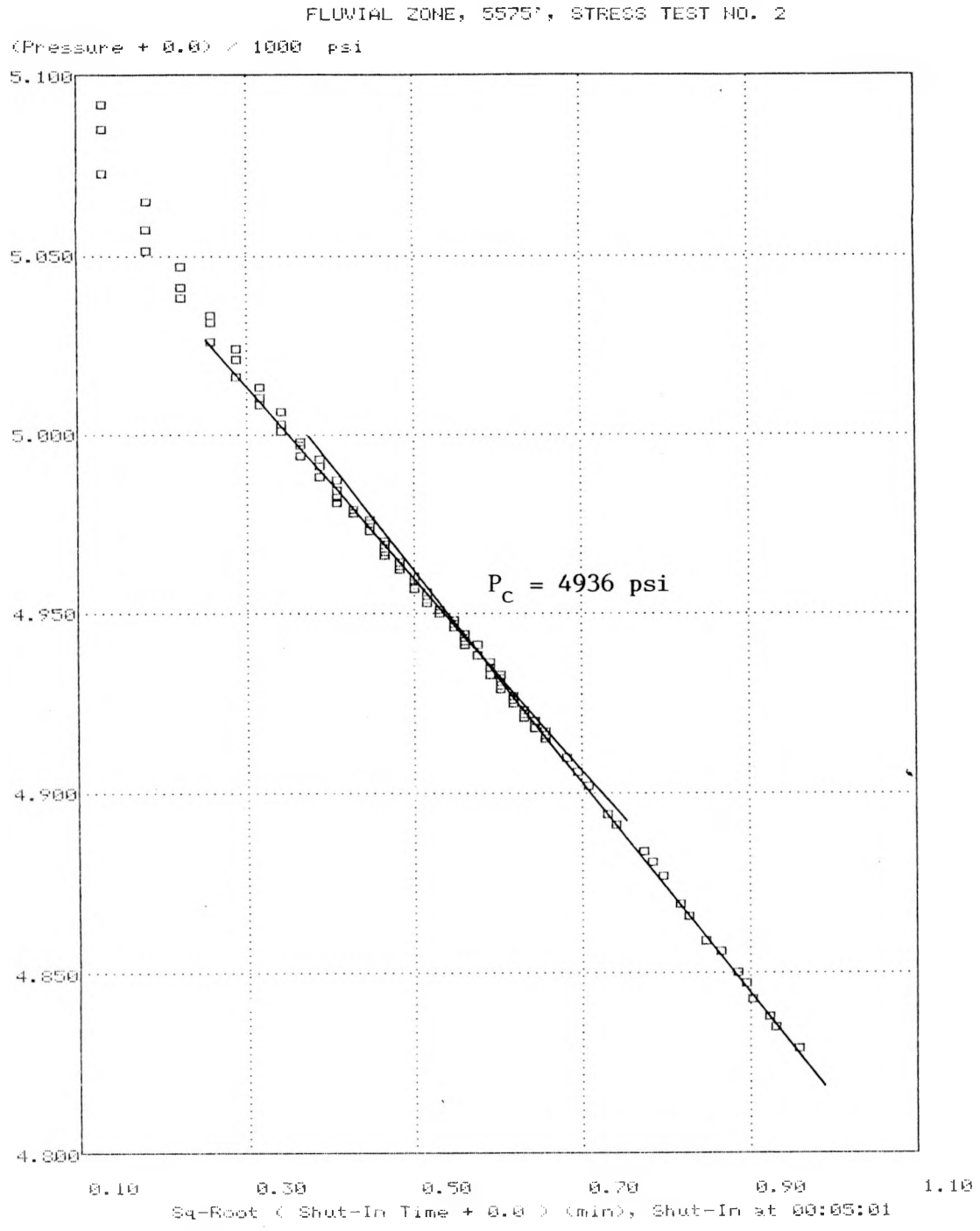


FIGURE A.118: Shale Stress Test (5575-5577'), Square-Root of Shut-In Time Plot of Test no. 2 Pressure Decline.

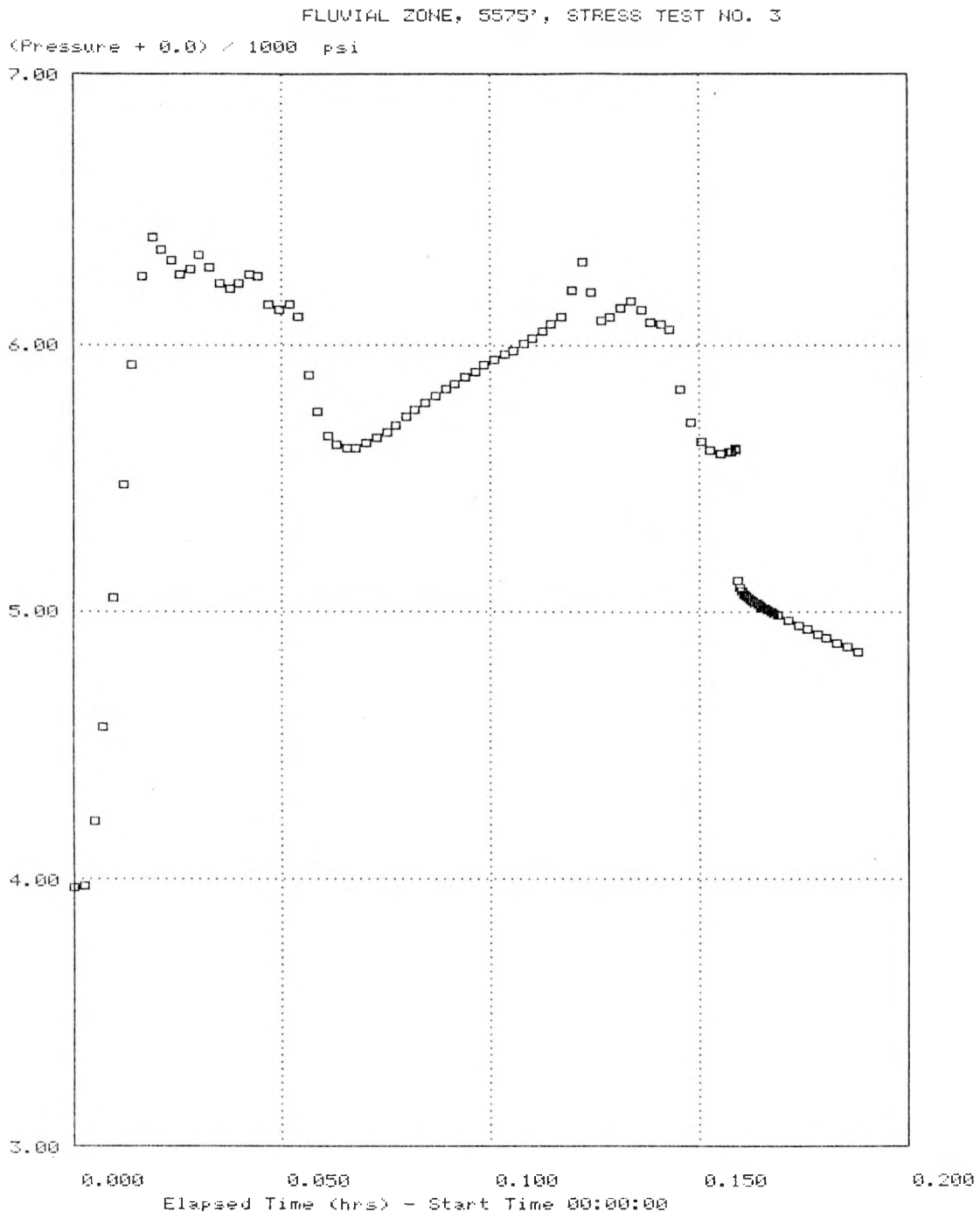


FIGURE A.119: Shale Stress Test (5575-5577'), Linear Plot of Test No. 3 Injection/Decline.

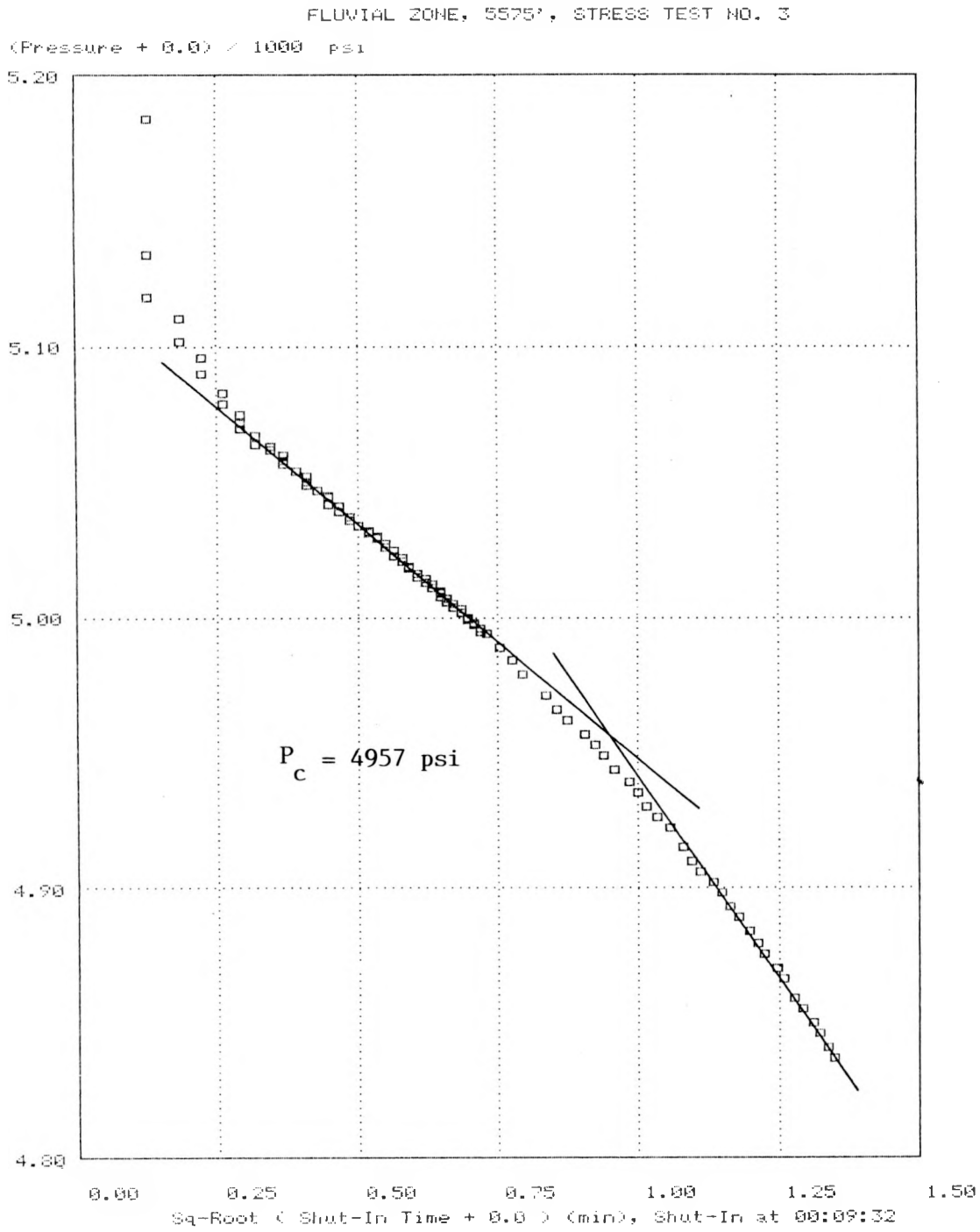


FIGURE A.120: Shale Stress Test (5575-5577'), Square-Root of Shut-In Time Plot of Test No. 3 Pressure Decline.

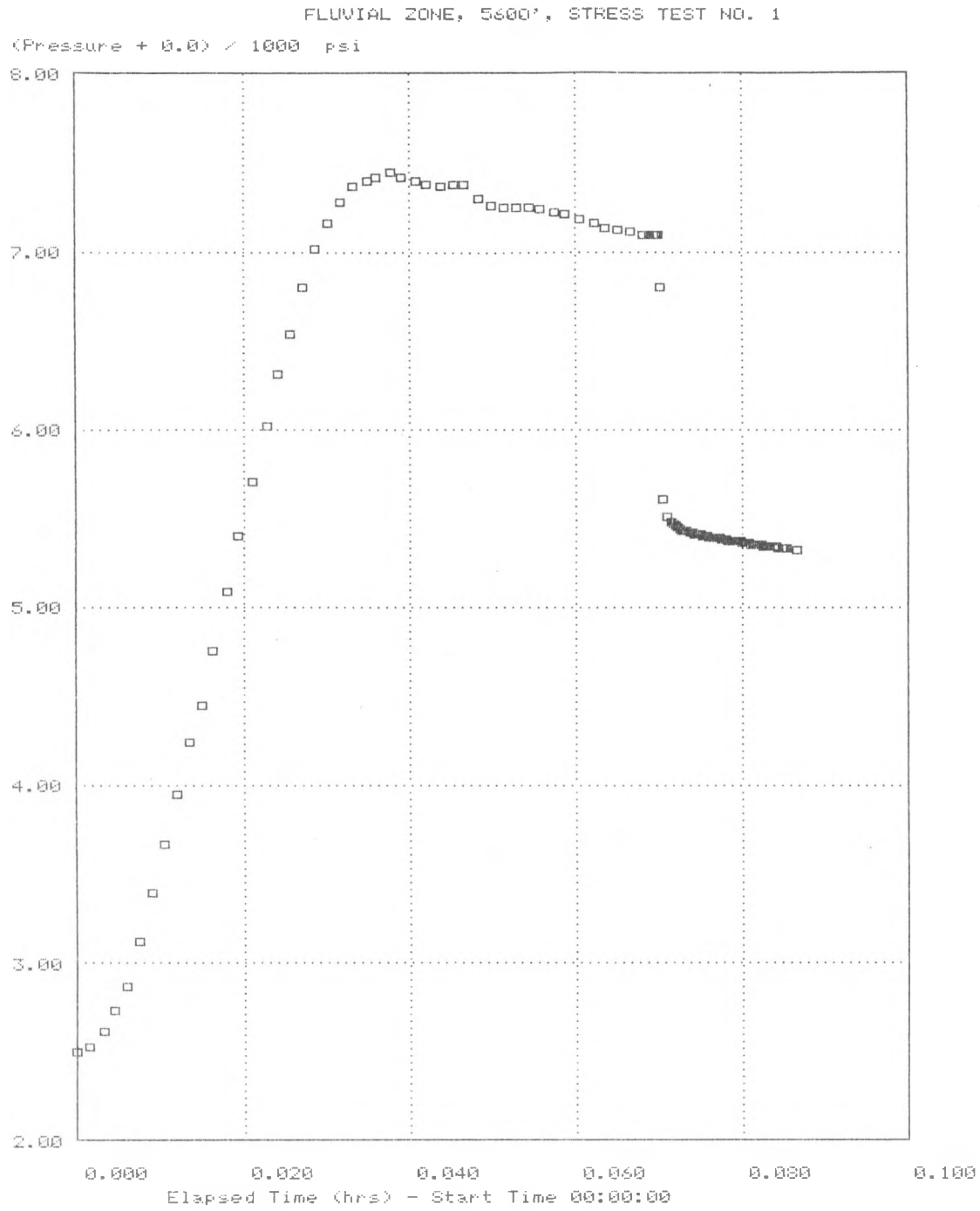


FIGURE A.121: Shale Stress Test (5600-5602'), Linear Plot of Test No. 1 Injection/Decline.

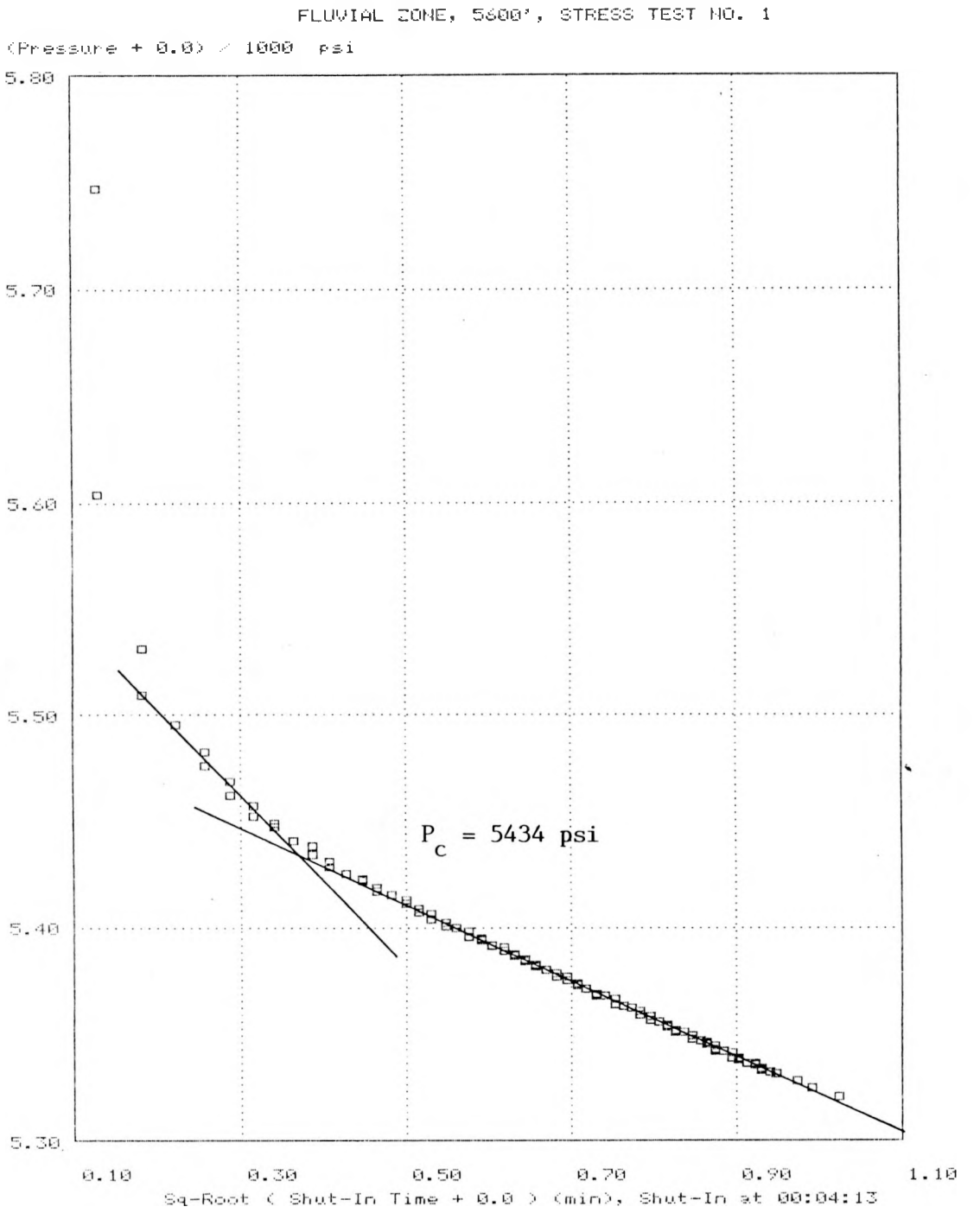


FIGURE A.122: Shale Stress Test (5600-5602'), Square-Root of Shut-In Time Plot of Test No. 1 Pressure Decline.

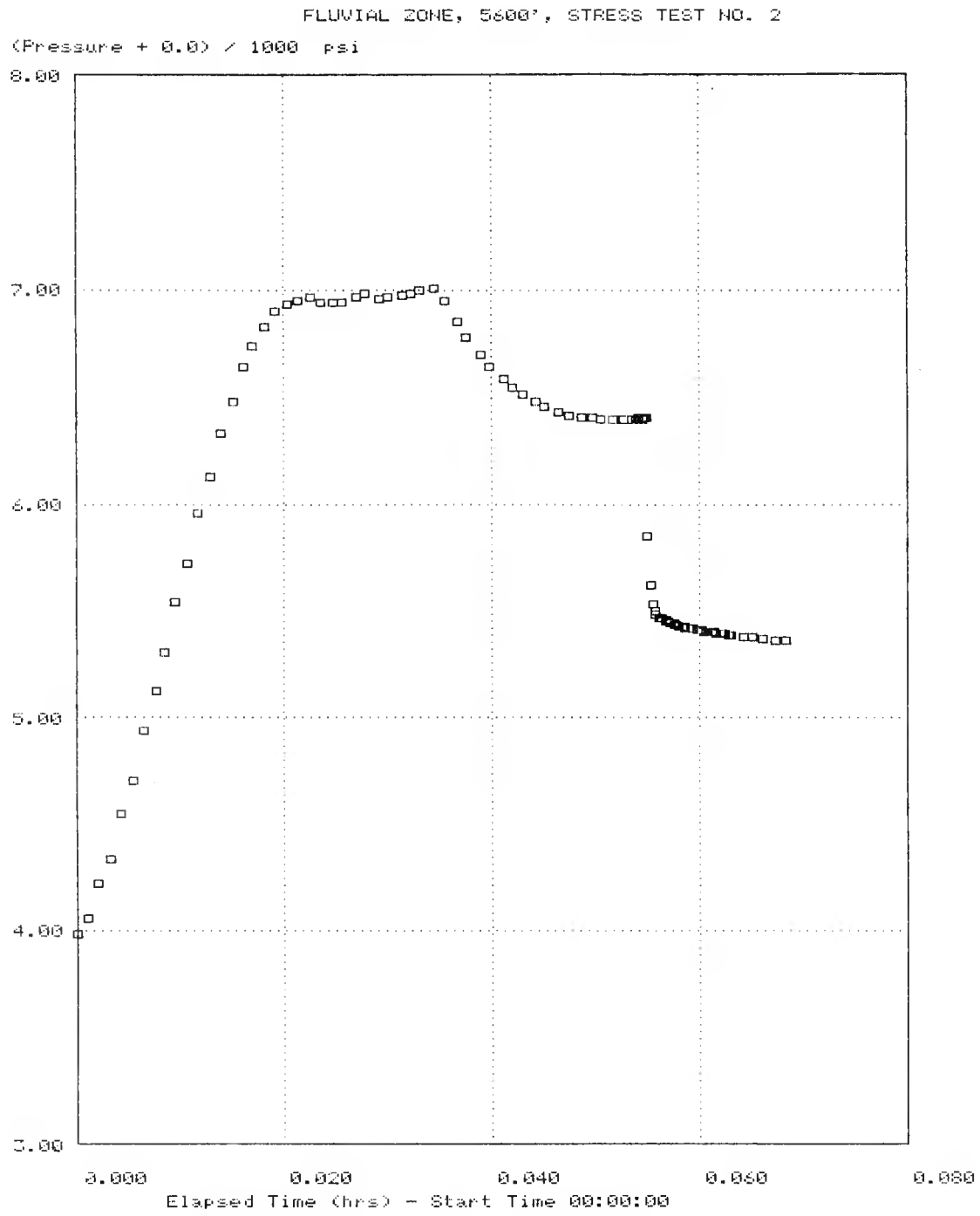


FIGURE A.123: Shale Stress Test (5600-5602'), Linear Plot of Test no. 2 injection/Decline.

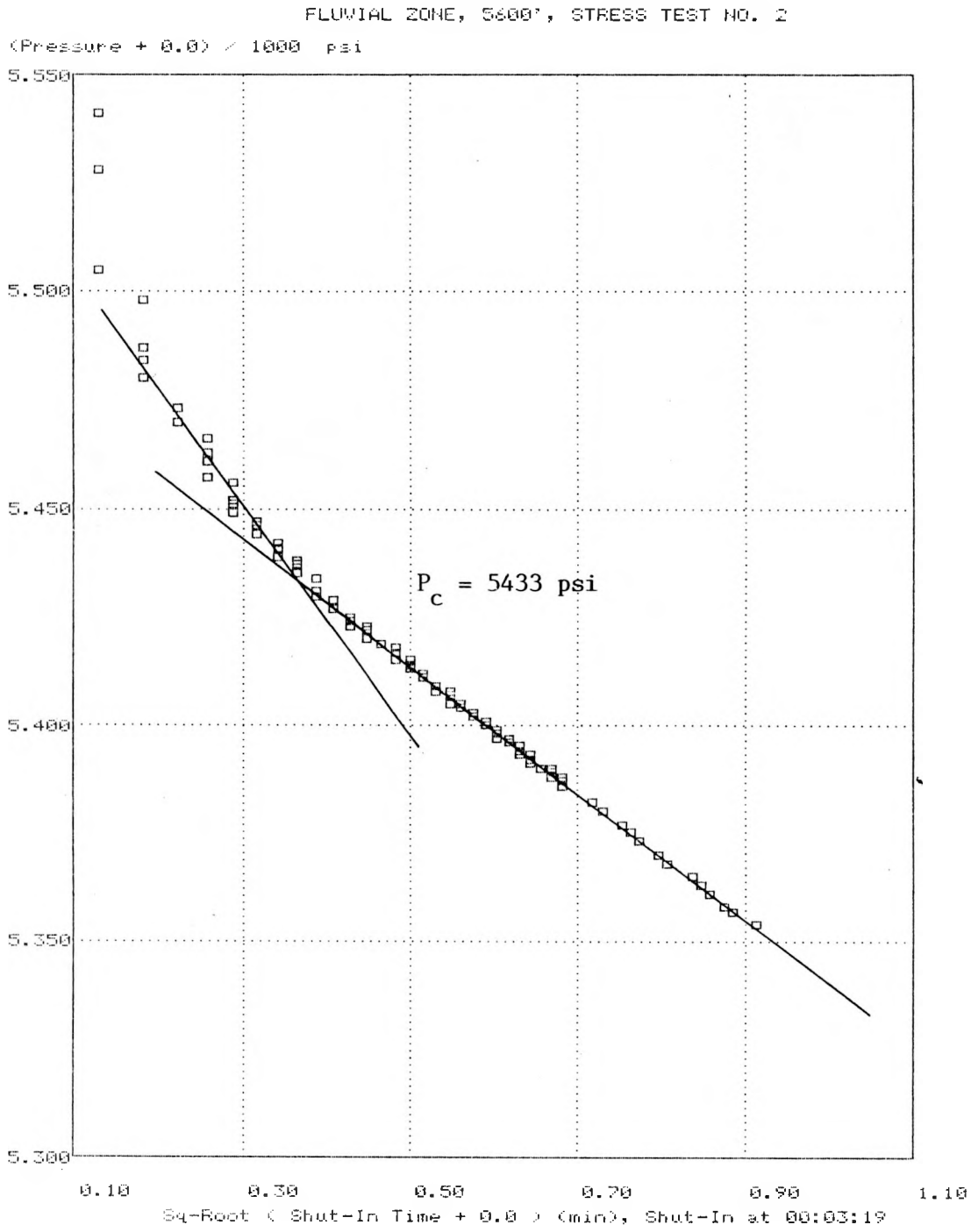


FIGURE A.124: Shale Stress Test (5600-5602'), Square-Root of Shut-In Time Plot of Test No. 2 Pressure Decline.

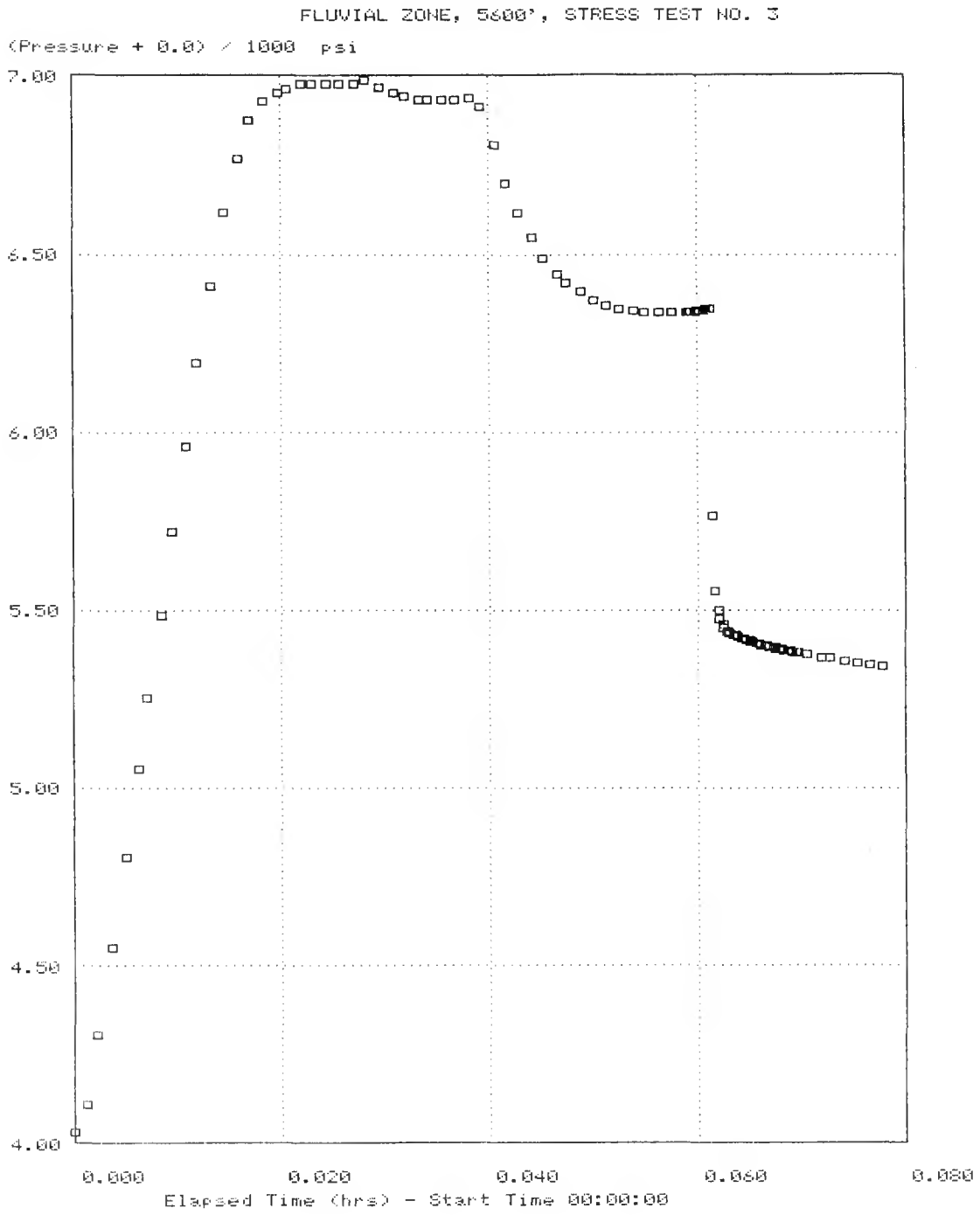


FIGURE A.125: Shale Stress Test (5600-5602'), Linear Plot of Test No. 3 Injection/Decline.

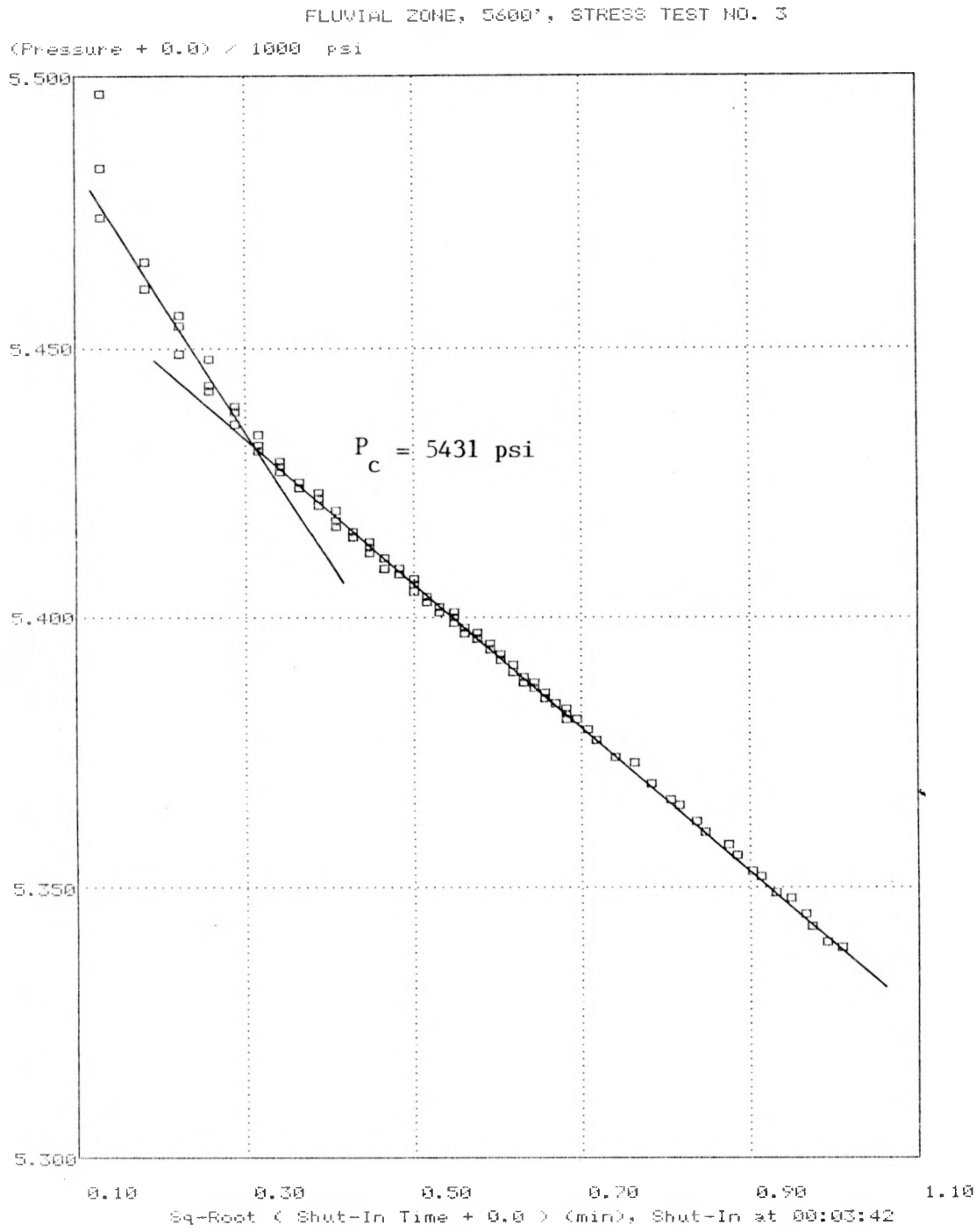


FIGURE A.126: Shale Stress Test (5600-5602'), Square-Root of Shut-In Time Plot of Test No. 3 Pressure Decline.

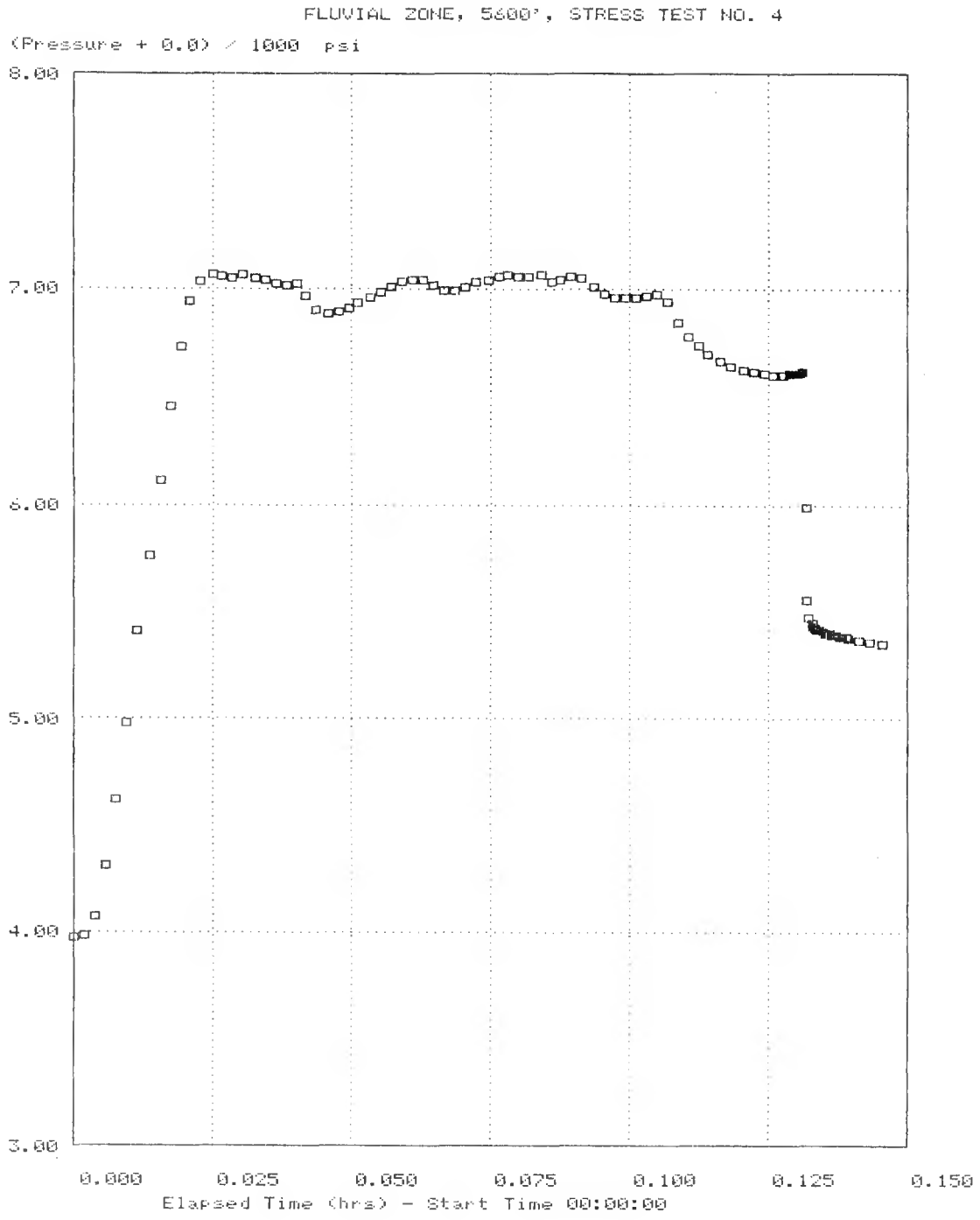


FIGURE A.127: Shale Stress Test (5600-5602'), Linear Plot of Test No. 4 injection/Decline.

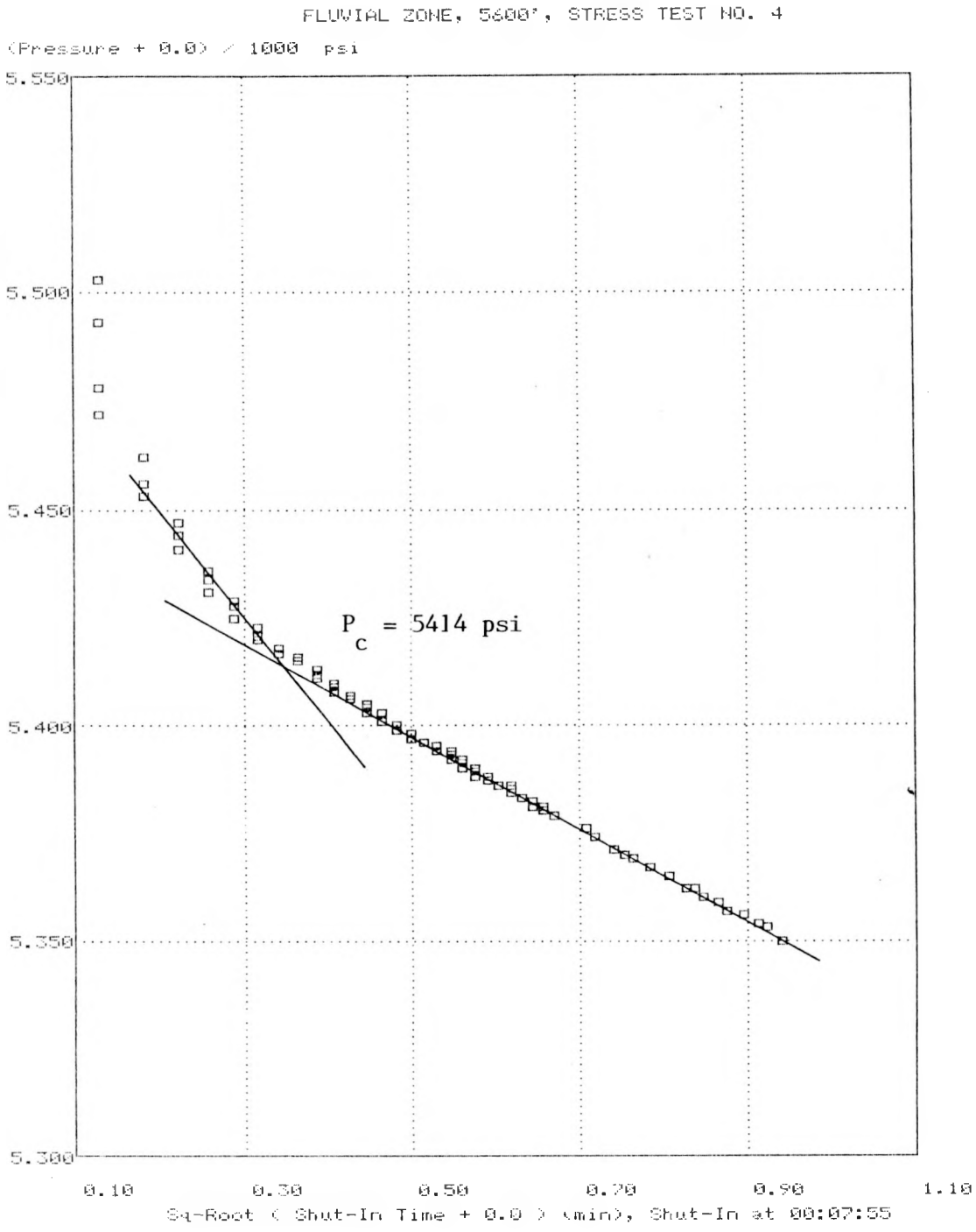


FIGURE A.128: Shale Stress Test (5600-5602'), Square-Root of Shut-In Time Plot of Test No. 4 Pressure Decline.

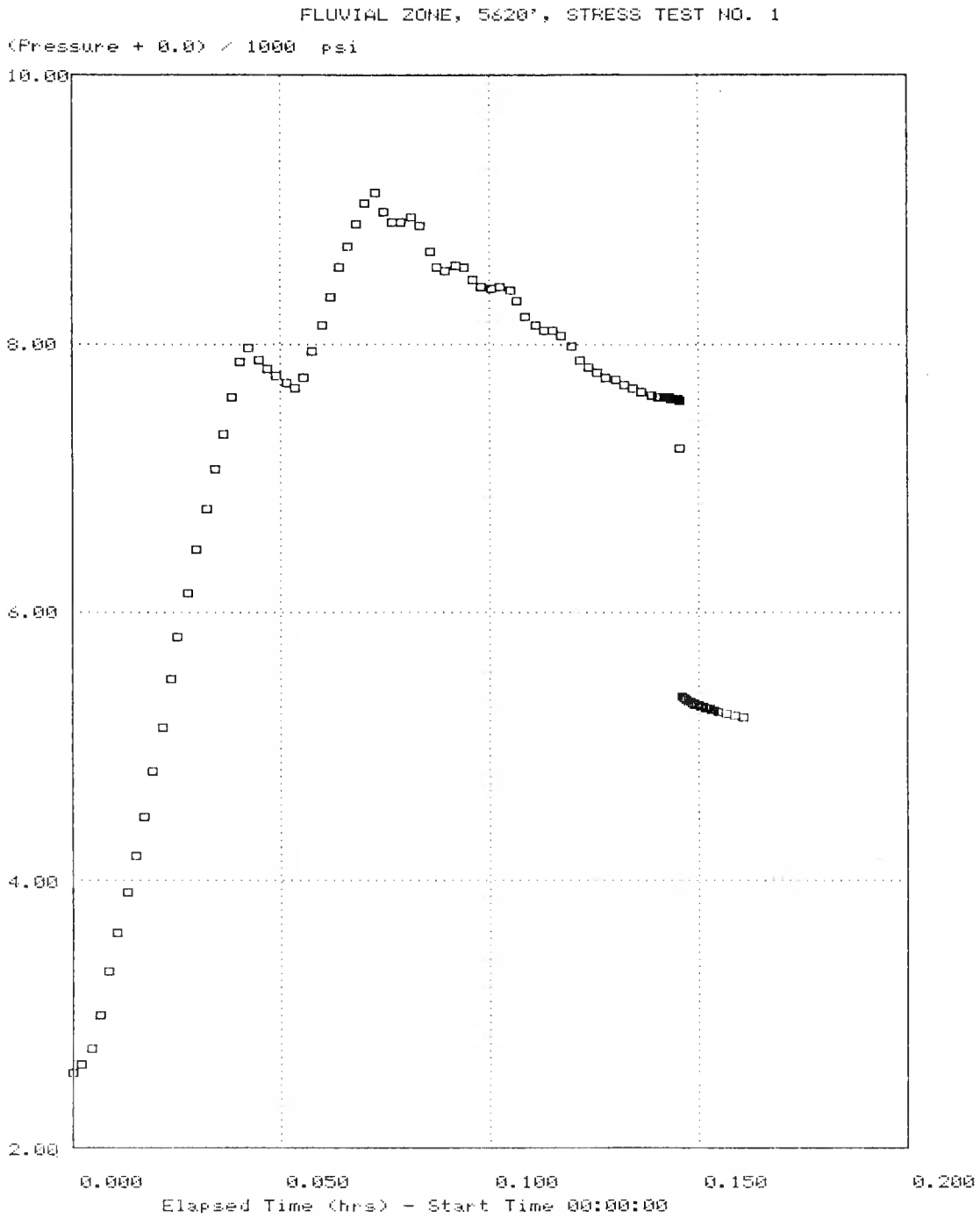


FIGURE A.129: Shale Stress Test (5620-5622'), Linear Plot of Test No. 1 Injection/Decline.

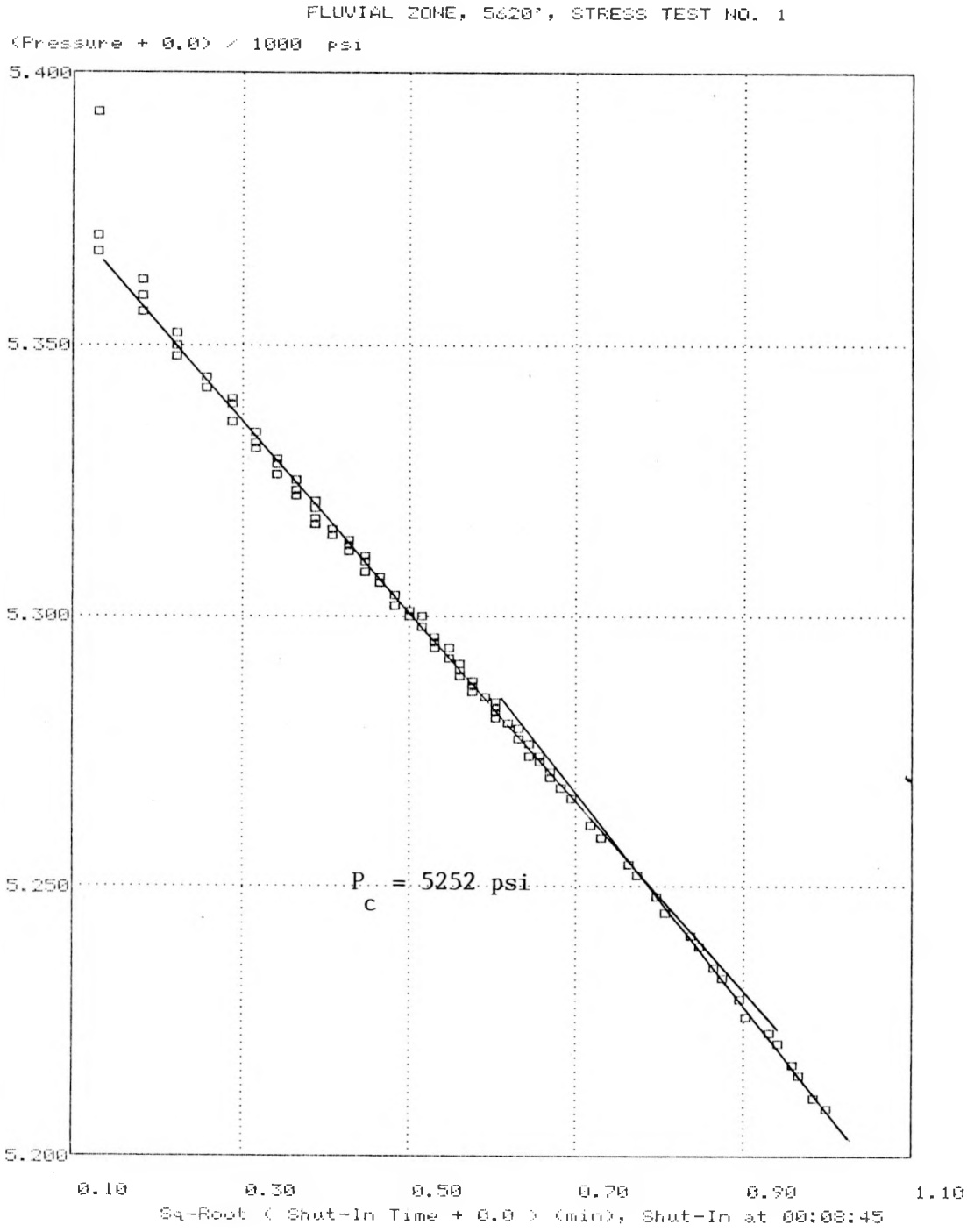


FIGURE A.130: Shale Stress Test (5620-5622'), Square-Root of Shut-In Time Plot of Test No. 1 Pressure Decline.

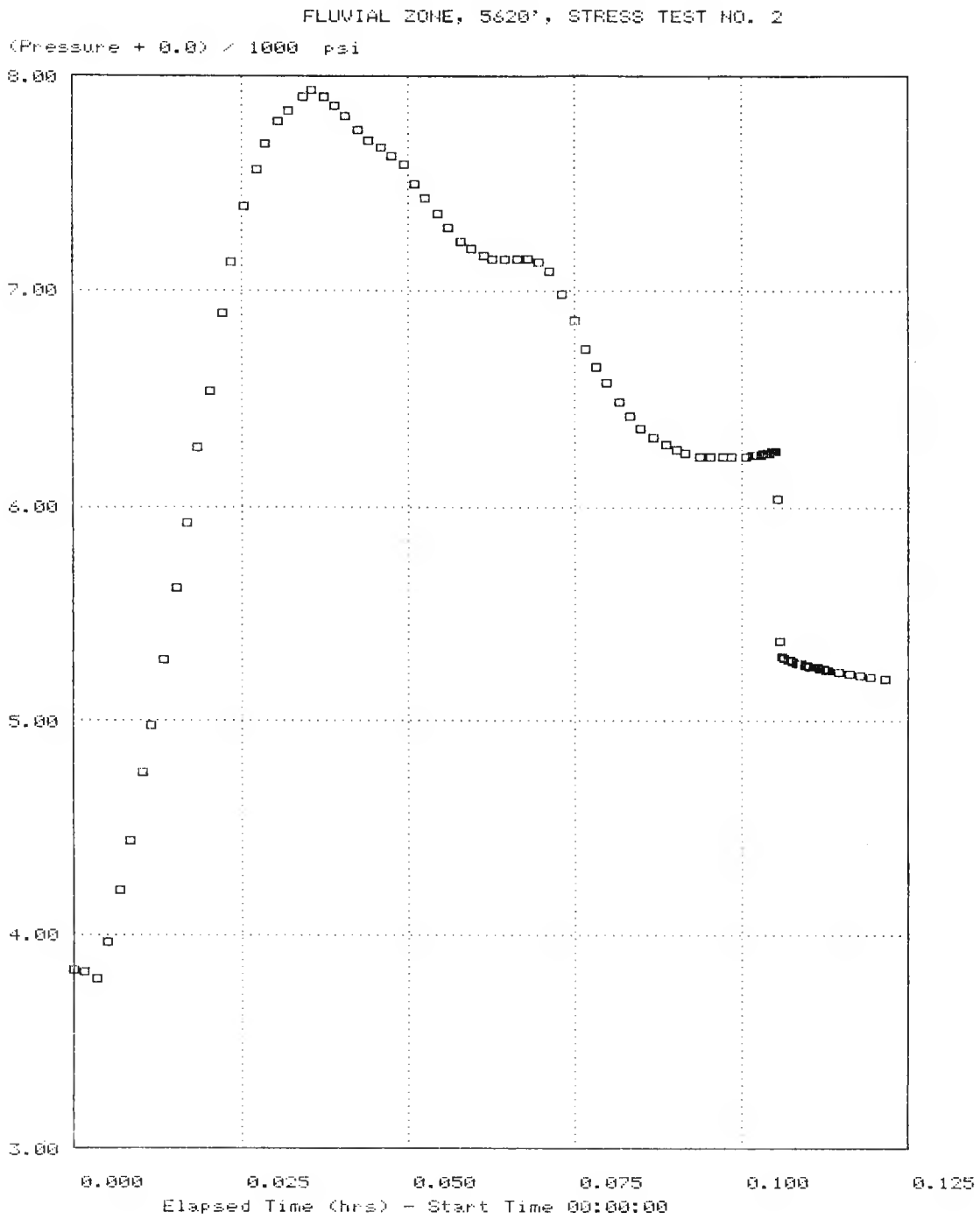


FIGURE A.131: Shale Stress Test (5620-5622'), Linear Plot of Test No. 2 Injection/Decline.

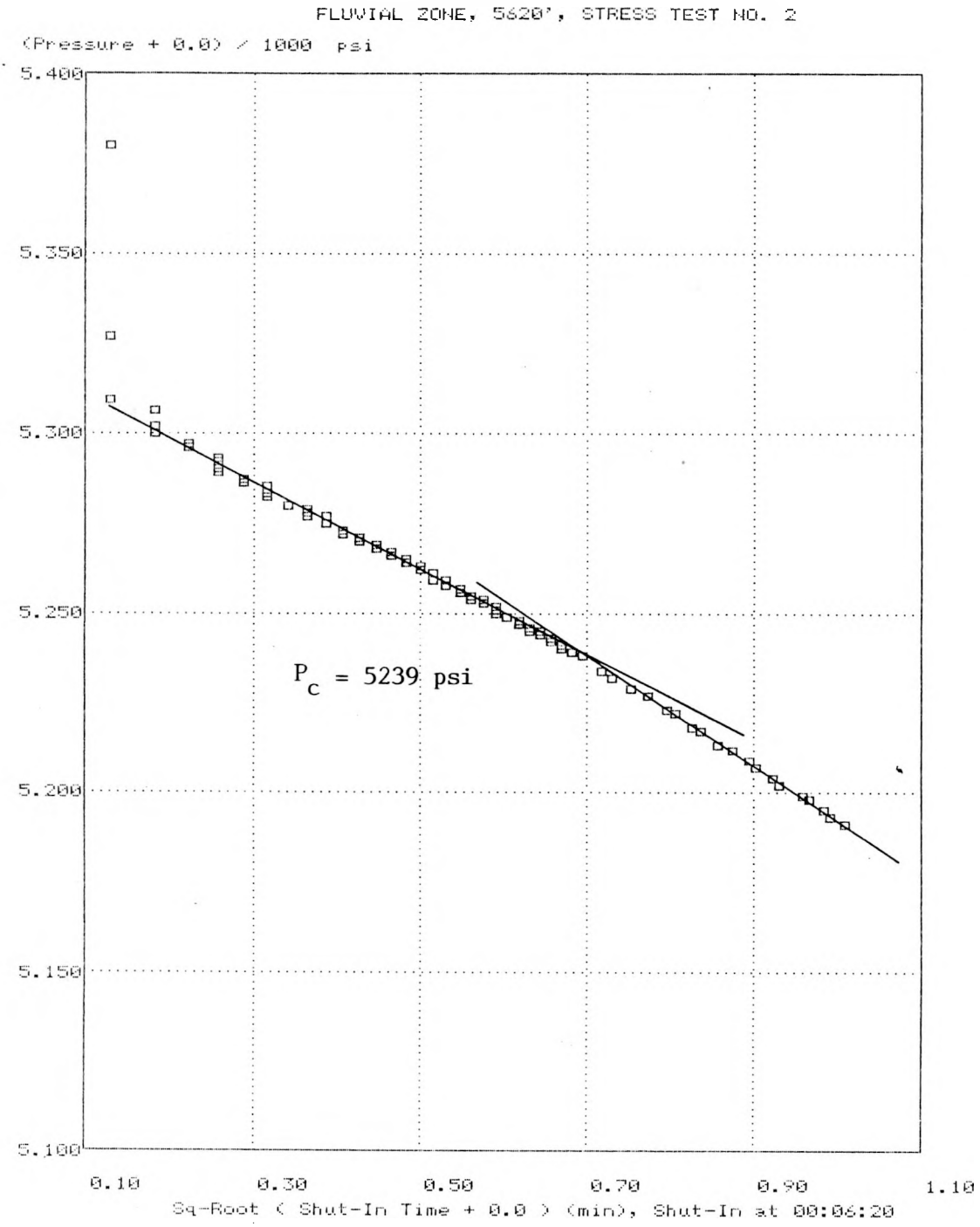


FIGURE A.132: Shale Stress Test (5620-5622'), Square-Root of Shut-In time Plot of Test No. 2 Pressure Decline.

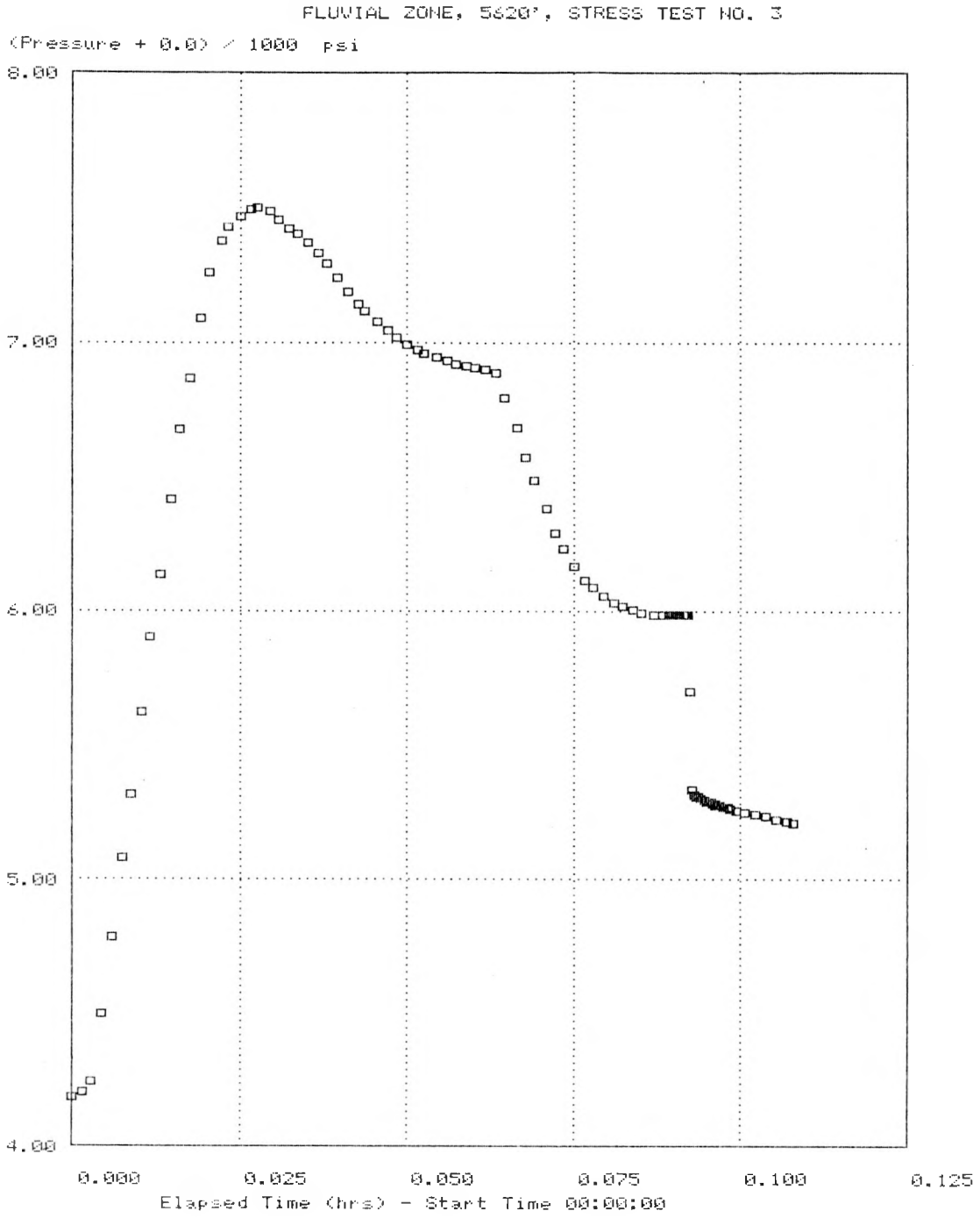


FIGURE A.133: Shale Stress Test (5620-5622'), Linear Plot of Test No. 3 Injection/Decline.

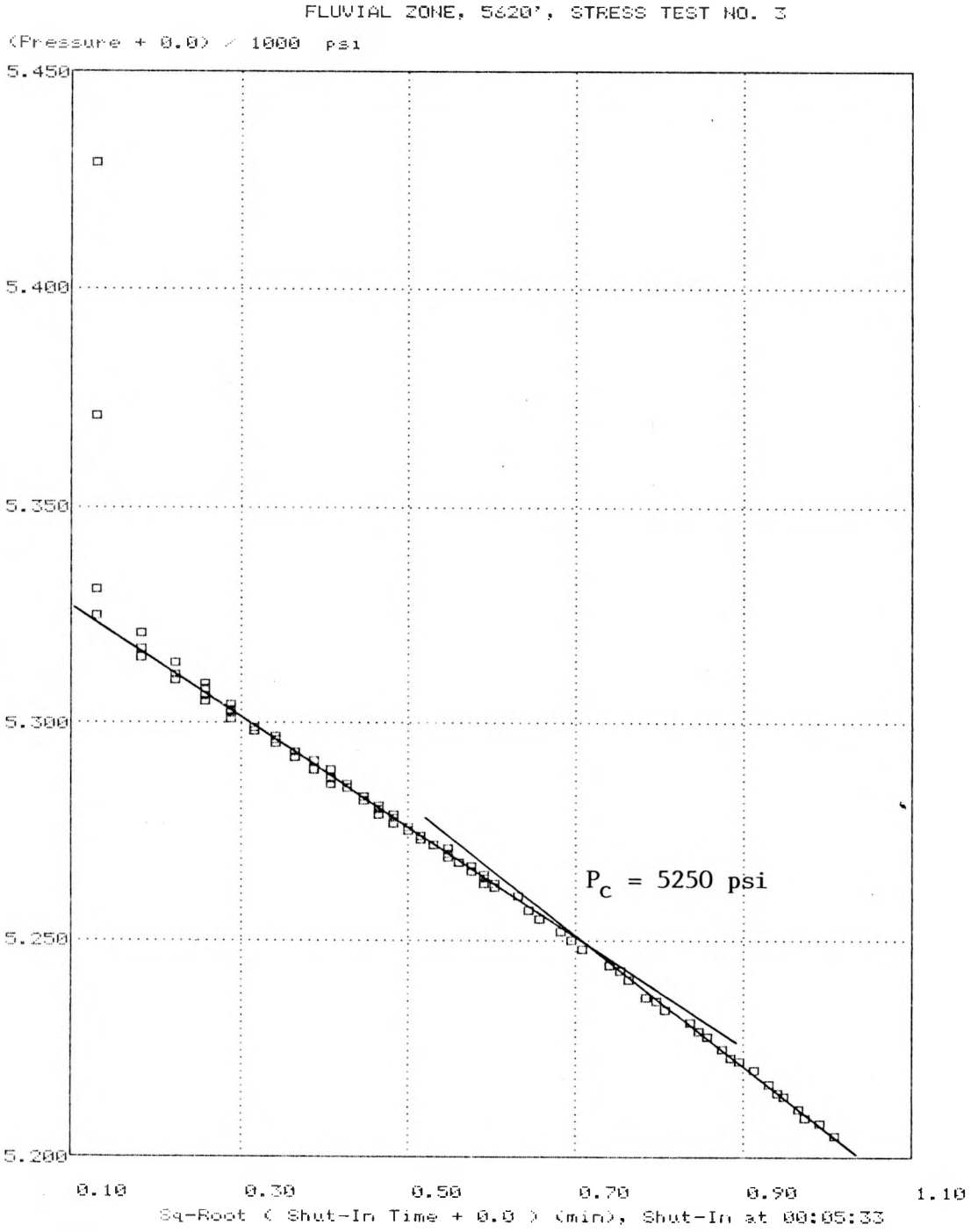


FIGURE A.134: Shale Stress Test (5620-5622'), Square-Root of Shut-In Time Plot of Test No. 3 Pressure Decline.

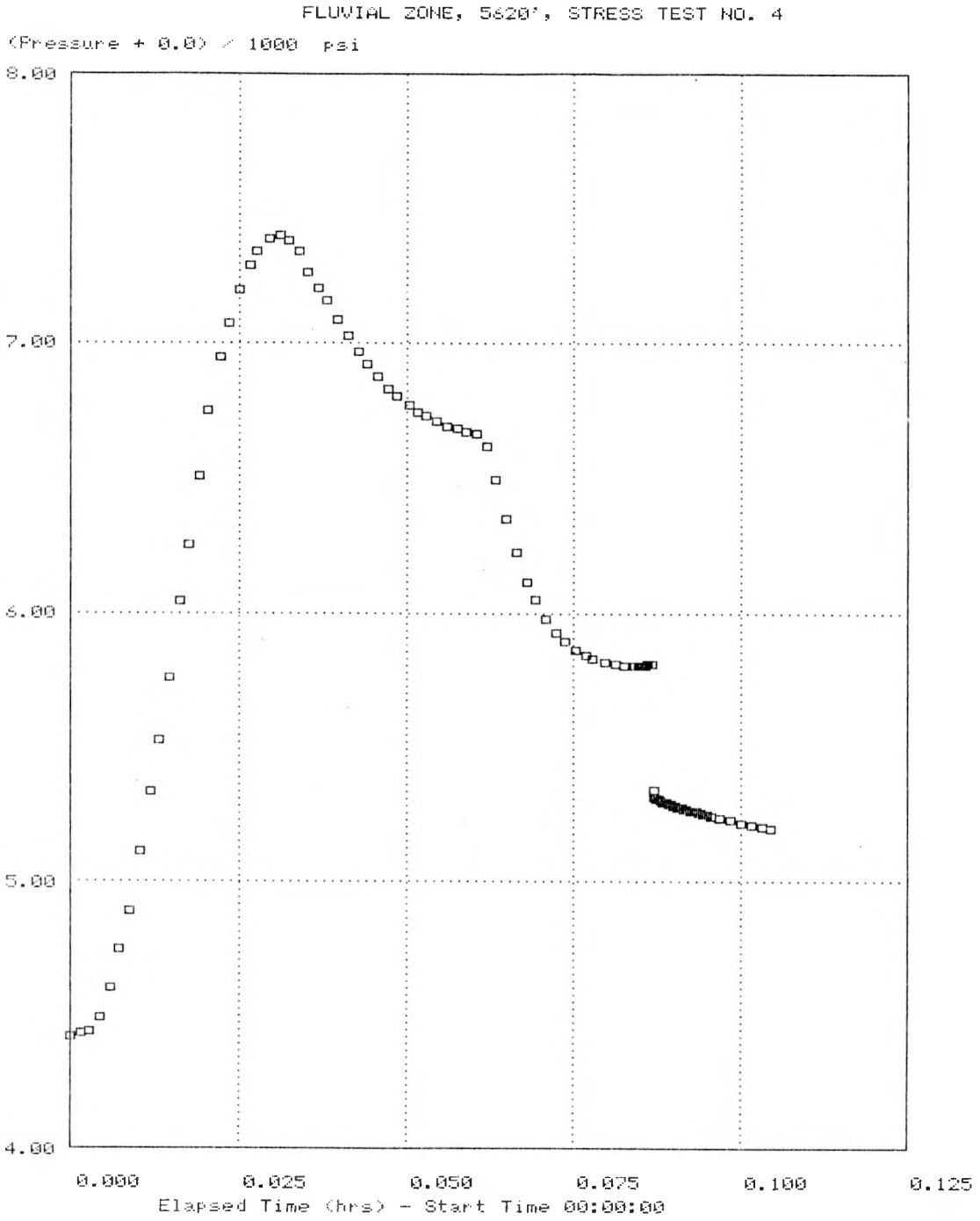


FIGURE A.135: Shale Stress Test (5620-5622'), Linear Plot of Test No. 4 Injection/Decline.

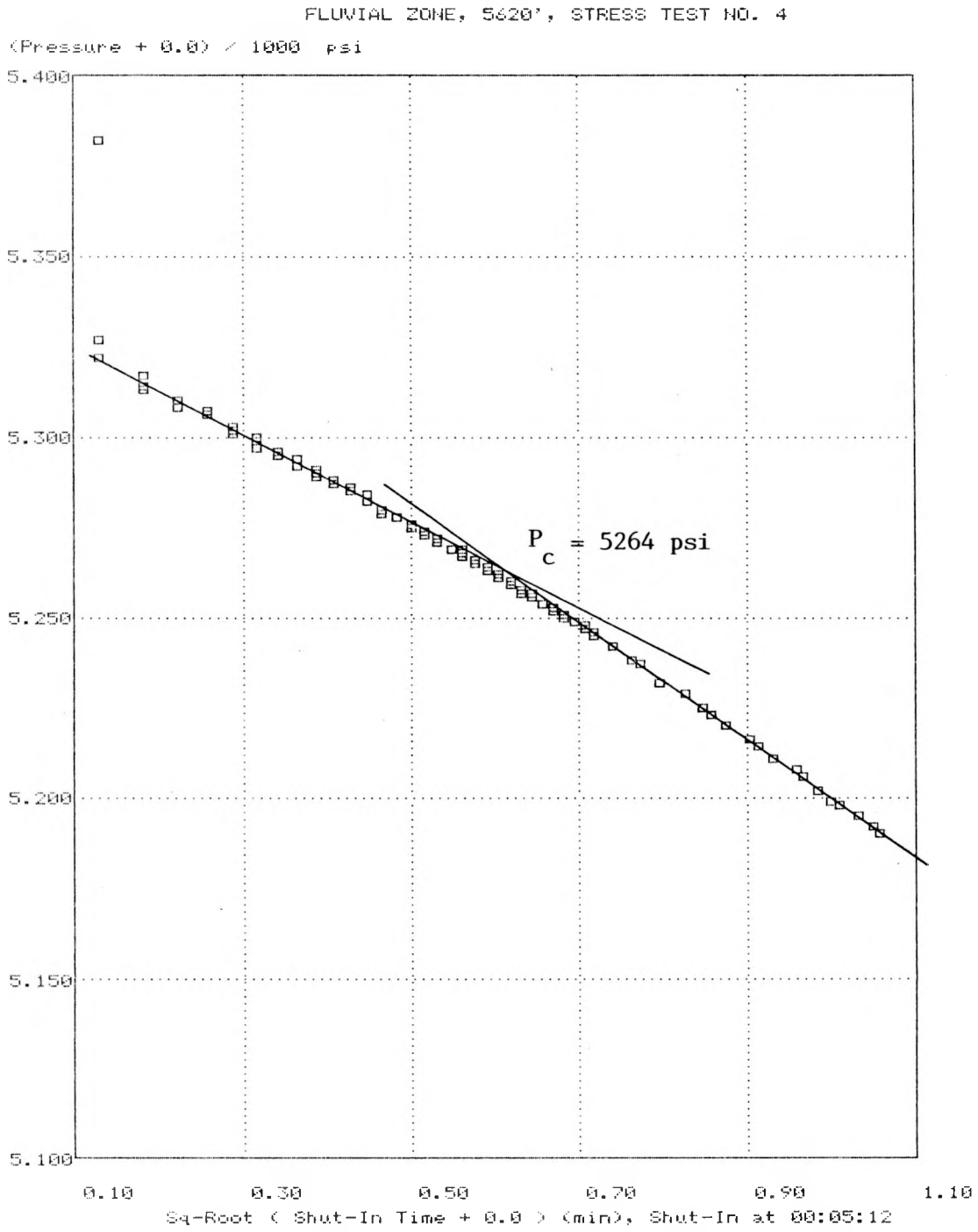


FIGURE A.136: Shale Stress Test (5620-5622'), Square-Root of Shut-In Time Plot of Test No. 4 Pressure Decline.

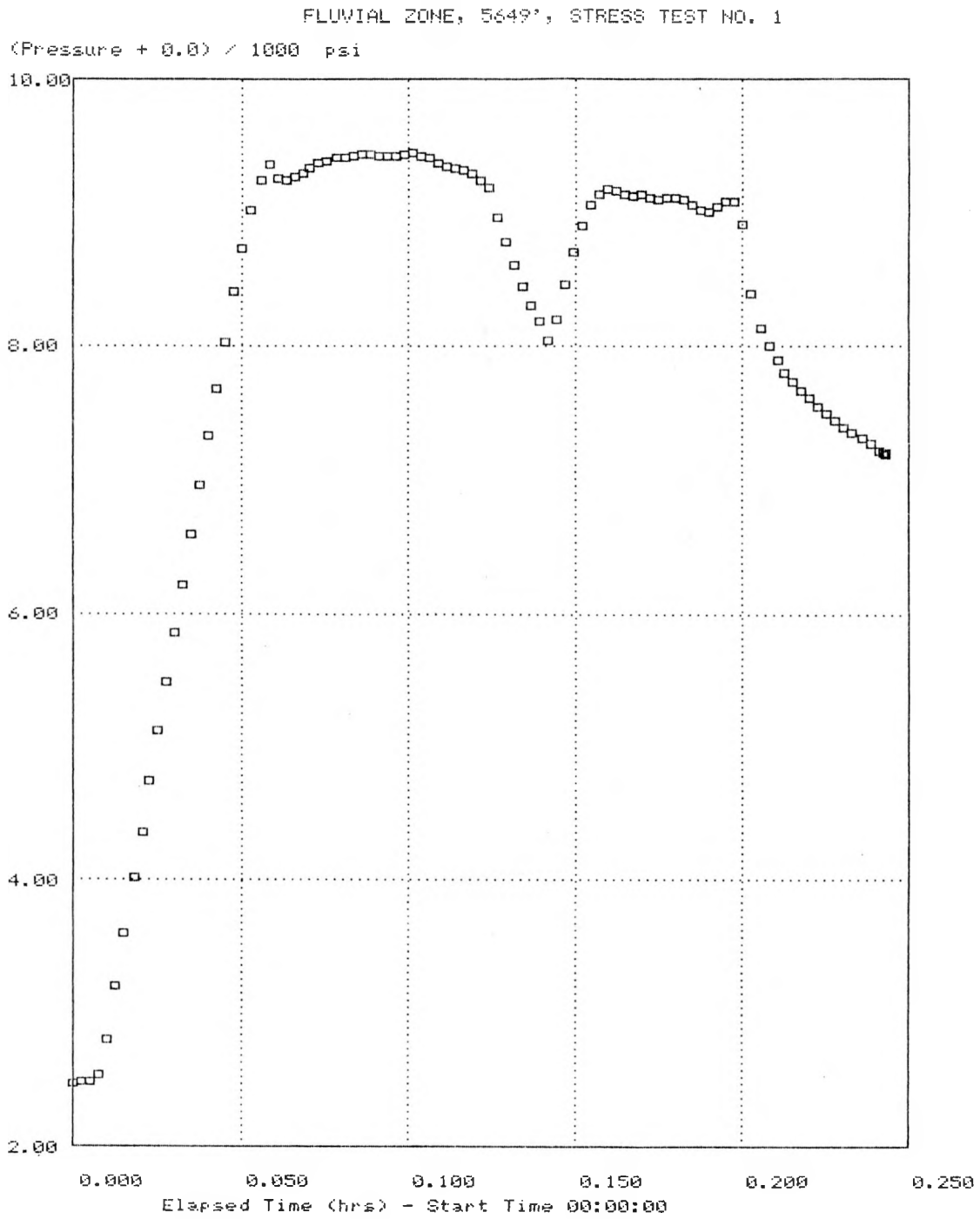


FIGURE A.137: Shale Stress Test (5649-5651'), Linear Plot of Test No. 1 Injection/Decline.

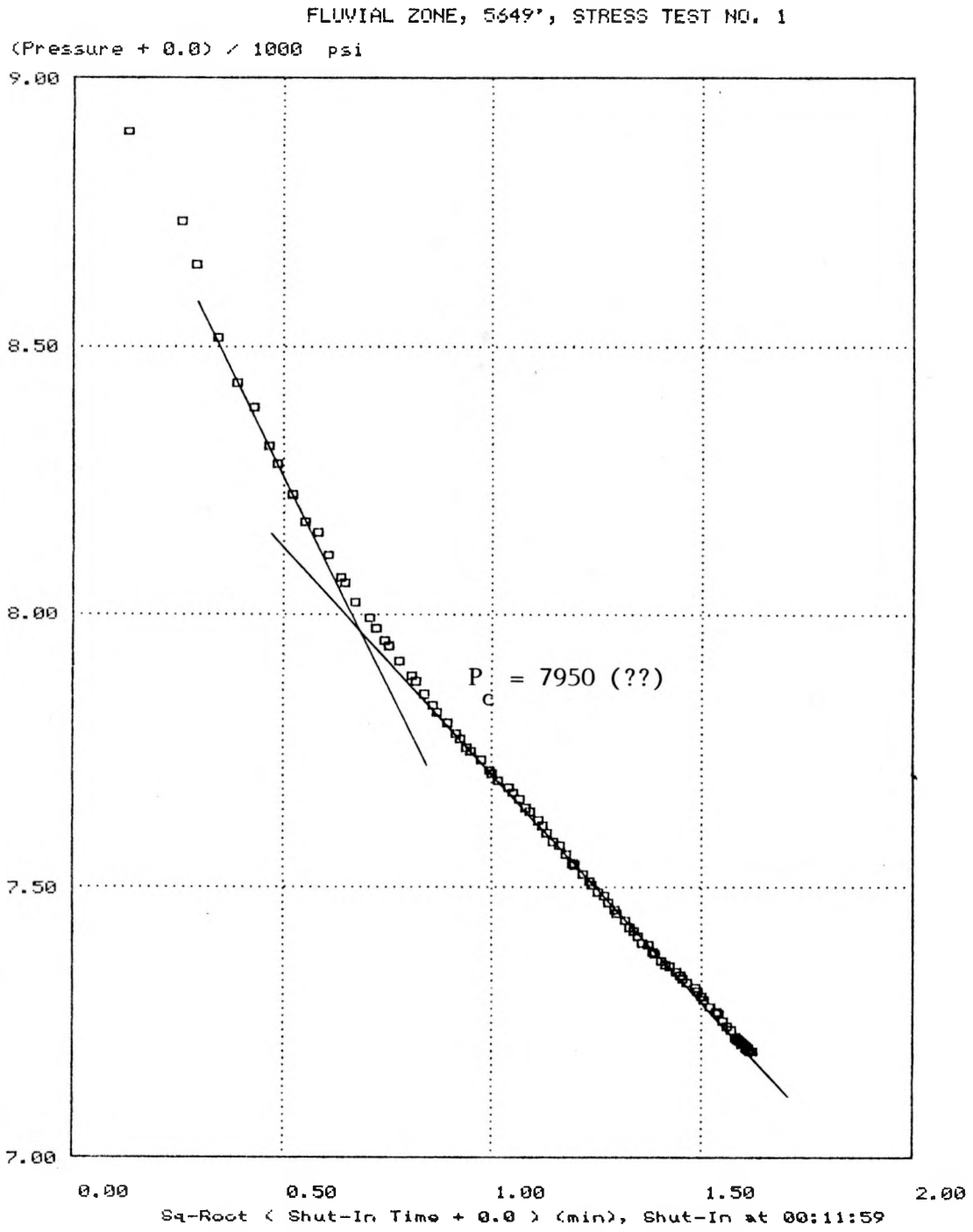


FIGURE A.138: Shale Stress Test (5649-5651'), Square-Root of Shut-In time Plot of Test No. 1 Pressure Decline.

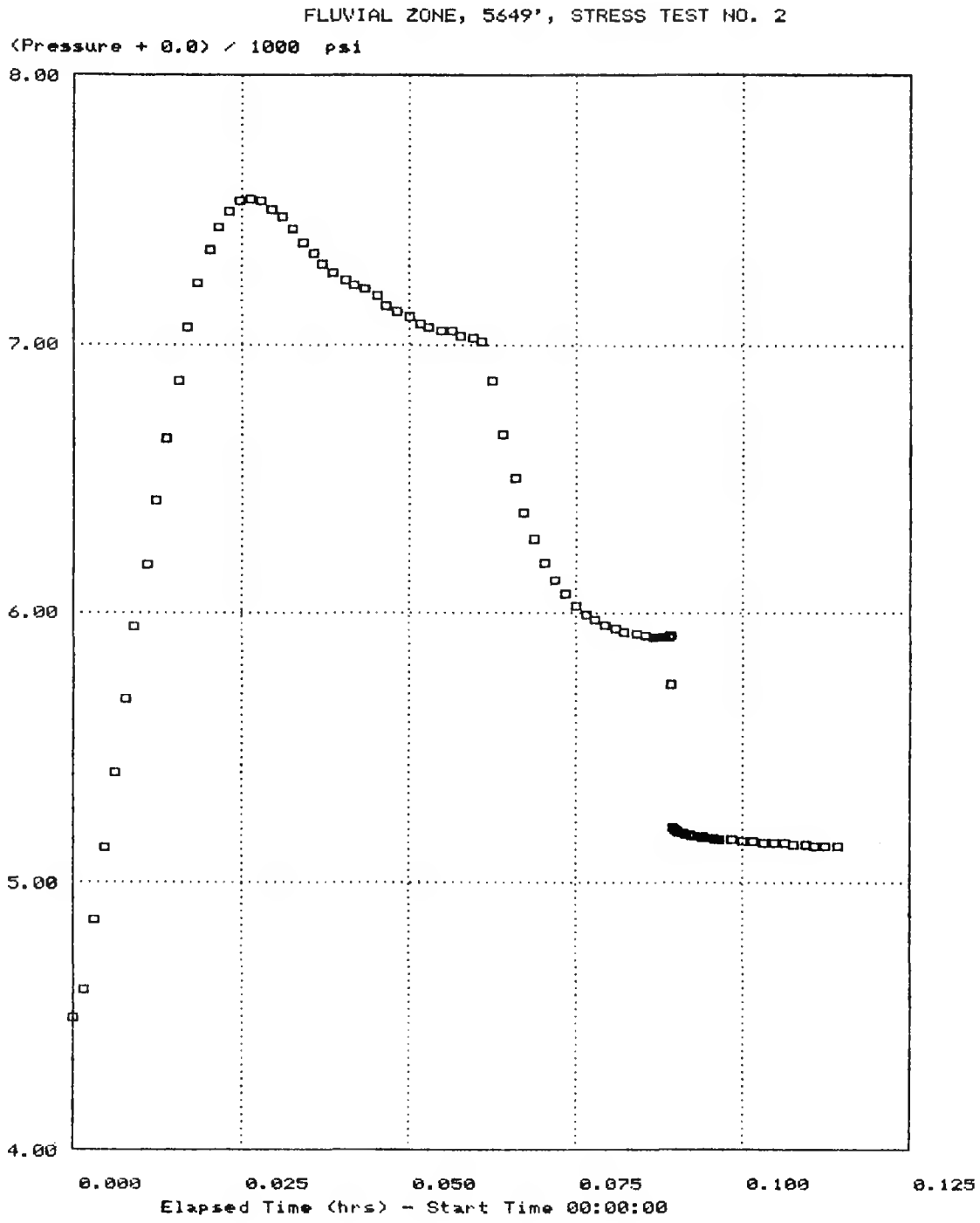


FIGURE A.139: Shale Stress Test (5649-5651'), Linear Plot of Test No. 2 Injection/Decline.

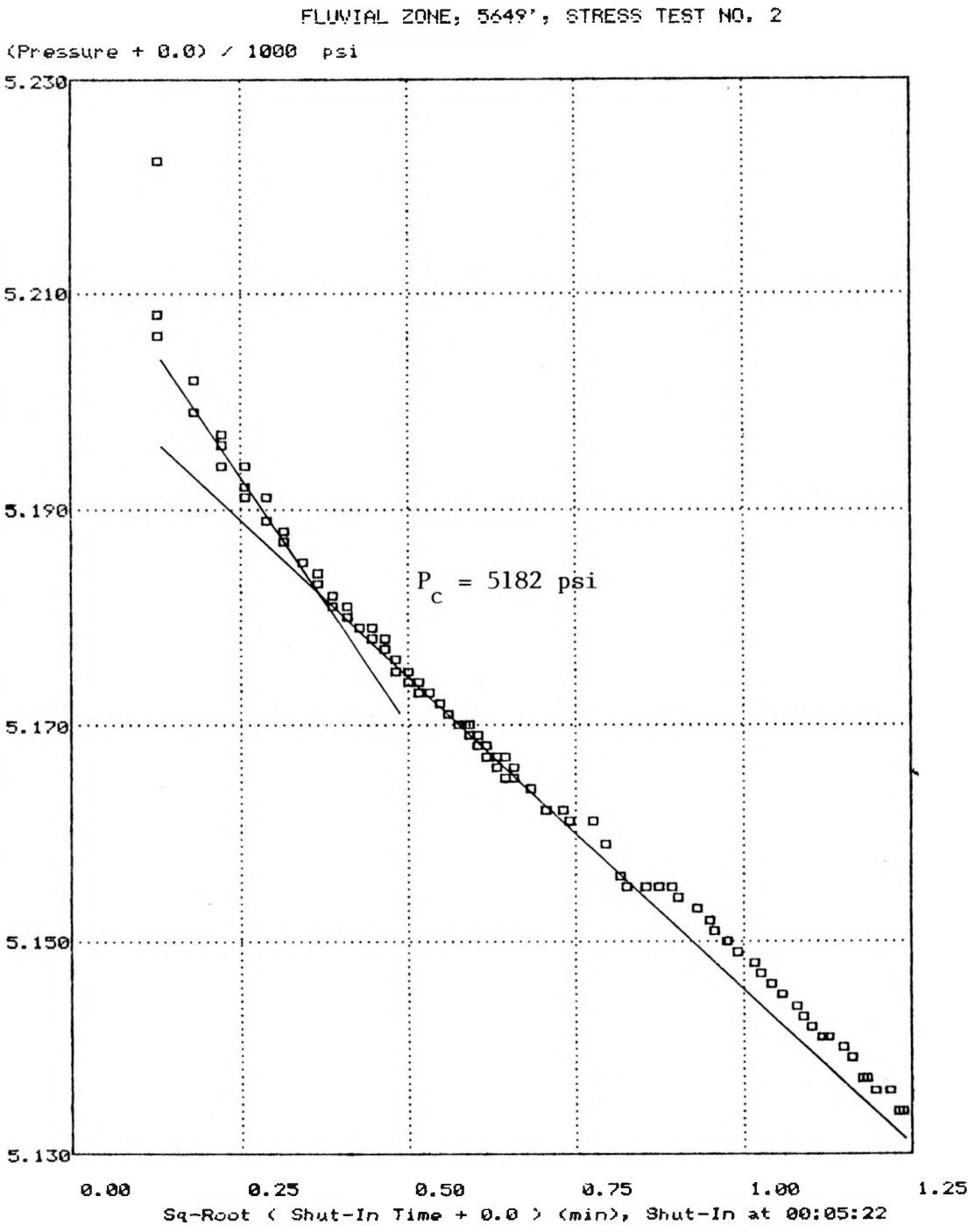


FIGURE A.140: Shale Stress Test (5649-5651'), Square-Root of Shut-In Time Plot of Test No. 2 Pressure Decline.

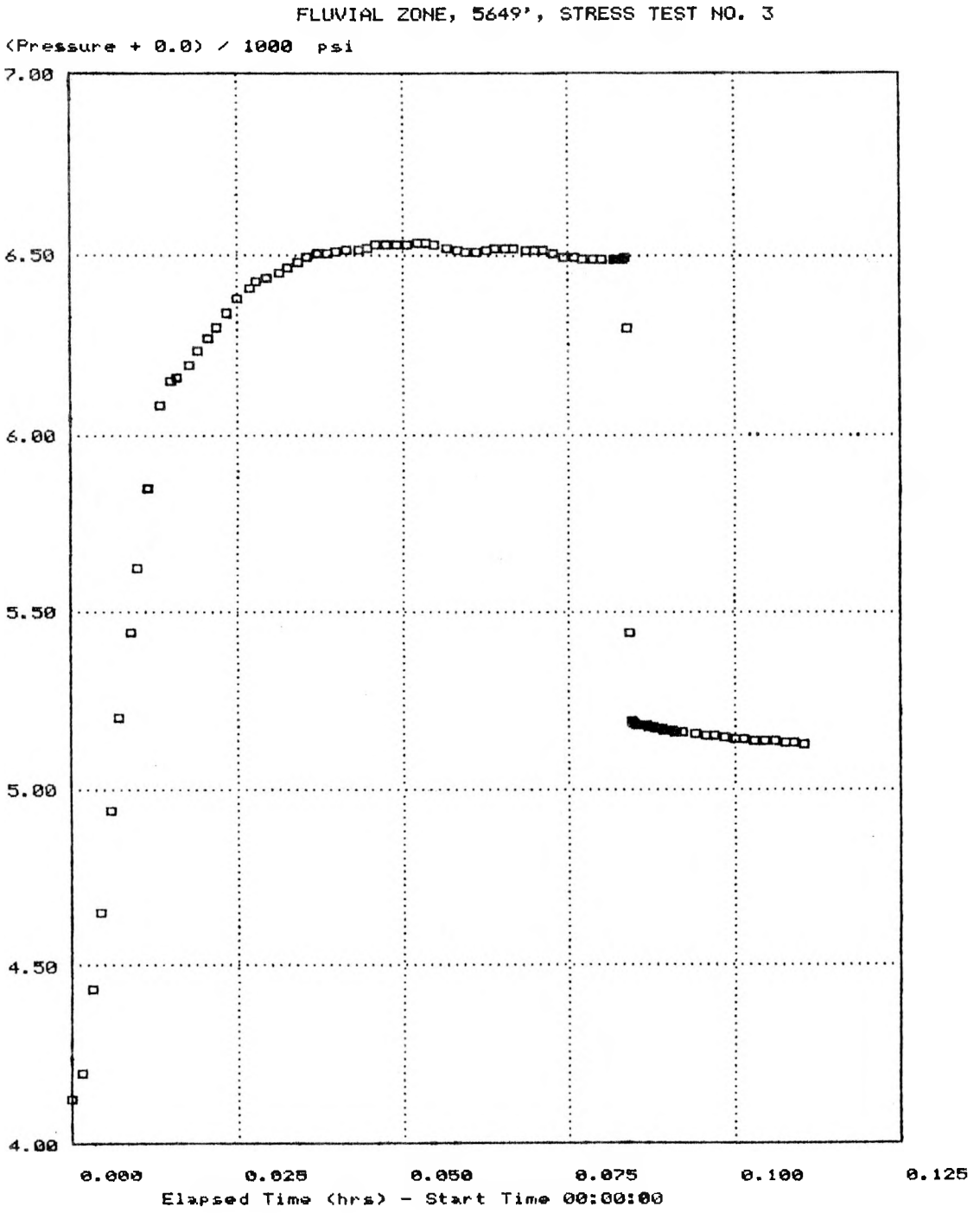


FIGURE A.141: Shale Stress Test (5649-5651'), Linear Plot of Test No. 3 Injection/Decline.

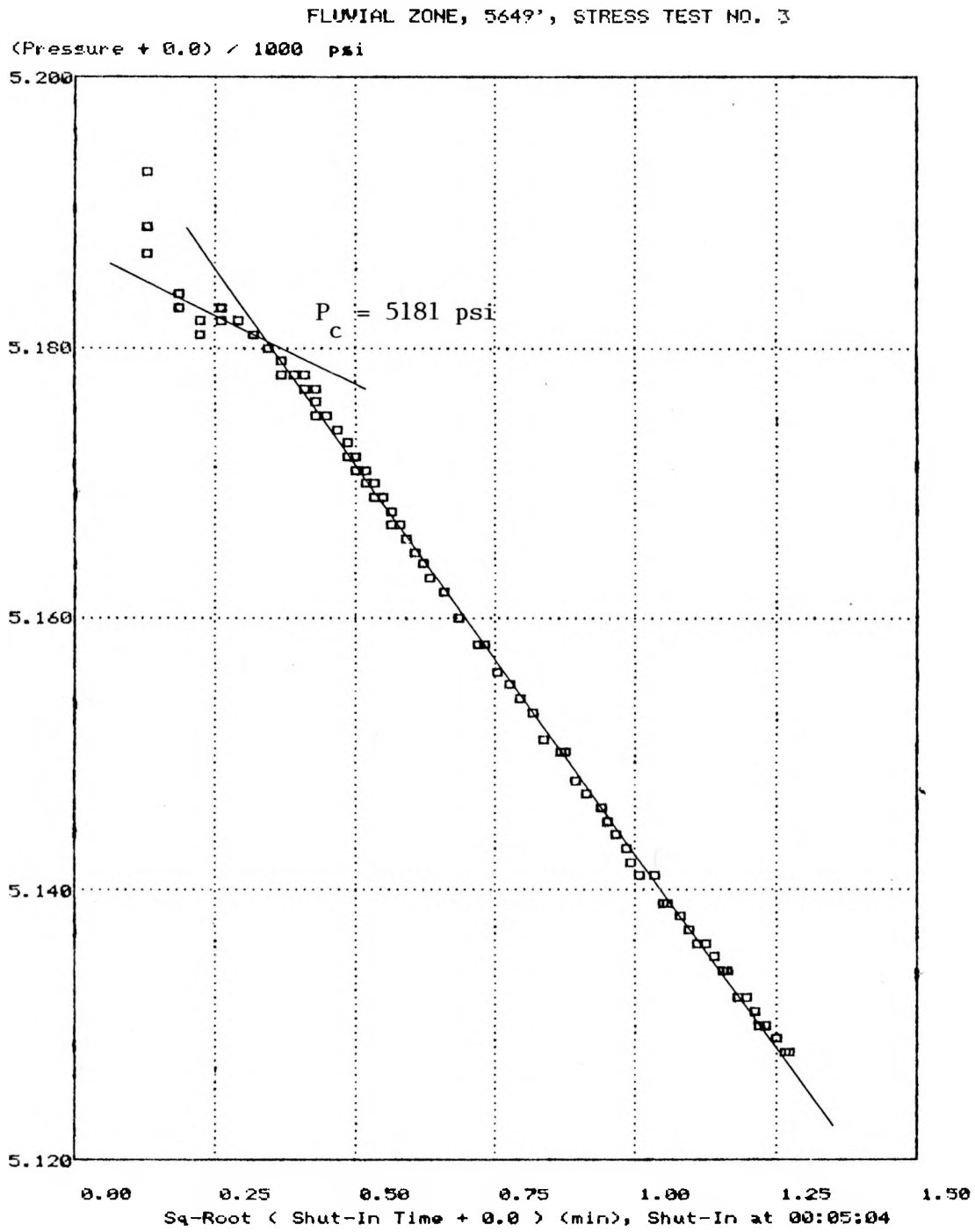


FIGURE A.142: Shale Stress Test (5649-5651'), Square-Root of Shut-In Time Plot of Test No. 3 Pressure Decline.

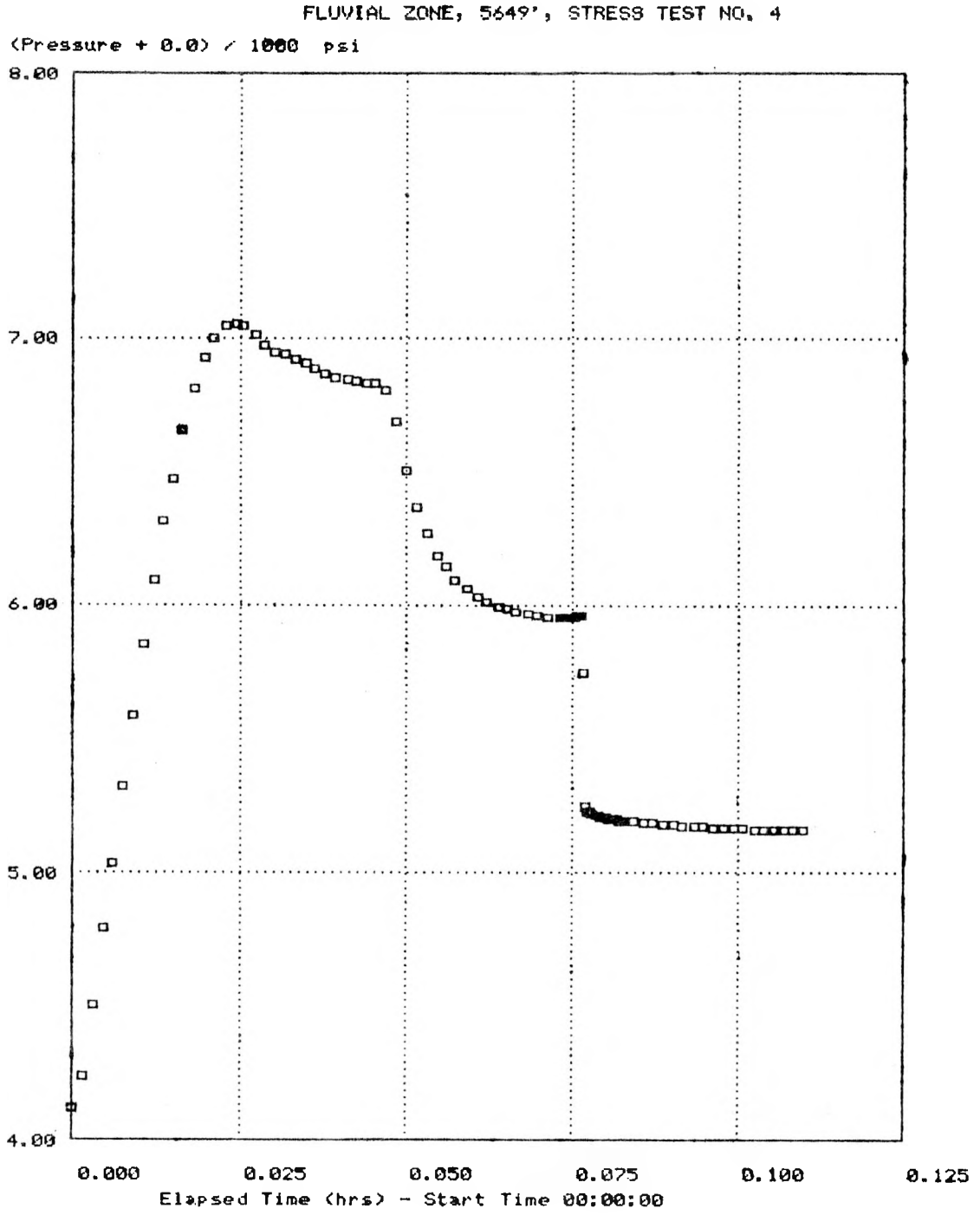


FIGURE A.143: Shale Stress Test (5649-5651'), Linear Plot of Test No. 4 Injection/Decline.

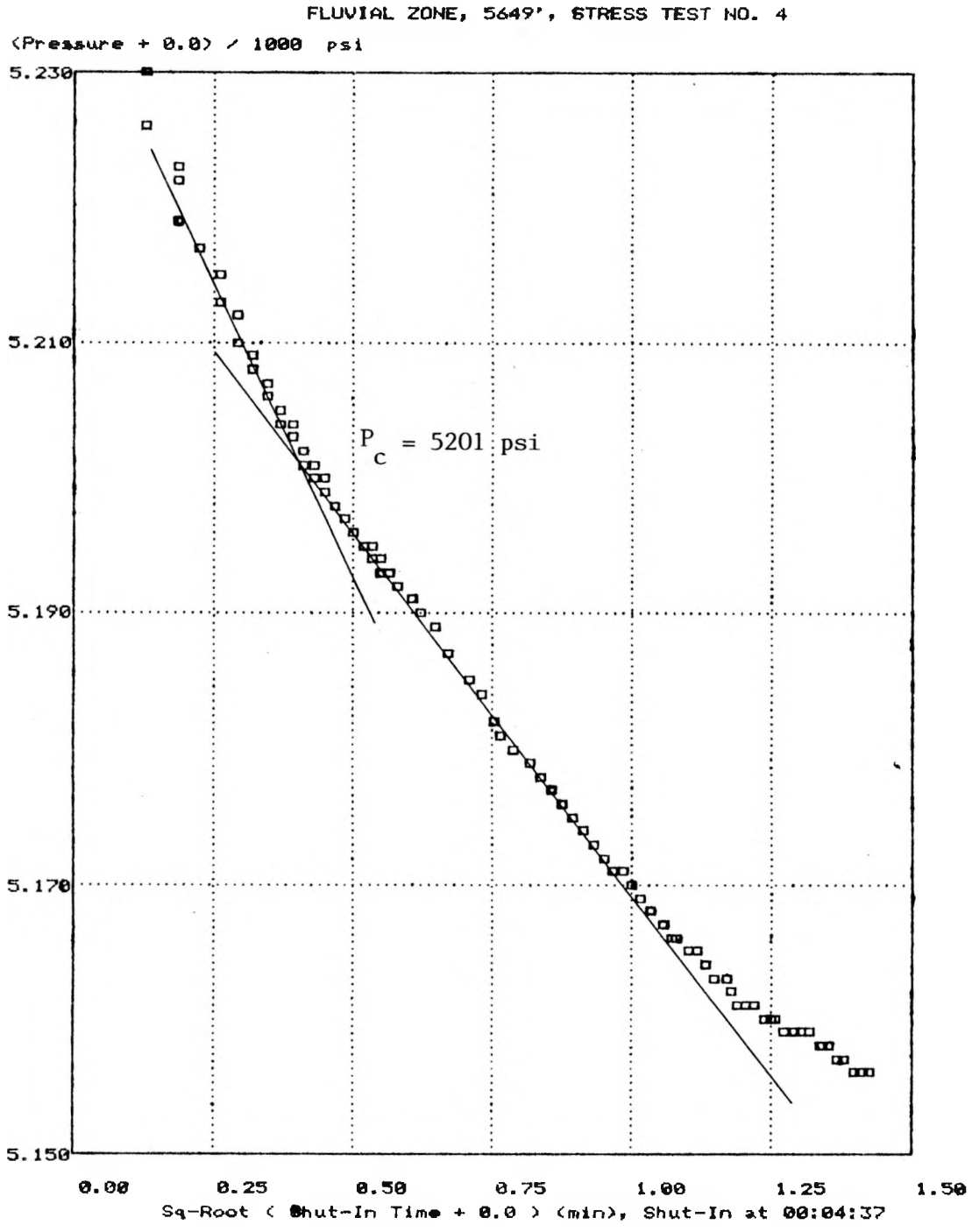


FIGURE A.144: Shale Stress Test (5649-5651'), Square-Root of Shut-In Time Plot of Test No. 4 Pressure Decline.

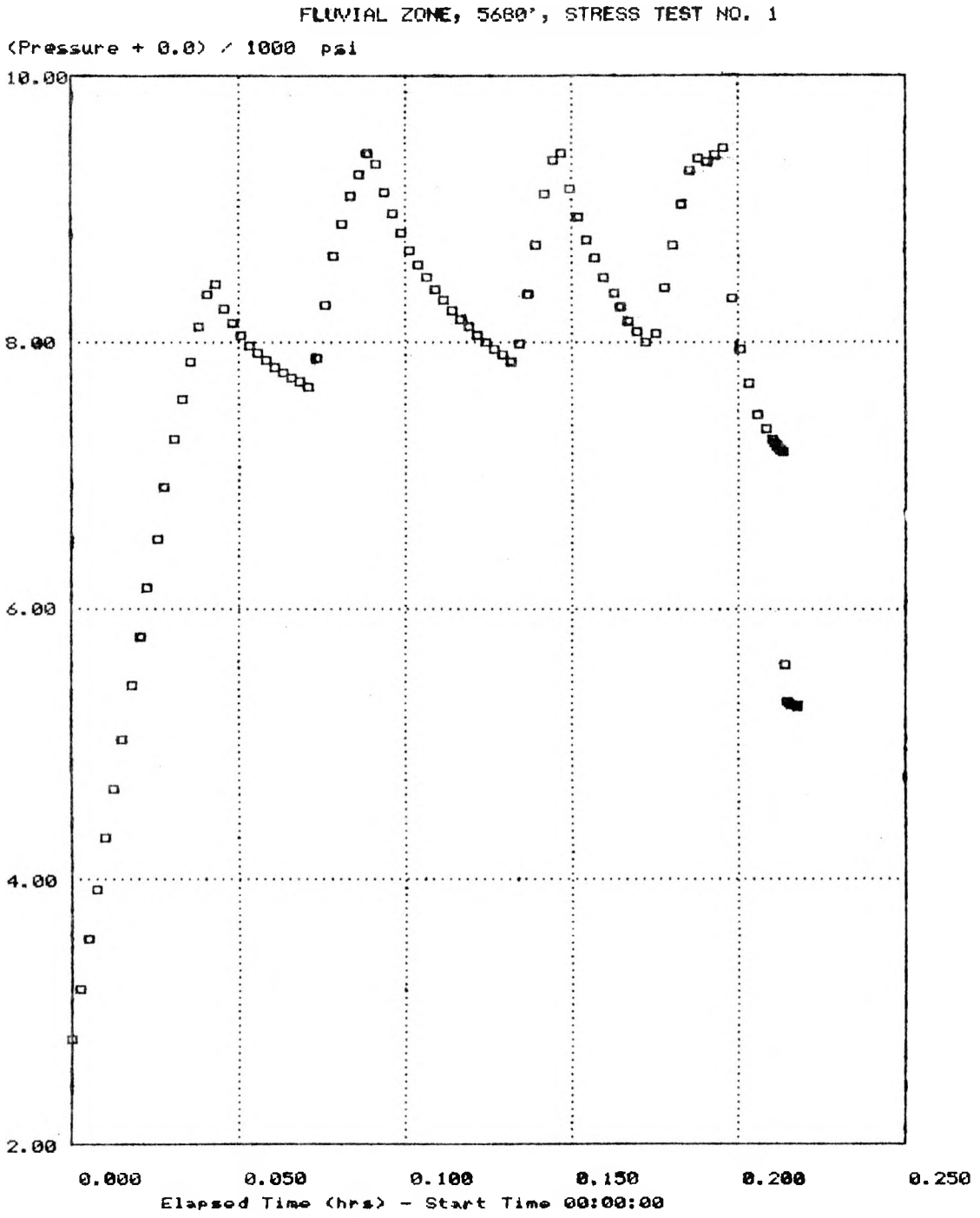


FIGURE A.145: Shale Stress Test (5680-5682'), Linear Plot of Test No. 1 Injection/Decline.

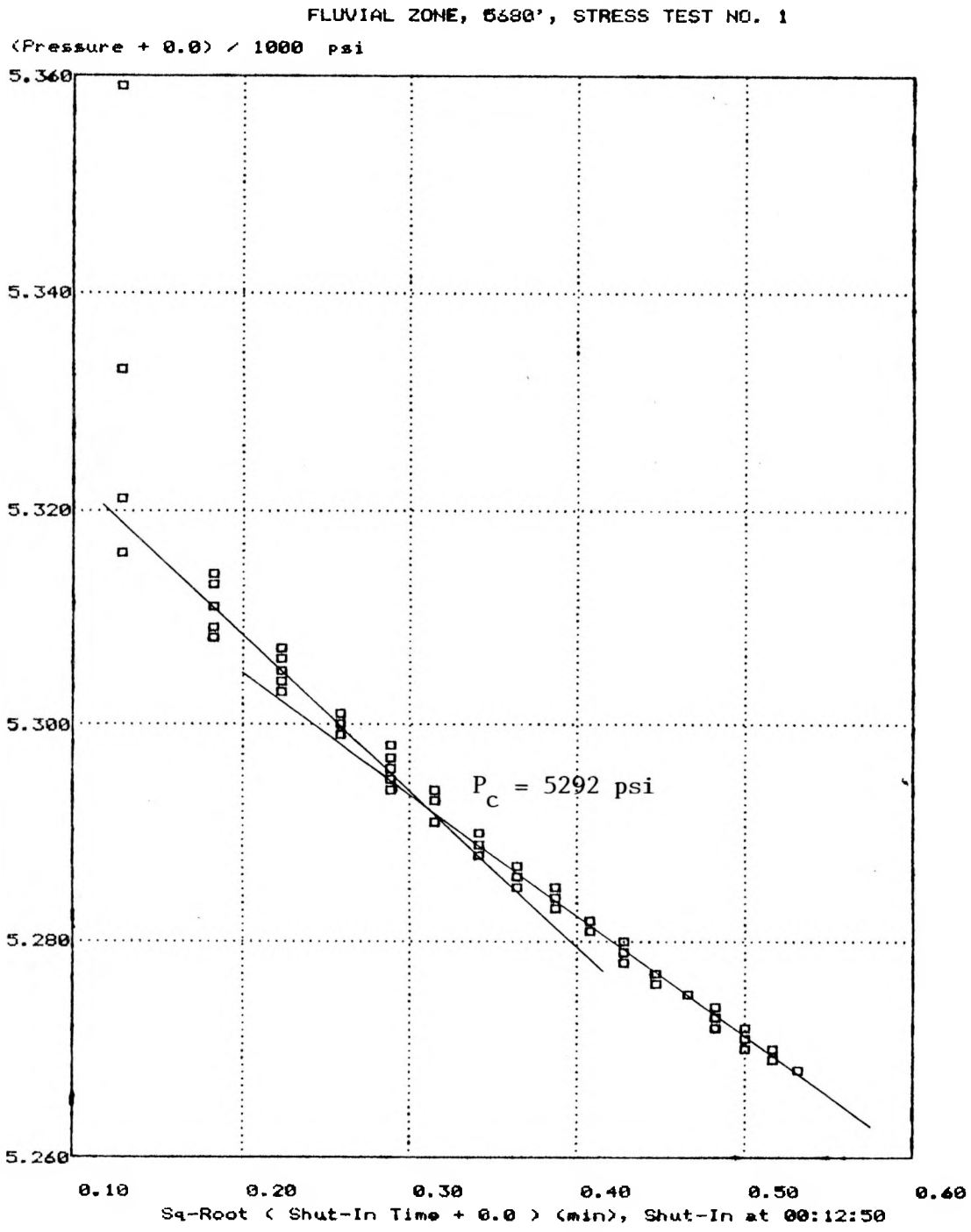


FIGURE A.146: Shale Stress Test (5680-5682'), Square-Root of Shut-In Time Plot of Test No. 1 Pressure Decline.

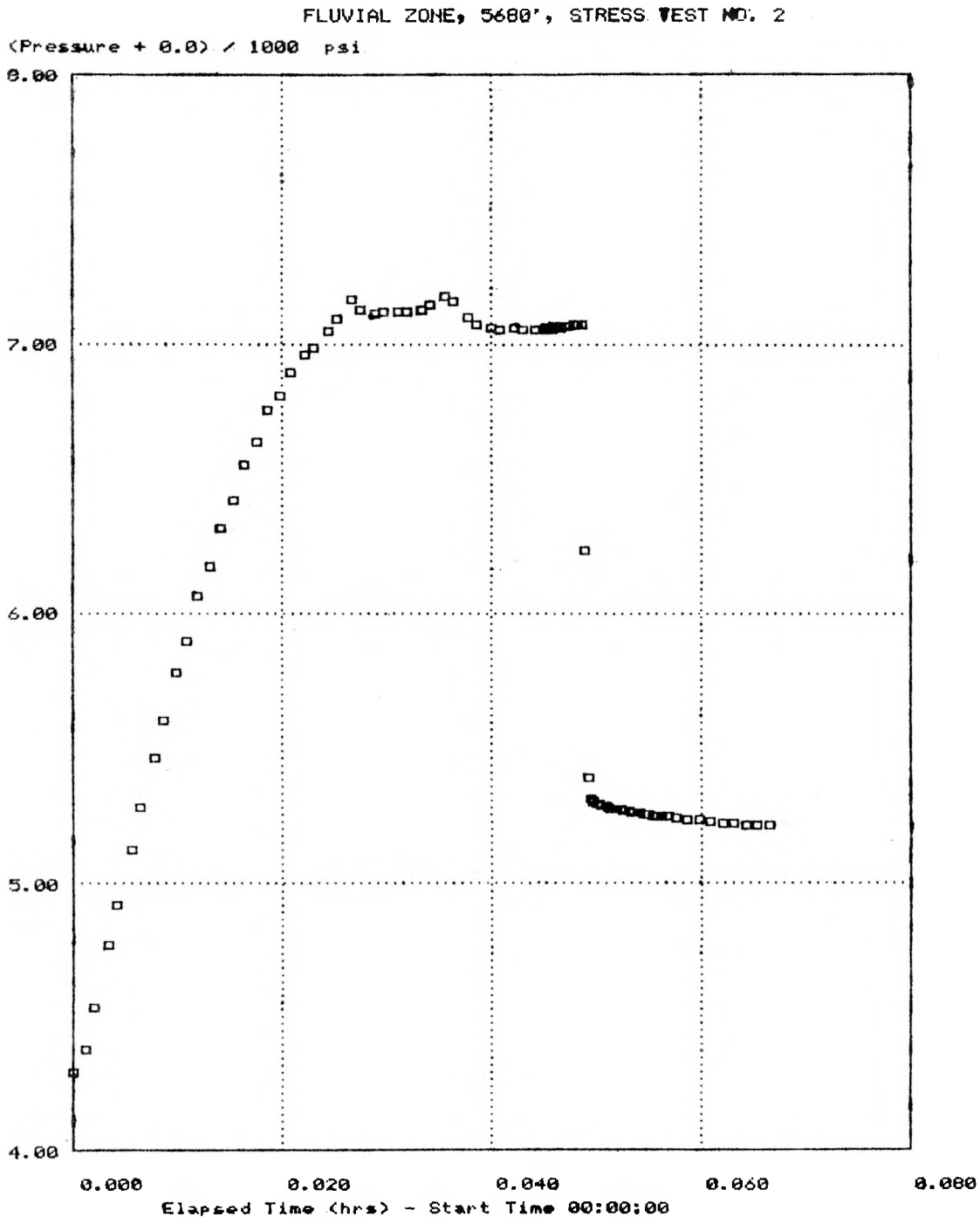


FIGURE A.147: Shale Stress Test (5680-5682'), Linear Plot of Test No. 2 Injection/Decline.

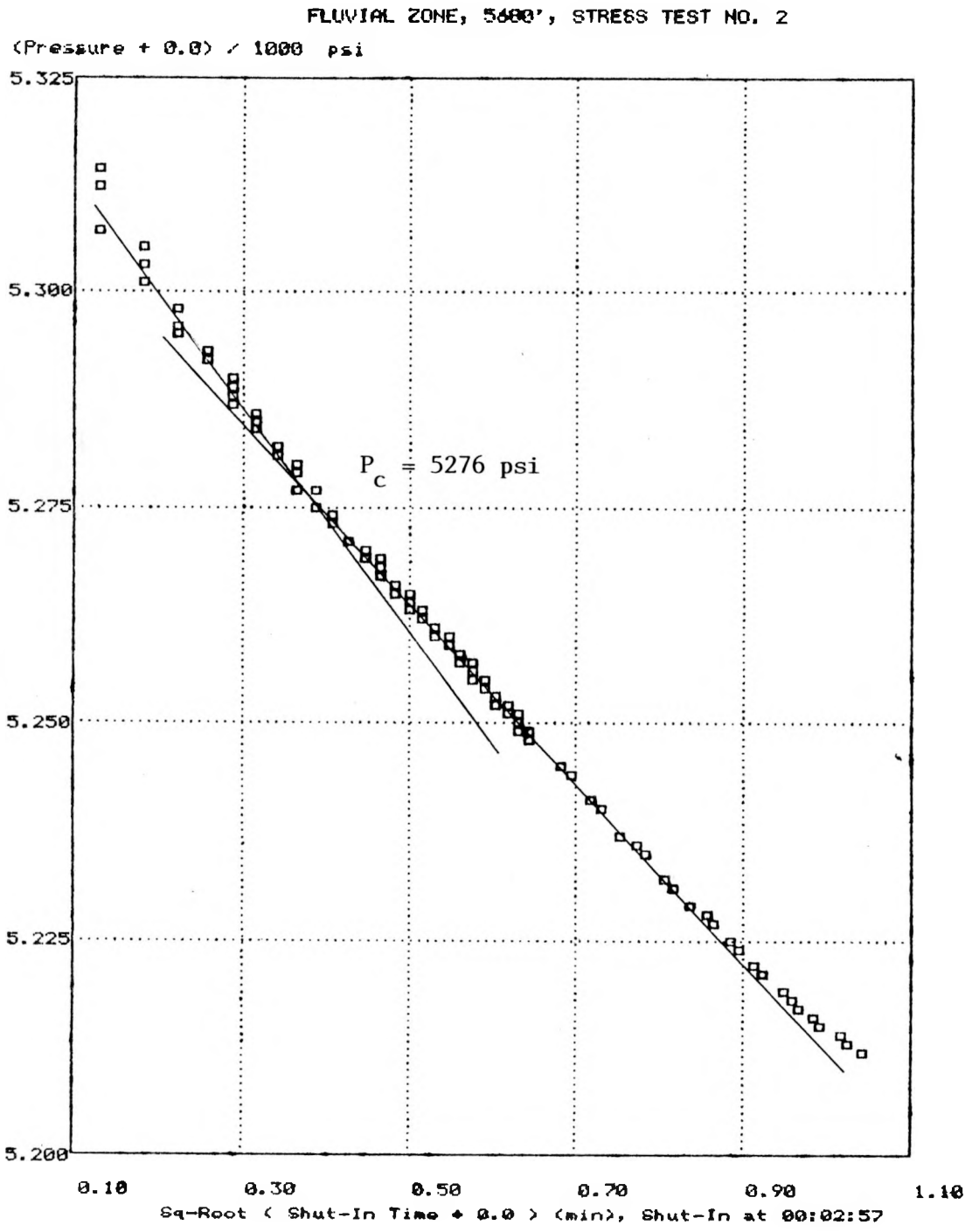


FIGURE A.148: Shale Stress Test (5680-5682'), Square-Root of Shut-In Time Plot of Test No. 2 Pressure Decline.

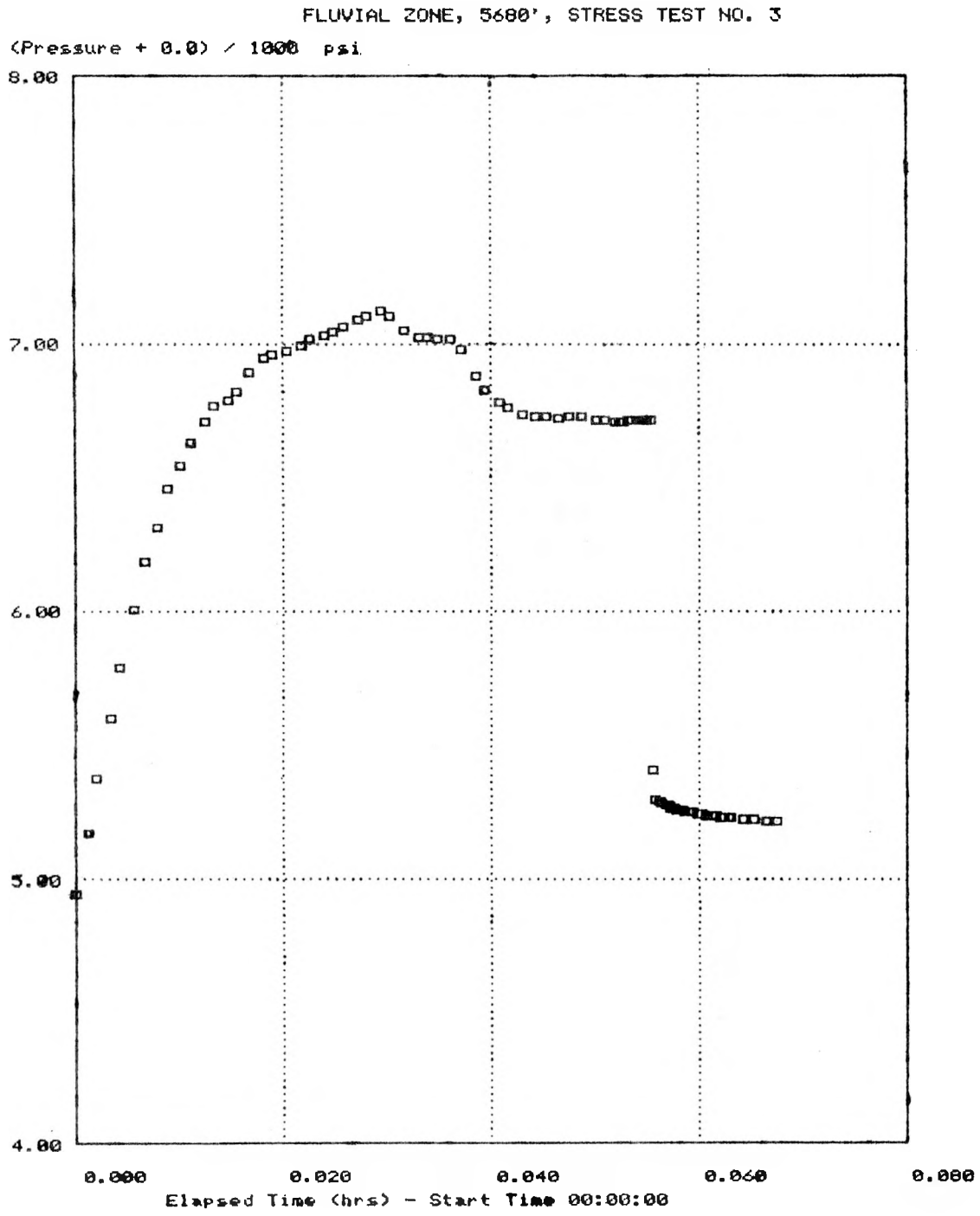


FIGURE A.149: Shale Stress Test (5680-5682'), Linear Plot of Test No. 3 Injection/Decline.

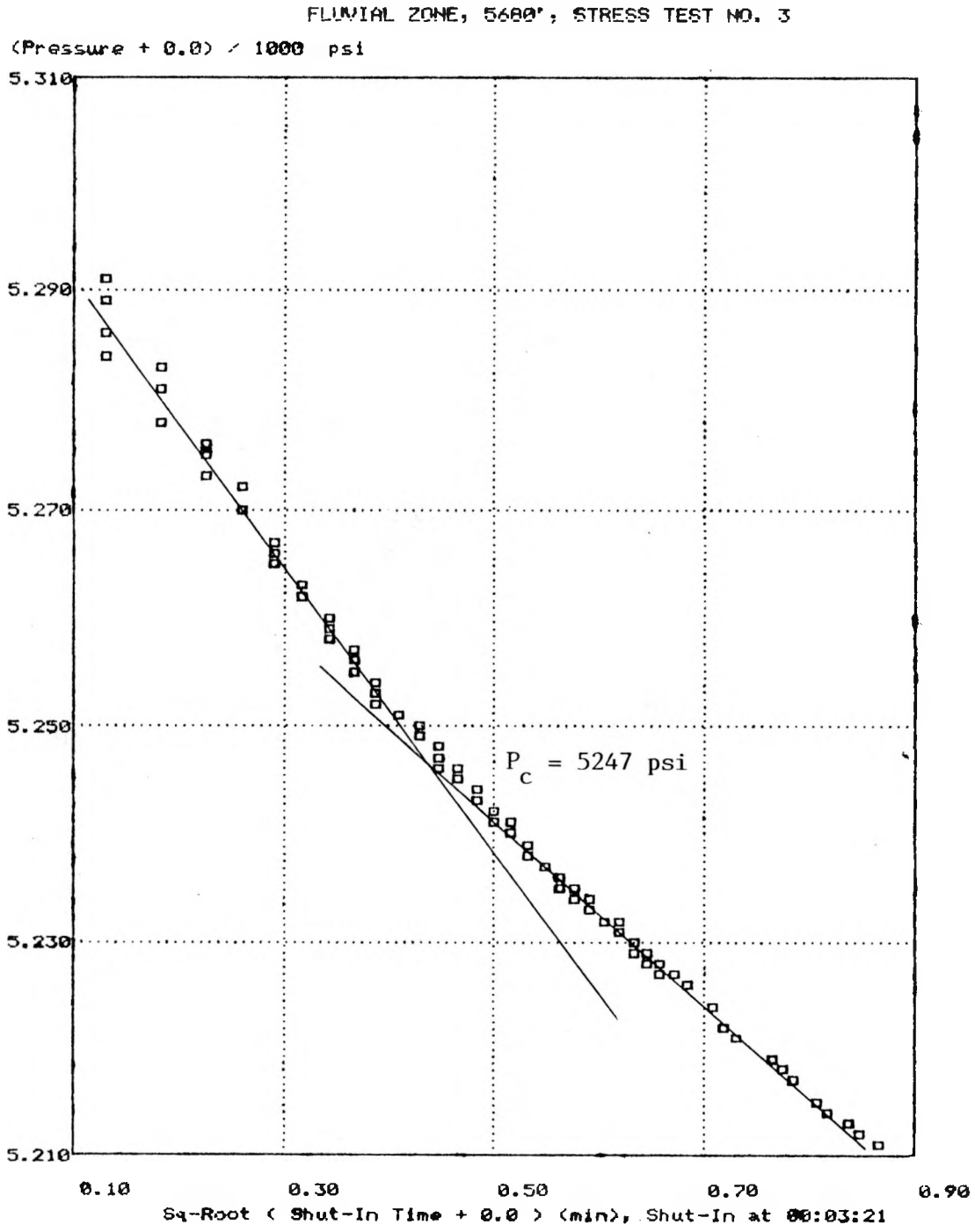


FIGURE A.150: Shale Stress Test (5680-5682'), Square-Root of Shut-In Time Plot of Test No. 3 Pressure Decline.

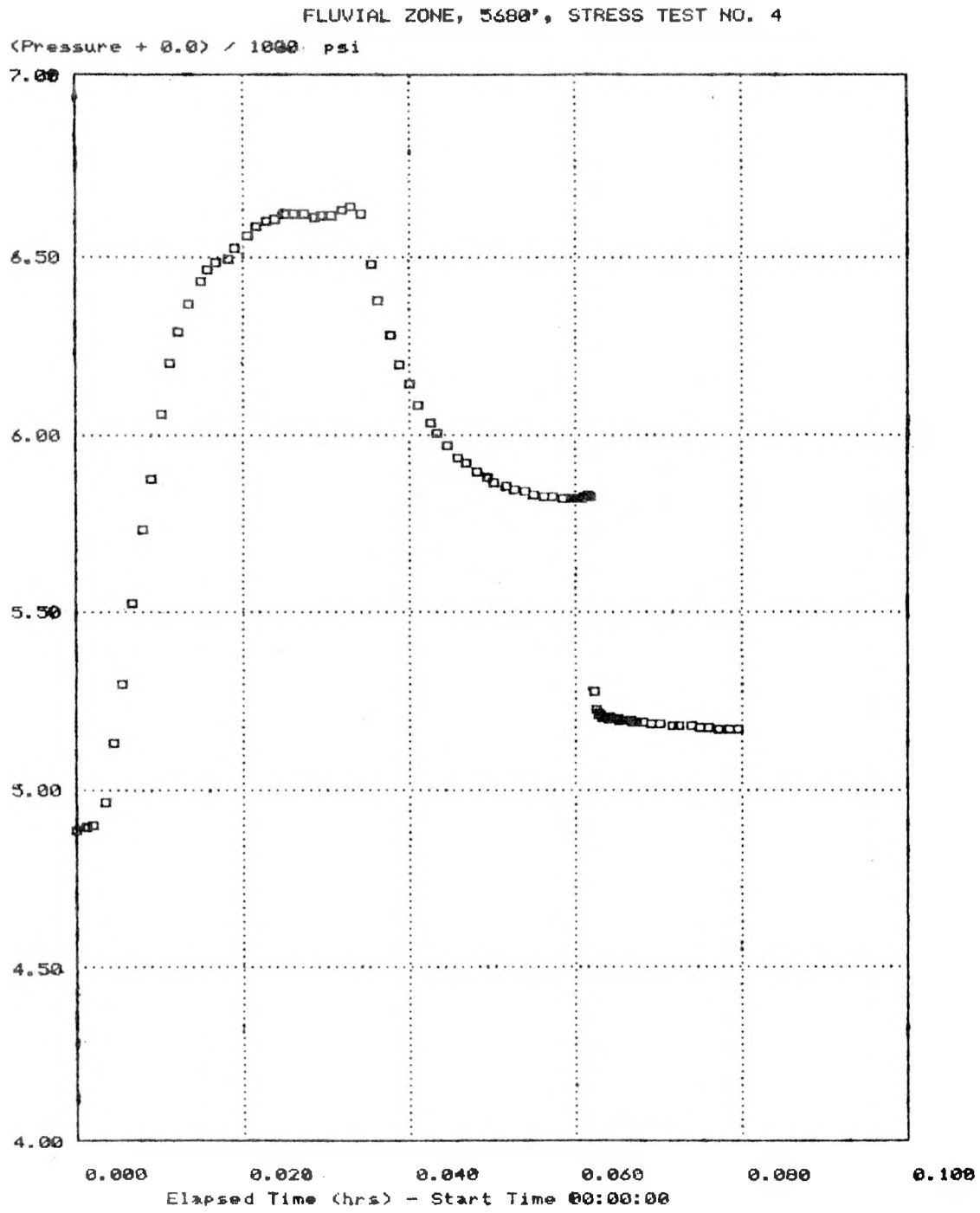


FIGURE A.151: Shale Stress Test (5680-5682'), Linear Plot of Test No. 4 Injection/Decline.

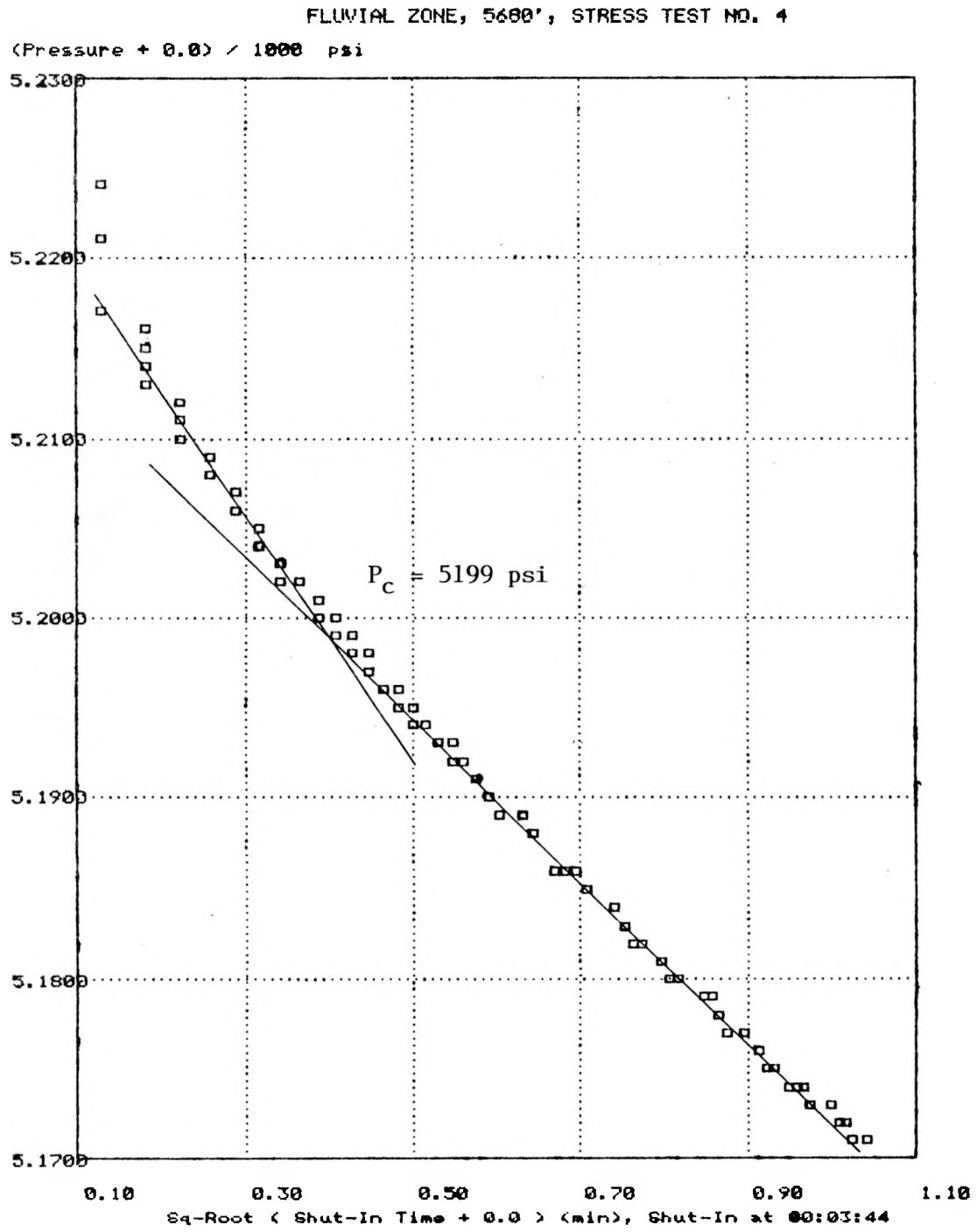


FIGURE A.152: Shale Stress Test (5680-5682'), Square-Root of Shut-In Time Plot of test No. 4 Pressure Decline.

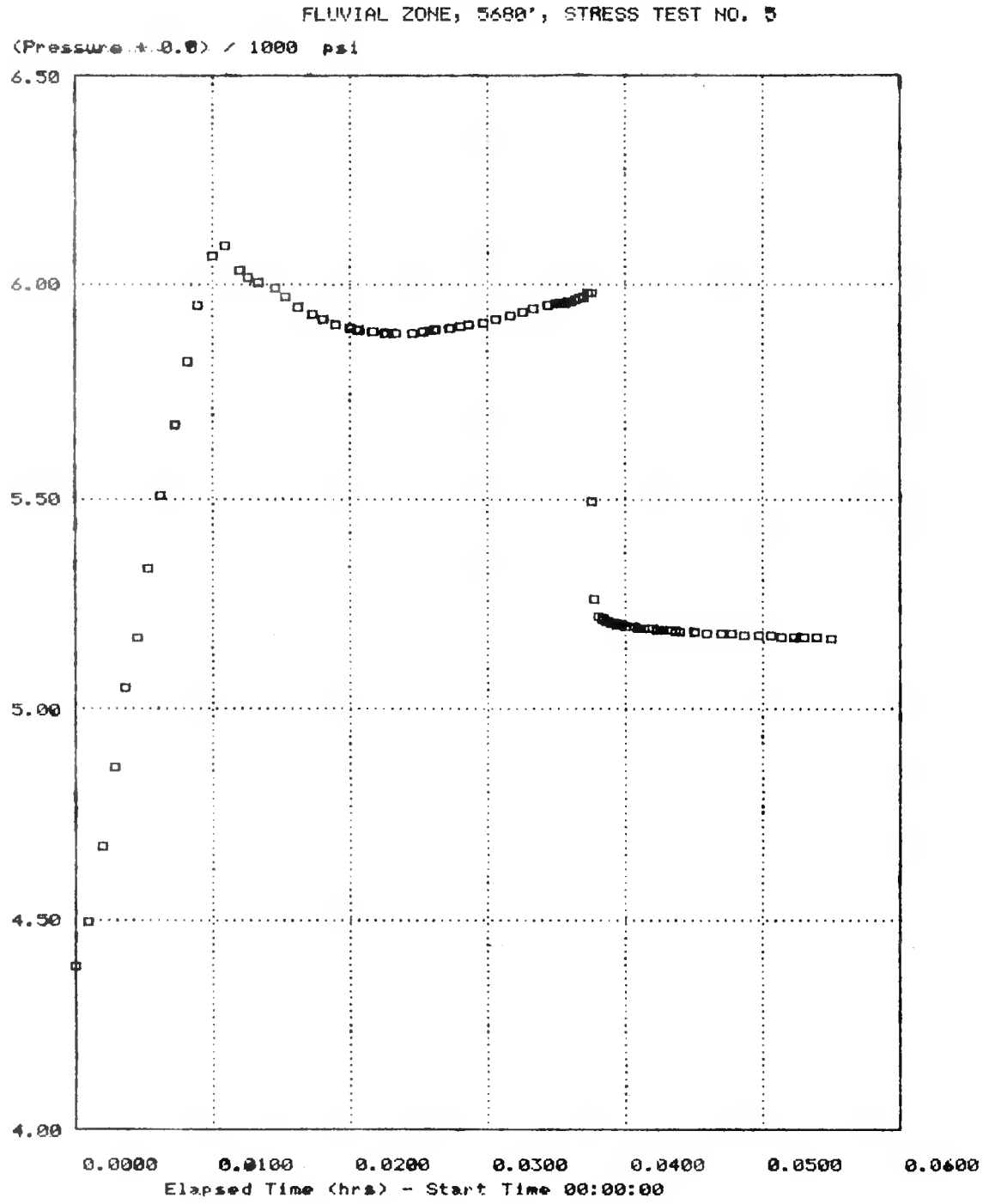


FIGURE A.153: Shale Stress Test (5680-5682'), Linear Plot of Test No. 5 Injection/Decline.

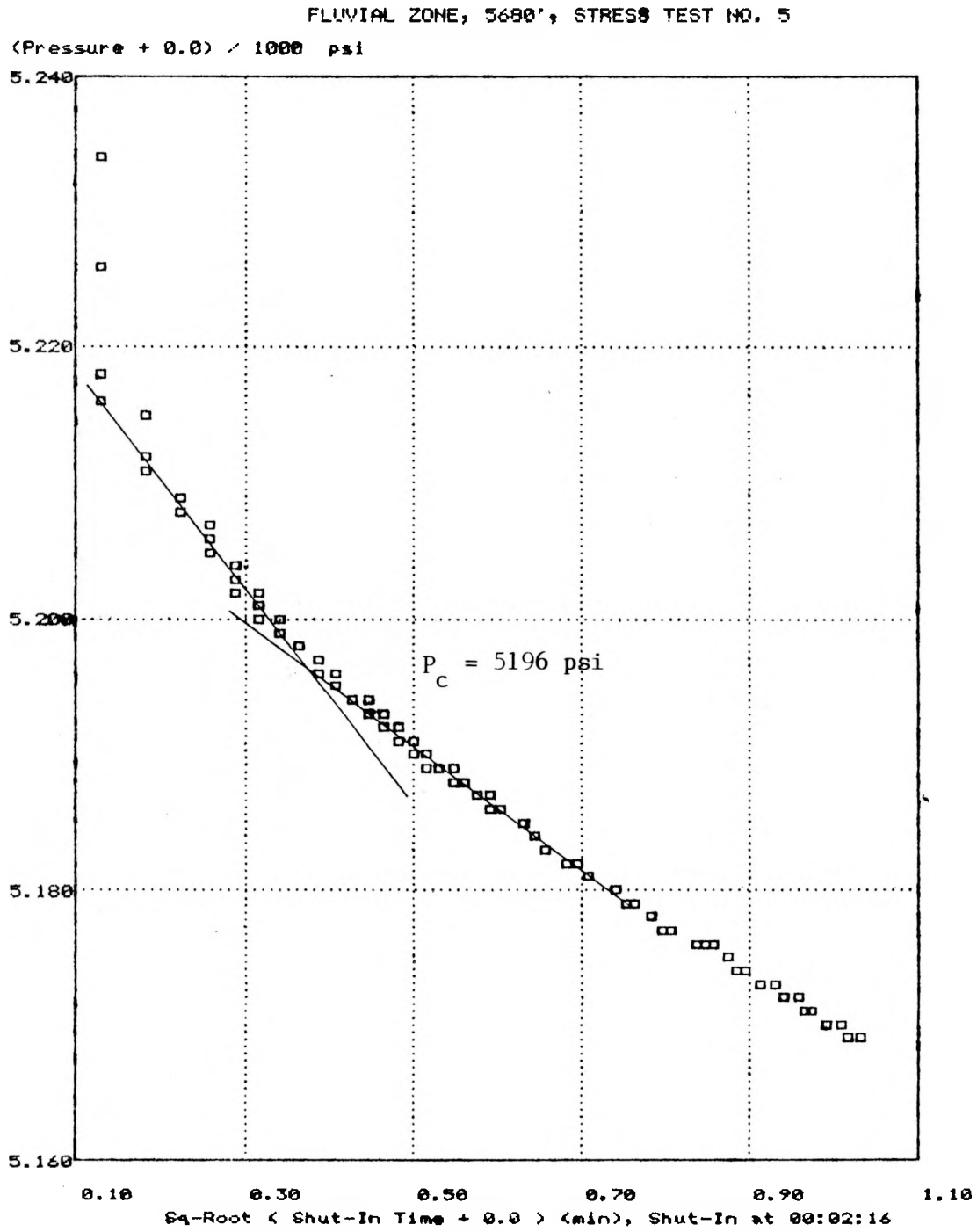


FIGURE A.154: Shale Stress Test (5680-5682'), Square-Root of Shut-In Time Plot of Test No. 5 Pressure Decline.

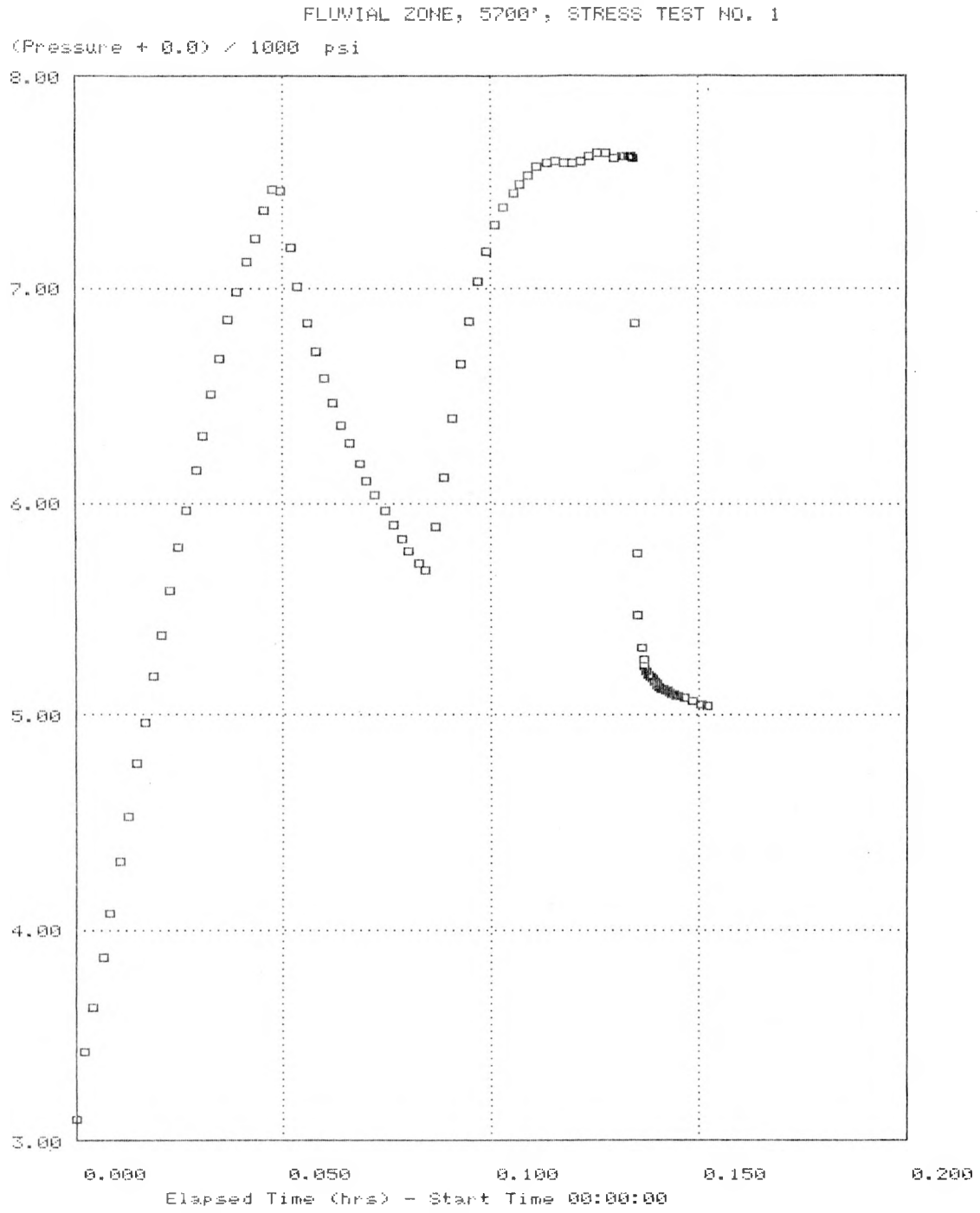


FIGURE A.155: Shale Stress Test (5700-5702'), Linear Plot of Test No. 1 Injection/Decline.

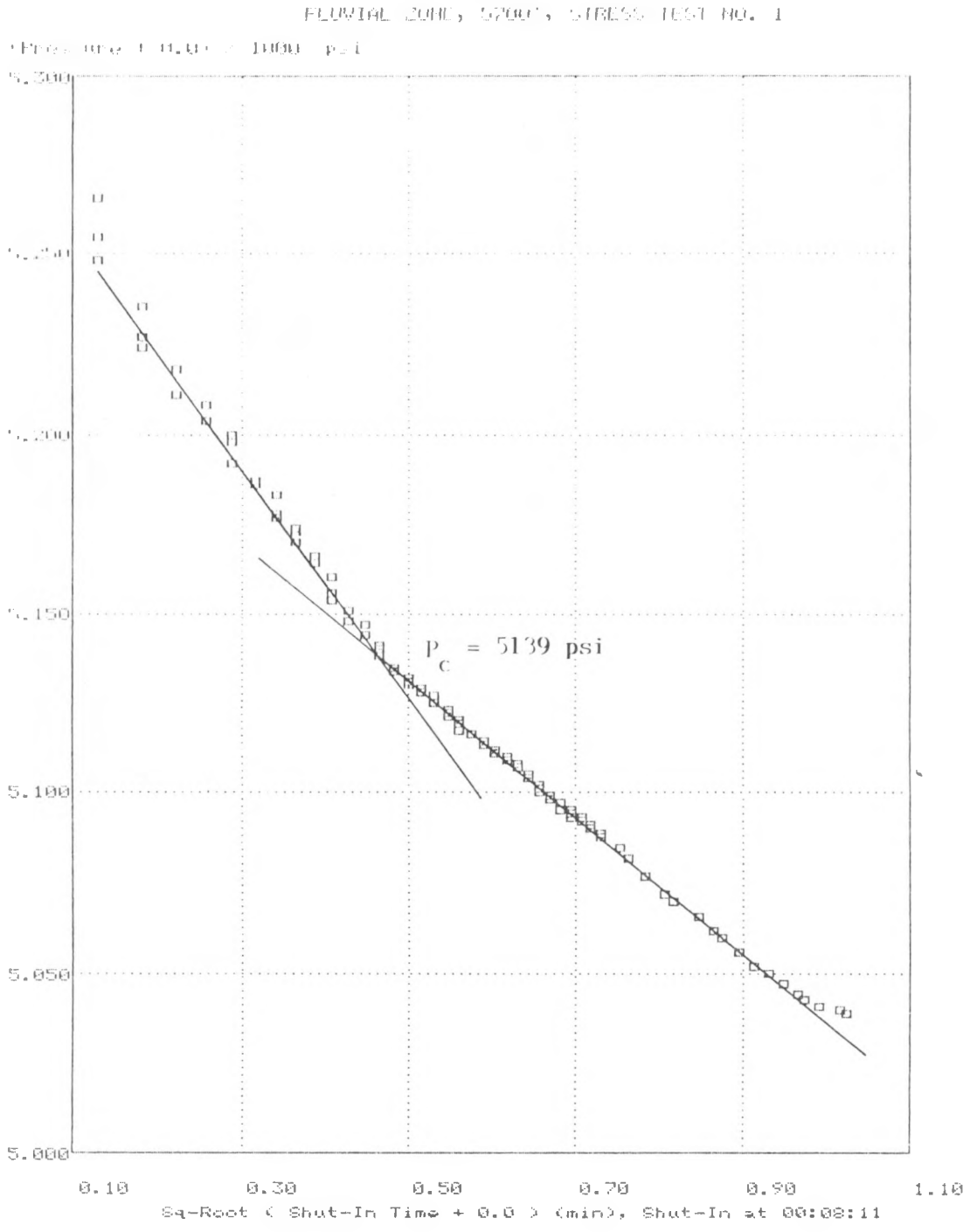


FIGURE A.156: Shale Stress Test (5700-5702'), Square-Root of Shut-In Time Plot of Test No.1 Pressure Decline.

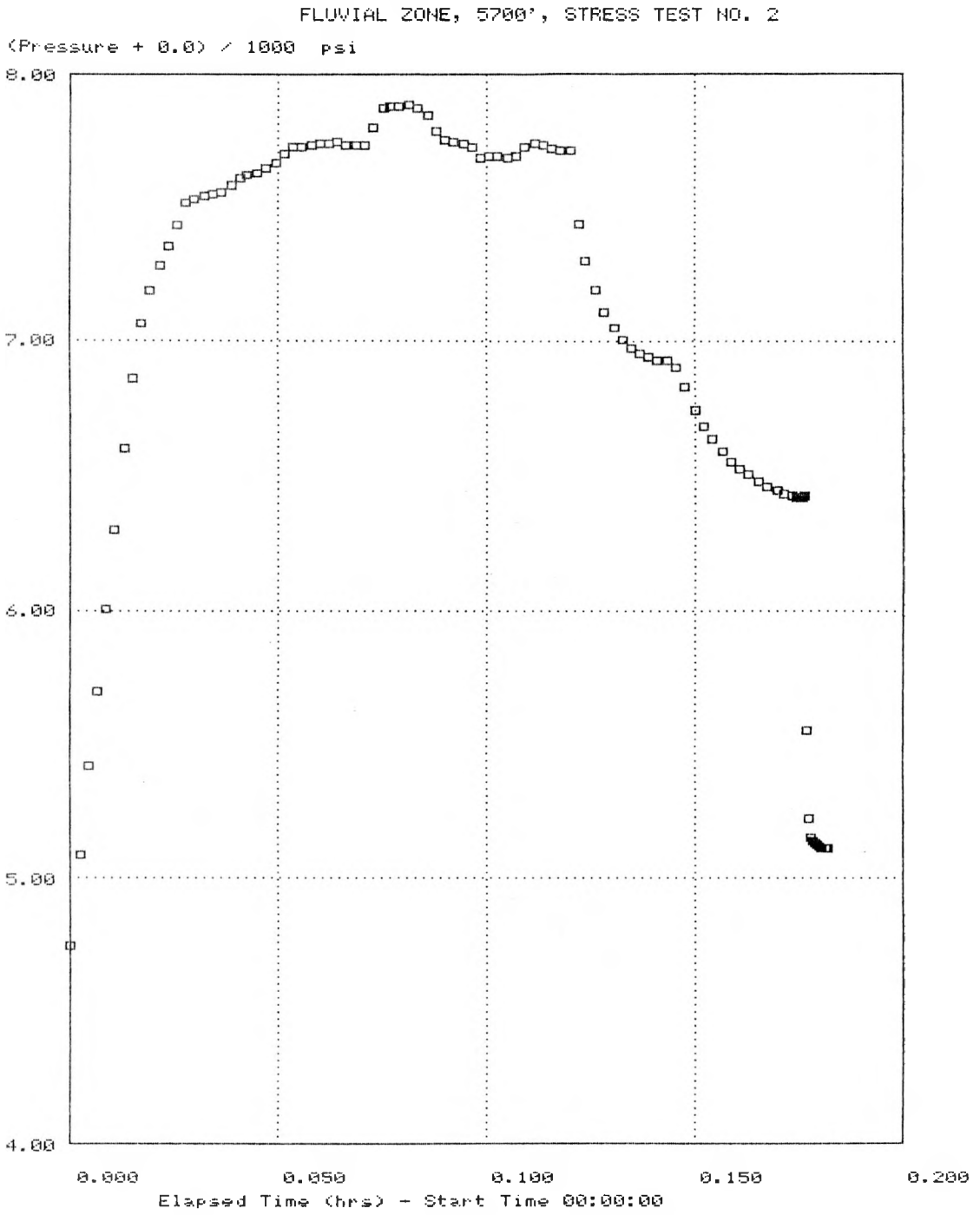


FIGURE A 157: Shale Stress Test (5700-5702'), Linear Plot of Test No. 2 Injection/Decline.

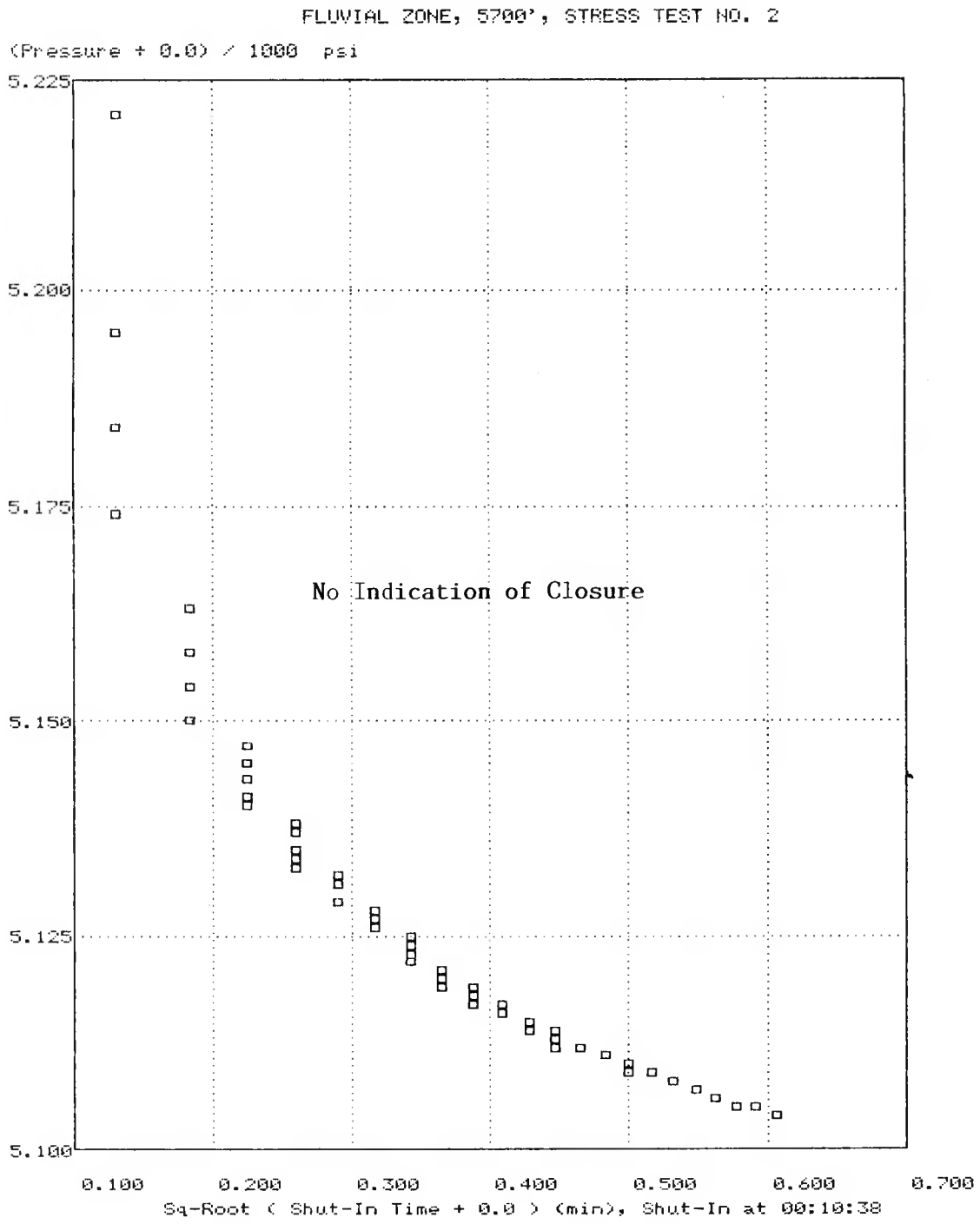


FIGURE A.158: Shale Stress Test (5700-5702'), Square-Root of Shut-In Time Plot of Test No. 2 Pressure Decline.

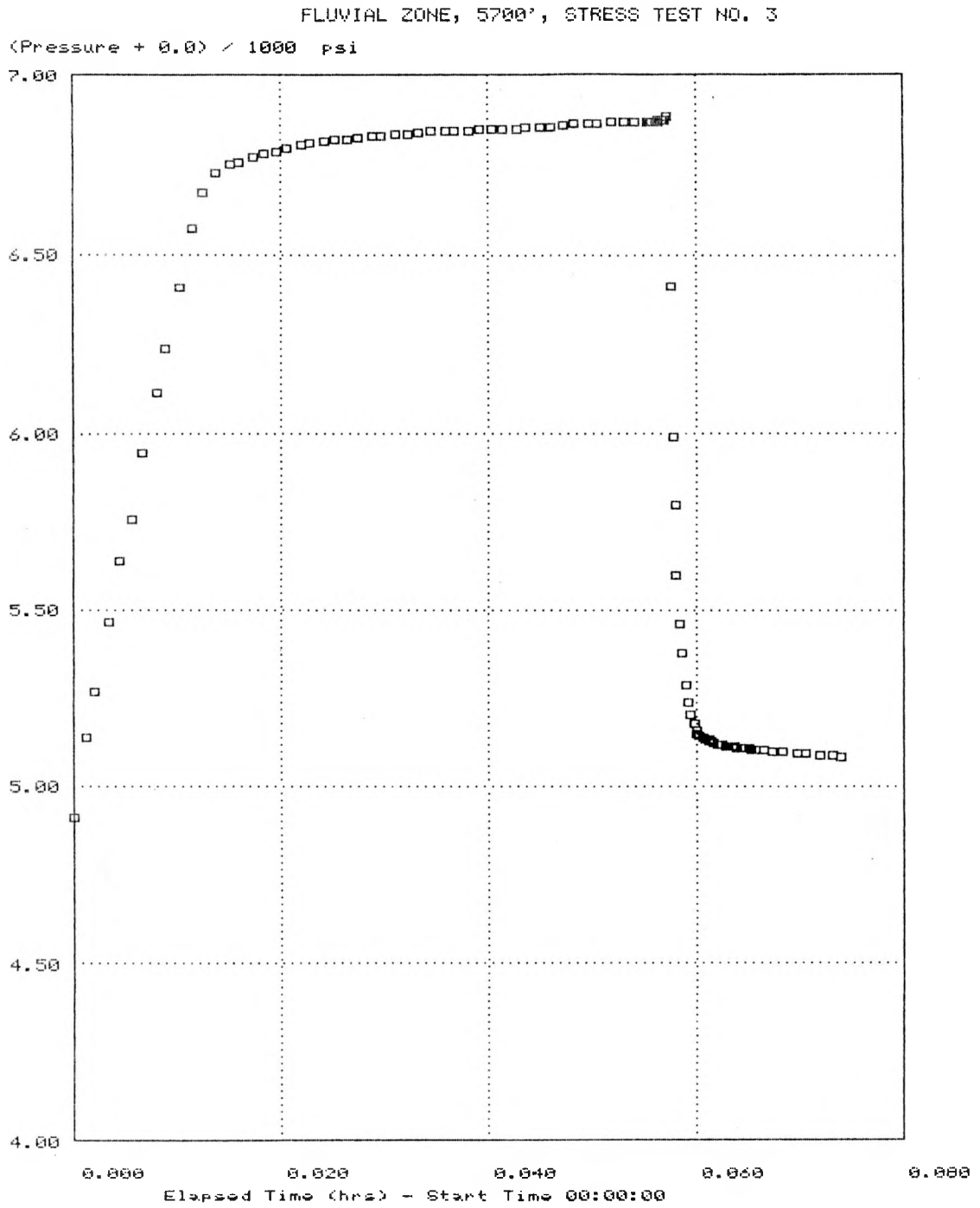


FIGURE A.159: Shale Stress Test (5700-5702') Linear Plot of Test No. 3 Injection/Decline.

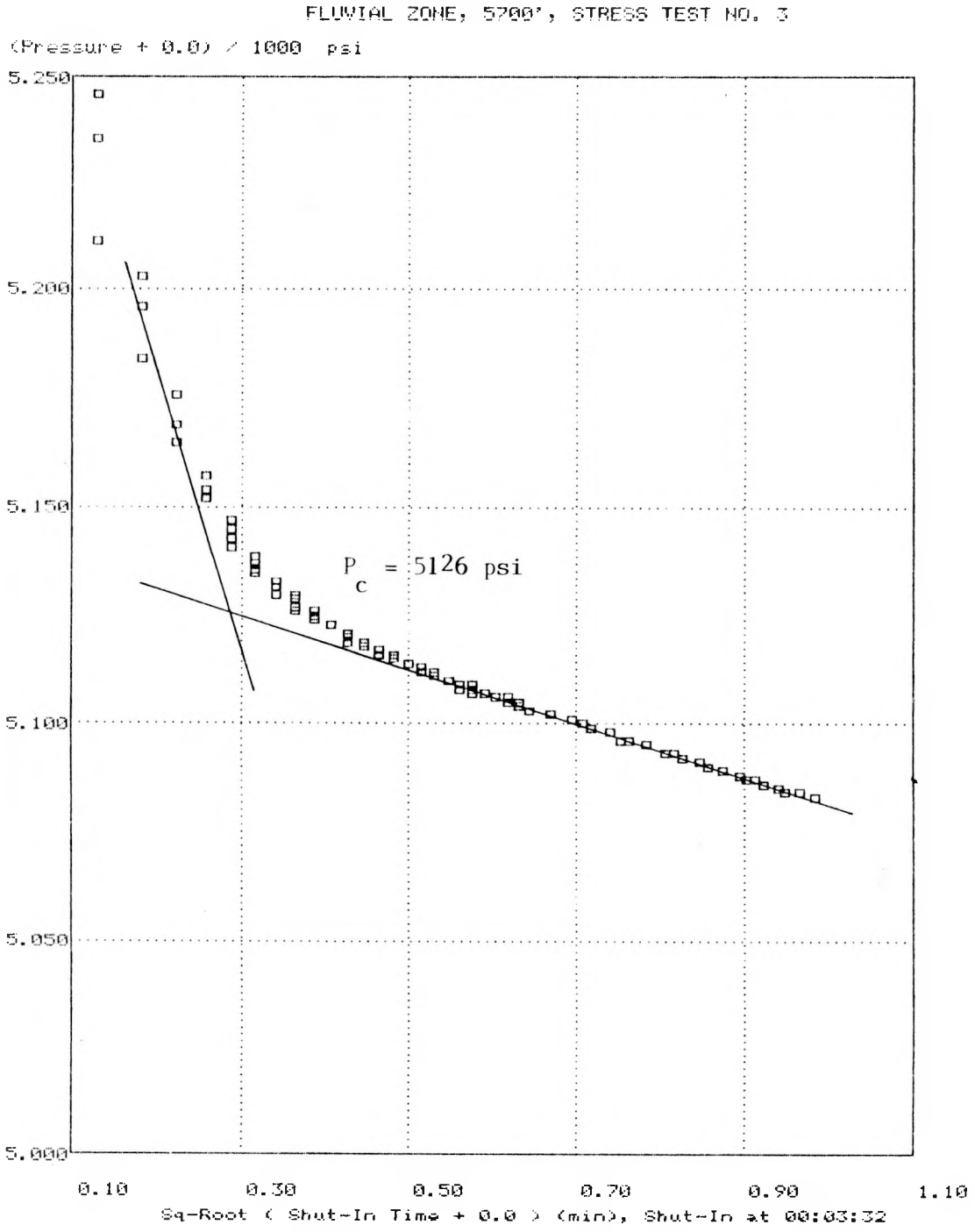


FIGURE A 160: Shale Stress Test (5700-5702' , Square-Root of Shut-In Time Plot of Test No.3 Pressure Decline.

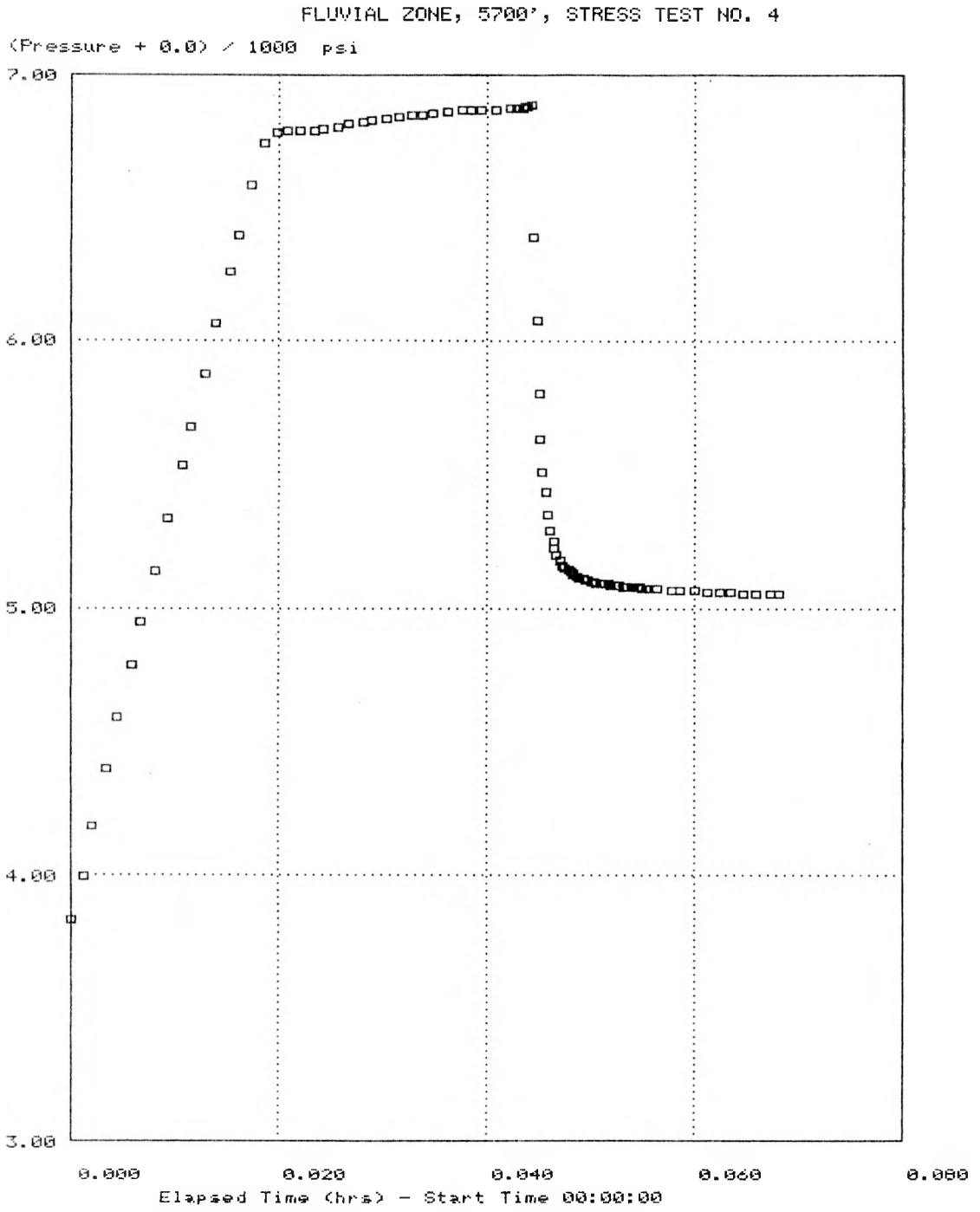


FIGURE A.161: Shale Stress Test (5700-5702'), Linear Plot of Test No. 4 Injection/Decline.

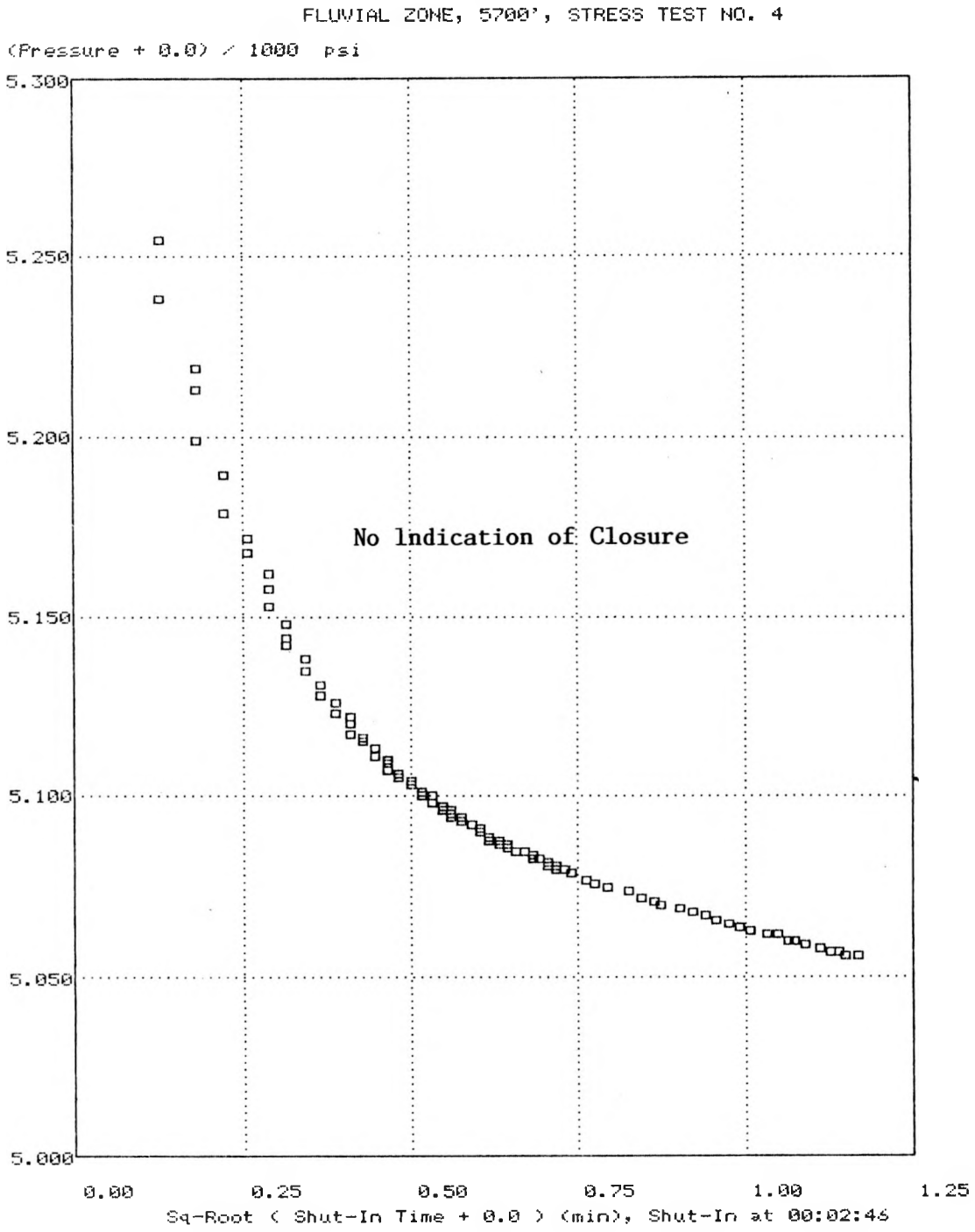


FIGURE A.162: Shale Stress Test (5700-5702'), Square-Root of Shut-In Time Plot of Test No. 4 Pressure Decline.

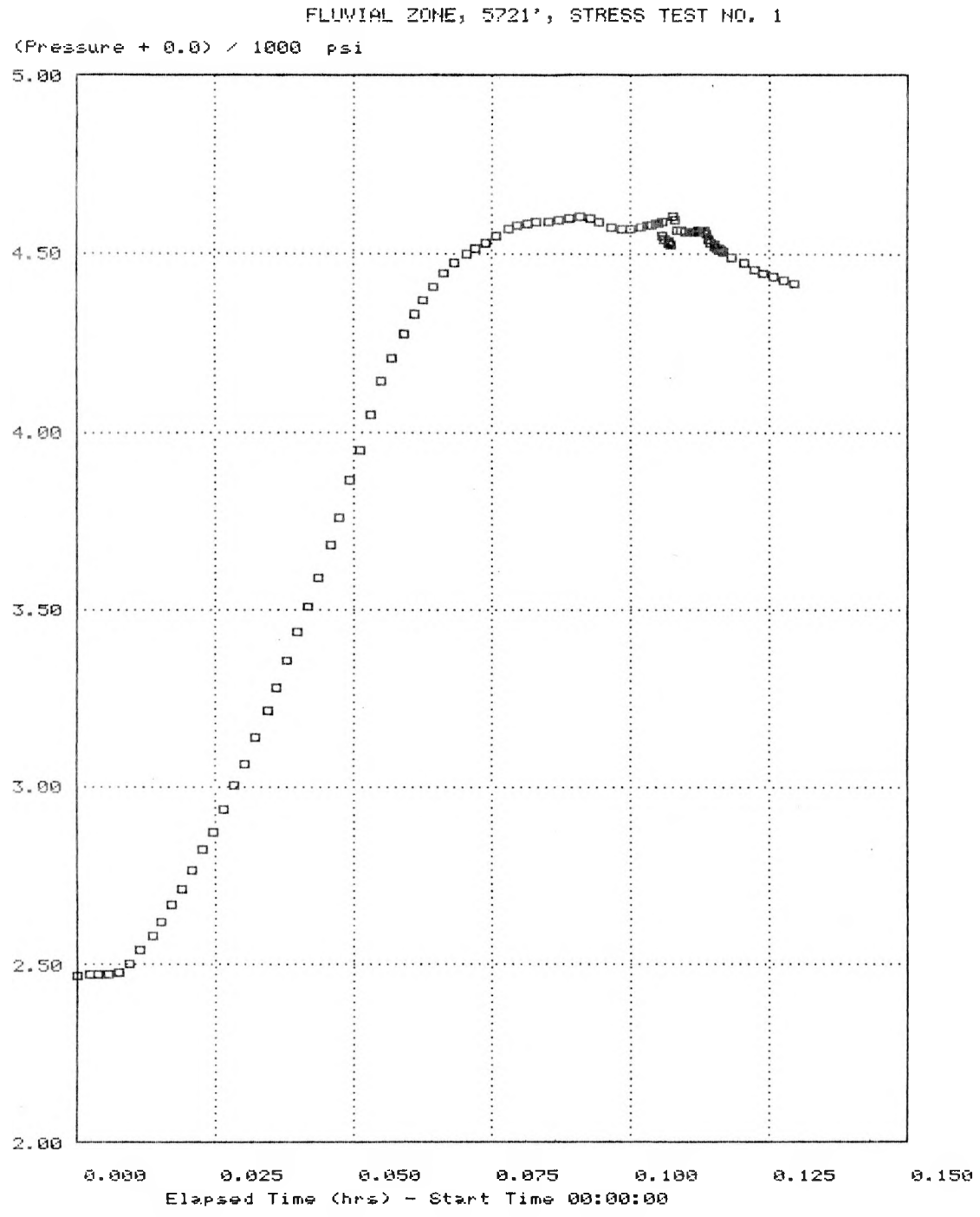


FIGURE A.163: Sandstone Stress Tests (5721-5723'), Linear Plot of Test No. 1 Injection/Decline.

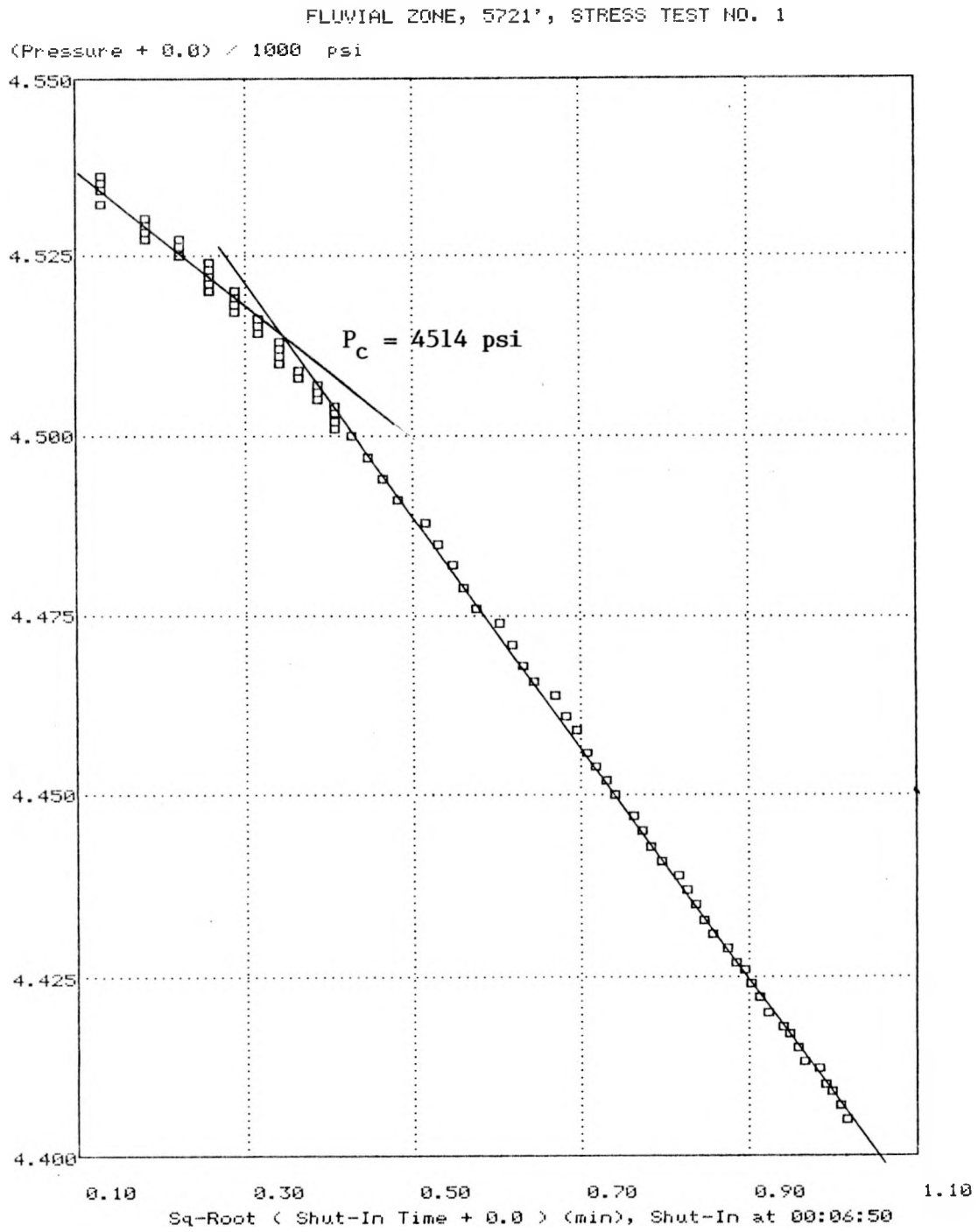


FIGURE A.164: Sandstone Stress Test (5721-5723'), Sqaure-Root of Shut-In Time Plot of Test No. 1 Pressure Decline.

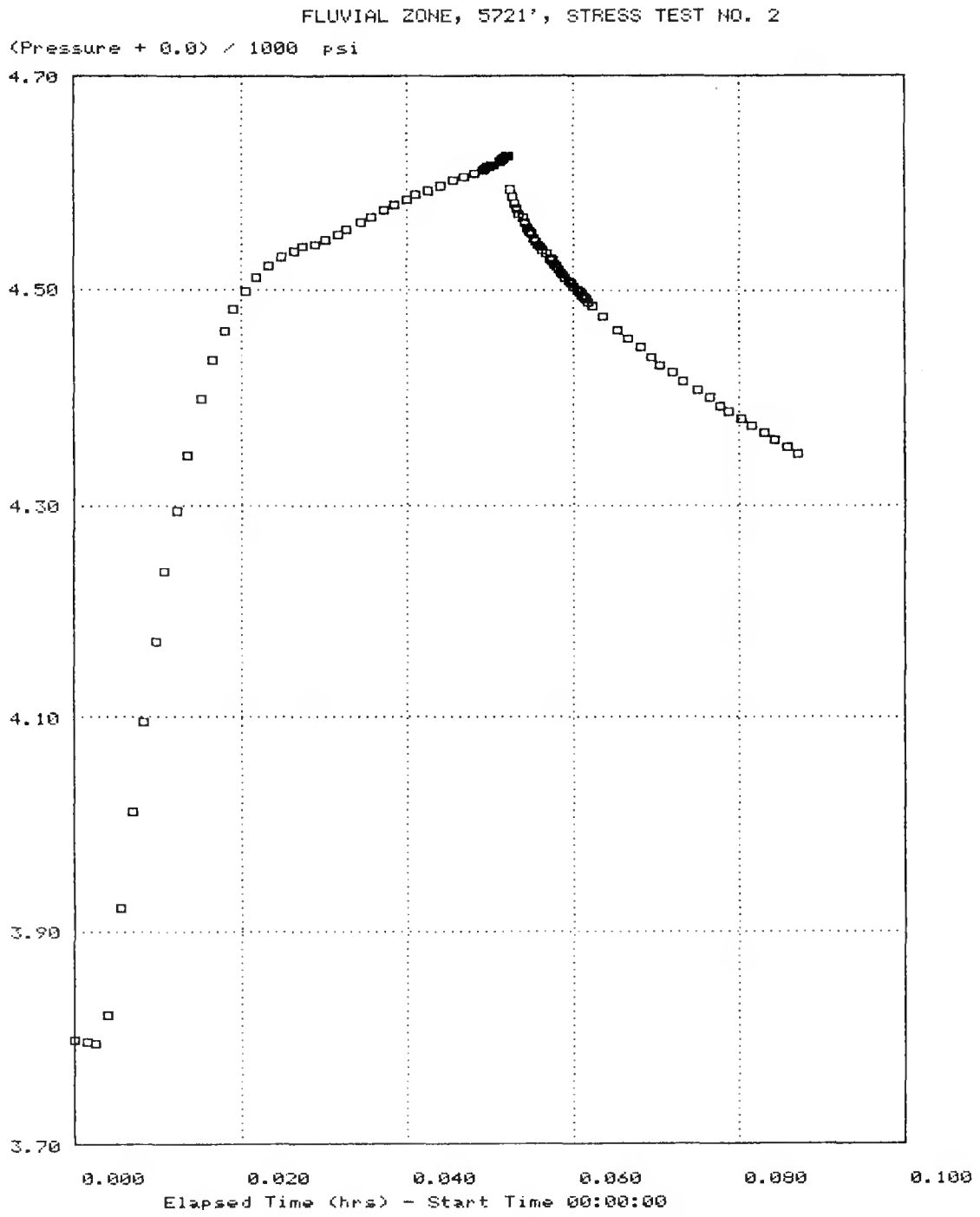


FIGURE A.165: Sandstone Stress Test (5721–5723'), Linear Plot of Test No. 2 Injection/Decline.

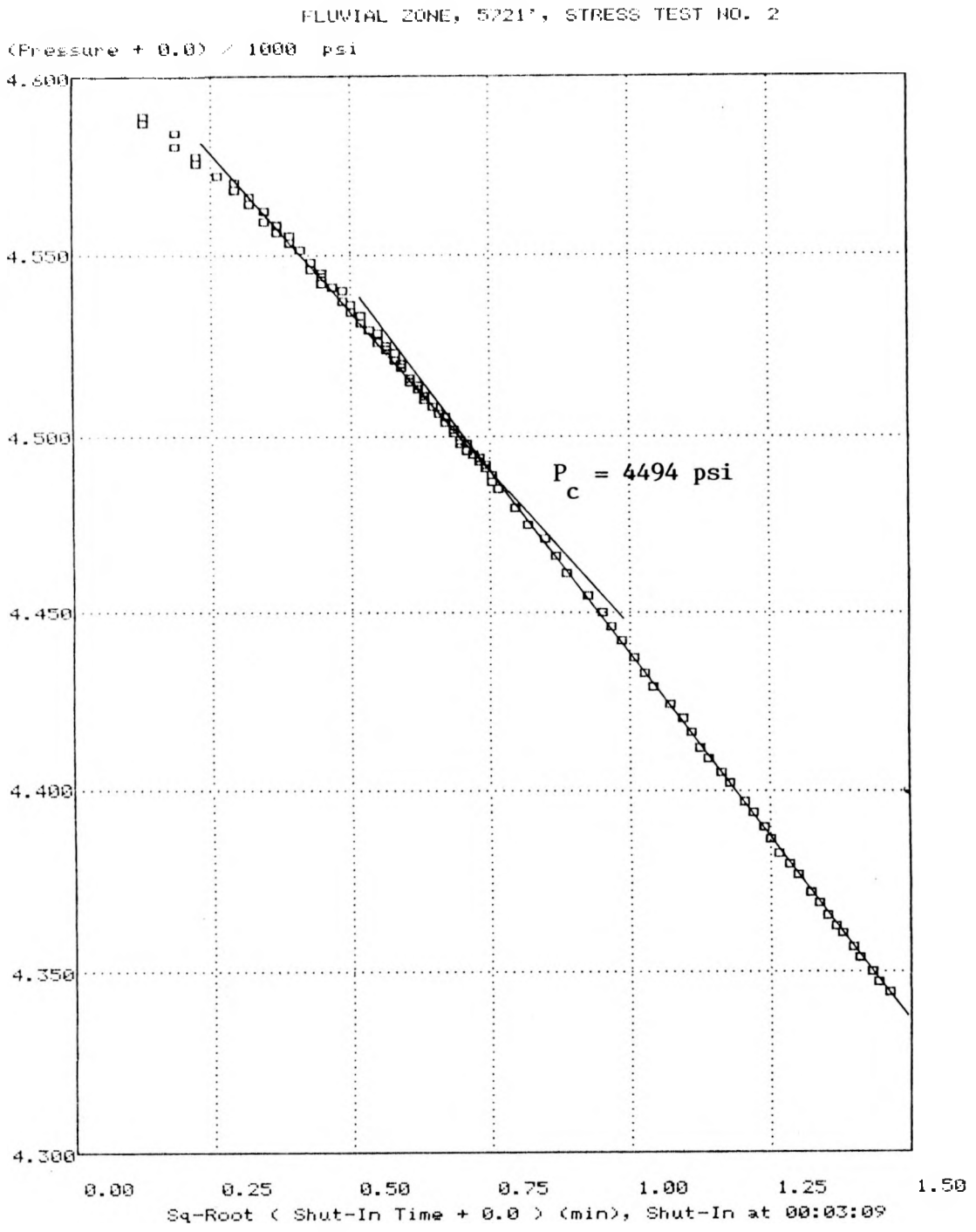


FIGURE A.166: Sandstone Stress Test (5721-5723'), Square-Root of Shut-In Time Plot of Test No. 2 Pressure Decline.

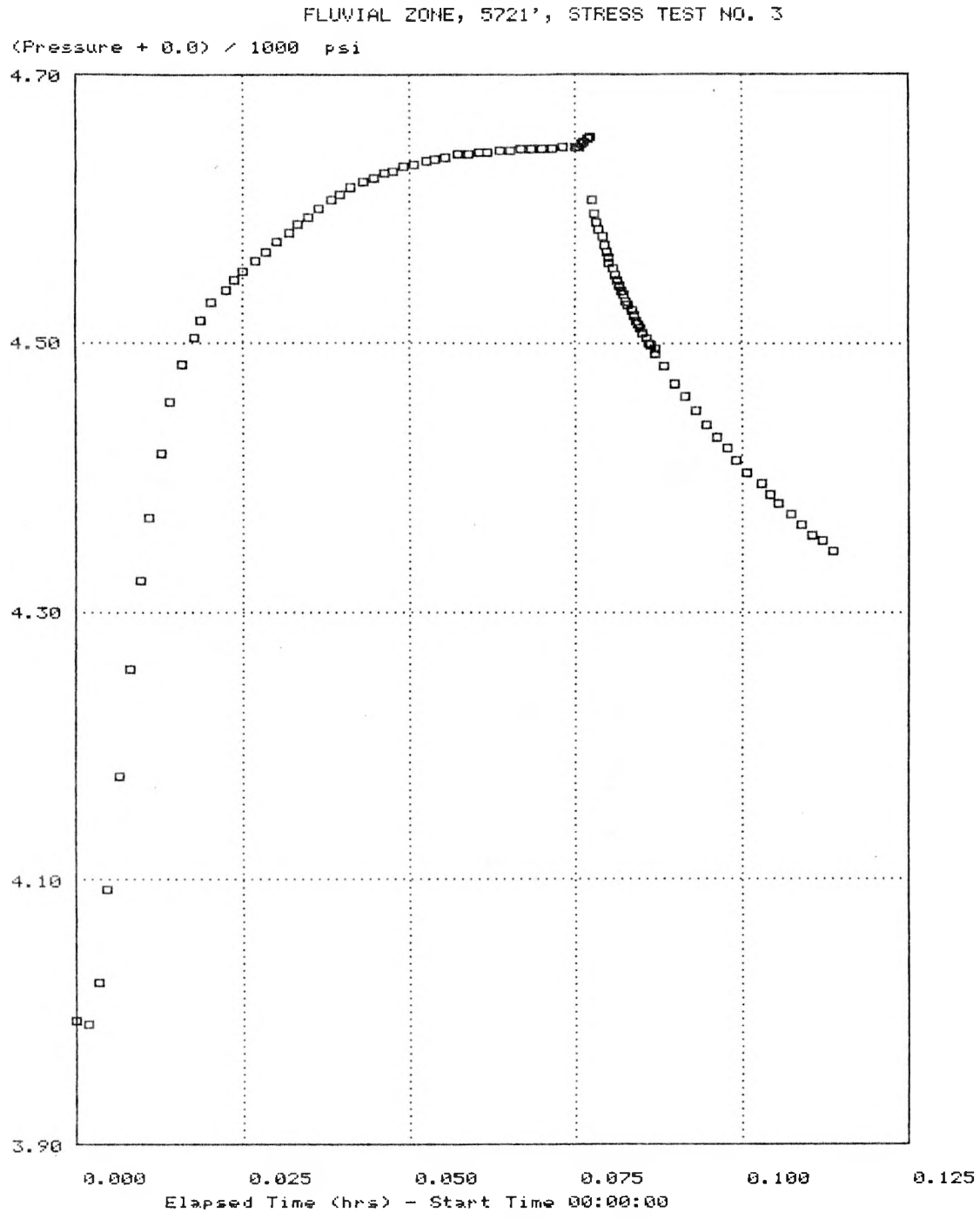


FIGURE A.167: Sandstone Stress Test (5721-5723'), Linear Plot of Test No. 3 Injection/Decline.

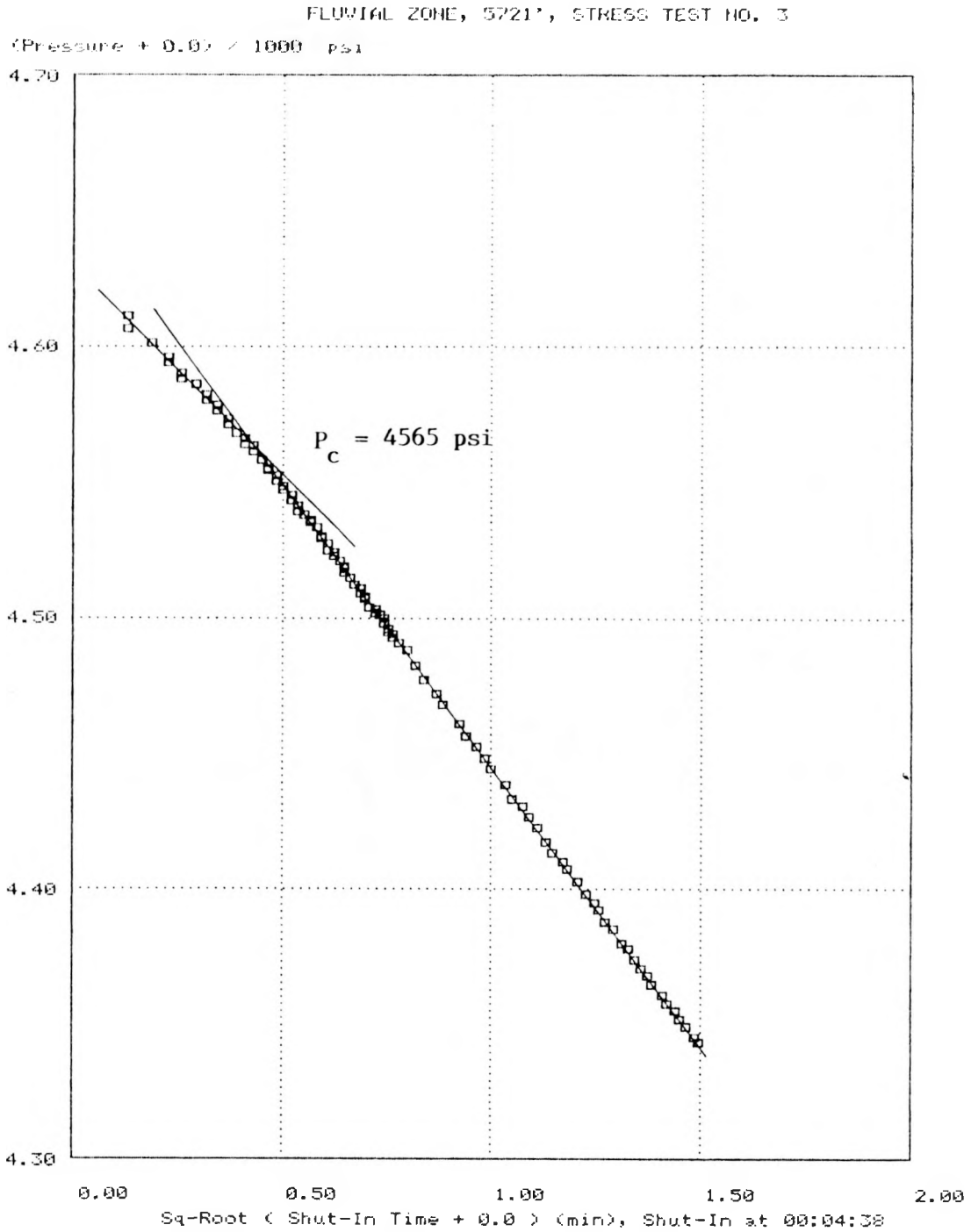


FIGURE A.168: Sandstone Stress Test (5721-5723'), Sqaure-Root of Shut-In Time Plot of Test No. 3 Pressure Decline.

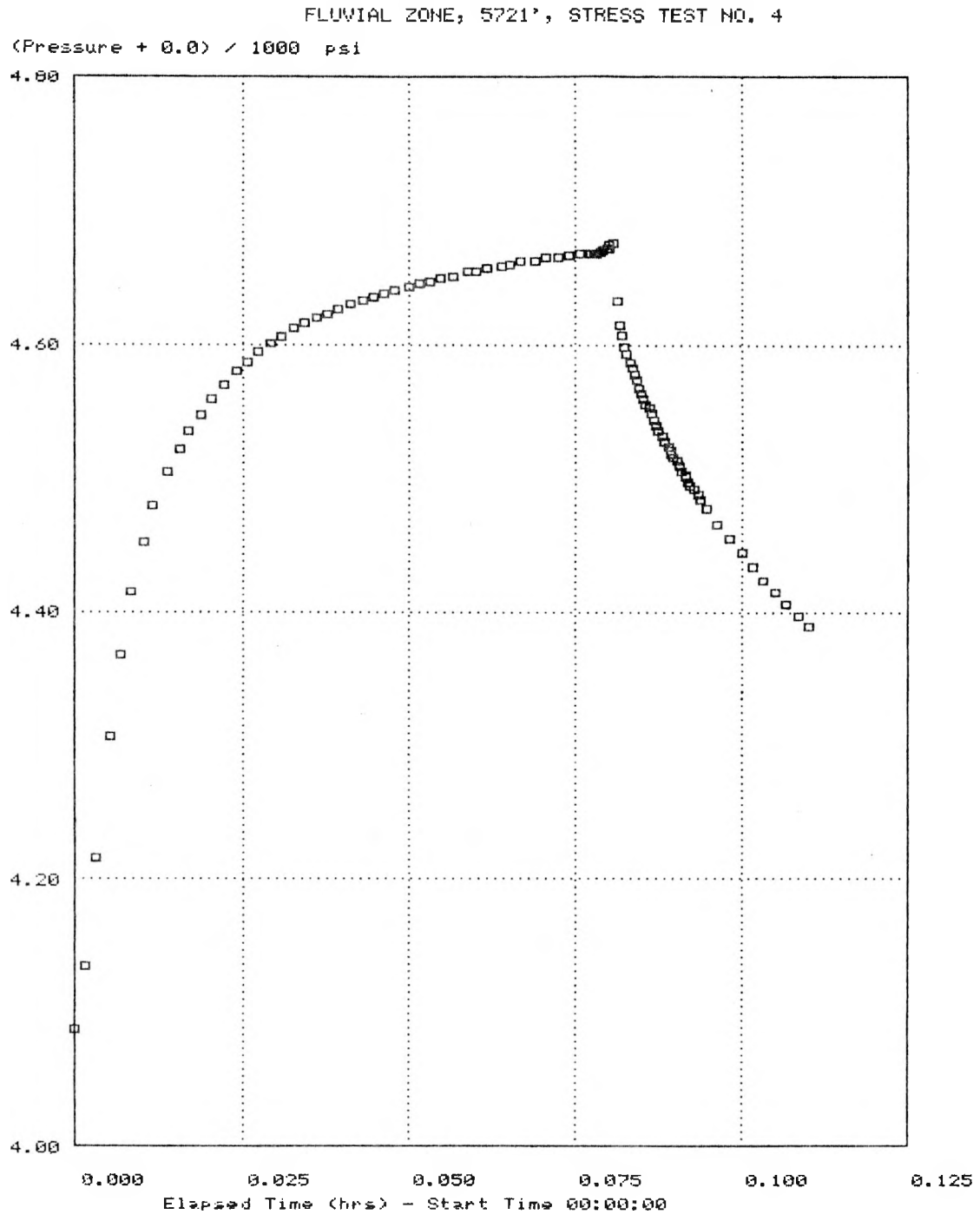


FIGURE A.169: Sandstone Stress Test (5721-5723'), Linear Plot of Test No. 4 Injection/Decline.

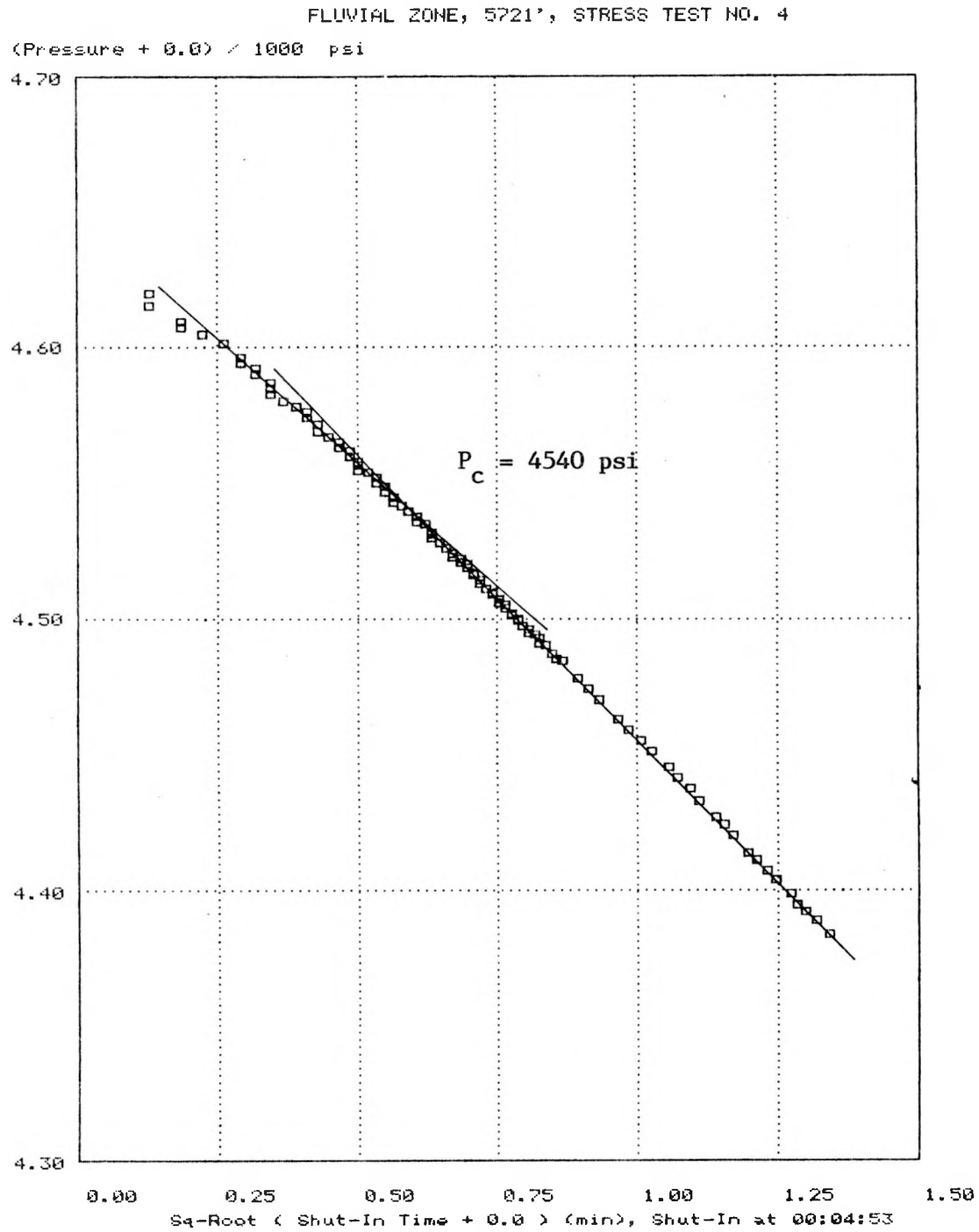


FIGURE A.170: Sandstone Stress Test (5721-5723'), Sqaure-Root of Shut-In Time Plot of Test No. 4 Pressure Decline.

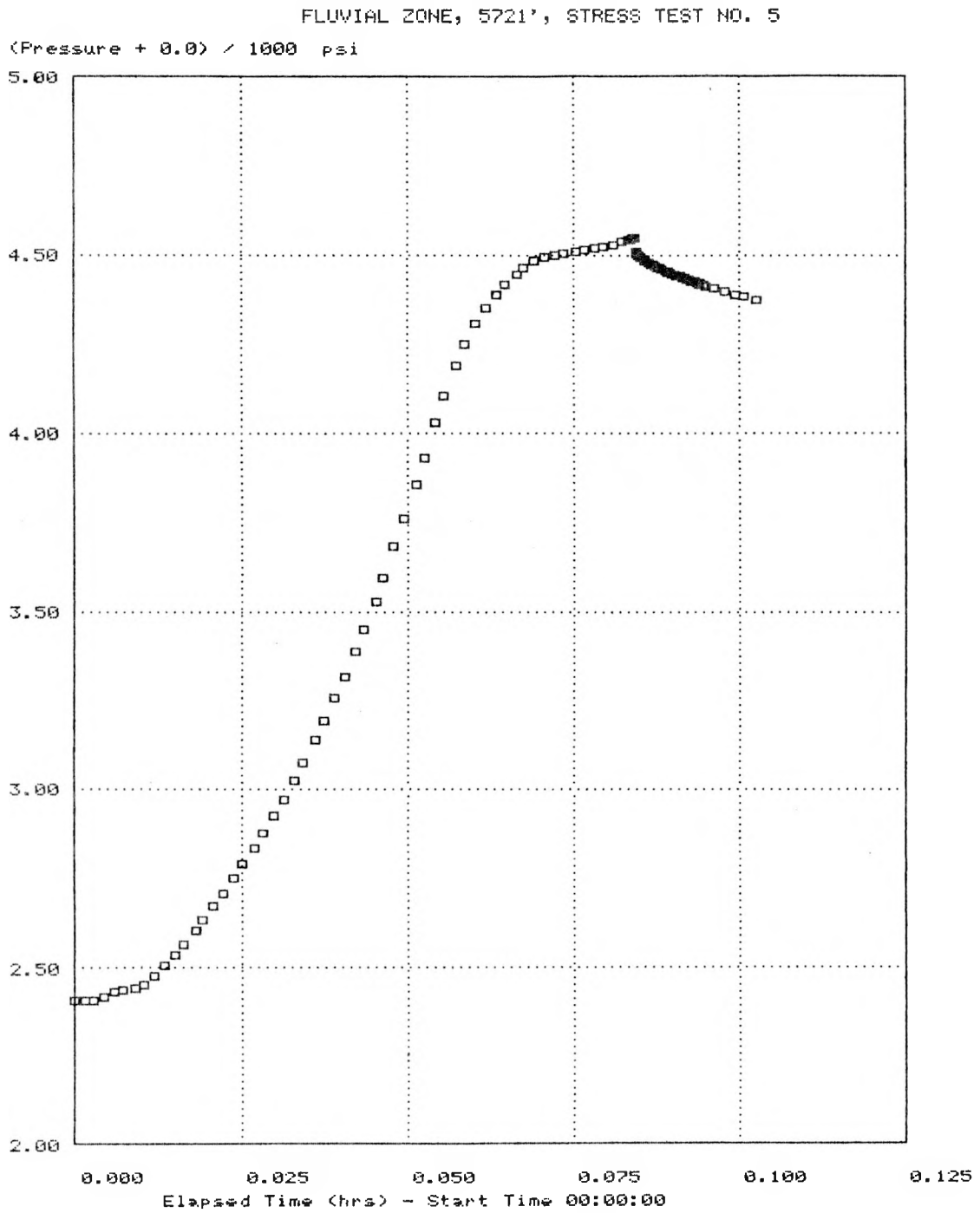


FIGURE A.171: Sandstone Stress Test (5721-5723'), Linear Plot of Test No. 5 Injection/Decline.

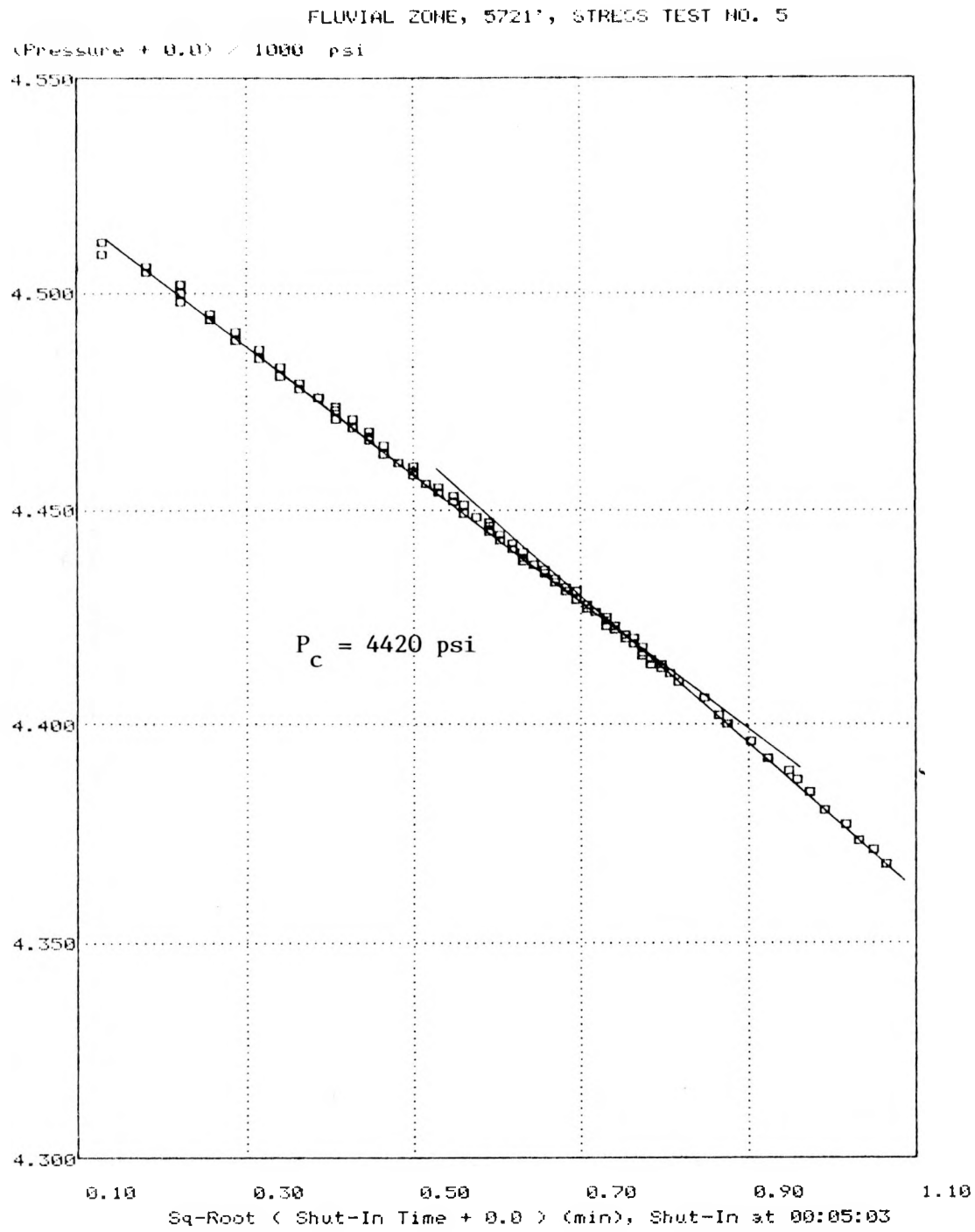


FIGURE A.172: Sandstone Stress Test (5721-5723'), Square-Root of Shut-In Time Plot of Test No. 5 Pressure Decline.

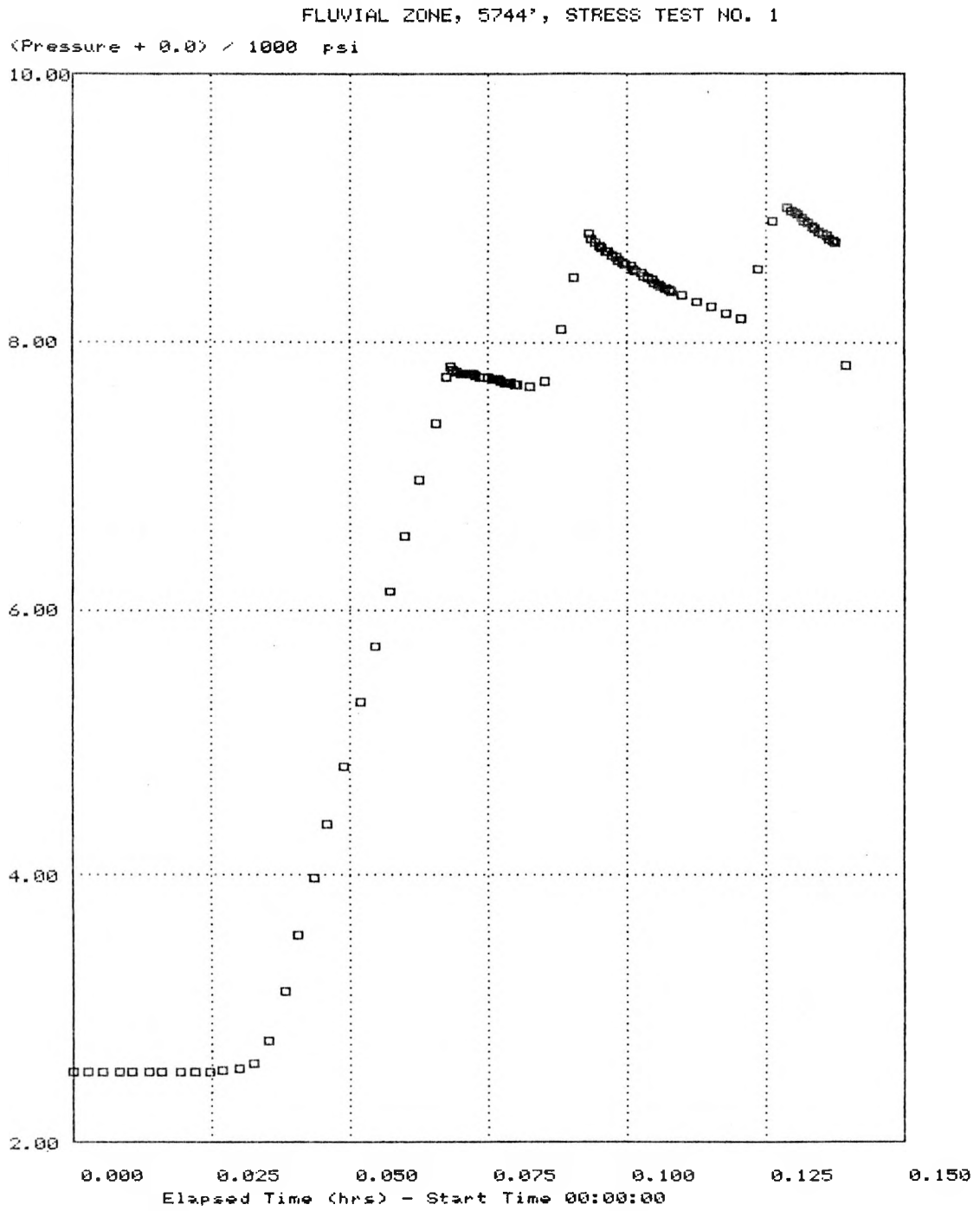


FIGURE A. 173: Shale Stress Test (5744-5746'), Linear Plot of Test No. 1 Injection/Decline.

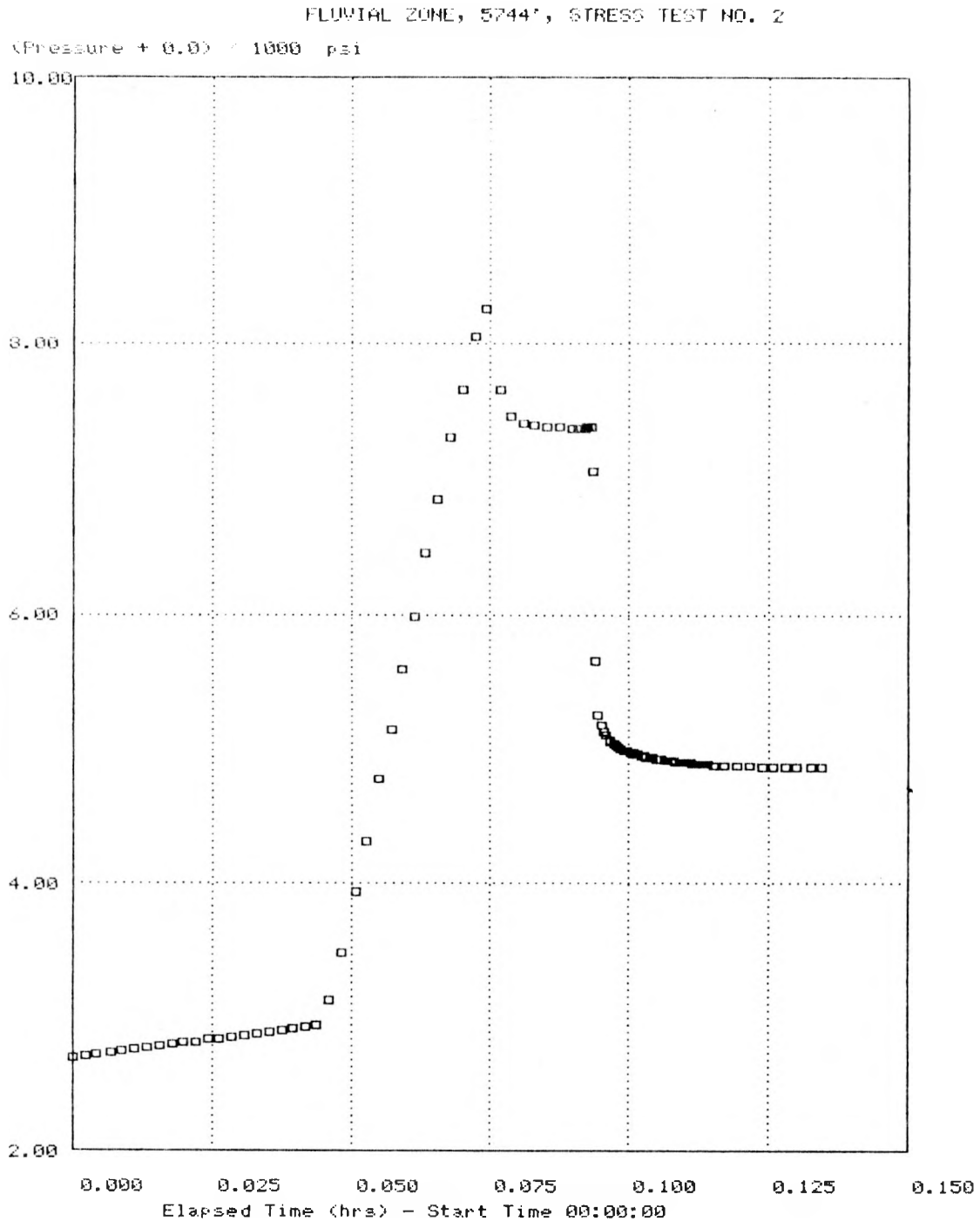


FIGURE A. 174: Shale Stress Test (5744-5746'), Linear Plot of Test No. 2 Injection/Decline.

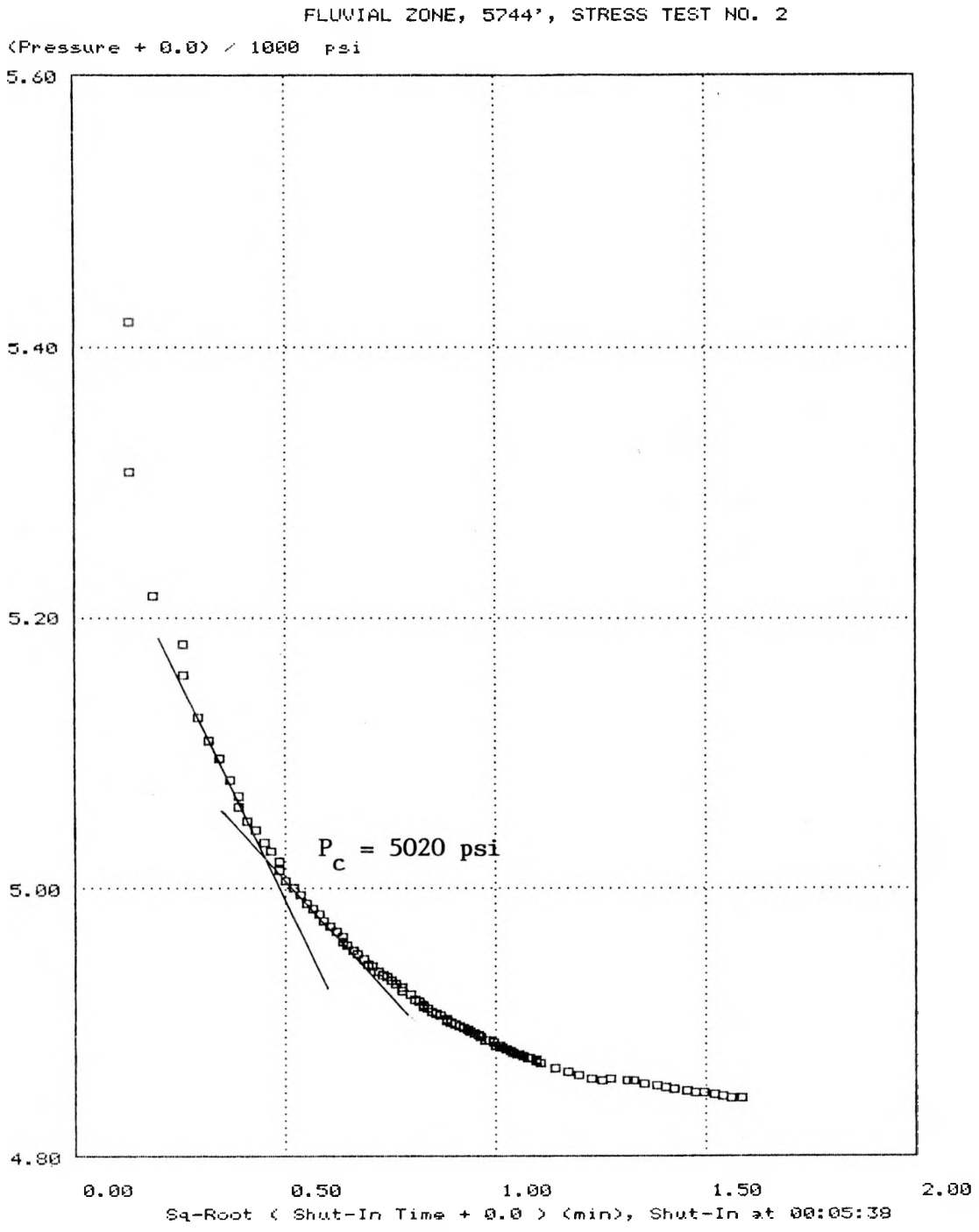


FIGURE A.175: Shale Stress Test (5744-5746'), Square-Root of Shut-In Time Plot of Test No. 2 Pressure Decline.

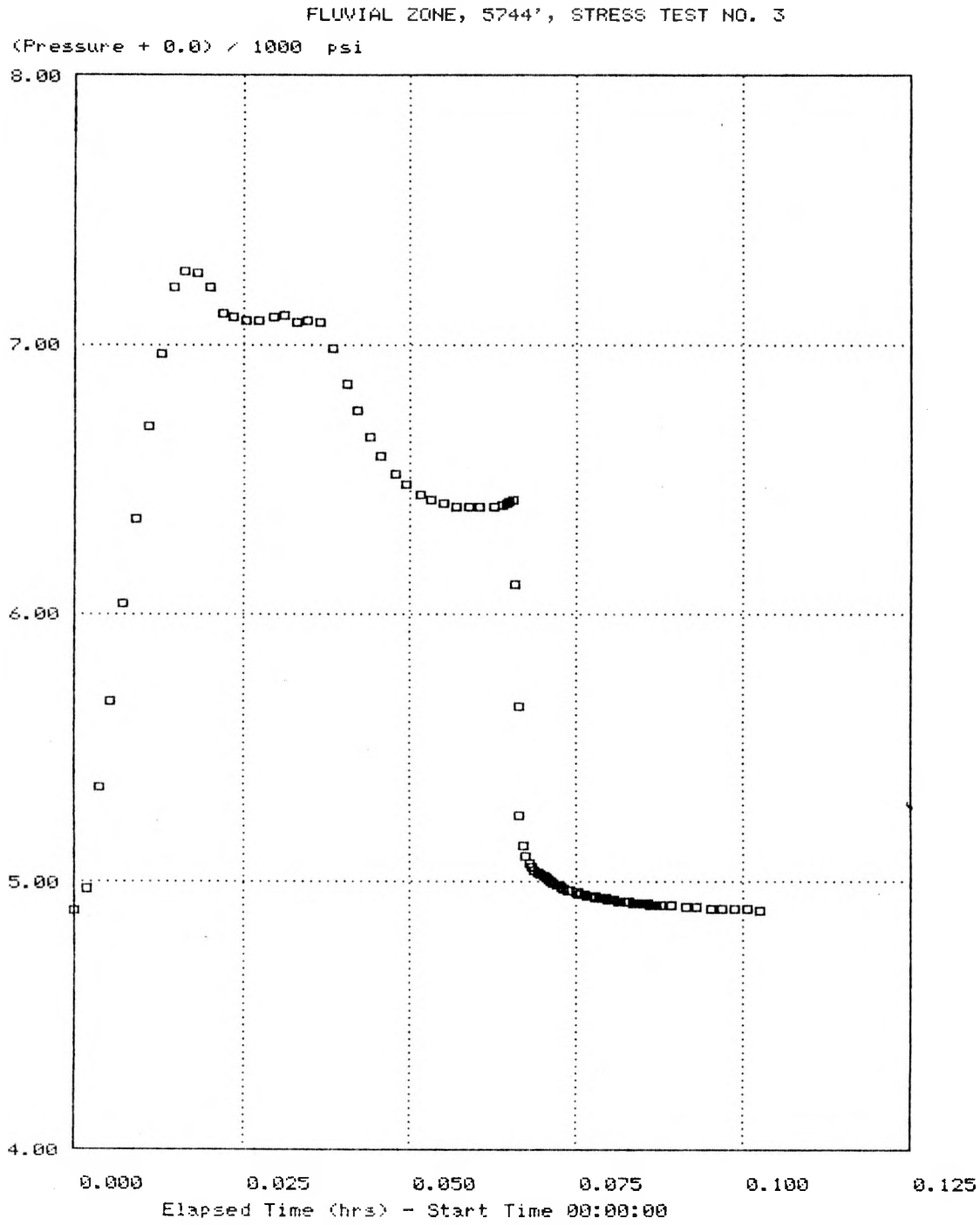


FIGURE A.176: Shale Stress Test (5744-5746'), Linear Plot of Test No. 3 Injection/Decline.

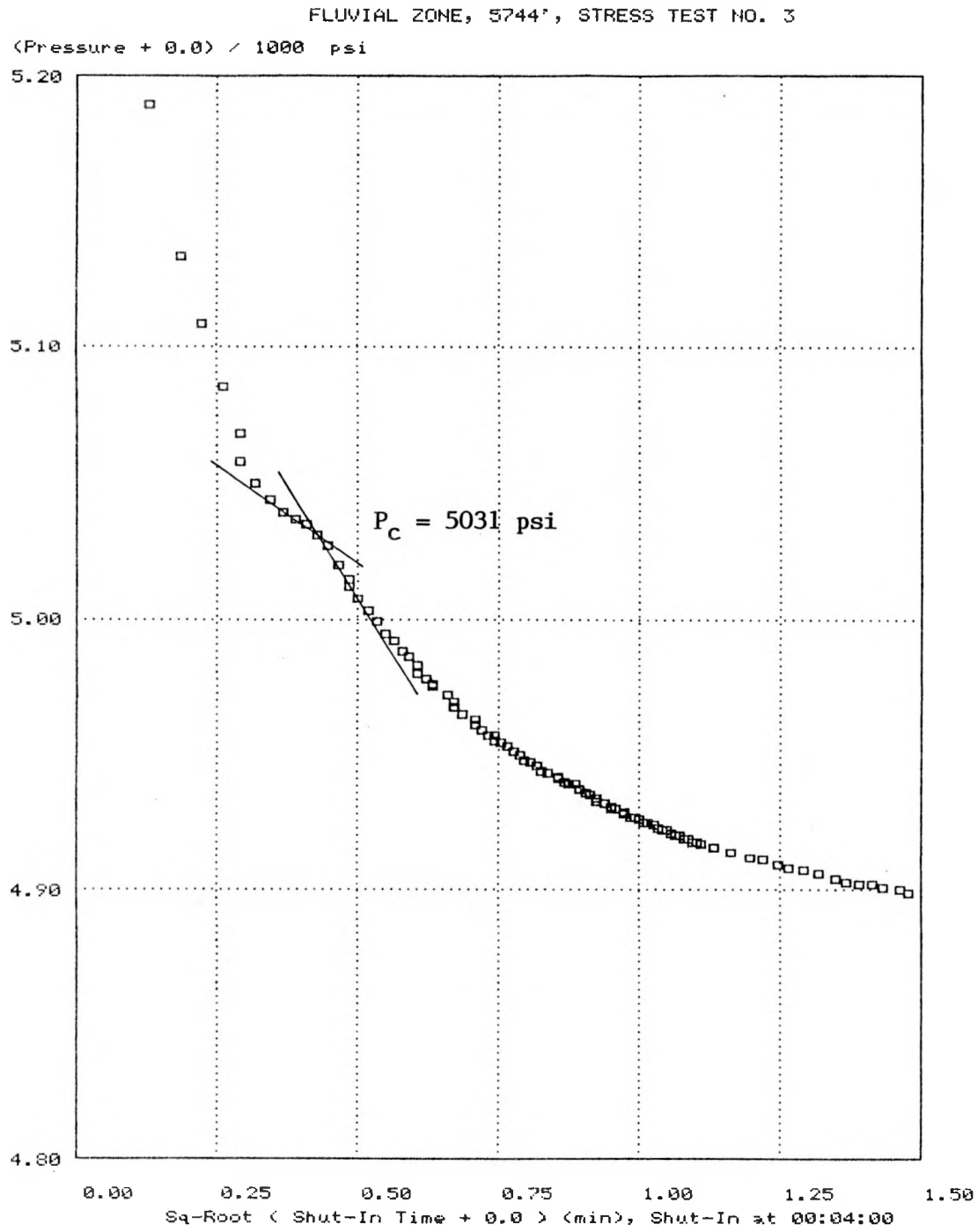


FIGURE A.177: Shale Stress Test (5744-5746'), Square-Root of Shut-In Time Plot of Test No. 3 Pressure Decline.

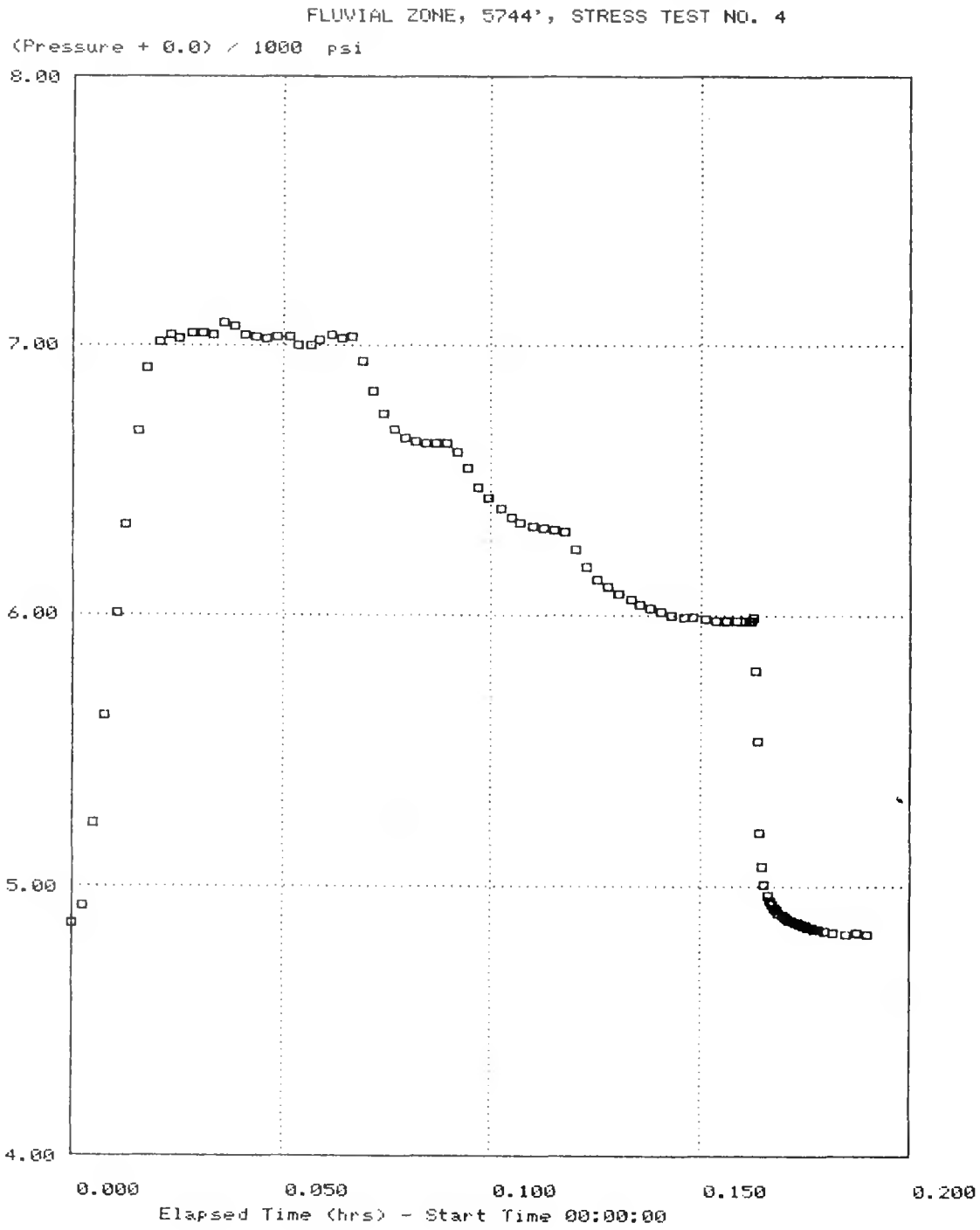


FIGURE A.178: Shale Stress Test (5744-5746'), Linear Plot of Test No. 4 Injection/Decline.

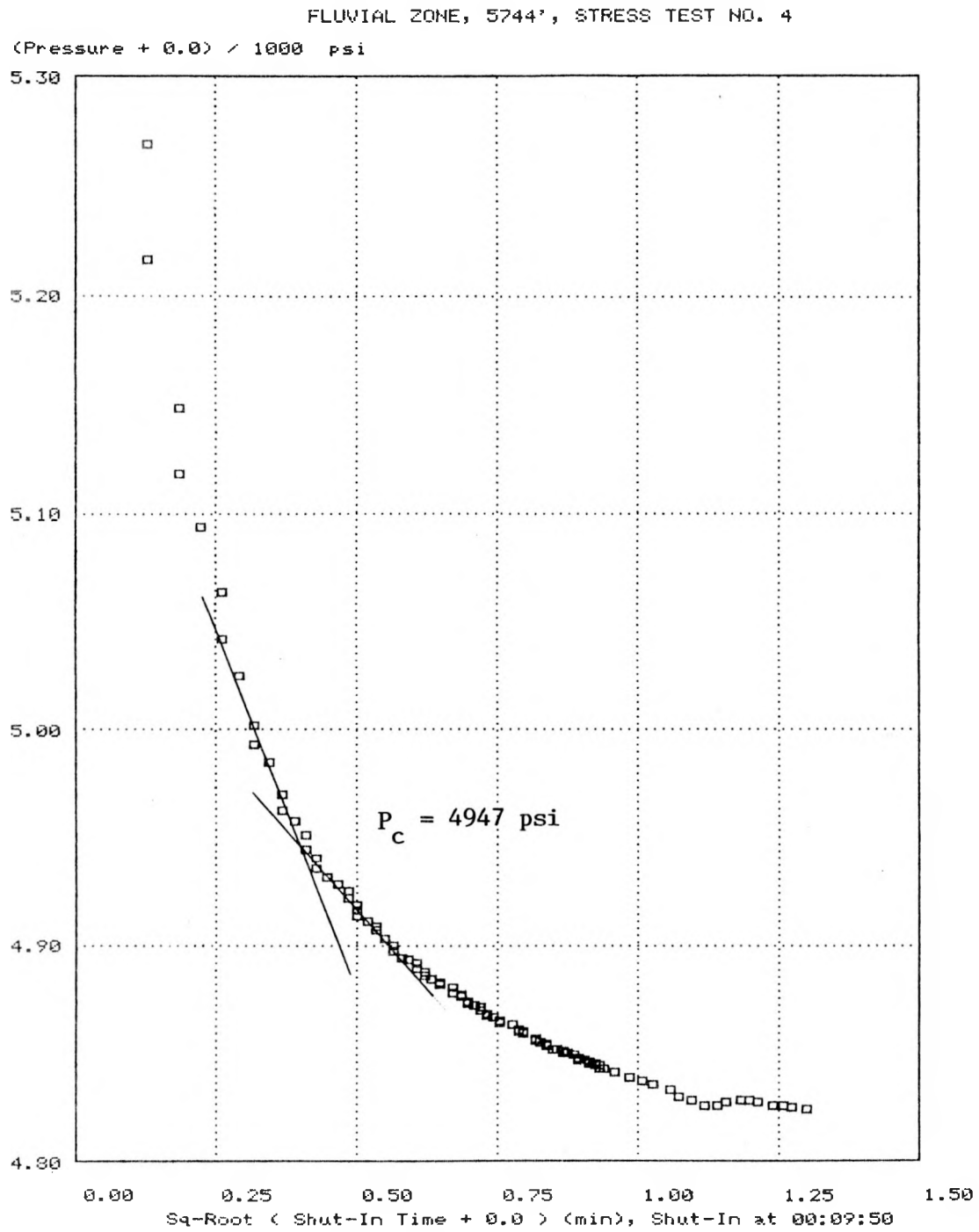


FIGURE A.179: Shale Stress Test (5744-5746'), Square-Root of Shut-In Time Plot of Test No. 4 Pressure Decline.

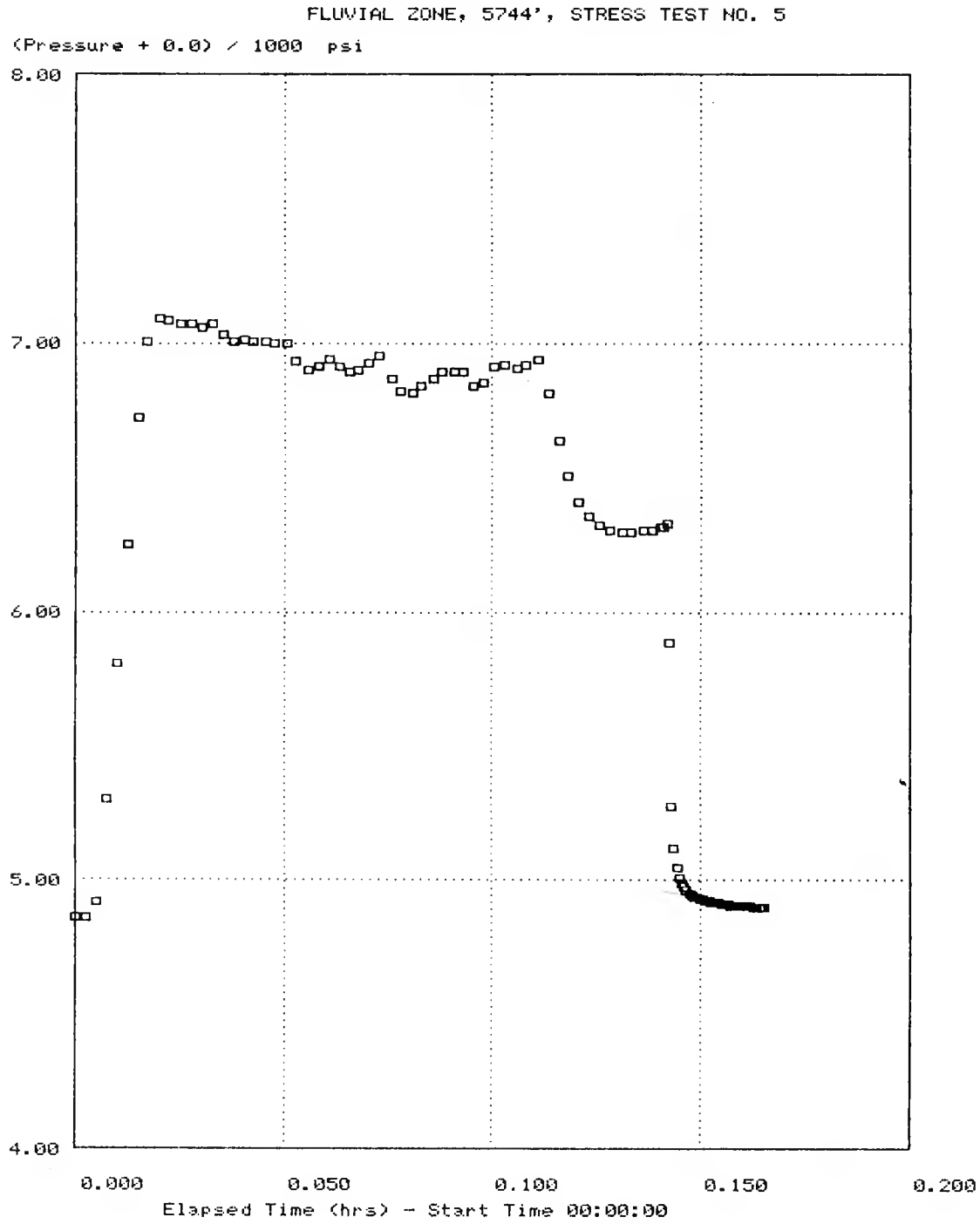


FIGURE A.180: Shale Stress Test (5744-5746'), Linear Plot of Test No. 5 Injection/Decline.

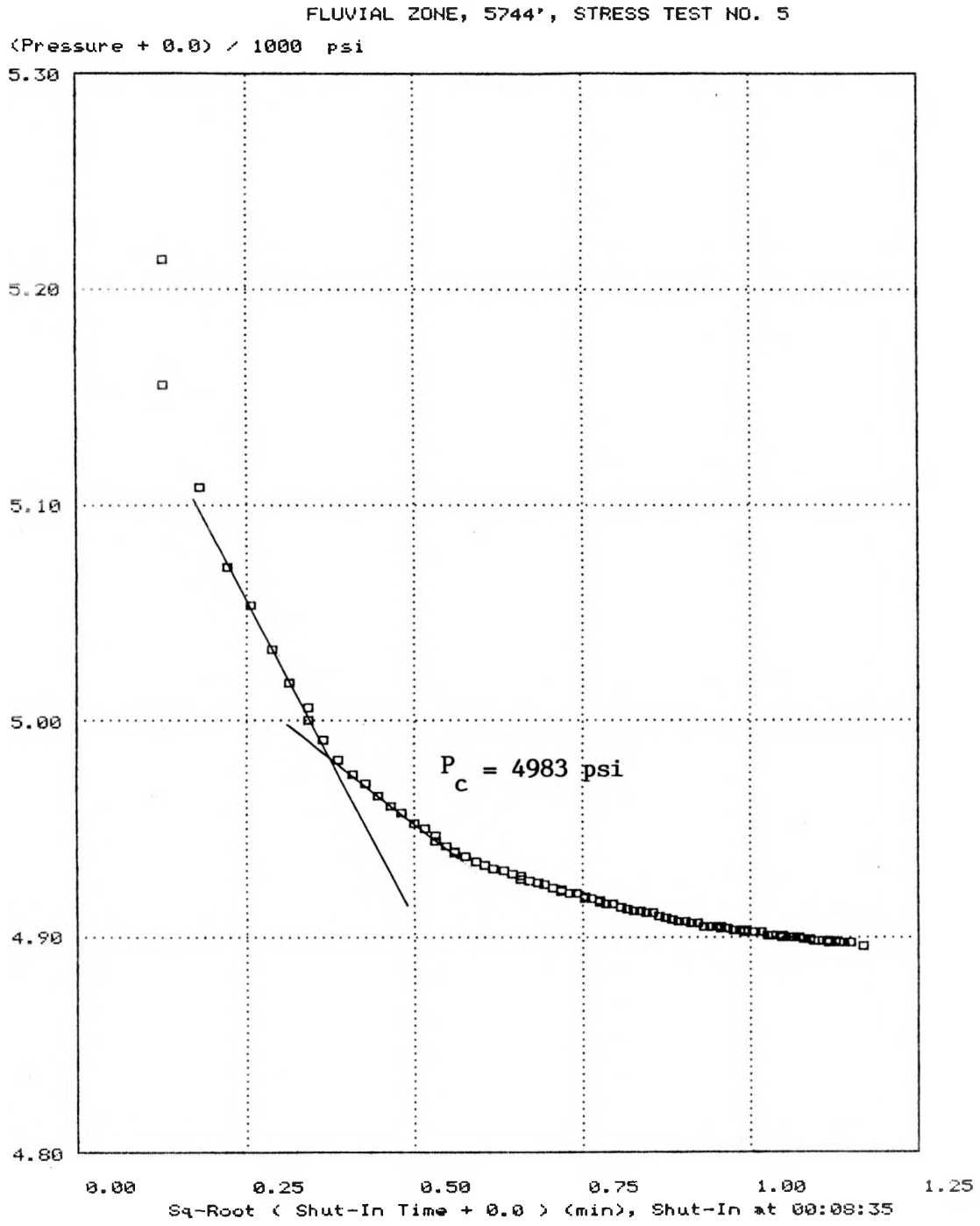


FIGURE A.181: Shale Stress Test (5744-5746'), Square-Root of Shut-In Time Plot of Test No. 5 Pressure Decline.

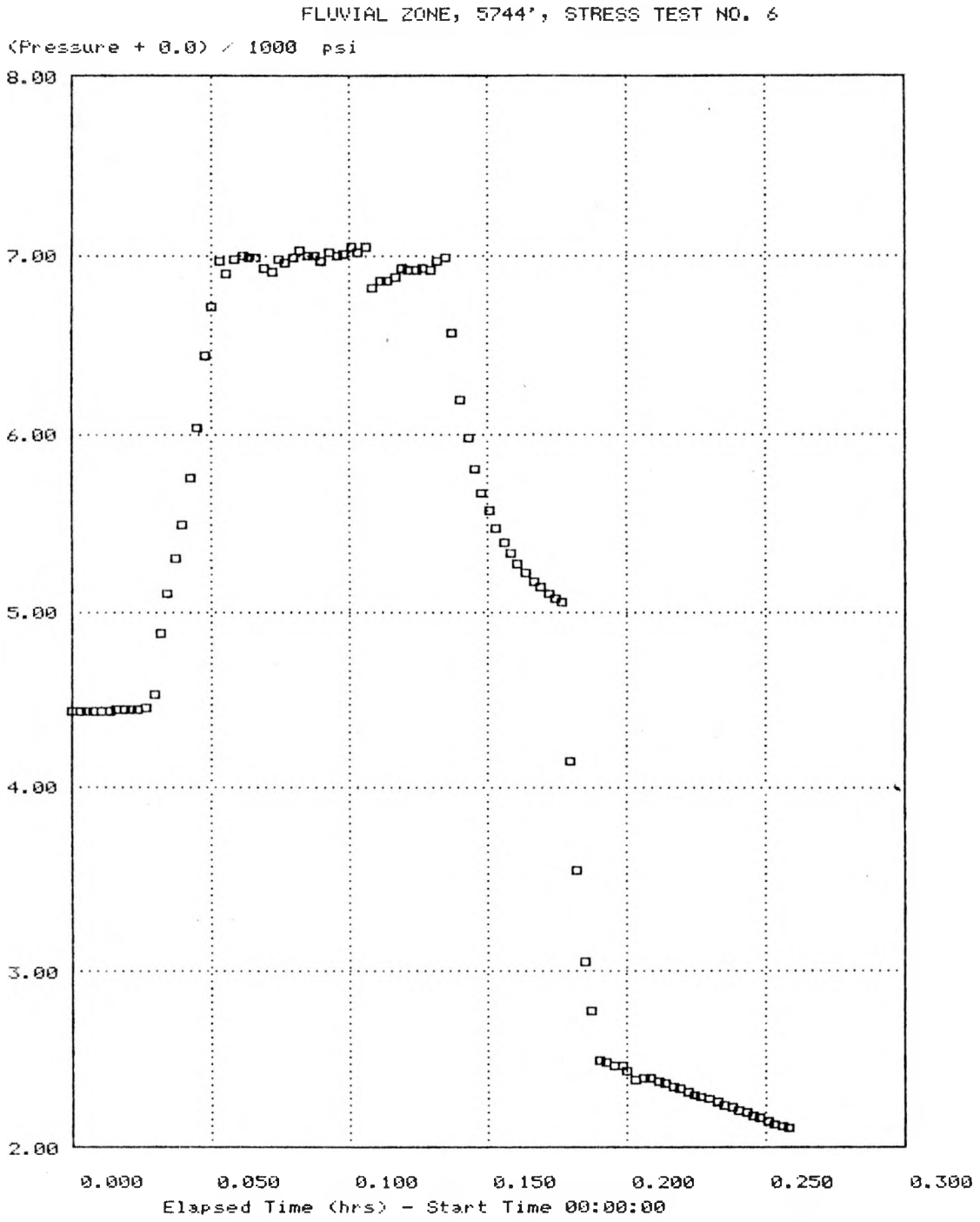


FIGURE A.182: Shale Stress Test (5744-5746'), Linear Plot of Test No. 6 Injection/Decline.

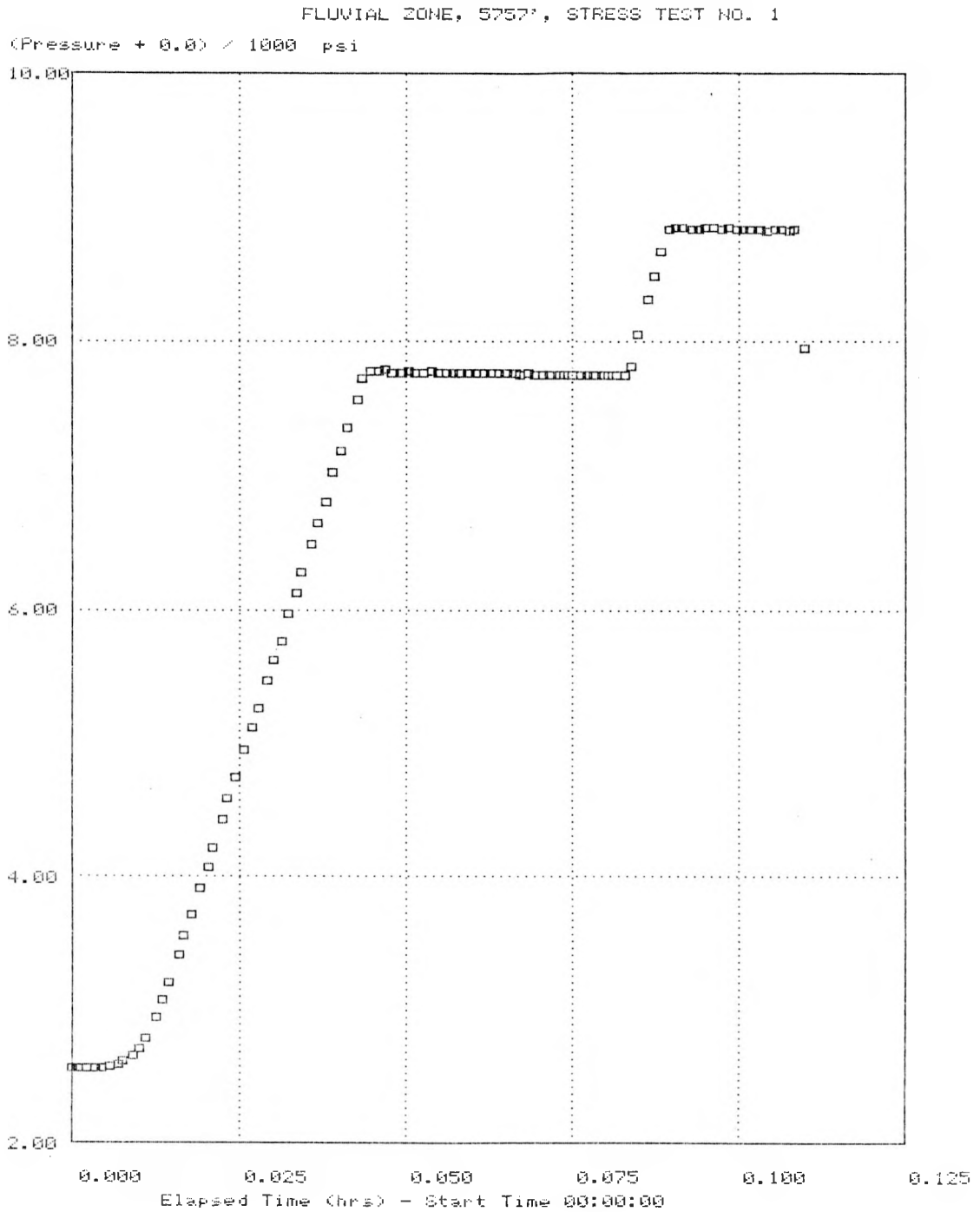


FIGURE A.183: Shale Stress Test (5757-5759'), Linear Plot of Test No. 1 Injection/Decline.

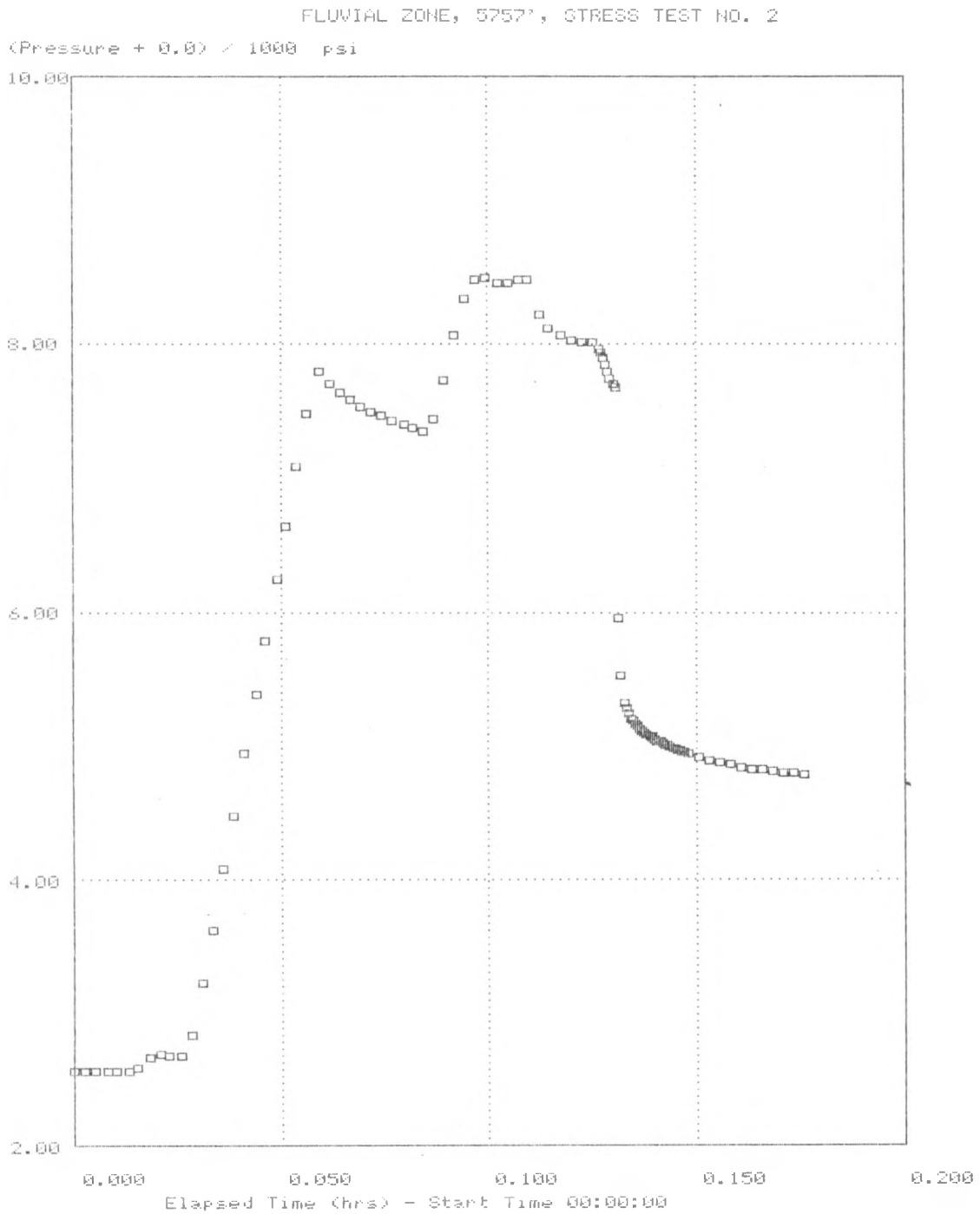


FIGURE A.184: Shale Stress Test (5757-5759'), Linear Plot of Test No. 2 Injection/Decline.

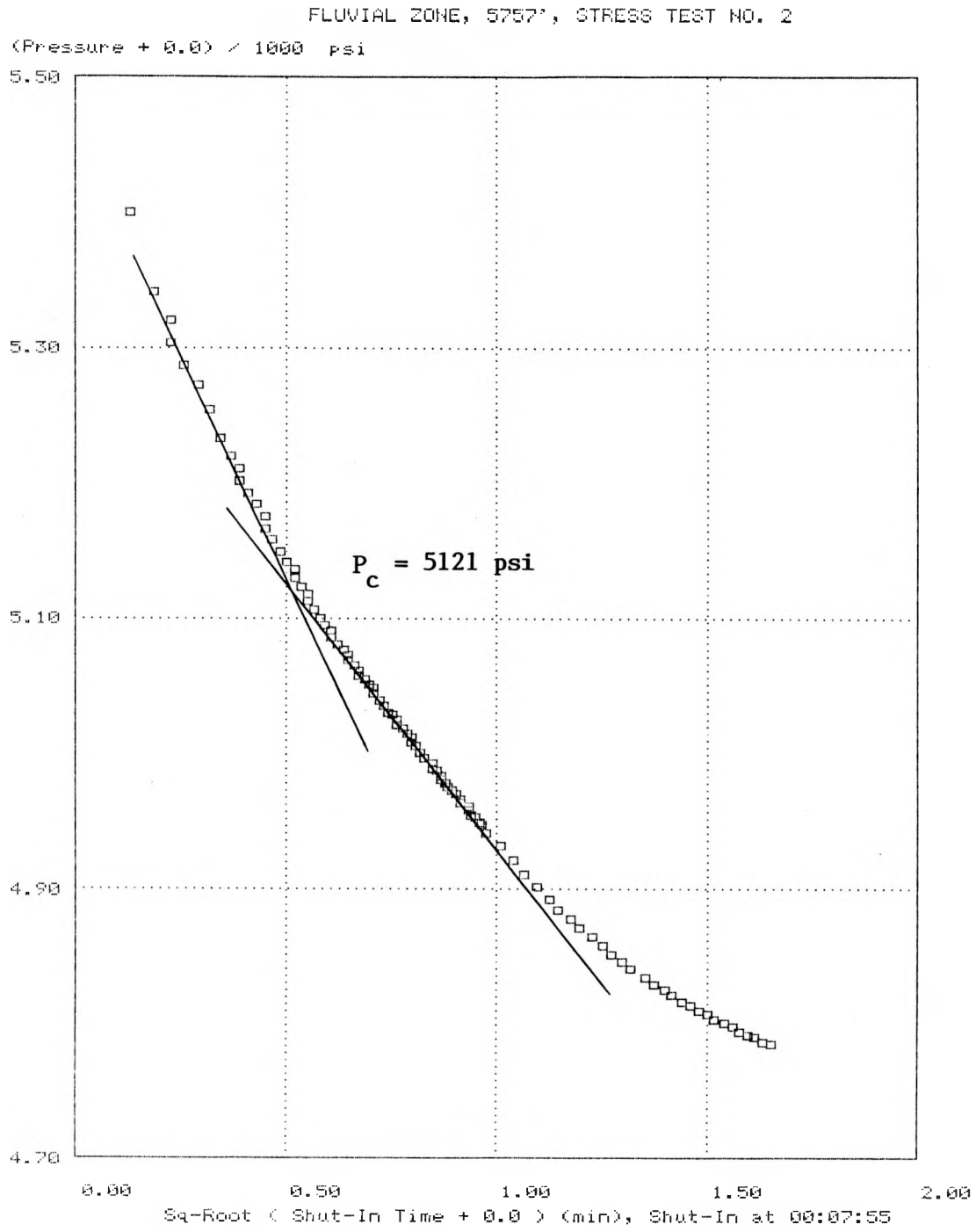


FIGURE A.185: Shale Stress Test (5757-5759'), Square-Root of Shut-In Time Plot of Test No. 2 Pressure Decline.

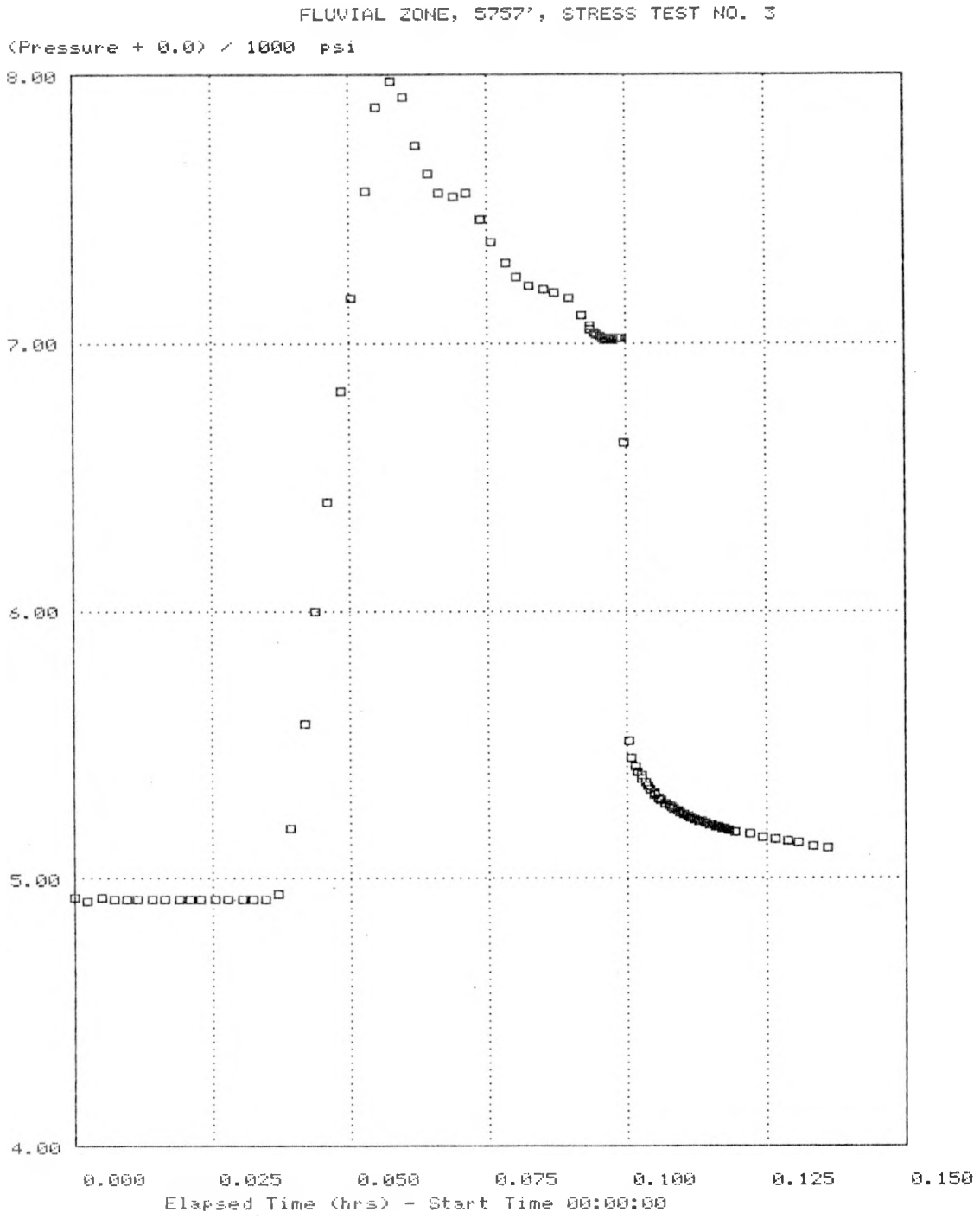


FIGURE A.186: Shale Stress Test (5757-5759'), Linear Plot of Test No. 3 Injection/Decline.

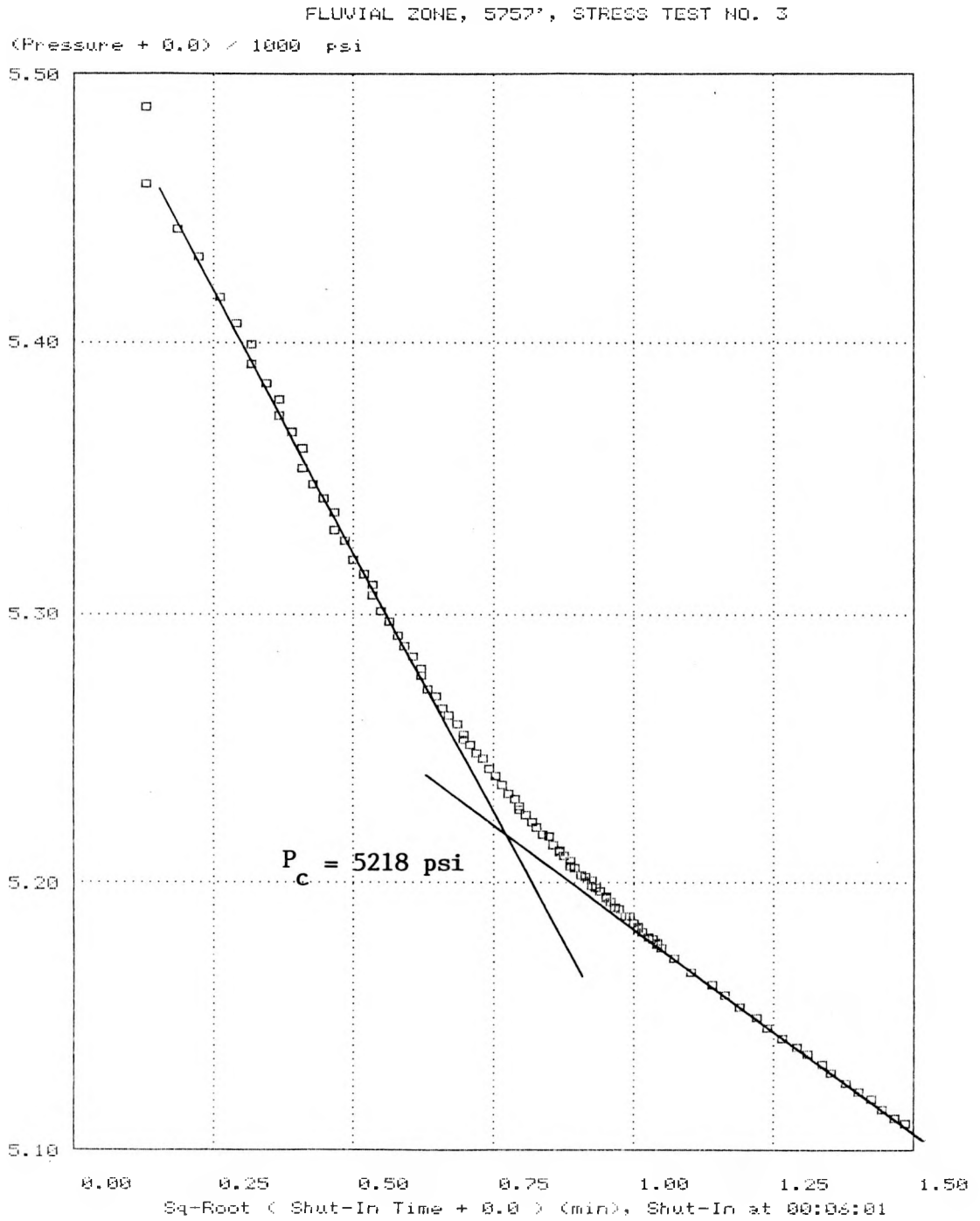


FIGURE A.187: Shale Stress Test (5757-5759'), Square-Root of Shut-In Time Plot of Test No. 3 Pressure Decline.

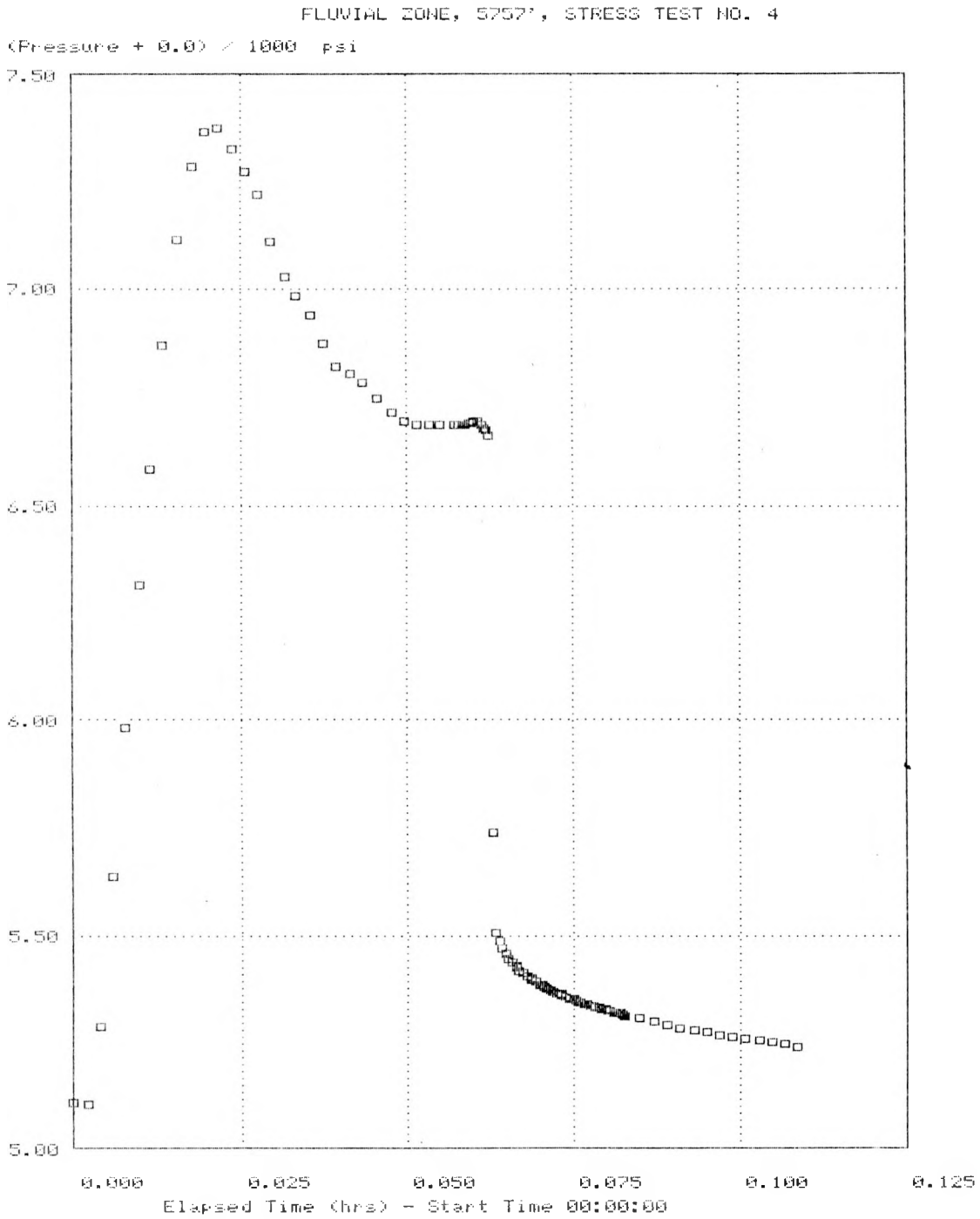


FIGURE A.188: Shale Stress Test (5757-5759'), Linear Plot of Test No. 4 Injection/Decline.

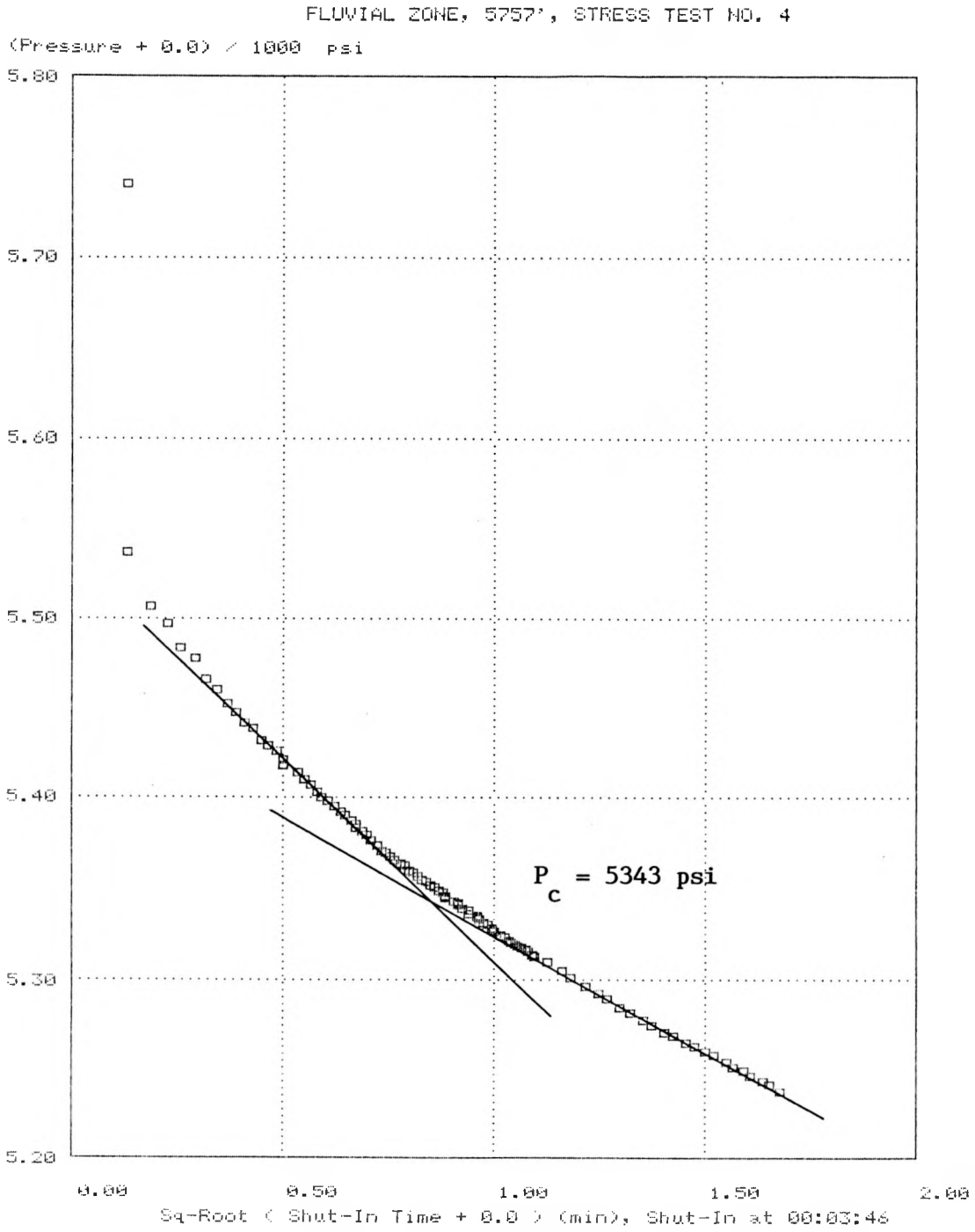


FIGURE A.189: Shale Stress Test (5757-5759'), Square-Root of Shut-In Time Plot of Test No. 4 Pressure Decline.

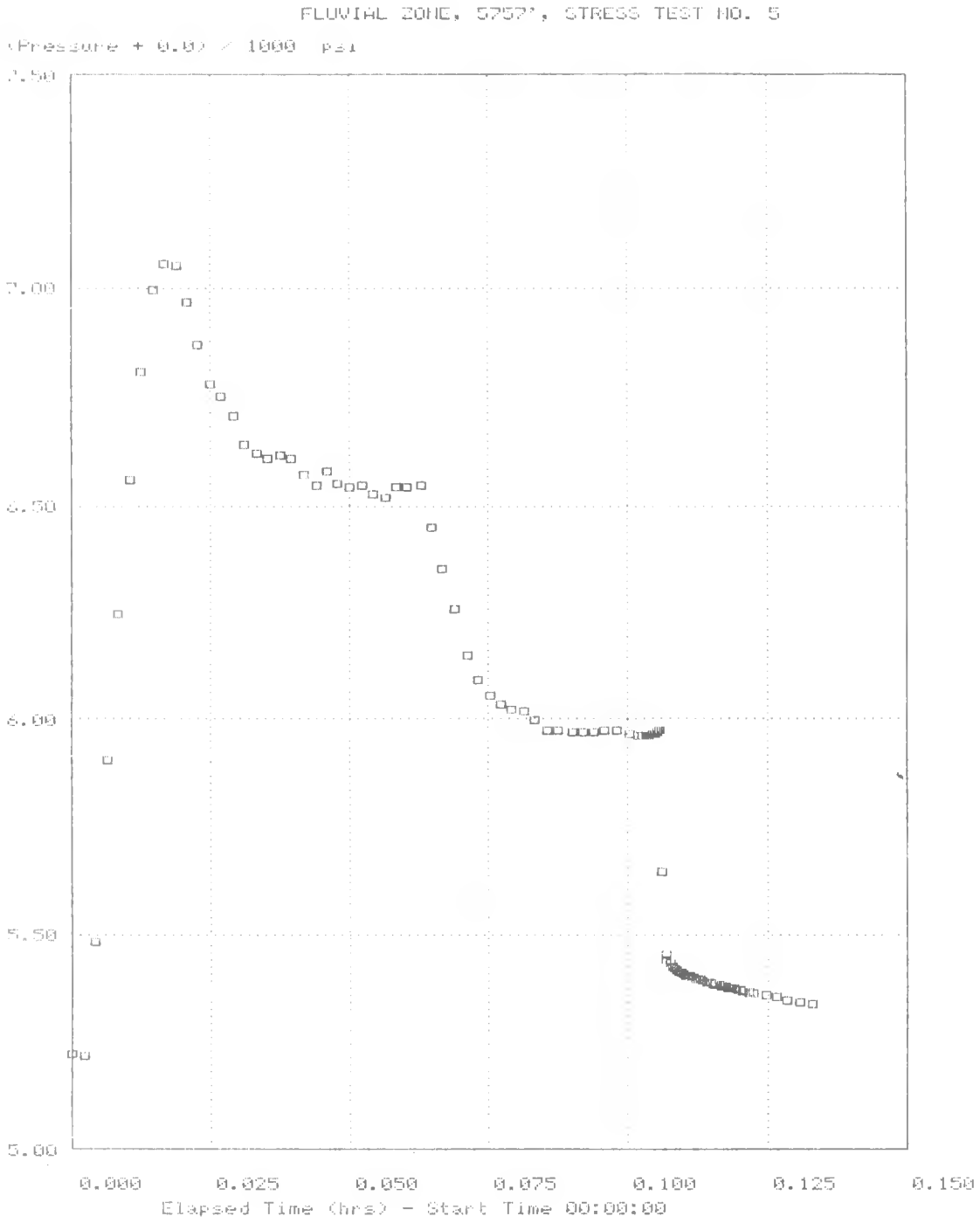


FIGURE A.190: Shale Stress Test (5757-5759'), Linear Plot of Test No. 5 Injection/Decline.

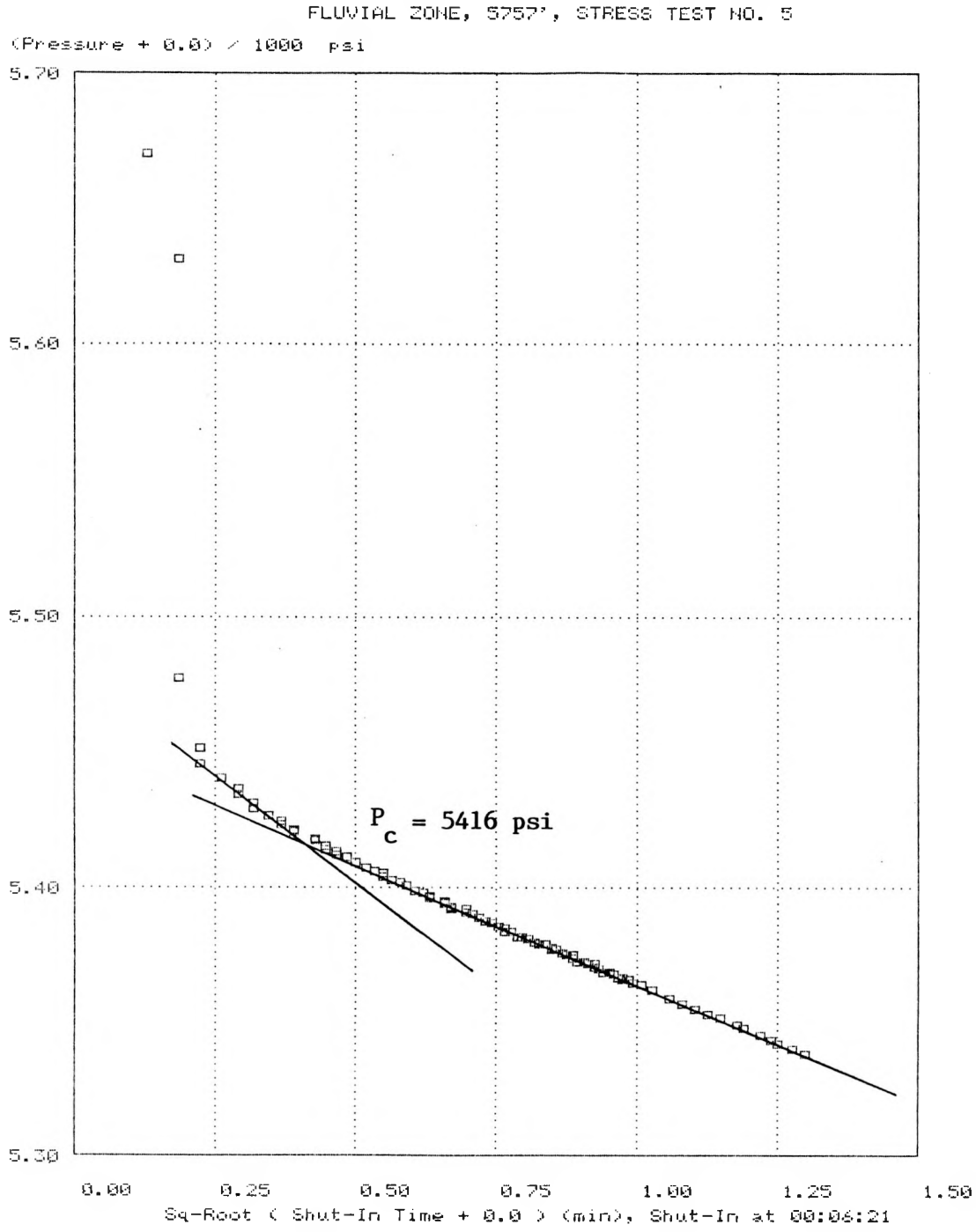


FIGURE A.191: Shale Stress Test (5757-5759'), Square-Root of Shut-In Time Plot of Test No. 5 Pressure Decline.

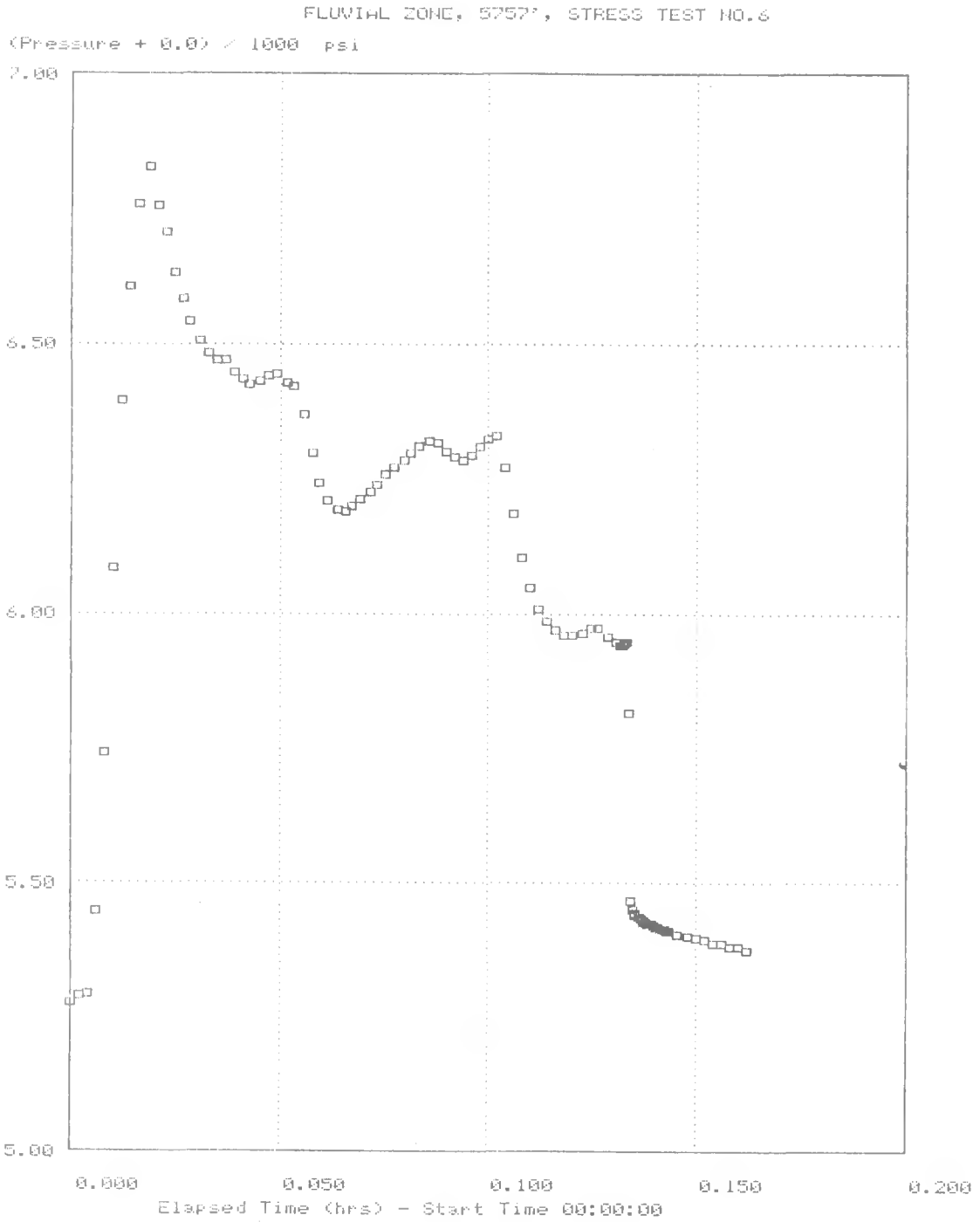


FIGURE A.192: Shale Stress Test (5757-5759'), Linear Plot of Test No. 6 Injection/Decline.

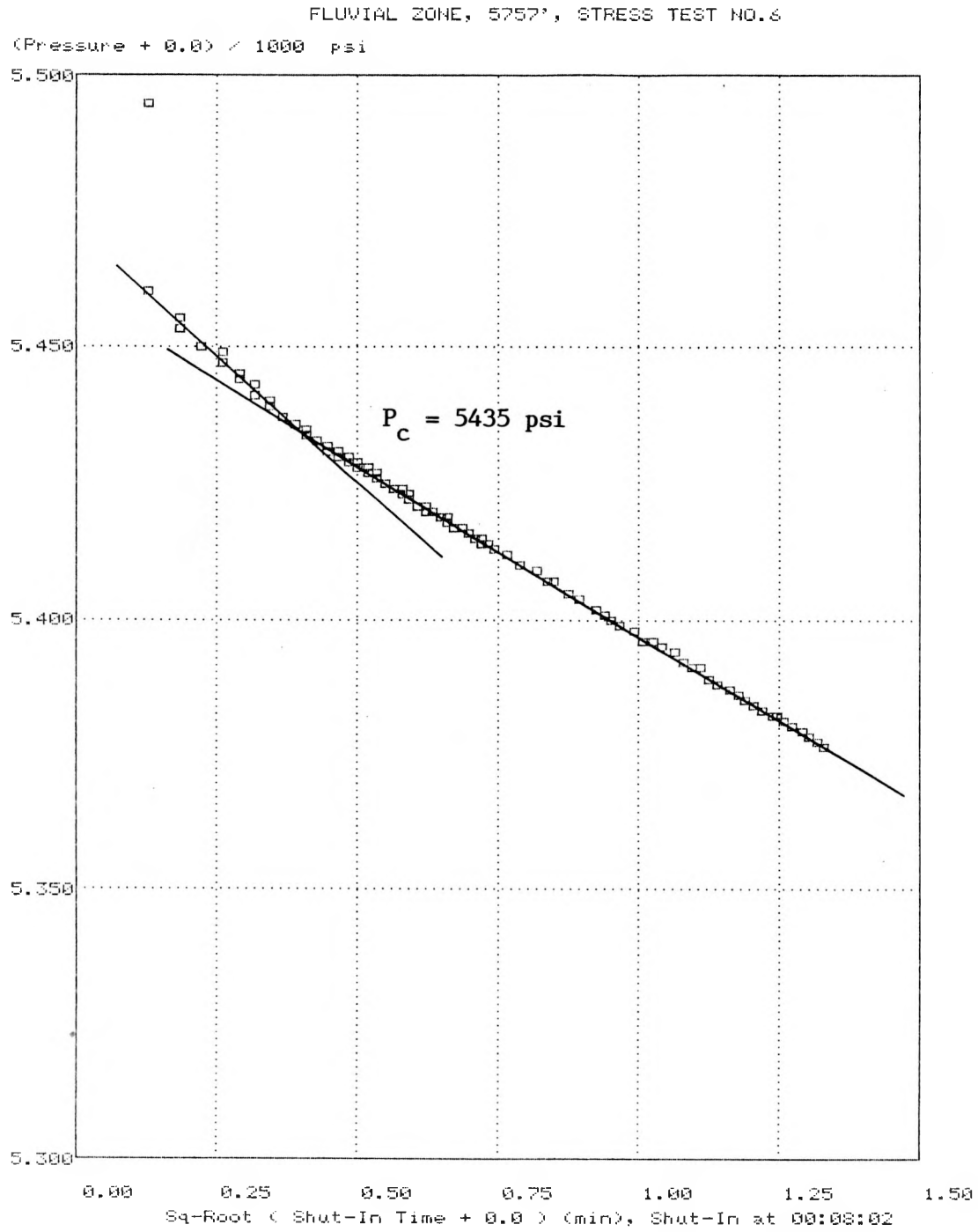


FIGURE A.193: Shale Stress Test (5757-5759'), Square-Root of Shut-In Time Plot of Test No. 6 Pressure Decline.

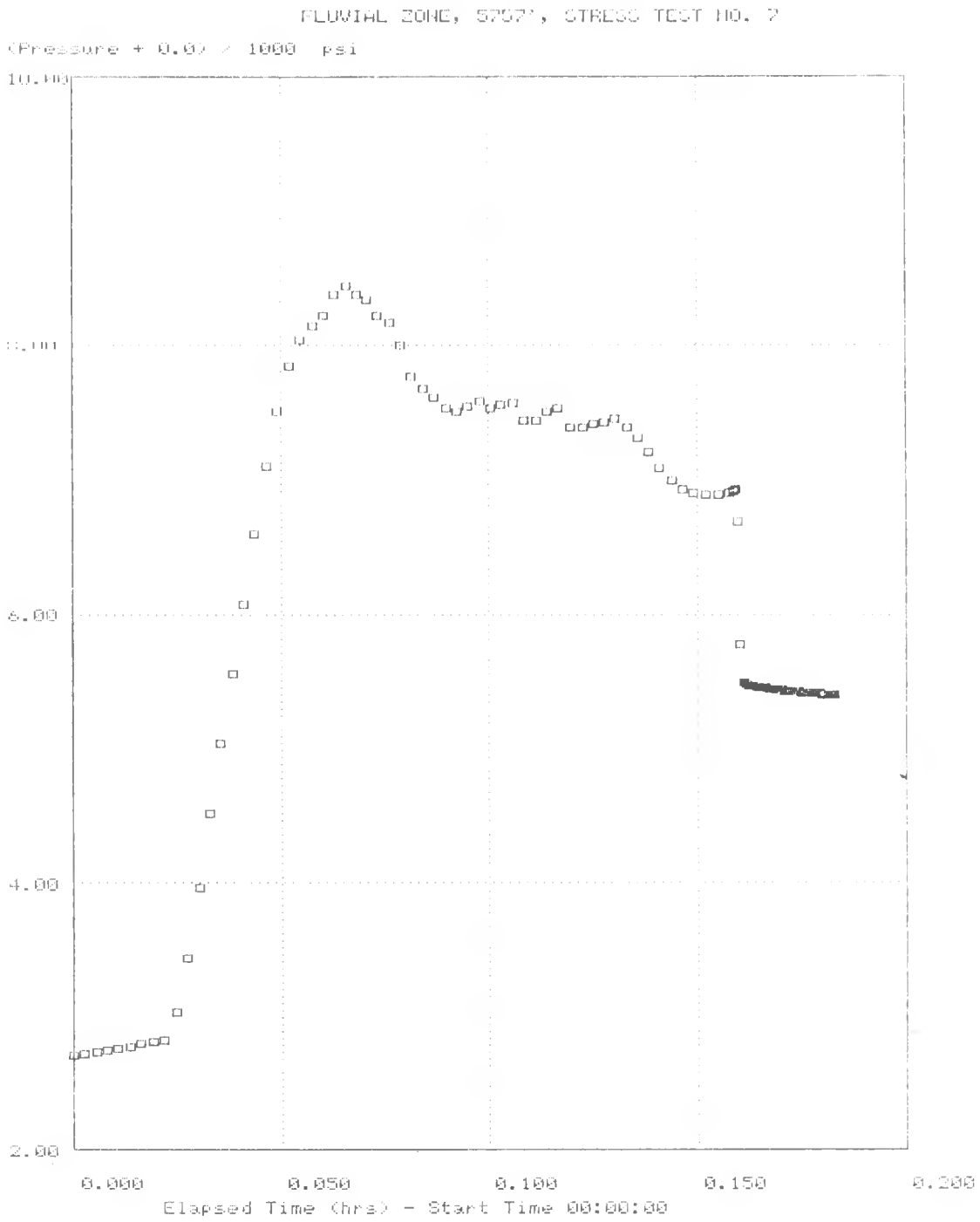


FIGURE A.194: Shale Stress Test (5757-5759'), Linear Plot of Test No. 7 Injection/Decline.

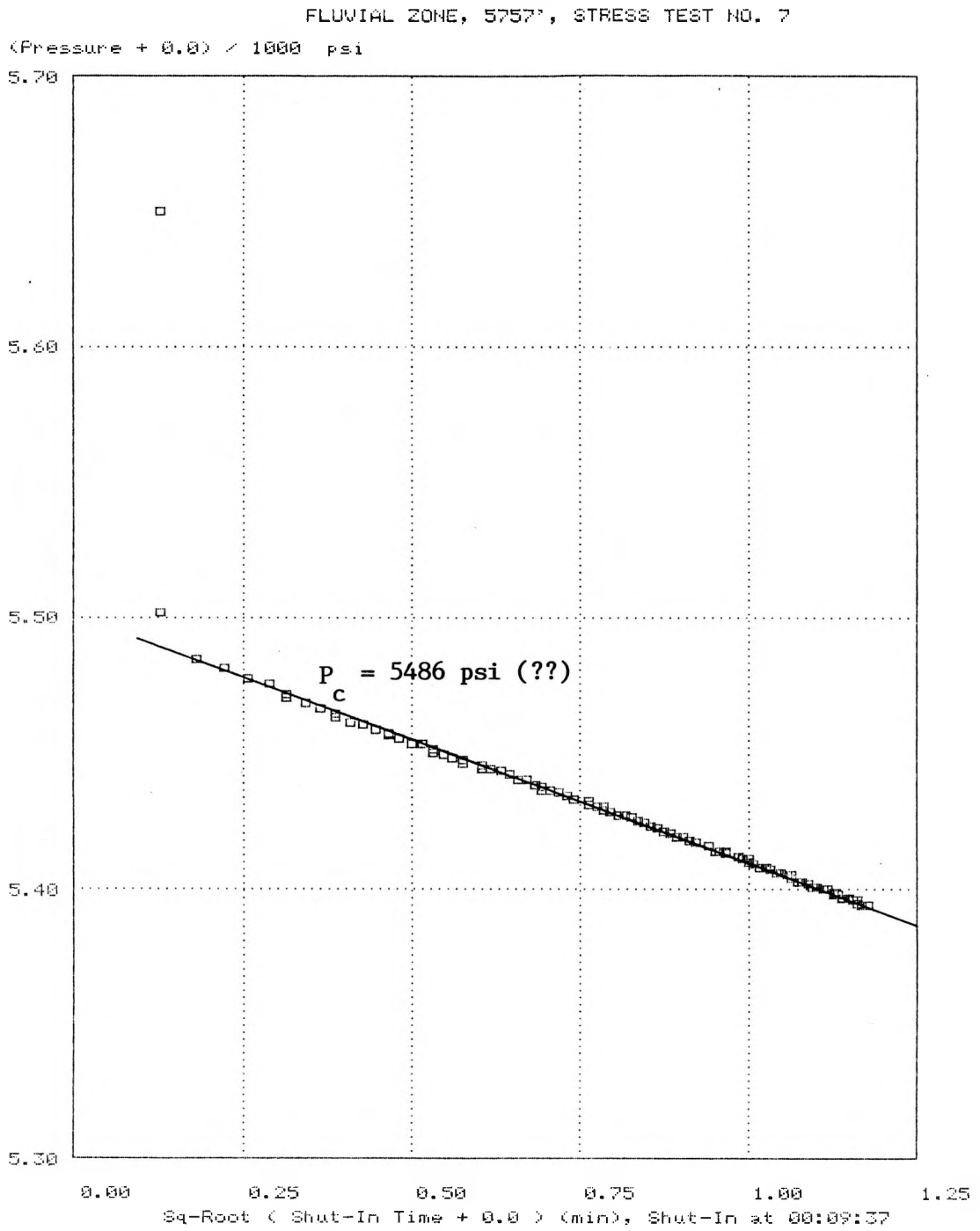


FIGURE A.195: Shale Stress Test (5757-5759'), Square-Root of Shut-In Time Plot of Test No. 7 Pressure Decline.

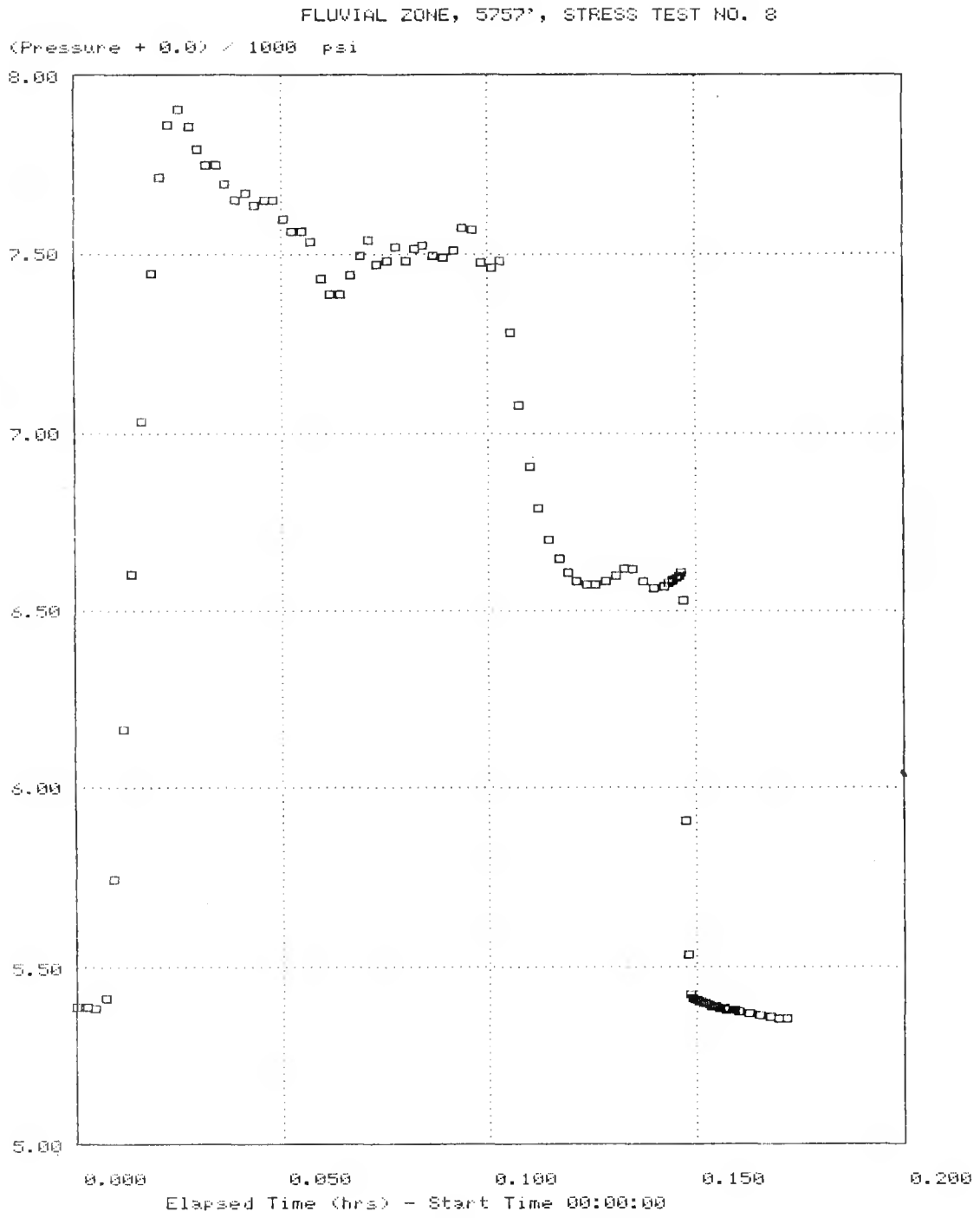


FIGURE A.196: Shale Stress Test (5757-5759'), Linear Plot of Test No. 8 Injection/Decline.

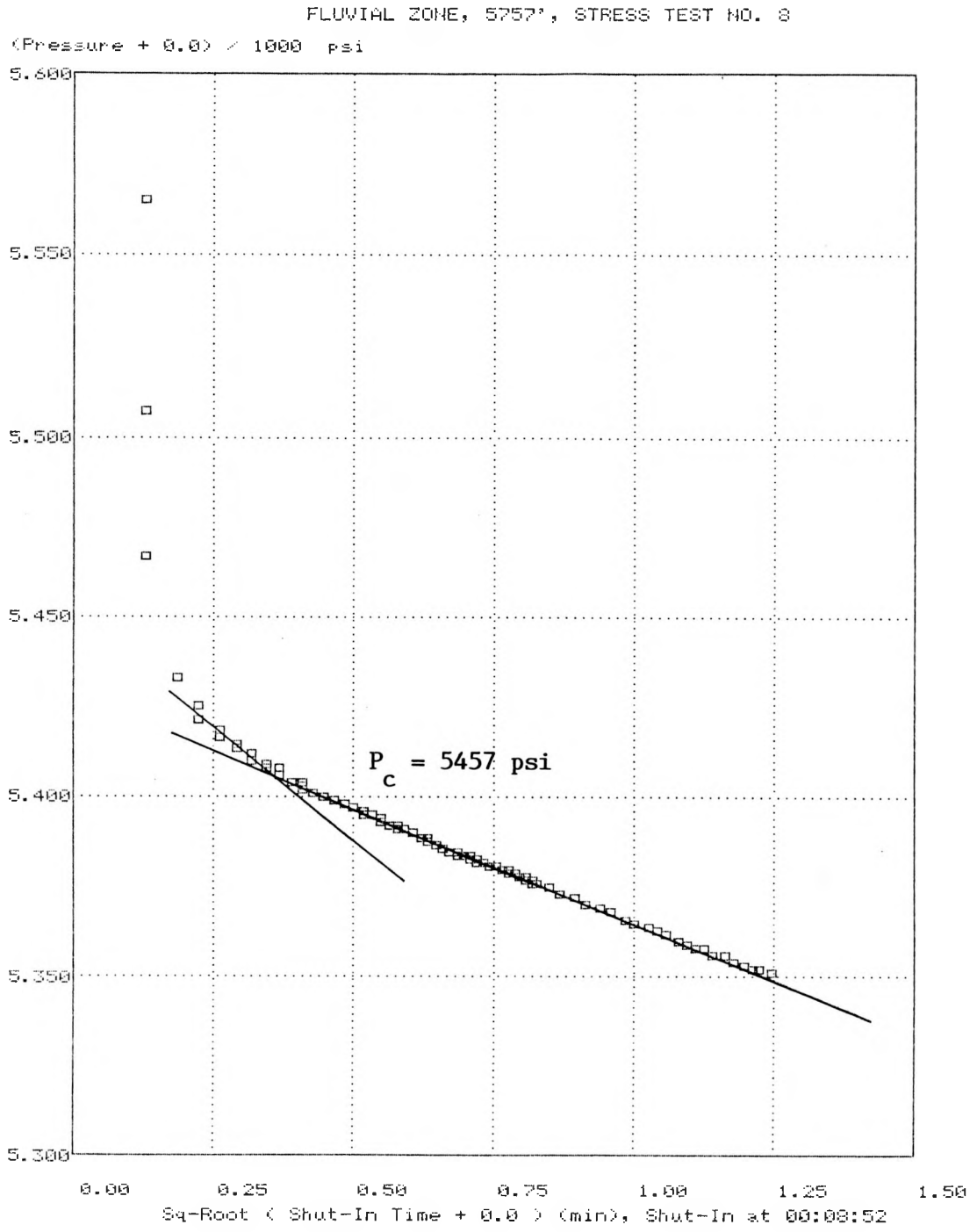


FIGURE A.197: Shale Stress Test (5757-5759') Square-Root of Shut-In Time Plot of Test No. 8 Pressure Decline.

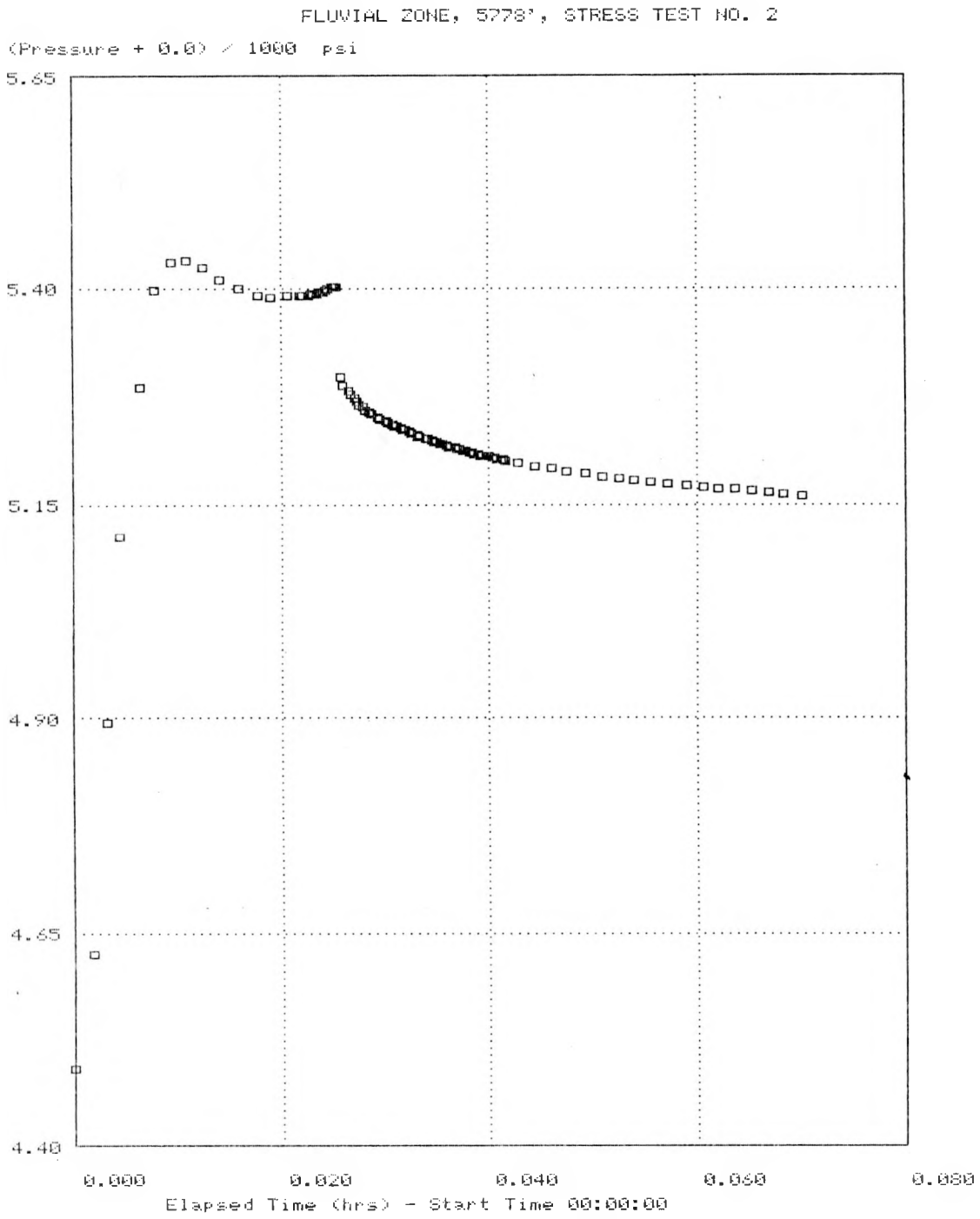


FIGURE A.198 Shale Stress Test (5778-5780'), Linear Plot of Test No. 2 Injection/Decline.

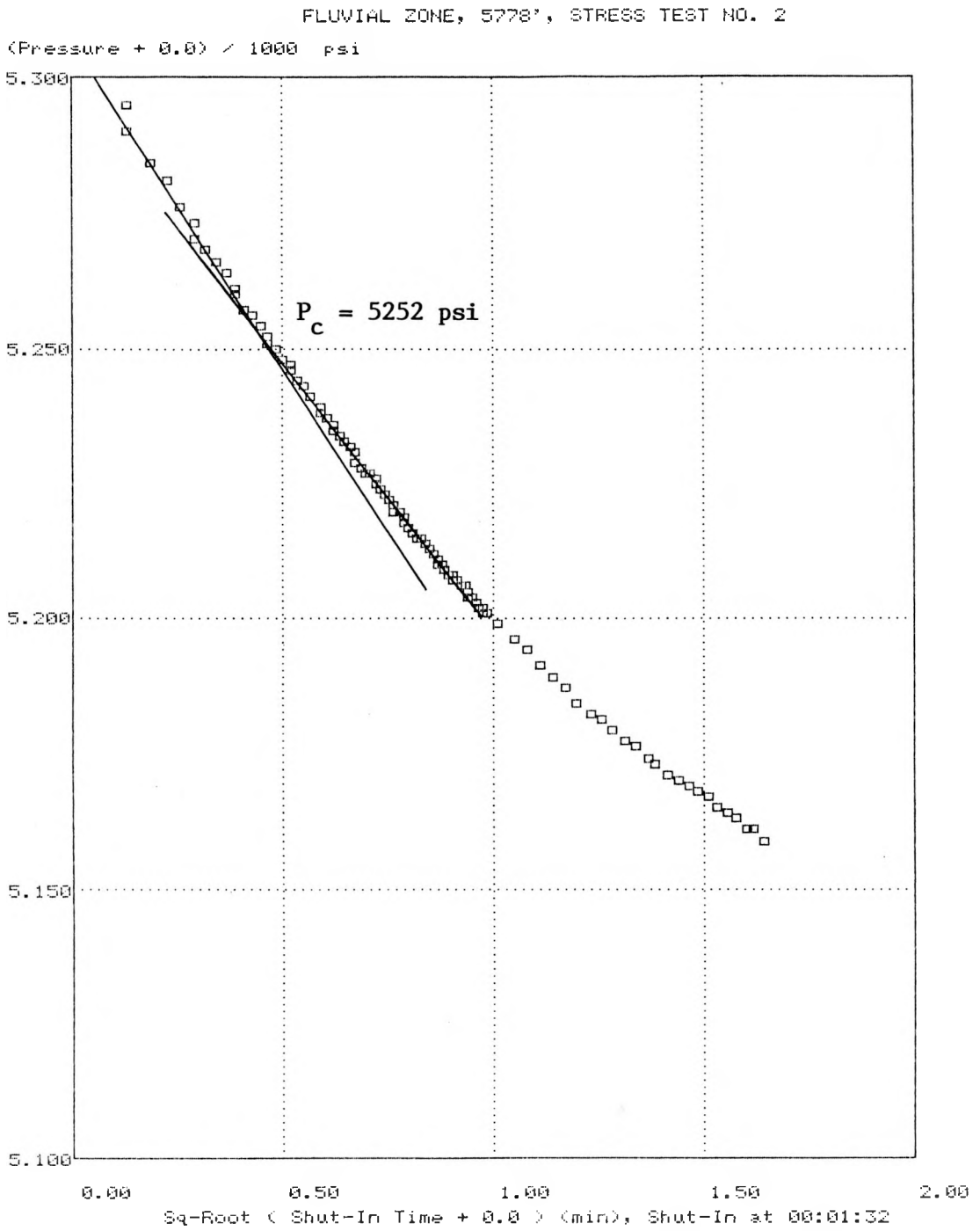


FIGURE A.199: Shale Stress Test (5778-5780'), Square-Root of Shut-In Time Plot of Test No. 2 Pressure Decline

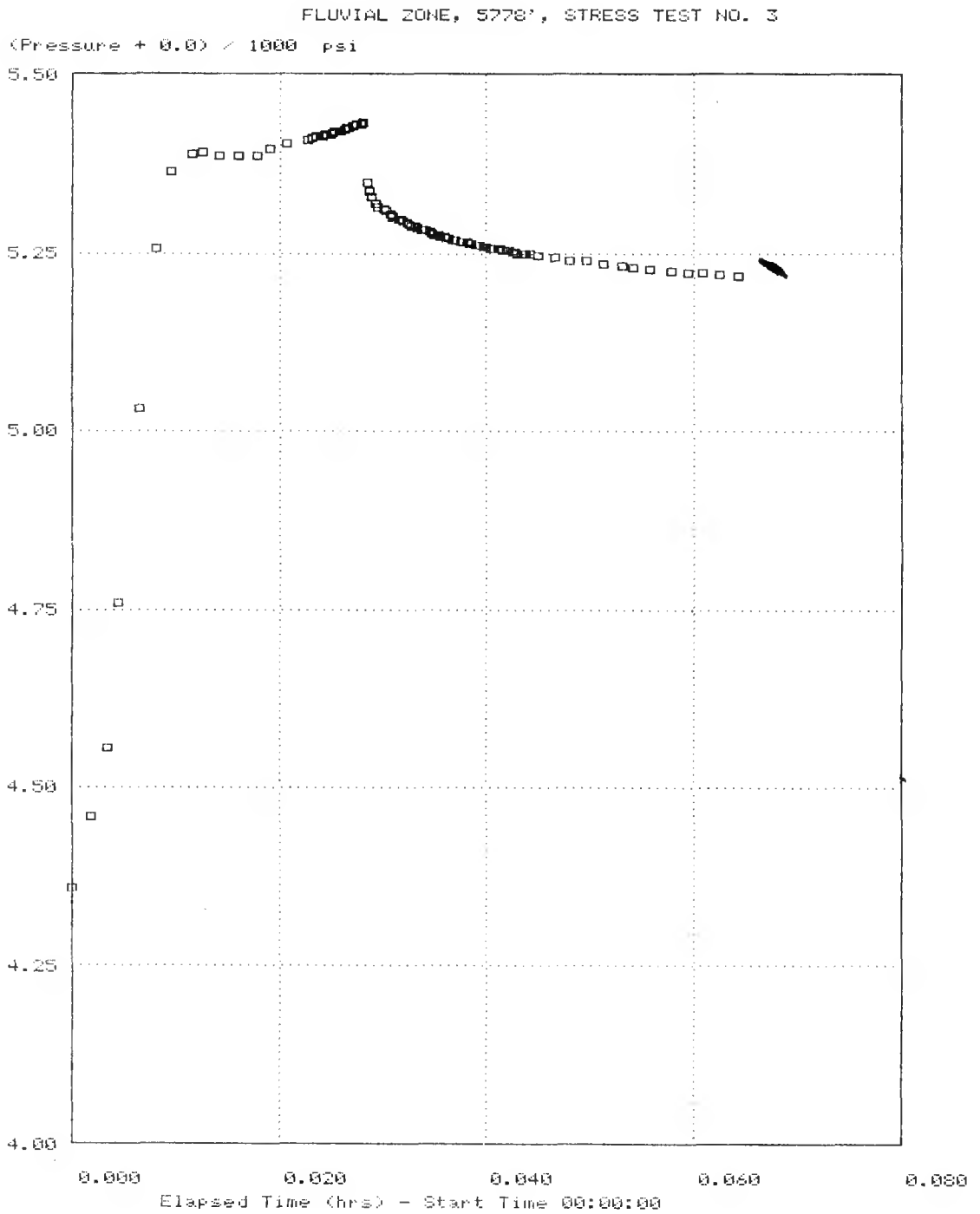


FIGURE A.200: Shale Stress Test (5778-5780'), Linear Plot of Test No. 3 Injection/Decline.

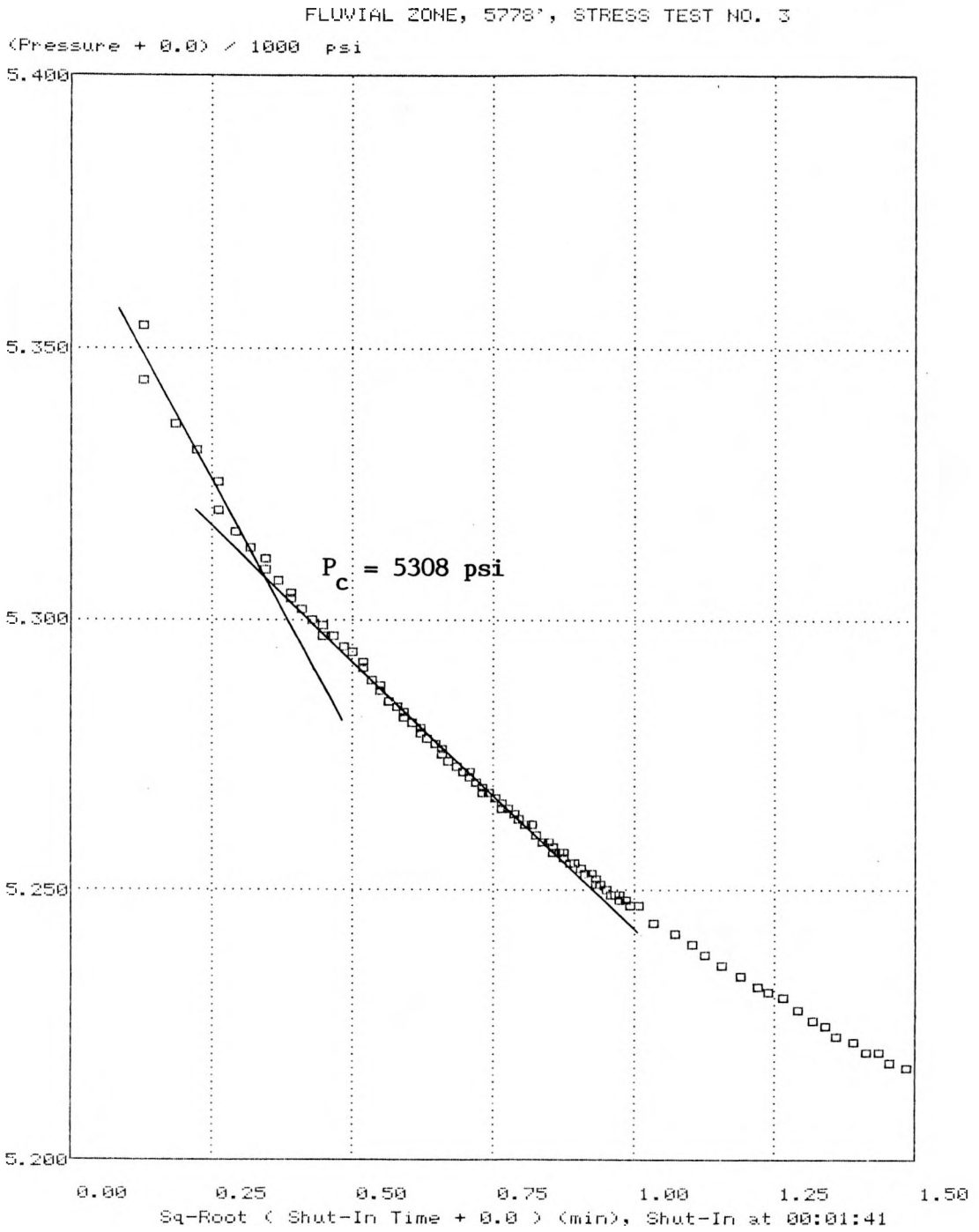


FIGURE A.201: Shale Stress Test (5778-5780'), Square-Root of Shut-In Time Plot of Test No. 3 Pressure Decline.

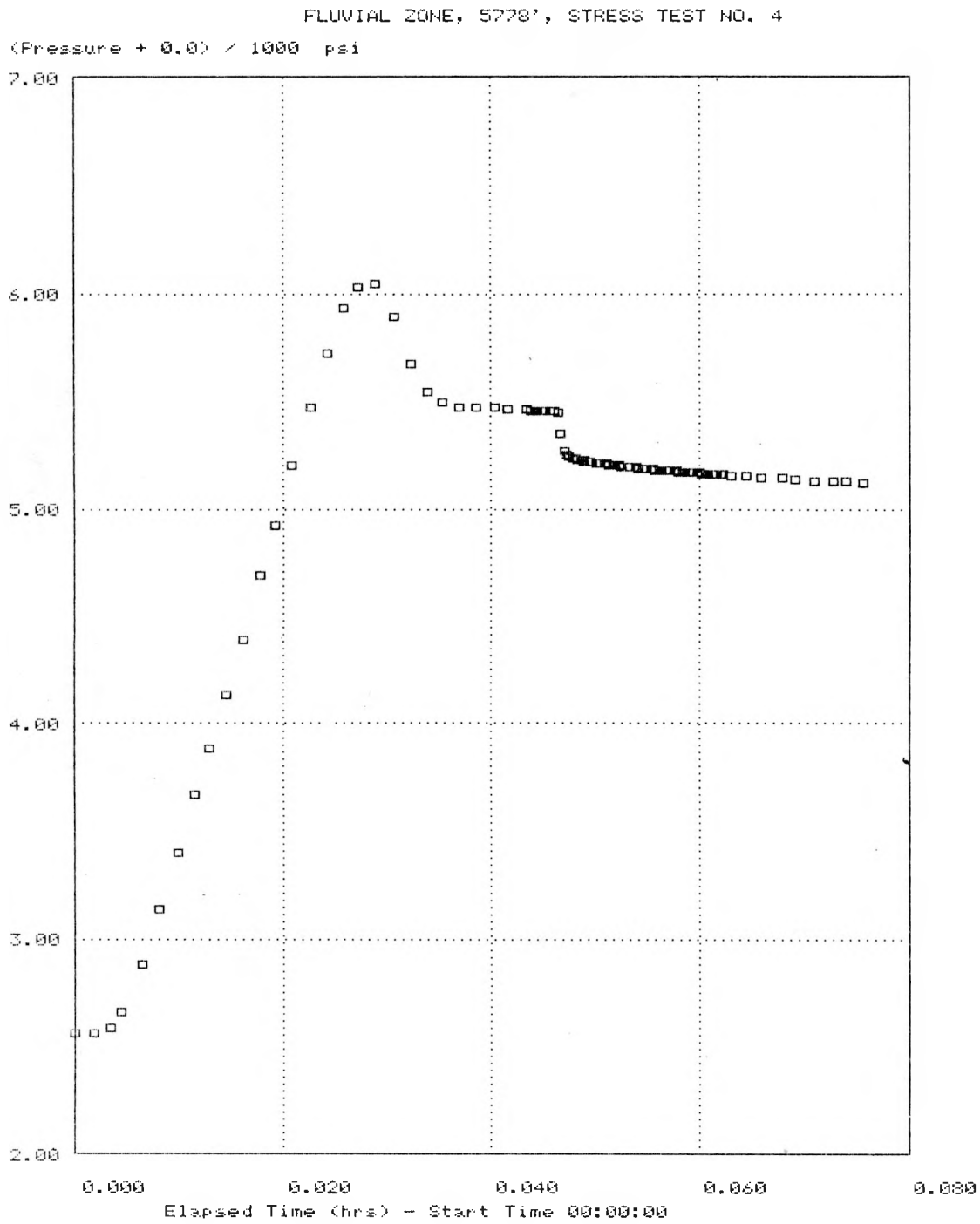


FIGURE A.202: Shale Stress Test (5778-5780'), Linear Plot of Test No. 4 Injection/Decline.

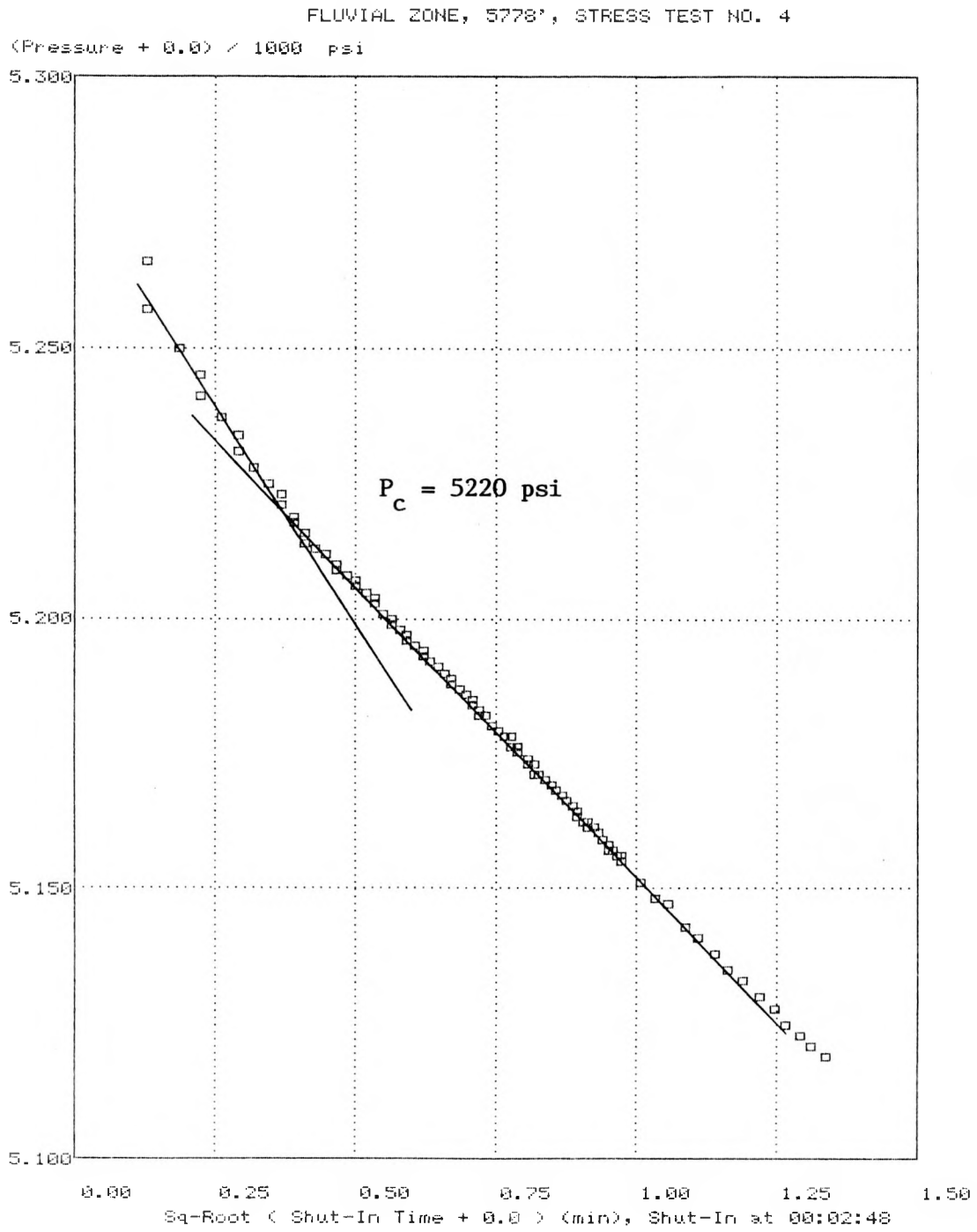


FIGURE A.203: Shale Stress Test (5778-5780'), Square-Root of Shut-In Time Plot of Test No. 4 Pressure Decline.

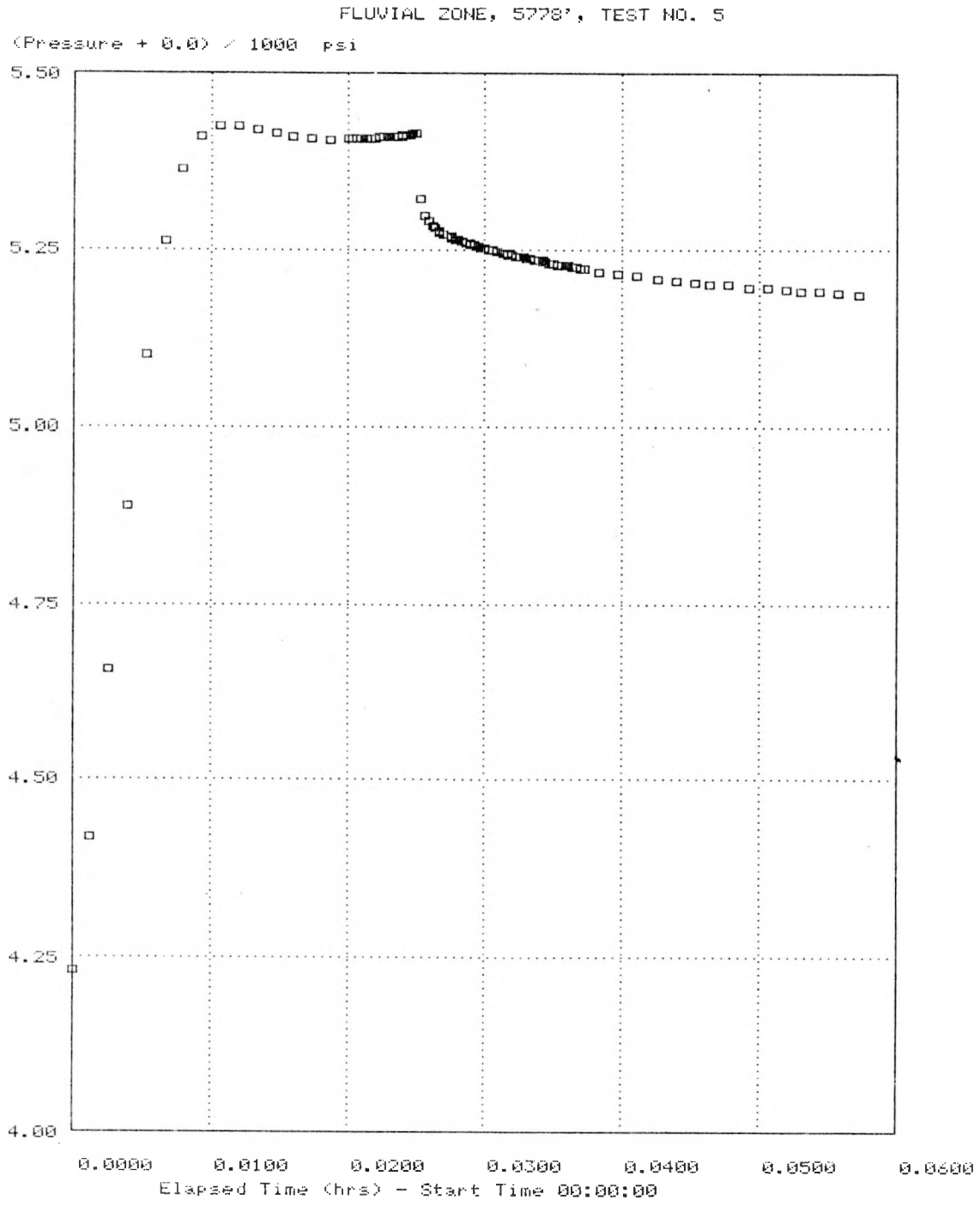


FIGURE A.204: Shale Stress Test (5778-5780'), Linear Plot of Test No. 5 Injection/Decline.

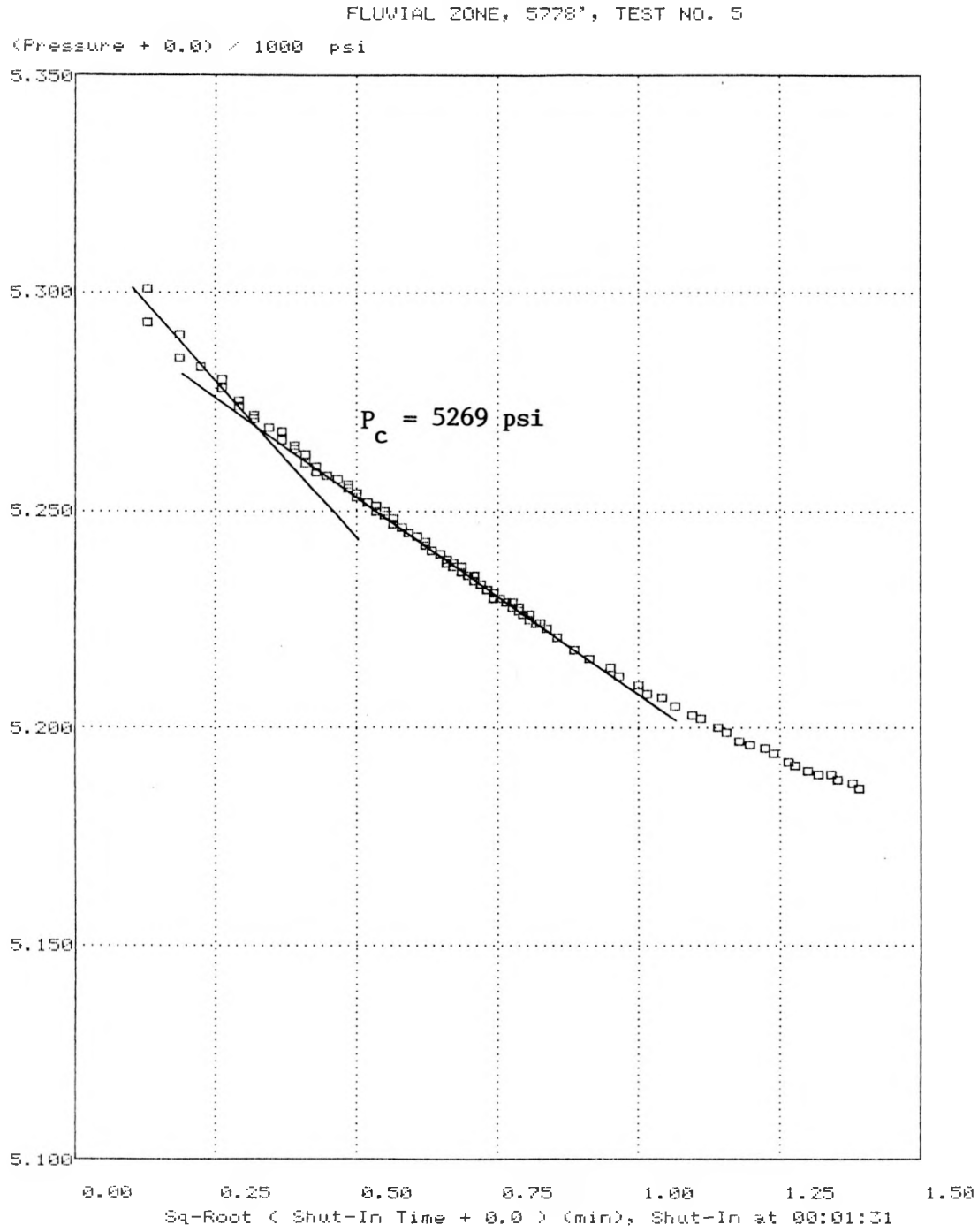


FIGURE A.205: Shale Stress Test (5778-5780'), Square-Root of Shut-In Time Plot of Test No. 5 Pressure Decline.

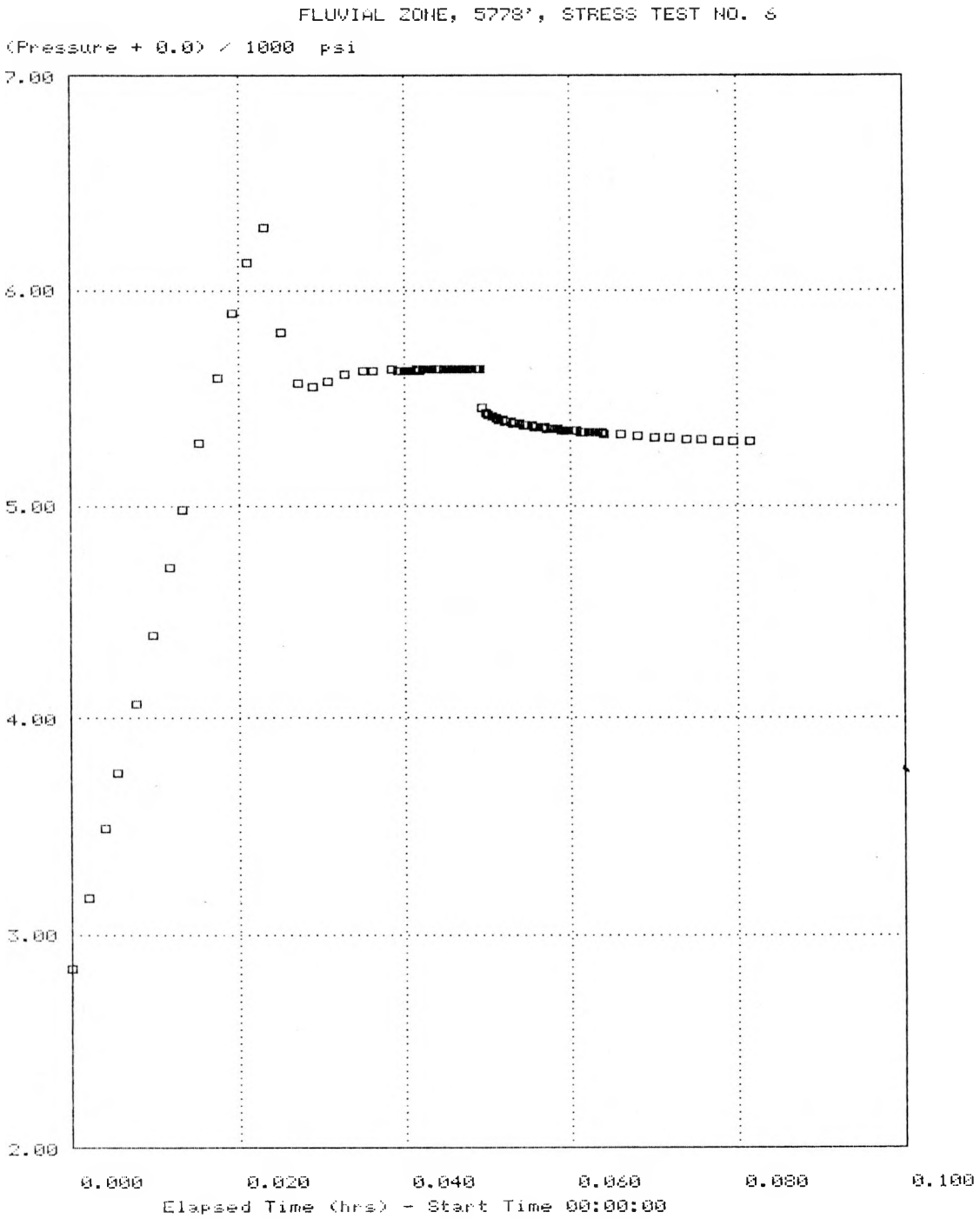


FIGURE A.206: Shale Stress Test (5778-5780'), Linear Plot of Test No. 6 Injection/Decline.

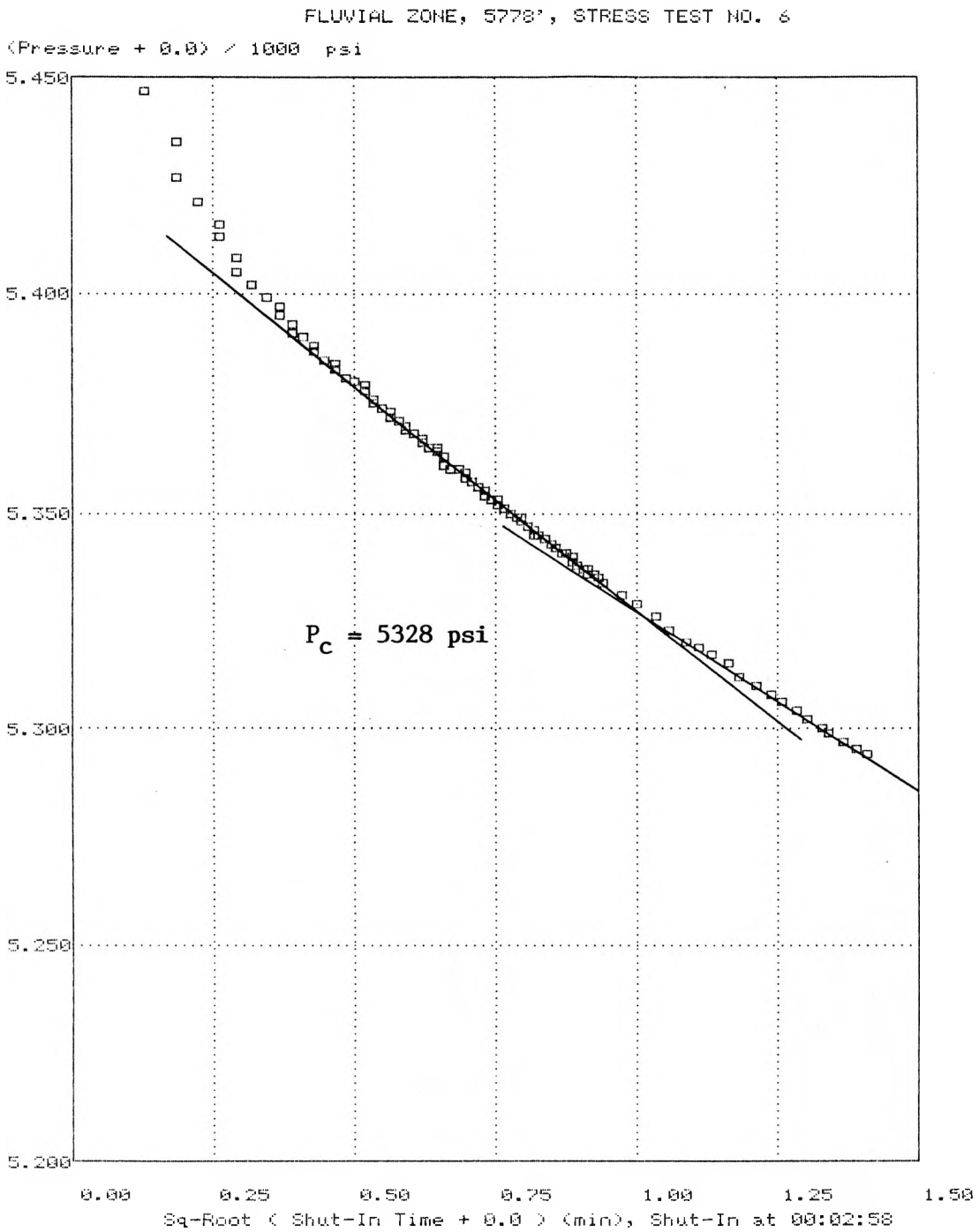


FIGURE A.207: Shale Stress Test (5778-5780'), Square-Root of Shut-In Time Plot of Test No. 6 Pressure Decline.

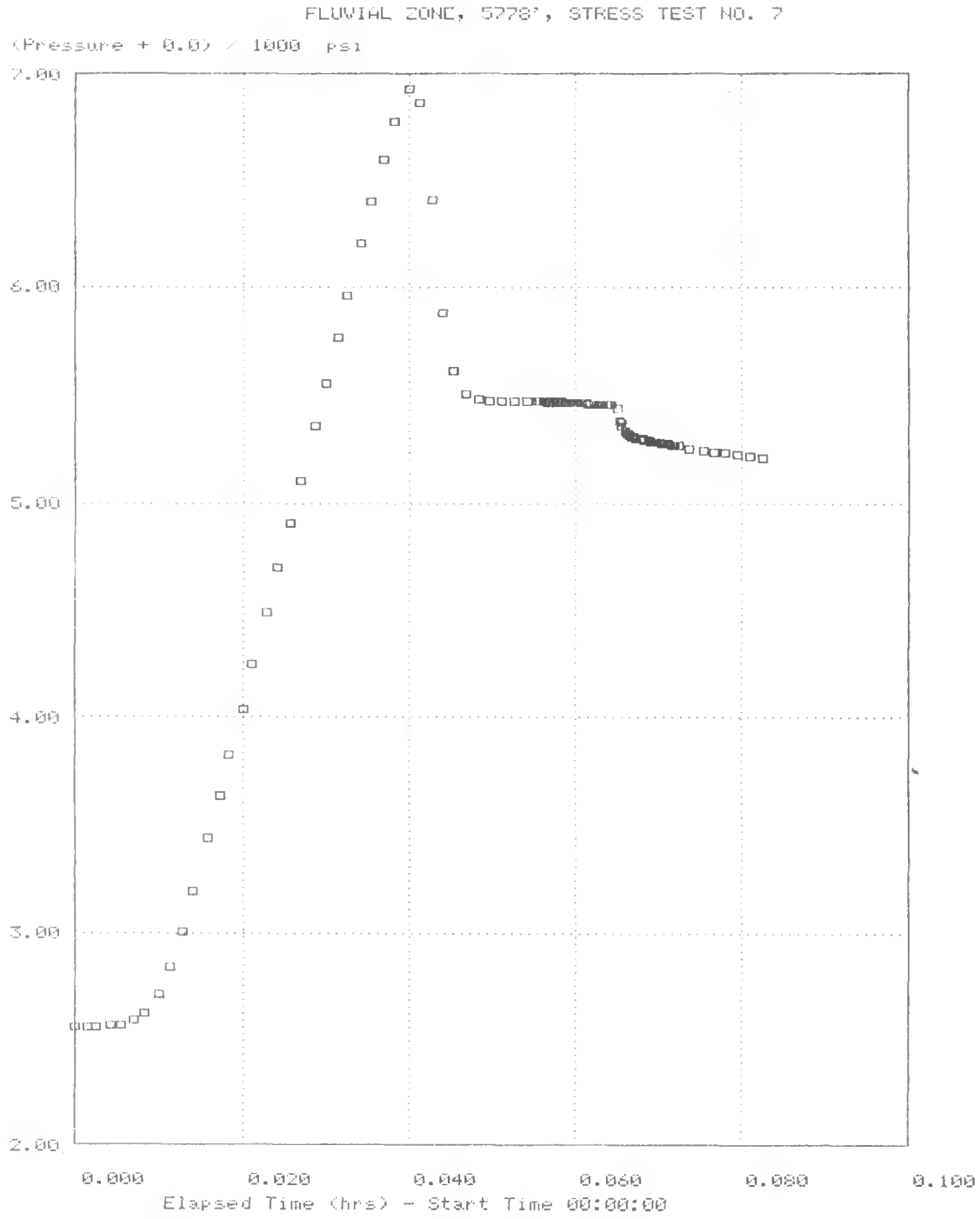


FIGURE A.208: Shale Stress Test (5778–5780'), Linear Plot of Test No. 7 Injection/Decline.

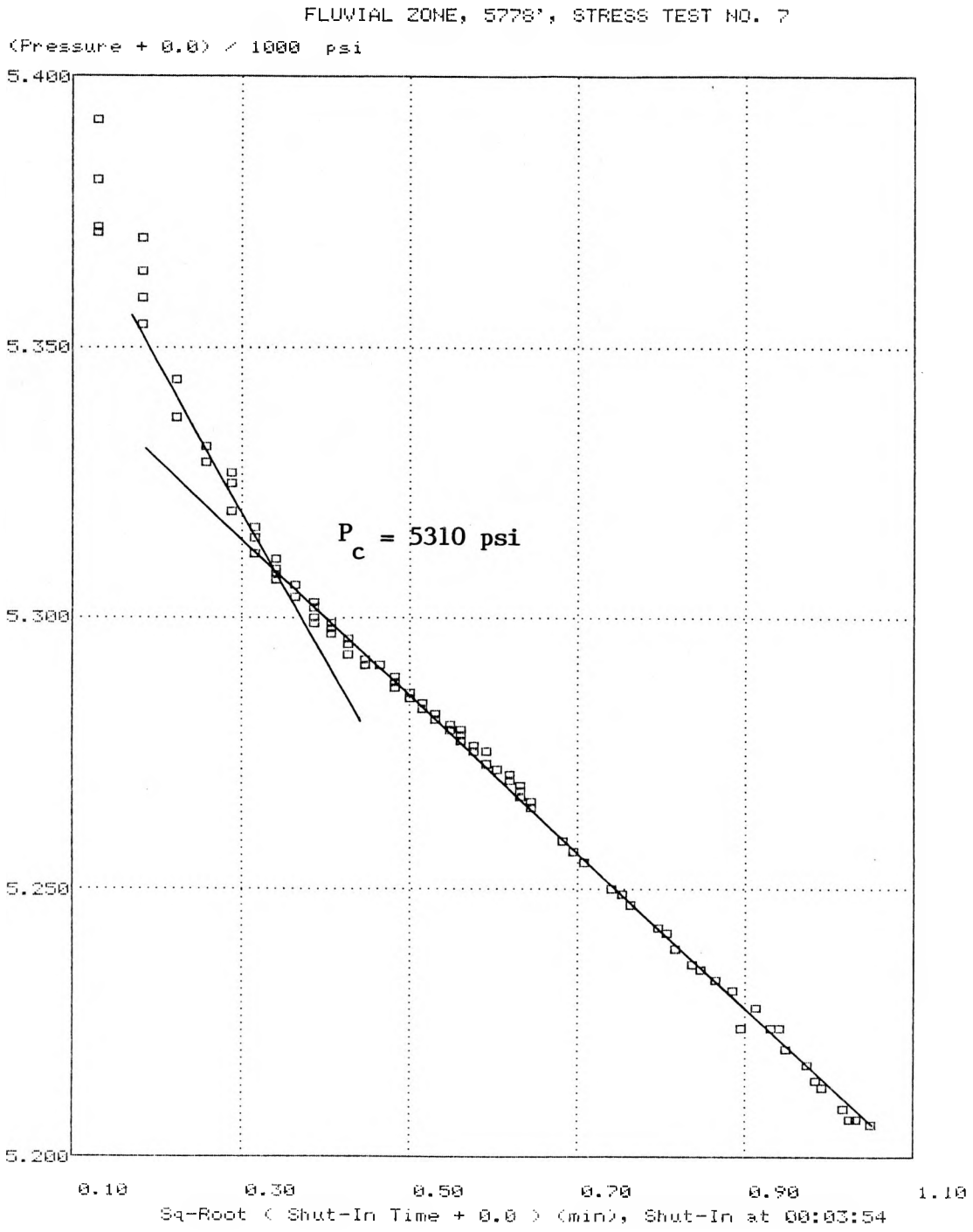


FIGURE A.209: Shale Stress Test (5778-5780'), Square Root of Shut-In Time Plot of Test No. 7 Pressure Decline.

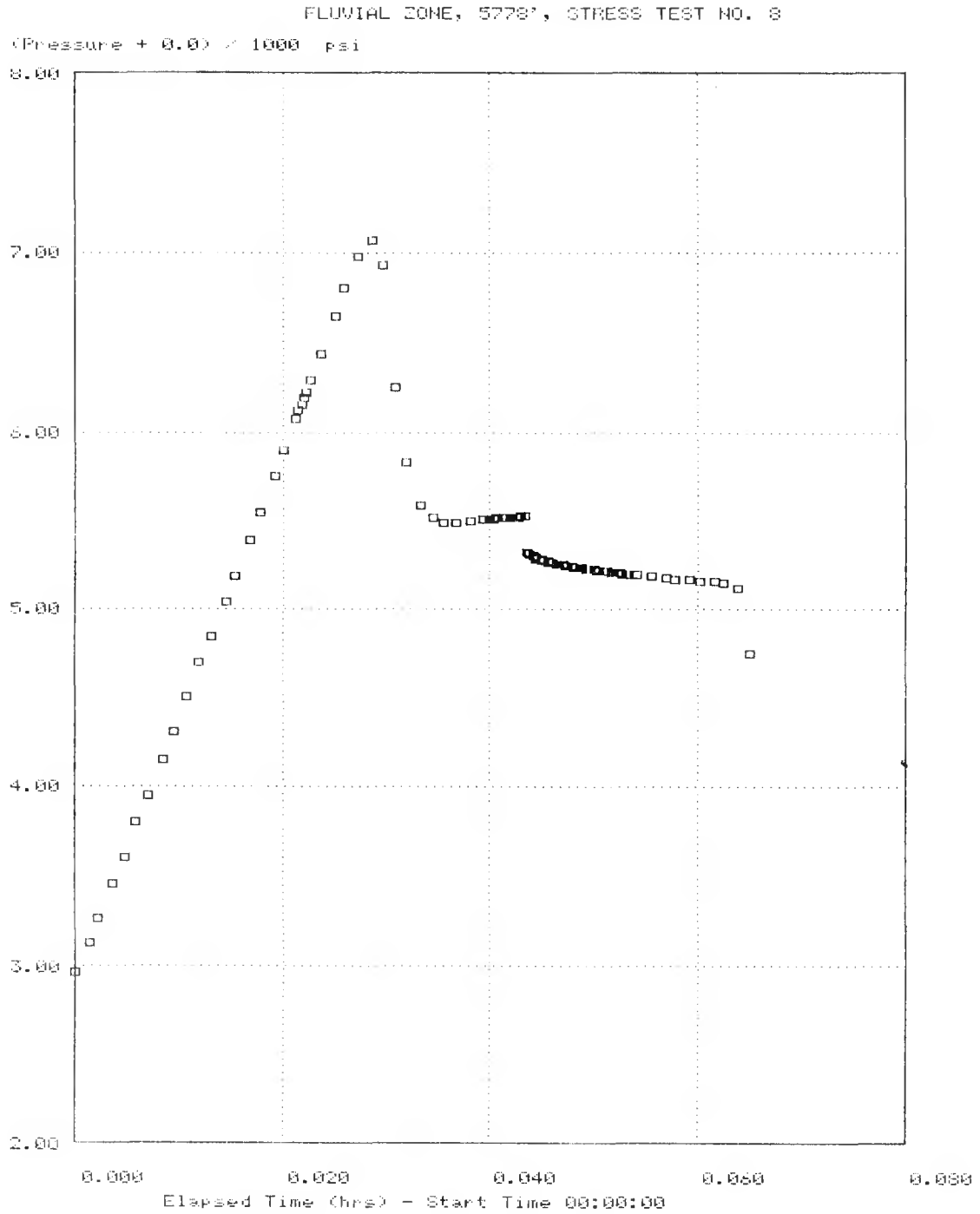


FIGURE A.210: Shale Stress Test (5778-5780'), Linear Plot of Test No. 8 Injection/Decline.

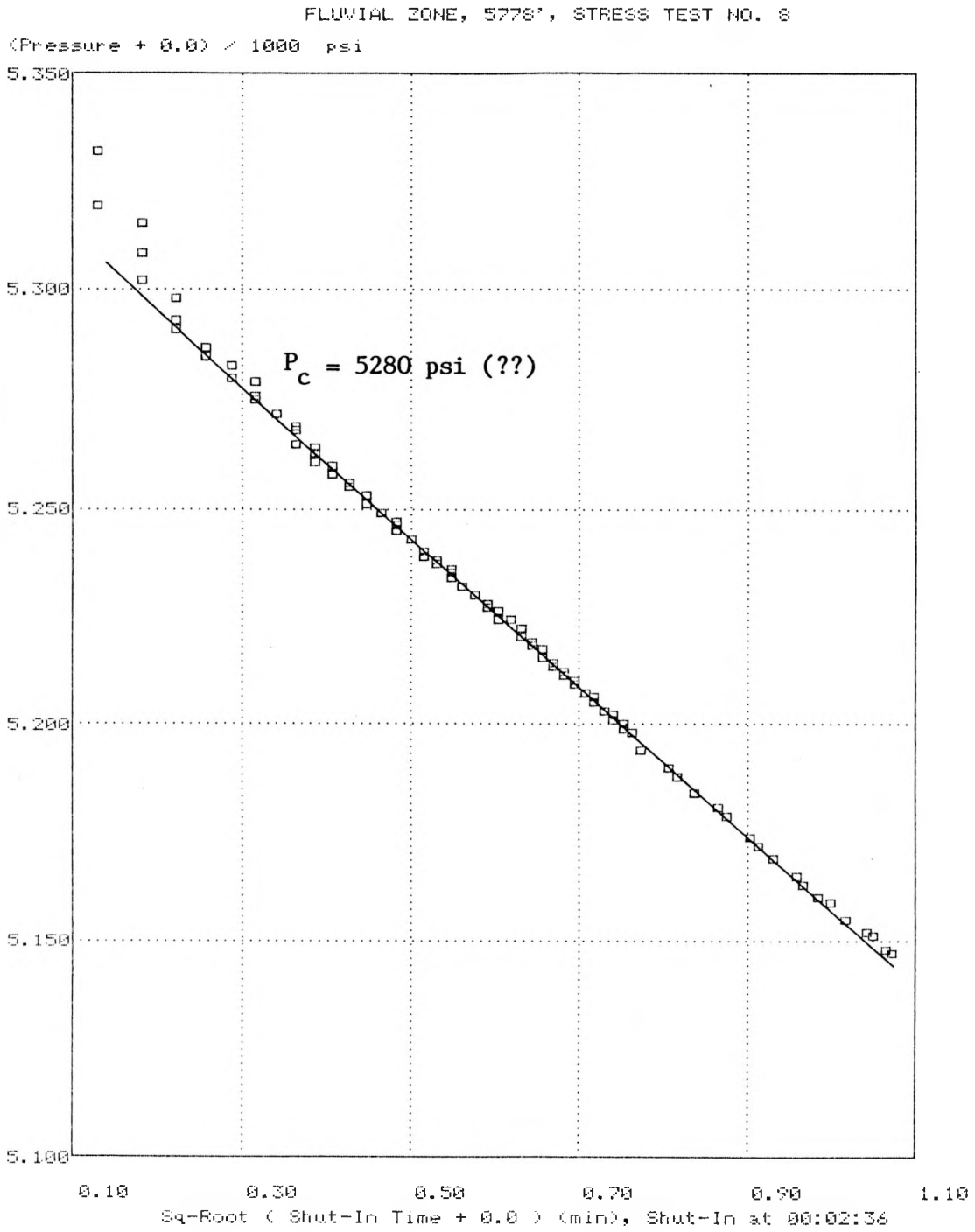


FIGURE A.211: Shale Stress Test (5778-5780'), Square-Root of Shut-In Time Plot of Test No. 8 Pressure Decline.

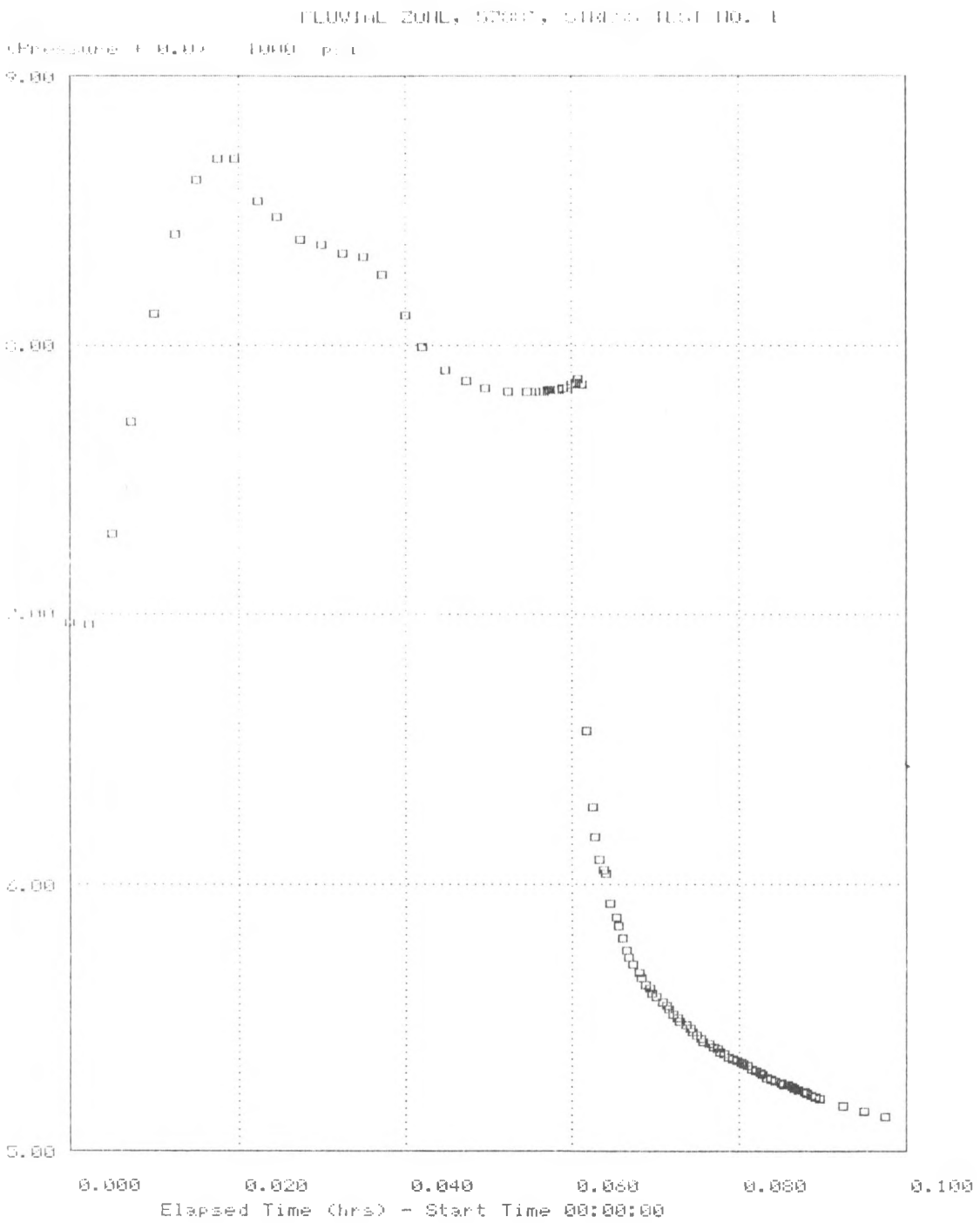


FIGURE A.212: Shale Stress Test (5788-5790'), Linear Plot of Test No. 1 Injection/Decline.

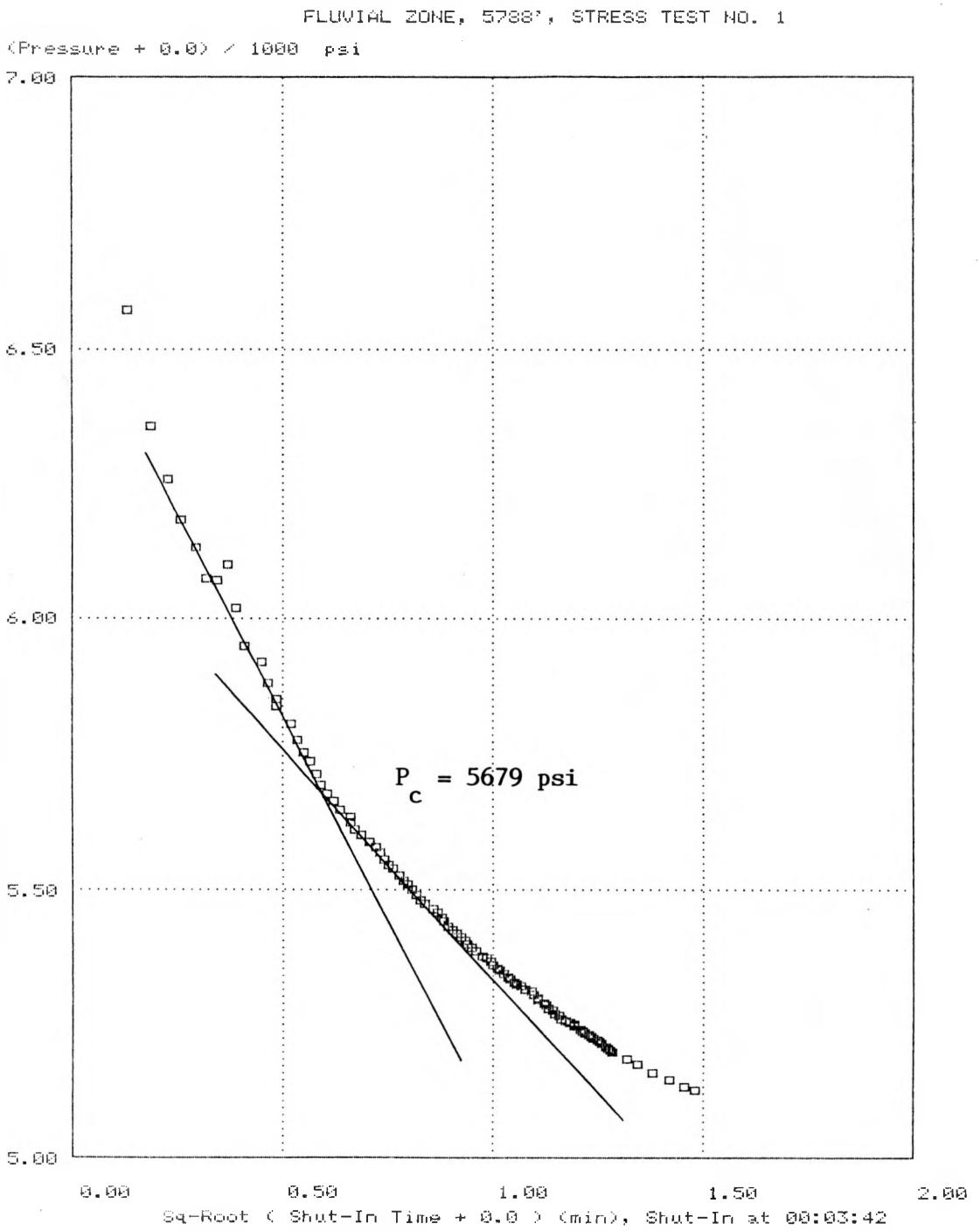


FIGURE A.213: Shale Stress Test (5788-5790'), Square-Root of Shut-In Time Plot of Test No. 1 Pressure Decline.

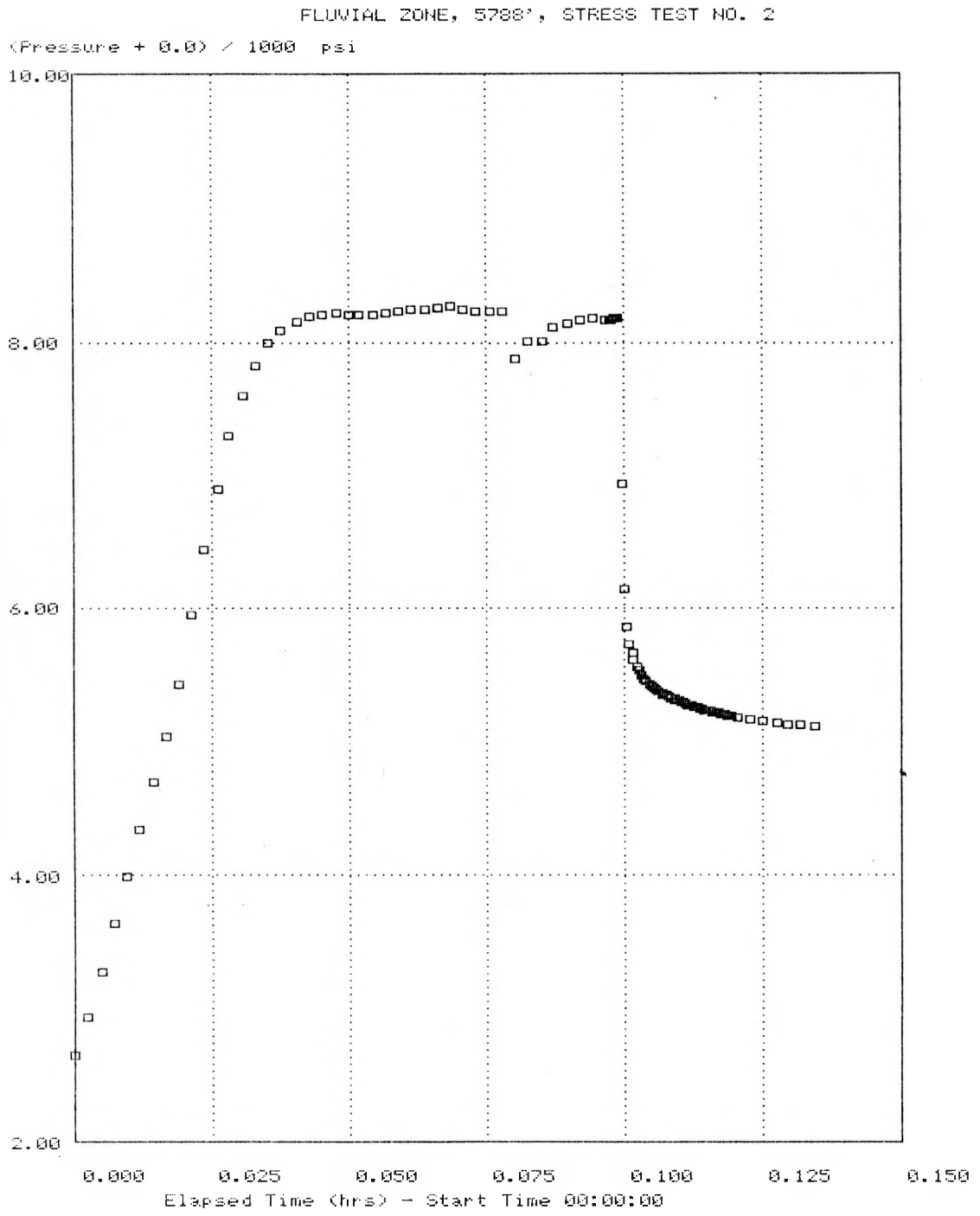


FIGURE A.214: Shale Stress Test (5788-5790'), Linear Plot of Test No. 2 Injection/Decline.

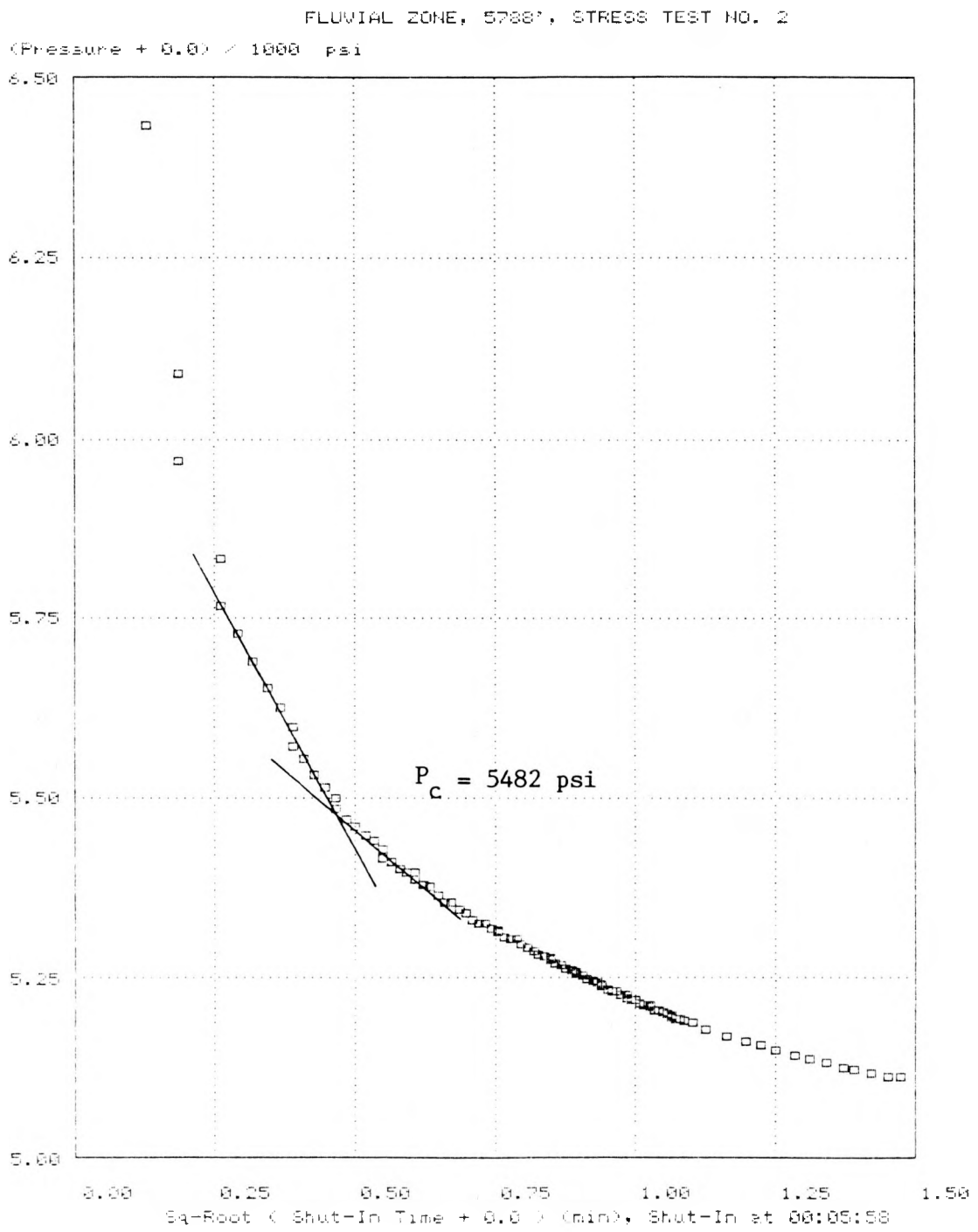


FIGURE A.215: Shale Stress Test (5788-5790'), Square-Root of Shut-In Time Plot of Test No. 2 Pressure Decline.

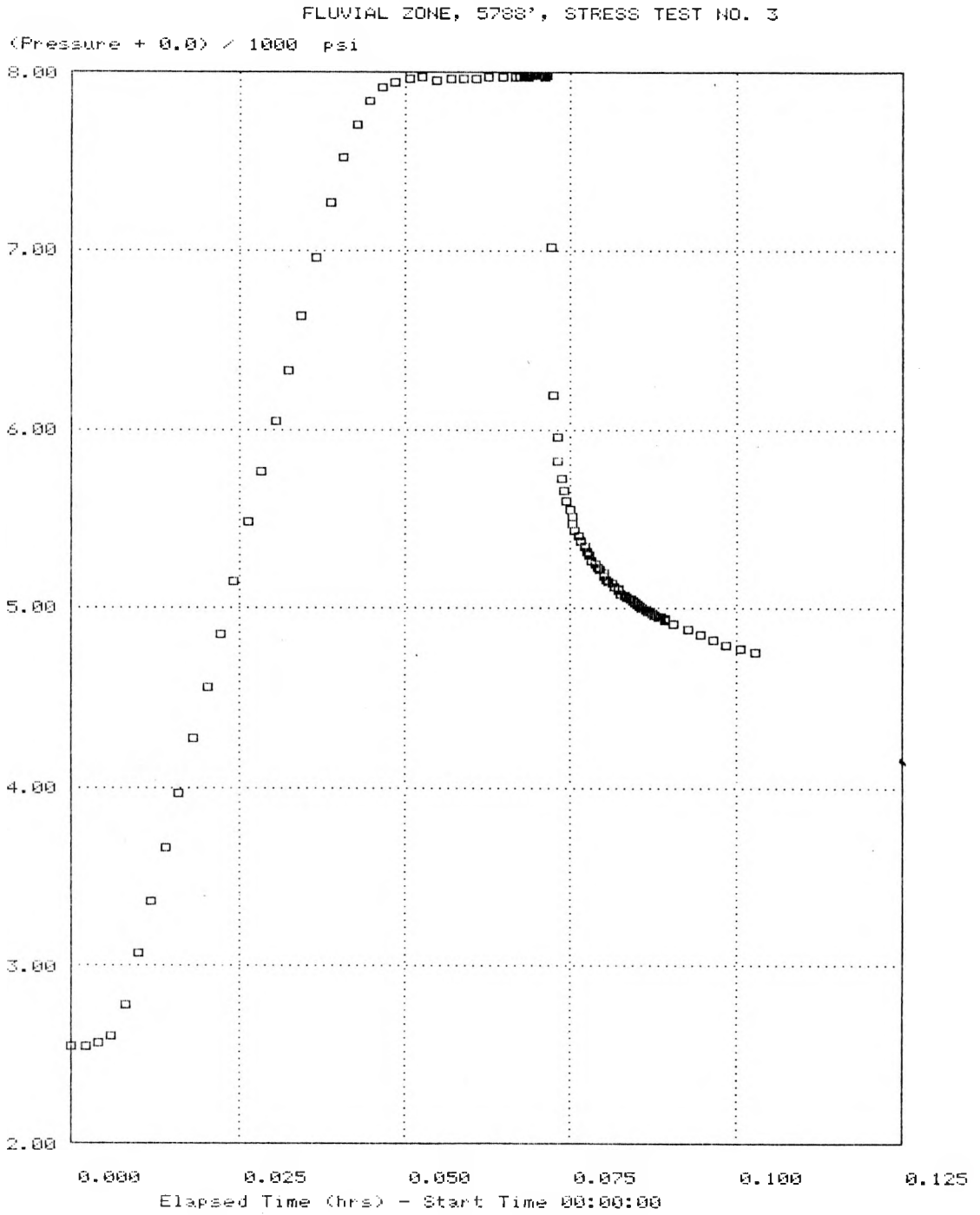


FIGURE A.216: Shale Stress Test (5788-5790'), Linear Plot of Test No. 3 Injection/Decline.

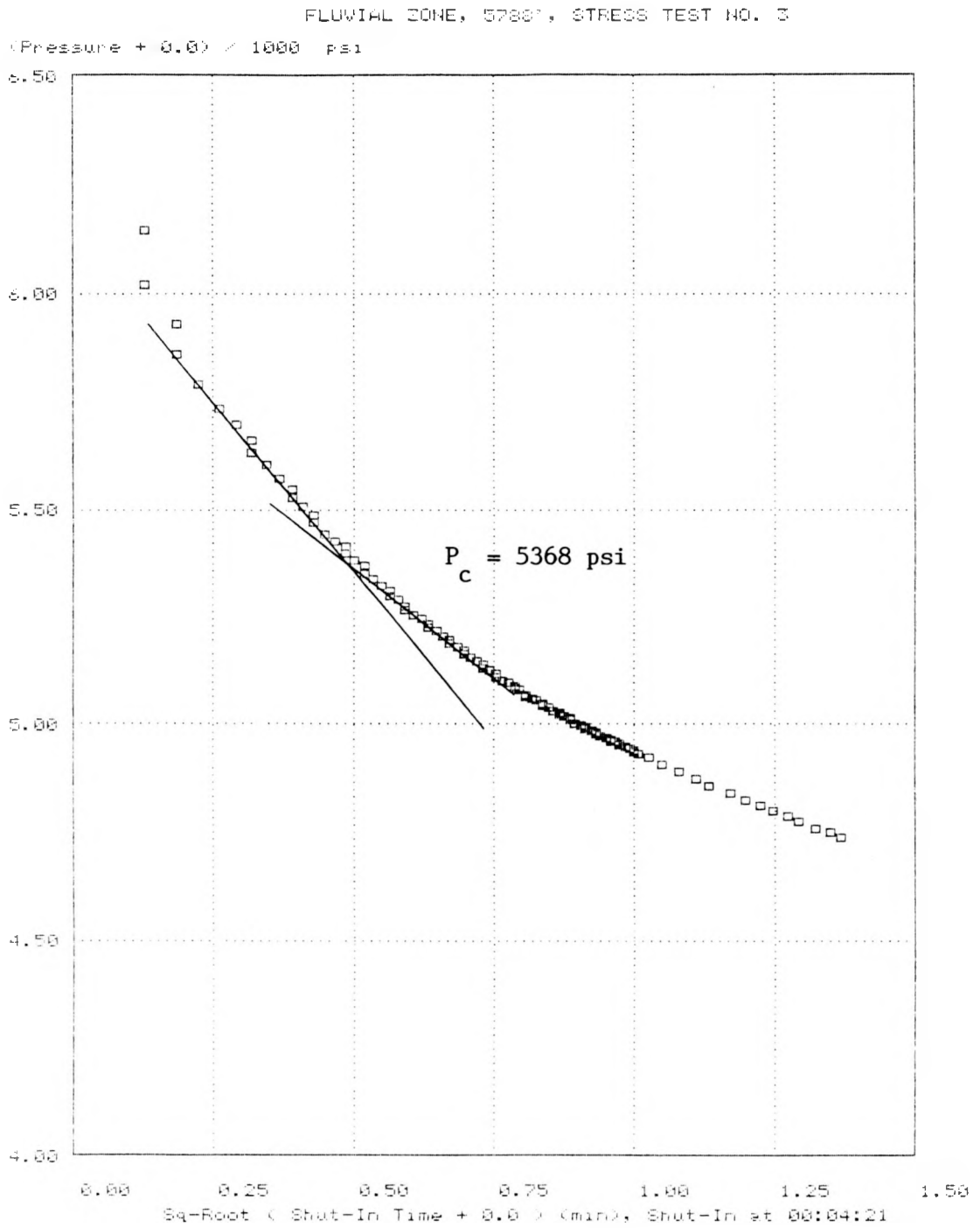


FIGURE A.217: Shale Stress Test (5788-5790'), Square-Root of Shut-In Time Plot of Test No. 3 Pressure Decline.

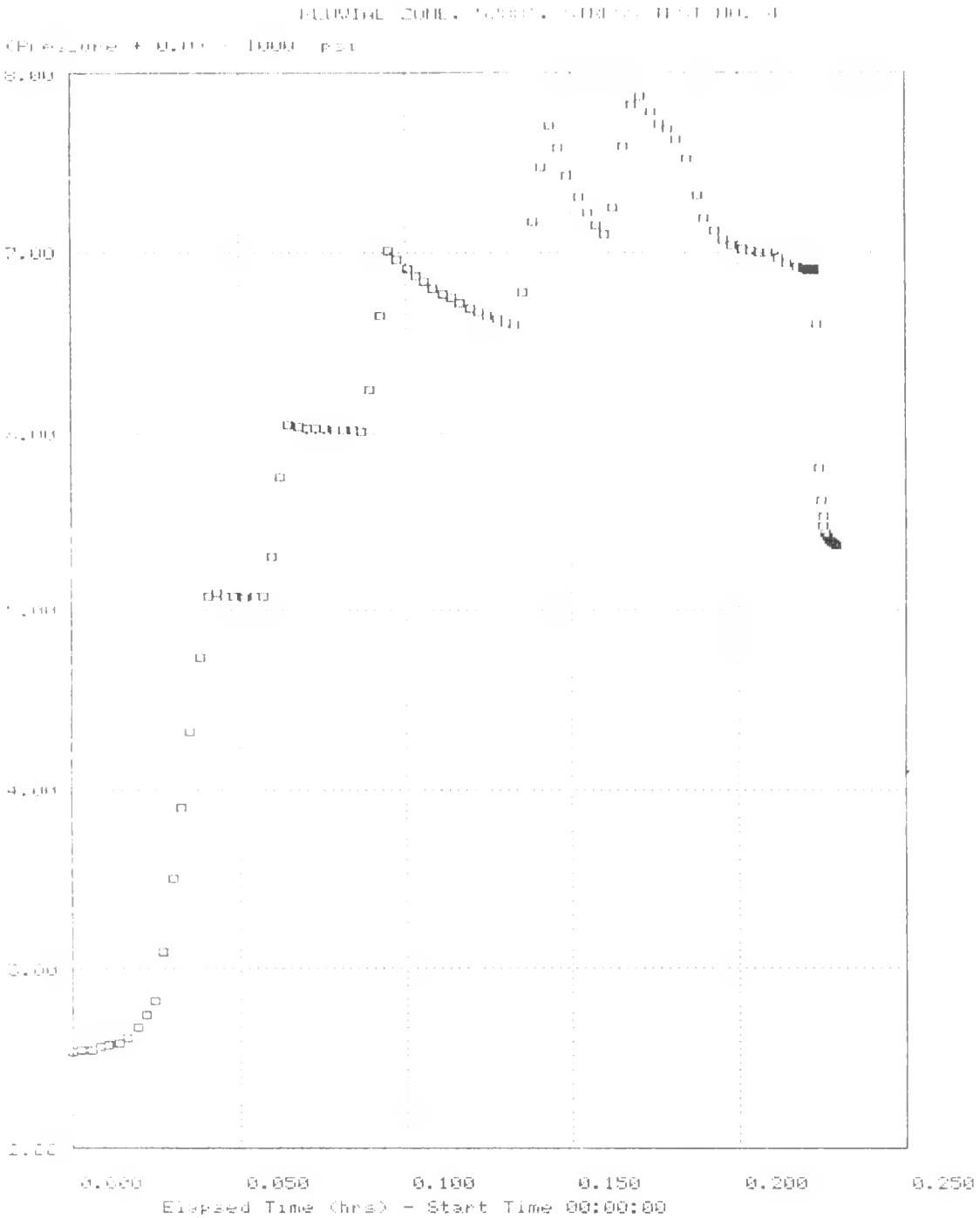


FIGURE A.218: Shale Stress Test (5788-5790'), Linear Plot of Test No. 4 Injection/Decline.

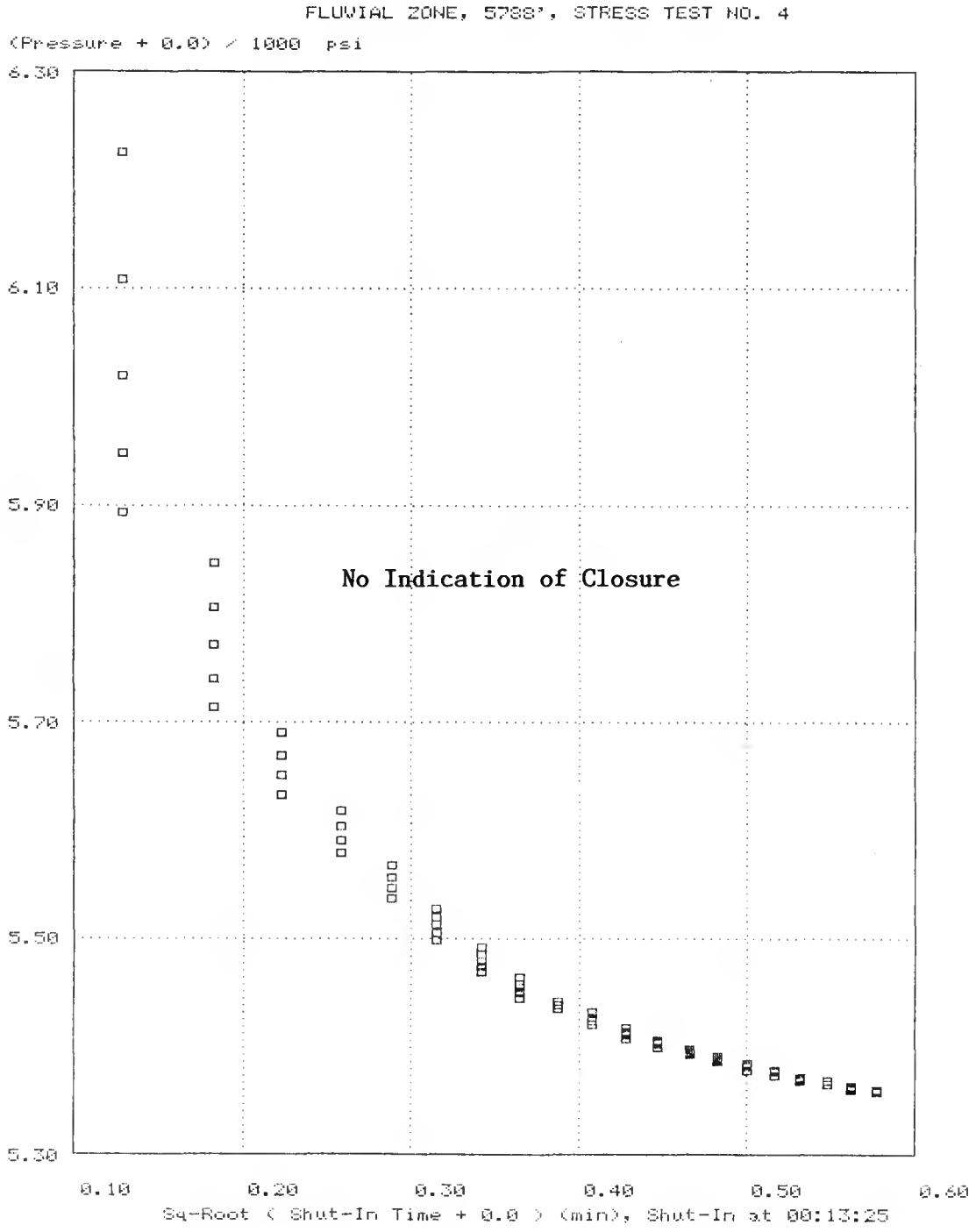


FIGURE A.219: Shale Stress Test (5788-5790'), Square-Root of Shut-In Time Plot of Test No. 4 Pressure Decline.

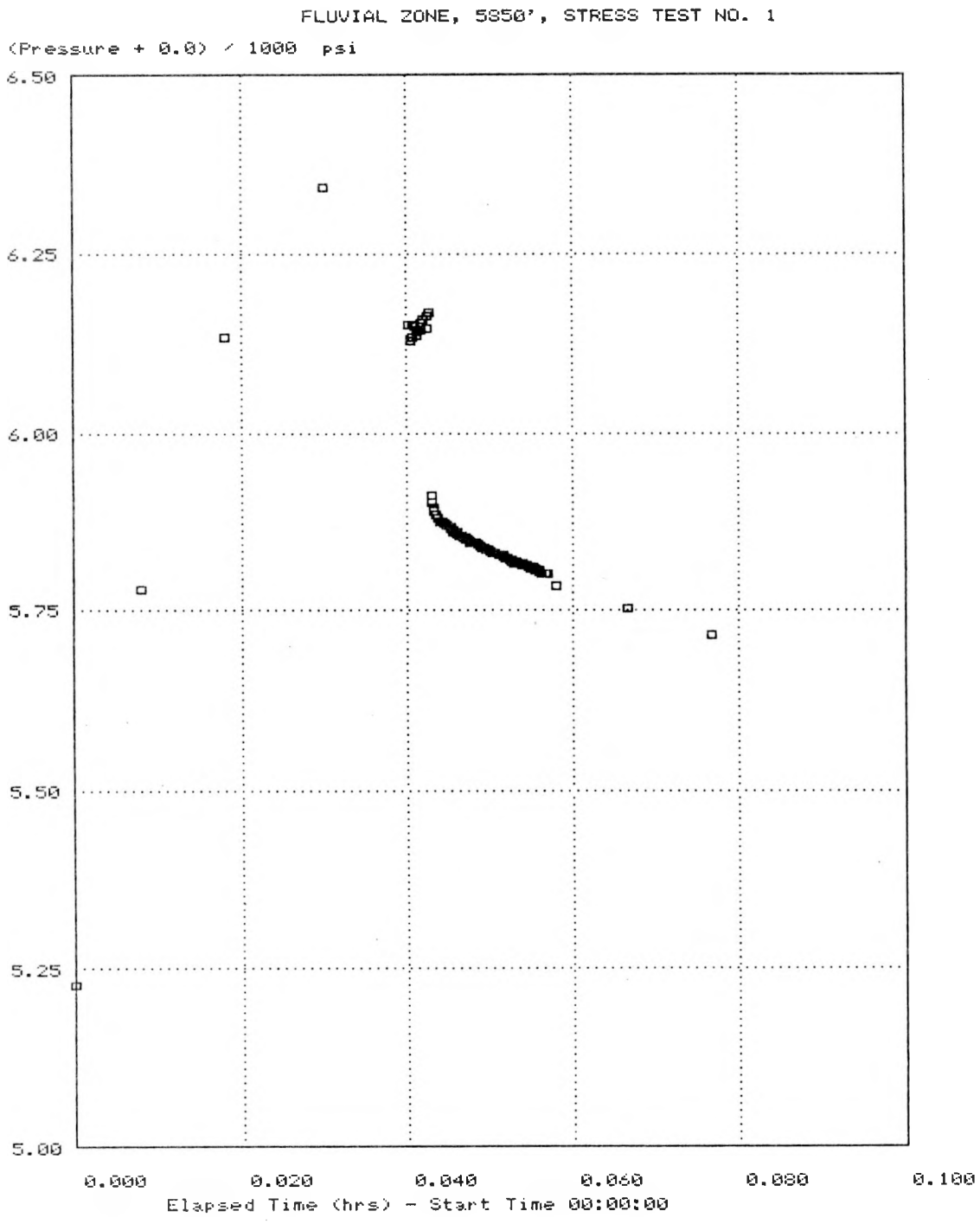


FIGURE A.220: Shale Stress Test (5850–5852'), Linear Plot of Test No. 1 Injection/Decline.

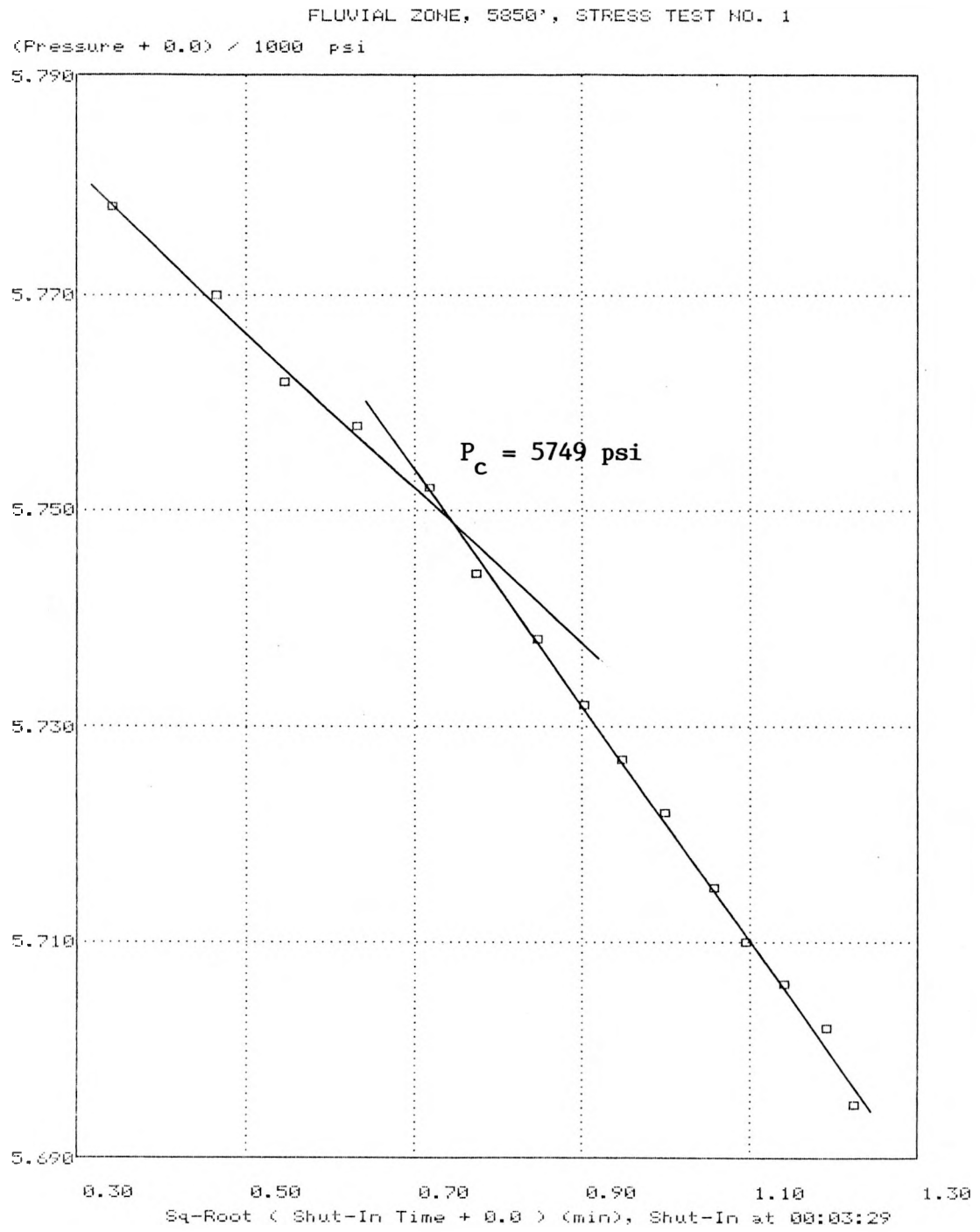


FIGURE A.221: Shale Stress Test (5850-5852'), Square-Root of Shut-In Time Plot of Test No. 1 Pressure Decline.

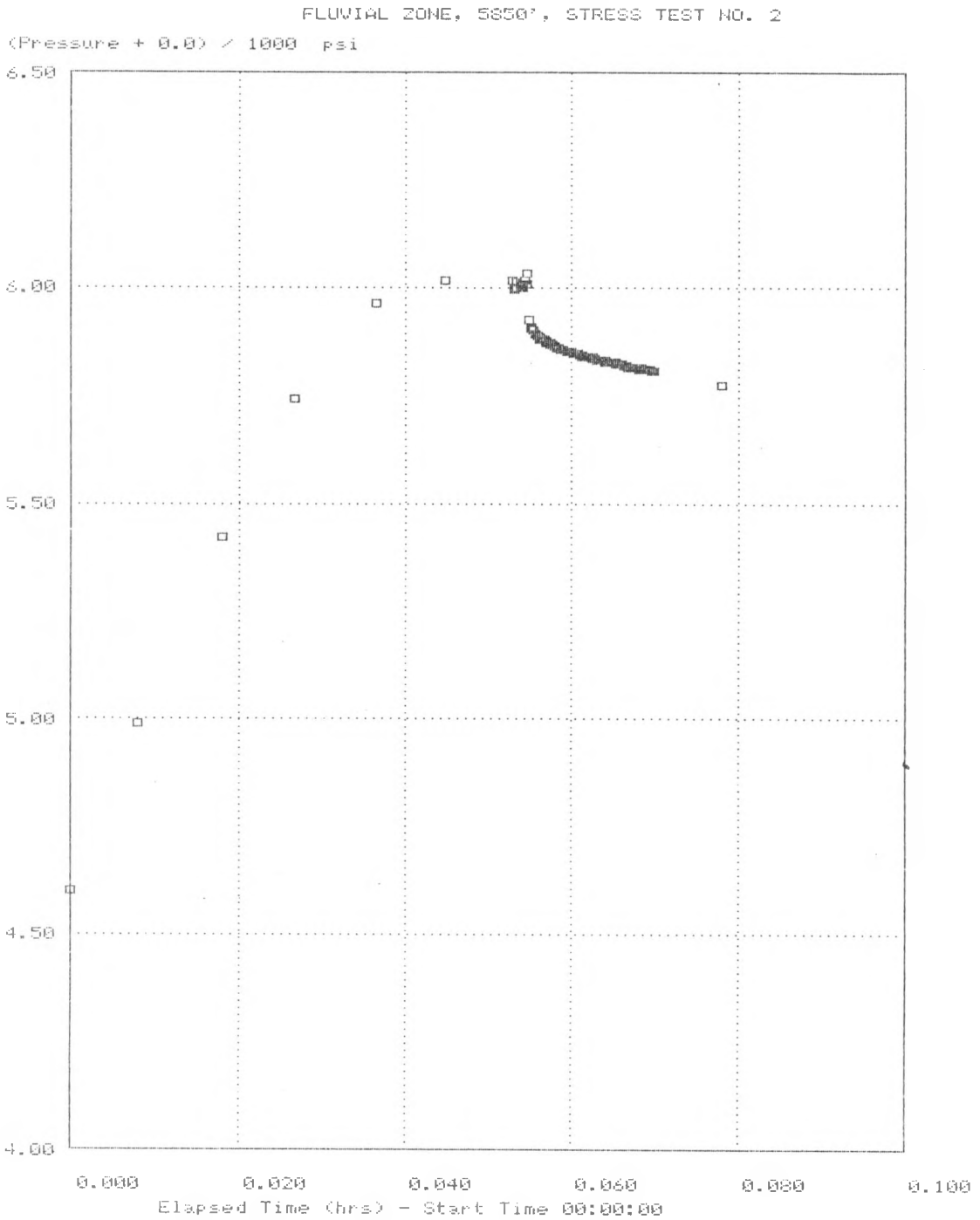


FIGURE A.222: Shale Stress Test (5850–5852'), Linear Plot of Test No. 2 Injection/Decline.

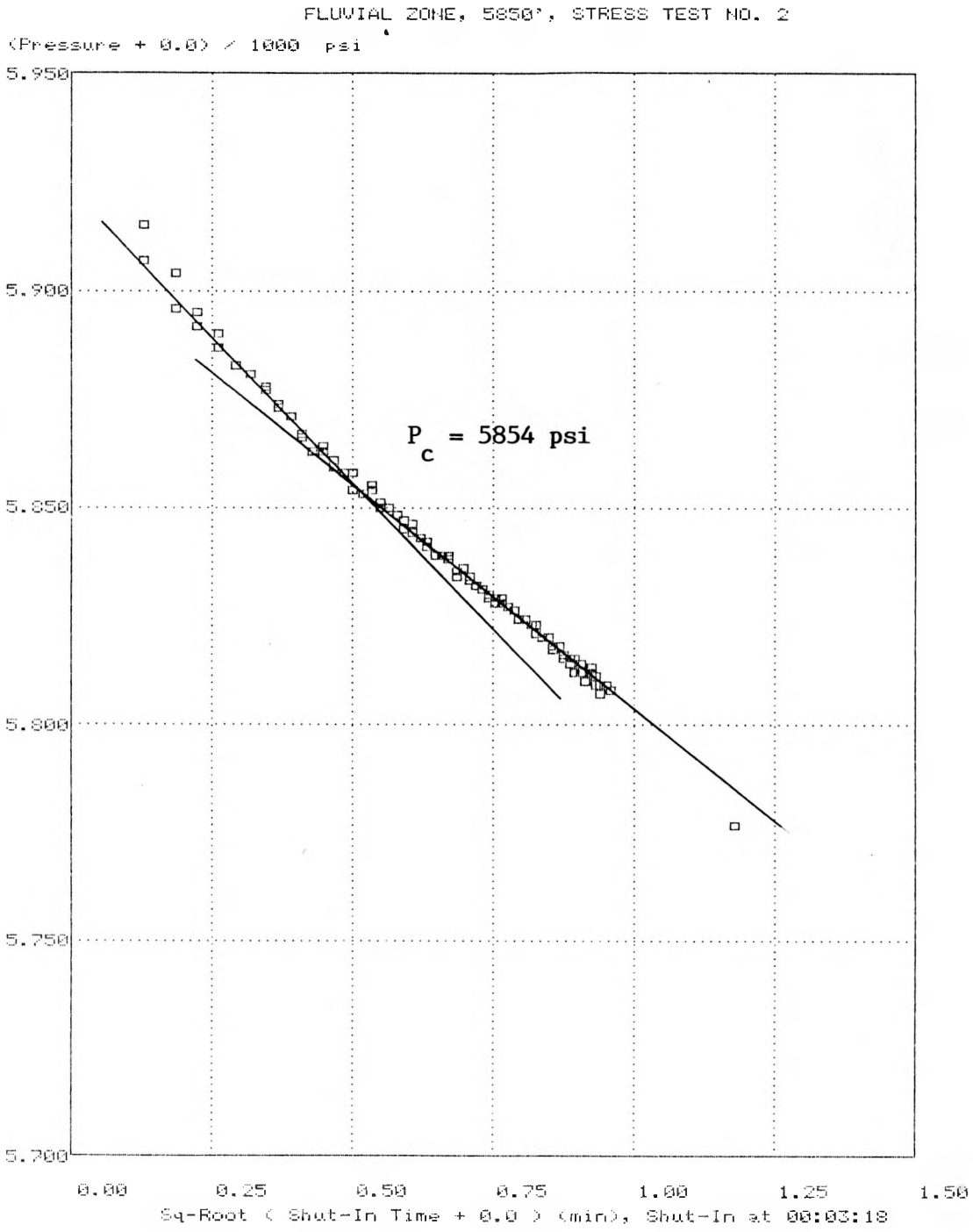


FIGURE A.223: Shale Stress Test (5850-5852'), Square-Root of Shut-In Time Plot of Test No. 2 Pressure Decline.

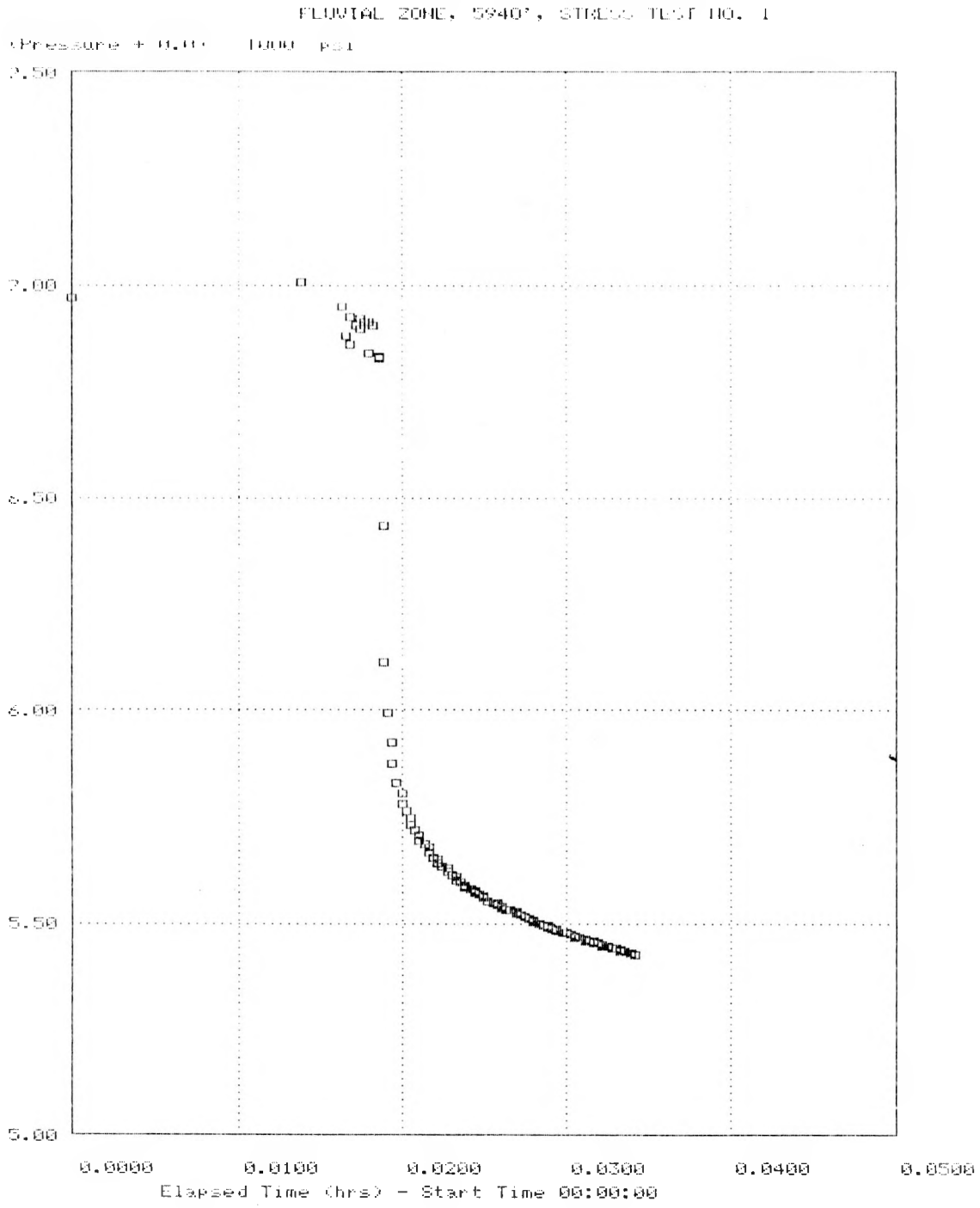


FIGURE A.224: Shale Stress Test (5940-5942'), Linear Plot of Test No. 1 Injection/Decline.

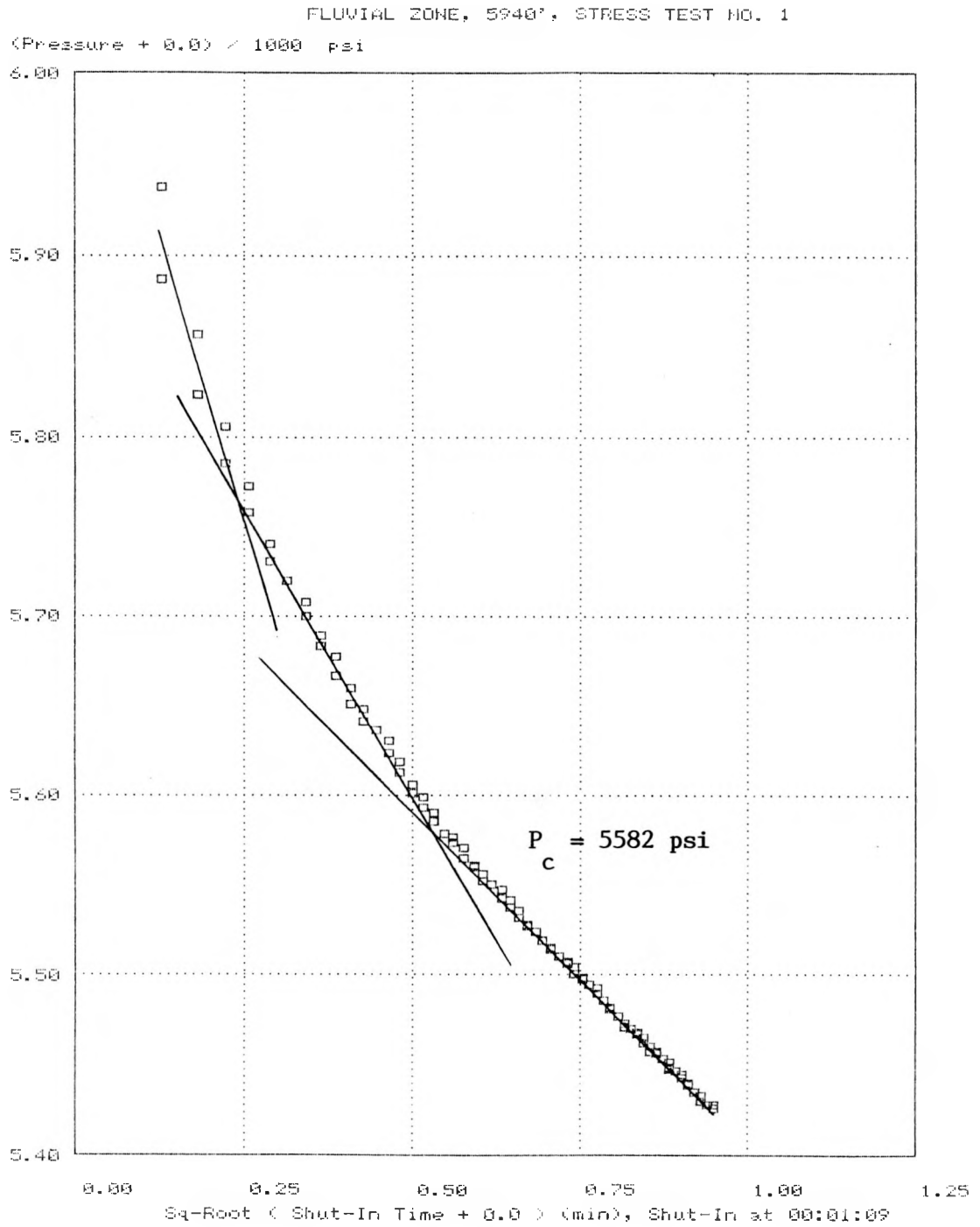


FIGURE A.225: Shale Stress Test (5940-5942'), Square-Root of Shut-In Time Plot of Test No. 1 Pressure Decline.

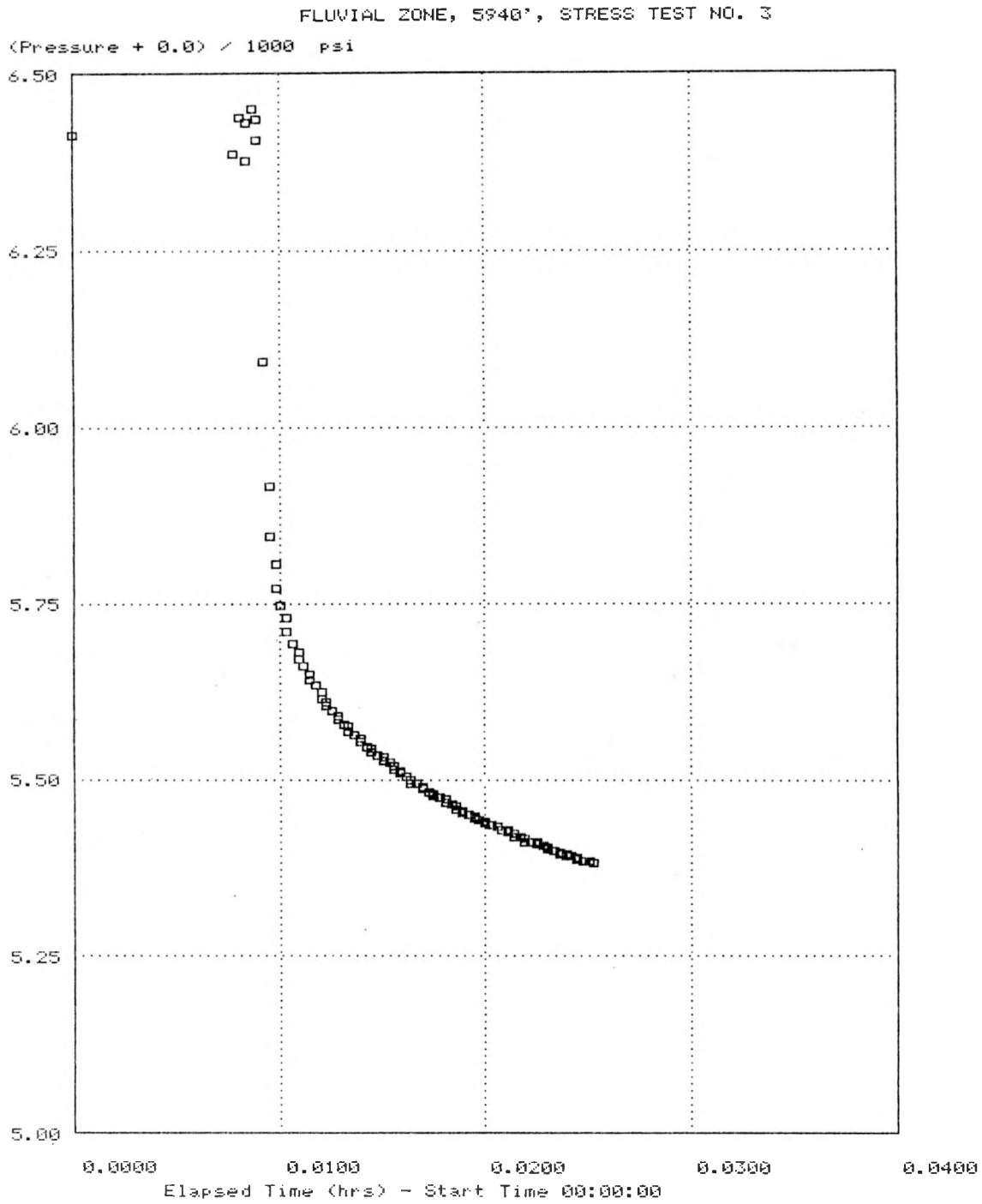


FIGURE A.226: Shale Stress Test (5940–5942'), Linear Plot of Test No. 3 Injection/Decline.

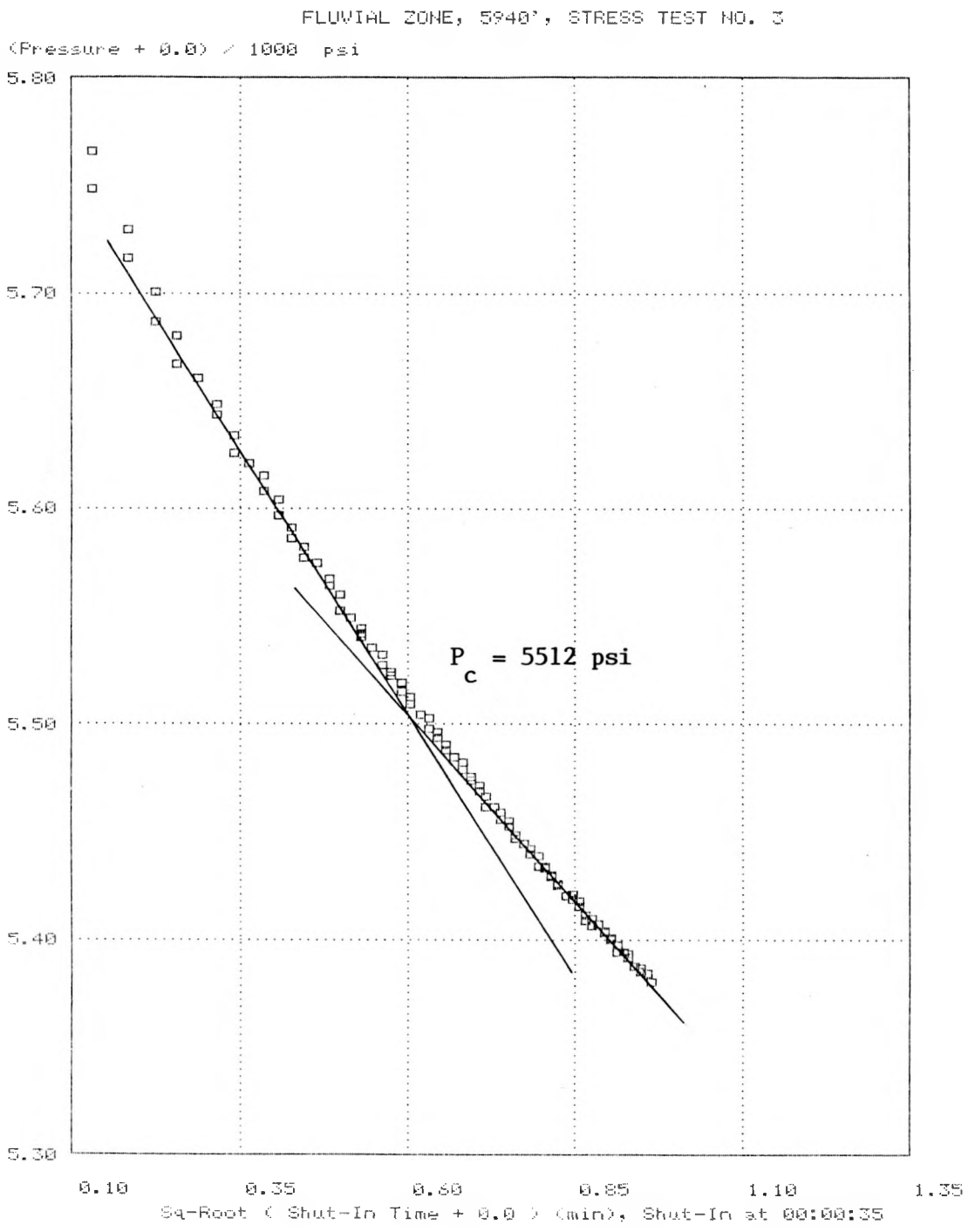


FIGURE A.227: Shale Stress Test (5940-5942'), Square-Root of Shut-In Time Plot of Test No. 3 Pressure Decline.

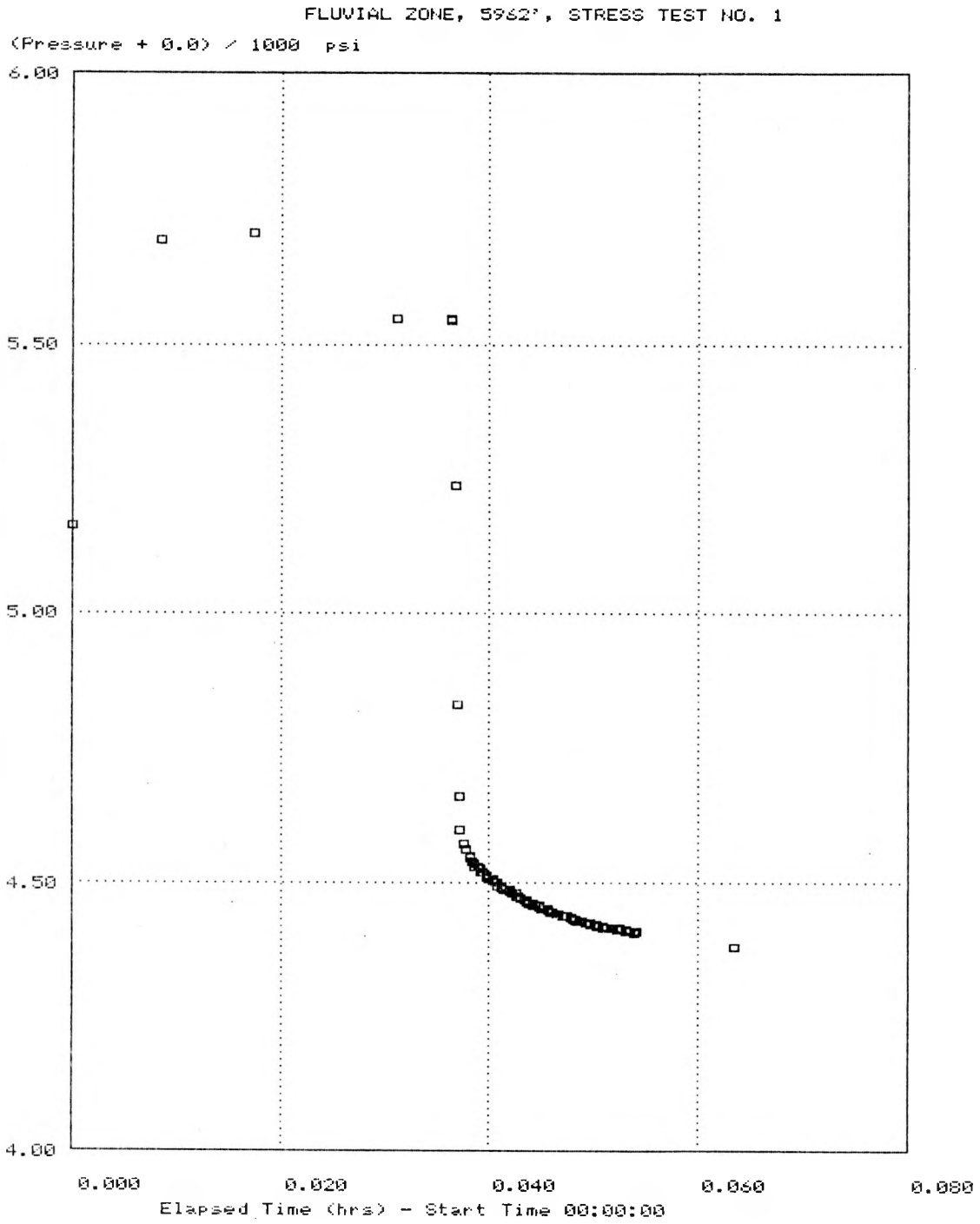


FIGURE A.228: Sandstone Stress Test (5962-5964'), Linear Plot of Test No. 1 Injection/Decline.

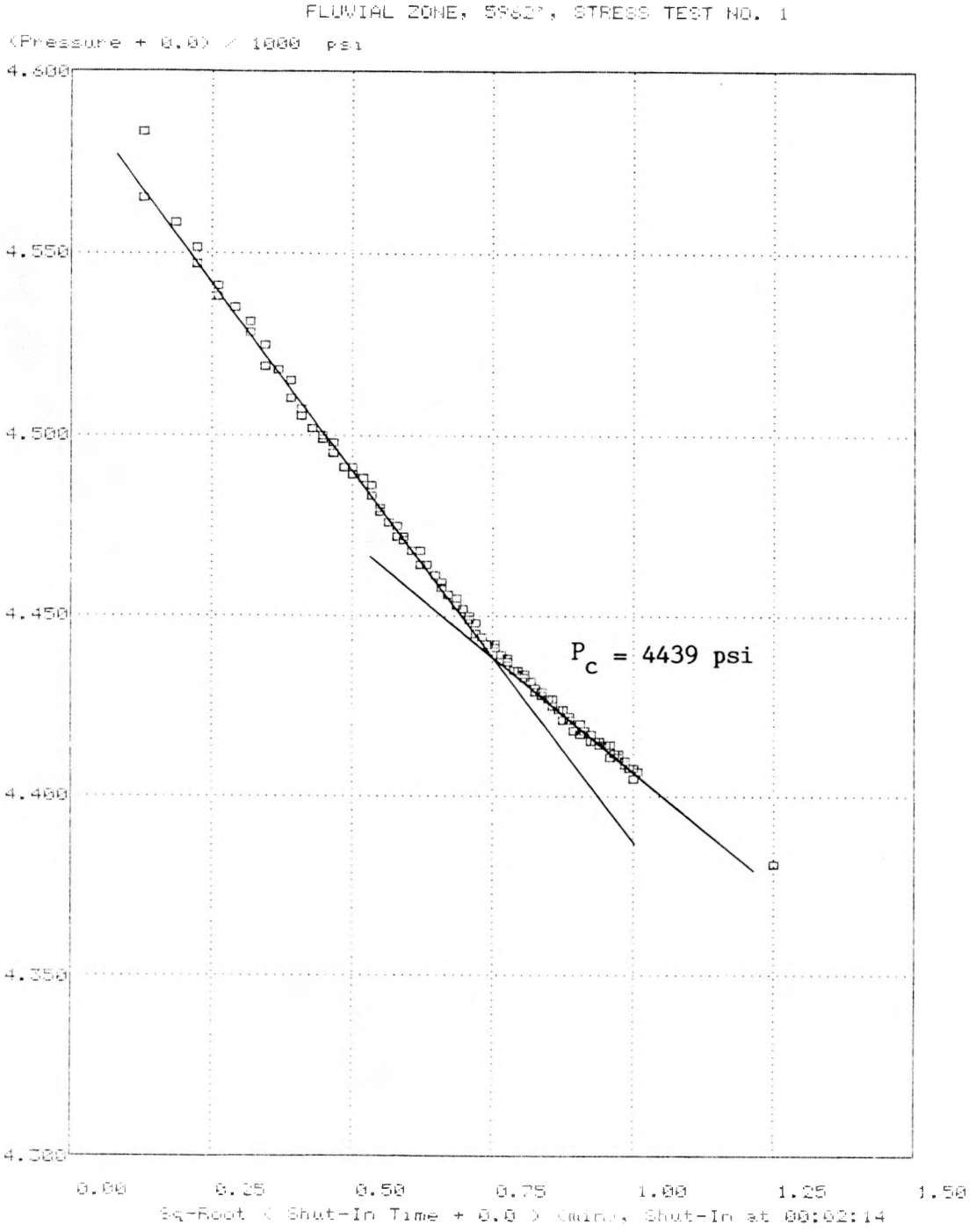


FIGURE A.229: Sandstone Stress Test (5962-5964'), Square-Root of Shut-In Time Plot of Test No. 1 Pressure Decline.

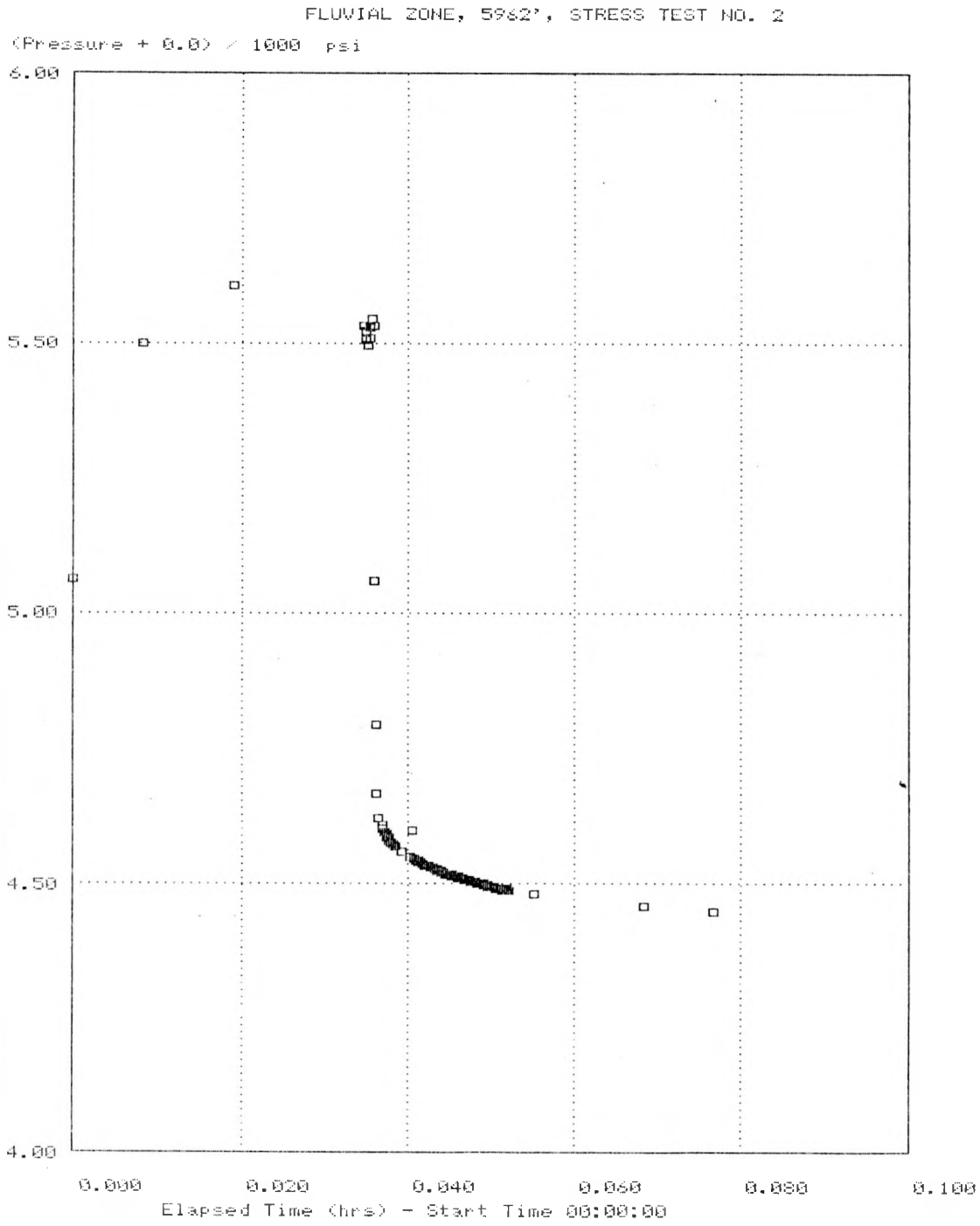


FIGURE A.230: Sandstone Stress Test (5962-5964'), Linear Plot of Test No. 2 Injection/Decline.

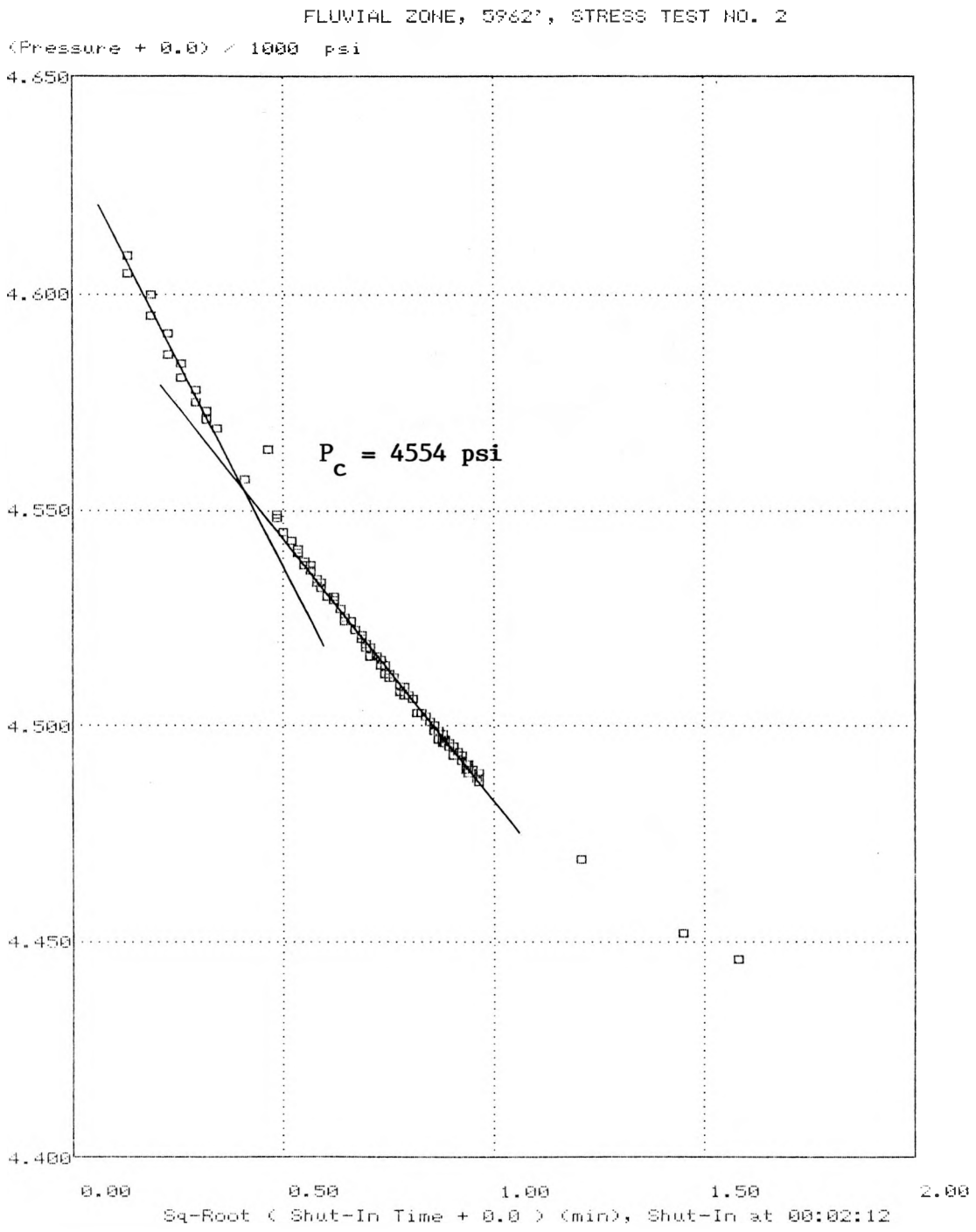


FIGURE A.231: Sandstone Stress Test (5962-5964'), Square-Root of Shut-In Time Plot of Test No. 2 Pressure Decline.

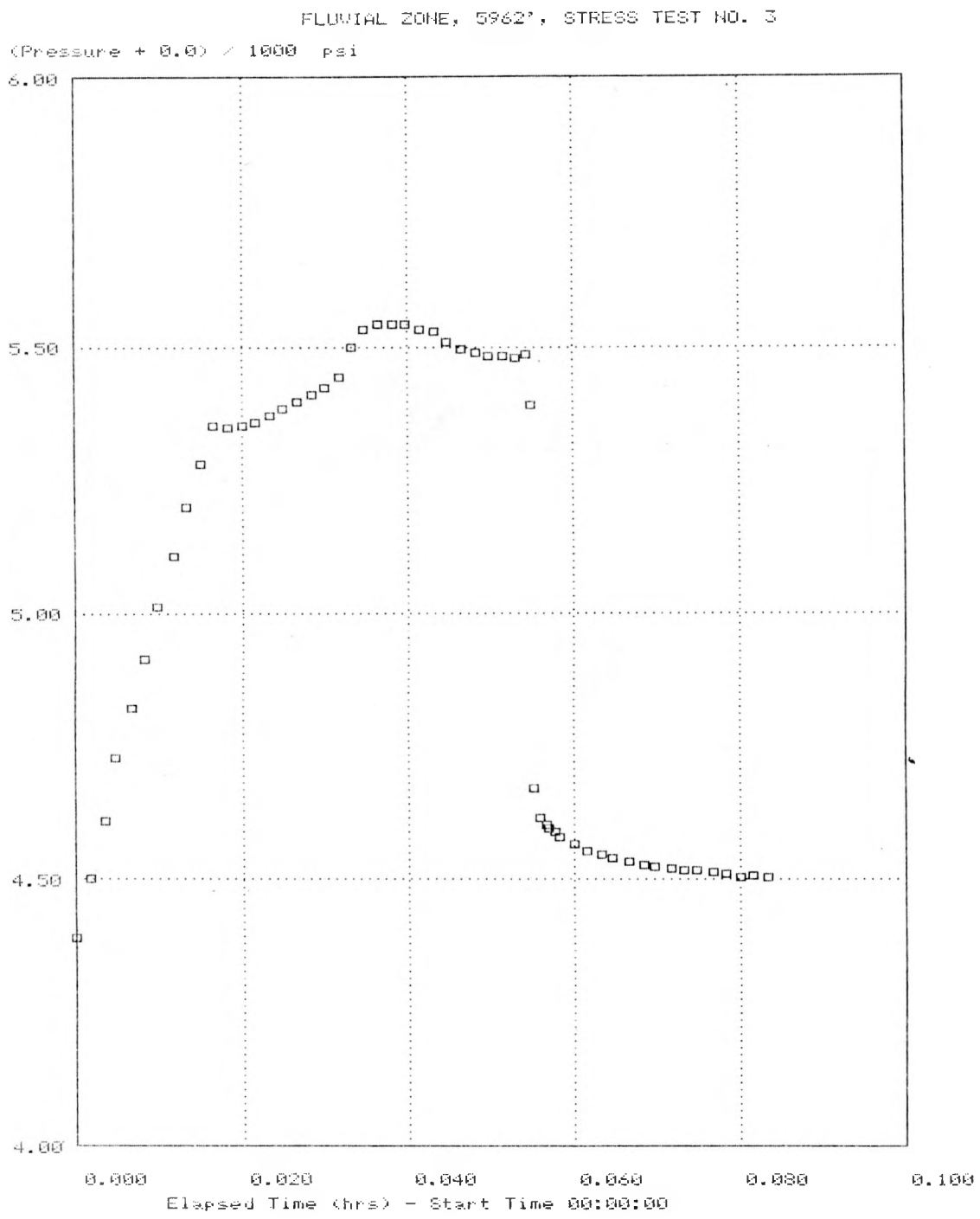


FIGURE A.232: Sandstone Stress Test (5962-5964'), Linear Plot of Test No. 3 Injection/Decline.

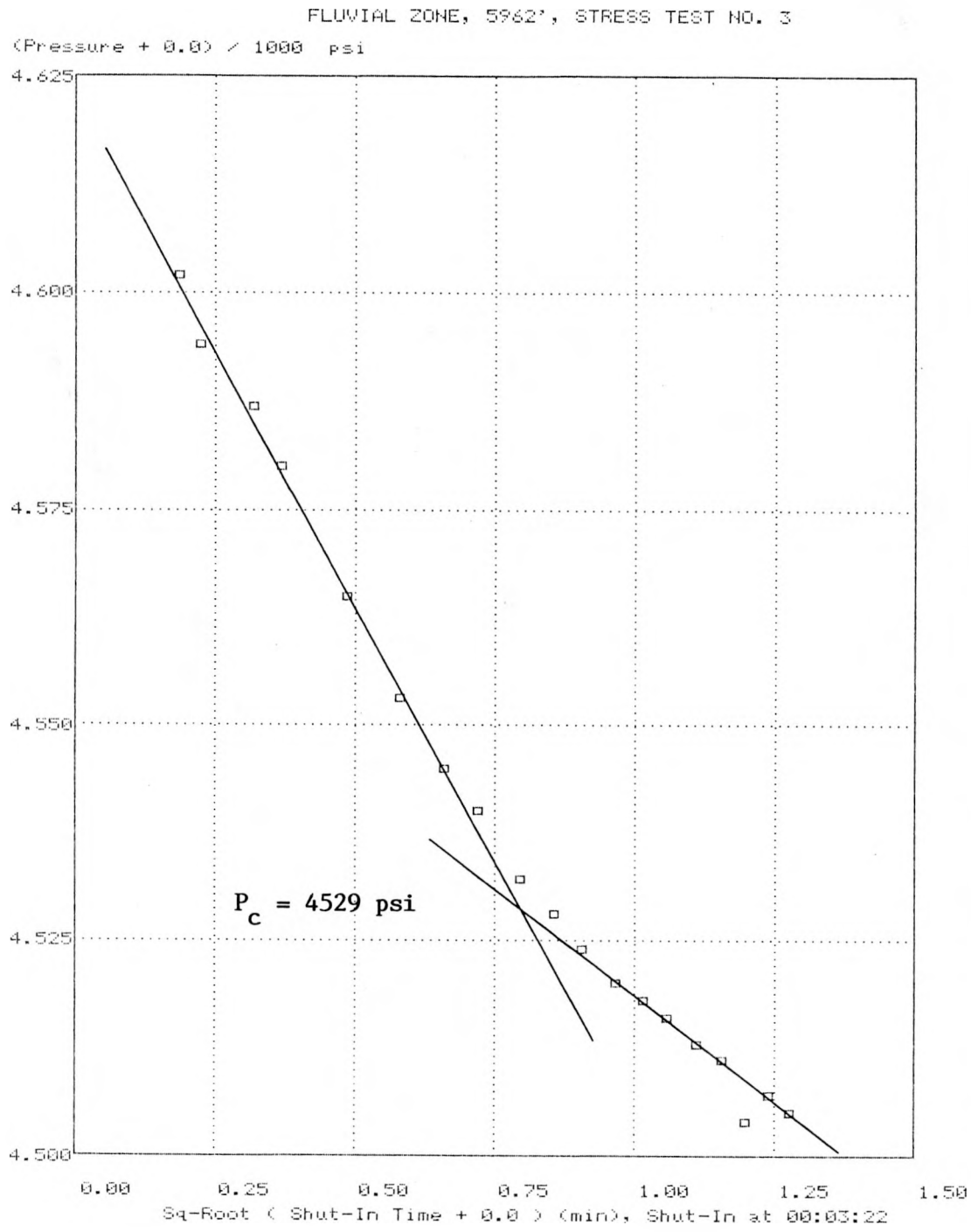


FIGURE A.233: Sandstone Stress Test (5962-5964'), Square-Root of Shut-In Time Plot of Test No. 3 Pressure Decline.

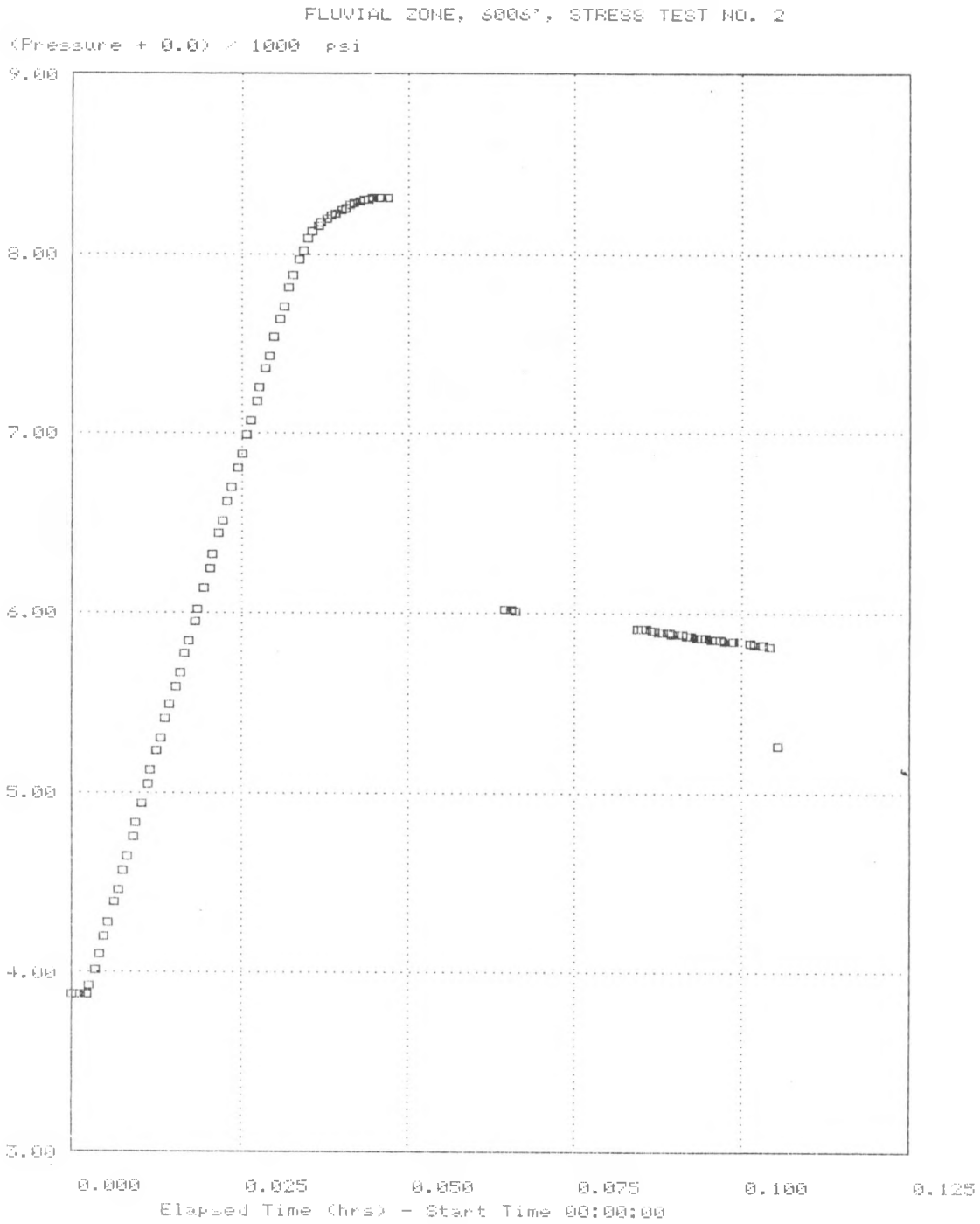


FIGURE A.234: Shale Stress Test (6006-6008'), Linear Plot of Test No. 2 Injection/Decline.

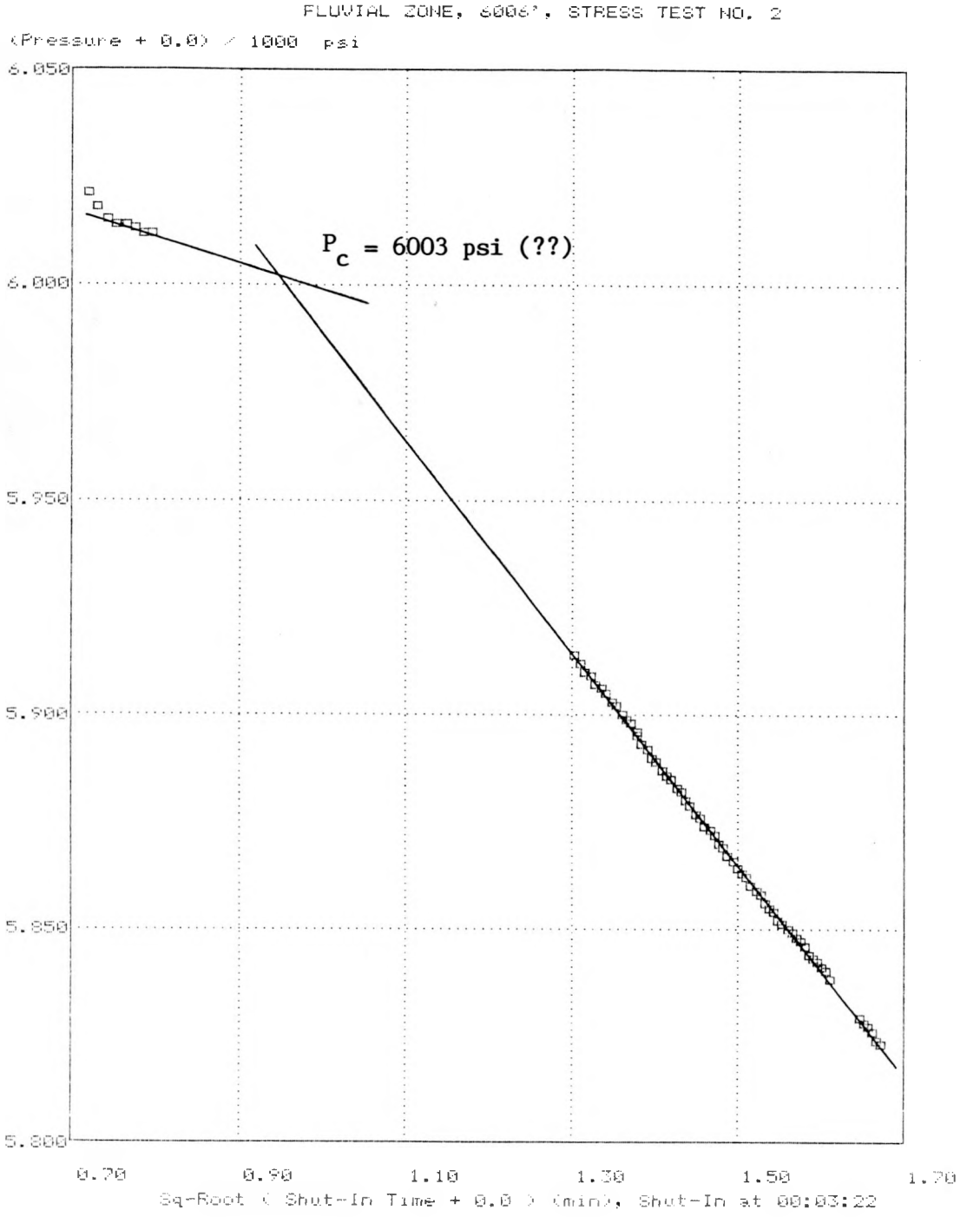


FIGURE A.235: Shale Stress Test (6006-6008'), Square-Root of Shut-In Time Plot of Test No. 2 Pressure Decline.

APPENDIX B

CALCULATIONS FOR LITHOLOGY AND ACOUSTIC DERIVED IN SITU STRESS LOGS

B.1: TABULAR RESULTS FOR GAMMA-RAY (LITHOLOGY) DERIVED IN SITU STRESS LOG FOR THE FLUVIAL ZONE.

DEPTH (ft)	GR	K-FACTOR	OB (psi)	Pr (psi)	Closure P (psi)
4320	40	0.155	4536	2505	2820
22	39	0.139	4538	2506	2788
24	38	0.124	4540	2507	2759
26	60	0.461	4542	2508	3446
28	58	0.431	4544	2509	3386
30	41	0.170	4546	2510	2856
32	50	0.308	4549	2511	3139
34	52	0.339	4551	2512	3203
36	47	0.262	4553	2513	3047
38	57	0.415	4555	2514	3361
40	45	0.231	4557	2515	2987
42	56	0.400	4559	2517	3334
44	39	0.139	4561	2518	2802
46	40	0.155	4563	2519	2836
48	47	0.262	4565	2520	3056
50	70	0.614	4567	2521	3777
52	108	1.0	4569	2522	4569
54	90	0.921	4571	2523	4409
56	40	0.155	4574	2524	2842
58	40	0.155	4576	2525	2843
60	38	0.124	4578	2526	2780
62	34	0.063	4580	2527	2656
64	38	0.124	4582	2529	2784
66	79	0.752	4584	2530	4075
68	95	0.997	4586	2531	4580
70	85	0.844	4588	2532	4267
72	106	1.0	4591	2533	4591
74	110	1.0	4593	2534	4593
76	110	1.0	4595	2535	4595
78	112	1.0	4597	2536	4597
80	110	1.0	4599	2537	4599
82	90	0.921	4601	2539	4438
84	81	0.783	4603	2540	4155
86	79	0.752	4605	2541	4093
88	83	0.814	4607	2542	4223
90	90	0.921	4609	2543	4446
92	43	0.201	4611	2544	2959
94	130	1.0	4613	2546	4613
96	148	1.0	4616	2547	4616
98	107	1.0	4618	2548	4618
4400	112	1.0	4620	2549	4620
02	110	1.0	4622	2550	4622
04	105	1.0	4624	2551	4624
06	100	1.0	4626	2553	4626
08	83	0.814	4628	2554	4242
10	100	1.0	4631	2555	4631
12	72	0.645	4633	2556	3896

DEPTH (ft)	GR	K-FACTOR	OB (psi)	Pr (psi)	Closure P (psi)
4414	80	0.768	4635	2557	4153
16	100	1.0			4637
18	117	1.0			4639
20	103	1.0			4641
22	94	0.982	4643	2562	4635
24	88	0.890	4645	2563	4416
26	107	1.0			4647
28	121	1.0			4649
30	110	1.0			4650
32	70	0.614	4654	2568	3849
34	63	0.507	4656	2569	3627
36	82	0.798	4658	2570	4236
38	52	0.339	4660	2571	3279
40	100	1.0			4662
42	105	1.0			4664
44	106	1.0			4666
46	98	1.0			4668
48	120	1.0			4670
50	82	0.798	4673	2578	4250
52	53	0.354	4675	2580	3322
54	90	0.921	4677	2581	4511
56	114	1.0			4679
58	116	1.0			4681
60	105	1.0			4683
62	99	1.0			4685
64	84	0.829	4687	2587	4328
66	109	1.0			4689
68	117	1.0			4691
70	132	1.0			4693
72	119	1.0			4695
74	127	1.0			4698
76	128	1.0			4700
78	110	1.0			4702
80	133	1.0			4704
82	122	1.0			4706
84	75	0.691	4708	2598	4056
86	98	1.0			4710
88	160	1.0			4712
90	160	1.0			4715
92	160	1.0			4717
94	140	1.0			4719
96	157	1.0			4721
98	160	1.0			4723
4500	160	1.0			4725
02	160	1.0			4727
04	160	1.0			4729
06	157	1.0		2611	4731
08	120	1.0			4733
10	120	1.0			4735
12	112	1.0			4737

DEPTH (ft)	GR	K-FACTOR	OB (psi)	Pr (psi)	Closure P (psi)
4514	72	0.645	4740	2616	3986
16	98	1.0			4741
18	118	1.0			4743
20	120	1.0			4745
22	110	1.0			4747
24	119	1.0			4749
26	100	1.0			4751
28	70	0.614	4754	2624	3932
30	53	0.354	4756	2625	3379
32	55	0.385	4758	2626	3447
34	43	0.201	4760	2628	3057
36	50	0.308	4762	2629	3286
38	48	0.277	4765	2630	3221
40	46	0.247	4767	2631	3159
42	44	0.185	4769	2632	3027
44	43	0.201	4771	2633	3063
46	60	0.461	4773	2635	3621
48	57	0.415	4775	2636	3524
50	50	0.308	4777	2637	3296
52	50	0.308	4779	2638	3297
54	52	0.339	4782	2639	3365
56	43	0.201	4784	2640	3071
58	90	0.921	4786	2642	4617
60	120	1.0			4788
62	100	1.0			4790
64	100	1.0			4792
66	81	0.783	4794	2646	4328
68	60	0.461	4796	2647	3638
70	46	0.247	4798	2649	3180
72	130	1.0			4801
74	90	0.921	4803	2651	4633
76	113	1.0			4805
78	82	0.798	4807	2653	4372
80	125	1.0			4809
82	120	1.0			4811
84	124	1.0			4813
86	119	1.0			4815
88	105	1.0			4817
90	70	0.614	4820	2660	3986
92	110	1.0			4822
94	103	1.0			4824
96	68	0.584	4826	2664	3927
98	80	0.768	4828	2665	4326
4600	140	1.0			4830
02	132	1.0		2667	4832
04	160	1.0			4834
06	160	1.0			4836
08	160	1.0			4838
10	143	1.0			4840
12	105	1.0			4842

DEPTH (ft)	GR	K-FACTOR	OB (psi)	Pr (psi)	Closure P (psi)
4614	85	0.844	4845	2674	4506
16	83	0.814	4847	2676	4443
18	93	0.967	4849	2677	4777
20	81	0.783	4851	2678	4379
22	113	1.0			4853
24	102	1.0			4855
26	95	0.997	4857	2681	4850
28	60	0.461	4859	2683	3686
30	55	0.385	4861	2684	3522
32	60	0.461	4864	2685	3690
34	80	0.768	4866	2686	4360
36	87	0.875	4868	2687	4595
38	70	0.614	4870	2688	4028
40	53	0.354	4872	2690	3462
42	130	1.0			4874
44	160	1.0			4876
46	153	1.0			4878
48	140	1.0			4880
50	130	1.0			4882
52	130	1.0			4884
54	60	0.461	4887	2698	3707
56	100	1.0			4889
58	60	0.461	4891	2700	3710
60	60	0.461	4893	2701	3712
62	120	1.0			4895
64	95	0.997	4897	2704	4890
66	90	0.921	4899	2705	4726
68	119	1.0			4901
70	93	0.967	4904	2707	4831
72	92	0.951	4906	2708	4798
74	80	0.768	4908	2709	4398
76	65	0.538	4910	2711	3894
78	106	1.0			4912
80	90	0.921	4914	2713	4740
82	160	1.0			4916
84	130	1.0			4918
86	100	1.0			4920
88	90	0.921	4922	2718	4748
90	90	0.921	4924	2719	4750
92	86	0.860	4926	2720	4617
94	82	0.798	4929	2721	4483
96	63	0.507	4931	2722	3842
98	86	0.860	4933	2723	4624
4700	90	0.921	4935	2724	4760
02	140	1.0			4937
04	160	1.0			4939
06	160	1.0			4941
08	160	1.0			4943
10	120	1.0			4945
12	160	1.0			4948

DEPTH (ft)	GR	K-FACTOR	OB (psi)	Pr (psi)	Closure P (psi)
4714	160	1.0		2730	4950
16	160	1.0			4952
18	160	1.0			4954
20	132	1.0			4956
22	142	1.0			4958
24	138	1.0			4960
26	160	1.0			4962
28	140	1.0			4964
30	120	1.0			4967
32	146	1.0			4969
34	140	1.0			4971
36	160	1.0			4973
38	160	1.0			4975
40	160	1.0			4977
42	146	1.0			4979
44	78	0.737	4981	2748	4394
46	140	1.0			4983
48	139	1.0			4985
50	141	1.0			4987
52	140	1.0			4990
54	100	1.0			4992
56	78	0.737	4994	2755	4405
58	85	0.844	4996	2756	4647
60	70	0.614	4998	2757	4133
62	80	0.768	5000	2758	4480
64	80	0.768	5002	2760	4482
66	73	0.660	5004	2761	4241
68	72	0.645	5006	2762	4209
70	80	0.768	5008	2763	4487
72	75	0.691	5011	2764	4317
74	69	0.599	5013	2765	4112
76	67	0.568	5015	2767	4044
78	70	0.614	5017	2768	4149
80	85	0.844	5019	2769	4668
82	85	0.844	5021	2770	4670
84	142	1.0			5023
86	125	1.0			5025
88	115	1.0			5027
90	120	1.0			5029
92	133	1.0			5032
94	142	1.0			5034
96	120	1.0			5036
98	90	0.921	5038	2779	4860
4800	120	1.0			5040
02	100	1.0			5042
04	119	1.0			5044
06	53	0.354	5046	2784	3585
08	100	1.0			5048
10	127	1.0			5050
12	125	1.0			5052

DEPTH (ft)	GR	K-FACTOR	OB (psi)	Pr (psi)	Closure P (psi)
4814	125	1.0			5055
16	120	1.0			5057
18	102	1.0			5059
20	73	0.660	5061	2792	4290
22	68	0.584	5063	2794	4119
24	66	0.553	5065	2795	4050
26	80	0.768	5067	2796	4540
28	102	1.0			5069
30	145	1.0			5071
32	160	1.0			5074
34	160	1.0			5076
36	90	0.921	5078	2802	4898
38	70	0.614	5080	2803	4201
40	68	0.584	5082	2804	4134
42	66	0.553	5084	2805	4065
44	61	0.477	5086	2807	3894
46	78	0.737	5088	2808	4488
48	103	1.0			5090
50	110	1.0			5092
52	110	1.0			5095
54	90	0.921	5097	2812	4916
56	66	0.553	5099	2814	4078
58	65	0.538	5101	2815	4045
60	130	1.0			5103
62	135	1.0			5105
64	138	1.0			5107
66	123	1.0			5109
68	130	1.0			5111
70	90	0.921	5113	2822	4932
72	87	0.875	5115	2823	4829
74	68	0.584	5118	2824	4164
76	59	0.446	5120	2825	3849
78	58	0.431	5122	2827	3816
80	90	0.921	5124	2828	4943
82	97	1.0			5126
84	128	1.0			5128
86	103	1.0			5130
88	120	1.0			5132
90	125	1.0		2834	5135
92	123	1.0			5137
94	110	1.0			5139
96	108	1.0			5141
98	70	0.614	5143	2838	4253
4900	47	0.262	5145	2840	3444
02	60	0.461	5147	2841	3904
04	62	0.492	5150	2842	3978
06	45	0.231	5152	2843	3376
08	43	0.201	5154	2844	3308
10	47	0.262	5156	2846	3451
12	140	1.0			5158

DEPTH (ft)	GR	K-FACTOR	OB (psi)	Pr (psi)	Closure P (psi)
4914	160	1.0			5160
16	160	1.0			5162
18	160	1.0			5164
20	87	0.875	5166	2851	4877
22	52	0.339	5168	2853	3638
24	53	0.354	5170	2854	3674
26	60	0.461	5172	2855	3923
28	53	0.354	5174	2856	3677
30	45	0.231	5176	2857	3393
32	47	0.262	5179	2859	3467
34	47	0.262	5181	2860	3468
36	45	0.231	5183	2861	3397
38	120	1.0			5185
40	108	1.0			5187
42	95	0.997	5189	2864	5182
44	79	0.752	5191	2866	4614
46	115	1.0			5193
48	133	1.0			5195
50	102	1.0			5197
52	100	1.0			5199
54	142	1.0			5201
56	123	1.0			5203
58	123	1.0			5205
60	133	1.0			5208
62	147	1.0			5210
64	152	1.0			5212
66	120	1.0			5214
68	120	1.0			5216
70	120	1.0			5219
72	105	1.0			5221
74	110	1.0			5223
76	139	1.0			5225
78	120	1.0			5227
80	145	1.0			5229
82	140	1.0			5231
84	130	1.0			5233
86	107	1.0		2890	5235
88	99	1.0			5237
90	103	1.0			5239
92	99	1.0			5241
94	107	1.0			5243
96	112	1.0			5246
98	100	1.0			5248
5000	80	0.768	5250	2899	4705
02	87	0.875	5252	2900	4958
04	85	0.844	5254	2901	4887
06	84	0.829	5256	2902	4853
08	84	0.829	5258	2903	4855
10	87	0.875	5260	2905	4966
12	90	0.921	5262	2906	5076

DEPTH (ft)	GR	K-FACTOR	OB (psi)	Pr (psi)	Closure P (psi)
5014	87	0.875	5265	2907	4970
16	83	0.814	5267	2908	4828
18	83	0.814	5269	2909	4830
20	82	0.798	5271	2910	4794
22	90	0.921	5273	2912	5086
24	135	1.0			5275
26	112	1.0			5277
28	88	0.890	5279	2915	5019
30	97	1.0			5282
32	96	1.0			5284
34	89	0.905	5286	2919	5061
36	80	0.768	5288	2920	4739
38	81	0.783	5290	2921	4776
40	83	0.814	5292	2922	4851
42	81	0.783	5294	2923	4779
44	89	0.905	5296	2925	5071
46	87	0.875	5298	2926	5002
48	85	0.844	5300	2927	4930
50	82	0.798	5302	2928	4822
52	80	0.768	5304	2929	4753
54	93	0.967	5307	2930	5229
56	160	1.0			5309
58	130	1.0			5311
60	125	1.0			5313
62	110	1.0			5315
64	135	1.0			5317
66	110	1.0			5319
68	130	1.0			5321
70	140	1.0			5323
72	120	1.0			5326
74	132	1.0		2940	5328
76	120	1.0			5330
78	128	1.0			5332
80	110	1.0		2944	5334
82	153	1.0			5336
84	125	1.0			5338
86	140	1.0			5340
88	140	1.0			5342
90	130	1.0			5345
92	90	0.921	5347	2951	5158
94	136	1.0			5349
96	130	1.0			5351
98	120	1.0			5353
5100	160	1.0			5355
02	160	1.0			5357
04	147	1.0			5359
06	130	1.0			5361
08	79	0.752	5363	2960	4767
10	160	1.0			5366
12	160	1.0			5368

DEPTH (ft)	GR	K-FACTOR	OB (psi)	Pr (psi)	Closure P (psi)
5114	150	1.0			5370
16	130	1.0			5372
18	79	0.752	5374	2966	4777
20	79	0.752	5376	2967	4779
22	78	0.737	5378	2968	4744
24	78	0.737	5380	2970	4746
26	79	0.752	5382	2971	4784
28	80	0.768	5384	2972	4824
30	80	0.768	5387	2973	4827
32	65	0.538	5389	2974	4273
34	137	1.0			5391
36	135	1.0			5393
38	119	1.0			5395
40	105	1.0			5397
42	160	1.0			5399
44	100	1.0			5401
46	73	0.660	5403	2982	4580
48	75	0.691	5405	2984	4657
50	70	0.614	5408	2985	4473
52	70	0.614	5410	2986	4474
54	140	1.0			5412
56	155	1.0			5414
58	160	1.0			5416
60	120	1.0			5418
62	100	1.0			5420
64	100	1.0			5422
66	105	1.0			5424
68	90	0.921	5426	2995	5234
70	82	0.798	5428	2997	4937
72	70	0.614	5431	2998	4492
74	48	0.277	5433	2999	3673
76	120	1.0		3000	5435
78	90	0.921	5437	3001	5245
80	93	0.967	5439	3003	5359
82	100	1.0			5441
84	118	1.0			5443
86	118	1.0			5445
88	102	1.0			5447
90	150	1.0			5450
92	160	1.0			5452
94	160	1.0			5454
96	160	1.0			5456
98	140	1.0			5458
5200	130	1.0			5460
02	110	1.0			5462
04	110	1.0			5464
06	80	0.768	5466	3018	4898
08	107	1.0			5468
10	95	0.997	5471	3020	5464
12	101	1.0			5473

DEPTH (ft)	GR	K-FACTOR	OB (psi)	Pr (psi)	Closure P (psi)
5214	105	1.0			5475
16	95	0.997	5477	3024	5470
18	115	1.0			5479
20	125	1.0			5481
22	100	1.0			5483
24	130	1.0			5485
26	125	1.0			5487
28	138	1.0			5989
30	107	1.0			5491
32	100	1.0			5494
34	90	0.921	5496	3034	5302
36	70	0.614	5498	3036	4548
38	70	0.614	5500	3037	4549
40	100	1.0			5502
42	120	1.0			5504
44	120	1.0			5506
46	142	1.0			5508
48	130	1.0			5510
50	152	1.0			5513
52	138	1.0			5515
54	160	1.0			5517
56	160	1.0			5519
58	140	1.0			5521
60	80	0.768	5523	3050	4949
62	93	0.967	5525	3051	5443
64	100	1.0			5527
66	105	1.0			5529
68	118	1.0			5531
70	118	1.0			5534
72	75	0.691	5536	3057	4770
74	100	1.0			5538
76	135	1.0			5540
78	118	1.0			5542
80	103	1.0			5544
82	130	1.0			5546
84	110	1.0			5548
86	92	0.951	5550	3065	5428
88	98	1.0			5552
90	70	0.614	5554	3067	4594
92	87	0.875	5556	3069	5245
94	56	0.400	5559	3070	4066
96	61	0.477	5561	3071	4259
98	63	0.507	5563	3072	4335
5300	86	0.860	5565	3073	5216
02	62	0.492	5567	3075	4301
04	60	0.461	5569	3076	4225
06	118	1.0			5571
08	110	1.0			5573
10	130	1.0			5575
12	110	1.0			5577

DEPTH (ft)	GR	K-FACTOR	OB (psi)	Pr (psi)	Closure P (psi)
5314	100	1.0			5579
16	140	1.0			5581
18	112	1.0			5584
20	140	1.0		3085	5586
22	137	1.0			5588
24	125	1.0			5590
26	110	1.0			5592
28	112	1.0			5594
30	125	1.0			5596
32	132	1.0			5598
34	120	1.0			5601
36	125	1.0			5603
38	115	1.0			5605
40	80	0.768	5607	3092	5024
42	82	0.798	5609	3093	5101
44	90	0.921	5611	3094	5412
46	122	1.0			5613
48	90	0.921	5615	3095	5416
50	80	0.768	5618	3096	5033
52	99	1.0			5620
54	89	0.905	5622	3098	5382
56	90	0.921	5624	3099	5425
58	120	1.0			5626
60	100	1.0			5628
62	132	1.0			5630
64	120	1.0			5632
66	150	1.0			5634
68	153	1.0		3103	5636
70	150	1.0			5639
72	100	1.0			5641
74	80	0.768	5643	3105	5054
76	60	0.461	5645	3106	4276
78	55	0.385	5647	3106	4084
80	120	1.0			5649
82	150	1.0			5651
84	150	1.0			5653
86	110	1.0			5655
88	72	0.645	5657	3110	4753
90	90	0.921	5660	3111	5459
92	77	0.722	5662	3112	4953
94	63	0.507	5664	3112	4406
96	118	1.0			5666
98	111	1.0			5668
5400	127	1.0			5670
02	100	1.0			5672
04	90	0.921	5674	3116	5472
06	102	1.0			5676
08	85	0.844	5679	3118	5279
10	100	1.0			5681
12	117	1.0			5683

DEPTH (ft)	GR	K-FACTOR	OB (psi)	Pr (psi)	Closure P (psi)
5414	112	1.0			5685
16	132	1.0			5687
18	140	1.0			5689
20	120	1.0			5691
22	108	1.0			5693
24	110	1.0			5695
26	110	1.0			5697
28	105	1.0			5699
30	68	0.584	5701	3129	4631
32	105	1.0			5704
34	121	1.0			5706
36	108	1.0			5708
38	113	1.0			5710
40	107	1.0			5712
42	100	1.0			5714
44	93	0.967	5716	3137	5631
46	110	1.0			5718
48	115	1.0			5720
50	140	1.0			5722
52	125	1.0			5725
54	127	1.0			5727
56	123	1.0			5729
58	160	1.0			5731
60	100	1.0			5733
62	80	0.768	5735	3164	5139
64	80	0.768	5737	3168	5141
66	102	1.0			5739
68	99	1.0			5741
70	102	1.0			5743
72	110	1.0			5746
74	107	1.0			5748
76	80	0.768	5750	3192	5156
78	65	0.538	5752	3196	4571
80	53	0.354	5754	3200	4104
82	59	0.446	5756	3200	4340
84	59	0.446	5758	3200	4341
86	60	0.461	5760	3200	4380
88	49	0.293	5762	3200	3951
90	73	0.660	5765	3200	4893
92	72	0.645	5767	3200	4856
94	60	0.461	5769	3200	4384
96	110	1.0			5771
98	142	1.0			5773
5500	92	0.951	5775	3200	5649
02	120	1.0			5777
04	85	0.844	5779	3200	5377
06	125	1.0			5781
08	75	0.691	5783	3200	4985
10	110	1.0			5786
12	80	0.768	5788	3200	5188

DEPTH (ft)	GR	K-FACTOR	OB (psi)	Pr (psi)	Closure P (psi)
5514	70	0.614	5790	3200	4790
16	100	1.0			5792
18	90	0.921	5794	3200	5589
20	105	1.0			5796
22	119	1.0			5798
24	90	0.921	5800	3200	5595
6	70	0.614	5802	3200	4798
28	126	1.0			5804
30	85	0.844	5806	3200	5399
32	67	0.568	5808	3200	4681
34	60	0.461	5810	3200	4403
36	50	0.308	5812	3200	4004
38	50	0.308	5815	3200	4005
40	48	0.277	5817	3200	3925
42	43	0.201	5819	3200	3726
44	45	0.231	5821	3200	3805
46	50	0.308	5823	3200	4008
48	47	0.262	5826	3200	3888
50	46	0.247	5828	3200	3849
52	47	0.262	5830	3200	3889
54	45	0.231	5832	3200	3808
56	55	0.385	5834	3200	4214
58	57	0.415	5836	3200	4294
60	50	0.308	5838	3200	4013
62	53	0.354	5840	3200	4135
64	60	0.461	5842	3200	4418
66	80	0.768	5844	3200	5231
68	100	1.0			5846
70	103	1.0			5848
72	100	1.0			5851
74	95	0.997	5853	3200	5845
76	90	0.921	5855	3200	5645
78	125	1.0			5857
80	120	1.0			5859
82	90	0.921	5861	3200	5651
84	100	1.0			5863
86	50	0.308	5865	3200	4021
88	70	0.614	5867	3200	4838
90	118	1.0			5870
92	120	1.0			5872
94	120	1.0			5874
96	100	1.0			5876
98	110	1.0			5878
5600	125	1.0		3200	5880
02	123	1.0			5882
04	90	0.921	5884	3208	5673
06	130	1.0			5886
08	130	1.0			5888
10	120	1.0			5890
12	102	1.0			5893

DEPTH (ft)	GR	K-FACTOR	OB (psi)	Pr (psi)	Closure P (psi)
5614	87	0.875	5895	3228	5562
16	82	0.798	5897	3232	5359
18	92	0.951	5899	3236	5769
20	107	1.0			5901
22	115	1.0			5903
24	100	1.0			5905
26	100	1.0			5907
28	105	1.0			5909
30	140	1.0			5911
32	135	1.0			5914
34	140	1.0			5916
36	85	0.844	5918	3251	5502
38	100	1.0			5920
40	125	1.0			5922
42	65	0.538	5924	3255	4691
44	60	0.461	5926	3257	4487
46	75	0.691	5928	3258	5103
48	120	1.0			5930
50	100	1.0			5933
52	87	0.875	5935	3262	5601
54	115	1.0			5937
56	125	1.0			5939
58	70	0.614	5941	3266	4908
60	100	1.0			5943
62	72	0.645	5945	3269	4995
64	90	0.921	5947	3270	5736
66	70	0.614	5949	3271	4915
68	82	0.798	5951	3272	5410
70	90	0.921	5954	3274	5742
72	85	0.844	5956	3275	5538
74	125	1.0			5958
76	100	1.0			5960
78	100	1.0			5962
80	100	1.0		3280	5964
82	79	0.752	5966	3281	5300
84	92	0.951	5968	3282	5836
86	73	0.660	5970	3283	5056
88	83	0.814	5972	3284	5472
90	80	0.768	5975	3285	5351
92	90	0.921	5977	3286	5764
94	68	0.584	5979	3287	4859
96	75	0.691	5981	3288	5149
98	79	0.752	5983	3289	5315
5700	130	1.0		3290	5985
02	145	1.0			5987
04	120	1.0			5989
06	80	0.768	5991	3293	5365
08	120	1.0			5993
10	100	1.0			5996
12	110	1.0			5998

DEPTH (ft)	GR	K-FACTOR	OB (psi)	Pr (psi)	Closure P (psi)
5714	87	0.875	6000	3297	5662
16	80	0.768	6002	3298	5375
18	80	0.768	6004	3299	5376
20	53	0.354	6006	3300	4258
22	51	0.323	6008	3300	4175
24	54	0.369	6010	3300	4300
26	55	0.385	6012	3300	4344
28	60	0.461	6014	3300	4551
30	107	1.0			6017
32	80	0.768	6019	3300	5388
34	79	0.752	6021	3300	5346
36	50	0.308	6023	3300	4139
38	62	0.492	6025	3300	4641
40	110	1.0			6027
42	60	0.461	6029	3300	4558
44	110	1.0		3300	6031
46	139	1.0			6033
48	120	1.0			6035
50	60	0.461	6038	3314	4570
52	80	0.768	6040	3318	5408
54	70	0.614	6042	3323	4992
56	90	0.921	6044	3328	5829
58	120	1.0			6046
60	127	1.0			6048
62	100	1.0			6050
64	85	0.844	6052	3368	5633
66	80	0.768	6054	3380	5434
68	110	1.0			6057
70	140	1.0			6059
72	90	0.921	6061	3416	5852
74	130	1.0			6063
76	120	1.0			6065
78	90	0.921	6067	3450	5860
80	85	0.844	6069	3450	5660
82	80	0.768	6071	3450	5463
84	80	0.844	6073	3450	5464
86	105	1.0			6075
88	120	1.0			6077
90	115	1.0			6080
92	120	1.0			6082
94	125	1.0			6084
96	110	1.0			6086
98	130	1.0			6087
5800	120	1.0			6089
02	95	0.997	6092	3450	6084
04	103	1.0			6094
06	95	0.997	6096	3450	6088
08	73	0.660	6098	3450	5198
10	79	0.752	6101	3450	5444
12	68	0.584	6103	3450	4999

DEPTH (ft)	GR	K-FACTOR	OB (psi)	Pr (psi)	Closure P (psi)
5814	110	1.0			6105
16	100	1.0			6107
18	62	0.492	6109	3450	4758
20	105	1.0			6111
22	82	0.798	6113	3450	5575
24	60	0.461	6115	3450	4679
26	52	0.339	6117	3450	4354
28	47	0.262	6120	3450	4150
30	60	0.461	6122	3450	4682
32	50	0.308	6124	3450	4274
34	50	0.308	6126	3450	4274
36	56	0.400	6128	3450	4521
38	52	0.339	6130	3450	4359
40	53	0.354	6132	3450	4399
42	80	0.768	6134	3450	5511
44	95	0.997	6136	3450	6128
46	123	1.0			6138
48	90	0.921	6140	3450	5927
50	93	0.967	6143	3450	6054
52	100	1.0			6145
54	110	1.0			6147
56	105	1.0			6149
58	112	1.0			6151
60	100	1.0			6153
62	75	0.691	6155	3458	5322
64	80	0.768	6157	3459	5531
66	100	1.0			6160
68	97	1.0		3462	6162
70	110	1.0			6164
72	130	1.0			6166
74	80	0.768	6168	3466	5541
76	120	1.0			6170
78	80	0.768	6172	3469	5545
80	139	1.0			6174
82	130	1.0			6176
84	87	0.875	6178	3473	5840
86	90	0.921	6180	3474	5966
88	82	0.798	6183	3475	5636
90	83	0.814	6185	3477	5681
92	105	1.0			6187
94	87	0.875	6189	3479	5850
96	80	0.768	6191	3481	5562
98	90	0.921	6193	3482	5979
5900	115	1.0			6195
02	90	0.921	6197	3485	5983
04	105	1.0			6199
06	108	1.0			6201
08	110	1.0			6203
10	90	0.912	6206	3490	5991
12	80	0.768	6208	3491	5578

DEPTH (ft)	GR	K-FACTOR	OB (psi)	Pr (psi)	Closure P (psi)
5914	82	0.798	6210	3493	5661
16	60	0.461	6212	3494	4747
18	95	0.997	6214	3495	6206
20	102	1.0			6216
22	60	0.461	6218	3498	4752
24	50	0.308	6220	3499	4337
26	72	0.645	6222	3500	5256
28	102	1.0			6224
30	140	1.0			6227
32	100	1.0			6229
34	53	0.354	6231	3506	4471
36	82	0.798	6233	3507	5682
38	122	1.0			6235
40	110	1.0		3510	6237
42	115	1.0			6239
44	115	1.0			6241
46	120	1.0			6243
48	98	1.0			6245
50	65	0.538	6248	3519	4987
52	105	1.0			6250
54	100	1.0			6252
56	60	0.461	6254	3525	4783
58	58	0.431	6256	3526	4703
60	59	0.446	6258	3528	4746
62	63	0.507	6260	3530	4914
64	65	0.538	6262	3531	5000
66	65	0.538	6264	3532	5002
68	66	0.553	6267	3533	5045
70	67	0.568	6269	3534	5087
72	80	0.768	6271	3535	5636
74	140	1.0			6273
76	125	1.0			6275
78	80	0.768	6277	3537	5641
80	60	0.461	6279	3538	4802
82	55	0.385	6282	3539	4595
84	53	0.354	6284	3540	4511
86	95	0.997	6286	3541	6278
88	80	0.768	6288	3542	5651
90	120	1.0			6290
92	120	1.0			6292
94	105	1.0			6294
96	79	0.752	6296	3545	5614
98	70	0.614	6298	3546	5236
6000	70	0.614	6300	3547	5237
02	105	1.0			6302
04	112	1.0			6304
06	105	1.0		3550	6306

B.2: TABULAR RESULTS FOR ACOUSTIC VELOCITY (SONIC) DERIVED IN SITU STRESS LOG FOR THE FLUVIAL ZONE.

DEPTH (ft)	K(LOG)	K(CORR)	OB (psi)	Pr (psi)	CLOSURE P (psi)
4388	0.435	1.0			4607
90	0.410	0.975	4609	2543	4557
92	0.235	0.363	4611	2544	3294
94	0.431	1.0			4613
96	0.471	1.0			4616
98	0.420	1.0			4618
4400	0.391	0.909	4620	2549	4432
02	0.433	1.0			4622
04	0.431	1.0			4624
06	0.374	0.849	4626	2553	4313
08	0.312	0.632	4628	2554	3865
10	0.385	0.888	4631	2555	4398
12	0.368	0.828	4633	2556	4276
14	0.277	0.510	4635	2557	3617
16	0.357	0.790	4637	2558	4200
18	0.422	1.0			4639
20	0.473	1.0			4641
22	0.397	0.930	4643	2562	4497
24	0.379	0.867	4645	2563	4368
26	0.473	1.0			4647
28	0.342	0.737	4649	2565	4101
30	0.435	1.0			4650
32	0.441	1.0			4654
34	0.307	0.615	4656	2569	3853
36	0.404	0.954	4658	2570	4562
38	0.295	0.573	4660	2571	3768
40	0.263	0.461	4662	2572	3535
42	0.366	0.821	4664	2573	4290
44	0.410	0.975	4666	2574	4614
46	0.422	1.0			4668
48	0.391	0.909	4670	2576	4479
50	0.437	1.0			4673
52	0.307	0.615	4675	2580	3868
54	0.274	0.500	4677	2581	3629
56	0.374	0.849	4679	2582	4362
58	0.420	1.0			4681
60	0.441	1.0			4683
62	0.429	1.0			4685
64	0.277	0.510	4687	2587	3658
66	0.269	0.482	4689	2588	3601
68	0.425	1.0			4691
70	0.416	0.996	4693	2590	4685
72	0.460	1.0			4695
74	0.362	0.807	4698	2592	4292
76	0.368	0.828	4700	2593	4338
78	0.376	0.856	4702	2594	4398
80	0.359	0.797	4704	2595	4276
82	0.464	1.0			4706

DEPTH (ft)	K(LOG)	K(CORR)	OB (psi)	Pr (psi)	CLOSURE P (psi)
4484	0.292	0.563	4708	2598	3786
86	0.253	0.426	4710	2599	3498
88	0.361	0.804	4713	2601	4299
90	0.395	0.923	4715	2602	4552
92	0.418	1.0			4717
94	0.391	0.909	4719	2604	4527
96	0.397	0.930	4721	2605	4573
98	0.389	0.902	4723	2606	4516
4500	0.447	1.0			4725
02	0.427	1.0			4727
04	0.403	0.950	4729	2610	4623
06	0.416	0.996	4731	2611	4723
08	0.429	1.0			4733
10	0.397	0.930	4735	2604	4587
12	0.344	0.744	4737	2615	4194
14	0.366	0.821	4740	2616	4360
16	0.337	0.720	4741	2617	4146
18	0.397	0.930	4743	2618	4594
20	0.425	1.0			4745
22	0.410	0.975	4747	2620	4694
24	0.416	0.996	4749	2621	4740
26	0.395	0.923	4751	2622	4587
28	0.355	0.783	4754	2624	4292
30	0.279	0.517	4756	2625	3727
32	0.272	0.493	4758	2626	3677
34	0.192	0.213	4760	2628	3082
36	0.215	0.293	4762	2629	3254
38	0.272	0.493	4765	2630	3683
40	0.299	0.587	4767	2631	3885
42	0.220	0.311	4769	2632	3297
44	0.164	0.115	4771	2633	2879
46	0.215	0.293	4773	2635	3261
48	0.190	0.206	4775	2636	3077
50	0.195	0.224	4777	2637	3116
52	0.236	0.367	4779	2638	3424
54	0.299	0.587	4782	2639	3897
56	0.299	0.587	4784	2640	3899
58	0.250	0.416	4786	2642	3534
** NO DATA: 4559-4669' **					
4670	0.185	0.189	4904	2707	3122
72	0.255	0.433	4906	2708	3660
74	0.332	0.702	4908	2709	4253
76	0.285	0.538	4910	2711	3894
78	0.381	0.874	4912	2712	4635
80	0.255	0.433	4914	2713	3666
82	0.252	0.423	4916	2714	3645
84	0.304	0.604	4918	2716	4046
86	0.190	0.206	4920	2717	3171
88	0.337	0.720	4922	2718	4305
90	0.420	1.0			4923
92	0.408	0.968	4924	2720	4855

DEPTH (ft)	K(LOG)	K(CORR)	OB (psi)	Pr (psi)	CLOSURE P (psi)
4694	0.321	0.660	4929	2721	4187
96	0.307	0.615	4931	2722	4081
98	0.239	0.377	4933	2723	3556
4700	0.256	0.437	4935	2724	3690
02	0.332	0.702	4937	2725	4278
04	0.305	0.608	4939	2726	4072
06	0.437	1.0			4941
08	0.447	1.0			4943
10	0.366	0.821	4945	2728	4548
12	0.362	0.807	4948	2729	4520
14	0.393	0.916	4950	2730	4764
16	0.425	1.0			4952
18	0.420	1.0			4954
20	0.418	1.0			4956
22	0.368	0.828	4958	2734	4575
24	0.383	0.881	4960	2735	4695
26	0.391	0.909	4962	2736	4759
28	0.323	0.671	4964	2737	4231
30	0.368	0.828	4967	2739	4584
32	0.397	0.930	4969	2740	4813
34	0.377	0.860	4971	2741	4659
36	0.381	0.874	4973	2743	4692
38	0.416	0.996	4975	2744	4966
40	0.433	1.0			4977
42	0.350	0.765	4979	2747	4454
44	0.391	0.909	4981	2748	4778
46	0.410	0.975	4983	2749	4927
48	0.433	1.0			4985
50	0.416	0.996	4987	2752	4978
52	0.391	0.909	4990	2753	4786
54	0.391	0.909	4992	2754	4788
56	0.372	0.842	4994	2755	4640
58	0.337	0.720	4996	2756	4369
60	0.218	0.304	4998	2757	3438
62	0.206	0.262	5000	2758	3345
64	0.279	0.517	5002	2760	3919
66	0.279	0.517	5004	2761	3921
68	0.295	0.573	5006	2762	4048
70	0.312	0.632	5008	2763	4182
72	0.289	0.552	5011	2764	4004
74	0.287	0.545	5013	2765	3990
76	0.277	0.510	5015	2767	3913
78	0.272	0.493	5017	2768	3877
80	0.271	0.489	5019	2769	3869
82	0.290	0.556	5021	2770	4022
84	0.335	0.713	5023	2771	4377
86	0.328	0.688	5025	2772	4322
88	0.403	0.950	5027	2773	4914
90	0.406	0.961	5029	2775	4941
92	0.418	1.0			5032
94	0.389	0.902	5034	2777	4813

DEPTH (ft)	K(LOG)	K(CORR)	OB (psi)	Pr (psi)	CLOSURE P (psi)
4796	0.385	0.888	5036	2778	4783
98	0.340	0.730	5038	2779	4428
4800	0.312	0.632	5040	2780	4208
02	0.348	0.758	5042	2782	4495
04	0.351	0.769	5044	2783	4522
06	0.279	0.517	5046	2784	3953
08	0.339	0.727	5048	2785	4430
10	0.471	1.0			5050
12	0.420	1.0			5052
14	0.376	0.856	5055	2788	4729
16	0.316	0.646	5057	2790	4254
18	0.393	0.916	5059	2791	4868
20	0.379	0.867	5061	2792	4759
22	0.340	0.730	5063	2794	4450
24	0.239	0.377	5065	2795	3651
26	0.256	0.437	5067	2796	3788
28	0.276	0.507	5069	2797	3949
30	0.385	0.888	5071	2799	4817
32	0.481	1.0			5074
34	0.464	1.0			5076
36	0.383	0.881	5078	2802	4807
38	0.174	0.150	5080	2803	3144
40	0.230	0.346	5082	2804	3592
42	0.256	0.437	5084	2805	3801
44	0.255	0.433	5086	2807	3794
46	0.287	0.545	5088	2808	4051
48	0.312	0.632	5090	2809	4251
50	0.340	0.730	5092	2810	4476
52	0.379	0.867	5095	2811	4791
54	0.316	0.646	5097	2812	4288
56	0.318	0.653	5099	2814	4306
58	0.393	0.916	5101	2815	4909
60	0.425	1.0			5103
62	0.395	0.923	5105	2818	4929
64	0.374	0.849	5107	2819	4762
66	0.447	1.0			5109
68	0.420	1.0			5111
70	0.406	0.961	5113	2822	5024
72	0.305	0.608	5115	2823	4217
74	0.376	0.856	5118	2824	4788
76	0.253	0.426	5120	2825	3803
78	0.200	0.241	5122	2827	3380
80	0.292	0.563	5124	2828	4121
82	0.318	0.653	5126	2829	4329
84	0.383	0.881	5128	2831	4855
86	0.340	0.730	5130	2832	4510
88	0.318	0.653	5132	2833	4334
90	0.339	0.727	5135	2834	4507
92	0.335	0.713	5137	2835	4476
94	0.312	0.632	5139	2836	4291
96	0.126	0	5141	2837	2837

DEPTH (ft)	K(LOG)	K(CORR)	OB (psi)	Pr (psi)	CLOSURE P (psi)
4898	0.208	0.269	5143	2838	3458
4900	0.166	0.122	5145	2840	3121
02	0.112	0	5147	2841	2841
04	0.230	0.346	5150	2842	3641
06	0.189	0.203	5152	2843	3312
08	0.259	0.447	5154	2844	3877
10	0.227	0.335	5156	2846	3620
12	0.253	0.426	5158	2847	3831
14	0.404	0.954	5160	2848	5054
16	0.432	1.0			5162
18	0.420	1.0			5164
20	0.319	0.657	5166	2851	4372
22	0.172	0.143	5168	2853	3184
24	0.171	0.140	5170	2854	3178
26	0.252	0.423	5172	2855	3835
28	0.164	0.115	5174	2856	3123
30	0.248	0.409	5176	2857	3805
32	0.235	0.363	5179	2859	3701
34	0.238	0.374	5181	2860	3728
36	0.277	0.510	5183	2861	4045
38	0.399	0.937	5185	2862	5039
40	0.350	0.765	5187	2863	4641
42	0.312	0.632	5189	2864	4333
44	0.266	0.472	5191	2866	3963
46	0.346	0.751	5193	2867	4614
48	0.401	0.944	5195	2868	5065
50	0.377	0.860	5197	2869	4871
52	0.357	0.790	5199	2871	4710
54	0.412	0.982	5201	2872	5159
56	0.391	0.909	5203	2873	4991
58	0.408	0.968	5205	2874	5130
60	0.433	1.0			5208
62	0.422	1.0			5210
64	0.374	0.849	5212	2877	4859
66	0.353	0.776	5214	2878	4691
68	0.410	0.975	5216	2879	5158
70	0.370	0.835	5219	2880	4833
72	0.302	0.597	5221	2882	4278
74	0.214	0.290	5223	2883	3562
76	0.248	0.409	5225	2884	3841
78	0.276	0.507	5227	2885	4072
80	0.387	0.895	5229	2887	4983
82	0.379	0.867	5231	2888	4919
84	0.366	0.821	5233	2889	4813
86	0.332	0.702	5235	2890	4536
88	0.316	0.646	5237	2892	4407
90	0.302	0.597	5239	2893	4294
92	0.285	0.538	5241	2894	4157
94	0.319	0.657	5243	2895	4438
96	0.316	0.646	5246	2897	4414
98	0.261	0.454	5248	2898	3965

DEPTH (ft)	K(LOG)	K(CORR)	OB (psi)	Pr (psi)	CLOSURE P (psi)
5000	0.277	0.510	5250	2899	4098
02	0.285	0.538	5252	2900	4165
04	0.277	0.510	5254	2901	4101
06	0.258	0.444	5256	2902	3947
08	0.256	0.437	5258	2903	3932
10	0.258	0.444	5260	2905	3951
12	0.285	0.538	5262	2906	4174
14	0.292	0.563	5265	2907	4235
16	0.285	0.538	5267	2908	4177
18	0.255	0.433	5269	2909	3931
20	0.229	0.342	5271	2910	3717
22	0.230	0.346	5273	2912	3279
24	0.289	0.552	5275	2913	4217
26	0.307	0.615	5277	2914	4367
28	0.274	0.500	5279	2915	4097
30	0.277	0.510	5282	2917	4123
32	0.274	0.500	5284	2918	4101
34	0.302	0.597	5286	2919	4332
36	0.271	0.489	5288	2920	4078
38	0.284	0.535	5290	2921	4188
40	0.290	0.556	5292	2922	4240
42	0.294	0.570	5294	2923	4274
44	0.253	0.426	5296	2925	3935
46	0.277	0.510	5298	2926	4136
48	0.314	0.639	5300	2927	4443
50	0.269	0.482	5302	2928	4072
52	0.217	0.300	5304	2929	3642
54	0.261	0.454	5307	2930	4009
56	0.397	0.930	5309	2931	5143
58	0.401	0.944	5311	2932	5178
60	0.353	0.776	5313	2933	4780
62	0.351	0.769	5315	2934	4765
64	0.376	0.856	5317	2935	4974
66	0.429	1.0			5319
68	0.408	0.968	5321	2937	5245
70	0.416	0.996	5323	2938	5313
72	0.385	0.888	5326	2939	5059
74	0.377	0.860	5328	2940	4994
76	0.359	0.797	5330	2941	4845
78	0.328	0.688	5332	2943	4587
80	0.333	0.706	5334	2944	4631
82	0.332	0.702	5336	2945	4623
84	0.355	0.783	5338	2947	4819
86	0.353	0.776	5340	2948	4804
88	0.340	0.730	5342	2949	4696
90	0.350	0.765	5345	2950	4782
92	0.245	0.398	5347	2951	3905
94	0.359	0.797	5349	2952	4862
96	0.385	0.888	5351	2953	5082
98	0.387	0.895	5353	2954	5101
5100	0.422	1.0			5355

DEPTH (ft)	K(LOG)	K(CORR)	OB (psi)	Pr (psi)	CLOSURE P (psi)
5102	0.425	1.0			5357
04	0.385	0.888	5359	2958	5090
06	0.355	0.783	5361	2959	4840
08	0.292	0.563	5363	2960	4313
10	0.302	0.597	5366	2961	4397
12	0.274	0.500	5368	2962	4165
14	0.264	0.465	5370	2964	4083
16	0.259	0.447	5372	2965	4041
18	0.269	0.482	5374	2966	4127
20	0.224	0.325	5376	2967	3750
22	0.147	0.172	5378	2968	3383
24	0.323	0.671	5380	2970	4587
26	0.379	0.867	5382	2971	5061
28	0.374	0.849	5384	2972	5020
30	0.299	0.587	5387	2973	4390
32	0.416	0.996	5389	2974	5379
34	0.307	0.615	5391	2976	4461
36	0.250	0.416	5393	2977	3982
38	0.245	0.398	5395	2978	3940
40	0.282	0.528	5397	2979	4256
42	0.285	0.538	5399	2980	4281
44	0.318	0.653	5401	2981	4561
46	0.395	0.922	5403	2982	5214
48	0.401	0.944	5405	2984	5269
50	0.370	0.835	5408	2985	5008
52	0.335	0.712	5410	2986	4712
54	0.379	0.867	5412	2987	5089
56	0.389	0.902	5414	2988	5176
58	0.372	0.842	5416	2989	5033
60	0.271	0.489	5418	2991	4178
62	0.309	0.622	5420	2992	4502
64	0.252	0.423	5422	2993	4020
66	0.297	0.580	5424	2994	4403
68	0.418	1.0			5426
70	0.385	0.888	5428	2997	5156
72	0.376	0.856	5431	2998	5081
74	0.429	1.0			5433
76	0.374	0.849	5435	3000	5067
78	0.318	0.653	5437	3001	4592
80	0.387	0.895	5439	3003	5183
82	0.366	0.821	5441	3004	5005
84	0.387	0.895	5443	3005	5187
86	0.418	1.0			5445
88	0.372	0.842	5447	3007	5061
90	0.362	0.807	5450	3008	4979
92	0.425	1.0			5452
94	0.420	1.0			5454
96	0.383	0.881	5456	3012	5165
98	0.515	1.0			5458
5200	0.443	1.0			5460
02	0.449	1.0			5462

DEPTH (ft)	K(LOG)	K(CORR)	OB (psi)	Pr (psi)	CLOSURE P (psi)
5204	0.437	1.0			5464
06	0.451	1.0			5466
08	0.344	0.744	5468	3019	4841
10	0.377	0.860	5471	3020	5128
12	0.362	0.807	5473	3021	5000
14	0.330	0.695	5475	3023	4727
16	0.389	0.902	5477	3024	5237
18	0.364	0.814	5479	3025	5023
20	0.335	0.713	5481	3026	4776
22	0.305	0.608	5483	3027	4520
24	0.312	0.632	5485	3029	4581
26	0.372	0.842	5487	3030	5099
28	0.340	0.730	5489	3031	4825
30	0.314	0.639	5491	3032	4603
32	0.263	0.461	5494	3033	4168
34	0.227	0.335	5496	3034	3859
36	0.230	0.346	5498	3036	3888
38	0.252	0.423	5500	3037	4079
40	0.222	0.318	5502	3038	3822
42	0.241	0.384	5504	3039	3986
44	0.280	0.521	5506	3040	4325
46	0.323	0.671	5508	3041	4696
48	0.393	0.916	5510	3042	5303
50	0.353	0.776	5513	3043	4960
52	0.393	0.916	5515	3045	5308
54	0.368	0.828	5517	3046	5092
56	0.431	1.0			5519
58	0.410	0.975	5521	3049	5459
60	0.359	0.797	5523	3050	5021
62	0.266	0.472	5525	3051	4219
64	0.322	0.667	5527	3052	4703
66	0.387	0.895	5529	3054	5269
68	0.381	0.874	5531	3055	5219
70	0.404	0.954	5534	3056	5420
72	0.404	0.954	5536	3057	5421
74	0.335	0.713	5538	3058	4826
76	0.379	0.867	5540	3059	5210
78	0.429	1.0			5542
80	0.377	0.860	5544	3062	5197
82	0.351	0.769	5546	3063	4972
84	0.372	0.842	5548	3064	5156
86	0.284	0.535	5550	3065	4394
88	0.271	0.489	5552	3066	4282
90	0.399	0.937	5554	3067	5397
92	0.370	0.835	5556	3069	5146
94	0.332	0.702	5559	3070	4817
96	0.294	0.570	5561	3071	4490
98	0.272	0.493	5563	3072	4300
5300	0.259	0.447	5565	3073	4187
02	0.302	0.597	5567	3075	4563
04	0.242	0.388	5569	3076	4043

DEPTH (ft)	K(LOG)	K(CORR)	OB (psi)	Pr (psi)	CLOSURE P (psi)
5306	0.227	0.335	5571	3077	3912
08	0.387	0.895	5573	3078	5311
10	0.427	1.0			5575
12	0.416	0.996	5577	3080	5567
14	0.351	0.769	5579	3081	5002
16	0.319	0.657	5581	3082	4724
18	0.368	0.828	5584	3083	5154
20	0.339	0.727	5586	3085	4903
22	0.385	0.888	5588	3085	5308
24	0.376	0.856	5590	3086	5229
26	0.377	0.860	5592	3087	5241
28	0.464	1.0			5594
30	0.395	0.923	5596	3088	5403
32	0.312	0.632	5598	3089	4675
34	0.353	0.776	5601	3090	5039
36	0.304	0.604	5603	3091	4608
38	0.372	0.842	5605	3091	5208
40	0.309	0.622	5607	3092	4656
42	0.305	0.608	5609	3093	4623
44	0.256	0.437	5611	3094	4194
46	0.399	0.937	5613	3094	5454
48	0.325	0.678	5615	3095	4804
50	0.335	0.713	5618	3096	4894
52	0.247	0.405	5620	3097	4119
54	0.272	0.493	5622	3098	4342
56	0.121	0			3099
58	0.227	0.335	5626	3099	3946
60	0.290	0.556	5628	3100	4506
62	0.332	0.702	5630	3101	4876
64	0.325	0.678	5632	3101	4817
66	0.350	0.765	5634	3102	5039
68	0.399	0.937	5636	3103	5476
70	0.401	0.944	5639	3103	5497
72	0.370	0.835	5641	3104	5222
74	0.351	0.769	5643	3105	5057
76	0.368	0.828	5645	3106	5208
78	0.325	0.678	5647	3106	4829
80	0.276	0.507	5649	3107	4396
82	0.348	0.758	5651	3107	5035
84	0.397	0.930	5653	3108	5475
86	0.395	0.923	5655	3109	5459
88	0.312	0.632	5657	3110	4720
90	0.287	0.545	5660	3111	4500
92	0.271	0.489	5662	3112	4359
94	0.211	0.279	5664	3112	3824
96	0.276	0.507	5666	3113	4407
98	0.305	0.608	5668	3114	4667
5400	0.359	0.797	5670	3114	5151
02	0.383	0.881	5672	3115	5368
04	0.326	0.681	5674	3116	4858
06	0.294	0.570	5676	3117	4576

DEPTH (ft)	K(LOG)	K(CORR)	OB (psi)	Pr (psi)	CLOSURE P (psi)
5408	0.189	0.203	5679	3118	3638
10	0.370	0.835	5681	3119	5258
12	0.359	0.797	5683	3120	5163
14	0.321	0.664	5685	3121	4823
16	0.326	0.681	5687	3122	4869
18	0.404	0.954	5689	3123	5571
20	0.389	0.902	5691	3124	5439
22	0.328	0.688	5693	3125	4892
24	0.325	0.678	5695	3126	4868
26	0.326	0.681	5697	3127	4877
28	0.416	0.996	5699	3128	5689
30	0.318	0.653	5702	3129	4809
32	0.299	0.587	5704	3130	4641
34	0.385	0.888	5706	3131	5418
36	0.297	0.580	5708	3133	4627
38	0.340	0.730	5710	3134	5014
40	0.337	0.720	5712	3135	4990
42	0.357	0.790	5714	3136	5173
44	0.376	0.856	5716	3137	5345
46	0.377	0.860	5718	3140	5357
48	0.370	0.835	5720	3143	5295
50	0.376	0.856	5722	3146	5351
52	0.376	0.856	5725	3149	5354
54	0.395	0.923	5727	3152	5529
56	0.376	0.856	5729	3152	5358
58	0.414	0.989	5731	3156	5703
60	0.342	0.737	5733	3160	5056
62	0.271	0.489	5735	3164	4421
64	0.300	0.591	5737	3168	4686
66	0.408	0.968	5739	3172	5657
68	0.395	0.923	5741	3176	5543
70	0.366	0.821	5743	3180	5284
72	0.391	0.909	5746	3184	5513
74	0.410	0.975	5748	3188	5684
76	0.366	0.821	5750	3192	5292
78	0.318	0.653	5752	3196	4865
80	0.328	0.688	5754	3200	4957
82	0.253	0.426	5756	3200	4289
84	0.292	0.563	5758	3200	4640
86	0.276	0.507	5760	3200	4498
88	0.215	0.293	5762	3200	3951
90	0.271	0.489	5765	3200	4454
92	0.290	0.556	5767	3200	4627
94	0.230	0.346	5769	3200	4089
96	0.408	0.968	5771	3200	5689
98	0.520	1.0			5773
5500	0.379	0.867	5775	3200	5433
02	0.362	0.807	5777	3200	5280
04	0.346	0.751	5779	3200	5137
06	0.319	0.657	5781	3200	4896
08	0.425	1.0			5783

DEPTH (ft)	K(LOG)	K(CORR)	OB (psi)	Pr (psi)	CLOSURE P (psi)
5510	0.307	0.615	5786	3200	4790
12	0.376	0.856	5788	3200	5415
14	0.316	0.646	5790	3200	4873
16	0.325	0.678	5792	3200	4957
18	0.385	0.888	5794	3200	5503
20	0.361	0.804	5796	3200	5287
22	0.403	0.950	5798	3200	5668
24	0.391	0.909	5800	3200	5563
26	0.305	0.608	5802	3200	4782
28	0.410	0.975	5804	3200	5739
30	0.376	0.856	5806	3200	5431
32	0.319	0.657	5808	3200	4913
34	0.280	0.521	5810	3200	4560
36	0.211	0.279	5812	3200	3929
38	0.236	0.367	5815	3200	4160
40	0.209	0.272	5817	3200	3912
42	0.175	0.154	5819	3200	3603
44	0.168	0.129	5821	3200	3538
46	0.168	0.129	5823	3200	3538
48	0.239	0.377	5826	3200	4190
50	0.200	0.241	5828	3200	3833
52	0.189	0.203	5830	3200	3734
54	0.199	0.238	5832	3200	3826
56	0.144	0.045	5834	3200	3319
58	0.224	0.325	5836	3200	4057
60	0.174	0.150	5838	3200	3596
62	0.174	0.150	5840	3200	3596
64	0.183	0.182	5842	3200	3681
66	0.115	0	5844	3200	3200
68	0.193	0.217	5846	3200	3774
70	0.300	0.591	5848	3200	4765
72	0.353	0.776	5851	3200	5257
74	0.312	0.632	5853	3200	4877
76	0.333	0.706	5855	3200	5074
78	0.361	0.804	5857	3200	5336
80	0.439	1.0			5859
82	0.376	0.856	5861	3200	5478
84	0.363	0.811	5863	3200	5360
86	0.326	0.681	5865	3200	5015
88	0.264	0.465	5867	3200	4440
90	0.348	0.758	5870	3200	5224
92	0.391	0.909	5872	3200	5629
94	0.404	0.954	5874	3200	5751
96	0.366	0.821	5876	3200	5397
98	0.366	0.821	5878	3200	5399
5600	0.403	0.950	5880	3200	5746
02	0.264	0.465	5882	3200	4447
04	0.433	1.0			5884
06	0.420	1.0			5886
08	0.502	1.0			5888
10	0.471	1.0			5890

DEPTH (ft)	K(LOG)	K(CORR)	OB (psi)	Pr (psi)	CLOSURE P (psi)
5612	0.359	0.797	5893	3224	5351
14	0.359	0.797	5895	3228	5354
16	0.314	0.639	5897	3232	4935
18	0.330	0.695	5899	3236	5087
20	0.376	0.856	5901	3238	5518
22	0.404	0.954	5903	3240	5781
24	0.391	0.909	5905	3241	5663
26	0.355	0.783	5907	3243	5329
28	0.370	0.835	5909	3245	5469
30	0.420	1.0			5911
32	0.418	1.0			5914
34	0.408	0.968	5916	3249	5831
36	0.355	0.783	5918	3251	5339
38	0.309	0.622	5920	3252	4911
40	0.344	0.744	5922	3254	5239
42	0.340	0.730	5924	3255	5203
44	0.305	0.608	5926	3257	4880
46	0.357	0.790	5928	3258	5367
48	0.339	0.727	5930	3259	5201
50	0.431	1.0			5933
52	0.350	0.765	5935	3262	5307
54	0.348	0.758	5937	3263	5290
56	0.395	0.923	5939	3265	5733
58	0.325	0.678	5941	3266	5080
60	0.372	0.842	5943	3267	5520
62	0.385	0.888	5945	3269	5645
64	0.328	0.688	5947	3270	5112
66	0.381	0.874	5949	3271	5612
68	0.307	0.615	5951	3272	4920
70	0.333	0.706	5954	3274	5166
72	0.359	0.797	5956	3275	5412
74	0.297	0.580	5958	3276	4832
76	0.362	0.807	5960	3278	5442
78	0.277	0.510	5962	3279	4647
80	0.350	0.765	5964	3280	5333
82	0.302	0.597	5966	3281	4884
84	0.335	0.713	5968	3282	5197
86	0.321	0.664	5970	3283	5067
88	0.323	0.671	5972	3284	5088
90	0.323	0.671	5975	3285	5090
92	0.314	0.639	5977	3286	5006
94	0.309	0.622	5979	3287	4961
96	0.271	0.489	5981	3288	4605
98	0.229	0.342	5983	3289	4210
5700	0.323	0.671	5985	3290	5098
02	0.379	0.867	5987	3291	5628
04	0.466	1.0			5989
06	0.335	0.713	5991	3293	5217
08	0.377	0.860	5993	3294	5615
10	0.307	0.615	5996	3295	4956
12	0.391	0.909	5998	3296	5752

DEPTH (ft)	K(LOG)	K(CORR)	OB (psi)	Pr (psi)	CLOSURE P (psi)
5714	0.337	0.720	6000	3297	5243
16	0.307	0.615	6002	3298	4961
18	0.274	0.500	6004	3299	4652
20	0.247	0.405	6006	3300	4396
22	0.227	0.335	6008	3300	4207
24	0.167	0.126	6010	3300	3641
26	0.159	0.098	6012	3300	3566
28	0.175	0.154	6014	3300	3718
30	0.285	0.538	6017	3300	4762
32	0.295	0.573	6019	3300	4858
34	0.263	0.461	6021	3300	4554
36	0.255	0.433	6023	3300	4479
38	0.276	0.507	6025	3300	4682
40	0.364	0.814	6027	3300	5520
42	0.379	0.867	6029	3300	5666
44	0.342	0.737	6031	3300	5313
46	0.346	0.751	6033	3300	5352
48	0.477	1.0			6035
50	0.495	1.0			6038
52	0.287	0.545	6040	3318	4801
54	0.328	0.688	6042	3323	5194
56	0.241	0.384	6044	3328	4371
58	0.295	0.573	6046	3338	4890
60	0.368	0.828	6048	3348	5584
62	0.387	0.895	6050	3358	5767
64	0.374	0.849	6052	3368	5647
66	0.376	0.856	6054	3380	5669
68	0.342	0.737	6057	3392	5356
70	0.408	0.968	6059	3404	5974
72	0.385	0.888	6061	3416	5765
74	0.330	0.695	6063	3428	5259
76	0.368	0.828	6065	3435	5613
78	0.332	0.702	6067	3450	5287
80	0.289	0.552	6069	3450	4896
82	0.385	0.888	6071	3450	5777
84	0.416	0.996	6073	3450	6063
86	0.267	0.475	6075	3450	4697
88	0.342	0.737	6077	3450	5386
90	0.362	0.807	6080	3450	5572
92	0.406	0.961	6082	3450	5979
94	0.393	0.916	6084	3450	5863
96	0.370	0.835	6086	3450	5651
98	0.362	0.807	6087	3450	5578
5800	0.451	1.0			6089
02	0.495	1.0			6092
04	0.339	0.727	6094	3450	5372
06	0.359	0.797	6096	3450	5559
08	0.314	0.639	6098	3450	5142
10	0.271	0.489	6101	3450	4746
12	0.307	0.615	6103	3450	5082
14	0.300	0.591	6105	3450	5019

DEPTH (ft)	K(LOG)	K(CORR)	OB (psi)	Pr (psi)	CLOSURE P (psi)
5816	0.401	0.944	6107	3450	5958
18	0.319	0.657	6109	3450	5197
20	0.300	0.591	6111	3450	5023
22	0.333	0.706	6113	3450	5330
24	0.330	0.695	6115	3450	5302
26	0.311	0.629	6117	3450	5128
28	0.250	0.416	6120	3450	4561
30	0.198	0.234	6122	3450	4075
32	0.238	0.374	6124	3450	4450
34	0.155	0.084	6126	3450	3675
36	0.208	0.269	6128	3450	4170
38	0.168	0.129	6130	3450	3796
40	0.147	0.056	6132	3450	3600
42	0.157	0.091	6134	3450	3694
44	0.289	0.552	6136	3450	4933
46	0.383	0.881	6138	3450	5818
48	0.330	0.695	6140	3450	5320
50	0.337	0.720	6143	3450	5389
52	0.323	0.671	6145	3451	5259
54	0.397	0.930	6147	3452	5958
56	0.376	0.856	6149	3454	5761
58	0.395	0.923	6151	3455	5943
60	0.416	0.996	6153	3457	6142
62	0.253	0.426	6155	3458	4607
64	0.344	0.744	6157	3459	5466
66	0.379	0.867	6160	3460	5801
68	0.340	0.730	6162	3462	5433
70	0.350	0.765	6164	3464	5530
72	0.335	0.713	6166	3465	5391
74	0.326	0.681	6168	3466	5306
76	0.353	0.776	6170	3467	5565
78	0.312	0.632	6172	3469	5177
80	0.383	0.881	6174	3471	5852
82	0.433	1.0			6176
84	0.328	0.688	6178	3473	5334
86	0.319	0.657	6180	3474	5252
88	0.277	0.510	6183	3475	4856
90	0.230	0.346	6185	3477	4414
92	0.220	0.311	6187	3478	4320
94	0.285	0.538	6189	3479	4937
96	0.280	0.521	6191	3481	4893
98	0.316	0.646	6193	3482	5233
5900	0.300	0.591	6195	3484	5086
02	0.309	0.622	6197	3485	5172
04	0.297	0.580	6199	3486	5060
06	0.305	0.608	6201	3488	5138
08	0.340	0.730	6203	3489	5470
10	0.319	0.657	6206	3490	5274
12	0.323	0.671	6208	3491	5314
14	0.295	0.573	6210	3493	5050
16	0.220	0.311	6212	3494	4339

DEPTH (ft)	K(LOG)	K(CORR)	OB (psi)	Pr (psi)	CLOSURE P (psi)
5918	0.236	0.367	6214	3495	4493
20	0.359	0.797	6216	3497	5664
22	0.233	0.356	6218	3498	4466
24	0.175	0.154	6220	3499	3918
26	0.302	0.597	6222	3500	5125
28	0.302	0.597	6224	3502	5127
30	0.404	0.954	6227	3503	6102
32	0.376	0.856	6229	3505	5837
34	0.287	0.545	6231	3506	4991
36	0.364	0.814	6233	3507	5726
38	0.395	0.923	6235	3509	6025
40	0.376	0.856	6237	3510	5844
42	0.370	0.835	6239	3511	5789
44	0.381	0.874	6241	3513	5897
46	0.376	0.856	6243	3515	5850
48	0.346	0.751	6245	3517	5566
50	0.312	0.632	6248	3519	5244
52	0.305	0.608	6250	3521	5180
54	0.287	0.545	6252	3523	5010
56	0.161	0.105	6254	3525	3812
58	0.202	0.248	6256	3526	4203
60	0.274	0.500	6258	3528	4893
62	0.307	0.615	6260	3530	5209
64	0.297	0.580	6262	3531	5115
66	0.171	0.140	6264	3532	3914
68	0.041	0	6267	3533	3533
70	0.200	0.241	6269	3534	4193
72	0.220	0.311	6271	3535	4386
74	0.058	0	6273	3535	3535
76	0.211	0.279	6275	3536	4300
78	0.239	0.377	6277	3537	4570
80	0.271	0.489	6279	3538	4878
82	0.282	0.528	6282	3539	4987
84	0.418	1.0			6284
86	0.328	0.688	6286	3541	5431
88	0.340	0.730	6288	3542	5547
90	0.357	0.790	6290	3543	5713
92	0.383	0.881	6292	3543	5965
94	0.376	0.856	6294	3544	5898
96	0.318	0.653	6296	3545	5341
98	0.297	0.580	6298	3546	5142
6000	0.304	0.604	6300	3547	5210

APPENDIX C

FRACTURE ANALYSIS SIMULATOR INPUT/OUTPUT

C.1: SIMULATION OF FLUVIAL "B" FOAM MINIFRAC iNJECTION/ DECLINE PRESSURE HISTORY MATCH.

Frac Summary * FLUVIAL B FOAM MINIFRAC
Filename: FLUV-B-M.FRK

Design Data		
FLUID LOSS:	Coefficient (ft/sqrt(min))	0.0007
	Spurt Loss (gal/100 sq ft)	0.00
FORMATION:	Modulus (MM psi)	5.00
	Fracture Height (ft)	25.0
	Fluid Loss Height (ft)	25.0
	Perforated Height (ft)	10.0
TEMPERATURE:	Bottom Hole (deg F)	160
PRESSURE:	Reservoir Pressure (psi)	3450.0
	Closure Pressure (psi)	4550.0
DEPTH:	Well Depth (ft)	5825

FORMATION LAYER DATA:

Depth	Stress at Top	Stress Grad	Modulus	Toughness
5570	5475.0	0.000	5.00	1.00
5719	4700.0	0.000	5.00	1.00
5739	5700.0	0.000	5.00	1.00
5825	4550.0	0.000	5.00	1.00
5850	5575.0	0.000	5.00	1.00
5886	5200.0	0.000	5.00	1.00
5927	5775.0	0.000	5.00	1.00
5953	4200.0	0.000	5.00	1.00
5980	5600.0	0.433	5.00	1.00

Fluid Pressure Gradient (psi/ft)		0.433
Fracture Top (ft)		5825
Fracture Bottom (ft)		5835

Calculated Results
from 3-D Simulator
STIMPLAN (TM) , NSI , Tulsa,OK
Licensed To: Internal Use - NSI Technologies

1/2 LENGTH:	'Hydraulic' length (ft)	893
	Propped length (ft)	0
PRESSURE:	Max Net Pressure (psi)	965
TIME:	Max Exposure to Form. Temp. (min) ..	13.9
	Time to Close (min)	80.0
RATE:	Fluid Loss Rate during pad (bpm) ...	0.0
EFFICIENCY:	at end of pumping schedule	0.67
PROPPANT:	Average In Situ Conc. (#/sq ft)	0.0
	Average Conductivity (md-ft)	0
HEIGHT:	Max Fracture Height (ft)	159
WIDTH:	Avg width at end of pumping (in) ...	0.06

STIMPLAN (TM). NSI Technologies, Tulsa, OK
Licensed To: Internal Use - NSI Technologies

WELL ID:
FLUVIAL B FOAM MINIFRAC

DEPTH:	Well Depth (ft)	5825
PRESSURE:	Reservoir Pressure (psi)	3450
	Closure Pressure (psi)	4550
TEMPERATURE:	Bottom Hole Temperature (deg F)	160

** Pumping Schedule **

Sl Vol (Mgal)	Fl Vol (Mgal)	Conc (ppg)	Rate (bpm)	Fluid Type	Prop Type	Cum Prop (M-lb)	Pump Time (min)
0.3	0.3	0.0	10.0	2	1	0.0	0.7
7.7	7.7	0.0	10.0	1	1	0.0	18.3

Total Slurry ...	8.0	Total Fluid ...	8.0
Total Proppant ...	0.0	Avg. Conc	0.0
Total Pump Time	19.0 min		

Proppant ID No. 1 20- 40 Ottawa_Snd

Specific Gravity	2.65
'Damage Factor'	0.70

Closure Pres (Mpsi)	0	2	4	8	16
KfW @ 2 #/sq ft (md-ft)	2000	2000	2000	2000	2000

Fluid ID No. 2 Nitrogen-Foam_Comb.

Specific Gravity 0.60

	@Welbor	@FormTmp	@1Hr	@2Hr	@4Hr	@8Hr
vis (cp @ 170 1/sec) .	5	5	5	5	5	5
non-Newtonian n'	0.50	0.50	0.50	0.50	0.50	0.50

Fluid ID No. 1	Foam_75_Qual,_20#-HPG,_150_F					
Specific Gravity					1.04	
Quality					75	
	@Welbor	@FormTmp	@1Hr	@2Hr	@4Hr	@8Hr
vis (cp @ 170 1/sec) .	50	40	30	20	10	10
non-Newtonian n'	0.52	0.52	0.52	0.57	0.57	0.57

Time History * NSI STIMPLAN 3-D Fracture Simulation
FLUVIAL B FOAM MINIFRAC

Time (min)	Pen (ft)	Pres (psi)	Rate (bpm)	Prop (PPG)	Sl Vol (MGal)	Eff-ciency	Loss (bpm)	Hght (ft)	W-Avg (in)
0.2	74	220	10.0	0.0	0.1	0.62	3.7	32	0.01
0.6	124	390	10.0	0.0	0.2	0.55	3.3	32	0.03
1.0	174	452	10.0	0.0	0.4	0.53	3.6	32	0.03
1.4	224	509	10.0	0.0	0.6	0.50	4.0	32	0.03
1.9	274	589	10.0	0.0	0.8	0.51	4.3	33	0.04
2.4	324	657	10.0	0.0	1.0	0.51	4.5	37	0.04
3.4	374	741	10.0	0.0	1.4	0.53	4.2	45	0.05
4.6	424	823	10.0	0.0	1.9	0.56	3.8	54	0.05
6.0	474	861	10.0	0.0	2.5	0.59	3.7	64	0.05
7.4	524	885	10.0	0.0	3.1	0.60	3.7	72	0.06
8.9	574	906	10.0	0.0	3.7	0.62	3.8	78	0.06
10.4	624	919	10.0	0.0	4.4	0.63	3.8	117	0.06
12.1	674	906	10.0	0.0	5.1	0.64	3.9	117	0.06
13.4	724	956	10.0	0.0	5.7	0.64	4.0	157	0.06
14.8	749	792	10.0	0.0	6.2	0.66	3.8	157	0.06
16.8	799	896	10.0	0.0	7.1	0.66	3.9	157	0.06
19.1	868	965	10.0	0.0	8.0	0.67	4.3	159	0.06
20.8	893	715	0.0	0.0	8.0	0.64	3.8	159	0.06
25.9	893	644	0.0	0.0	8.0	0.58	2.8	159	0.05
32.3	893	572	0.0	0.0	8.0	0.51	2.4	159	0.05
39.7	893	501	0.0	0.0	8.0	0.45	2.1	159	0.04
48.0	893	429	0.0	0.0	8.0	0.39	1.9	159	0.03
57.0	893	358	0.0	0.0	8.0	0.32	1.7	159	0.03
66.6	893	286	0.0	0.0	8.0	0.26	1.5	159	0.02
76.9	893	215	0.0	0.0	8.0	0.19	1.4	159	0.02
87.8	893	143	0.0	0.0	8.0	0.13	1.3	159	0.01
99.1	893	72	0.0	0.0	8.0	0.06	1.2	159	0.01

GEOMETRY SUMMARY * At End of Pumping Schedule
FLUVIAL B FOAM MINIFRAC

Dstnce (ft)	Press (psi)	W-Avg (in)	Q (bpm)	Sh-Rate (1/sec)	Hght (ft) Total	Up	Dn	Prop	Bank Fraction	Prop (PSF)
24	962	0.11	4.9	89	159	37	111	141	0.00	0.00
61	954	0.06	4.5	287	155	35	110	137	0.00	0.00
99	945	0.06	4.3	299	149	31	108	133	0.00	0.00
149	930	0.05	4.1	452	121	24	87	108	0.00	0.00
199	917	0.07	3.9	326	80	20	50	56	0.00	0.00
249	903	0.07	3.7	343	76	19	48	53	0.00	0.00
299	890	0.07	3.6	372	73	17	45	50	0.00	0.00
349	875	0.07	3.5	408	69	16	43	47	0.00	0.00
399	860	0.07	3.3	427	64	14	41	43	0.00	0.00
449	843	0.06	3.2	463	61	13	38	41	0.00	0.00
499	824	0.06	3.0	499	57	13	34	39	0.00	0.00
549	803	0.06	2.8	517	53	12	31	37	0.00	0.00
599	785	0.06	2.7	567	50	12	29	36	0.00	0.00
649	782	0.05	2.4	606	49	11	28	35	0.00	0.00
699	729	0.05	2.1	689	45	9	26	32	0.00	0.00
736	690	0.05	1.8	653	41	7	24	30	0.00	0.00
774	674	0.06	1.6	547	35	4	21	27	0.00	0.00
833	425	0.04	1.1	813	32	3	19	24	0.00	0.00

FLUID SUMMARY * At End of Pumping Schedule
FLUVIAL B FOAM MINIFRAC

Stage No	Gone	Fluid ID	Prop ID	Pos (ft)	Concentration In	Now	Desgn	Fl (MGal)	Vol Ex Tim (min)	Temp (deg F)	Visc (cp)	Fall Frac
1	1	2	1	868	0.0	0.0	0.0	0.1	2.8	160	1	0.00
1	1	2	1	868	0.0	0.0	0.0	0.2	3.2	160	1	0.00
1	1	2	1	868	0.0	0.0	0.0	0.3	5.9	160	1	0.00
2	1	1	1	868	0.0	0.0	0.0	0.4	7.0	160	10	0.00
2	1	1	1	868	0.0	0.0	0.0	0.6	9.6	160	10	0.00
2	1	1	1	868	0.0	0.0	0.0	0.8	10.6	160	10	0.00
2	1	1	1	868	0.0	0.0	0.0	1.0	12.9	160	11	0.00
2	0	1	1	862	0.0	0.0	0.0	1.4	13.9	160	11	0.00
2	0	1	1	828	0.0	0.0	0.2	1.9	11.2	160	11	0.00
2	0	1	1	742	0.0	0.0	0.5	2.5	9.7	160	13	0.00
2	0	1	1	622	0.0	0.0	0.7	3.1	6.7	160	14	0.00
2	0	1	1	502	0.0	0.0	0.9	3.7	5.2	160	15	0.00
2	0	1	1	392	0.0	0.0	0.9	4.3	2.2	160	16	0.00
2	0	1	1	292	0.0	0.0	0.9	5.0	0.0	160	17	0.00
2	0	1	1	207	0.0	0.0	0.9	5.5	0.0	108	20	0.00
2	0	1	1	140	0.0	0.0	0.9	6.1	0.0	84	23	0.00
2	0	1	1	76	0.0	0.0	1.0	6.8	0.0	78	27	0.00
2	0	1	1	22	0.0	0.0	1.0	7.8	0.0	73	41	0.00

C.2: PRESSURE HISTORY MATCH OF FLUVIAL "B" FOAM FRACTURE TREATMENT USING SAME INPUT PARAMETERS USED TO HISTORY MATCH THE MINIFRAC.

Frac Summary * FLUVIAL B FOAM MINIFRAC
Filename: FLUV-B-M.FRK

Design Data		
FLUID LOSS:	Coefficient (ft/sqrt(min))	0.0005
	Spurt Loss (gal/100 sq ft)	0.00
FORMATION:	Modulus (MM psi)	5.00
	Fracture Height (ft)	25.0
	Fluid Loss Height (ft)	25.0
	Perforated Height (ft)	10.0
TEMPERATURE:	Bottom Hole (deg F)	160
PRESSURE:	Reservoir Pressure (psi)	3450.0
	Closure Pressure (psi)	4550.0
DEPTH:	Well Depth (ft)	5825

FORMATION LAYER DATA:

Depth	Stress at Top	Stress Grad	Modulus	Toughness
5570	5475.0	0.000	5.00	1.00
5719	4700.0	0.000	5.00	1.00
5739	5700.0	0.000	5.00	1.00
5825	4550.0	0.000	5.00	1.00
5850	5575.0	0.000	5.00	1.00
5886	5200.0	0.000	5.00	1.00
5927	5775.0	0.000	5.00	1.00
5953	4200.0	0.000	5.00	1.00
5980	5600.0	0.433	5.00	1.00

Fluid Pressure Gradient (psi/ft)		0.433
Fracture Top (ft)		5825
Fracture Bottom (ft)		5835

Calculated Results from 3-D Simulator STIMPLAN (TM) , NSI , Tulsa,OK Licensed To: Internal Use - NSI Technologies		
1/2 LENGTH:	'Hydraulic' length (ft)	1487
	Propped length (ft)	775
PRESSURE:	Max Net Pressure (psi)	983
TIME:	Max Exposure to Form. Temp. (min) ..	44.9
	Time to Close (min)	347.3
RATE:	Fluid Loss Rate during pad (bpm) ...	2.5
EFFICIENCY:	at end of pumping schedule	0.74
PROPPANT:	Average In Situ Conc. (#/sq ft)	0.3
	Average Conductivity (md-ft)	719
HEIGHT:	Max Fracture Height (ft)	288
WIDTH:	Avg width at end of pumping (in) ...	0.07

STIMPLAN (TM). NSI Technologies, Tulsa, OK
Licensed To: Internal Use - NSI Technologies

WELL ID:
FLUVIAL B FOAM MINIFRAC

DEPTH:	Well Depth (ft)	5825
PRESSURE:	Reservoir Pressure (psi)	3450
	Closure Pressure (psi)	4550
TEMPERATURE:	Bottom Hole Temperature (deg F)	160

** Pumping Schedule **

Sl Vol (Mgal)	Fl Vol (Mgal)	Conc (ppg)	Rate (bpm)	Fluid Type	Prop Type	Cum Prop (M-lb)	Pump Time (min)
8.0	8.0	0.0	11.0	1	1	0.0	17.3
1.2	1.2	1.0	11.0	1	1	1.2	2.7
0.1	0.1	0.0	0.2	1	1	1.2	11.9
1.3	1.3	1.0	11.0	1	1	2.5	2.9
2.8	2.5	3.0	11.0	1	1	10.0	6.0
6.5	5.6	4.0	11.0	1	1	32.5	14.0

Total Slurry ...	20.0	Total Fluid ...	18.7
Total Proppant ...	32.5	Avg. Conc	1.7
Total Pump Time	54.9 min		

Proppant ID No. 1 — 20- 40 Pro-Flow

Specific Gravity	3.15
'Damage Factor'	0.80

Closure Pres (Mpsi)	0	2	4	8	16
KfW @ 2 #/sq ft (md-ft)	11000	10500	9200	5400	950

Fluid ID No. 1 — Foam_75_Qual,_20#-HPG,_150_F

Specific Gravity	1.04
Quality	75

	@Welbor	@FormTmp	@1Hr	@2Hr	@4Hr	@8Hr
vis (cp @ 170 1/sec) .	50	40	30	20	10	10
non-Newtonian n'	0.52	0.52	0.52	0.57	0.57	0.57

Time History * NSI STIMPLAN 3-D Fracture Simulation
FLUVIAL B FOAM MINIFRAC

Time (min)	Pen (ft)	Pres (psi)	Rate (bpm)	Prop (PPG)	Sl Vol (MGal)	Eff-ciency	Loss (bpm)	Hght (ft)	W-Avg (in)
0.3	75	433	11.0	0.0	0.1	0.80	2.1	44	0.02
1.0	125	779	11.0	0.0	0.5	0.73	1.8	44	0.05
1.8	175	909	11.0	0.0	0.8	0.72	1.9	67	0.05
2.6	225	882	11.0	0.0	1.2	0.73	2.1	71	0.06
3.4	275	902	11.0	0.0	1.6	0.74	2.3	77	0.06
4.2	325	902	11.0	0.0	2.0	0.74	2.5	78	0.06
5.1	375	914	11.0	0.0	2.3	0.74	2.6	81	0.06
6.0	425	918	11.0	0.0	2.8	0.75	2.8	122	0.06
7.2	475	890	11.0	0.0	3.3	0.75	2.8	122	0.06
8.1	525	941	11.0	0.0	3.8	0.75	2.9	148	0.06
9.7	575	862	11.0	0.0	4.5	0.75	2.8	148	0.06
11.0	625	931	11.0	0.0	5.1	0.76	2.9	148	0.07
12.1	675	959	11.0	0.0	5.6	0.76	3.0	160	0.06
14.1	725	865	11.0	0.0	6.5	0.76	2.9	160	0.07
15.6	775	931	11.0	0.0	7.2	0.76	2.9	160	0.07
16.9	825	969	11.0	0.0	7.8	0.76	3.1	165	0.07
20.0	888	838	11.0	0.0	9.3	0.77	3.0	165	0.07
23.7	938	808	0.2	0.0	9.3	0.73	2.7	165	0.07
25.3	963	792	0.2	0.0	9.3	0.73	2.6	165	0.06
26.7	988	781	0.2	0.0	9.3	0.72	2.6	165	0.06
28.2	1013	768	0.2	0.0	9.3	0.71	2.6	165	0.06
30.1	1038	747	0.2	0.0	9.4	0.70	2.6	165	0.06
31.9	1056	729	0.2	0.0	9.4	0.68	2.4	165	0.05
35.3	1106	869	11.0	1.0	10.9	0.70	2.5	165	0.06
37.7	1156	937	11.0	3.0	12.0	0.70	2.7	165	0.07
39.6	1206	982	11.0	3.0	12.9	0.71	2.8	247	0.06
43.7	1256	848	11.0	3.0	14.8	0.71	2.7	247	0.07
46.8	1306	933	11.0	4.0	16.2	0.72	2.7	247	0.07
49.0	1356	983	11.0	4.0	17.3	0.73	2.9	288	0.07
52.9	1406	873	11.0	4.0	19.1	0.74	2.8	288	0.07
54.9	1437	916	11.0	4.0	20.0	0.74	2.7	288	0.07
58.2	1487	879	0.0	0.0	20.0	0.73	2.8	288	0.07
75.3	1487	791	0.0	0.0	20.0	0.66	1.9	288	0.06
98.4	1487	703	0.0	0.0	20.0	0.58	1.6	288	0.06
126.9	1487	615	0.0	0.0	20.0	0.51	1.4	288	0.05
160.1	1487	527	0.0	0.0	20.0	0.44	1.2	288	0.04
196.7	1487	440	0.0	0.0	20.0	0.38	1.1	288	0.04
235.6	1487	352	0.0	0.0	20.0	0.31	0.9	288	0.03
275.0	1487	264	0.0	0.0	20.0	0.25	0.9	288	0.02
328.3	1487	176	0.0	0.0	20.0	0.24	0.8	288	0.03
402.2	1487	88	0.0	0.0	20.0	0.21	0.7	288	0.03

GEOMETRY SUMMARY * At End of Pumping Schedule
FLUVIAL B FOAM MINIFRAC

Dstnce (ft)	Press (psi)	W-Avg (in)	Q (bpm)	Sh-Rate (1/sec)	Hght (ft) Total	Up	Dn	Prop	Bank Fraction	Prop (PSF)
25	915	0.17	5.4	23	288	62	216	257	0.01	0.43
63	913	0.15	4.6	28	252	52	189	227	0.01	0.38
100	908	0.12	4.3	69	167	39	118	143	0.01	0.31
150	902	0.11	4.0	69	164	39	115	143	0.01	0.28
200	895	0.11	3.7	69	161	39	112	143	0.01	0.21
250	888	0.10	3.4	72	156	35	110	138	0.01	0.20
300	880	0.10	3.1	75	150	31	108	133	0.01	0.10
350	872	0.07	2.8	160	121	25	87	109	0.01	0.05
400	861	0.07	2.7	227	81	21	51	57	0.01	0.05
450	852	0.07	2.6	234	78	19	49	55	0.01	0.05
500	841	0.07	2.5	242	75	18	47	52	0.00	0.05
550	831	0.07	2.4	252	72	17	45	49	0.00	0.04
600	820	0.07	2.3	263	68	15	43	46	0.00	0.00
650	809	0.07	2.3	277	65	14	41	43	0.00	0.00
700	797	0.07	2.2	287	62	13	38	41	0.00	0.00
750	784	0.07	2.1	297	59	13	36	40	0.00	0.00
800	771	0.07	2.0	308	56	13	33	38	0.00	0.00
857	755	0.06	1.9	326	52	12	30	36	0.00	0.00
913	738	0.06	1.8	333	50	12	28	35	0.00	0.00
951	726	0.06	1.8	334	49	11	28	35	0.00	0.00
976	718	0.06	1.7	338	48	11	27	34	0.00	0.00
1001	710	0.06	1.7	341	47	10	27	34	0.00	0.00
1026	702	0.06	1.6	345	46	10	26	33	0.00	0.00
1047	694	0.06	1.6	348	45	9	26	33	0.00	0.00
1081	682	0.06	1.6	358	44	9	26	32	0.00	0.00
1131	663	0.06	1.5	359	44	9	26	32	0.00	0.00
1181	641	0.06	1.4	361	44	9	26	32	0.00	0.00
1231	615	0.05	1.3	367	44	9	26	32	0.00	0.00
1281	579	0.05	1.2	382	44	9	26	32	0.00	0.00
1331	521	0.05	1.1	424	44	9	26	32	0.00	0.00
1381	393	0.03	0.9	628	44	9	26	32	0.00	0.00
1421	164	0.01	0.6	2355	44	9	26	32	0.00	0.00

FLUID SUMMARY * At End of Pumping Schedule
FLUVIAL B FOAM MINIFRAC

Stage No	Stage Gone	Fluid ID	Prop ID	Pos (ft)	Concentration In	Concentration Now	Concentration Desgn	Fl Vol (MGal)	Ex Tim (min)	Temp (deg F)	Visc (cp)	Fall Frac
1	1	1	1	1437	0.0	0.0	0.0	0.1	12.9	160	10	0.00
1	1	1	1	1437	0.0	0.0	0.0	0.5	17.0	160	13	0.00
1	1	1	1	1437	0.0	0.0	0.0	0.8	23.9	160	11	0.00
1	1	1	1	1437	0.0	0.0	0.0	1.2	29.8	160	11	0.00
1	1	1	1	1437	0.0	0.0	0.0	1.6	34.0	160	12	0.00
1	1	1	1	1437	0.0	0.0	0.0	2.0	38.7	160	10	0.00
1	1	1	1	1437	0.0	0.0	0.0	2.3	43.3	160	6	0.00
1	1	1	1	1437	0.0	0.0	0.0	2.8	44.9	160	5	0.00
1	0	1	1	1399	0.0	0.0	0.4	3.3	42.3	160	9	0.00
1	0	1	1	1352	0.0	0.0	1.0	3.7	40.8	160	12	0.00
1	0	1	1	1268	0.0	0.0	1.6	4.4	35.5	160	14	0.00
1	0	1	1	1161	0.0	0.0	2.2	5.0	32.0	160	14	0.00
1	0	1	1	1057	0.0	0.0	2.6	5.4	20.3	160	15	0.00
1	0	1	1	914	0.0	0.0	3.1	6.3	17.4	160	16	0.00
1	0	1	1	759	0.0	0.0	3.5	6.9	15.2	160	17	0.00
1	0	1	1	646	0.0	0.0	3.7	7.4	8.6	160	18	0.00
1	0	1	1	580	0.0	0.0	3.8	7.6	8.6	160	19	0.00
2	0	1	1	481	1.0	1.1	3.7	8.7	0.0	160	20	0.31
3	0	1	1	396	0.0	0.0	3.6	8.7	0.0	160	21	0.00
3	0	1	1	394	0.0	0.0	3.7	8.7	0.0	160	21	0.00
3	0	1	1	392	0.0	0.0	3.7	8.7	0.0	160	21	0.00
3	0	1	1	391	0.0	0.0	3.7	8.7	0.0	160	21	0.00
3	0	1	1	389	0.0	0.0	3.7	8.8	0.0	160	21	0.00
3	0	1	1	387	0.0	0.0	3.7	8.8	0.0	160	21	0.00
4	0	1	1	338	1.0	1.0	3.8	9.9	0.0	95	34	0.14
5	0	1	1	286	3.0	3.2	3.8	10.1	0.0	89	42	0.11
5	0	1	1	255	3.0	3.2	3.8	11.1	0.0	86	43	0.08
5	0	1	1	208	3.0	3.1	3.9	11.9	0.0	83	44	0.07
5	0	1	1	176	3.0	3.1	3.8	12.4	0.0	81	45	0.05
6	0	1	1	137	4.0	4.2	3.8	13.5	0.0	78	45	0.05
6	0	1	1	87	4.0	4.1	4.0	14.8	0.0	75	53	0.02
6	0	1	1	54	4.0	4.0	4.0	15.6	0.0	73	73	0.01
6	0	1	1	30	4.0	4.1	3.9	17.2	0.0	72	77	0.01
6	0	1	1	8	4.0	4.0	4.0	18.0	0.0	72	77	0.00

PROPPANT SUMMARY * At End of Pumping Schedule
FLUVIAL B FOAM MINIFRAC

Lb/Sq-Ft Lost to Embedment 0.050

Distance (ft)	KfW (md-ft)	Proppant Concentration (lb/sq foot) Prop ID--> 1
25	1306	0.40
63	1133	0.40
100	891	0.30
150	784	0.30
200	553	0.20
250	508	0.20
300	183	0.10
350	0	0.00
400	0	0.00
450	17	0.10
500	6	0.10
550	0	0.00
600	0	0.00
650	0	0.00
700	0	0.00
750	0	0.00
800	0	0.00
857	0	0.00
913	0	0.00
951	0	0.00
976	0	0.00
1001	0	0.00
1026	0	0.00
1047	0	0.00
1081	0	0.00
1131	0	0.00
1181	0	0.00
1231	0	0.00
1281	0	0.00
1331	0	0.00
1381	0	0.00
1421	0	0.00

Average Conductivity (md-ft) 567

PROPPANT SUMMARY * At Fracture Closure
FLUVIAL B FOAM MINIFRAC

Lb/Sq-Ft Lost to Embedment 0.050

Distance (ft)	KfW (md-ft)	Proppant Concentration (lb/sq foot) Prop ID--> 1
25	267	0.10
63	296	0.10
100	346	0.10
150	366	0.20
200	377	0.20
250	422	0.20
300	552	0.20
350	655	0.20
400	995	0.30
450	1203	0.40
500	1267	0.40
550	1360	0.40
600	1145	0.40
650	1135	0.40
700	799	0.30
750	115	0.10
800	0	0.00
857	0	0.00
913	0	0.00
951	0	0.00
976	0	0.00
1001	0	0.00
1026	0	0.00
1047	0	0.00
1081	0	0.00
1131	0	0.00
1181	0	0.00
1231	0	0.00
1281	0	0.00
1331	0	0.00
1381	0	0.00
1421	0	0.00
1462	0	0.00

Average Conductivity (md-ft) 720

C.3: PRESSURE HISTORY MATCH OF FLUVIAL "B" FOAM FRACTURE TREATMENT WITH INCREASED BOUNDARY STRESS, CONSTANT PRESSURE MODE, AND EXTENDED MID-TREATMENT SHUT-IN DECLINE.

Frac Summary * FLUVIAL B FOAM MINIFRAC
Filename: FLUV-B-M.FRK

Design Data		
FLUID LOSS:	Coefficient (ft/sqrt(min))	0.0005
	Spurt Loss (gal/100 sq ft)	0.00
FORMATION:	Modulus (MM psi)	5.00
	Fracture Height (ft)	25.0
	Fluid Loss Height (ft)	25.0
	Perforated Height (ft)	10.0
TEMPERATURE:	Bottom Hole (deg F)	160
PRESSURE:	Reservoir Pressure (psi)	3450.0
	Closure Pressure (psi)	4550.0
DEPTH:	Well Depth (ft)	5825

FORMATION LAYER DATA:

Depth	Stress at Top	Stress Grad	Modulus	Toughness
5570	5475.0	0.000	5.00	1.00
5719	4700.0	0.000	5.00	1.00
5739	6000.0	0.000	5.00	1.00
5825	4550.0	0.000	5.00	1.00
5850	6000.0	0.000	5.00	1.00
5886	5200.0	0.000	5.00	1.00
5927	5775.0	0.000	5.00	1.00
5953	4200.0	0.000	5.00	1.00
5980	5600.0	0.433	5.00	1.00

Fluid Pressure Gradient (psi/ft)		0.433
Fracture Top (ft)		5825
Fracture Bottom (ft)		5835

Calculated Results
from 3-D Simulator
STIMPLAN (TM) , NSI , Tulsa,OK
Licensed To: Internal Use - NSI Technologies

1/2 LENGTH:	'Hydraulic' length (ft)	1088
	Propped length (ft)	121
PRESSURE:	Max Net Pressure (psi)	1008
TIME:	Max Exposure to Form. Temp. (min) ..	16.0
	Time to Close (min)	105.5
RATE:	Fluid Loss Rate during pad (bpm) ...	5.1
EFFICIENCY:	at end of pumping schedule	0.64
PROPPANT:	Average In Situ Conc. (#/sq ft)	0.1
	Average Conductivity (md-ft)	16
HEIGHT:	Max Fracture Height (ft)	79
WIDTH:	Avg width at end of pumping (in) ...	0.07

STIMPLAN (TM). NSI Technologies, Tulsa, OK
Licensed To: Internal Use - NSI Technologies

WELL ID:
FLUVIAL B FOAM MINIFRAC

DEPTH:	Well Depth (ft)	5825
PRESSURE:	Reservoir Pressure (psi)	3450
	Closure Pressure (psi)	4550
TEMPERATURE:	Bottom Hole Temperature (deg F)	160

** Pumping Schedule **

Sl Vol (Mgal)	Fl Vol (Mgal)	Conc (ppg)	Rate (bpm)	Fluid Type	Prop Type	Cum Prop (M-lb)	Pump Time (min)
8.0	8.0	0.0	11.0	1	1	0.0	17.3
1.2	1.2	1.0	11.0	1	1	1.2	2.7

Total Slurry ...	9.2	Total Fluid ...	9.2
Total Proppant ...	1.2	Avg. Conc	0.1
Total Pump Time	20.0 min		

Proppant ID No. 1 — 20- 40 Pro-Flow

Specific Gravity	3.15
'Damage Factor'	0.80

Closure Pres (Mpsi)	0	2	4	8	16
KfW @ 2 #/sq ft (md-ft)	11000	10500	9200	5400	950

Fluid ID No. 1 — Foam_75_Qual,_20#-HPG,_150_F

Specific Gravity	1.04
Quality	75

	@Welbor	@FormTmp	@1Hr	@2Hr	@4Hr	@8Hr
vis (cp @ 170 1/sec) .	50	40	20	10	10	10
non-Newtonian n'	0.52	0.52	0.52	0.57	0.57	0.57

Time History * NSI STIMPLAN 3-D Fracture Simulation
FLUVIAL B FOAM MINIFRAC

Time (min)	Pen (ft)	Pres (psi)	Rate (bpm)	Prop (PPG)	Sl Vol (MGal)	Eff-ciency	Loss (bpm)	Hght (ft)	W-Avg (in)
0.2	71	490	11.0	0.0	0.1	0.78	2.2	41	0.02
0.8	121	827	11.0	0.0	0.4	0.72	1.9	60	0.04
1.6	171	915	11.0	0.0	0.7	0.73	1.9	70	0.05
2.4	221	909	11.0	0.0	1.1	0.74	2.1	72	0.05
3.2	271	911	11.0	0.0	1.5	0.75	2.3	72	0.06
4.0	321	923	11.0	0.0	1.9	0.76	2.5	73	0.06
4.8	371	934	11.0	0.0	2.3	0.77	2.7	74	0.06
5.7	421	949	11.0	0.0	2.6	0.77	2.8	75	0.06
6.6	471	958	11.0	0.0	3.0	0.77	3.0	76	0.06
7.4	521	968	11.0	0.0	3.5	0.77	3.1	76	0.06
8.4	571	980	11.0	0.0	3.9	0.77	3.2	77	0.07
9.3	621	991	11.0	0.0	4.3	0.77	3.3	78	0.07
10.3	671	1000	11.0	0.0	4.7	0.77	3.4	78	0.07
11.2	721	1008	11.0	0.0	5.2	0.77	3.5	79	0.07
12.3	771	1008	11.0	0.0	5.7	0.76	2.5	79	0.07
13.4	821	1008	11.0	0.0	6.2	0.74	3.4	79	0.07
14.6	871	1008	11.0	0.0	6.8	0.72	3.8	79	0.07
15.9	921	1008	11.0	0.0	7.3	0.70	4.1	79	0.07
17.2	971	1007	11.0	0.0	8.0	0.68	4.5	79	0.07
18.7	1021	1007	11.0	0.0	8.6	0.66	4.9	79	0.07
20.0	1063	1008	11.0	1.0	9.3	0.64	5.1	79	0.07
20.7	1088	949	0.0	0.0	9.3	0.63	3.7	79	0.07
26.3	1088	854	0.0	0.0	9.3	0.57	2.5	79	0.06
33.9	1088	759	0.0	0.0	9.3	0.51	2.1	79	0.05
43.1	1088	664	0.0	0.0	9.3	0.44	1.8	79	0.05
53.8	1088	569	0.0	0.0	9.3	0.38	1.5	79	0.04
66.0	1088	474	0.0	0.0	9.3	0.32	1.4	79	0.03
79.4	1088	379	0.0	0.0	9.3	0.25	1.2	79	0.03
93.9	1088	285	0.0	0.0	9.3	0.19	1.1	79	0.02
109.3	1088	190	0.0	0.0	9.3	0.13	1.0	79	0.01
125.5	1088	95	0.0	0.0	9.3	0.07	0.9	79	0.01

GEOMETRY SUMMARY * At End of Pumping Schedule
FLUVIAL B FOAM MINIFRAC

Dstnce (ft)	Press (psi)	W-Avg (in)	Q (bpm)	Sh-Rate (1/sec)	Hght (ft) Total	Up	Dn	Prop	Bank Fraction	Prop (PSF)
23	1003	0.08	3.4	223	79	26	43	59	0.00	0.09
58	994	0.08	3.4	226	78	25	43	59	0.00	0.11
96	985	0.08	3.4	231	78	25	43	58	0.00	0.07
146	973	0.08	3.3	238	77	25	42	57	0.00	0.00
196	960	0.08	3.3	245	76	24	42	57	0.00	0.00
246	948	0.08	3.3	253	75	24	41	56	0.00	0.00
296	936	0.08	3.3	262	75	24	41	55	0.00	0.00
346	923	0.08	3.4	278	74	23	41	54	0.00	0.00
396	910	0.08	3.4	296	73	23	40	54	0.00	0.00
446	897	0.07	3.4	314	72	22	39	53	0.00	0.00
496	883	0.07	3.4	330	70	21	39	51	0.00	0.00
546	868	0.07	3.3	346	68	20	37	49	0.00	0.00
596	853	0.07	3.2	364	65	19	36	47	0.00	0.00
646	836	0.07	3.1	384	63	18	35	44	0.00	0.00
696	818	0.07	2.9	409	60	17	33	42	0.00	0.00
746	797	0.06	2.8	439	56	15	31	39	0.00	0.00
796	772	0.06	2.5	481	52	13	29	35	0.00	0.00
846	740	0.06	2.3	544	48	11	27	31	0.00	0.00
896	695	0.05	2.0	658	43	8	24	26	0.00	0.00
946	655	0.05	1.7	799	36	5	21	20	0.00	0.00
996	539	0.04	1.4	862	30	3	18	15	0.00	0.00
1042	301	0.02	1.0	1949	30	3	18	15	0.00	0.00

FLUID SUMMARY * At End of Pumping Schedule
FLUVIAL B FOAM MINIFRAC

Stage No	Gone	Fluid ID	Prop ID	Pos (ft)	Concentration In	Now	Desgn	Fl Vol (MGal)	Ex Tim (min)	Temp (deg F)	Visc (cp)	Fall Frac
1	1	1	1	1063	0.0	0.0	0.0	0.1	9.6	160	8	0.00
1	1	1	1	1063	0.0	0.0	0.0	0.4	14.0	160	9	0.00
1	1	1	1	1063	0.0	0.0	0.0	0.7	16.0	160	6	0.00
1	0	1	1	1051	0.0	0.0	0.1	1.1	15.8	160	6	0.00
1	0	1	1	1014	0.0	0.0	0.2	1.5	14.9	160	8	0.00
1	0	1	1	945	0.0	0.0	0.4	1.9	13.2	160	11	0.00
1	0	1	1	865	0.0	0.0	0.6	2.2	12.4	160	12	0.00
1	0	1	1	790	0.0	0.0	0.7	2.6	11.4	160	13	0.00
1	0	1	1	720	0.0	0.0	0.8	3.0	9.6	160	14	0.00
1	0	1	1	651	0.0	0.0	0.9	3.4	8.6	160	15	0.00
1	0	1	1	583	0.0	0.0	0.9	3.8	7.6	160	15	0.00
1	0	1	1	516	0.0	0.0	1.0	4.2	5.4	160	16	0.00
1	0	1	1	451	0.0	0.0	1.0	4.6	4.1	160	17	0.00
1	0	1	1	389	0.0	0.0	0.9	5.1	2.8	160	18	0.00
1	0	1	1	332	0.0	0.0	0.8	5.6	0.0	160	19	0.00
1	0	1	1	280	0.0	0.0	0.7	6.1	0.0	139	21	0.00
1	0	1	1	231	0.0	0.0	0.7	6.6	0.0	90	24	0.00
1	0	1	1	181	0.0	0.0	0.6	7.2	0.0	85	24	0.00
1	0	1	1	131	0.0	0.0	0.6	7.8	0.0	81	25	0.00
1	0	1	1	105	0.0	0.0	0.6	7.8	0.0	78	25	0.00
2	0	1	1	79	1.0	1.7	0.6	8.4	0.0	77	25	0.05
2	0	1	1	28	1.0	1.4	0.7	9.0	0.0	72	26	0.02

PROPPANT SUMMARY * At End of Pumping Schedule
FLUVIAL B FOAM MINIFRAC

Lb/Sq-Ft Lost to Embedment 0.050

Distance (ft)	KfW (md-ft)	Proppant Concentration (lb/sq foot) Prop ID--> 1
23	146	0.10
58	211	0.10
96	54	0.10
146	0	0.00
196	0	0.00
246	0	0.00
296	0	0.00
346	0	0.00
396	0	0.00
446	0	0.00
496	0	0.00
546	0	0.00
596	0	0.00
646	0	0.00
696	0	0.00
746	0	0.00
796	0	0.00
846	0	0.00
896	0	0.00
946	0	0.00
996	0	0.00
1042	0	0.00

Average Conductivity (md-ft) 121

PROPPANT SUMMARY * At Fracture Closure
FLUVIAL B FOAM MINIFRAC

Lb/Sq-Ft Lost to Embedment 0.050

Distance (ft)	KfW (md-ft)	Proppant Concentration (lb/sq foot) Prop ID--> 1
23	6	0.10
58	7	0.10
96	28	0.10
146	0	0.00
196	0	0.00
246	0	0.00
296	0	0.00
346	0	0.00
396	0	0.00
446	0	0.00
496	0	0.00
546	0	0.00
596	0	0.00
646	0	0.00
696	0	0.00
746	0	0.00
796	0	0.00
846	0	0.00
896	0	0.00
946	0	0.00
996	0	0.00
1042	0	0.00
1075	0	0.00

Average Conductivity (md-ft) 16

C.4: SIMULATION OF EXTENDED CONSTANT PRESSURE MODE FOR FLUVIAL "B" FOAM FRACTURING TREATMENT TO EVALUATE EXCESS LEAK-OFF AS REASON FOR ABNORMAL PRESSURE INCREASE.

Frac Summary * FLUVIAL B FOAM MINIFRAC
Filename: FLUV-B-M.FRK

Design Data		
FLUID LOSS:	Coefficient (ft/sqrt(min))	0.0005
	Spurt Loss (gal/100 sq ft)	0.00
FORMATION:	Modulus (MM psi)	5.00
	Fracture Height (ft)	25.0
	Fluid Loss Height (ft)	25.0
	Perforated Height (ft)	10.0
TEMPERATURE:	Bottom Hole (deg F)	160
PRESSURE:	Reservoir Pressure (psi)	3450.0
	Closure Pressure (psi)	4550.0
DEPTH:	Well Depth (ft)	5825

FORMATION LAYER DATA:

Depth	Stress at Top	Stress Grad	Modulus	Toughness
5570	5475.0	0.000	5.00	1.00
5719	4700.0	0.000	5.00	1.00
5739	6000.0	0.000	5.00	1.00
5825	4550.0	0.000	5.00	1.00
5850	6000.0	0.000	5.00	1.00
5886	5200.0	0.000	5.00	1.00
5927	5775.0	0.000	5.00	1.00
5953	4200.0	0.000	5.00	1.00
5980	5600.0	0.433	5.00	1.00

Fluid Pressure Gradient (psi/ft)		0.433
Fracture Top (ft)		5825
Fracture Bottom (ft)		5835

Calculated Results from 3-D Simulator STIMPLAN (TM) , NSI , Tulsa,OK Licensed To: Internal Use - NSI Technologies		
1/2 LENGTH:	'Hydraulic' length (ft)	1571
	Propped length (ft)	775
PRESSURE:	Max Net Pressure (psi)	1017
TIME:	Max Exposure to Form. Temp. (min) ..	34.1
	Time to Close (min)	51.2
RATE:	Fluid Loss Rate during pad (bpm) ...	4.4
EFFICIENCY:	at end of pumping schedule	0.41
PROPPANT:	Average In Situ Conc. (#/sq ft)	0.4
	Average Conductivity (md-ft)	1021
HEIGHT:	Max Fracture Height (ft)	79
WIDTH:	Avg width at end of pumping (in) ...	0.06

STIMPLAN (TM). NSI Technologies, Tulsa, OK
Licensed To: Internal Use - NSI Technologies

WELL ID:
FLUVIAL B FOAM MINIFRAC

DEPTH:	Well Depth (ft)	5825
PRESSURE:	Reservoir Pressure (psi)	3450
	Closure Pressure (psi)	4550
TEMPERATURE:	Bottom Hole Temperature (deg F)	160

** Pumping Schedule **

Sl Vol (Mgal)	Fl Vol (Mgal)	Conc (ppg)	Rate (bpm)	Fluid Type	Prop Type	Cum Prop (M-lb)	Pump Time (min)
8.0	8.0	0.0	11.0	1	1	0.0	17.3
1.2	1.2	1.0	11.0	1	1	1.2	2.7
1.3	1.3	1.0	11.0	1	1	2.5	2.9
2.8	2.5	3.0	11.0	1	1	10.1	6.1
6.5	5.6	4.0	11.0	1	1	32.5	14.0

Total Slurry ...	19.9	Total Fluid ...	18.6
Total Proppant ...	32.5	Avg. Conc	1.7
Total Pump Time	43.0 min		

Proppant ID No. 1 — 20- 40 Pro-Flow

Specific Gravity	3.15
'Damage Factor'	0.80

Closure Pres (Mpsi)	0	2	4	8	16
KfW @ 2 #/sq ft (md-ft)	11000	10500	9200	5400	950

Fluid ID No. 1 — Foam_75_Qual,_20#-HPG,_150_F

Specific Gravity	1.04
Quality	75

	@Welbor	@FormTmp	@1Hr	@2Hr	@4Hr	@8Hr
vis (cp @ 170 1/sec)	50	40	20	10	10	10
non-Newtonian n'	0.52	0.52	0.52	0.57	0.57	0.57

Time History * NSI STIMPLAN 3-D Fracture Simulation
FLUVIAL B FOAM MINIFRAC

Time (min)	Pen (ft)	Pres (psi)	Rate (bpm)	Prop (PPG)	Sl Vol (MGal)	Eff-ciency	Loss (bpm)	Hght (ft)	W-Avg (in)
0.3	75	465	11.0	0.0	0.1	0.80	2.1	40	0.03
0.9	125	811	11.0	0.0	0.4	0.71	1.9	59	0.04
1.8	175	890	11.0	0.0	0.8	0.73	1.9	69	0.05
2.6	225	891	11.0	0.0	1.2	0.74	2.0	71	0.05
3.4	275	908	11.0	0.0	1.6	0.75	2.3	72	0.06
4.3	325	916	11.0	0.0	2.0	0.75	2.5	73	0.06
5.1	375	930	11.0	0.0	2.3	0.75	2.7	74	0.06
5.9	425	940	11.0	0.0	2.8	0.75	2.8	74	0.06
6.8	475	953	11.0	0.0	3.2	0.75	3.0	75	0.06
7.7	525	964	11.0	0.0	3.6	0.75	3.1	76	0.06
8.6	575	973	11.0	0.0	4.0	0.75	3.2	77	0.07
9.6	625	985	11.0	0.0	4.4	0.75	3.3	77	0.07
10.6	675	994	11.0	0.0	4.9	0.75	3.4	78	0.07
11.6	725	1003	11.0	0.0	5.4	0.75	3.5	78	0.07
12.6	775	1013	11.0	0.0	5.8	0.75	3.6	79	0.07
13.7	825	1013	11.0	0.0	6.3	0.74	2.3	79	0.07
14.8	875	1013	11.0	0.0	6.8	0.73	3.1	79	0.07
16.0	925	1013	11.0	0.0	7.4	0.71	3.6	79	0.07
17.3	975	1013	11.0	0.0	8.0	0.69	4.1	79	0.07
18.7	1025	1013	11.0	1.0	8.6	0.67	4.4	79	0.07
20.2	1075	1013	11.0	1.0	9.3	0.65	4.6	79	0.07
21.7	1125	1013	11.0	1.0	10.1	0.63	4.9	79	0.07
23.4	1175	1013	11.0	1.0	10.8	0.61	5.3	79	0.07
25.2	1225	1013	11.0	3.0	11.6	0.59	5.6	79	0.07
27.1	1275	1013	11.0	3.0	12.5	0.56	5.8	79	0.07
29.1	1325	1014	11.0	3.0	13.5	0.54	6.1	79	0.07
31.4	1375	1014	11.0	4.0	14.5	0.52	6.4	79	0.07
33.8	1425	1016	11.0	4.0	15.7	0.49	6.9	79	0.07
36.6	1475	1016	11.0	4.0	16.9	0.46	7.2	79	0.07
39.7	1525	1016	11.0	4.0	18.4	0.44	7.4	79	0.06
43.0	1571	1017	11.0	4.0	19.9	0.41	7.7	79	0.06
50.9	1571	915	0.0	0.0	19.9	0.37	2.5	79	0.06
60.3	1571	814	0.0	0.0	19.9	0.33	2.3	79	0.05
70.9	1571	712	0.0	0.0	19.9	0.29	2.0	79	0.05
82.3	1571	610	0.0	0.0	19.9	0.25	1.8	79	0.04
94.2	1571	508	0.0	0.0	19.9	0.22	1.6	79	0.03

GEOMETRY SUMMARY * At End of Pumping Schedule
FLUVIAL B FOAM MINIFRAC

Dstnce (ft)	Press (psi)	W-Avg (in)	Q (bpm)	Sh-Rate (1/sec)	Hght (ft) Total	Up	Dn	Prop	Bank Fraction	Prop (PSF)
25	1011	0.08	1.8	116	79	26	44	60	0.06	0.60
63	998	0.08	1.8	118	79	26	43	59	0.07	0.66
100	983	0.08	1.8	122	78	25	43	58	0.09	0.79
150	962	0.08	1.7	127	77	25	42	58	0.09	0.64
200	942	0.08	1.7	132	76	25	42	57	0.09	0.66
250	921	0.08	1.7	137	76	24	42	56	0.08	0.61
300	903	0.08	1.7	143	75	24	41	55	0.07	0.55
350	888	0.07	1.7	148	74	23	41	55	0.06	0.37
400	875	0.07	1.6	153	73	23	40	54	0.05	0.34
450	863	0.07	1.7	162	73	23	40	53	0.04	0.31
500	852	0.07	1.7	171	72	22	40	53	0.04	0.24
550	841	0.07	1.7	180	71	22	39	52	0.02	0.09
600	830	0.07	1.7	187	70	22	39	51	0.02	0.08
650	819	0.07	1.7	195	69	21	38	50	0.02	0.07
700	808	0.07	1.7	202	68	21	38	49	0.01	0.05
750	798	0.07	1.7	209	67	20	37	49	0.01	0.03
800	786	0.07	1.7	216	66	20	37	48	0.00	0.00
850	775	0.06	1.7	224	65	19	36	46	0.00	0.00
900	762	0.06	1.6	231	64	19	35	46	0.00	0.00
950	749	0.06	1.6	242	63	18	35	45	0.00	0.00
1000	736	0.06	1.5	255	61	17	34	43	0.00	0.00
1050	723	0.06	1.5	268	59	16	33	41	0.00	0.00
1100	708	0.06	1.4	282	57	15	32	39	0.00	0.00
1150	693	0.06	1.4	299	54	14	30	37	0.00	0.00
1200	676	0.05	1.3	319	51	13	29	34	0.00	0.00
1250	656	0.05	1.2	346	48	11	27	31	0.00	0.00
1300	636	0.05	1.1	379	45	9	25	28	0.00	0.00
1350	614	0.05	1.0	387	41	7	23	25	0.00	0.00
1400	581	0.05	1.0	386	39	7	22	23	0.00	0.00
1450	533	0.04	0.9	416	39	7	22	23	0.00	0.00
1500	446	0.04	0.8	509	39	7	22	23	0.00	0.00
1548	270	0.02	0.5	969	39	7	22	23	0.00	0.00

FLUID SUMMARY * At End of Pumping Schedule
FLUVIAL B FOAM MINIFRAC

Stage No	Gone	Fluid ID	Prop ID	Pos (ft)	Concentration In	Now	Desgn	Fl (MGal)	Vol Ex Tim (min)	Temp (deg F)	Visc (cp)	Fall Frac
1	1	1	1	1571	0.0	0.0	0.0	0.1	11.9	160	8	0.00
1	1	1	1	1571	0.0	0.0	0.0	0.4	15.3	160	9	0.00
1	1	1	1	1571	0.0	0.0	0.0	0.8	20.4	160	9	0.00
1	1	1	1	1571	0.0	0.0	0.0	1.2	24.3	160	9	0.00
1	1	1	1	1571	0.0	0.0	0.0	1.6	27.9	160	9	0.00
1	1	1	1	1571	0.0	0.0	0.0	2.0	31.8	160	7	0.00
1	1	1	1	1571	0.0	0.0	0.0	2.3	34.1	160	7	0.00
1	0	1	1	1553	0.0	0.0	0.2	2.7	33.2	160	7	0.00
1	0	1	1	1522	0.0	0.0	0.6	3.1	31.3	160	9	0.00
1	0	1	1	1472	0.0	0.0	1.1	3.5	30.3	160	11	0.00
1	0	1	1	1403	0.0	0.0	1.5	4.0	29.3	160	11	0.00
1	0	1	1	1322	0.0	0.0	2.0	4.4	27.1	160	12	0.00
1	0	1	1	1235	0.0	0.0	2.3	4.8	26.0	160	13	0.00
1	0	1	1	1151	0.0	0.0	2.6	5.2	24.7	160	14	0.00
1	0	1	1	1071	0.0	0.0	2.7	5.6	22.0	160	15	0.00
1	0	1	1	996	0.0	0.0	2.6	6.1	20.4	160	16	0.00
1	0	1	1	926	0.0	0.0	2.5	6.6	18.8	160	16	0.00
1	0	1	1	858	0.0	0.0	2.4	7.1	18.8	160	17	0.00
1	0	1	1	790	0.0	0.0	2.4	7.6	15.2	160	18	0.00
2	0	1	1	724	1.0	1.8	2.2	8.2	13.3	160	19	0.55
2	0	1	1	661	1.0	1.7	2.2	8.8	11.1	160	20	0.50
3	0	1	1	628	1.0	2.4	1.6	8.8	11.1	160	20	0.48
3	0	1	1	593	1.0	1.9	2.1	9.5	6.2	160	21	0.43
3	0	1	1	536	1.0	1.9	2.1	10.0	6.2	160	22	0.38
4	0	1	1	505	3.0	7.8	1.6	10.2	3.2	160	23	0.28
4	0	1	1	469	3.0	6.9	1.8	11.0	0.0	160	24	0.25
4	0	1	1	410	3.0	7.6	1.7	11.8	0.0	160	25	0.21
4	0	1	1	353	3.0	8.3	1.6	12.7	0.0	98	30	0.18
5	0	1	1	324	4.0	21.1	1.1	12.7	0.0	87	31	0.12
5	0	1	1	294	4.0	13.6	1.4	13.7	0.0	87	31	0.12
5	0	1	1	236	4.0	15.3	1.3	14.8	0.0	83	32	0.09
5	0	1	1	176	4.0	16.9	1.2	16.0	0.0	80	33	0.08
5	0	1	1	114	4.0	19.2	1.1	17.4	0.0	76	34	0.06
5	0	1	1	41	4.0	12.2	1.5	18.8	0.0	72	36	0.03

PROPPANT SUMMARY * At End of Pumping Schedule
FLUVIAL B FOAM MINIFRAC

Lb/Sq-Ft Lost to Embedment 0.050

Distance (ft)	KfW (md-ft)	Proppant Concentration (lb/sq foot) Prop ID--> 1
25	1811	0.60
63	2032	0.70
100	2435	0.80
150	1968	0.60
200	2031	0.70
250	1844	0.60
300	1669	0.60
350	1075	0.40
400	971	0.30
450	852	0.30
500	637	0.20
550	120	0.10
600	93	0.10
650	52	0.10
700	12	0.10
750	0	0.00
800	0	0.00
850	0	0.00
900	0	0.00
950	0	0.00
1000	0	0.00
1050	0	0.00
1100	0	0.00
1150	0	0.00
1200	0	0.00
1250	0	0.00
1300	0	0.00
1350	0	0.00
1400	0	0.00
1450	0	0.00
1500	0	0.00
1548	0	0.00

Average Conductivity (md-ft) 1144

PROPPANT SUMMARY * At Fracture Closure
FLUVIAL B FOAM MINIFRAC

Lb/Sq-Ft Lost to Embedment 0.050

Distance (ft)	KfW (md-ft)	Proppant Concentration (lb/sq foot) Prop ID--> 1
25	1437	0.50
63	1445	0.50
100	1641	0.50
150	1934	0.60
200	1827	0.60
250	1722	0.60
300	1570	0.50
350	1425	0.50
400	1287	0.40
450	842	0.30
500	774	0.30
550	649	0.20
600	495	0.20
650	398	0.20
700	55	0.10
750	59	0.10
800	0	0.00
850	0	0.00
900	8	0.00
950	0	0.00
1000	0	0.00
1050	0	0.00
1100	0	0.00
1150	0	0.00
1200	0	0.00
1250	0	0.00
1300	0	0.00
1350	0	0.00
1400	0	0.00
1450	0	0.00
1500	0	0.00
1548	0	0.00

Average Conductivity (md-ft) 1021

C.5: SIMULATION OF FLUVIAL "C" MINIFRAC NO. 1 WITHOUT CONSTANT PRESSURE MODE.

Frac Summary * FLUVIAL C FOAM MINIFRAC NO. 1
Filename: FLUV-C-M.FRK

Design Data		
FLUID LOSS:	Coefficient (ft/sqrt(min))	0.0004
	Spurt Loss (gal/100 sq ft)	0.00
FORMATION:	Modulus (MM psi)	4.00
	Fracture Height (ft)	17.0
	Fluid Loss Height (ft)	22.0
	Perforated Height (ft)	13.0
TEMPERATURE:	Bottom Hole (deg F)	160
PRESSURE:	Reservoir Pressure (psi)	3400.0
	Closure Pressure (psi)	4727.0
DEPTH:	Well Depth (ft)	5722

FORMATION LAYER DATA:

Depth	Stress at Top	Stress Grad	Modulus	Toughness
5300	5400.0	0.000	5.00	1.00
5532	3800.0	0.000	5.00	1.00
5570	5550.0	0.000	5.00	1.00
5719	4727.0	0.000	4.00	1.00
5739	6000.0	0.000	5.00	1.00
5825	4550.0	0.000	5.00	1.00
5850	6000.0	0.000	5.00	1.00
5886	5200.0	0.000	5.00	1.00
5927	5775.0	0.000	5.00	1.00
5953	4200.0	0.000	5.00	1.00
5980	5600.0	0.433	5.00	1.00

Fluid Pressure Gradient (psi/ft)		0.433
Fracture Top (ft)		5722
Fracture Bottom (ft)		5735

Calculated Results
from 3-D Simulator
STIMPLAN (TM) , NSI , Tulsa,OK
Licensed To: Internal Use - NSI Technologies

1/2 LENGTH:	'Hydraulic' length (ft)	1926
	Propped length (ft)	0
PRESSURE:	Max Net Pressure (psi)	896
TIME:	Max Exposure to Form. Temp. (min) ..	20.6
	Time to Close (min)	151.9
RATE:	Fluid Loss Rate during pad (bpm) ...	0.0
EFFICIENCY:	at end of pumping schedule	0.73
PROPPANT:	Average In Situ Conc. (#/sq ft)	0.0
	Average Conductivity (md-ft)	0
HEIGHT:	Max Fracture Height (ft)	185
WIDTH:	Avg width at end of pumping (in) ...	0.05

STIMPLAN (TM). NSI Technologies, Tulsa, OK
Licensed To: Internal Use - NSI Technologies

WELL ID:
FLUVIAL C FOAM MINIFRAC NO. 1
DEPTH: Well Depth (ft) 5722
PRESSURE: Reservoir Pressure (psi) 3400
Closure Pressure (psi) 4727
TEMPERATURE: Bottom Hole Temperature (deg F) 160

** Pumping Schedule **

Sl Vol (Mgal)	Fl Vol (Mgal)	Conc (ppg)	Rate (bpm)	Fluid Type	Prop Type	Cum Prop (M-lb)	Pump Time (min)
1.0	1.0	0.0	11.0	2	1	0.0	2.2
11.9	11.9	0.0	11.0	1	1	0.0	25.7

Total Slurry ... 12.9 Total Fluid ... 12.9
Total Proppant ... 0.0 Avg. Conc 0.0
Total Pump Time 27.8 min

Proppant ID No. 1 20- 40 Pro-Flow

Specific Gravity 3.15
'Damage Factor' 0.80

Closure Pres (Mpsi)	0	2	4	8	16
kfW @ 2 #/sq ft (md-ft)	11000	10500	9200	5400	950

Fluid ID No. 2 Nitrogen-Foam_Comb.

Specific Gravity 0.60

	@Wellbor	@FormTmp	@1Hr	@2Hr	@4Hr	@8Hr
vis (cp @ 170 1/sec) .	25	20	15	15	10	10
non-Newtonian n'	0.52	0.52	0.52	0.57	0.57	0.57

Fluid ID No. 1	Foam_75_Qual,_20#-HPG,_150_F					
Specific Gravity					1.04	
Quality					75	
	@Welbor	@FormTmp	@1Hr	@2Hr	@4Hr	@8Hr
vis (cp @ 170 1/sec) .	20	15	10	7	7	7
non-Newtonian n'	0.52	0.52	0.52	0.57	0.57	0.57

Time History * NSI STIMPLAN 3-D Fracture Simulation
FLUVIAL C FOAM MINIFRAC NO. 1

Time (min)	Pen (ft)	Pres (psi)	Rate (bpm)	Prop (PPG)	Sl Vol (MGal)	Eff-ciency	Loss (bpm)	Hght (ft)	W-Avg (in)
0.2	80	452	11.0	0.0	0.1	0.78	2.1	33	0.02
0.7	155	626	11.0	0.0	0.3	0.66	2.0	43	0.03
1.4	230	697	11.0	0.0	0.6	0.65	2.2	48	0.04
2.1	305	715	11.0	0.0	1.0	0.65	2.4	50	0.04
2.9	380	739	11.0	0.0	1.3	0.65	2.6	52	0.04
3.7	455	758	11.0	0.0	1.7	0.65	2.8	53	0.05
4.6	530	780	11.0	0.0	2.1	0.66	2.9	54	0.05
5.4	605	797	11.0	0.0	2.5	0.67	3.1	61	0.05
6.4	680	803	11.0	0.0	3.0	0.68	3.2	69	0.05
7.4	755	814	11.0	0.0	3.4	0.69	3.3	79	0.05
8.4	830	820	11.0	0.0	3.9	0.70	3.5	85	0.05
9.4	905	826	11.0	0.0	4.4	0.70	3.5	91	0.05
10.6	980	836	11.0	0.0	4.9	0.71	3.6	99	0.05
11.7	1055	837	11.0	0.0	5.4	0.71	3.7	101	0.05
12.8	1130	852	11.0	0.0	5.9	0.72	3.8	113	0.05
14.1	1205	834	11.0	0.0	6.5	0.72	3.8	113	0.05
15.2	1280	865	11.0	0.0	7.0	0.72	4.0	123	0.05
16.6	1355	843	11.0	0.0	7.7	0.72	4.0	123	0.05
17.9	1430	876	11.0	0.0	8.3	0.72	4.0	135	0.05
19.4	1505	849	11.0	0.0	9.0	0.72	4.0	135	0.05
20.9	1580	883	11.0	0.0	9.7	0.72	4.1	153	0.05
22.5	1655	862	11.0	0.0	10.4	0.72	4.1	153	0.05
24.1	1730	896	11.0	0.0	11.1	0.72	4.1	185	0.05
25.2	1768	795	11.0	0.0	11.7	0.73	4.0	185	0.05
27.9	1869	874	11.0	0.0	12.9	0.73	4.2	185	0.05
28.8	1907	834	0.0	0.0	12.9	0.73	4.0	185	0.05
30.1	1926	925	0.0	0.0	12.9	0.72	3.7	185	0.05
38.1	1926	742	0.0	0.0	12.9	0.65	2.7	185	0.05
48.6	1926	660	0.0	0.0	12.9	0.57	2.3	185	0.04
61.4	1926	577	0.0	0.0	12.9	0.50	2.0	185	0.04
76.6	1926	495	0.0	0.0	12.9	0.42	1.7	185	0.03
93.8	1926	412	0.0	0.0	12.9	0.36	1.5	185	0.03
113.0	1926	330	0.0	0.0	12.9	0.29	1.4	185	0.02
133.8	1926	247	0.0	0.0	12.9	0.22	1.2	185	0.02
156.2	1926	165	0.0	0.0	12.9	0.14	1.1	185	0.01
179.7	1926	82	0.0	0.0	12.9	0.07	1.0	185	0.01

GEOMETRY SUMMARY * At End of Pumping Schedule
FLUVIAL C FOAM MINIFRAC NO. 1

Dstnce (ft)	Press (psi)	W-Avg (in)	Q (bpm)	Sh-Rate (1/sec)	Hght (ft) Total	Up	Dn	Prop	Bank Fraction	Prop (PSF)
22	873	0.07	5.5	193	185	146	26	156	0.00	0.00
62	870	0.07	5.2	206	173	135	25	143	0.00	0.00
118	864	0.07	4.9	245	152	116	23	120	0.00	0.00
193	854	0.07	4.5	296	128	94	21	95	0.00	0.00
268	841	0.07	4.2	306	117	85	19	86	0.00	0.00
343	828	0.06	3.9	322	105	74	18	77	0.00	0.00
418	815	0.06	3.6	345	93	64	16	67	0.00	0.00
493	801	0.06	3.4	382	81	53	14	57	0.00	0.00
568	787	0.06	3.3	452	67	42	13	46	0.00	0.00
643	770	0.06	3.1	548	55	31	11	37	0.00	0.00
718	753	0.06	3.0	561	54	30	11	36	0.00	0.00
793	736	0.06	2.9	574	53	30	11	35	0.00	0.00
868	719	0.06	2.8	587	52	29	10	35	0.00	0.00
943	701	0.06	2.7	602	51	28	10	34	0.00	0.00
1018	683	0.06	2.6	618	50	27	10	33	0.00	0.00
1093	665	0.05	2.5	636	49	26	10	33	0.00	0.00
1168	645	0.05	2.4	657	48	25	9	32	0.00	0.00
1243	625	0.05	2.3	682	46	24	9	31	0.00	0.00
1318	603	0.05	2.1	716	45	23	9	30	0.00	0.00
1393	580	0.05	2.0	760	44	22	9	29	0.00	0.00
1468	554	0.04	1.9	826	42	21	8	28	0.00	0.00
1543	527	0.04	1.7	905	41	20	8	27	0.00	0.00
1618	501	0.04	1.5	1014	39	18	8	26	0.00	0.00
1693	444	0.03	1.3	1397	36	15	7	24	0.00	0.00
1749	404	0.03	1.0	1209	32	13	7	22	0.00	0.00
1819	279	0.02	0.8	1740	29	10	6	20	0.00	0.00

FLUID SUMMARY * At End of Pumping Schedule
FLUVIAL C FOAM MINIFRAC NO. 1

Stage No	Gone	Fluid ID	Prop ID	Pos (ft)	Concentration In	Now	Desgn	Fl Vol (MGal)	Ex Tim (min)	Temp (deg F)	Visc (cp)	Fall Frac
1	1	2	1	1869	0.0	0.0	0.0	0.1	6.8	160	3	0.00
1	1	2	1	1869	0.0	0.0	0.0	0.3	9.0	160	3	0.00
1	1	2	1	1869	0.0	0.0	0.0	0.6	10.6	160	3	0.00
1	1	2	1	1869	0.0	0.0	0.0	1.0	12.2	160	3	0.00
1	1	2	1	1869	0.0	0.0	0.0	1.0	14.8	160	3	0.00
2	1	1	1	1869	0.0	0.0	0.0	1.3	18.4	160	2	0.00
2	1	1	1	1869	0.0	0.0	0.0	1.7	19.6	160	3	0.00
2	0	1	1	1853	0.0	0.0	0.1	2.1	20.6	160	3	0.00
2	0	1	1	1798	0.0	0.0	0.2	2.5	19.6	160	3	0.00
2	0	1	1	1692	0.0	0.0	0.4	3.0	17.6	160	3	0.00
2	0	1	1	1562	0.0	0.0	0.6	3.4	16.5	160	4	0.00
2	0	1	1	1432	0.0	0.0	0.7	3.8	15.4	160	4	0.00
2	0	1	1	1297	0.0	0.0	0.8	4.3	11.9	160	4	0.00
2	0	1	1	1160	0.0	0.0	0.9	4.8	10.6	160	4	0.00
2	0	1	1	1019	0.0	0.0	0.9	5.3	7.9	160	5	0.00
2	0	1	1	882	0.0	0.0	1.0	5.8	6.4	160	5	0.00
2	0	1	1	746	0.0	0.0	1.0	6.4	4.8	160	5	0.00
2	0	1	1	620	0.0	0.0	1.0	6.9	0.0	160	5	0.00
2	0	1	1	514	0.0	0.0	1.0	7.5	0.0	160	6	0.00
2	0	1	1	426	0.0	0.0	1.0	8.1	0.0	97	8	0.00
2	0	1	1	348	0.0	0.0	1.0	8.8	0.0	97	8	0.00
2	0	1	1	273	0.0	0.0	1.0	9.4	0.0	83	9	0.00
2	0	1	1	202	0.0	0.0	1.0	10.2	0.0	80	9	0.00
2	0	1	1	139	0.0	0.0	1.0	10.9	0.0	76	10	0.00
2	0	1	1	92	0.0	0.0	1.0	11.4	0.0	75	10	0.00
2	0	1	1	37	0.0	0.0	1.0	12.5	0.0	72	11	0.00

C.6: SIMULATION OF FLUVIAL "C" MINIFRAC NO. 1 WITH CONSTANT PRESSURE MODE.

Frac Summary * FLUVIAL C FOAM MINIFRAC NO. 1
Filename: FLUV-C-M.FRK

Design Data		
FLUID LOSS:	Coefficient (ft/sqrt(min))	0.0004
	Spurt Loss (gal/100 sq ft)	0.00
FORMATION:	Modulus (MM psi)	4.00
	Fracture Height (ft)	17.0
	Fluid Loss Height (ft)	22.0
	Perforated Height (ft)	13.0
TEMPERATURE:	Bottom Hole (deg F)	160
PRESSURE:	Reservoir Pressure (psi)	3400.0
	Closure Pressure (psi)	4727.0
DEPTH:	Well Depth (ft)	5722

FORMATION LAYER DATA:

Depth	Stress at Top	Stress Grad	Modulus	Toughness
5300	5700.0	0.000	5.00	1.00
5532	3800.0	0.000	5.00	1.00
5570	5700.0	0.000	5.00	1.00
5719	4727.0	0.000	4.00	1.00
5739	6000.0	0.000	5.00	1.00
5825	4550.0	0.000	5.00	1.00
5850	6000.0	0.000	5.00	1.00
5886	5200.0	0.000	5.00	1.00
5927	5775.0	0.000	5.00	1.00
5953	4200.0	0.000	5.00	1.00
5980	5600.0	0.433	5.00	1.00

Fluid Pressure Gradient (psi/ft)		0.433
Fracture Top (ft)		5722
Fracture Bottom (ft)		5735

Calculated Results
from 3-D Simulator
STIMPLAN (TM) , NSI , Tulsa,OK
Licensed To: Internal Use - NSI Technologies

1/2 LENGTH:	'Hydraulic' length (ft)	2295
	Propped length (ft)	0
PRESSURE:	Max Net Pressure (psi)	863
TIME:	Max Exposure to Form. Temp. (min) ..	19.9
	Time to Close (min)	66.1
RATE:	Fluid Loss Rate during pad (bpm) ...	0.0
EFFICIENCY:	at end of pumping schedule	0.51
PROPPANT:	Average In Situ Conc. (#/sq ft)	0.0
	Average Conductivity (md-ft)	0
HEIGHT:	Max Fracture Height (ft)	53
WIDTH:	Avg width at end of pumping (in) ...	0.05

STIMPLAN (TM). NSI Technologies, Tulsa, OK
Licensed To: Internal Use - NSI Technologies

WELL ID:
FLUVIAL C FOAM MINIFRAC NO. 1

DEPTH:	Well Depth (ft)	5722
PRESSURE:	Reservoir Pressure (psi)	3400
	Closure Pressure (psi)	4727
TEMPERATURE:	Bottom Hole Temperature (deg F)	160

** Pumping Schedule **

Sl Vol (Mgal)	Fl Vol (Mgal)	Conc (ppg)	Rate (bpm)	Fluid Type	Prop Type	Cum Prop (M-lb)	Pump Time (min)
1.0	1.0	0.0	11.0	2	1	0.0	2.2
11.9	11.9	0.0	11.0	1	1	0.0	25.7

Total Slurry ...	12.9	Total Fluid ...	12.9
Total Proppant ...	0.0	Avg. Conc	0.0
Total Pump Time	27.8 min		

Proppant ID No. 1 — 20- 40 Pro-Flow

Specific Gravity					3.15
'Damage Factor'					0.80
Closure Pres (Mpsi)	0	2	4	8	16
KfW @ 2 #/sq ft (md-ft)	11000	10500	9200	5400	950

Fluid ID No. 2 — Nitrogen-Foam_Comb.

Specific Gravity 0.60

	@Welbor	@FormTmp	@1Hr	@2Hr	@4Hr	@8Hr
vis (cp @ 170 1/sec) .	25	20	15	15	10	10
non-Newtonian n'	0.52	0.52	0.52	0.57	0.57	0.57

Fluid ID No. 1	Foam_75_Qual,_20#-HPG,_150_F					
Specific Gravity					1.04	
Quality					75	
	@Welbor	@FormTmp	@1Hr	@2Hr	@4Hr	@8Hr
vis (cp @ 170 1/sec) .	15	10	7	7	7	7
non-Newtonian n'	0.52	0.52	0.52	0.57	0.57	0.57

Time History * NSI STIMPLAN 3-D Fracture Simulation
FLUVIAL C FOAM MINIFRAC NO. 1

Time (min)	Pen (ft)	Pres (psi)	Rate (bpm)	Prop (PPG)	Sl Vol (MGal)	Eff (cone/)	Loss (bpm)	Hght (ft)	W Avg (in)
0.1	58	428	11.0	0.0	0.1	0.70	1.9	31	0.02
0.4	108	577	11.0	0.0	0.2	0.67	1.9	38	0.03
0.8	158	645	11.0	0.0	0.4	0.66	2.0	42	0.04
1.2	208	662	11.0	0.0	0.5	0.66	2.2	43	0.04
1.6	258	681	11.0	0.0	0.7	0.66	2.4	44	0.04
2.0	308	702	11.0	0.0	0.9	0.65	2.5	45	0.04
2.5	358	722	11.0	0.0	1.2	0.65	2.6	46	0.04
3.0	408	737	11.0	0.0	1.4	0.65	2.8	47	0.05
3.6	458	748	11.0	0.0	1.6	0.65	2.9	48	0.05
4.1	508	760	11.0	0.0	1.9	0.65	3.0	48	0.05
4.6	558	771	11.0	0.0	2.1	0.66	3.2	49	0.05
5.1	608	780	11.0	0.0	2.4	0.67	3.3	49	0.05
5.6	658	789	11.0	0.0	2.6	0.67	3.4	50	0.05
6.1	708	796	11.0	0.0	2.8	0.68	3.6	50	0.05
6.6	758	803	11.0	0.0	3.1	0.68	3.7	50	0.05
7.1	808	809	11.0	0.0	3.3	0.68	3.8	51	0.05
7.7	858	815	11.0	0.0	3.5	0.68	3.9	51	0.05
8.2	908	820	11.0	0.0	3.8	0.69	4.0	51	0.05
8.7	958	825	11.0	0.0	4.0	0.69	4.1	52	0.05
9.2	1008	829	11.0	0.0	4.3	0.69	4.2	52	0.05
9.7	1058	834	11.0	0.0	4.5	0.69	4.3	52	0.05
10.2	1108	838	11.0	0.0	4.7	0.69	4.4	52	0.06
10.7	1158	841	11.0	0.0	4.9	0.69	4.6	52	0.05
11.2	1208	844	11.0	0.0	5.2	0.69	4.7	52	0.05
11.6	1258	847	11.0	0.0	5.4	0.69	4.8	53	0.05
12.1	1308	849	11.0	0.0	5.6	0.69	4.9	53	0.05
12.6	1358	852	11.0	0.0	5.8	0.69	5.0	53	0.05
13.1	1408	856	11.0	0.0	6.1	0.68	5.1	53	0.05
13.6	1458	858	11.0	0.0	6.3	0.68	5.2	53	0.05
14.1	1508	863	11.0	0.0	6.6	0.68	5.2	53	0.05
14.7	1558	863	11.0	0.0	6.8	0.68	3.8	53	0.05
15.3	1608	863	11.0	0.0	7.1	0.67	4.3	53	0.05
16.0	1658	863	11.0	0.0	7.4	0.66	4.6	53	0.05
16.7	1708	863	11.0	0.0	7.7	0.65	4.8	53	0.05
17.4	1758	863	11.0	0.0	8.1	0.64	5.0	53	0.05
18.2	1808	863	11.0	0.0	8.4	0.63	5.1	53	0.05
19.1	1858	863	11.0	0.0	8.8	0.62	5.3	53	0.05
20.0	1908	863	11.0	0.0	9.3	0.61	5.4	53	0.05
20.9	1958	863	11.0	0.0	9.7	0.59	5.6	53	0.05
22.0	2008	863	11.0	0.0	10.2	0.58	5.7	53	0.05
23.1	2058	863	11.0	0.0	10.7	0.56	5.8	53	0.05
24.3	2108	863	11.0	0.0	11.2	0.55	5.9	53	0.05
25.5	2158	863	11.0	0.0	11.8	0.53	6.1	53	0.05
26.8	2208	863	11.0	0.0	12.4	0.52	6.1	53	0.05
27.9	2245	863	11.0	0.0	12.9	0.51	6.6	53	0.05
28.5	2295	776	0.0	0.0	12.9	0.49	4.5	53	0.05
33.9	2295	698	0.0	0.0	12.9	0.44	3.5	53	0.05
39.3	2295	621	0.0	0.0	12.9	0.39	3.2	53	0.04
62.5	2295	78	0.0	0.0	12.9	0.05	1.8	53	0.01

GEOMETRY SUMMARY * At End of Pumping Schedule
FLUVIAL C FOAM MINIFRAC NO. 1

Dstnce (ft)	Press (psi)	W-Avg (in)	Q (bpm)	Sh-Rate (1/sec)	Hght (ft) Total	Up	Dn	Prop	Bank Fraction	Prop (PSF)
17	860	0.07	3.0	432	53	27	14	40	0.00	0.00
46	856	0.07	3.0	436	53	27	14	39	0.00	0.00
83	850	0.07	2.9	441	53	26	14	39	0.00	0.00
133	843	0.07	2.9	448	53	26	13	39	0.00	0.00
183	835	0.07	2.9	455	52	26	13	39	0.00	0.00
233	827	0.07	2.9	462	52	26	13	38	0.00	0.00
283	819	0.07	2.8	471	51	25	13	38	0.00	0.00
333	811	0.06	2.8	480	51	25	13	38	0.00	0.00
383	802	0.06	2.8	489	51	25	13	37	0.00	0.00
433	794	0.06	2.8	499	50	25	13	37	0.00	0.00
483	786	0.06	2.8	509	50	24	13	37	0.00	0.00
533	777	0.06	2.8	518	50	24	13	37	0.00	0.00
583	770	0.06	2.7	527	49	24	12	36	0.00	0.00
633	763	0.06	2.8	549	49	24	12	36	0.00	0.00
683	757	0.06	2.8	570	49	23	12	36	0.00	0.00
733	749	0.06	2.8	589	48	23	12	36	0.00	0.00
783	742	0.06	2.9	607	48	23	12	35	0.00	0.00
833	735	0.06	2.9	622	48	23	12	35	0.00	0.00
883	727	0.06	2.8	636	47	22	12	35	0.00	0.00
933	720	0.06	2.8	648	47	22	12	35	0.00	0.00
983	712	0.06	2.8	660	47	22	12	34	0.00	0.00
1033	704	0.06	2.8	671	46	22	12	34	0.00	0.00
1083	696	0.06	2.7	682	46	21	12	34	0.00	0.00
1133	687	0.06	2.7	692	45	21	11	33	0.00	0.00
1183	678	0.05	2.6	704	45	21	11	33	0.00	0.00
1233	669	0.05	2.6	723	45	20	11	33	0.00	0.00
1283	660	0.05	2.5	738	44	20	11	32	0.00	0.00
1333	650	0.05	2.5	755	43	19	11	31	0.00	0.00
1383	640	0.05	2.4	774	42	19	10	31	0.00	0.00
1433	630	0.05	2.3	794	41	18	10	30	0.00	0.00
1483	619	0.05	2.3	817	40	17	10	29	0.00	0.00
1533	608	0.05	2.2	842	39	16	10	28	0.00	0.00
1583	596	0.05	2.1	870	38	16	9	28	0.00	0.00
1633	584	0.05	2.1	902	37	15	9	27	0.00	0.00
1683	571	0.05	2.0	939	35	14	9	26	0.00	0.00
1733	557	0.05	1.9	982	34	13	8	25	0.00	0.00
1783	541	0.04	1.8	1034	32	12	8	23	0.00	0.00
1833	525	0.04	1.7	1098	31	11	7	22	0.00	0.00
1883	506	0.04	1.6	1178	29	9	7	21	0.00	0.00
1933	486	0.04	1.5	1285	27	8	6	19	0.00	0.00
1983	467	0.04	1.4	1402	25	6	6	18	0.00	0.00
2033	448	0.04	1.3	1407	23	5	5	16	0.00	0.00
2083	416	0.04	1.2	1473	22	4	5	16	0.00	0.00
2133	372	0.03	1.0	1654	22	4	5	16	0.00	0.00
2183	308	0.03	0.9	2048	22	4	5	16	0.00	0.00
2227	187	0.02	0.7	4184	22	4	5	16	0.00	0.00

FLUID SUMMARY * At End of Pumping Schedule
FLUVIAL C FOAM MINIFRAC NO. 1

Stage No	Gone	Fluid ID	Prop ID	Pos (ft)	Concentration In	Now	Desgn	Fl (MGal)	Vol Ex Tim (min)	Temp (deg F)	Visc (cp)	Fall Frac
1	1	2	1	2245	0.0	0.0	0.0	0.1	4.3	160	3	0.00
1	1	2	1	2245	0.0	0.0	0.0	0.2	5.3	160	3	0.00
1	1	2	1	2245	0.0	0.0	0.0	0.4	6.4	160	3	0.00
1	1	2	1	2245	0.0	0.0	0.0	0.5	8.1	160	3	0.00
1	1	2	1	2245	0.0	0.0	0.0	0.7	9.1	160	3	0.00
1	1	2	1	2245	0.0	0.0	0.0	0.9	9.1	160	2	0.00
1	1	2	1	2245	0.0	0.0	0.0	1.0	10.6	160	3	0.00
2	1	1	1	2245	0.0	0.0	0.0	1.2	11.7	160	1	0.00
2	1	1	1	2245	0.0	0.0	0.0	1.4	13.2	160	1	0.00
2	1	1	1	2245	0.0	0.0	0.0	1.6	14.7	160	1	0.00
2	1	1	1	2245	0.0	0.0	0.0	1.9	16.1	160	2	0.00
2	1	1	1	2245	0.0	0.0	0.0	2.1	17.8	160	2	0.00
2	1	1	1	2245	0.0	0.0	0.0	2.4	19.3	160	1	0.00
2	1	1	1	2245	0.0	0.0	0.0	2.6	19.9	160	1	0.00
2	0	1	1	2216	0.0	0.0	0.1	2.8	19.4	160	1	0.00
2	0	1	1	2174	0.0	0.0	0.2	3.1	18.4	160	2	0.00
2	0	1	1	2109	0.0	0.0	0.3	3.3	17.9	160	2	0.00
2	0	1	1	2025	0.0	0.0	0.4	3.5	17.4	160	2	0.00
2	0	1	1	1935	0.0	0.0	0.5	3.8	16.4	160	2	0.00
2	0	1	1	1848	0.0	0.0	0.6	4.0	15.9	160	2	0.00
2	0	1	1	1765	0.0	0.0	0.6	4.2	15.5	160	2	0.00
2	0	1	1	1685	0.0	0.0	0.7	4.5	14.5	160	2	0.00
2	0	1	1	1607	0.0	0.0	0.7	4.7	13.4	160	3	0.00
2	0	1	1	1533	0.0	0.0	0.8	4.9	13.4	160	3	0.00
2	0	1	1	1465	0.0	0.0	0.8	5.1	12.3	160	3	0.00
2	0	1	1	1399	0.0	0.0	0.8	5.3	11.7	160	3	0.00
2	0	1	1	1334	0.0	0.0	0.8	5.5	11.0	160	3	0.00
2	0	1	1	1268	0.0	0.0	0.9	5.8	9.5	160	3	0.00
2	0	1	1	1202	0.0	0.0	0.9	6.0	9.5	160	3	0.00
2	0	1	1	1133	0.0	0.0	0.9	6.2	8.7	160	3	0.00
2	0	1	1	1063	0.0	0.0	0.9	6.4	7.8	160	3	0.00
2	0	1	1	992	0.0	0.0	0.9	6.7	5.9	160	3	0.00
2	0	1	1	922	0.0	0.0	0.9	7.0	4.8	160	3	0.00
2	0	1	1	852	0.0	0.0	0.8	7.3	4.8	160	3	0.00
2	0	1	1	783	0.0	0.0	0.8	7.6	3.7	160	3	0.00
2	0	1	1	715	0.0	0.0	0.7	7.9	1.2	160	3	0.00
2	0	1	1	648	0.0	0.0	0.7	8.3	0.0	160	3	0.00
2	0	1	1	581	0.0	0.0	0.6	8.7	0.0	150	4	0.00
2	0	1	1	516	0.0	0.0	0.6	9.1	0.0	91	5	0.00
2	0	1	1	449	0.0	0.0	0.6	9.5	0.0	88	5	0.00
2	0	1	1	381	0.0	0.0	0.6	10.0	0.0	85	5	0.00
2	0	1	1	312	0.0	0.0	0.6	10.5	0.0	82	5	0.00
2	0	1	1	242	0.0	0.0	0.6	11.0	0.0	80	5	0.00
2	0	1	1	171	0.0	0.0	0.5	11.6	0.0	77	5	0.00
2	0	1	1	100	0.0	0.0	0.5	12.2	0.0	74	6	0.00
2	0	1	1	32	0.0	0.0	0.6	12.6	0.0	71	6	0.00

C.7: SIMULATION OF FLUVIAL "C" MINIFRAC NO. 2

Frac Summary * FLUVIAL C FOAM MINIFRAC NO. 2
Filename: FLUV2-C.FRK

Design Data		
FLUID LOSS:	Coefficient (ft/sqrt(min))	0.0008
	Spurt Loss (gal/100 sq ft)	0.00
FORMATION:	Modulus (MM psi)	4.00
	Fracture Height (ft)	17.0
	Fluid Loss Height (ft)	22.0
	Perforated Height (ft)	13.0
TEMPERATURE:	Bottom Hole (deg F)	160
PRESSURE:	Reservoir Pressure (psi)	3400.0
	Closure Pressure (psi)	4727.0
DEPTH:	Well Depth (ft)	5722

FORMATION LAYER DATA:

Depth	Stress at Top	Stress Grad	Modulus	Toughness
5300	5400.0	0.000	5.00	1.00
5532	3800.0	0.000	5.00	1.00
5570	5550.0	0.000	5.00	1.00
5719	4727.0	0.000	4.00	1.00
5739	6000.0	0.000	5.00	1.00
5825	4550.0	0.000	5.00	1.00
5850	6000.0	0.000	5.00	1.00
5886	5200.0	0.000	5.00	1.00
5927	5775.0	0.000	5.00	1.00
5953	4200.0	0.000	5.00	1.00
5980	5600.0	0.433	5.00	1.00

Fluid Pressure Gradient (psi/ft)		0.433
Fracture Top (ft)		5722
Fracture Bottom (ft)		5735

Calculated Results
from 3-D Simulator
STIMPLAN (TM) , NSI , Tulsa,OK
Licensed To: Internal Use - NSI Technologies

1/2 LENGTH:	'Hydraulic' length (ft)	1774
	Propped length (ft)	175
PRESSURE:	Max Net Pressure (psi)	920
TIME:	Max Exposure to Form. Temp. (min) ..	29.6
	Time to Close (min)	110.4
RATE:	Fluid Loss Rate during pad (bpm) ...	5.8
EFFICIENCY:	at end of pumping schedule	0.51
PROPPANT:	Average In Situ Conc. (#/sq ft)	0.1
	Average Conductivity (md-ft)	20
HEIGHT:	Max Fracture Height (ft)	286
WIDTH:	Avg width at end of pumping (in) ...	0.05

STIMPLAN (TM). NSI Technologies, Tulsa, OK
Licensed To: Internal Use - NSI Technologies

WELL ID:
FLUVIAL C FOAM MINIFRAC NO. 1

DEPTH:	Well Depth (ft)	5722
PRESSURE:	Reservoir Pressure (psi)	3400
	Closure Pressure (psi)	4727
TEMPERATURE:	Bottom Hole Temperature (deg F)	160

** Pumping Schedule **

Sl Vol (Mgal)	Fl Vol (Mgal)	Conc (ppg)	Rate (bpm)	Fluid Type	Prop Type	Cum Prop (M-lb)	Pump Time (min)
2.2	2.2	0.0	10.0	2	1	0.0	5.2
5.0	5.0	0.0	10.0	3	1	0.0	11.9
2.4	2.4	0.0	10.0	1	1	0.0	5.7
2.0	2.0	0.2	10.0	1	1	0.4	4.8
2.0	2.0	0.5	10.0	1	1	1.4	4.8
2.0	1.9	0.8	10.0	1	1	2.9	4.7
2.0	1.9	1.0	10.0	1	1	4.9	4.9
5.9	5.9	0.0	10.0	1	1	4.9	14.1

Total Slurry ...	23.6	Total Fluid ...	23.4
Total Proppant ...	4.9	Avg. Conc	0.2
Total Pump Time	56.2 min		

Proppant ID No. 1 — 20- 40 Ottawa_Snd

Specific Gravity					2.65
'Damage Factor'					0.70
Closure Pres (Mpsi)	0	2	4	8	16
KfW @ 2 #/sq ft (md-ft)	4800	3850	2750	990	50

Fluid ID No. 2 — NITROGEN

Specific Gravity 0.60

	@Welbor	@FormTmp	@1Hr	@2Hr	@4Hr	@8Hr
vis (cp @ 170 1/sec) .	1	1	1	1	1	1
non-Newtonian n'	0.57	0.57	0.57	0.57	0.57	0.57

Fluid ID No. 3	NITROGEN					
Specific Gravity					0.60	
	@Welbor	@FormTmp	@1Hr	@2Hr	@4Hr	@8Hr
vis (cp @ 170 1/sec) .	2	2	2	2	2	2
non-Newtonian n'	0.57	0.57	0.57	0.57	0.57	0.57

Fluid ID No. 1	Foam_75_Qual,_20#-HPG,_150_F					
Specific Gravity					1.04	
Quality					75	
	@Welbor	@FormTmp	@1Hr	@2Hr	@4Hr	@8Hr
vis (cp @ 170 1/sec) .	35	25	20	15	10	10
non-Newtonian n'	0.52	0.52	0.52	0.52	0.57	0.57

Time History * NSI STIMPLAN 3-D Fracture Simulation
FLUVIAL C FOAM MINIFRAC NO. 1

Time (min)	Pen (ft)	Pres (psi)	Rate (bpm)	Prop (PPG)	Sl Vol (MGal)	Eff-ciency	Loss (bpm)	Hght (ft)	W-Avg (in)
0.2	75	163	10.0	0.0	0.1	0.57	4.2	34	0.01
0.4	125	221	10.0	0.0	0.2	0.47	4.2	34	0.01
0.7	175	250	10.0	0.0	0.3	0.44	4.6	34	0.02
0.9	225	260	10.0	0.0	0.4	0.41	5.1	34	0.02
1.3	275	270	10.0	0.0	0.5	0.39	5.5	34	0.02
1.6	325	279	10.0	0.0	0.7	0.37	5.7	34	0.02
2.0	375	287	10.0	0.0	0.8	0.36	6.0	34	0.02
2.4	425	296	10.0	0.0	1.0	0.35	6.2	34	0.02
2.8	475	304	10.0	0.0	1.2	0.34	6.3	34	0.02
3.3	525	311	10.0	0.0	1.4	0.33	6.5	34	0.02
3.7	575	319	10.0	0.0	1.6	0.32	6.6	34	0.02
4.2	625	326	10.0	0.0	1.8	0.31	6.7	34	0.02
4.8	675	332	10.0	0.0	2.0	0.30	6.8	34	0.02
5.3	725	339	10.0	0.0	2.2	0.30	6.9	34	0.02
5.9	775	347	10.0	0.0	2.5	0.29	7.1	34	0.02
6.5	825	365	10.0	0.0	2.8	0.28	7.1	34	0.02
7.2	875	385	10.0	0.0	3.0	0.28	7.1	34	0.02
8.0	925	405	10.0	0.0	3.3	0.28	7.1	34	0.02
8.8	975	422	10.0	0.0	3.7	0.28	7.0	35	0.02
9.7	1025	436	10.0	0.0	4.1	0.28	6.9	36	0.03
10.6	1075	449	10.0	0.0	4.5	0.27	6.9	37	0.03
11.7	1125	461	10.0	0.0	4.9	0.28	6.8	38	0.03
12.7	1175	470	10.0	0.0	5.3	0.28	6.9	38	0.03
13.6	1225	478	10.0	0.0	5.7	0.27	6.9	39	0.03
14.6	1275	484	10.0	0.0	6.1	0.27	7.0	39	0.03
15.6	1325	491	10.0	0.0	6.5	0.27	7.1	39	0.03
16.5	1375	495	10.0	0.0	7.0	0.27	7.2	40	0.03
17.5	1425	502	10.0	0.0	7.4	0.27	7.3	40	0.03
18.6	1475	559	10.0	0.0	7.8	0.26	7.3	42	0.03
19.9	1525	673	10.0	0.0	8.4	0.27	7.2	47	0.03
21.7	1575	763	10.0	0.0	9.1	0.27	6.9	52	0.03
24.3	1625	840	10.0	0.0	10.2	0.29	6.4	78	0.03
28.4	1675	898	10.0	0.2	11.9	0.31	5.8	117	0.04
33.3	1688	913	10.0	0.5	14.0	0.35	5.0	176	0.04
38.7	1691	891	10.0	0.8	16.3	0.40	4.4	252	0.04
43.0	1697	866	10.0	1.0	18.1	0.43	4.0	252	0.05
44.2	1700	913	10.0	0.0	18.6	0.45	3.9	263	0.04
46.1	1706	796	10.0	0.0	19.4	0.47	3.8	263	0.04
48.6	1719	869	10.0	0.0	20.4	0.48	3.8	263	0.05
51.0	1744	920	10.0	0.0	21.5	0.49	4.0	286	0.05
54.3	1756	763	10.0	0.0	22.8	0.51	3.8	286	0.05
56.2	1767	803	10.0	0.0	23.6	0.51	3.6	286	0.05
57.2	1774	792	0.0	0.0	23.6	0.52	3.7	286	0.05
66.7	1774	713	0.0	0.0	23.6	0.46	3.2	286	0.04
77.6	1774	634	0.0	0.0	23.6	0.41	3.0	286	0.04
90.0	1774	554	0.0	0.0	23.6	0.36	2.7	286	0.03
103.7	1774	475	0.0	0.0	23.6	0.31	2.5	286	0.03
118.3	1774	396	0.0	0.0	23.6	0.26	2.3	286	0.02
133.9	1774	317	0.0	0.0	23.6	0.22	2.1	286	0.02
150.0	1774	238	0.0	0.0	23.6	0.17	2.0	286	0.02
166.6	1774	158	0.0	0.0	23.6	0.12	1.9	286	0.01

GEOMETRY SUMMARY * At End of Pumping Schedule
FLUVIAL C FOAM MINIFRAC NO. 1

Dstnce (ft)	Press (psi)	W-Avg (in)	Q (bpm)	Sh-Rate (1/sec)	Hght (ft) Total	Up	Dn	Prop	Bank Fraction	Prop (PSF)
25	802	0.10	5.1	61	286	239	34	185	0.01	0.01
63	801	0.08	4.5	98	239	192	34	174	0.01	0.01
100	799	0.08	4.3	95	238	191	34	174	0.01	0.01
150	796	0.08	3.9	88	238	192	33	174	0.01	0.01
200	793	0.08	3.5	99	221	179	29	170	0.01	0.02
250	787	0.07	3.2	157	171	134	25	141	0.02	0.06
300	779	0.06	2.9	197	143	108	22	110	0.02	0.06
350	770	0.06	2.7	223	125	92	20	92	0.03	0.06
400	760	0.06	2.5	233	114	82	19	84	0.03	0.05
450	750	0.06	2.4	245	104	73	17	75	0.03	0.05
500	740	0.06	2.3	263	93	64	16	67	0.02	0.05
550	731	0.06	2.1	289	81	54	14	58	0.03	0.05
600	721	0.06	2.0	327	69	43	13	48	0.03	0.05
650	711	0.06	1.9	385	57	33	11	38	0.04	0.04
700	701	0.06	1.9	394	54	31	11	36	0.03	0.03
750	689	0.06	1.8	392	53	30	11	36	0.02	0.02
800	678	0.05	1.7	391	53	29	10	35	0.02	0.01
850	665	0.05	1.6	391	52	29	10	35	0.01	0.01
900	652	0.05	1.5	392	51	28	10	34	0.01	0.01
950	639	0.05	1.5	394	50	27	10	33	0.01	0.01
1000	625	0.05	1.4	397	49	26	10	33	0.00	0.00
1050	610	0.05	1.3	400	48	26	10	32	0.00	0.00
1100	595	0.05	1.2	405	47	25	9	32	0.00	0.00
1150	578	0.05	1.2	410	46	24	9	31	0.00	0.00
1200	561	0.05	1.1	417	45	23	9	30	0.00	0.00
1250	542	0.04	1.0	427	44	22	9	29	0.00	0.00
1300	523	0.04	0.9	439	43	21	9	29	0.00	0.00
1350	501	0.04	0.9	455	41	20	8	28	0.00	0.00
1400	478	0.04	0.8	475	40	19	8	27	0.00	0.00
1450	453	0.04	0.7	503	38	17	8	26	0.00	0.00
1500	424	0.04	0.7	543	36	16	7	24	0.00	0.00
1550	392	0.03	0.6	602	34	14	7	23	0.00	0.00
1600	354	0.03	0.5	657	34	14	7	23	0.00	0.00
1650	310	0.03	0.5	750	34	14	7	23	0.00	0.00
1681	277	0.02	0.4	791	34	14	7	23	0.00	0.00
1689	268	0.02	0.4	802	34	14	7	23	0.00	0.00
1694	262	0.02	0.4	825	34	14	7	23	0.00	0.00
1698	257	0.02	0.4	835	34	14	7	23	0.00	0.00
1703	250	0.02	0.3	861	34	14	7	23	0.00	0.00
1713	236	0.02	0.3	928	34	14	7	23	0.00	0.00
1731	200	0.02	0.3	1175	34	14	7	23	0.00	0.00
1756	180	0.02	0.2	1082	34	14	7	23	0.00	0.00

FLUID SUMMARY * At End of Pumping Schedule
FLUVIAL C FOAM MINIFRAC NO. 1

Stage No	Gone	Fluid ID	Prop ID	Pos (ft)	Concentration In	Now	Desgn	Fl Vol (MGal)	Ex Tim (min)	Temp (deg F)	Visc (cp)	Fall Frac
1	1	2	1	1767	0.0	0.0	0.0	0.1	1.3	160	0	0.00
1	1	2	1	1767	0.0	0.0	0.0	0.2	1.3	160	0	0.00
1	1	2	1	1767	0.0	0.0	0.0	0.3	1.8	160	0	0.00
1	1	2	1	1767	0.0	0.0	0.0	0.4	1.9	160	0	0.00
1	1	2	1	1767	0.0	0.0	0.0	0.5	2.1	160	0	0.00
1	1	2	1	1767	0.0	0.0	0.0	0.7	2.2	160	0	0.00
1	1	2	1	1767	0.0	0.0	0.0	0.8	2.9	160	0	0.00
1	1	2	1	1767	0.0	0.0	0.0	1.0	3.0	160	0	0.00
1	1	2	1	1767	0.0	0.0	0.0	1.2	3.2	160	0	0.00
1	1	2	1	1767	0.0	0.0	0.0	1.4	3.4	160	0	0.00
1	1	2	1	1767	0.0	0.0	0.0	1.6	3.1	160	0	0.00
1	1	2	1	1767	0.0	0.0	0.0	1.8	3.3	160	0	0.00
1	1	2	1	1767	0.0	0.0	0.0	2.0	4.2	160	0	0.00
1	1	2	1	1767	0.0	0.0	0.0	2.2	4.6	160	0	0.00
2	1	3	1	1767	0.0	0.0	0.0	2.2	5.6	160	0	0.00
2	1	3	1	1767	0.0	0.0	0.0	2.5	4.3	160	0	0.00
2	1	3	1	1767	0.0	0.0	0.0	2.8	5.6	160	0	0.00
2	1	3	1	1767	0.0	0.0	0.0	3.0	5.7	160	0	0.00
2	1	3	1	1767	0.0	0.0	0.0	3.3	5.8	160	0	0.00
2	1	3	1	1767	0.0	0.0	0.0	3.7	6.9	160	0	0.00
2	1	3	1	1767	0.0	0.0	0.0	4.1	6.9	160	0	0.00
2	1	3	1	1767	0.0	0.0	0.0	4.5	7.0	160	0	0.00
2	1	3	1	1767	0.0	0.0	0.0	4.9	7.6	160	0	0.00
2	1	3	1	1767	0.0	0.0	0.0	5.3	8.9	160	0	0.00
2	1	3	1	1767	0.0	0.0	0.0	5.7	11.3	160	1	0.00
2	1	3	1	1767	0.0	0.0	0.0	6.1	14.8	160	1	0.00
2	1	3	1	1767	0.0	0.0	0.0	6.5	13.8	160	1	0.00
2	1	3	1	1767	0.0	0.0	0.0	7.0	17.9	160	1	0.00
2	1	3	1	1767	0.0	0.0	0.0	7.2	16.8	160	1	0.00
3	1	1	1	1767	0.0	0.0	0.0	7.4	24.3	160	7	0.00
3	1	1	1	1767	0.0	0.0	0.0	7.8	26.6	160	5	0.00
3	1	1	1	1767	0.0	0.0	0.0	8.4	29.6	160	6	0.00
3	0	1	1	1741	0.0	0.0	0.0	9.1	28.9	160	5	0.00
3	0	1	1	1664	0.0	0.0	0.2	9.6	28.9	160	7	0.00
4	0	1	1	1537	0.2	0.6	0.3	10.2	24.4	160	8	1.00
4	0	1	1	1294	0.2	0.4	0.5	11.6	19.2	160	9	1.00
5	0	1	1	1094	0.5	0.0	1.0	11.9	19.2	160	9	1.00
5	0	1	1	975	0.5	0.0	1.0	13.6	7.9	160	10	1.00
6	0	1	1	653	0.8	1.0	0.8	13.9	5.4	160	10	0.73
6	0	1	1	505	0.8	0.9	0.9	15.5	0.0	147	13	0.35
7	0	1	1	360	1.0	1.1	0.9	16.1	0.0	88	17	0.26
7	0	1	1	275	1.0	1.0	1.0	17.5	0.0	84	20	0.12
8	0	1	1	212	0.0	0.0	1.0	17.8	0.0	80	26	0.00
8	0	1	1	192	0.0	0.0	1.0	18.3	0.0	80	26	0.00
8	0	1	1	163	0.0	0.0	1.0	19.1	0.0	78	28	0.00
8	0	1	1	125	0.0	0.0	1.0	20.1	0.0	76	27	0.00
8	0	1	1	83	0.0	0.0	1.0	21.1	0.0	75	27	0.00
8	0	1	1	42	0.0	0.0	1.0	22.4	0.0	72	32	0.00
8	0	1	1	11	0.0	0.0	1.0	23.1	0.0	71	34	0.00

PROPPANT SUMMARY * At End of Pumping Schedule
FLUVIAL C FOAM MINIFRAC NO. 1

Lb/Sq-Ft Lost to Embedment 0.050

Distance (ft)	KfW (md-ft)	Proppant Concentration (lb/sq foot) Prop ID--> 1
25	8	0.00
63	8	0.00
100	8	0.00
150	8	0.00
200	0	0.00
250	5	0.10
300	9	0.10
350	7	0.10
400	0	0.10
450	0	0.00
500	0	0.00
550	0	0.00
600	0	0.00
650	0	0.00
700	0	0.00
750	0	0.00
800	0	0.00
850	8	0.00
900	8	0.00
950	6	0.00
1000	2	0.00
1050	0	0.00
1100	0	0.00
1150	0	0.00
1200	0	0.00
1250	0	0.00
1300	0	0.00
1350	0	0.00
1400	0	0.00
1450	0	0.00
1500	0	0.00
1550	0	0.00
1600	0	0.00
1650	0	0.00
1681	0	0.00
1689	0	0.00
1694	0	0.00
1698	0	0.00
1703	0	0.00
1713	0	0.00
1731	0	0.00
1756	0	0.00

Average Conductivity (md-ft) 6

PROPPANT SUMMARY * At Fracture Closure
FLUVIAL C FOAM MINIFRAC NO. 1

Lb/Sq-Ft Lost to Embedment 0.050

Distance (ft)	KfW (md-ft)	Proppant Concentration (lb/sq foot) Prop ID--> 1
25	8	0.00
63	8	0.00
100	8	0.00
150	8	0.00
200	0	0.00
250	0	0.00
300	0	0.00
350	0	0.00
400	0	0.00
450	0	0.00
500	8	0.10
550	21	0.10
600	31	0.10
650	50	0.10
700	49	0.10
750	30	0.10
800	11	0.10
850	0	0.00
900	0	0.00
950	0	0.00
1000	2	0.00
1050	0	0.00
1100	0	0.00
1150	0	0.00
1200	0	0.00
1250	0	0.00
1300	0	0.00
1350	0	0.00
1400	0	0.00
1450	0	0.00
1500	0	0.00
1550	0	0.00
1600	0	0.00
1650	0	0.00
1681	0	0.00
1689	0	0.00
1694	0	0.00
1698	0	0.00
1703	0	0.00
1713	0	0.00
1731	0	0.00
1756	0	0.00
1771	0	0.00

Average Conductivity (md-ft) 20

C.8: SIMULATION OF FLUVIAL "C" MINIFRAC NO. 2 WITH INCREASED FLUID VISCOSITY THROUGH CONSTANT PRESSURE MODE.

Frac Summary * FLUVIAL C FOAM MINIFRAC NO. 2
Filename: FLUV2-C.FRK

Design Data		
FLUID LOSS:	Coefficient (ft/sqrt(min))	0.0008
	Spurt Loss (gal/100 sq ft)	0.00
FORMATION:	Modulus (MM psi)	4.00
	Fracture Height (ft)	17.0
	Fluid Loss Height (ft)	22.0
	Perforated Height (ft)	13.0
TEMPERATURE:	Bottom Hole (deg F)	160
PRESSURE:	Reservoir Pressure (psi)	3400.0
	Closure Pressure (psi)	4727.0
DEPTH:	Well Depth (ft)	5722

FORMATION LAYER DATA:

Depth	Stress at Top	Stress Grad	Modulus	Toughness
5300	5700.0	0.000	5.00	1.00
5532	3800.0	0.000	5.00	1.00
5570	5700.0	0.000	5.00	1.00
5719	4727.0	0.000	4.00	1.00
5739	6000.0	0.000	5.00	1.00
5825	4550.0	0.000	5.00	1.00
5850	6000.0	0.000	5.00	1.00
5886	5200.0	0.000	5.00	1.00
5927	5775.0	0.000	5.00	1.00
5953	4200.0	0.000	5.00	1.00
5980	5600.0	0.433	5.00	1.00

Fluid Pressure Gradient (psi/ft)		0.433
Fracture Top (ft)		5722
Fracture Bottom (ft)		5735

Calculated Results
from 3-D Simulator
STIMPLAN (TM) , NSI , Tulsa,OK
Licensed To: Internal Use - NSI Technologies

1/2 LENGTH:	'Hydraulic' length (ft)	1717
	Propped length (ft)	72
PRESSURE:	Max Net Pressure (psi)	1029
TIME:	Max Exposure to Form. Temp. (min) ..	23.1
	Time to Close (min)	63.6
RATE:	Fluid Loss Rate during pad (bpm) ...	5.3
EFFICIENCY:	at end of pumping schedule	0.56
PROPPANT:	Average In Situ Conc. (#/sq ft)	0.1
	Average Conductivity (md-ft)	15
HEIGHT:	Max Fracture Height (ft)	185
WIDTH:	Avg width at end of pumping (in) ...	0.06

STIMPLAN (TM). NSI Technologies, Tulsa, OK
Licensed To: Internal Use - NSI Technologies

WELL ID:
FLUVIAL C FOAM MINIFRAC NO. 2
DEPTH: Well Depth (ft) 5722
PRESSURE: Reservoir Pressure (psi) 3400
Closure Pressure (psi) 4727
TEMPERATURE: Bottom Hole Temperature (deg F) 160

** Pumping Schedule **

Sl Vol (Mgal)	Fl Vol (Mgal)	Conc (ppg)	Rate (bpm)	Fluid Type	Prop Type	Cum Prop (M-lb)	Pump Time (min)
2.4	2.4	0.0	10.0	1	1	0.0	5.7
2.0	2.0	0.2	10.0	1	1	0.4	4.8
2.0	2.0	0.5	10.0	1	1	1.4	4.8
2.0	1.9	0.8	10.0	1	1	2.9	4.7
2.0	1.9	1.0	10.0	1	1	4.9	4.9
5.9	5.9	0.0	10.0	1	1	4.9	14.1

Total Slurry ... 16.4 Total Fluid ... 16.2
Total Proppant ... 4.9 Avg. Conc 0.3
Total Pump Time 39.0 min

Proppant ID No. 1 20- 40 Ottawa_Snd

Specific Gravity 2.65
'Damage Factor' 0.70

Closure Pres (Mpsi)	0	2	4	8	16
KfW @ 2 #/sq ft (md-ft)	4800	3850	2750	990	50

Fluid ID No. 1 Foam_75_Qual,_20#-HPG,_150_F

Specific Gravity 1.04
Quality 75

	@Welbor	@FormTmp	@1Hr	@2Hr	@4Hr	@8Hr
vis (cp @ 170 1/sec) .	35	25	20	15	10	10
non-Newtonian n'	0.52	0.52	0.52	0.52	0.57	0.57

Time History * NSI STIMPLAN 3-D Fracture Simulation
FLUVIAL C FOAM MINIFRAC NO. 1

Time (min)	Pen (ft)	Pres (psi)	Rate (bpm)	Prop (PPG)	Sl Vol (MGal)	Eff-ciency	Loss (bpm)	Hght (ft)	W-Avg (in)
0.2	66	435	10.0	0.0	0.1	0.68	3.3	30	0.02
0.6	116	587	10.0	0.0	0.3	0.59	3.2	37	0.03
1.1	166	661	10.0	0.0	0.4	0.59	3.4	42	0.04
1.6	216	684	10.0	0.0	0.7	0.59	3.7	44	0.04
2.1	266	709	10.0	0.0	0.9	0.59	4.0	45	0.04
2.7	316	732	10.0	0.0	1.1	0.59	4.3	47	0.04
3.3	366	754	10.0	0.0	1.4	0.59	4.5	48	0.05
4.0	416	776	10.0	0.0	1.7	0.59	4.7	49	0.05
4.7	466	795	10.0	0.0	2.0	0.59	4.8	50	0.05
5.4	516	814	10.0	0.0	2.3	0.58	5.0	51	0.05
6.2	566	832	10.0	0.0	2.6	0.59	5.1	51	0.05
7.0	616	847	10.0	0.2	2.9	0.58	5.3	52	0.05
7.8	666	863	10.0	0.2	3.3	0.58	5.4	53	0.05
8.7	716	878	10.0	0.2	3.7	0.58	5.5	54	0.05
9.6	766	892	10.0	0.2	4.0	0.58	5.6	55	0.05
10.5	816	904	10.0	0.2	4.4	0.57	5.7	63	0.05
11.6	866	907	10.0	0.5	4.9	0.57	5.6	66	0.05
12.6	916	923	10.0	0.5	5.3	0.57	5.7	75	0.05
13.7	966	923	10.0	0.5	5.8	0.57	5.8	77	0.06
14.8	1016	940	10.0	0.5	6.2	0.57	5.8	86	0.05
16.1	1066	934	10.0	0.5	6.8	0.57	5.8	86	0.06
17.3	1116	961	10.0	0.8	7.3	0.57	5.9	98	0.06
18.8	1166	936	10.0	0.8	7.9	0.57	5.8	98	0.06
20.1	1216	972	10.0	0.8	8.5	0.56	5.8	104	0.06
21.6	1266	962	10.0	1.0	9.1	0.56	5.8	104	0.06
23.1	1316	991	10.0	1.0	9.7	0.56	5.9	117	0.06
24.9	1366	955	10.0	1.0	10.5	0.56	5.8	117	0.06
26.5	1416	995	10.0	0.0	11.2	0.56	5.8	118	0.06
28.3	1466	998	10.0	0.0	11.9	0.56	5.8	124	0.06
30.1	1516	995	10.0	0.0	12.6	0.56	5.8	124	0.06
31.8	1566	1016	10.0	0.0	13.4	0.56	5.9	156	0.06
34.2	1616	967	10.0	0.0	14.4	0.56	5.7	156	0.06
36.2	1666	1009	10.0	0.0	15.2	0.56	5.7	156	0.06
38.0	1716	1029	10.0	0.0	16.0	0.56	5.8	185	0.06
39.0	1717	882	10.0	0.0	16.4	0.56	5.0	185	0.06
44.5	1717	794	0.0	0.0	16.4	0.51	4.4	185	0.05
51.0	1717	706	0.0	0.0	16.4	0.45	4.0	185	0.05
58.3	1717	618	0.0	0.0	16.4	0.40	3.6	185	0.04
66.3	1717	529	0.0	0.0	16.4	0.35	3.2	185	0.04
74.8	1717	441	0.0	0.0	16.4	0.29	3.0	185	0.03
83.8	1717	353	0.0	0.0	16.4	0.24	2.8	185	0.02
93.1	1717	265	0.0	0.0	16.4	0.19	2.6	185	0.02
102.6	1717	176	0.0	0.0	16.4	0.14	2.4	185	0.01

GEOMETRY SUMMARY * At End of Pumping Schedule
FLUVIAL C FOAM MINIFRAC NO. 2

Dstnce (ft)	Press (psi)	W-Avg (in)	Q (bpm)	Sh-Rate (1/sec)	Hght (ft) Total	Up	Dn	Prop	Bank Fraction	Prop (PSF)
21	867	0.07	5.0	185	185	134	37	149	0.01	0.01
54	837	0.07	4.6	199	175	126	35	141	0.01	0.01
91	809	0.07	4.3	227	160	115	32	128	0.02	0.01
141	865	0.07	3.7	207	140	99	28	110	0.02	0.02
191	912	0.07	3.4	203	123	85	25	96	0.02	0.02
241	891	0.07	3.3	216	117	80	24	91	0.03	0.02
291	868	0.07	3.2	231	110	74	23	85	0.03	0.02
341	848	0.07	3.0	244	103	68	22	80	0.03	0.03
391	828	0.06	2.8	258	96	62	21	74	0.04	0.03
441	807	0.06	2.7	275	88	56	19	68	0.05	0.03
491	784	0.06	2.5	295	81	50	18	62	0.06	0.04
541	758	0.06	2.3	324	73	43	17	55	0.06	0.04
591	786	0.06	2.1	309	64	36	16	48	0.07	0.06
641	846	0.07	2.0	287	56	29	14	42	0.07	0.09
691	849	0.07	2.0	293	54	27	14	40	0.07	0.09
741	835	0.07	2.0	306	53	26	14	39	0.07	0.08
791	821	0.07	2.0	318	52	26	13	39	0.07	0.08
841	807	0.06	1.9	330	52	25	13	38	0.07	0.07
891	791	0.06	1.9	341	51	25	13	38	0.07	0.07
941	776	0.06	1.9	353	50	24	13	37	0.07	0.06
991	760	0.06	1.8	365	49	24	13	36	0.06	0.05
1041	743	0.06	1.8	376	49	23	12	36	0.04	0.03
1091	726	0.06	1.8	388	48	23	12	35	0.02	0.01
1141	708	0.06	1.7	400	47	22	12	35	0.00	0.00
1191	689	0.06	1.6	412	46	21	12	34	0.00	0.00
1241	669	0.05	1.5	424	45	21	11	33	0.00	0.00
1291	648	0.05	1.5	437	44	20	11	32	0.00	0.00
1341	625	0.05	1.4	450	43	19	11	31	0.00	0.00
1391	600	0.05	1.3	464	42	18	10	31	0.00	0.00
1441	573	0.05	1.2	479	40	17	10	30	0.00	0.00
1491	540	0.04	1.0	498	39	16	10	28	0.00	0.00
1541	498	0.04	0.9	530	37	15	9	27	0.00	0.00
1591	437	0.04	0.7	600	34	13	8	25	0.00	0.00
1641	393	0.03	0.5	644	32	11	8	23	0.00	0.00
1692	238	0.02	0.3	934	27	8	6	20	0.00	0.00

FLUID SUMMARY * At End of Pumping Schedule
FLUVIAL C FOAM MINIFRAC NO. 2

Stage No	Stage Gone	Fluid ID	Prop ID	Pos (ft)	Concentration In	Concentration Now	Concentration Design	Fl Vol (MGal)	Ex Tim (min)	Temp (deg F)	Visc (cp)	Fall Frac
1	1	1	1	1717	0.0	0.0	0.0	0.1	3.5	160	4	0.00
1	1	1	1	1717	0.0	0.0	0.0	0.3	4.2	160	4	0.00
1	1	1	1	1717	0.0	0.0	0.0	0.4	5.3	160	4	0.00
1	1	1	1	1717	0.0	0.0	0.0	0.7	6.4	160	4	0.00
1	1	1	1	1717	0.0	0.0	0.0	0.9	7.6	160	4	0.00
1	1	1	1	1717	0.0	0.0	0.0	1.1	8.4	160	4	0.00
1	1	1	1	1717	0.0	0.0	0.0	1.4	9.9	160	4	0.00
1	1	1	1	1717	0.0	0.0	0.0	1.7	11.6	160	4	0.00
1	1	1	1	1717	0.0	0.0	0.0	2.0	11.4	160	4	0.00
1	1	1	1	1717	0.0	0.0	0.0	2.3	12.0	160	4	0.00
1	1	1	1	1717	0.0	0.0	0.0	2.4	13.4	160	4	0.00
2	1	1	1	1717	0.2	44.2	0.0	2.6	14.1	160	4	0.00
2	1	1	1	1717	0.2	44.2	0.0	2.9	16.6	160	4	0.00
2	1	1	1	1717	0.2	44.2	0.0	3.3	17.3	160	4	0.00
2	1	1	1	1717	0.2	44.2	0.0	3.7	19.9	160	5	0.00
2	1	1	1	1717	0.2	44.2	0.0	4.0	20.9	160	4	0.00
2	1	1	1	1717	0.2	44.2	0.0	4.4	22.8	160	6	0.00
3	1	1	1	1717	0.5	0.0	1.0	4.9	23.1	160	6	1.00
3	0	1	1	1678	0.5	0.0	1.0	5.3	21.9	160	7	1.00
3	0	1	1	1613	0.5	0.0	1.0	5.8	19.1	160	8	1.00
3	0	1	1	1523	0.5	0.0	1.0	6.2	19.1	160	8	1.00
3	0	1	1	1454	0.5	0.0	1.0	6.4	17.7	160	8	1.00
4	0	1	1	1400	0.8	0.0	1.0	6.7	16.2	160	9	1.00
4	0	1	1	1317	0.8	0.0	1.0	7.2	16.2	160	9	1.00
4	0	1	1	1202	0.8	0.0	1.0	7.8	12.8	160	9	1.00
4	0	1	1	1080	0.8	0.0	1.0	8.3	11.1	160	10	1.00
5	0	1	1	1020	1.0	0.0	1.0	8.4	11.1	160	10	1.00
5	0	1	1	950	1.0	1.4	0.7	9.0	9.4	160	10	0.89
5	0	1	1	819	1.0	1.2	0.8	9.6	5.6	160	11	0.70
5	0	1	1	677	1.0	1.1	0.9	10.3	3.4	160	11	0.51
6	0	1	1	538	0.0	0.0	1.0	11.0	1.4	160	11	0.00
6	0	1	1	430	0.0	0.0	0.9	11.6	0.0	133	13	0.00
6	0	1	1	340	0.0	0.0	0.9	12.4	0.0	88	16	0.00
6	0	1	1	262	0.0	0.0	0.9	13.1	0.0	84	17	0.00
6	0	1	1	183	0.0	0.0	0.9	14.0	0.0	79	18	0.00
6	0	1	1	107	0.0	0.0	1.0	14.9	0.0	76	18	0.00
6	0	1	1	49	0.0	0.0	1.0	15.6	0.0	72	19	0.00
6	0	1	1	12	0.0	0.0	1.0	16.0	0.0	71	20	0.00

PROPPANT SUMMARY * At End of Pumping Schedule
FLUVIAL C FOAM MINIFRAC NO. 2

Lb/Sq-Ft Lost to Embedment 0.050

Distance (ft)	KfW (md-ft)	Proppant Concentration (lb/sq foot) Prop ID--> 1
21	7	0.00
54	6	0.00
91	0	0.00
141	0	0.00
191	0	0.00
241	0	0.00
291	0	0.00
341	0	0.00
391	0	0.00
441	0	0.00
491	0	0.00
541	0	0.00
591	8	0.10
641	32	0.10
691	32	0.10
741	30	0.10
791	23	0.10
841	20	0.10
891	16	0.10
941	6	0.10
991	0	0.00
1041	0	0.00
1091	0	0.00
1141	0	0.00
1191	0	0.00
1241	0	0.00
1291	0	0.00
1341	0	0.00
1391	0	0.00
1441	0	0.00
1491	0	0.00
1541	0	0.00
1591	0	0.00
1641	0	0.00
1692	0	0.00

Average Conductivity (md-ft) 19

PROPPANT SUMMARY * At Fracture Closure
FLUVIAL C FOAM MINIFRAC NO. 2

Lb/Sq-Ft Lost to Embedment 0.050

Distance (ft)	KfW (md-ft)	Proppant Concentration (lb/sq foot) Prop ID--> 1
21	7	0.00
54	6	0.00
91	0	0.00
141	0	0.00
191	0	0.00
241	0	0.00
291	0	0.00
341	0	0.00
391	0	0.00
441	0	0.00
491	0	0.00
541	0	0.00
591	1	0.10
641	8	0.10
691	15	0.10
741	18	0.10
791	26	0.10
841	30	0.10
891	35	0.10
941	26	0.10
991	2	0.10
1041	0	0.00
1091	0	0.00
1141	0	0.00
1191	0	0.00
1241	0	0.00
1291	0	0.00
1341	0	0.00
1391	0	0.00
1441	0	0.00
1491	0	0.00
1541	0	0.00
1591	0	0.00
1641	0	0.00
1692	0	0.00

Average Conductivity (md-ft) 15

C.9: SIMULATION OF FLUVIAL "C" MINIFRAC NO. 2 WITH INCREASED FLUID VISCOSITY THROUGH CONSTANT PRESSURE MODE AND DECREASED VISCOSITY IN EARLY TIME.

Frac Summary * FLUVIAL C FOAM MINIFRAC NO. 2
Filename: FLUV2-C.FRK

Design Data		
FLUID LOSS:	Coefficient (ft/sqrt(min))	0.0007
	Spurt Loss (gal/100 sq ft)	0.00
FORMATION:	Modulus (MM psi)	4.00
	Fracture Height (ft)	17.0
	Fluid Loss Height (ft)	22.0
	Perforated Height (ft)	13.0
TEMPERATURE:	Bottom Hole (deg F)	160
PRESSURE:	Reservoir Pressure (psi)	3400.0
	Closure Pressure (psi)	4727.0
DEPTH:	Well Depth (ft)	5722

FORMATION LAYER DATA:

Depth	Stress at Top	Stress Grad	Modulus	Toughness
5300	5700.0	0.000	5.00	1.00
5532	3800.0	0.000	5.00	1.00
5570	5700.0	0.000	5.00	1.00
5719	4727.0	0.000	4.00	1.00
5739	6000.0	0.000	5.00	1.00
5825	4550.0	0.000	5.00	1.00
5850	6000.0	0.000	5.00	1.00
5886	5200.0	0.000	5.00	1.00
5927	5775.0	0.000	5.00	1.00
5953	4200.0	0.000	5.00	1.00
5980	5600.0	0.433	5.00	1.00

Fluid Pressure Gradient (psi/ft)		0.433
Fracture Top (ft)		5722
Fracture Bottom (ft)		5735

Calculated Results
from 3-D Simulator
STIMPLAN (TM) , NSI , Tulsa,OK
Licensed To: Internal Use - NSI Technologies

1/2 LENGTH:	'Hydraulic' length (ft)	1722
	Propped length (ft)	73
PRESSURE:	Max Net Pressure (psi)	1026
TIME:	Max Exposure to Form. Temp. (min) ..	23.2
	Time to Close (min)	74.0
RATE:	Fluid Loss Rate during pad (bpm) ...	4.8
EFFICIENCY:	at end of pumping schedule	0.57
PROPPANT:	Average In Situ Conc. (#/sq ft)	0.1
	Average Conductivity (md-ft)	20
HEIGHT:	Max Fracture Height (ft)	179
WIDTH:	Avg width at end of pumping (in) ...	0.06

STIMPLAN (TM). NSI Technologies, Tulsa, OK
Licensed To: Internal Use - NSI Technologies

WELL ID:
FLUVIAL C FOAM MINIFRAC NO. 1
DEPTH: Well Depth (ft) 5722
PRESSURE: Reservoir Pressure (psi) 3400
Closure Pressure (psi) 4727
TEMPERATURE: Bottom Hole Temperature (deg F) 160

** Pumping Schedule **

Sl Vol (Mgal)	Fl Vol (Mgal)	Conc (ppg)	Rate (bpm)	Fluid Type	Prop Type	Cum Prop (M-lb)	Pump Time (min)
2.4	2.4	0.0	10.0	3	1	0.0	5.7
2.0	2.0	0.2	10.0	1	1	0.4	4.8
2.0	2.0	0.5	10.0	1	1	1.4	4.8
2.0	1.9	0.8	10.0	1	1	2.9	4.7
2.0	1.9	1.0	10.0	1	1	4.9	4.9
5.9	5.9	0.0	10.0	1	1	4.9	14.1

Total Slurry ... 16.4 Total Fluid ... 16.2
Total Proppant ... 4.9 Avg. Conc 0.3
Total Pump Time 39.0 min

Proppant ID No. 1 20- 40 Ottawa_Snd

Specific Gravity 2.65
'Damage Factor' 0.70

Closure Pres (Mpsi)	0	2	4	8	16
KfW @ 2 #/sq ft (md-ft)	4800	3850	2750	990	50

Fluid ID No. 3 NITROGEN

Specific Gravity 0.60

	@Welbor	@FormTmp	@1Hr	@2Hr	@4Hr	@8Hr
vis (cp @ 170 1/sec) .	15	15	15	15	10	10
non-Newtonian n'	0.57	0.57	0.57	0.57	0.57	0.57

Fluid ID No. 1	Foam_75_Qual,_20#-HPG,_150_F					
Specific Gravity					1.04	
Quality					75	
	@Welbor	@FormTmp	@1Hr	@2Hr	@4Hr	@8Hr
vis (cp @ 170 1/sec) .	35	25	20	15	10	10
non-Newtonian n'	0.52	0.52	0.52	0.52	0.57	0.57

Time History * NSI STIMPLAN 3-D Fracture Simulation
FLUVIAL C FOAM MINIFRAC NO. 1

Time (min)	Pen (ft)	Pres (psi)	Rate (bpm)	Prop (PPG)	Sl Vol (MGal)	Eff-ciency	Loss (bpm)	Hght (ft)	W-Avg (in)
0.2	67	395	10.0	0.0	0.1	0.69	3.1	29	0.02
0.5	117	528	10.0	0.0	0.2	0.57	3.1	35	0.03
1.0	167	588	10.0	0.0	0.4	0.56	3.3	39	0.03
1.5	217	607	10.0	0.0	0.6	0.55	3.5	41	0.04
2.0	267	628	10.0	0.0	0.8	0.54	3.8	42	0.04
2.6	317	648	10.0	0.0	1.1	0.53	4.0	43	0.04
3.2	367	666	10.0	0.0	1.3	0.52	4.2	44	0.04
3.8	417	683	10.0	0.0	1.6	0.52	4.3	45	0.04
4.5	467	699	10.0	0.0	1.9	0.51	4.5	45	0.04
5.3	517	714	10.0	0.0	2.2	0.50	4.6	46	0.04
6.0	567	728	10.0	0.0	2.5	0.50	4.7	47	0.05
6.8	617	748	10.0	0.2	2.9	0.49	4.8	48	0.05
7.7	667	780	10.0	0.2	3.2	0.49	4.9	49	0.05
8.6	717	808	10.0	0.2	3.6	0.49	5.0	50	0.05
9.5	767	833	10.0	0.2	4.0	0.49	5.1	51	0.05
10.4	817	856	10.0	0.2	4.4	0.50	5.2	52	0.05
11.3	867	876	10.0	0.2	4.8	0.51	5.3	53	0.05
12.3	917	895	10.0	0.5	5.2	0.51	5.4	56	0.05
13.3	967	910	10.0	0.5	5.6	0.52	5.4	66	0.05
14.5	1017	917	10.0	0.5	6.1	0.52	5.4	72	0.05
15.6	1067	934	10.0	0.5	6.6	0.53	5.4	82	0.05
16.9	1117	933	10.0	0.8	7.1	0.53	5.4	83	0.05
18.3	1167	961	10.0	0.8	7.7	0.54	5.4	98	0.05
19.9	1217	939	10.0	0.8	8.4	0.54	5.3	98	0.06
21.3	1267	979	10.0	0.8	9.0	0.55	5.3	108	0.06
23.0	1317	954	10.0	1.0	9.7	0.55	5.3	108	0.06
24.5	1367	992	10.0	1.0	10.3	0.56	5.4	117	0.06
26.2	1417	967	10.0	1.0	11.0	0.56	5.3	117	0.06
27.7	1467	1003	10.0	0.0	11.7	0.56	5.4	124	0.06
29.5	1517	983	10.0	0.0	12.4	0.56	5.4	124	0.06
31.1	1567	1015	10.0	0.0	13.1	0.56	5.5	149	0.06
33.3	1617	971	10.0	0.0	14.0	0.57	5.4	149	0.06
35.1	1667	1010	10.0	0.0	14.8	0.57	5.4	149	0.06
36.9	1717	1026	10.0	0.0	15.5	0.57	5.5	179	0.06
39.0	1722	936	10.0	0.0	16.4	0.57	4.8	179	0.06
45.2	1722	843	0.0	0.0	16.4	0.52	3.9	179	0.05
52.6	1722	749	0.0	0.0	16.4	0.46	3.6	179	0.05
60.9	1722	655	0.0	0.0	16.4	0.41	3.2	179	0.04
70.2	1722	562	0.0	0.0	16.4	0.35	2.9	179	0.04
80.2	1722	468	0.0	0.0	16.4	0.30	2.6	179	0.03
90.8	1722	375	0.0	0.0	16.4	0.24	2.4	179	0.02
101.8	1722	281	0.0	0.0	16.4	0.19	2.2	179	0.02
113.1	1722	187	0.0	0.0	16.4	0.14	2.1	179	0.01

GEOMETRY SUMMARY * At End of Pumping Schedule
FLUVIAL C FOAM MINIFRAC NO. 1

Dstnce (ft)	Press (psi)	W-Avg (in)	Q (bpm)	Sh-Rate (1/sec)	Hght (ft) Total	Up	Dn	Prop	Bank Fraction	Prop (PSF)
21	931	0.08	5.0	168	179	130	36	144	0.01	0.01
54	920	0.08	4.5	170	168	121	34	135	0.01	0.01
92	916	0.07	4.1	181	153	109	31	122	0.02	0.01
142	928	0.07	3.5	185	132	92	27	103	0.02	0.02
192	926	0.07	3.3	194	121	83	25	94	0.02	0.02
242	915	0.07	3.2	201	114	78	23	89	0.02	0.02
292	903	0.07	3.0	209	107	72	22	83	0.03	0.02
342	891	0.07	2.9	218	100	66	21	77	0.03	0.03
392	879	0.07	2.7	228	92	59	20	71	0.04	0.03
442	867	0.07	2.6	238	85	53	19	65	0.04	0.04
492	854	0.07	2.4	253	77	47	18	59	0.05	0.04
542	840	0.07	2.3	271	69	40	16	52	0.06	0.05
592	841	0.07	2.1	280	61	33	15	46	0.08	0.09
642	847	0.07	2.0	297	54	27	14	40	0.07	0.09
692	835	0.07	2.0	312	53	27	14	40	0.07	0.09
742	822	0.07	2.0	325	53	26	13	39	0.07	0.08
792	810	0.06	2.0	338	52	26	13	39	0.07	0.07
842	796	0.06	2.0	350	51	25	13	38	0.07	0.07
892	783	0.06	2.0	362	51	25	13	37	0.07	0.07
942	769	0.06	2.0	375	50	24	13	37	0.07	0.06
992	754	0.06	1.9	386	49	24	12	36	0.05	0.04
1042	739	0.06	1.9	398	48	23	12	36	0.02	0.02
1092	724	0.06	1.8	410	48	23	12	35	0.01	0.01
1142	708	0.06	1.8	421	47	22	12	34	0.00	0.00
1192	691	0.06	1.7	433	46	21	11	34	0.00	0.00
1242	673	0.05	1.6	445	45	21	11	33	0.00	0.00
1292	654	0.05	1.5	457	44	20	11	32	0.00	0.00
1342	635	0.05	1.5	470	43	19	11	32	0.00	0.00
1392	614	0.05	1.4	482	42	19	10	31	0.00	0.00
1442	591	0.05	1.3	494	41	18	10	30	0.00	0.00
1492	566	0.05	1.1	506	40	17	10	29	0.00	0.00
1542	537	0.04	1.0	519	38	16	9	28	0.00	0.00
1592	501	0.04	0.8	537	36	15	9	27	0.00	0.00
1642	468	0.03	0.6	547	35	13	8	25	0.00	0.00
1692	312	0.03	0.3	636	28	9	6	20	0.00	0.00
1719	118	0.01	0.1	715	28	9	6	20	0.00	0.00

FLUID SUMMARY * At End of Pumping Schedule
FLUVIAL C FOAM MINIFRAC NO. 1

Stage No	Stage Gone	Fluid ID	Prop ID	Pos (ft)	Concentration In	Concentration Now	Concentration Desgn	Fl Vol (MGal)	Ex Tim (min)	Temp (deg F)	Visc (cp)	Fall Frac
1	1	3	1	1722	0.0	0.0	0.0	0.1	2.7	160	3	0.00
1	1	3	1	1722	0.0	0.0	0.0	0.2	3.4	160	3	0.00
1	1	3	1	1722	0.0	0.0	0.0	0.4	4.4	160	3	0.00
1	1	3	1	1722	0.0	0.0	0.0	0.6	5.6	160	3	0.00
1	1	3	1	1722	0.0	0.0	0.0	0.8	5.9	160	3	0.00
1	1	3	1	1722	0.0	0.0	0.0	1.1	7.1	160	3	0.00
1	1	3	1	1722	0.0	0.0	0.0	1.3	7.7	160	3	0.00
1	1	3	1	1722	0.0	0.0	0.0	1.6	7.9	160	3	0.00
1	1	3	1	1722	0.0	0.0	0.0	1.9	9.4	160	3	0.00
1	1	3	1	1722	0.0	0.0	0.0	2.2	9.8	160	3	0.00
1	1	3	1	1722	0.0	0.0	0.0	2.4	10.3	160	3	0.00
2	1	1	1	1722	0.2	44.2	0.0	2.5	13.4	160	4	0.00
2	1	1	1	1722	0.2	44.2	0.0	2.9	15.6	160	4	0.00
2	1	1	1	1722	0.2	44.2	0.0	3.2	17.9	160	4	0.00
2	1	1	1	1722	0.2	44.2	0.0	3.6	17.8	160	4	0.00
2	1	1	1	1722	0.2	44.2	0.0	4.0	20.4	160	4	0.00
2	1	1	1	1722	0.2	44.2	0.0	4.4	21.4	160	4	0.00
2	1	1	1	1722	0.2	44.2	0.0	4.4	23.2	160	8	0.00
3	1	1	1	1722	0.5	0.0	1.0	4.8	22.9	160	7	1.00
3	0	1	1	1699	0.5	0.0	1.0	5.2	21.7	160	7	1.00
3	0	1	1	1649	0.5	0.0	1.0	5.6	20.3	160	8	1.00
3	0	1	1	1566	0.5	0.0	1.0	6.1	20.3	160	8	1.00
3	0	1	1	1478	0.5	0.0	1.0	6.4	17.3	160	8	1.00
4	0	1	1	1427	0.8	0.0	1.0	6.5	17.3	160	8	1.00
4	0	1	1	1356	0.8	0.0	1.0	7.1	15.8	160	9	1.00
4	0	1	1	1234	0.8	0.0	1.0	7.6	14.2	160	9	1.00
4	0	1	1	1097	0.8	0.0	1.0	8.3	11.0	160	9	1.00
4	0	1	1	1018	0.8	0.0	1.0	8.3	11.0	160	10	1.00
5	0	1	1	953	1.0	1.5	0.7	8.9	9.3	160	10	0.93
5	0	1	1	817	1.0	1.2	0.8	9.5	5.8	160	10	0.72
5	0	1	1	676	1.0	1.1	0.9	10.1	3.8	160	11	0.53
5	0	1	1	593	1.0	1.1	0.9	10.3	2.0	160	12	0.41
6	0	1	1	530	0.0	0.0	1.0	10.8	2.0	160	12	0.00
6	0	1	1	444	0.0	0.0	0.9	11.4	0.0	146	13	0.00
6	0	1	1	358	0.0	0.0	0.9	12.2	0.0	89	17	0.00
6	0	1	1	281	0.0	0.0	0.9	12.8	0.0	84	18	0.00
6	0	1	1	206	0.0	0.0	0.9	13.7	0.0	81	19	0.00
6	0	1	1	135	0.0	0.0	1.0	14.4	0.0	77	20	0.00
6	0	1	1	79	0.0	0.0	1.0	15.1	0.0	74	20	0.00
6	0	1	1	27	0.0	0.0	1.0	16.0	0.0	71	21	0.00

PROPPANT SUMMARY * At End of Pumping Schedule
FLUVIAL C FOAM MINIFRAC NO. 1

Lb/Sq-Ft Lost to Embedment 0.050

Distance (ft)	KfW (md-ft)	Proppant Concentration (lb/sq foot) Prop ID--> 1
21	7	0.00
54	8	0.00
92	0	0.00
142	0	0.00
192	0	0.00
242	0	0.00
292	0	0.00
342	0	0.00
392	0	0.00
442	0	0.00
492	0	0.00
542	0	0.00
592	32	0.10
642	32	0.10
692	31	0.10
742	26	0.10
792	21	0.10
842	20	0.10
892	14	0.10
942	8	0.10
992	0	0.00
1042	0	0.00
1092	6	0.00
1142	0	0.00
1192	0	0.00
1242	0	0.00
1292	0	0.00
1342	0	0.00
1392	0	0.00
1442	0	0.00
1492	0	0.00
1542	0	0.00
1592	0	0.00
1642	0	0.00
1692	0	0.00
1719	0	0.00

Average Conductivity (md-ft) 19

PROPPANT SUMMARY * At Fracture Closure
FLUVIAL C FOAM MINIFRAC NO. 1

Lb/Sq-Ft Lost to Embedment 0.050

Distance (ft)	KfW (md-ft)	Proppant Concentration (lb/sq foot) Prop ID--> 1
21	7	0.00
54	8	0.00
92	0	0.00
142	0	0.00
192	0	0.00
242	0	0.00
292	0	0.00
342	0	0.00
392	0	0.00
442	0	0.00
492	0	0.00
542	0	0.00
592	9	0.10
642	12	0.10
692	19	0.10
742	23	0.10
792	33	0.10
842	30	0.10
892	30	0.10
942	23	0.10
992	0	0.00
1042	0	0.00
1092	0	0.00
1142	0	0.00
1192	0	0.00
1242	0	0.00
1292	0	0.00
1342	0	0.00
1392	0	0.00
1442	0	0.00
1492	0	0.00
1542	0	0.00
1592	0	0.00
1642	0	0.00
1692	0	0.00
1719	0	0.00

Average Conductivity (md-ft) 20

C.10: SIMULATION OF INITIAL ATTEMPT TO HISTORY MATCH THE FLUVIAL "E" FOAM MINIFRAC INJECTION/DECLINE PRESSURES.

Frac Summary * FLUVIAL E FOAM MINIFRAC
Filename: FLUV-E-M.FRK

Design Data		
FLUID LOSS:	Coefficient (ft/sqrt(min))	0.0020
	Spurt Loss (gal/100 sq ft)	0.00
FORMATION:	Modulus (MM psi)	4.00
	Fracture Height (ft)	30.0
	Fluid Loss Height (ft)	15.0
	Perforated Height (ft)	10.0
TEMPERATURE:	Bottom Hole (deg F)	160
PRESSURE:	Reservoir Pressure (psi)	3200.0
	Closure Pressure (psi)	4520.0
DEPTH:	Well Depth (ft)	5540

FORMATION LAYER DATA:

Depth	Stress at Top	Stress Grad	Modulus	Toughness
5300	5800.0	0.000	5.00	1.00
5480	4500.0	0.000	5.00	1.00
5495	5800.0	0.000	6.00	1.00
5532	4520.0	0.000	4.00	1.00
5570	5800.0	0.000	6.00	1.00
5719	4727.0	0.000	4.00	1.00
5739	6000.0	0.000	5.00	1.00
5825	4550.0	0.000	5.00	1.00
5850	6000.0	0.000	5.00	1.00
5886	5200.0	0.000	5.00	1.00
5927	5775.0	0.000	5.00	1.00
5953	4200.0	0.000	5.00	1.00
5980	5600.0	0.433	5.00	1.00

Fluid Pressure Gradient (psi/ft)		0.433
Fracture Top (ft)		5540
Fracture Bottom (ft)		5550

Calculated Results
from 3-D Simulator
STIMPLAN (TM) , NSI , Tulsa,OK
Licensed To: Internal Use - NSI Technologies

1/2 LENGTH:	'Hydraulic' length (ft)	1674
	Propped length (ft)	0
PRESSURE:	Max Net Pressure (psi)	762
TIME:	Max Exposure to Form. Temp. (min) ..	15.4
	Time to Close (min)	36.3
RATE:	Fluid Loss Rate during pad (bpm) ...	0.0
EFFICIENCY:	at end of pumping schedule	0.47
PROPPANT:	Average In Situ Conc. (#/sq ft)	0.0
	Average Conductivity (md-ft)	0
HEIGHT:	Max Fracture Height (ft)	89
WIDTH:	Avg width at end of pumping (in) ...	0.07

STIMPLAN (TM). NSI Technologies, Tulsa, OK
Licensed To: Internal Use - NSI Technologies

WELL ID:
FLUVIAL E FOAM MINIFRAC

DEPTH:	Well Depth (ft)	5540
PRESSURE:	Reservoir Pressure (psi)	3200
	Closure Pressure (psi)	4520
TEMPERATURE:	Bottom Hole Temperature (deg F)	160

** Pumping Schedule **

Sl Vol (Mgal)	Fl Vol (Mgal)	Conc (ppg)	Rate (bpm)	Fluid Type	Prop Type	Cum Prop (M-lb)	Pump Time (min)
9.1	9.1	0.0	23.0	3	1	0.0	9.4
2.0	2.0	0.0	23.0	2	1	0.0	2.1
4.3	4.3	0.0	23.0	2	1	0.0	4.4
1.9	1.9	0.0	21.0	2	1	0.0	2.2
5.3	5.3	0.0	20.0	2	1	0.0	6.3
1.4	1.4	0.0	21.0	2	1	0.0	1.6

Total Slurry ...	23.9	Total Fluid ...	23.9
Total Proppant ...	0.0	Avg. Conc	0.0
Total Pump Time	25.9 min		

Proppant ID No. 1 — 20- 40 Pro-Flow

Specific Gravity					3.15
'Damage Factor'					0.80
Closure Pres (Mpsi)	0	2	4	8	16
KfW @ 2 #/sq ft (md-ft)	11000	10500	9200	5400	950

Fluid ID No. 3 — nitrogen-water

Specific Gravity					0.60	
	@Welbor	@FormTmp	@1Hr	@2Hr	@4Hr	@8Hr
vis (cp @ 170 1/sec)	7	7	7	7	7	7
non-Newtonian n'	0.57	0.57	0.57	0.57	0.57	0.57

Fluid ID No. 2	75_Q_foam,_20#_gel					
Specific Gravity					0.60	
	@Welbor	@FormTmp	@1Hr	@2Hr	@4Hr	@8Hr
vis (cp @ 170 1/sec) .	50	27	15	10	10	10
non-Newtonian n'	0.42	0.52	0.53	0.57	0.57	0.57

Time History * NSI STIMPLAN 3-D Fracture Simulation
FLUVIAL E FOAM MINIFRAC

Time (min)	Pen (ft)	Pres (psi)	Rate (bpm)	Prop (PPG)	Sl Vol (MGal)	Eff-ciency	Loss (bpm)	Hght (ft)	W-Avg (in)
0.1	84	298	23.0	0.0	0.1	0.62	8.4	33	0.02
0.6	159	537	23.0	0.0	0.6	0.55	7.3	49	0.04
1.1	234	594	23.0	0.0	1.1	0.56	7.6	73	0.05
1.8	309	577	23.0	0.0	1.8	0.56	8.1	73	0.05
2.6	384	566	23.0	0.0	2.5	0.56	8.5	73	0.06
3.5	459	561	23.0	0.0	3.3	0.56	8.8	73	0.06
4.4	534	563	23.0	0.0	4.2	0.56	9.2	73	0.06
5.3	609	569	23.0	0.0	5.2	0.55	9.6	73	0.06
6.3	684	573	23.0	0.0	6.1	0.54	10.0	73	0.06
7.3	759	578	23.0	0.0	7.1	0.54	10.4	74	0.07
8.4	834	583	23.0	0.0	8.1	0.53	10.8	74	0.07
9.4	909	588	23.0	0.0	9.1	0.52	11.1	75	0.07
10.5	984	596	23.0	0.0	10.2	0.52	11.4	75	0.07
11.7	1059	624	23.0	0.0	11.3	0.51	11.6	77	0.07
13.0	1134	649	23.0	0.0	12.5	0.51	11.7	79	0.07
14.4	1209	673	23.0	0.0	13.9	0.50	11.8	81	0.07
15.9	1284	693	23.0	0.0	15.3	0.50	11.8	83	0.07
17.5	1359	704	21.0	0.0	16.8	0.49	11.7	84	0.07
19.4	1434	721	21.0	0.0	18.5	0.48	11.6	85	0.07
20.5	1471	724	20.0	0.0	19.4	0.48	11.3	86	0.07
22.4	1546	741	20.0	0.0	21.0	0.47	11.5	87	0.07
23.7	1584	747	20.0	0.0	22.1	0.47	11.1	87	0.07
24.9	1621	752	20.0	0.0	23.1	0.47	11.1	88	0.07
25.9	1655	762	21.0	0.0	24.0	0.47	10.9	89	0.07
26.7	1674	685	0.0	0.0	24.0	0.45	10.9	89	0.07
29.4	1674	617	0.0	0.0	24.0	0.41	9.1	89	0.06
32.5	1674	548	0.0	0.0	24.0	0.36	8.3	89	0.06
36.0	1674	480	0.0	0.0	24.0	0.32	7.6	89	0.05
39.7	1674	411	0.0	0.0	24.0	0.27	7.0	89	0.04
43.6	1674	343	0.0	0.0	24.0	0.23	6.5	89	0.03
47.9	1674	274	0.0	0.0	24.0	0.18	6.1	89	0.03
52.4	1674	206	0.0	0.0	24.0	0.14	5.7	89	0.02
57.2	1674	137	0.0	0.0	24.0	0.09	5.4	89	0.01
62.3	1674	69	0.0	0.0	24.0	0.05	5.1	89	0.01

GEOMETRY SUMMARY * At End of Pumping Schedule
FLUVIAL E FOAM MINIFRAC

Dstnce (ft)	Press (psi)	W-Avg (in)	Q (bpm)	Sh-Rate (1/sec)	Hght (ft) Total	Up	Dn	Prop	Bank Fraction	Prop (PSF)
23	757	0.10	10.5	406	89	33	45	66	0.00	0.00
65	747	0.10	10.3	411	88	33	45	65	0.00	0.00
121	734	0.10	10.2	422	87	32	44	64	0.00	0.00
196	717	0.10	9.9	434	85	32	44	63	0.00	0.00
271	699	0.09	9.5	449	84	31	43	61	0.00	0.00
346	680	0.09	9.2	465	82	30	42	59	0.00	0.00
421	662	0.09	8.9	484	81	29	41	58	0.00	0.00
496	645	0.09	8.5	500	79	29	41	56	0.00	0.00
571	629	0.09	8.2	510	78	28	40	55	0.00	0.00
646	612	0.08	7.8	521	77	27	39	53	0.00	0.00
721	595	0.08	7.5	533	75	27	39	52	0.00	0.00
796	578	0.08	7.1	545	74	26	38	50	0.00	0.00
871	559	0.08	6.7	559	72	25	37	49	0.00	0.00
946	540	0.08	6.4	575	71	24	36	47	0.00	0.00
1021	520	0.07	6.0	592	69	23	35	45	0.00	0.00
1096	498	0.07	5.6	626	66	22	34	42	0.00	0.00
1171	475	0.07	5.1	663	63	20	33	38	0.00	0.00
1246	451	0.06	4.7	712	58	18	31	34	0.00	0.00
1321	424	0.06	4.2	781	53	15	29	29	0.00	0.00
1396	395	0.06	3.7	884	48	11	26	23	0.00	0.00
1453	368	0.05	3.2	987	42	8	24	17	0.00	0.00
1509	342	0.04	2.8	1499	36	5	22	14	0.00	0.00
1565	308	0.04	1.9	1852	31	1	20	11	0.00	0.00
1603	252	0.03	1.6	2273	31	1	20	11	0.00	0.00
1638	147	0.02	1.0	4397	31	1	20	11	0.00	0.00

FLUID SUMMARY * At End of Pumping Schedule
FLUVIAL E FOAM MINIFRAC

Stage No	Gone	Fluid ID	Prop ID	Pos (ft)	Concentration In	Now	Desgn	Fl Vol (MGal)	Ex Tim (min)	Temp (deg F)	Visc (cp)	Fall Frac
1	1	3	1	1655	0.0	0.0	0.0	0.1	2.9	160	1	0.00
1	1	3	1	1655	0.0	0.0	0.0	0.6	4.0	160	1	0.00
1	1	3	1	1655	0.0	0.0	0.0	1.1	5.3	160	1	0.00
1	1	3	1	1655	0.0	0.0	0.0	1.8	6.7	160	1	0.00
1	1	3	1	1655	0.0	0.0	0.0	2.5	8.1	160	1	0.00
1	1	3	1	1655	0.0	0.0	0.0	3.3	8.8	160	1	0.00
1	1	3	1	1655	0.0	0.0	0.0	4.2	10.9	160	1	0.00
1	1	3	1	1655	0.0	0.0	0.0	5.2	11.7	160	1	0.00
1	1	3	1	1655	0.0	0.0	0.0	6.1	13.6	160	1	0.00
1	1	3	1	1655	0.0	0.0	0.0	7.1	15.4	160	1	0.00
1	1	3	1	1655	0.0	0.0	0.0	8.1	15.4	160	1	0.00
1	0	3	1	1575	0.0	0.0	0.2	9.1	14.3	160	2	0.00
2	0	2	1	1516	0.0	0.0	0.3	9.1	14.3	160	5	0.00
2	0	2	1	1445	0.0	0.0	0.3	10.2	11.8	160	6	0.00
2	0	2	1	1324	0.0	0.0	0.4	11.0	11.8	160	7	0.00
3	0	2	1	1260	0.0	0.0	0.5	11.3	10.3	160	8	0.00
3	0	2	1	1180	0.0	0.0	0.6	12.5	8.7	160	8	0.00
3	0	2	1	1043	0.0	0.0	0.6	13.8	6.9	160	8	0.00
3	0	2	1	899	0.0	0.0	0.7	15.2	5.5	160	9	0.00
4	0	2	1	750	0.0	0.0	0.8	16.7	4.0	160	9	0.00
4	0	2	1	651	0.0	0.0	0.8	17.1	2.3	160	9	0.00
5	0	2	1	571	0.0	0.0	0.8	18.2	1.1	160	9	0.00
5	0	2	1	469	0.0	0.0	0.9	19.1	0.0	160	10	0.00
5	0	2	1	347	0.0	0.0	0.9	20.7	0.0	105	12	0.00
5	0	2	1	221	0.0	0.0	0.9	21.8	0.0	82	14	0.00
5	0	2	1	146	0.0	0.0	1.0	22.3	0.0	78	14	0.00
6	0	2	1	101	0.0	0.0	1.0	22.7	0.0	76	14	0.00
6	0	2	1	41	0.0	0.0	1.0	23.6	0.0	72	15	0.00

C.11: FLUVIAL "E" FOAM MINIFRAC PRESSURE HISTORY MATCH WITH CHANGES IN FLUID VISCOSITY.

Frac Summary * FLUVIAL E FOAM FRACTURE TREATMENT
Filename: FLUV-E-M.FRK

Design Data		
FLUID LOSS:	Coefficient (ft/sqrt(min))	0.0020
	Spurt Loss (gal/100 sq ft)	0.00
FORMATION:	Modulus (MM psi)	4.00
	Fracture Height (ft)	30.9
	Fluid Loss Height (ft)	15.0
	Perforated Height (ft)	10.0
TEMPERATURE:	Bottom Hole (deg F)	160
PRESSURE:	Reservoir Pressure (psi)	3200.0
	Closure Pressure (psi)	4520.0
DEPTH:	Well Depth (ft)	5540

FORMATION LAYER DATA:

Depth	Stress at Top	Stress Grad	Modulus	Toughness
5300	5800.0	0.000	5.00	1.00
5480	4500.0	0.000	5.00	1.00
5495	5800.0	0.000	6.00	1.00
5532	4520.0	0.000	4.00	1.00
5570	5800.0	0.000	6.00	1.00
5719	4727.0	0.000	4.00	1.00
5739	6000.0	0.000	5.00	1.00
5825	4550.0	0.000	5.00	1.00
5850	6000.0	0.000	5.00	1.00
5886	5200.0	0.000	5.00	1.00
5927	5775.0	0.000	5.00	1.00
5953	4200.0	0.000	5.00	1.00
5980	5600.0	0.433	5.00	1.00

Fluid Pressure Gradient (psi/ft)	0.433
Fracture Top (ft)	5540
Fracture Bottom (ft)	5550

Calculated Results
from 3-D Simulator
STIMPLAN (TM) , NSI , Tulsa,OK
Licensed To: Internal Use - NSI Technologies

1/2 LENGTH:	'Hydraulic' length (ft)	1621
	Propped length (ft)	0
PRESSURE:	Max Net Pressure (psi)	940
TIME:	Max Exposure to Form. Temp. (min) ..	16.0
	Time to Close (min)	45.0
RATE:	Fluid Loss Rate during pad (bpm) ...	0.0
EFFICIENCY:	at end of pumping schedule	0.55
PROPPANT:	Average In Situ Conc. (#/sq ft)	0.0
	Average Conductivity (md-ft)	0
HEIGHT:	Max Fracture Height (ft)	102
WIDTH:	Avg width at end of pumping (in) ...	0.08

STIMPLAN (TM). NSI Technologies, Tulsa, OK
Licensed To: Internal Use - NSI Technologies

WELL ID:
FLUVIAL E FOAM FRACTURE TREATMENT

DEPTH:	Well Depth (ft)	5540
PRESSURE:	Reservoir Pressure (psi)	3200
	Closure Pressure (psi)	4520
TEMPERATURE:	Bottom Hole Temperature (deg F)	160

** Pumping Schedule **

Sl Vol (Mgal)	Fl Vol (Mgal)	Conc (ppg)	Rate (bpm)	Fluid Type	Prop Type	Cum Prop (M-lb)	Pump Time (min)
9.1	9.1	0.0	23.0	3	1	0.0	9.4
2.0	2.0	0.0	23.0	1	1	0.0	2.1
4.3	4.3	0.0	23.0	1	1	0.0	4.5
1.9	1.9	0.0	21.0	2	1	0.0	2.2
5.5	5.5	0.0	20.0	2	1	0.0	6.5
1.6	1.6	0.0	21.0	2	1	0.0	1.8

Total Slurry ...	24.4	Total Fluid ...	24.4
Total Proppant ...	0.0	Avg. Conc	0.0
Total Pump Time	26.5 min		

Proppant ID No. 1 20- 40 Pro-Flow

Specific Gravity					3.15
'Damage Factor'					0.80
Closure Pres (Mpsi)	0	2	4	8	16
KfW @ 2 #/sq ft (md-ft)	11000	10500	9200	5400	950

Fluid ID No. 3 nitrogen-water

Specific Gravity 0.60

	@Welbor	@FormTmp	@1Hr	@2Hr	@4Hr	@8Hr
vis (cp @ 170 1/sec) .	7	7	7	7	7	7
non-Newtonian n'	0.57	0.57	0.57	0.57	0.57	0.57

Fluid ID No. 1	Thick_gel,_tank_bottom					
Specific Gravity					1.04	
Quality					75	
	@Welbor	@FormTmp	@1Hr	@2Hr	@4Hr	@8Hr
vis (cp @ 170 1/sec) .	400	100	20	10	10	10
non-Newtonian n'	0.27	0.27	0.52	0.57	0.57	0.57

Fluid ID No. 2	75_Q_foam,_20#_gel					
Specific Gravity					0.60	
	@Welbor	@FormTmp	@1Hr	@2Hr	@4Hr	@8Hr
vis (cp @ 170 1/sec) .	75	50	15	10	10	10
non-Newtonian n'	0.36	0.42	0.53	0.57	0.57	0.57

Time History * NSI STIMPLAN 3-D Fracture Simulation
FLUVIAL E FOAM FRACTURE TREATMENT

Time (min)	Pen (ft)	Pres (psi)	Rate (bpm)	Prop (PPG)	Sl Vol (MGal)	Eff-ciency	Loss (bpm)	Hght (ft)	W-Avg (in)
0.1	84	298	23.0	0.0	0.1	0.62	8.4	33	0.02
0.6	159	537	23.0	0.0	0.6	0.55	7.3	49	0.04
1.1	234	594	23.0	0.0	1.1	0.56	7.6	73	0.05
1.8	309	577	23.0	0.0	1.8	0.56	8.1	73	0.05
2.6	384	566	23.0	0.0	2.5	0.56	8.5	73	0.06
3.5	459	561	23.0	0.0	3.3	0.56	8.8	73	0.06
4.4	534	563	23.0	0.0	4.2	0.56	9.2	73	0.06
5.3	609	569	23.0	0.0	5.2	0.55	9.6	73	0.06
6.3	684	573	23.0	0.0	6.1	0.54	10.0	73	0.06
7.3	759	578	23.0	0.0	7.1	0.54	10.4	74	0.07
8.4	834	583	23.0	0.0	8.1	0.53	10.8	74	0.07
9.4	909	588	23.0	0.0	9.1	0.52	11.1	75	0.07
10.5	984	593	23.0	0.0	10.2	0.52	11.4	75	0.07
11.8	1059	756	23.0	0.0	11.4	0.51	11.4	85	0.07
13.7	1134	865	23.0	0.0	13.3	0.52	10.9	94	0.07
15.6	1209	912	23.0	0.0	15.1	0.52	10.6	99	0.07
17.3	1284	940	23.0	0.0	16.8	0.53	10.8	102	0.08
19.1	1359	916	21.0	0.0	18.3	0.54	11.0	102	0.08
20.9	1434	893	20.0	0.0	19.8	0.54	11.1	102	0.08
22.9	1509	879	20.0	0.0	21.5	0.55	11.2	102	0.08
24.1	1546	863	20.0	0.0	22.5	0.55	10.9	102	0.08
25.4	1584	861	20.0	0.0	23.6	0.55	10.8	102	0.08
26.5	1611	866	21.0	0.0	24.6	0.55	10.2	102	0.08
27.3	1621	793	0.0	0.0	24.6	0.54	10.1	102	0.08
31.0	1621	714	0.0	0.0	24.6	0.49	8.2	102	0.07
35.4	1621	634	0.0	0.0	24.6	0.43	7.5	102	0.06
40.3	1621	555	0.0	0.0	24.6	0.38	6.7	102	0.05
45.6	1621	476	0.0	0.0	24.6	0.33	6.1	102	0.05
51.5	1621	396	0.0	0.0	24.6	0.27	5.6	102	0.04
57.7	1621	317	0.0	0.0	24.6	0.22	5.2	102	0.03
64.4	1621	238	0.0	0.0	24.6	0.16	4.9	102	0.02
71.4	1621	159	0.0	0.0	24.6	0.11	4.6	102	0.02

GEOMETRY SUMMARY * At End of Pumping Schedule
FLUVIAL E FOAM FRACTURE TREATMENT

Dstnce (ft)	Press (psi)	W-Avg (in)	Q (bpm)	Sh-Rate (1/sec)	Hght (ft) Total	Up	Dn	Prop	Bank Fraction	Prop (PSF)
23	862	0.11	10.6	282	102	40	52	81	0.00	0.00
65	853	0.11	10.4	287	100	39	51	78	0.00	0.00
121	840	0.11	10.3	297	97	38	49	75	0.00	0.00
196	821	0.11	10.1	310	94	36	48	72	0.00	0.00
271	801	0.11	9.8	323	92	35	47	70	0.00	0.00
346	781	0.10	9.5	335	91	34	46	68	0.00	0.00
421	761	0.10	9.2	347	89	34	45	67	0.00	0.00
496	744	0.10	8.8	354	88	33	45	65	0.00	0.00
571	727	0.10	8.4	359	86	32	44	64	0.00	0.00
646	709	0.10	8.0	365	85	31	43	62	0.00	0.00
721	686	0.09	7.7	361	83	30	42	60	0.00	0.00
796	661	0.09	7.3	374	81	29	41	58	0.00	0.00
871	635	0.09	6.9	390	78	28	40	55	0.00	0.00
946	609	0.08	6.5	407	76	27	39	53	0.00	0.00
1021	582	0.08	6.0	423	74	26	38	50	0.00	0.00
1096	554	0.08	5.5	437	72	25	37	48	0.00	0.00
1171	524	0.07	4.9	456	69	24	36	45	0.00	0.00
1246	492	0.07	4.4	474	65	21	33	40	0.00	0.00
1321	447	0.06	3.8	538	58	18	31	34	0.00	0.00
1396	381	0.05	3.0	679	51	14	27	26	0.00	0.00
1471	314	0.04	2.4	1104	42	8	24	16	0.00	0.00
1528	290	0.03	1.6	1859	32	2	20	12	0.00	0.00
1565	227	0.03	1.3	2343	31	1	20	11	0.00	0.00
1598	116	0.01	0.9	5819	31	1	20	11	0.00	0.00

FLUID SUMMARY * At End of Pumping Schedule
FLUVIAL E FOAM FRACTURE TREATMENT

Stage No	Gone	Fluid ID	Prop ID	Pos (ft)	Concentration In	Now	Desgn	Fl Vol (MGal)	Ex Tim (min)	Temp (deg F)	Visc (cp)	Fall Frac
1	1	3	1	1611	0.0	0.0	0.0	0.1	2.9	160	1	0.00
1	1	3	1	1611	0.0	0.0	0.0	0.6	4.0	160	1	0.00
1	1	3	1	1611	0.0	0.0	0.0	1.1	5.3	160	1	0.00
1	1	3	1	1611	0.0	0.0	0.0	1.8	6.7	160	1	0.00
1	1	3	1	1611	0.0	0.0	0.0	2.5	8.1	160	1	0.00
1	1	3	1	1611	0.0	0.0	0.0	3.3	7.9	160	1	0.00
1	1	3	1	1611	0.0	0.0	0.0	4.2	10.6	160	1	0.00
1	1	3	1	1611	0.0	0.0	0.0	5.2	13.2	160	1	0.00
1	1	3	1	1611	0.0	0.0	0.0	6.1	14.0	160	1	0.00
1	1	3	1	1611	0.0	0.0	0.0	7.1	15.9	160	1	0.00
1	1	3	1	1611	0.0	0.0	0.0	8.1	16.0	160	1	0.00
1	0	3	1	1510	0.0	0.0	0.2	9.1	14.8	160	2	0.00
2	0	1	1	1373	0.0	0.0	0.5	10.1	11.3	160	12	0.00
2	0	1	1	1240	0.0	0.0	0.7	11.1	11.3	160	14	0.00
3	0	1	1	1163	0.0	0.0	0.7	11.4	11.3	160	15	0.00
3	0	1	1	1035	0.0	0.0	0.9	13.1	7.7	160	16	0.00
3	0	1	1	825	0.0	0.0	1.0	14.9	4.1	160	18	0.00
3	0	1	1	708	0.0	0.0	1.0	15.2	4.1	160	18	0.00
4	0	2	1	639	0.0	0.0	0.8	16.5	2.5	160	15	0.00
4	0	2	1	556	0.0	0.0	0.8	17.2	1.2	160	16	0.00
5	0	2	1	495	0.0	0.0	0.9	18.0	1.2	160	16	0.00
5	0	2	1	404	0.0	0.0	0.9	19.5	0.0	136	18	0.00
5	0	2	1	283	0.0	0.0	0.9	21.1	0.0	86	21	0.00
5	0	2	1	182	0.0	0.0	0.9	22.1	0.0	80	21	0.00
5	0	2	1	126	0.0	0.0	1.0	22.6	0.0	77	22	0.00
6	0	2	1	87	0.0	0.0	1.0	23.1	0.0	75	22	0.00
6	0	2	1	33	0.0	0.0	1.0	24.1	0.0	72	23	0.00

C.12: SIMULATION OF FLUVIAL "E" FOAM FRACTURE TREATMENT.

Frac Summary * FLUVIAL E FOAM FRACTURE TREATMENT
Filename: FLUV-E-M.FRK

Design Data		
FLUID LOSS:	Coefficient (ft/sqrt(min))	0.0015
	Spurt Loss (gal/100 sq ft)	0.00
FORMATION:	Modulus (MM psi)	4.00
	Fracture Height (ft)	30.9
	Fluid Loss Height (ft)	15.0
	Perforated Height (ft)	10.0
TEMPERATURE:	Bottom Hole (deg F)	160
PRESSURE:	Reservoir Pressure (psi)	3200.0
	Closure Pressure (psi)	4520.0
DEPTH:	Well Depth (ft)	5540

FORMATION LAYER DATA:

Depth	Stress at Top	Stress Grad	Modulus	Toughness
5300	5800.0	0.000	5.00	1.00
5480	4500.0	0.000	5.00	1.00
5495	5800.0	0.000	6.00	1.00
5532	4520.0	0.000	4.00	1.00
5570	5800.0	0.000	6.00	1.00
5719	4727.0	0.000	4.00	1.00
5739	6000.0	0.000	5.00	1.00
5825	4550.0	0.000	5.00	1.00
5850	6000.0	0.000	5.00	1.00
5886	5200.0	0.000	5.00	1.00
5927	5775.0	0.000	5.00	1.00
5953	4200.0	0.000	5.00	1.00
5980	5600.0	0.433	5.00	1.00

Fluid Pressure Gradient (psi/ft)		0.433
Fracture Top (ft)		5540
Fracture Bottom (ft)		5550

Calculated Results
from 3-D Simulator
STIMPLAN (TM) , NSI , Tulsa,OK
Licensed To: Internal Use - NSI Technologies

1/2 LENGTH:	'Hydraulic' length (ft)	2320
	Propped length (ft)	2100
PRESSURE:	Max Net Pressure (psi)	1043
TIME:	Max Exposure to Form. Temp. (min) ..	36.9
	Time to Close (min)	132.3
RATE:	Fluid Loss Rate during pad (bpm) ...	6.3
EFFICIENCY:	at end of pumping schedule	0.62
PROPPANT:	Average In Situ Conc. (#/sq ft)	0.2
	Average Conductivity (md-ft)	611
HEIGHT:	Max Fracture Height (ft)	142
WIDTH:	Avg width at end of pumping (in) ...	0.11

STIMPLAN (TM). NSI Technologies, Tulsa, OK
Licensed To: Internal Use - NSI Technologies

WELL ID:
FLUVIAL E FOAM FRACTURE TREATMENT

DEPTH:	Well Depth (ft)	5540
PRESSURE:	Reservoir Pressure (psi)	3200
	Closure Pressure (psi)	4520
TEMPERATURE:	Bottom Hole Temperature (deg F)	160

** Pumping Schedule **

Sl Vol (Mgal)	Fl Vol (Mgal)	Conc (ppg)	Rate (bpm)	Fluid Type	Prop Type	Cum Prop (M-lb)	Pump Time (min)
2.0	2.0	0.0	17.0	3	1	0.0	2.8
4.0	4.0	0.0	23.0	2	1	0.0	4.1
6.0	6.0	0.0	23.0	1	1	0.0	6.2
8.0	7.8	0.5	23.0	2	4	3.9	8.3
5.2	5.0	1.0	23.0	2	1	8.9	5.4
10.0	9.0	3.0	23.0	2	1	35.9	10.4
11.5	10.0	4.0	23.0	2	1	75.9	11.9

Total Slurry ...	46.7	Total Fluid ...	43.8
Total Proppant ...	75.9	Avg. Conc	1.7
Total Pump Time	49.1 min		

Proppant ID No. 4 20- 40 Ottawa_Snd

Specific Gravity					2.65
'Damage Factor'					0.70
Closure Pres (Mpsi)	0	2	4	8	16
KfW @ 2 #/sq ft (md-ft)	4800	3850	2750	990	50

Fluid ID No. 3 nitrogen-water

Specific Gravity 0.60

	@Welbor	@FormTmp	@1Hr	@2Hr	@4Hr	@8Hr
vis (cp @ 170 1/sec) .	7	7	7	7	7	7
non-Newtonian n'	0.57	0.57	0.57	0.57	0.57	0.57

Fluid ID No. 2	75_Q_foam,_20#_gel					
Specific Gravity					0.60	
	@Welbor	@FormTmp	@1Hr	@2Hr	@4Hr	@8Hr
vis (cp @ 170 1/sec) .	75	50	15	10	10	10
non-Newtonian n'	0.36	0.42	0.53	0.57	0.57	0.57

Fluid ID No. 1	Thick_gel,_tank_bottom					
Specific Gravity					1.04	
Quality					75	
	@Welbor	@FormTmp	@1Hr	@2Hr	@4Hr	@8Hr
vis (cp @ 170 1/sec) .	400	100	20	10	10	10
non-Newtonian n'	0.27	0.27	0.52	0.57	0.57	0.57

Proppant ID No. 1	20- 40 Pro-Flow				
Specific Gravity					3.15
'Damage Factor'					0.80
Closure Pres (Mpsi)	0	2	4	8	16
kfW @ 2 #/sq ft (md-ft)	11000	10500	9200	5400	950

Time History * NSI STIMPLAN 3-D Fracture Simulation
FLUVIAL E FOAM FRACTURE TREATMENT

Time (min)	Pen (ft)	Pres (psi)	Rate (bpm)	Prop (PPG)	Sl Vol (MGal)	Eff-ciency	Loss (bpm)	Hght (ft)	W-Avg (in)
0.3	104	233	17.0	0.0	0.2	0.69	5.1	44	0.03
1.2	179	458	17.0	0.0	0.9	0.61	4.3	58	0.05
2.2	254	517	17.0	0.0	1.6	0.60	4.4	66	0.05
2.8	300	500	17.0	0.0	2.0	0.58	4.2	67	0.05
3.6	375	530	23.0	0.0	2.8	0.59	5.7	69	0.06
4.4	450	579	23.0	0.0	3.6	0.59	6.3	72	0.06
5.3	525	612	23.0	0.0	4.5	0.59	6.7	75	0.06
6.4	600	643	23.0	0.0	5.4	0.59	6.9	78	0.07
7.4	675	670	23.0	0.0	6.5	0.59	7.1	80	0.07
8.7	750	724	23.0	0.0	7.7	0.60	7.3	84	0.07
10.0	825	804	23.0	0.0	9.0	0.60	7.3	89	0.07
12.5	900	886	23.0	0.0	11.4	0.62	6.7	96	0.08
15.5	975	979	23.0	0.0	14.3	0.65	6.2	104	0.09
17.9	1050	976	23.0	0.5	16.6	0.67	6.3	106	0.10
19.9	1125	972	23.0	0.5	18.6	0.68	6.6	106	0.10
21.7	1200	976	23.0	0.5	20.3	0.68	7.0	107	0.11
23.4	1275	980	23.0	1.0	21.9	0.68	7.4	107	0.11
25.0	1350	983	23.0	1.0	23.5	0.68	7.7	107	0.11
26.6	1425	984	23.0	1.0	25.0	0.67	8.0	107	0.11
28.3	1500	988	23.0	1.0	26.7	0.67	8.2	108	0.11
30.1	1575	992	23.0	3.0	28.4	0.66	8.3	108	0.11
31.9	1650	997	23.0	3.0	30.1	0.65	8.5	108	0.11
34.3	1725	1013	23.0	3.0	32.4	0.65	8.4	110	0.11
36.6	1800	1024	23.0	3.0	34.7	0.65	8.3	111	0.11
38.8	1875	1031	23.0	3.0	36.8	0.64	8.5	111	0.11
40.8	1950	1036	23.0	4.0	38.8	0.64	8.7	130	0.11
43.2	2025	1027	23.0	4.0	41.1	0.63	8.7	130	0.11
45.2	2100	1036	23.0	4.0	43.1	0.63	8.9	130	0.11
47.2	2175	1043	23.0	4.0	44.9	0.62	9.1	142	0.11
49.1	2245	1034	23.0	4.0	46.8	0.62	9.2	142	0.11
51.5	2320	940	0.0	0.0	46.8	0.60	9.3	142	0.10
60.3	2320	846	0.0	0.0	46.8	0.54	6.7	142	0.09
71.2	2320	752	0.0	0.0	46.8	0.48	5.9	142	0.08
83.5	2320	658	0.0	0.0	46.8	0.43	5.1	142	0.07
97.2	2320	564	0.0	0.0	46.8	0.37	4.6	142	0.06
111.8	2320	470	0.0	0.0	46.8	0.32	4.1	142	0.05
126.8	2320	376	0.0	0.0	46.8	0.27	3.8	142	0.05
141.7	2320	282	0.0	0.0	46.8	0.22	3.5	142	0.04
156.3	2320	188	0.0	0.0	46.8	0.18	3.3	142	0.03
181.4	2320	94	0.0	0.0	46.8	0.15	3.0	142	0.03

GEOMETRY SUMMARY * At End of Pumping Schedule
FLUVIAL E FOAM FRACTURE TREATMENT

Dstnce (ft)	Press (psi)	W-Avg (in)	Q (bpm)	Sh-Rate (1/sec)	Hght (ft) Total	Up	Dn	Prop	Bank Fraction	Prop (PSF)
33	1032	0.12	11.6	186	142	63	69	126	0.04	0.35
85	1028	0.13	10.9	196	111	45	57	91	0.04	0.41
141	1018	0.13	10.8	200	111	45	56	90	0.04	0.39
216	1004	0.13	10.7	205	109	44	56	89	0.03	0.39
277	992	0.13	10.6	208	109	43	55	88	0.03	0.39
337	981	0.13	10.5	213	108	43	55	87	0.03	0.38
412	966	0.12	10.4	218	106	42	54	85	0.03	0.38
487	952	0.12	10.3	225	105	42	53	84	0.03	0.38
562	938	0.12	10.2	233	104	41	53	83	0.03	0.37
637	925	0.12	10.1	240	103	41	52	82	0.03	0.34
712	913	0.12	10.1	246	102	40	52	81	0.03	0.30
787	900	0.12	10.0	251	101	40	51	80	0.03	0.29
862	888	0.12	9.9	258	100	39	51	79	0.03	0.29
937	875	0.11	9.8	264	99	39	51	78	0.03	0.28
1012	863	0.11	9.7	270	99	38	50	77	0.03	0.28
1087	852	0.11	9.6	277	98	38	50	76	0.02	0.27
1162	840	0.11	9.5	284	97	38	49	75	0.02	0.25
1237	829	0.11	9.4	290	96	37	49	74	0.02	0.15
1312	818	0.11	9.4	297	95	37	48	73	0.01	0.10
1387	807	0.11	9.3	306	93	36	48	71	0.01	0.09
1462	796	0.11	9.2	313	93	35	47	70	0.01	0.09
1537	784	0.10	9.1	321	92	35	47	69	0.01	0.06
1612	770	0.10	8.8	326	91	34	46	68	0.01	0.05
1687	756	0.10	8.4	324	90	34	46	67	0.01	0.05
1762	743	0.10	7.8	341	88	33	45	65	0.01	0.04
1837	727	0.09	7.1	347	82	30	42	59	0.01	0.04
1912	707	0.09	6.3	360	75	26	38	51	0.00	0.03
1987	675	0.09	5.4	381	66	22	34	42	0.00	0.00
2062	634	0.08	4.4	456	56	17	29	31	0.00	0.00
2137	538	0.08	3.8	448	44	11	23	19	0.00	0.00
2210	281	0.04	2.5	1087	44	11	23	19	0.00	0.00

FLUID SUMMARY * At End of Pumping Schedule
FLUVIAL E FOAM FRACTURE TREATMENT

Stage No	Gone	Fluid ID	Prop ID	Pos (ft)	Concentration In	Now	Desgn	Fl Vol (MGal)	Ex Tim (min)	Temp (deg F)	Visc (cp)	Fall Frac
1	1	3	1	2245	0.0	0.0	0.0	0.2	6.7	160	2	0.00
1	1	3	1	2245	0.0	0.0	0.0	0.9	9.6	160	3	0.00
1	1	3	1	2245	0.0	0.0	0.0	1.6	14.2	160	3	0.00
1	1	3	1	2245	0.0	0.0	0.0	2.0	15.7	160	3	0.00
2	1	2	1	2245	0.0	0.0	0.0	2.0	15.7	160	9	0.00
2	1	2	1	2245	0.0	0.0	0.0	2.8	20.2	160	8	0.00
2	1	2	1	2245	0.0	0.0	0.0	3.6	22.6	160	8	0.00
2	1	2	1	2245	0.0	0.0	0.0	4.5	26.2	160	9	0.00
2	1	2	1	2245	0.0	0.0	0.0	5.4	27.4	160	9	0.00
2	1	2	1	2245	0.0	0.0	0.0	6.0	30.4	160	8	0.00
3	1	1	1	2245	0.0	0.0	0.0	6.5	36.8	160	6	0.00
3	1	1	1	2245	0.0	0.0	0.0	7.7	36.9	160	6	0.00
3	0	1	1	2207	0.0	0.0	0.3	9.0	34.2	160	7	0.00
3	0	1	1	2096	0.0	0.0	1.4	11.2	31.5	160	12	0.00
3	0	1	1	1982	0.0	0.0	2.3	11.8	31.5	160	14	0.00
4	0	2	4	1895	0.5	1.1	1.7	13.9	27.4	160	11	0.67
4	0	2	4	1771	0.5	0.9	2.0	16.1	25.6	160	12	0.49
4	0	2	4	1655	0.5	0.8	2.3	17.8	22.4	160	12	0.41
4	0	2	4	1563	0.5	0.8	2.5	19.1	20.7	160	12	0.36
5	0	2	1	1515	1.0	1.5	2.5	19.4	20.7	160	13	0.47
5	0	2	1	1463	1.0	1.5	2.6	20.9	18.9	160	13	0.39
5	0	2	1	1373	1.0	1.4	2.8	22.3	15.1	160	14	0.34
5	0	2	1	1283	1.0	1.4	2.9	23.7	12.7	160	15	0.30
5	0	2	1	1232	1.0	1.3	3.0	23.9	12.7	160	15	0.28
6	0	2	1	1185	3.0	4.0	3.0	25.2	12.7	160	15	0.28
6	0	2	1	1094	3.0	3.9	3.1	26.7	10.5	160	16	0.22
6	0	2	1	994	3.0	3.8	3.2	28.3	6.2	160	17	0.18
6	0	2	1	877	3.0	3.6	3.3	30.3	4.0	160	18	0.15
6	0	2	1	743	3.0	3.5	3.4	32.3	2.0	160	19	0.12
6	0	2	1	660	3.0	3.4	3.5	32.8	2.0	160	20	0.10
7	0	2	1	599	4.0	4.6	3.5	34.2	0.0	160	20	0.13
7	0	2	1	499	4.0	4.4	3.6	35.9	0.0	108	24	0.07
7	0	2	1	377	4.0	4.3	3.7	37.9	0.0	85	26	0.05
7	0	2	1	255	4.0	4.2	3.8	39.6	0.0	80	28	0.04
7	0	2	1	146	4.0	4.2	3.9	41.3	0.0	76	28	0.02
7	0	2	1	47	4.0	4.1	3.9	42.9	0.0	72	30	0.01

PROPPANT SUMMARY * At End of Pumping Schedule
FLUVIAL E FOAM FRACTURE TREATMENT

Lb/Sq-Ft Lost to Embedment 0.050

Distance (ft)	KfW (md-ft)	Proppant Concentration (lb/sq foot) Prop ID--> 1	4
33	1026	0.30	0.00
85	1211	0.40	0.00
141	1172	0.40	0.00
216	1158	0.40	0.00
277	1153	0.40	0.00
338	1140	0.40	0.00
413	1127	0.40	0.00
488	1118	0.40	0.00
563	1080	0.40	0.00
638	974	0.30	0.00
713	840	0.30	0.00
788	823	0.30	0.00
863	812	0.30	0.00
938	784	0.30	0.00
1013	763	0.30	0.00
1088	733	0.30	0.00
1163	682	0.20	0.00
1238	331	0.10	0.00
1313	152	0.10	0.00
1388	141	0.10	0.00
1463	120	0.10	0.00
1538	19	0.00	0.00
1613	1	0.00	0.10
1688	0	0.00	0.00
1763	0	0.00	0.00
1838	0	0.00	0.00
1913	0	0.00	0.00
1988	2	0.00	0.00
2063	0	0.00	0.00
2138	0	0.00	0.00
2210	0	0.00	0.00

Average Conductivity (md-ft) 704

PROPPANT SUMMARY * At Fracture Closure
FLUVIAL E FOAM FRACTURE TREATMENT

Lb/Sq-Ft Lost to Embedment 0.050

Distance (ft)	KfW (md-ft)	Proppant Concentration (lb/sq foot) Prop ID--> 1	4
33	468	0.20	0.00
85	587	0.20	0.00
141	554	0.20	0.00
216	584	0.20	0.00
277	634	0.20	0.00
338	645	0.20	0.00
413	678	0.20	0.00
488	703	0.20	0.00
563	741	0.30	0.00
638	839	0.30	0.00
713	928	0.30	0.00
788	1061	0.40	0.00
863	1397	0.40	0.00
938	1503	0.50	0.00
1013	1225	0.40	0.00
1088	790	0.30	0.00
1163	728	0.30	0.00
1238	716	0.30	0.00
1313	730	0.30	0.00
1388	687	0.20	0.00
1463	603	0.20	0.00
1538	499	0.20	0.00
1613	143	0.10	0.00
1688	123	0.10	0.00
1763	84	0.10	0.00
1838	9	0.00	0.10
1913	11	0.00	0.10
1988	24	0.00	0.10
2063	18	0.00	0.10
2138	0	0.00	0.00
2210	0	0.00	0.00
2283	0	0.00	0.00

Average Conductivity (md-ft) 612